

GEOLOGY, GEOCHRONOLOGY, AND TECTONIC EVOLUTION OF THE
BROOKVILLE TERRANE, SOUTHERN NEW BRUNSWICK

by

Christopher E. White

Submitted in partial fulfillment of the requirements
for the degree of Doctor of Philosophy

at

Dalhousie University
Halifax, Nova Scotia
December, 1995

© Copyright by Christopher E. White, 1995



National Library
of Canada

Acquisitions and
Bibliographic Services Branch

395 Wellington Street
Ottawa, Ontario
K1A 0N4

Bibliothèque nationale
du Canada

Direction des acquisitions et
des services bibliographiques

395, rue Wellington
Ottawa (Ontario)
K1A 0N4

Your file *Votre référence*

Our file *Notre référence*

The author has granted an irrevocable non-exclusive licence allowing the National Library of Canada to reproduce, loan, distribute or sell copies of his/her thesis by any means and in any form or format, making this thesis available to interested persons.

L'auteur a accordé une licence irrévocable et non exclusive permettant à la Bibliothèque nationale du Canada de reproduire, prêter, distribuer ou vendre des copies de sa thèse de quelque manière et sous quelque forme que ce soit pour mettre des exemplaires de cette thèse à la disposition des personnes intéressées.

The author retains ownership of the copyright in his/her thesis. Neither the thesis nor substantial extracts from it may be printed or otherwise reproduced without his/her permission.

L'auteur conserve la propriété du droit d'auteur qui protège sa thèse. Ni la thèse ni des extraits substantiels de celle-ci ne doivent être imprimés ou autrement reproduits sans son autorisation.

ISBN 0-612-15898-5

Canada

Name

Dissertation Abstracts International is arranged by broad, general subject categories. Please select the one subject which most nearly describes the content of your dissertation. Enter the corresponding four-digit code in the spaces provided.

Geology

SUBJECT TERM

0372

U·M·I

SUBJECT CODE

Subject Categories

THE HUMANITIES AND SOCIAL SCIENCES

COMMUNICATIONS AND THE ARTS

Architecture 0729
 Art History 0377
 Cinema 0900
 Dance 0378
 Fine Arts 0357
 Information Science 0723
 Journalism 0391
 Library Science 0399
 Mass Communications 0708
 Music 0413
 Speech Communication 0459
 Theater 0465

EDUCATION

General 0515
 Administration 0514
 Adult and Continuing 0516
 Agricultural 0517
 Art 0273
 Bilingual and Multicultural 0282
 Business 0688
 Community College 0275
 Curriculum and Instruction 0727
 Early Childhood 0518
 Elementary 0524
 Finance 0277
 Guidance and Counseling 0519
 Health 0680
 Higher 0745
 History of 0520
 Home Economics 0278
 Industrial 0521
 Language and Literature 0279
 Mathematics 0280
 Music 0522
 Philosophy of 0998
 Physical 0523

Psychology 0525
 Reading 0535
 Religious 0527
 Sciences 0714
 Secondary 0533
 Social Sciences 0534
 Sociology of 0340
 Special 0529
 Teacher Training 0530
 Technology 0710
 Tests and Measurements 0288
 Vocational 0747

LANGUAGE, LITERATURE AND LINGUISTICS

Language
 General 0679
 Ancient 0289
 Linguistics 0290
 Modern 0291
 Literature
 General 0401
 Classical 0294
 Comparative 0295
 Medieval 0297
 Modern 0298
 African 0316
 American 0591
 Asian 0305
 Canadian (English) 0352
 Canadian (French) 0355
 English 0593
 Germanic 0311
 Latin American 0312
 Middle Eastern 0315
 Romance 0313
 Slavic and East European 0314

PHILOSOPHY, RELIGION AND THEOLOGY

Philosophy 0422
 Religion
 General 0318
 Biblical Studies 0321
 Clergy 0319
 History of 0320
 Philosophy of 0322
 Theology 0469

SOCIAL SCIENCES

American Studies 0323
 Anthropology
 Archaeology 0324
 Cultural 0326
 Physical 0327
 Business Administration
 General 0310
 Accounting 0272
 Banking 0770
 Management 0454
 Marketing 0338
 Canadian Studies 0385
 Economics
 General 0501
 Agricultural 0503
 Commerce-Business 0505
 Finance 0508
 History 0509
 Labor 0510
 Theory 0511
 Folklore 0358
 Geography 0366
 Gerontology 0351
 History
 General 0578

Ancient 0579
 Medieval 0581
 Modern 0582
 Black 0328
 African 0331
 Asia, Australia and Oceania 0332
 Canadian 0334
 European 0335
 Latin American 0336
 Middle Eastern 0333
 United States 0337
 History of Science 0585
 Law 0398
 Political Science
 General 0613
 International Law and
 Relations 0616
 Public Administration 0617
 Recreation 0814
 Social Work 0452
 Sociology
 General 0626
 Criminology and Penology 0627
 Demography 0938
 Ethnic and Racial Studies 0631
 Individual and Family
 Studies 0628
 Industrial and Labor
 Relations 0629
 Public and Social Welfare 0630
 Social Structure and
 Development 0700
 Theory and Methods 0344
 Transportation 0709
 Urban and Regional Planning 0999
 Women's Studies 0453

THE SCIENCES AND ENGINEERING

BIOLOGICAL SCIENCES

Agriculture
 General 0473
 Agronomy 0285
 Animal Culture and
 Nutrition 0475
 Animal Pathology 0476
 Food Science and
 Technology 0359
 Forestry and Wildlife 0478
 Plant Culture 0479
 Plant Pathology 0480
 Plant Physiology 0817
 Range Management 0777
 Wood Technology 0746
 Biology
 General 0306
 Anatomy 0287
 Biostatistics 0308
 Botany 0309
 Cell 0379
 Ecology 0329
 Entomology 0353
 Genetics 0369
 Limnology 0793
 Microbiology 0410
 Molecular 0307
 Neuroscience 0317
 Oceanography 0416
 Physiology 0433
 Radiation 0821
 Veterinary Science 0778
 Zoology 0472
 Biophysics
 General 0786
 Medical 0760
 EARTH SCIENCES
 Biogeochemistry 0425
 Geochemistry 0996

Geodesy 0370
 Geology 0372
 Geophysics 0373
 Hydrology 0388
 Mineralogy 0411
 Paleontology 0345
 Paleobotany 0426
 Paleocology 0418
 Paleozoology 0985
 Paleontology 0427
 Physical Geography 0368
 Physical Oceanography 0415

HEALTH AND ENVIRONMENTAL SCIENCES

Environmental Sciences 0768
 Health Sciences
 General 0566
 Audiology 0300
 Chemotherapy 0992
 Dentistry 0567
 Education 0350
 Hospital Management 0769
 Human Development 0758
 Immunology 0982
 Medicine and Surgery 0564
 Mental Health 0347
 Nursing 0569
 Nutrition 0570
 Obstetrics and Gynecology 0380
 Occupational Health and
 Therapy 0354
 Ophthalmology 0381
 Pathology 0571
 Pharmacology 0419
 Pharmacy 0572
 Physical Therapy 0382
 Public Health 0573
 Radiology 0574
 Recreation 0575

Speech Pathology 0460
 Toxicology 0323
 Home Economics 0386

PHYSICAL SCIENCES

Pure Sciences
 Chemistry
 General 0485
 Agricultural 0749
 Analytical 0486
 Biochemistry 0487
 Inorganic 0488
 Nuclear 0738
 Organic 0490
 Pharmaceutical 0491
 Physical 0494
 Polymer 0495
 Radiation 0754
 Mathematics 0405
 Physics
 General 0605
 Acoustics 0986
 Astronomy and
 Astrophysics 0606
 Atmospheric Science 0608
 Atomic 0748
 Electronics and Electricity 0607
 Elementary Particles and
 High Energy 0798
 Fluid and Plasma 0759
 Molecular 0609
 Nuclear 0610
 Optics 0752
 Radiation 0756
 Solid State 0611
 Statistics 0463
 Applied Sciences
 Applied Mechanics 0346
 Computer Science 0984

Engineering
 General 0537
 Aerospace 0538
 Agricultural 0539
 Automotive 0540
 Biomedical 0541
 Chemical 0542
 Civil 0543
 Electronics and Electrical 0544
 Heat and Thermodynamics 0348
 Hydraulic 0545
 Industrial 0546
 Marine 0547
 Materials Science 0794
 Mechanical 0548
 Metallurgy 0743
 Mining 0551
 Nuclear 0552
 Packaging 0549
 Petroleum 0765
 Sanitary and Municipal 0554
 System Science 0790
 Geotechnology 0428
 Operations Research 0796
 Plastics Technology 0795
 Textile Technology 0994

PSYCHOLOGY

General 0621
 Behavioral 0384
 Clinical 0622
 Developmental 0620
 Experimental 0623
 Industrial 0624
 Personality 0625
 Physiological 0989
 Psychobiology 0349
 Psychometrics 0632
 Social 0451



"Perhaps no other area of similar size in Canada has presented so many geological problems as has that which includes and immediately surrounds the city of Saint John, New Brunswick."

F.J. Alcock, 1938 p. 1.

TABLE OF CONTENTS

	Page
Table of Contents	v
List of Figures	xii
List of Tables	xvi
List of Plates	xvi
Abstract	xx
Acknowledgements	xxi

CHAPTER 1: INTRODUCTION

1.1. Introduction	1
1.2. Previous Work and Geological Setting	4
1.2.1. Late 1960's to Middle 1970's	4
1.2.2. Middle 1970's to Early 1980's	8
1.2.3. Early 1980's to present	12
1.3. Purpose and Scope of this Study	15
1.4. Location and Access	16
1.5. Method of Study	17

CHAPTER 2: DEFINITION AND DESCRIPTION OF MAP UNITS

2.1. Justification	23
2.2. Green Head Group	23
2.2.1. Ashburn Formation	24
2.2.2. Martinon Formation	28
2.2.3. Hammondvale Metamorphic Unit	32
2.3. Brookville Gneiss	33
2.4. Dipper Harbour Volcanic Unit	37
2.5. Plutonic Units	39
2.6. Cambrian to Ordovician Units	39
2.7. Devonian to Carboniferous Units	41
2.7.1. Northeastern Zone	41
2.7.2. Southwestern Zone	42
2.8. Triassic Units	44

	Page
CHAPTER 3: STRUCTURAL GEOLOGY	
3.1. Introduction	56
3.2. Criteria for Distinguishing Structural History	57
3.3. pre-Late Proterozoic Deformation (D_1)	57
3.3.1. D_{MFI} Structures in the Martinon Formation	58
3.3.2. D_{AFI} Structures in the Ashburn Formation	59
3.3.2.1. D_{AFIa} Structures	59
3.3.2.2. D_{AFIb} Structures	61
3.3.3. Northwest-Southeast-trending folds in Ashburn Formation	62
3.3.4. MacKay Highway shear zone	62
3.3.5. Brookville Gneiss	64
3.3.6. Timing of D_1 Deformation	65
3.4. Plutonism	66
3.5. Faults	67
3.5.1. Middle Paleozoic Faults and Related Fabrics (D_2)	69
3.5.1.1. Spruce Lake shear zone	69
3.5.1.2. Long Island shear zone	70
3.5.1.3. Deformed Granitoid rocks	71
3.5.2. Late Paleozoic Faults and Related Fabrics ($D_{3,1}$)	71
3.5.2.1. New River Beach-Kennebecasis Fault	71
3.5.2.2. Caledonia-Clover Hill Fault	73
3.5.2.3. Milkish Head Fault	75
3.5.2.4. Ragged Point Fault	76
3.5.2.5. Ragged Head Fault	77
3.5.2.6. Lepreau River Fault	77
3.5.3. Musquash-Dipper Harbour thrust belt ($D_{3,2}$)	71
3.5.3.1. $D_{3,2a}$ structures	78
3.5.3.2. $D_{3,2b}$ structures	80
3.5.4. Mesozoic Faults and Related Fabrics (D_4)	83

	Page
3.6. Dykes and Deformation	84
3.7. Summary	85
 CHAPTER 4: VOLCANIC AND PLUTONIC ROCKS OF THE BROOKVILLE TERRANE	
4.1. Introduction	104
4.2. Volcanic Units	105
4.2.1. Rhyolitic unit	105
4.2.2. Andesitic to dacitic unit	106
4.2.3. Mixed andesitic to rhyolitic unit	107
4.2.4. Petrochemistry	107
4.3. Plutonic Units	108
4.3.1. Orthogneiss	109
4.3.1.1. Petrochemistry	109
4.3.2. Granitoid Plutons	110
4.3.2.1. Mineralogy	112
4.3.2.2. Petrochemistry	115
4.3.3. Gabbroic to Ultramafic Plutons	118
4.3.3.1. Mineralogy	119
4.3.3.2. Petrochemistry	122
4.4. Dykes	123
4.4.1. Basaltic to andesitic dykes	124
4.4.2. Petrochemistry	125
4.4.3. Dacitic to rhyodactic dykes	126
4.4.4. Pegmatite and aplite dykes	126
4.5. Conditions of Crystallization in the ca. 548 to 537 Ma plutonic units	127
4.6. Tectonic Setting	129
4.7. Summary	132
 CHAPTER 5: METAMORPHIC ROCKS OF THE BROOKVILLE TERRANE	
5.1. Introduction	166
5.2. Petrography and Mineral Assemblages	167

	Page
5.2.1. Brookville Gneiss	167
5.2.1.1. Paragneiss	167
5.2.1.2. Migmatitic Paragneiss	170
5.2.1.3. Marble and Calc-silicate Gneiss	173
5.2.1.4. Orthogneiss	175
5.2.2. MacKay Highway shear zone	176
5.2.2.1. Gneissic Boudins	177
5.2.2.2. Pelitic Blastomylonitic Schists	178
5.2.2.3. Calc-silicate Blastomylonites	179
5.2.2.4. Marble Blastomylonites	180
5.2.3. Green Head Group	181
5.2.3.1. Regional metamorphic rocks	182
5.2.3.2a. Low-grade (Zone A) rocks	183
5.2.3.2b. Low-grade (Zone B) rocks	184
5.2.3.3. Medium-grade rocks	186
5.2.3.4. High-grade rocks	189
5.2.4. Hammondvale metamorphic unit	192
5.3. Mineral Chemistry	194
5.3.1. Brookville Gneiss and MacKay Highway shear zone	195
5.3.1.1. Biotite	195
5.3.1.2. Cordierite	196
5.3.1.3. Feldspar	197
5.3.1.4. Garnet	197
5.3.1.5. Clinopyroxene	198
5.3.1.6. Amphibole	198
5.3.1.7. Muscovite	199
5.3.1.8. Other phases	199
5.3.2. Ashburn Formation	200
5.3.2.1. Mica	200
5.3.2.2. Amphibole	200

	Page
5.3.2.3. Clinopyroxene	200
5.3.2.4. Plagioclase	201
5.3.3.5. Other phases	201
5.3.3. Hammondvale metamorphic unit	202
5.3.3.1. Mica	202
5.3.3.2. Garnet	203
5.3.3.3. Plagioclase	203
5.3.3.4. Other phases	203
5.4. Metamorphic Conditions	204
5.4.1. Introduction	204
5.4.2. Brookville Gneiss and MacKay Highway shear zone	204
5.4.2.1. Paragneiss and migmatitic paragneiss	204
5.4.2.2. Marble	207
5.4.2.3. Pelitic blastomylonite	208
5.4.2.4. Geothermobarometry	209
5.4.2.5. Summary of metamorphic conditions	211
5.4.3. Green Head Group	212
5.4.4. Hammondvale metamorphic unit	217
5.5. Summary	219
 CHAPTER 6: GEOCHRONOLOGY	
6.1. Introduction	248
6.2. Previous Geochronology	249
6.2.1. K-Ar Data	249
6.2.2. Rb-Sr Data	250
6.2.3. Early U-Pb Data	251
6.3. Present Geochronology	252
6.3.1. U-Pb Data from Plutonic Units	252
6.3.1.1. Fairville Granite	253
6.3.1.2. Ludgate Lake Granodiorite	254

	Page
6.3.2. $^{40}\text{Ar}/^{39}\text{Ar}$ Data from Plutonic Units	255
6.3.2.1. Fairville Granite	256
6.3.2.2. French Village Quartz Diorite	257
6.3.2.3. Rockwood Park Granodiorite	257
6.3.2.4. Renforth Pluton	258
6.3.2.5. Shadow Lake Granodiorite	259
6.3.3. $^{40}\text{Ar}/^{39}\text{Ar}$ Data from the Brookville Gneiss	260
6.3.4. $^{40}\text{Ar}/^{39}\text{Ar}$ Data from the Green Head Group	261
6.3.5. $^{40}\text{Ar}/^{39}\text{Ar}$ Data from the Hammondvale Metamorphic Unit	262
6.4. Interpretation	264
6.4.1. Previous Age Determinations	264
6.4.2. Closure Temperatures	266
6.4.3. Brookville Gneiss	268
6.4.4. Plutonic Units	270
6.4.5. Dipper Harbour Volcanic Unit	273
6.4.6. Green Head Group	274
6.4.7. MacKay Highway Shear Zone	276
6.4.8. Hammondvale Metamorphic Unit	277
6.4.9. Partial Argon Loss from $^{40}\text{Ar}/^{39}\text{Ar}$ Minerals	278
6.5. Thermal History	280
6.6. Summary	282
 CHAPTER 7: DISCUSSION	
7.1. Comparisons with Previous Interpretation	307
7.1.1. Green Head Group	307
7.1.2. Brookville Gneiss	312
7.1.3. Plutonic and Volcanic Units	314
7.2. Relationship of Brookville terrane to Adjacent Areas	317
7.2.1. Caledonia Terrane	317
7.2.2. Kingston Complex	319

	Page
7.2.3. New River Belt	321
7.2.4. Timing of Terrane Amalgamation	322
7.3. Regional Correlations	323
7.4. Implications for Palinspastic Restoration	325
CHAPTER 8: CONCLUSIONS	330
APPENDIX A: HISTORICAL PERSPECTIVE (pre-1966)	333
APPENDIX B: PLUTONS AND THEIR FIELD RELATIONSHIPS	
B.1. Introduction	349
B.2. Dioritic to Granodioritic Plutons	
B.2.1. Ludgate Lake Granodiorite	349
B.2.2. Spruce Lake Pluton	350
B.2.3. Rockwood Park Granodiorite	350
B.2.4. French Village Quartz Diorite and other dioritic plutons	351
B.2.5. Belmont Tonalite	352
B.2.6. Perch Lake Granodiorite	353
B.2.7. Shadow Lake Granodiorite	353
B.2.8. Talbot Road Granodiorite	354
B.2.9. Renforth Pluton	355
B.2.10. Enclaves	356
B.3. MONZOGRANITIC TO GRANODIORITIC PLUTONS	
B.3.1. Fairville Granite	357
B.3.2. Chalet Lake Granite	357
B.3.3. Gayton granite	358
B.3.4. Hammond River Granite	358
B.3.5. Milkish Head Pluton	360
B.3.6. Hanson Stream Granodiorite	361
B.3.7. Lepreau Pluton	361
B.3.8. Lepreau Harbour Granodiorite	362
B.4. SYENOGANITIC TO MONZOGRANITIC PLUTONS	

	Page
B.4.1. Henderson Brook Granite	362
B.4.2. Musquash Harbour, Jarvies Lakes, Cranberry Head, Prince of Wales, and Harvey Hill granites	363
B.5. DEFORMED GRANITOID ROCK	365
B.6. GABBROIC TO ULTRAMAFIC PLUTONS	366
B.7. DYKE ROCKS	367
B.7.1. Basaltic to Andesitic Dykes	367
B.7.2. Dacitic to Rhyodacitic Dykes	369
B.7.3. Pegmatites and Aplites	369
 APPENDIX C: GEOCHEMICAL DATA FOR IGNEOUS UNITS	
C.1. Modal Analysis	375
C.2. Major and Trace Element Data	379
C.3. Mineral Chemistry Data	395
APPENDIX D: MINERAL CHEMISTRY DATA FOR METAMORPHIC UNITS	427
APPENDIX E: GEOCHRONOLOGICAL DATA	
E.1. U-Pb Analytical Techniques and Data	456
E.2. ⁴⁰ Ar/ ³⁹ Ar Analytical Techniques, Error Analysis, Interpretation of age spectra, and Data	459
E.3. Conversion of ³⁷ Ar/ ³⁹ Ar to Ca/K	478
E.4. Location and Description of Samples	479
REFERENCES	490
 LIST OF FIGURES	
Figure 1.1. Pre-Silurian tectonostratigraphic divisions in the northern Appalachian Orogen	19
Figure 1.2. Schematic strstigraphic succession of the Avalon terrane	20
Figure 1.3. Simplified geology map of southern New Brunswick	21
Figure 2.1. Simplified geology map of the Brookville terrane	45
Figure 3.1. Summary of D _{MP1} and D _{AF1a} structural data	88
Figure 3.2. Cross section A-A'	89
Figure 3.3. Summary of D _{AF1b} structural data	90

	Page
Figure 3.4. Summary of structural data from the MacKay Highway shear zone, Brookville Gneiss, and plutonic units	91
Figure 3.5. Summary of structural data from various shear zones in the Brookville terrane	92
Figure 3.6. Summary of structural data from the Musquash-Dipper Harbour thrust belt	93
Figure 3.7. Cross sections B-B' and C-C'	94
Figure 4.1. Ternary plots of modal quartz, plagioclase, and K-feldspar for volcanic and plutonic units in the Brookville terrane	135
Figure 4.2a. Major element variation diagrams for SiO ₂ against TiO ₂ and Al ₂ O ₃	140
Figure 4.2b. Major element variation diagrams for SiO ₂ against Fe ₂ O ₃ ^T and MnO	141
Figure 4.2c. Major element variation diagrams for SiO ₂ against MgO and CaO	142
Figure 4.2d. Major element variation diagrams for SiO ₂ against Na ₂ O and K ₂ O	143
Figure 4.2e. Major element variation diagrams for SiO ₂ against P ₂ O ₅	144
Figure 4.3a. Trace element variation diagrams for SiO ₂ against Rb and Ba	145
Figure 4.3b. Trace element variation diagrams for SiO ₂ against Sr and Y	146
Figure 4.3c. Trace element variation diagrams for SiO ₂ against Nb and Zr	147
Figure 4.3d. Trace element variation diagrams for SiO ₂ against Ga and Zn	148
Figure 4.3e. Trace element variation diagrams for SiO ₂ against Ni and V	149
Figure 4.3f. Trace element variation diagrams for SiO ₂ against Pb and Th	150
Figure 4.3g. Trace element variation diagrams for SiO ₂ against Cr	151
Figure 4.4. A/CNK against SiO ₂ variation diagram	152
Figure 4.5. Na ₂ O + K ₂ O against SiO ₂	153
Figure 4.6. AFM ternary plot	154
Figure 4.7. Feldspar compositions from plutonic units	155
Figure 4.8. Hornblende compositions from plutonic units	156

	Page
Figure 4.9. Biotite compositions from plutonic units	157
Figure 4.10. Chondrite normalized REE patterns from plutonic units	158
Figure 4.11. Ternary plots of modal a) plagioclase, orthopyroxene, and clinopyroxene; b) olivine, orthopyroxene, and clinopyroxene; c) plagioclase, pyroxene, and olivine for gabbroic and ultramafic units . .	159
Figure 4.12. Ternary plots of modal quartz, plagioclase, and K-feldspar for dykes	160
Figure 4.13. Pressure versus temperature emplacement thermobarometry for plutonic units	161
Figure 4.14. FeO^T/MgO against Zr + Nb + Y variation diagram . .	162
Figure 4.15. Rb against Y + Nb tectonic discrimination diagram for plutonic units	162
Figure 4.16. Ti - Zr - Y tectonic discrimination diagram for mafic dykes	164
Figure 5.1. Ternary plots of modal quartz, plagioclase, and K-feldspar for leucosomes in the Brookville Gneiss . .	221
Figure 5.2. Simplified geology map of the Saint John area showing the distribution of metamorphic isograds	222
Figure 5.3. Simplified geology map of the Hammond River area showing the distribution of metamorphic isograds . . .	223
Figure 5.4. Biotite compositions from metamorphic units	224
Figure 5.5. A'F'M' projection diagrams for samples from the Brookville Gneiss	225
Figure 5.6. Feldspar compositions from metamorphic units	226
Figure 5.7. Clinopyroxene compositions from metamorphic units	227
Figure 5.8. Amphibole compositions from metamorphic units . . .	228
Figure 5.9. Muscovite compositions from metamorphic units . . .	229
Figure 5.10. Petrogenetic grid for the Brookville Gneiss	230
Figure 5.11. T - XCO_2 diagrams for marble samples in the Brookville Gneiss	231
Figure 5.12. T - XCO_2 diagrams for marble samples in the Ahburn Formation	232
Figure 5.13. Petrogenetic grid for the Hammondvale metamorphic unit	233
Figure 6.1. Location map for figures in Chapter 6 showing sample sites and ages	284

	Page
Figure 6.2. Detailed geology map of the Saint John River area showing sample sites and ages	285
Figure 6.3. U-Pb concordia diagrams for Fairville Granite and Ludgate Lake Granodiorite	286
Figure 6.4. $^{40}\text{Ar}/^{39}\text{Ar}$ age spectra from hornblende and biotite in the plutonic units	287
Figure 6.5. Detailed geology map of the Renforth area showing sample sites and ages	289
Figure 6.6. Detailed geology map of the Drury Cove area showing sample sites and ages	290
Figure 6.7. $^{40}\text{Ar}/^{39}\text{Ar}$ age spectra from phlogopite in marble samples from the Brookville Gneiss	291
Figure 6.8. Detailed geology map of the Drury Cove area showing sample sites and ages	292
Figure 6.9. $^{40}\text{Ar}/^{39}\text{Ar}$ age spectra from phlogopite and muscovite in samples from the Ashburn Formation	293
Figure 6.10. Detailed geology map of the Hammondvale area showing sample sites and ages	294
Figure 6.11. $^{40}\text{Ar}/^{39}\text{Ar}$ age spectra from muscovite in samples from the Hammondvale metamorphic unit	295
Figure 6.12. U-Pb concordia diagrams for samples from the Brookville Gneiss	296
Figure 6.13. U-Pb concordia diagrams for samples from the Rockwood Park Granodiorite and the French Village Quartz Diorite	297
Figure 6.14. Histogram of ages versus number of analyses	298
Figure 6.15. Temperature versus time diagram for dated samples from the Brookville terrane	299
Figure 7.1. Schematic comparative stratigraphic columns for present versus previous interpretations	328
Figure 7.2. Schematic comparative stratigraphic columns for various terranes and belts in southern New Brunswick	329
MAP A. Regional 1:50 0000 geological map of the study area	back pocket
MAP B. Geological map of the Saint John area	back pocket
MAP C. Geological map of the MacKay Highway shear zone	back pocket
MAP D. Geochemical sample locations	back pocket

	Page
LIST OF TABLES	
Table 2.1. Summary of field characteristics in the metamorphic and volcanic units	46
Table 2.2a. Summary of field characteristics of the dioritic to granodioritic plutons	47
Table 2.2b. Summary of field characteristics of the monzogranitic to granodioritic plutons	49
Table 2.2c. Summary of field characteristics of the syenogranitic to monzogranitic plutons	51
Table 2.2d. Summary of field characteristics of the gabbroic and ultramafic plutons	52
Table 2.3. Summary of field characteristics of the sedimentary units	53
Table 3.1. Summary of deformations and related structures	95
Table 4.1. Estimates of pressures and temperatures of crystallization in plutonic units	165
Table 5.1. List of mineral assemblages in the metamorphic rocks	234
Table 5.2. Estimates of metamorphic temperatures in the Brookville Gneiss	237
Table 5.3. List of reactions used to construct T - XCO ₂ diagrams (Fig. 5.11)	238
Table 5.4. List of reactions used to construct P-T diagram for the Hammondvale metamorphic unit (Fig. 5.11)	239
Table 6.1. Summary of early age determinations from the Brookville terrane	300
Table 6.2. Summary of recent age determinations from the Brookville terrane	302
Table 6.3. Closure temperatures	304
Table A.1. Summary chart	back pocket
Table B.1. Previous names used for plutonic units in the Brookville terrane	370
Table E.1. U-Pb data from Fairville, Ludgate Lake, and French Village plutons	458

LIST OF PLATES

Plate 1a. Outcrop showing textural heterogeneity typical of marble in the Ashburn Formation	54
Plate 1b. The stromatolite <i>Archaeozoon acadense</i> from relatively undeformed marble in the Ashburn Formation along the northwestern tip of Green Head Island	54

	Page
Plate 1c. A rare occurrence of finely laminated siltstone (dark) and small-scale trough cross-bedded sandstone (light) in the Martinon Formation	54
Plate 1d. A poorly sorted quartzite-marble pebble conglomerate interbedded with a thin calcareous sandstone in the Martinon Formation	54
Plate 1e. A poorly sorted carbonate-siliciclastic sedimentary breccia in the Martinon Formation	54
Plate 1f. Folded, cordierite-bearing migmatitic paragneiss from the Brookville Gneiss	54
Plate 2a. Alternating marble layers in the Ashburn Formation dipping steeply to the southeast with a dark grey siliciclastic boudin	98
Plate 2b. Large dolomite boudins surrounded by anastomosing calcite layers in the Ashburn Formation	98
Plate 2c. Marble layers in Ashburn Formation deformed into a steeply southeast-inclined, northeast-plunging, tight fold	98
Plate 2d. Cross section through a complex sheath fold in medium-grained marble of the Ashburn Formation	98
Plate 3a. Roadcut along the MacKay Highway showing a portion of the MacKay Highway shear zone	100
Plate 3b. Carbonate blastomylonite in the MacKay Highway shear zone deformed into a steeply southeast-inclined, moderately southwest-plunging, tight folds	100
Plate 3c. Carbonate blastomylonite in the MacKay Highway shear zone showing a pervasive moderately northeast-plunging intersection lineation	100
Plate 3d. A narrow, northeast-trending, steeply southeast-dipping, coarse-grained marble shear zone cutting folded marbles of the Ashburn Formation	100
Plate 4a. Finely laminated, shallowly southeast-dipping calcite ultramylonite associated with the Musquash - Dipper Harbour thrust belt	102
Plate 4b. Finely laminated, shallowly southeast-dipping calcite ultramylonite associated with the Musquash - Dipper Harbour thrust belt with numerous asymmetric quartzite boudins	102
Plate 4c. Massive to finely laminated, subhorizontal calcite mylonite associated with the Musquash - Dipper Harbour thrust belt. Large dioritic boudin in marble	102
Plate 4d. Photomicrograph of calcite ultramylonite with shear bands associated with the Musquash - Dipper Harbour thrust belt	102

	Page
Plate 5a. Photomicrograph of a typical quartzo- feldspathic and biotite-rich layer in paragneiss of the Brookville Gneiss	240
Plate 5b. Photomicrograph of the typical mineralogy of hornblende-bearing paragneiss in the Brookville Gneiss	240
Plate 5c. Photomicrograph of medium-grained marble from the Brookville Gneiss with granoblastic calcite, and subidioblastic phlogopite and diopside	240
Plate 5d. Photomicrograph of medium-grained amphibolite from the Brookville Gneiss with subidioblastic hornblende and minor xenoblastic clinopyroxene and biotite	240
Plate 6a. Photomicrograph of medium-grained, foliated, paragneissic boudin in MacKay Highway shear zone	242
Plate 6b. Photomicrograph of fine-grained, strongly foliated, granoblastic pelitic blastomylonite from the margin of a gneissic boudin	242
Plate 6c. Photomicrograph of medium-grained, calc-silicate blastomylonite from the MacKay Highway shear zone that consists of subidioblastic diopside with minor granoblastic calcite and idioblastic phlogopite	242
Plate 6d. Photomicrograph of medium-grained marble blastomylonite from the MacKay Highway shear zone that consists of granoblastic calcite with minor subidioblastic diopside, garnet, and rounded quartz	242
Plate 7a. Photomicrograph of medium-grained, strongly foliated and crenulated mica schist from the Ashburn Formation in the Drury Cove area	244
Plate 7b. Photomicrograph of fine-grained, well laminated siltstone from Zone B in the Ashburn Formation	244
Plate 7c. Photomicrograph of spotted hornfels from the Martinon Formation	244
Plate 7d. Photomicrograph of medium-grained, cordierite -bearing schist from the Ashburn Formation close to the contact with the Fairville Granite	244
Plate 8a. Photomicrograph of a large albite porphyroblast in a schist from the Hammondvale metamorphic unit with inclusions of elongate quartz, biotite, opaque minerals, epidote, and muscovite	246
Plate 8b. Photomicrograph of smaller albite porphyroblast in a schist from the Hammondvale metamorphic unit with curved inclusion trail defined by elongate quartz and epidote	246
Plate 8c. Photomicrograph of medium-grained muscovite- rich marble from the Hammondvale metamorphic unit with randomly oriented subidioblastic muscovite	246

	Page
Plate 8d. Photomicrograph of strongly foliated amphibolite from the Hammondvale metamorphic unit	246
Plate 9a. Photomicrograph of a typical aliquot of unabraded, acicular zircons from the Fairville Granite . . .	305
Plate 9b. Photomicrograph of same aliquot of zircon abraded about 80%	305
Plate 9c. Photomicrograph of an aliquot of unabraded, acicular zircons from the Ludgate Lake Granodiorite	305
Plate 9d. Photomicrograph of an aliquot of much less abundant, unabraded, equant zircons from the Ludgate Lake Granodiorite	305
Plate 9e. Photomicrograph of an aliquot of unabraded titanite from the Ludgate Lake Granodiorite	305
Plate 9f. Photomicrograph of same aliquot of titanite abraded about 80%	305

ABSTRACT

The Brookville terrane of southern New Brunswick consists of the Green Head Group, Brookville Gneiss, Dipper Harbour volcanic unit, and associated plutonic units. The Mesoproterozoic Green Head Group is mainly a low-grade platformal sequence of carbonate and pelitic rocks that is in faulted contact along a ductile shear zone with the low-pressure/high-temperature Brookville Gneiss, composed of cordierite-bearing paragneiss, amphibolite, tonalitic to granodioritic orthogneiss, minor marble and quartzite. The paragneiss has a maximum depositional age of ca. 641 Ma, the orthogneiss has an igneous crystallization age of ca. 605 Ma, and peak regional amphibolite facies metamorphism occurred at ca. 564 Ma. Hence, the Brookville Gneiss is younger than the Green Head Group and does not represent basement; however, the original relationship between these units is unclear. The Green Head Group was moderately to intensely folded prior to the Late Neoproterozoic regional deformation and amphibolite facies metamorphism associated with the prolonged juxtaposition of the Brookville Gneiss with adjacent parts of the Ashburn Formation of the Green Head Group. Based on contrasts in age and metamorphic conditions, the ca. 610 Ma high-pressure/low-temperature Hammondvale metamorphic unit is not a high-grade metamorphic equivalent of the Green Head Group and is excluded from the Brookville terrane.

The Late Neoproterozoic Dipper Harbour volcanic unit consists of rhyolitic to andesitic tuffs with minor siltstone and marble, preserved in a Carboniferous thrust in the southwestern part of the terrane.

Twenty-six granitoid plutons in the Brookville terrane are broadly grouped on the basis of composition into: 1) diorite to granodiorite; 2) monzogranite to granodiorite; and 3) syenogranite to monzogranite suites. They have I-type, calc-alkaline characteristics and have yielded crystallization and cooling ages from ca. 548 to 500 Ma. They are exposed at more shallow crustal levels in the southwest, where they are associated with the Dipper Harbour volcanic unit, compared to the northeast, where they intruded the Brookville Gneiss and Green Head Group. Although the isotopic ages obtained from the Brookville terrane span the Neoproterozoic-Cambrian boundary, the tectonothermal history of the terrane is not compatible with the transition from Late Neoproterozoic magmatic arc to stable Cambrian platform that is recorded in the adjacent Caledonia terrane (Avalon terrane *sensu stricto*). Thus, the Brookville terrane is interpreted to have been a distinct tectono-stratigraphic assemblage in the Neoproterozoic through early Paleozoic. It is correlated with the Bras d'Or terrane of Cape Breton Island and parts of the Hermitage Flexure of southern Newfoundland.

ACKNOWLEDGEMENTS

I thank Dr. Bocky Jamieson and Dr. Sandra Barr for excellent supervision and critical reading of the text which led to considerable clarification in the expression of my ideas. Thanks go also to Dr. Nick Culshaw for his interest and helpful structural advice and Dr. Peter Reynolds for unlimited use of the $^{40}\text{Ar}/^{39}\text{Ar}$ laboratory and assistance in interpretation of $^{40}\text{Ar}/^{39}\text{Ar}$ results.

I gratefully acknowledge Dr. Greg Dunning for providing use of the U-Pb laboratory at Memorial University and his guidance and assistance in interpretation of the U-Pb results and Sherry Dunsworth for technical assistance in every step of the procedure. Keith Taylor for technical assistance in the $^{40}\text{Ar}/^{39}\text{Ar}$ dating analyses, and Don Osburn for preparing regular and polished thin sections at a moment's notice, and Bob MacKay for assisting in microprobe analysis. I appreciated the use of office and laboratory facilities in the Geology Department at Acadia University.

The thesis greatly benefited from field discussions with Damian Nance, Ken Currie, Malcolm McLeod, Sue Johnson, Art Ruitenberg, Clint St. Peter, Les Fyffe, and Steve McCutcheon, and many others participants who were involved in numerous field trips to southern New Brunswick. Malcolm Hoar, Brookville Lime Company, is thanked for allowing access to marble quarries in the area.

Thanks goes to my fellow graduate students in the Earth Science Department at Dalhousie University and Acadia University, especially John Ketchum, Robbi Hicks, Charlie Walls, and Brent Miller for insightful and often lively discussions.

Last, but not least, I thank Judy White for her patience, understanding, and many sacrifices during the course of this thesis.

Financial support was provided by a Dalhousie University Graduate Scholarship and a Natural Science and Engineering Research Council operating grants to Dr. Sandra Barr, Dr. Becky Jamieson, and Nick Culshaw.

CHAPTER 1

INTRODUCTION

1.1. INTRODUCTION

In recent years the stratigraphic succession around the Saint John area in southern New Brunswick has been regarded as typical of a belt of rocks along the southeastern margin of the northern Appalachian orogen referred to as the Avalon Zone or Terrane (Fig. 1.1) (Williams, 1978, 1979; Williams and Hatcher, 1983; Zen, 1983). The generally accepted view was that its stratigraphy (Fig. 1.2) consisted of Late Precambrian (Neoproterozoic) volcanic-sedimentary successions (Coldbrook Group) and co-genetic plutonic rocks (Golden Grove Suite), overlain by an early Paleozoic platformal sequence (Saint John Group) containing Acado-Baltic fossils (Skehan et al., 1978; O'Brien et al., 1983; Rast and Skehan, 1983; Skehan and Rast, 1983; Keppie, 1985, 1989; Currie, 1986a, 1988a; Nance, 1986b, 1987a, 1988, 1990; Fyffe and Fricker, 1987; Skehan, 1988; Dallmeyer et al., 1990; Nance et al., 1990, 1991; Keppie and Dostal, 1991; Keppie et al., 1991; Murphy et al., 1992).

These units were interpreted to overlie a Middle Precambrian (Mesoproterozoic) platformal sequence (Green Head Group and Martinon Formation) of marble, quartzite and metasiltstone. A gneissic unit (Brookville Gneiss) associated with the Green Head Group was variably considered to be: a) part of the Golden Grove Suite (Cumming, 1916; Hayes and Howell, 1937; Belyea, 1939, 1944, 1945; Ruitenberg et al., 1975, 1979); b) a high-grade, migmatitic portion of the Green Head Group (Alcock, 1938; Leavitt, 1963; Richards, 1971; O'Brien, 1976; Rast et al., 1976a, b; Wardle, 1978); c) a deeper crustal level of the Coldbrook Group that represents the metamorphic infrastructure of the "Avalon Terrane" (Dallmeyer et al., 1990; Keppie et al., 1991; Nance et al., 1991; Dallmeyer and Nance, 1992); or d) an older, Aphebian to

Grenvillian (Palaeoproterozoic to Mesoproterozoic), remobilized and partially melted continental basement upon which the remaining stratified rocks were deposited (Wardle, 1978; Currie, et al., 1981; Currie, 1983, 1984, 1986a, 1987a, b, c, 1988a, b; Olszewski and Gaudette, 1982; O'Brien et al., 1983; Nance, 1986b, 1987a, 1988, 1990; Nance et al., 1990, 1991).

The northwest margin of the Avalon Terrane was interpreted to be marked by a bimodal dyke swarm and associated plutonic units termed the Kingston Complex (Currie, 1984). This zone is bordered by the Lubec-Belleisle and Pocologan mylonite zones (Brown and Helmstaedt, 1970; Rast and Dickson, 1982) and was thought to be Late Precambrian (Neoproterozoic) based on apparently overlying early Paleozoic successions (Fig. 1.2). This zone was interpreted to record the initial Late Precambrian (Neoproterozoic) formation of the Iapetus Ocean (Rast and Currie, 1976; Rast, 1979; Rast and Dickson, 1982; Dickson, 1983; Currie, 1984, 1986a, 1988a, b; Nance, 1987a, 1988, 1990; Nance et al., 1990).

Carboniferous units in the Saint John area have traditionally been subdivided into three packages: a) coarse conglomerate and arkose of the Kennebecasis Formation; b) interbedded volcanic and sedimentary rocks of the Mispec Group; and c) sedimentary rocks with plant fragments of the Lancaster Formation. Rocks of Triassic age (Lepreau and Quaco formations) occur as small fault-bounded basins along the Bay of Fundy (Stringer, 1978; Nadon and Middleton, 1985).

The results of the present study and other recent work in the area have demonstrated that the assumption of stratigraphic continuity in southern New Brunswick (e.g. Fig. 1.2) is not valid and geological interpretations therefore require major revisions. The changes are summarized as follows:

1. The Brookville Gneiss has a maximum detrital zircon age of ca. 640 Ma (Bevier et al., 1990; White et al., 1990a, b, c) and therefore does not represent an ancient continental basement to the Green Head Group as

previously interpreted. Based on its Neohelikian (Mesoproterozoic) stromatolite age (Hofmann, 1974) and ca 1200 Ma detrital zircon ages (D. Davis, written communication, 1995), the Green Head Group appears to be older than the gneiss previously considered to be its basement.

2. The Golden Grove Suite intruded only the Green Head Group and Brookville Gneiss and is generally younger than plutonic units associated with the Coldbrook Group to the southeast (Barr et al., 1990a; White et al., 1990a, b, c; Bevier et al., 1991; White and Barr, 1991a, in press; Dallmeyer and Nance, 1992; White, 1994; Barr and White, in press) and older than plutonic units in the Kingston Complex (e.g. McLeod et al., 1994).

3. The Coldbrook Group is in faulted contact (Caledonia-Clover Hill Fault) with these units and therefore may not stratigraphically overlie the Green Head Group, Brookville Gneiss, and associated plutons (e.g. White et al., 1990).

4. The Kingston Complex and associated mylonite zones to the northwest are in faulted contact (New River Beach-Kennebecasis Fault) with the Green Head Group, Brookville Gneiss, and Golden Grove Suite (Rast and Dickson, 1982; Dickson, 1983; Leger and Williams, 1986; Currie, 1988a; Eby and Currie, 1993). Recent work indicates a Silurian to Early Devonian age for much, if not all, of this Complex (Dallmeyer and Nance, 1989; Doig et al., 1990; Casseday et al., 1991; McLeod et al., 1994).

These results led Barr and White (1989, 1991a, 1994, 1996, in press) and White and Barr (1991, in press) to propose that the Green Head Group, Brookville Gneiss and associated plutonic units comprise a "Brookville terrane". The Brookville terrane is distinct from the volcanic-sedimentary sequences of the Coldbrook Group, associated plutons, and overlying Cambrian to Ordovician units that comprise the "Caledonia terrane" to the southeast and older than the Silurian to Devonian igneous units of the Kingston Complex to the northwest.

This study has significant regional implications because the previously accepted but apparently inaccurate interpretation of

stratigraphic succession in the Saint John area has been widely cited as characteristic of the entire Avalon terrane (Currie, 1983, 1986a, 1988a; O'Brien et al., 1983; Keppie, 1985, 1989; Nance, 1986b, 1987a, 1988, 1990; Murphy and Nance, 1989; Nance et al., 1990, 1991; Keppie and Dostal, 1991; Keppie et al., 1991; Rast and Skehan, 1991).

1.2. PREVIOUS WORK AND GEOLOGICAL SETTING

The literature pertaining to geological investigations in southern New Brunswick spans over 150 years. A vast number of contradictory views and opinions on the geological features in this area have been published. For this reason, a detailed historical account of previous work is presented in Appendix A. A summary of recent work and general geological setting is presented below.

1.2.1. Late-1960's to Middle-1970's

By the late-1960's, the stratigraphy of southern New Brunswick appeared to be firmly established (see Appendix A). However, geological work in the area continued to better constrain the timing of igneous, metamorphic, and deformational events. Rogers (1967, 1970) described the tectonic evolution of the Appalachian region and concluded that the Green Head Group was post-Grenville (<1000 Ma) in age. He suggested that the Green Head Group was deformed, metamorphosed, and intruded by granites prior to the deposition of the Coldbrook Group. The Saint John Group was interpreted to unconformably overlies strongly deformed volcanic rocks of the Coldbrook Group. He agreed with Poole et al. (1964) that certain plutonic rocks associated with the Green Head Group are Precambrian in age; however, radiometric dates suggested that the majority were Devonian. Based on textural and structural evidence Helmstaedt (1968) suggested that the Golden Grove Intrusives were Devonian and dykes and sills within the Kingston Complex were related to

these plutons.

During the late 1960's the Coldbrook and Saint John groups were regarded as part of a widespread belt of rocks that formed the southeastern margin of the Canadian Appalachian Orogen. This belt of rocks was referred to as the Avalon Platform or Zone (e.g. Poole, 1967; Poole et al., 1970) after the "type area" established by Williams (1964) in southeastern Newfoundland.

Although citing considerable evidence supporting an Archean (Palaeoproterozoic) age for the Green Head Group, Poole (1967), Poole et al. (1970), and Poole and Rodgers (1972) favoured a post-Grenville Hadrynian (Neoproterozoic) age. They suggested that the platformal deposits of the Green Head Group accumulated on a stable Grenville or older basement that is not now exposed, and interpreted the Late Hadrynian Coldbrook Group to overlie the Green Head Group, with "uncertain relations". These volcanic rocks were interpreted to be overlain by a redbed package that graded upward into Late Hadrynian-Early Cambrian "quartzite" (Glen Falls Formation of Hayes and Howell, 1937) at the base of the Cambrian-Ordovician Saint John Group. Poole (1967) postulated a Middle Ordovician age for the Golden Grove Intrusives and Milkish Head Pluton. However, citing numerous K-Ar and Rb-Sr radiometric dates, he later concluded that they are middle to late Devonian (Poole et al., 1970) and/or Cambrian to Ordovician (Poole and Rodgers, 1972). However, the presence of granitic cobbles in conglomerates related to both the Coldbrook Group and the redbed package suggested that plutonism and/or deformation occurred prior to deposition of the Coldbrook Group (Poole, 1967; Poole et al., 1970; Poole and Rodgers, 1972; Rodgers, 1972). Gneisses in the Green Head Group were interpreted to be the result of Early Paleozoic metamorphism.

Ruitenbergh (1969) described and mapped various mineral occurrences throughout the study area. Like Alcock (1948), he interpreted many of the mafic sills in the Green Head Group as minor basaltic and andesitic flows and concluded that this group is Precambrian or Lower Paleozoic.

He recognized a belt of Silurian and/or Lower Devonian sedimentary rocks along the coast southwest of Saint John (previously assigned to the Carboniferous Mispic Group by Alcock, 1959) and, citing radiometric dates, suggested that the Golden Grove Intrusives are Devonian.

Subhas (1970) carried out a detailed stratigraphical and structural investigation in the Musquash-Chance Harbour area. Using structural evidence, he agreed with Ruitenberg (1969) on a Devonian age for the Golden Grove Intrusives. He considered the Milkish Head Pluton part of the Golden Grove Intrusives, as opposed to the previous interpretation of MacKenzie (1964) and Poole (1967). Subhas (1970) introduced the names Cranberry and Musquash granites for divisions of the Golden Grove Intrusives near the coast, and mapped what he interpreted as contact metamorphic aureoles around these plutons. Subhas (1970) concluded that the host rocks to these granites should be assigned a pre-Middle Devonian age and called them the Musquash Head Group (previously Silurian and/or Lower Devonian sedimentary rocks of Ruitenberg, 1969 and the Carboniferous Mispic Group of Alcock, 1959). He assigned an Archean to Early Paleozoic age to the Green Head Group.

The Precambrian age assigned to the Coldbrook Group had been based on the overlying fossiliferous Lower Cambrian Saint John Group (e.g. Hayes and Howell, 1937; Alcock, 1938). Fairbairn et al. (1966) tried to date the Coldbrook Group using Rb-Sr whole-rock analyses; however, the resulting date of 468 Ma was too young to be Precambrian. Cormier (1969) also attempted to verify a Precambrian age using Rb-Sr whole-rock analyses. His results indicated an age of ca. 750 Ma for the volcanic rocks and a Devonian age (ca. 370 Ma) for regional metamorphism in the area.

Schenk (1971), Williams et al. (1972) and Potter et al. (1972) reinstated the earlier idea of lithological correlation of the Green Head Group with the Grenville Province of the Canadian Shield (see Appendix A). They concluded that the Hadrynian Coldbrook Group was deposited on a deformed Green Head Group basement. However, Potter et al. (1972)

suggested that biotite gneiss associated with the marbles might represent an even older basement. The Cambrian-Ordovician Saint John Group was considered to lie conformably on the Coldbrook Group by Schenk (1971) and Williams et al. (1972), whereas Potter et al. (1972) postulated a faulted contact.

According to Schenk (1971) and Williams et al. (1972) Precambrian granitic rocks are of two ages in southern New Brunswick. The Golden Grove Intrusives and Milkish Head Pluton are Late Hadrynian based on K-Ar ages and the lack of intrusive rocks in the Cambrian Saint John Group, whereas the granite gneisses associated with these plutons were considered part of a Helikian (Mesoproterozoic) basement intrusive sequence. Based on K-Ar ages and discordant relationships with foliated country rocks, Schenk (1971) and Williams et al. (1972) suggested the existence of mid-Devonian granites. Potter et al. (1972) suggested a Precambrian and Devonian age for plutonism in the area.

R. Grant (1972) mapped the northwestern margin of the study area including the Kingston Complex. He suggested that the Golden Grove Intrusives were pre-tectonic and probably Precambrian in age. Gneisses associated with the plutonic rocks were considered to be Green Head Group equivalents. The Kingston Complex was interpreted as Precambrian in age and grouped with the Coldbrook Group.

Based on structural relationships, Richards (1971) and Brown (1972) inferred that the upper Green Head Group is interlayered with the overlying Precambrian Coldbrook Group, and that the Cambrian Saint John Group rests conformably on the volcanic rocks. This conformable group of units was interpreted to represent a relict continental margin which was deformed in post-Early Ordovician time and intruded during the mid-Devonian and mid-Carboniferous. The presence of granite cobbles in conglomerates associated with the Coldbrook Group suggested an additional period of plutonism in the Precambrian (Brown, 1972). Based on structural evidence, Brown (1972) confirmed a Carboniferous age for the sedimentary, volcanic, and plutonic rocks of the Mispec Group.

Richards (1971) agreed with Poole et al. (1970) that the gneisses associated with the Green Head Group formed as the result of Late Paleozoic metamorphism.

Poole and Rodgers (1972), Patel (1973), and Ruitenberg et al. (1973a, b, c) refuted the interpretation of Richards (1971) and Brown (1972) for a conformable sequence in the Saint John area and noted that contacts between the Green Head Group and Coldbrook Group are everywhere faulted. They suggested that the stratigraphic nature of the contact between the Coldbrook Group and Cambrian sedimentary rocks is unclear and may be either conformable or disconformable. Ruitenberg et al. (1973a) suggested that the Cambrian rocks are mainly in faulted contact with the Coldbrook and Green Head groups. Poole and Rodgers (1972) and Ruitenberg et al. (1973a) concluded that the Green Head Group lithologies pass laterally into schist and gneiss, although Poole and Rodgers inferred that some schist and gneiss may underlie the Green Head Group. Based on radiometric dates, they suggested that the igneous rocks that intruded the Green Head and Coldbrook groups are Paleozoic in age (Ordovician, Devonian, and Carboniferous), whereas Poole (in Wanless et al., 1972, 1973) suggested a Late Precambrian and/or Cambrian to Ordovician age for plutonism. Rast and Stringer (1974) later suggested a Devonian age for plutonism.

1.2.2. Middle 1970's to Early-1980's

By the early- to mid-1970's, the age of the Coldbrook Group appeared firmly established as Precambrian; however, the age of the Green Head Group was only known as pre-Coldbrook. The only direct assessment of the age was that of Hofmann (1974) who proposed a Neohelikian or Middle Riphean age (Mesoproterozoic) based on stromatolites. However, he also noted that the age of the stromatolites could be anywhere in the range from Aphebian to Hadrynian.

Poole (1976), O'Brien (1976) and Rast et al. (1976a, b) made

regional correlations between the Precambrian and Lower Paleozoic rocks of the Avalon Zone in the Appalachian Orogen. O'Brien (1976) and Rast et al. (1976a, b) concluded that the Neohelikian Green Head Group accumulated on a cratonic basement (not now exposed) and was highly deformed, metamorphosed, and intruded by variety of syn- to post-kinematic plutonic rocks in late Neohelikian or early Hadrynian. They interpreted gneisses in the Green Head Group to be the result of selective metamorphism of clastic horizons prior to deposition of the Coldbrook Group, and not a crystalline basement equivalent to the Canadian Shield (cf. Poole, 1976), supporting the interpretation of Wardle and O'Brien (1973). These rocks were interpreted to be unconformably overlain by late Hadrynian volcanic rocks of the Coldbrook Group and intruded by a suite of plutonic rocks and mafic dykes and unconformably overlain by the Saint John Group. The gross structure of the area was thought to be an anticlinorium, cored by the Green Head Group and flanked by the Coldbrook and Saint John groups.

Butt (1976) performed the first geochemical study in the area on a small intrusion of granite in the Musquash area (portion of the Lepreau Pluton of Ruitenberg et al., 1975) termed the Musquash Stock. He concluded that the Musquash Stock intruded a metamorphosed complex of Precambrian gabbro and diorite and inferred a late Precambrian to mid-Devonian age for the stock.

Ruitenberg et al. (1975, 1977, 1979), Giles and Ruitenberg (1977) and McCutcheon et al. (1982) provided the first systematic subdivision of the Coldbrook Group, and simplified versions of the stratigraphy of the Green Head Group following Leavitt and Hamilton (1962). The Brookville Gneiss was mapped as intrusive, grouped with the other plutons northeast of the Saint John River, and collectively referred to as the Golden Grove Intrusive Complex. (This thesis study area broadly coincides with their Western Intrusive Belt). Based on K-Ar and Rb-Sr dates they concluded that the Golden Grove Intrusive Complex is Late Precambrian-Early Paleozoic in age. However, southwest of the river,

the plutonic rocks were divided into the Ordovician and older(?) granodiorite and quartz diorite of the Musquash Pluton, Upper Silurian and younger(?) granodiorite and quartz diorite of the Lepreau and Milkish Head plutons, and Carboniferous leucogranite of the Chance Harbour Intrusions and the Grand Bay Pluton. They also suggested that the Kennebecasis Formation should be included in the uppermost part of the Mispic Group and that this group may extend into the Devonian.

Wardle (1978) described the rock types in the Saint John area in detail. He replaced the Ashburn Formation of the lower Green Head Group with three stratigraphic units: 1) the Lily Lake Formation, a clastic sequence forming the lower part; 2) the Drury Cove Formation, a limestone and dolomite sequence in the middle part; 3) the Narrows Formation, an interlayered clastic and carbonate sequence forming the upper part. These divisions agreed with the informal units previously established by Hamilton (1965, 1968) (see Appendix A). Wardle excluded the gneisses from the Golden Grove Suite and divided them into three geographically separate packages termed the Brookville, Rockwood Park and Pleasant Point gneisses, the latter two predominantly orthogneisses. Rast et al. (1976a, b) and Wardle (1978) believed that these orthogneisses were intrusive diapirs into the Green Head Group and that the Brookville Gneiss was a highly metamorphosed equivalent of the upper clastic part of the Lily Lake Formation. However, Wardle (1978) and Nance (1982) considered that the bulk of the Green Head Group lies within the greenschist facies. Wardle (1978) concluded that the Coldbrook Group accumulated on a deformed Green Head Group basement and both were subsequently intruded by the late Precambrian Golden Grove Suite prior to the unconformable deposition of the Cambrian rocks. This view was supported by numerous subsequent workers (e.g. Schenk, 1978; O'Brien et al., 1983; Rast and Skehan, 1983; Skehan and Rast, 1983).

Wardle (1978) re-examined the Carboniferous system in the Saint John area. He agreed with Alcock (1938, 1959) and van de Poll (1970) that the Kennebecasis Formation unconformably overlies the Green Head

Group and should be assigned to the Lower Mississippian. Wardle (1978), citing structural evidence by Rast and Grant (1973a), suggested that the long established internal stratigraphy of the Pennsylvanian-Mississippian Mispec Group should be reversed with the West Beach Formation older than the Balls Lake Formation. The Pennsylvanian Lancaster Formation was confirmed to lie unconformably on the Mispec Group. These relationships were also confirmed by Strong et al. (1979) who conducted a geochemical survey on these inferred Carboniferous mafic rocks. The calc-alkaline affinity suggested that subduction may have influenced Carboniferous tectonic processes (Strong et al., 1979) and Keppie (1982) proposed the closure of a small ocean basin between New Brunswick and Nova Scotia in the Carboniferous.

Rast et al. (1978a) studied the rocks in the southwestern portion of the thesis area along the New River Beach Fault. He interpreted the rocks northwest of the fault to be related to the Precambrian Coldbrook Group, intruded by a dyke swarm, and mylonitized during the latest Precambrian. The dykes were interpreted by Rast (1979) and Rast and Dickson (1982) to record the initial opening of the Iapetus ocean in the late Precambrian.

Rast et al. (1978b) studied the deformed Carboniferous rocks southwest of Saint John (Mispec Group of Alcock, 1959) and mapped what was interpreted as a series of nappe complexes confirming the earlier work of Rast and Grant (1973b). The Chance Harbour nappe complex extends southwest from Musquash Harbour to Dipper Harbour. It consists of strongly deformed and mildly metamorphosed sedimentary rocks of the Dipper Harbour and Chance Harbour beds overlain by volcanic rocks of the Meadow Cove volcanic unit (Rast et al., 1978b). The Lancaster Formation was interpreted to overlie these older units. The Saint John nappe complex extends northeast from Musquash Harbour to Lorneville Harbour. It consists of sedimentary rocks of the Lorneville Beds, overlain by basic volcanics of the Lorneville Volcanics and unconformably overlain by the Lancaster Formation. Rast et al. (1978a, b) concluded that these

nappes were intruded by Carboniferous plutonic rocks (Chance Harbour Intrusions of Ruitenberg et al. 1975, 1979) based on the apparent gradation of granite into rhyolite that is interlayered with sedimentary rocks of the Lancaster Formation. Deformation associated with these nappes has been correlated with the Late Paleozoic Variscan or Hercynian orogeny in Europe or the Alleghanian orogeny of the southern Appalachian orogen (Rast and Grant, 1973a, b; Rast and Currie, 1976; Rast et al., 1978a, b; Ruitenberg and McCutcheon, 1980). This deformation is equivalent to the Maritime Disturbance of Poole (1967). Carboniferous rocks of the nappe complex were interpreted to be regionally metamorphosed to low grades based on the presence of chloritoid, biotite, and garnet (Rast et al., 1978b; Murray, 1988).

Based on structural evidence, Parker (1984) extended the Saint John nappe complex of Rast et al. (1978a, b) from Lorneville Harbour to east of Saint John. He subdivided the complex into the lower Saint John Harbour and Mispic nappes consisting of Carboniferous rocks overthrust by intensely deformed Precambrian rocks of the Tiner Point nappe. He disagreed with Rast et al. (1978a, b) on the age of plutonic units in the Musquash Harbour area and suggested a Precambrian age for the granitic rocks.

1.2.3. Early-1980's to present

Currie et al. (1981) and Currie (1983) re-examined the geology in the Saint John area. All the gneisses in the Saint John area were grouped under the term Brookville Gneiss and interpreted to represent Archean basement, reactivated and diapirically emplaced into the Green Head Group during the intrusion of the Golden Grove Suite at ca. 800 Ma. Based on cross-cutting dykes in the Green Head Group and Golden Grove Suite, Currie (1983) concluded that the late Hadrynian Coldbrook Group initially rested unconformably on these units. As a result of U-Pb zircon and Rb-Sr whole-rock isotopic dating of the Brookville Gneiss,

Olszewski et al. (1980) and Olszewski and Gaudette (1982) concluded that the gneiss is older than 800 Ma, and shows inheritance of an older component, substantiating the interpretation of Currie et al. (1981). Their work also suggested a major period of deformation, metamorphism and intrusion in the Devonian and Carboniferous. Hence, the Brookville Gneiss was considered to represent a continental basement upon which the overlying Green Head Group accumulated (e.g. Currie, 1983, 1984, 1985, 1986a, b, 1987a, b, c, 1988a, b, 1989a, b; O'Brien et al., 1983; Keppie, 1985, 1989; Nance, 1986b, 1987a, 1988, 1990; Murphy and Nance, 1989; Nance et al., 1990; Currie and Hunt, 1991; Keppie et al., 1991).

Currie and Nance (1983), Currie (1984), McCutcheon (1984, 1985), Nance (1985, 1986a, 1987b), Caudill and Nance (1986), Caudill (1989) and Watters (1993) revised the Carboniferous "Mispec Group" stratigraphy, southeast of, and within the study area. They suggested that the West Beach Formation ("Lorneville Volcanics" of Rast et al., 1978b) is lithologically similar to the Coldbrook Group and removed it from the Mispec Group. They concluded that the Balls Lake Formation grades laterally and vertically into the Lancaster and that these rest unconformably on the Hadrynian West Beach Formation. Pickerill et al. (1985) suggested that the Kennebecasis Formation was a distal equivalent of the Memramcook Formation to the northeast and is Devonian to Carboniferous in age. The name Mispec Group was abandoned (Nance, 1987b) and Currie (1992) resurrected the term "Lorneville Beds" for the West Beach Formation which he considered to be of "Eocambrian" age.

Dickson (1983) mapped and described many of the plutons located southwest of Saint John River and subdivided the igneous rocks based on age, degree of deformation, lithology and field relations. The Hepburn Basin Granite (part of the Chance Harbour Intrusions of Ruitenberg et al., 1975, 1979) was interpreted by Dickson (1983) to be of Helikian age, based on a nonconformable contact with an overlying Green Head Group stromatolite-bearing limestone. However, McCutcheon (1981, 1984, 1985) suggested that the stromatolitic limestone belongs to the

Carboniferous Windsor Group (Parleeville Formation) and is not related to the Green Head Group. The Milkish Head Complex, which included the Lepreau and Musquash plutons of Ruitenberg et al. (1975, 1979), was interpreted to be Precambrian based on the Rb-Sr data of Poole (1980). Granitic rocks in the Chance Harbour area were interpreted to have intruded Carboniferous sedimentary rocks, based on K-Ar ages. Dickson (1983) also agreed with earlier work (e.g. Rast et al., 1978a, b) that the associated volcanic and sedimentary rocks should be correlated with the Carboniferous Mispic Group of Alcock (1938, 1959). This view was supported by Stringer and Burke (1985); however, McCutcheon (1981, 1984, 1985) and Currie (1987b, 1989a) remapped the volcanic rocks as Precambrian. Currie (1983, 1985, 1987b, 1989a) subdivided the Milkish Head Complex of Dickson (1983) into a series of Precambrian plutons collectively assigned to the Golden Grove Intrusive Suite and placed only the Carboniferous sedimentary rocks in the Mispic Group. Based on a U-Pb zircon age of ca. 555 Ma, the volcanic rocks (Meadow Cove volcanic unit of Rast et al., 1978b) were grouped with the Precambrian Coldbrook Group (Zain Eldeen, 1991; Zain Eldeen et al., 1991). The Carboniferous plutonic units of Ruitenberg et al. (1975, 1979) and Dickson (1983) yielded a U-Pb zircon age of ca. 550 Ma and was correlated with the Golden Grove Suite (Currie and Hunt, 1991). However, based on field evidence, Rast and Skehan (1991) continued to argue for a Carboniferous age for the Meadow Cove volcanic unit and associated granitoid rocks. McLeod et al. (1994) changed the name of the Meadow Cove volcanic unit to the Dipper Harbour volcanic unit after the main area of exposure.

McCutcheon and Ruitenberg (1987) excluded the Milkish Head and Mayflower Lake plutons from the Golden Grove Intrusive Complex, because "these plutons are geographically separate, appear to have intruded the Coldbrook Group, and lack the mafic dykes that are characteristic of the Golden Grove suite" in the Kingston Complex. This interpretation led McCutcheon and Ruitenberg (1987) to suggest that the Milkish Head and

Mayflower Lake plutons may be coeval with the Kingston Complex. However, Deveau (1989) and White and Deveau (1989) included these plutons in the Golden Grove Suite based on their petrographic and geochemical characteristics.

Currie (1989b, 1991) mapped sections of the Green Head Group west of Saint John and concluded that the Martinon Formation should be excluded from this group and, based on lithological grounds, included in the Coldbrook Group.

By the late-1980's and early-1990's the names, lithologies, and ages for major units in southern New Brunswick appeared to be firmly established (Fig. 1.2) and this stratigraphy was used in numerous models to explain the evolution of the "Avalon terrane" (e.g. Keppie, 1989; Murphy and Nance, 1989; Keppie et al., 1991; Nance et al., 1991). However, as a result of the present study and related work in the Saint John area, the Brookville Gneiss, Green Head Group, and associated plutonic rocks have been suggested to form a distinct tectono-stratigraphic belt (Brookville terrane) different from rocks of the Caledonia terrane which are more typical of the Avalon Terrane *sensu stricto*. Other workers agree with some of the differences between the two terranes (e.g. Keppie et al., 1991; Dallmeyer et al., 1990; Dallmeyer and Nance, 1990; Murphy et al., 1990; Nance et al., 1991; Nance and Dallmeyer, 1994). However, they suggested that these contrasts represent different crustal levels of exposure of the same terrane (Avalon Composite Terrane).

1.3. PURPOSE AND SCOPE OF THIS STUDY

Although the stratigraphy in southern New Brunswick is widely accepted, considerable confusion and debate still exists regarding the absolute age of these units and their stratigraphic relationships. Much of the published data presented on the geology of southern New Brunswick have been repeated and re-interpreted by later workers without

contributing any new information, and erroneous and unconfirmed conclusions have been perpetuated in the literature and later became "fact".

This project focuses on the Green Head Group, Brookville Gneiss, and Golden Grove Suite in the "Brookville terrane". It attempts to resolve the relationships within and among these units, as well as their relationship to adjacent units of the Caledonia terrane and Kingston Complex, by a combination of detailed field mapping, structural studies, geochronology, and petrochemistry. The project consists of four fundamental components:

1. Clarification of field relationships and petrological characteristics of rock units in and adjacent to this terrane.
2. Determination of the ages of these units and the timing and nature of their deformation and metamorphism.
3. Interpretation of the tectonic significance of igneous and meta-igneous units.
4. Comparison of these units to other possibly correlative rocks in the northern Appalachian orogen.

1.4. LOCATION AND ACCESS

The Green Head Group, Brookville Gneiss and associated plutonic units (Brookville terrane) form a narrow, northeast-trending belt that is entirely confined to the area between the Caledonia-Clover Hill Fault to the southeast and the New River Beach-Kennebecasis Fault to the northwest (Fig. 1.3). This belt of rocks is exposed from Maces Bay in the southwest to Titusville in the northeast over a distance of 75 km. Rare inliers, drill core, and geophysical evidence indicate that the terrane can be traced under the Carboniferous cover, northwestward as far as Prince Edward Island. The terrane may also extend an additional 25 km offshore to the southwest to The Wolves islands. The study area

includes parts of the National Topographic Series map sheets 21G/1 (Musquash), 12G/8 (Saint John), 21H/5 (Loch Lomond) and 21H/12 (Sussex).

Access and rock exposure is excellent in and around the city of Saint John and includes a number of roads, paths, and power lines. Access is more limited northeast and southwest of the city but still reasonably good, mainly by secondary roads, streams, paths and power lines. The coastline provides excellent outcrop exposure with long stretches of near vertical cliffs, however, these sections are accessible only by boat, even at low tide. The larger lakes in the area also enable access by boat.

1.5. METHODS OF STUDY

Detailed field mapping and sampling were conducted during the 1988 to 1993 field seasons using as base maps orthophotomaps (1:10,000 scale) published in 1971 by the New Brunswick Department of Natural Resources. Statistical analysis of field orientation data (e.g. bedding, foliation, lineation etc.) using the computer software program STERONET (1993) was completed to assist in the geometric analysis and interpretation of field data.

Mapping was accompanied by the collection of approximately 1100 rock samples. Slabs of the granitoid rocks, orthogneiss and paragneiss were stained for K-feldspar, and modal compositions determined. About 600 thin sections were prepared for petrographic studies. This includes sections used by Deveau (1989) for his B.Sc. Honours thesis and Grammatikopoulos (1992) for his M.Sc. thesis. Mineral chemistry on polished thin sections was investigated using the JEOL 733 Superprobe at the Dalhousie University Regional Electron Microprobe Laboratory, Halifax, Nova Scotia.

Approximately 80 samples were selected from plutonic and related rocks for major and trace element analysis using the Regional X-ray Fluorescence Laboratory at Saint Mary's University, Halifax, Nova

Scotia. These data were supplemented by 28 samples from the study area previously analyzed by the same methods (Deveau, 1989; Grammatikopoulos, 1992). Seven of these samples were then selected for rare-earth element analysis by Induced Coupled Plasma-Mass Spectrometry at Memorial University in St. John's, Newfoundland and combined with 10 samples previously analyzed by the same method (Deveau, 1989; Grammatikopoulos, 1992; Whalen et al., 1994).

Seven samples from plutonic and metamorphic rocks were selected for $^{40}\text{Ar}/^{39}\text{Ar}$ dating and analyzed in an AEI MS-10 mass spectrometer at Dalhousie University in Halifax, Nova Scotia. In addition a detailed U-Pb study of zircon and titanite from 2 plutonic units was completed at Memorial University of Newfoundland under the supervision of Dr. G. Dunning.

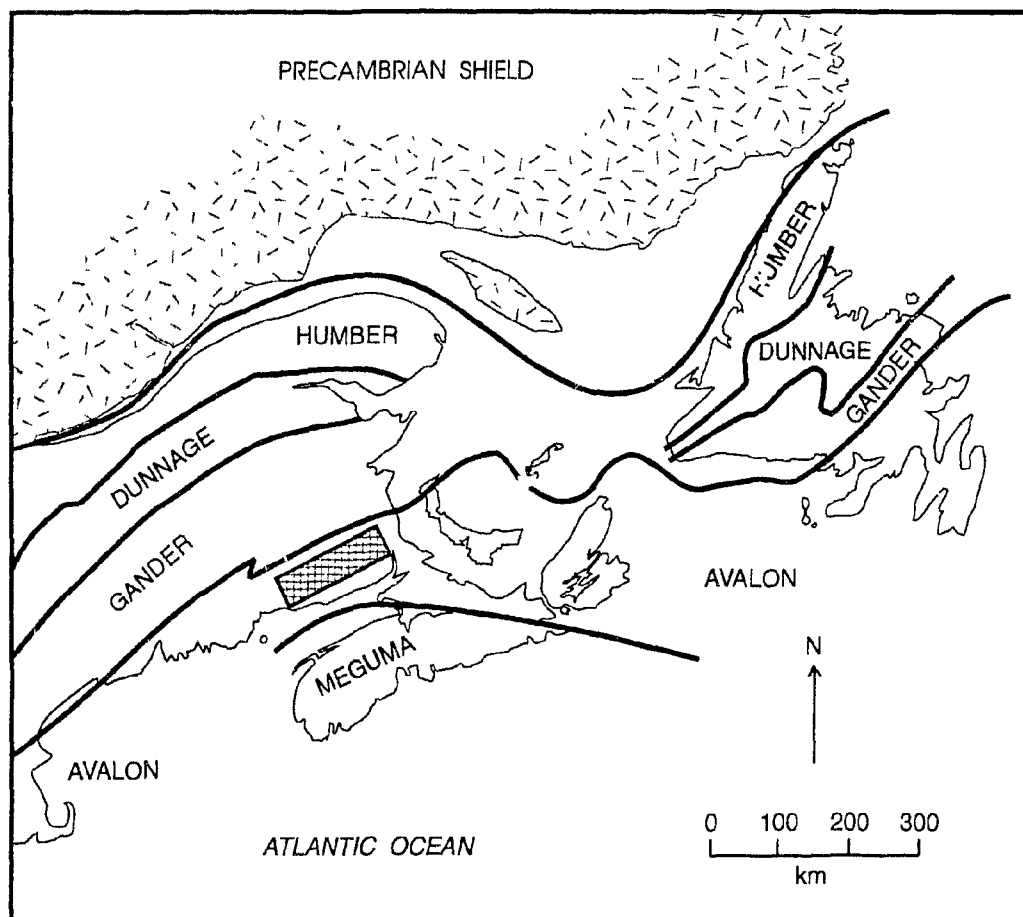


Figure 1.1. Distribution of the five pre-Silurian tectonostratigraphic zones or terranes in the northern Appalachian Orogen after Williams and Hatcher (1983). Box schematically outlines the present study area.

AVALON TERRANE

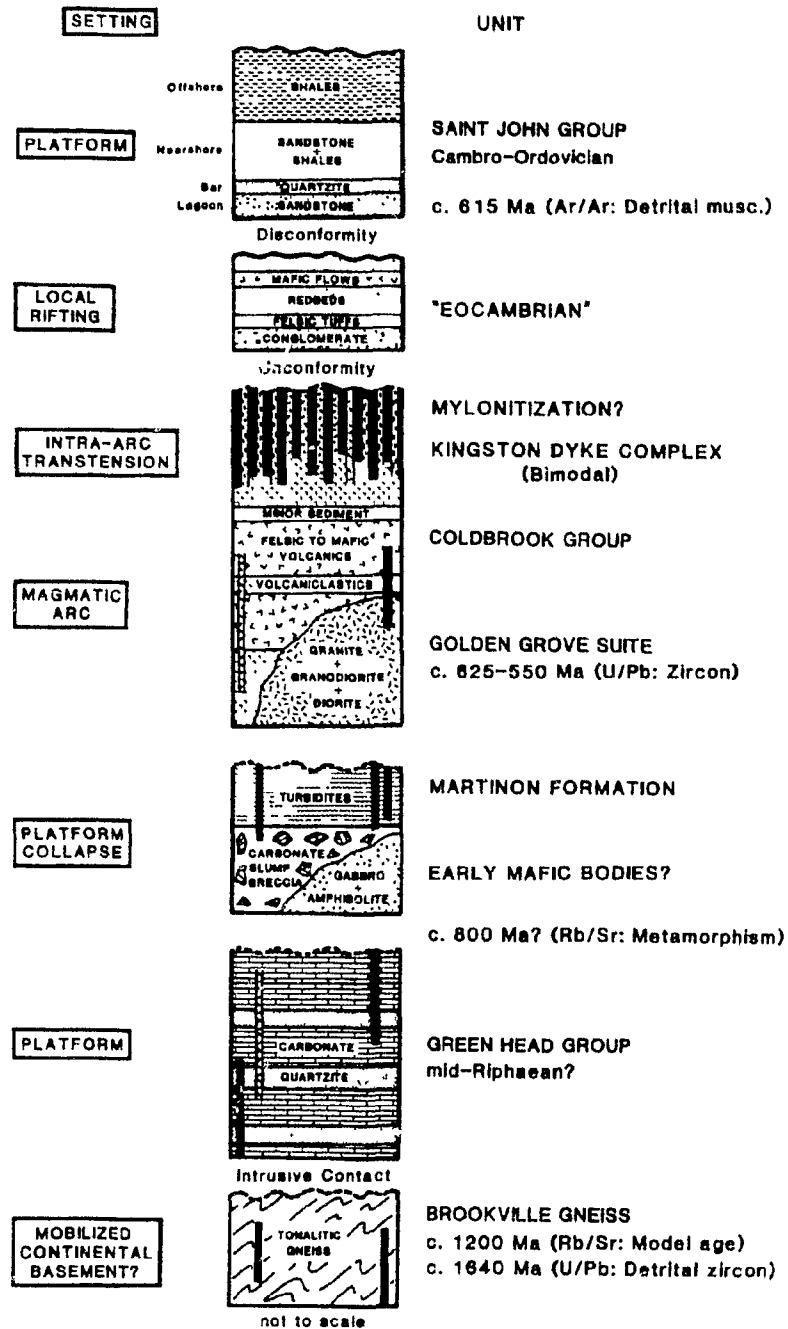


Figure 1.2. Schematic stratigraphic succession assumed to exist in the Avalon terrane in southern New Brunswick showing facies development, tectonism, and nomenclature prior to this study. Diagram after Nance (1990).

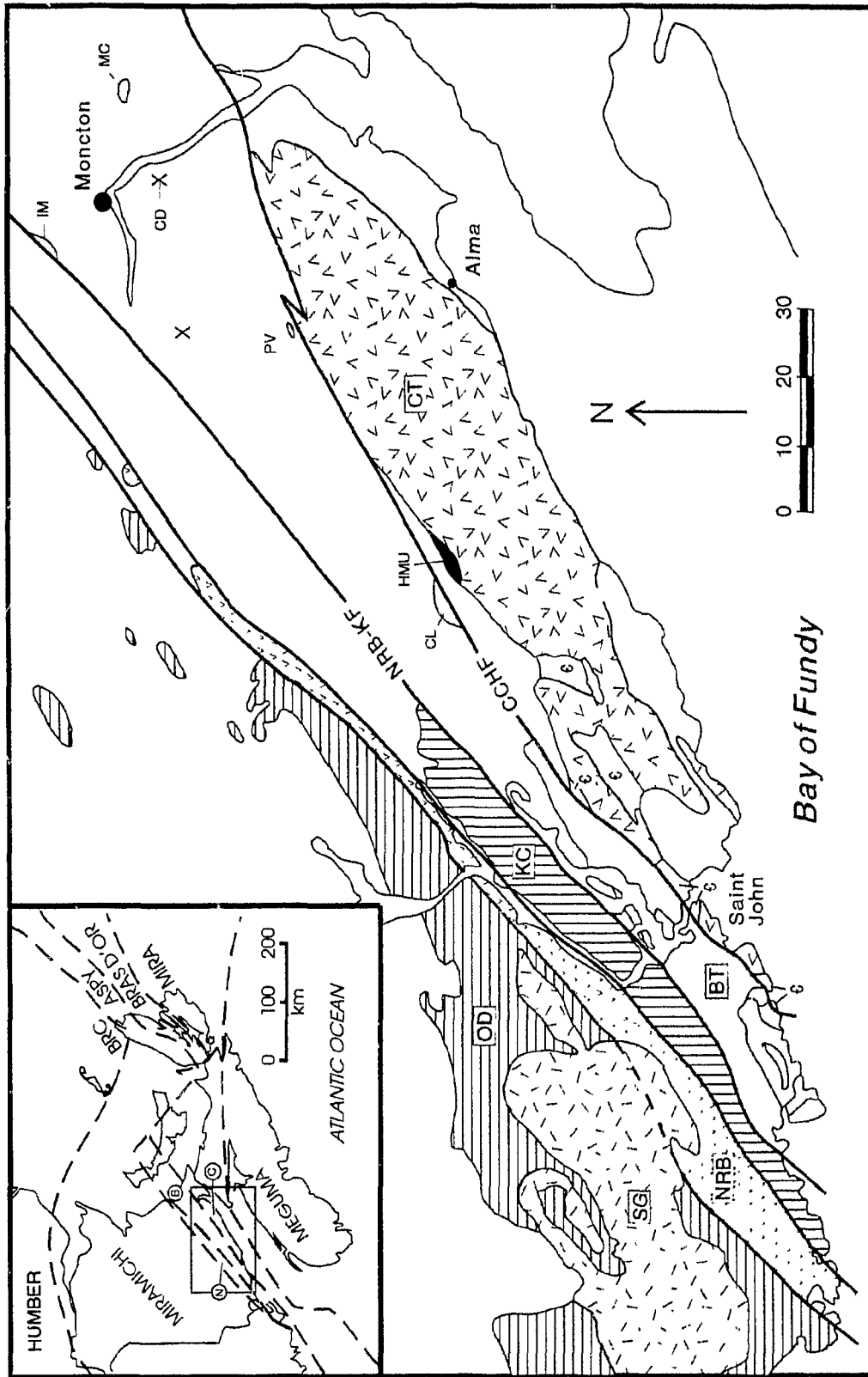
Figure 1.3. Simplified geology map showing the distribution of the Brookville terrane and other major rock units and faults in southern New Brunswick.

Units: CT = Caledonia terrane (Barr and White, 1989); HMU = Hammondvale metamorphic unit (Barr and White, 1991a); C = Cambrian to Ordovician Saint John Group; BT = Brookville terrane (Barr and White, 1989); KB = Kingston Complex (Currie, 1984); NRB = New River Belt (Johnson and McLeod, 1994); OD = Ordovician to Devonian stratified rocks; SG = Silurian to Devonian St. George Batholith.

Faults: CCHF = Caledonia-Clover Hill Fault; NRB-KF = New River Beach-Kennebecasis Fault.

Inliers of Brookville terrane: CL = Cassidy Lake inlier; PV = Pleasantvale inlier; IM = Indian Mountain inlier; MC = Memramcook inlier; X = drill core than intersects Brookville terrane (CD = Coverdale Pluton). Unpatterned areas are Upper Devonian and younger cover units.

Inset map: Teconostratigraphic terranes in New Brunswick and Nova Scotia after Barr and Raeside (1989). BRC = Blair River Complex; N = New River Belt; B = Brookville terrane; C = Caledonia terrane.



CHAPTER 2

DEFINITION AND DESCRIPTION OF MAP UNITS

2.1. JUSTIFICATION

Although portions of the study area have been included in regional scale mapping (e.g. Leavitt, 1963; Brown, 1972; Ruitenberg et al., 1979; Currie, 1985, 1987b, 1989a; Barr and White, 1991b; McLeod et al., 1994), as well as in more detailed localized studies (e.g. Hamilton, 1965, 1968; Subhas, 1970; Richards, 1971; Wardle, 1978; Dickson, 1983; Deveau, 1989), the complexity of units and field relationships still remain poorly understood and controversial. This was largely because of the assumption that a continuous stratigraphy existed in southern New Brunswick and geological interpretations attempted to conform with this framework. Confusion and controversy over the relationships among sedimentary, metamorphic, and igneous units led to contradictory interpretations that were incorporated into regional tectonic models for the Canadian Appalachian Orogen (see Appendix A and section 1.2). Detailed mapping to better define map units and establish field relations is critical to the understanding and interpretation of the area. The purpose of this chapter is to describe the redefined map units and their contact relationships with an intent to clarify the current controversial aspects of the geology in the Saint John area.

2.2. GREEN HEAD GROUP

The Green Head Group extends from Hammond River in the northeast to the Musquash Harbour area in the southwest and is the largest map unit in the Brookville terrane (Fig. 2.1, Map A). The Green Head Group in the Saint John area was mapped in considerable detail by Leavitt and Hamilton (1962), Leavitt (1963), Hamilton (1965, 1968), Wardle (1978),

and Nance (1982) and subdivided into two broad lithological units termed the Ashburn and Martinon formations. These formations were first established by Leavitt and Hamilton (1962) and Leavitt (1963) and retained here.

A small area of schist and marble to the northeast in the Hammondvale area (Fig. 1.3) was previously included with the Ashburn Formation (McCutcheon, 1978; Ruitenberg et al., 1979) and termed the Hammondvale Metamorphic unit by Barr and White (1991a) or the Hammondvale Schist (McLeod et al., 1994). These units are described below and a summary of the main field characteristics is presented in Table 2.1.

2.2.1. Ashburn Formation

Northeast of the Saint John River, the Ashburn Formation is located in three linear belts (Fig. 2.1, Map A). The main belt extends northeast from Green Head Island to Kennebecasis Bay area. Another large belt occurs farther northeast, in the Hammond River area where it is almost entirely surrounded by granitoid rocks. A thin belt is located southeast of the main body and extends northeast from the Saint John River along the Caledonia-Clover Hill Fault. Slivers of the Ashburn Formation also occur along the Caledonia-Clover Hill Fault to the northeast and in drill core that penetrated the Carboniferous Moncton Sub-Basin (Fig. 1.3). Clasts of marble interpreted to belong to the Ashburn Formation occur in conglomerates of the Devonian to Carboniferous Horton Group east of Moncton (St. Peter, personal communication, 1992).

Rocks of the Ashburn Formation also occur southwest of Saint John in a belt extending from Green Head Island to Musquash Harbour, along the northwestern margin of the Caledonia-Clover Hill Fault. A thin east-trending belt of Ashburn Formation occurs north of the Martinon Formation and as fault slivers along the New River Beach Fault (Fig.

2.1, Map A).

The Ashburn Formation is dominantly a carbonate unit that consists of calcite and dolomite marble with rare marble conglomerate. Other lithologies include meta-siltstone, spotted hornfels, quartzite, and mica schist.

The majority of the calcite marble in the Ashburn Formation is white to dark grey to light green, medium- to coarse-grained, and generally banded on a scale of 5 to 25 cm (Plate 1a). Locally the marbles are very coarse-grained near intrusive contacts (e.g. French Village area) and are clearly the result of contact metamorphism. Very fine-grained (locally aphanitic) calcite marbles are common and in places exhibit rhythmic layering (1 mm to 1 cm). The banding is typically folded into tight and isoclinal structures and locally displays sheath fold patterns. These rocks are interpreted to be calcite ultramytonites. They occur throughout the Ashburn Formation but are best developed proximal to the Caledonia-Clover Hill Fault in Saint John and the Musquash Harbour area where they correspond to Unit 3 of Wardle (1978). Wardle (1978, p. 37) considered these aphanitic "parallel-laminae cherty carbonates" to be algal in origin. The medium- to coarse-grained marbles are also folded into tight to isoclinal structures and locally display sheath fold geometries (Chapter 3).

Dolomite marbles are less abundant than the calcite marbles. They are easily distinguished from calcite marbles by the "cross-hatched" fissuring on weathered surfaces and they tend to be more resistant to erosion. They are typically massive (up to 50 m), pink to cream-coloured, lens-shaped, and generally concordant to layering in the calcite marbles. Discordant dolomite is locally developed and appears to be associated with brittle fault zones and to "cross-cut" the layering in the calcite marble. These dolomites are probably secondary in origin as described by Leavitt (1963) and Wardle (1978).

Locally the carbonate rocks contain the stromatolite Archaeozoon acadense (Matthew, 1890a), preserved in low-strain lenses. These

columnar stromatolites are commonly highly distorted and difficult to recognize in the field. However, on the northwestern tip of Green Head Island, pristine examples are preserved (Plate 1b) and locally interlayered with black meta-siltstone. Hofmann (1974) assigned a Neohelikian (Mesoproterozoic) age to these features but suggested they could be as young as 750-880 Ma (written communication, 1991).

Carbonate conglomerates are poorly preserved in the Ashburn Formation and have only been found in one location on the west shore of South Bay. Here a thin (1-2 m) white to light grey marble pebble conglomerate is exposed in banded marble. It contains rounded clasts of marble and rare quartzite and is matrix-supported. It is not associated with any pelitic material. Carbonate conglomerates are found along the east shore in the Narrows of the Saint John River but these are associated with spotted hornfels and included in the Martinon Formation (see section 2.2.2).

Areas of massive to finely bedded, black to grey to rust brown, meta-siltstone occur throughout the Ashburn Formation. They range in size from large mappable lens-shaped units to thin (<10 cm) boudinaged layers. Graded bedding and slump structures are locally preserved. These meta-siltstones are identical to lithologies in the Martinon Formation.

Like the meta-siltstone, spotted hornfels occurs throughout the Ashburn Formation, especially near plutonic contacts. They are also abundant in areas adjacent to the Caledonia-Clover Hill Fault, in and southwest of Saint John. The hornfels is typically grey, massive to moderately banded (5 to 25 cm) and locally interlayered with marble, thin (<50 cm) white quartzite, and calcite mylonite. It is intensely spotted with small (<1 cm), dark grey, oval patches of cordierite commonly retrogressed to large crystals of muscovite. The porphyroblasts are concentrated along primary bedding. Wardle (1978) reported the presence of andalusite but this was not confirmed in this study.

Abundant quartzite occurs in the Ashburn Formation adjacent to the Caladonia-Clover Hill Fault and Drury Cove area. It is generally white to light grey, fine-grained, thinly (5 - 25 cm) to massively (<10 m) layered, and locally displays small-scale cross-bedding. Ripple marks and graded beds were reported by Wardle (1978) but none were observed during the present study. Locally the quartzite is well laminated, with laminations defined by alternating biotite-rich and poor layers. These rocks were termed gneissic quartzites by Leavitt (1978). Wardle (1978) considered the quartzite and hornfels to be the protolith of paragneissic units in the Brookville Gneiss.

Mica schists are not common in the Ashburn Formation and occur only in the Drury Cove and Hammond River areas. Mica schists are typically grey, well foliated, medium- to rarely coarse-grained, and commonly spotted with small (<5 mm) oval patches of cordierite retrogressed to sericite. The foliation is usually kinked and defined by chlorite, muscovite, and minor biotite.

All siliciclastic horizons in the Ashburn Formation are highly fractured, exhibit little lateral continuity, and occur as variably sized boudins in the carbonate rocks. Extreme warping of marble layering around these boudins and the local preservation of pristine pre-deformation structures and textures indicate the high ductility of the marble.

The grade of metamorphism in the Ashburn Formation is difficult to determine because the marble is generally monomineralic. Metamorphic grade is best ascertained by studies of the pelitic rocks and is generally at albite-epidote hornfels facies; however, close to plutons metamorphic grade increases to hornblende-hornfels facies and rarely pyroxene-hornfels facies. Mica schist in the Drury Cove and Hammond River areas preserve what is interpreted to be a regional greenschist facies metamorphism with a well developed cleavage. Greenschist-facies metamorphism in the Drury Cove area is associated with the ductile shear zone (MacKay Highway shear zone of Nance and Dallmeyer, 1994) that

separates the Ashburn Formation from the Brookville Gneiss.

2.2.2. Martinon Formation

The main body of the Martinon Formation is located west of Saint John and occupies a large area north of Ludgate Lake (Fig. 2.1, Map A). Rocks interpreted to be part of the Martinon Formation occur on Green Head Island and in the area northeast of the Saint John River (Fig. 2.1, Map A, Map B) where they correspond to the Narrows Formation (Unit 8) of Wardle (1978). The Martinon Formation consists dominantly of meta-siltstone and spotted hornfels, with minor banded calc-silicate rocks, quartzite, conglomerate and rare marble (Table 2.1). New outcrops of the Martinon Formation along Highway 7, southwest of the Saint John River, have exposed new units and greatly added to the understanding of this formation.

The meta-siltstone is typically grey to black, fine-grained, and featureless. Sedimentary structures are generally difficult to find, but on weathered surfaces, primary sedimentary features are recognizable (Plate 1c). However, some outcrops lack such features, and this suggests that the thickness of beds is greater than the dimensions of the outcrop. Locally the meta-siltstone is interlayered with light grey meta-sandstone. The meta-sandstone is generally fine-grained and commonly forms thin (<10 cm) beds and channel-like structures. Associated with the meta-siltstone is minor, white to dark grey, fine-grained, massive quartzite. It typically forms layers less than 2 metres wide that cannot be traced more than 50 metres along strike. Rarely the quartzite has thin (<10 cm), matrix-supported, conglomeratic lenses with clasts of quartzite and black meta-siltstone. Other sedimentary structures include graded and flaser bedding, cross-laminations, and channel-fill structures.

Close to plutonic contacts, the meta-siltstone is hornfelsic and spotted with cordierite. These lithologies are identical to those in

the Ashburn Formation (Chapter 5).

Some units (up to several tens of metres thick) have a very chaotic appearance and may contain large irregular blocks (up to 10 metres) of white marble and minor black meta-siltstone. Contacts between the large blocks and the matrix are highly irregular and commonly interdigitate. Locally it is clear that fragments of marble have been detached from the larger blocks. This feature is best exposed along Highway 7 near the northern contact with the Ashburn Formation.

The next most abundant lithology is well banded (1 mm to 1 cm), white to light green to dark grey calc-silicate rocks. These are abundant in the Green Head Island area. The calc-silicate rocks typically have a striped appearance and in the southern part of the Martinon Formation, where they have been contact metamorphosed, they have been interpreted previously as gneisses (Dickson, 1983). These laminated rocks display abundant sedimentary features and preserve soft-sediment deformation structures. Some of the soft-sediment folds are associated with finely laminated, undisturbed meta-siltstone. These small-scale folds are interpreted to be penecontemporaneous with slumping or debris flows. Wardle (1978) suggested that this sequence of lithologies closely resembles the classical turbidite model proposed by Bouma (1962).

Other lithologies that are characteristic of the Martinon Formation include a variety of conglomerates. Quartzite pebble conglomerate is common throughout the formation and is more extensive than previously recognized (c.f. Leavitt, 1963; Wardle, 1978; Dickson, 1983; Currie, 1991). The conglomerate layers are generally 1-2 metres in thickness. They are typically unsorted, matrix-supported with rounded, white to light grey, fine-grained quartzite clasts (<5 cm in diameter) and minor black siltstone and rare fine-grained marble clasts. They are commonly set in a dark grey to black meta-siltstone matrix and rarely in a carbonate-meta-siltstone matrix. Black meta-siltstone associated with the conglomerate is typically chaotically folded.

Quartzite-marble pebble to boulder conglomerates are rare and are known to occur only on the west coast of Green Head Island, the Narrows on the Saint John River, and in the Pokiok area (Leavitt, 1963; Wardle, 1978; and this study). They range in thickness from 1-2 metres on Green Head Island and between 10-50 metres in the Narrows and Pokiok areas (Leavitt, 1963; Wardle, 1978). Clast content varies but is dominantly well-rounded quartzite with minor slab-like cobbles of calcitic and dolomitic marble (Plate 1d). The conglomerates on Green Head Island and in the Narrows were reported to contain stromatolite cobble and boulder debris by Leavitt (1963) and Wardle (1978). The stromatolite clasts in the conglomerate on Green Head Island were confirmed in this study but were not located in the Narrows. The conglomerate is poorly sorted and the matrix varies from light grey to black, fine-grained feldspathic sandstone to calcareous sandstone. The texture varies from clast- to matrix-supported. The conglomerates along the Narrows are locally interbedded with black laminated meta-siltstone and spotted hornfels that are enclosed in marble and may represent large boudins or primary channel fills.

Marble pebble-cobble conglomerate is well exposed on Highway 7 and is also associated with the conglomerates in the Saint John River area. The carbonate clasts are mainly sub-rounded and display a 1-5 mm paler-coloured rind. In places, the clasts are very angular and slab-like and the rocks resemble sedimentary breccias. Minor white quartzite and black meta-siltstone clasts are well-rounded and pebble-sized. The matrix in the conglomerate is grey to buff, carbonate to sandy-carbonate and the texture is generally matrix supported. These carbonate conglomerates are locally cut by graded sandy channels. Toward the northern contact with the Ashburn Formation, the carbonate clasts are flattened into the cleavage plane, as noted by Wardle (1978).

Clasts within the conglomeratic units appear to be intraformational in character. No exotic clasts were observed.

Sedimentary siliciclastic and carbonate breccias are rarely

developed in the Martinon Formation and are best exposed near the northern contact with the Ashburn Formation along Highway 7. This lithology consists of very irregularly shaped fragments of light grey carbonate and dark grey-brown meta-siltstone which commonly display evidence of soft-sediment deformation. This lithology was considered by Leavitt (1963) to be a deformed conglomerate, whereas Wardle (1978) interpreted it to represent a submarine slide breccia. Following the terminology of Hsu (1974) these chaotic deposits are better classified as olistostromes (Plate 1e) based on two lines of evidence:

1. the olistoliths show very little variation in composition compared to the clasts in conglomerates. Large olistoliths are primarily angular white marble with subsidiary black meta-siltstone. Smaller olistoliths are commonly rounded and may have been eroded prior to incorporation into the basin by debris flows. Following the definition of Hsu (1974) many of the conglomerates described in section 2.2.2. are genetically associated with olistostromes. The lack of exotic fragments and the homogeneity of the clasts combined with the lack of a sheared matrix suggests that a depositional process was involved in the production of the olistostrome, not a tectonic process (Hsu, 1974; Bailey et al., 1989; R.H. Bailey, 1992 personal communication).

2. all primary sedimentary features indicate soft sediment deformation. Intricate infolding of silt and fine sand with delicate wisps of mud along the margins of the olistoliths suggests transport in a plastic or cohesive matrix. Following the classification proposed by Postma (1986) this is termed a cohesive debris flow deposit.

A third criterion essential to the definition of an olistostrome is that it is stratigraphically concordant on all scales (Hsu, 1974). Due to the lack of outcrop exposure this cannot be satisfactorily proven. However, along strike northeast and southwest of the olistostrome exposed on Highway 7 are numerous quartzite and carbonate-bearing conglomerates which are interpreted to be correlative. Also

isolated outcrops of marble were found along strike and may represent poorly exposed olistoliths.

Metamorphic grade in the Martinon Formation is generally at albite-epidote hornfels facies and increases to hornblende-hornfels facies in proximity to intrusive bodies (Chapter 5).

The contact between the Ashburn and Martinon formations has been variously interpreted (see Appendix A). Field work in conjunction with this study suggests a sheared contact, with marble of the adjacent Ashburn Formation commonly deformed into tight (locally sheath) folds and containing varied-scale rafts/boudins of dark-coloured pelitic rocks. However, along the northeastern contact (Map B) lithologies of the Ashburn and Martinon formations are relatively undeformed and clearly interlayered. This suggests that the original contacts were locally interlayered and the Martinon and Ashburn formations are interpreted to be lateral facies equivalents (section 7.1.1).

2.2.3. Hammondvale metamorphic unit

The Hammondvale metamorphic unit (Barr and White, 1991a) is located approximately 15 km south of Sussex and forms a narrow belt along the northwestern margin of the Caledonia terrane (Fig. 1.3). This unit consists of mica-albite schist which is locally garnet-bearing and interlayered with minor marble and amphibolite. It is faulted against sedimentary, volcanic, and igneous rocks of the ca. 550 Ma Coldbrook Group. The northwest margin is unconformably overlain by fossiliferous limestone of the Carboniferous (Visean) Windsor Group and from drill core the schists can be traced under the Carboniferous cover to the northwest (McCutcheon, 1978) towards the Caledonia-Clover Hill Fault.

The schist is generally dark grey, fine- to medium-grained, with a well developed foliation. Where garnet is present (<1 mm) the schist usually has a pinkish hue. These schists are foliated on a scale of one millimetre to one centimetre, being defined by alternating layers of

albite- and muscovite-rich bands. Quartz stringers (<1 cm by <30 cm) commonly lie parallel to the foliation. In areas where muscovite is absent the rock displays a massive, featureless texture with large (<5 mm) subidioblastic feldspar porphyroblasts. Locally the schists exhibit a strong mineral lineation defined by elongate quartz ribbons and asymmetric albite and garnet porphyroclasts.

Marble bands are locally abundant in the schist. They are typically dark to light grey, fine- to medium-grained, and thinly banded (<5 mm). The marble occurs as thin (1 to 2 m wide) bands that commonly display gradational contacts with associated schist.

Minor dark grey to black, thin (<1 m) amphibolite layers are fine-grained and thinly laminated (<2 mm) with alternating feldspar and amphibole-rich layers and commonly lie parallel to foliations in the schist. The amphibolite displays sharp contacts with the schist and the original protolith is interpreted to be mafic dykes or sills. The Hammondvale metamorphic unit displays a unique metamorphic mineral assemblage characteristic of a low-temperature/high-pressure metamorphism (Chapter 5).

Fine-grained, pink, syenogranite dykes (<2 m) intrude the Hammondvale Metamorphic unit. Although these metamorphic rocks are in faulted contact with the Caledonia terrane, the syenogranitic dykes are interpreted to be related to the ca. 550 Ma Bonnell Brook Pluton.

2.3. BROOKVILLE GNEISS

The Brookville Gneiss is a locally migmatitic (Plate 1f), biotite-cordierite-K-feldspar-bearing paragneiss with minor sillimanite, hornblende, and andalusite (Table 2.1). Commonly associated with the paragneiss are minor calc-silicate and marble layers and rare feldspar-rich quartzite. The paragneiss is generally dark grey to pinky-grey, fine- to medium-grained, with a well developed gneissic foliation. The paragneiss is thinly layered (1 mm to 1 cm wide) and defined by

alternating biotite-rich, and quartzo-feldspathic bands. Where hornblende is present it usually defines a moderate to well developed lineation. Sillimanite-bearing paragneiss is common throughout the Brookville Gneiss, but is abundant in the Mackay Highway shear zone (Chapter 5). The migmatitic gneiss has light grey to pink, medium- to rarely coarse-grained, generally thin (1 to 10 cm wide) leucosomes and melanosomes, where present, are generally black, fine- to medium-grained, and thin (1 mm to 1 cm wide). Leucosomes are typically boudinaged parallel to gneissic layering and locally isoclinally folded and discordant to the gneissosity. Following the classification of Mehnert (1971) the dominant migmatitic structures are stromatic.

Calc-silicate layers are not common in the paragneiss. They are typically white to light green, coarse-grained, commonly boudinaged parallel to the gneissic layering. Marble bands (1 to 2 m wide) are typically white to light green, coarse-grained with a granoblastic texture, and commonly boudinaged parallel to the gneissosity. Weak layering is commonly observed. Feldspar-rich quartzite layers are light grey, medium-grained, and relatively thin (<50 cm). These layers are commonly parallel to gneissic layering, but locally they are tightly folded.

Metamorphic grade, as determined from the mineral assemblage cordierite + biotite + K-feldspar + sillimanite in the paragneiss, indicates low-pressure/high-temperature metamorphism, characteristic of the upper amphibolite facies (Chapter 5).

Associated with the paragneiss are sheets of granodioritic to tonalitic orthogneiss. They are typically grey, medium-grained, and moderately to strongly foliated. The foliation (<5 mm wide) is defined by alternating biotite-rich and quartzo-feldspathic layers. Biotite schlieren are commonly elongate parallel to the foliation. The orthogneiss commonly exhibits a strong mineral lineation defined by elongate aggregates of feldspar and quartz.

Amphibolites in the Indiantown area are interpreted to be related

to the Brookville Gneiss. They are thinly (2 mm) to thickly banded (<10 cm), medium-grained with alternating hornblende/biotite-rich and plagioclase-rich layers. Locally the plagioclase and hornblende define a weak east-west-trending horizontal lineation. The amphibolite contains small (<5 cm x <2 cm), finer-grained, lens-shaped amphibolite inclusions that are interpreted to represent pre-metamorphic mafic dykes. The amphibolite is associated with lenses and dykelets of foliated tonalite that generally lie parallel to the foliation but are locally cross-cutting and isoclinally folded. They are texturally and mineralogically identical to the tonalitic varieties in the granodioritic to tonalitic orthogneiss. It is unclear if the tonalitic stringers represent a metamorphic segregation from the amphibolite or is related to the intrusion of the orthogneiss. In the Indiantown area the amphibolite is completely enclosed by plutonic units.

Amphibolite layers within the paragneiss are rare. They are commonly dark green, thin (<1 m) and boudinaged parallel to the gneissic foliation. They generally have sharp contacts with the gneiss and are interpreted to be pre-metamorphic mafic dykes or sills, possibly related to the amphibolite in the Indiantown area.

The paragneiss and orthogneiss are intruded by rare, light grey, fine- to medium-grained granodiorite dykes/sills. The dykes are generally thin (<2 m), weakly to moderately foliated, and concordant with the gneissic foliation but are locally cross-cutting and boudinaged. These are interpreted to be pre- to syn-metamorphic and correspond to the quartz diorite dykes described by Wardle (1978, p. 142). The Brookville Gneiss is intruded by unfoliated pink, fine- to coarse-grained pegmatite dykes which are locally cut by fine-grained mafic dykes.

Wardle (1978) divided the gneiss in the Saint John area into three separate units, termed the Brookville, Rockwood Park, and Pleasant Point gneisses, based on geographic location. However, subsequent studies have grouped these units together under the term Brookville Gneiss (e.g.

Currie et al., 1981; and this study). The geographic locations of Wardle (1978) are retained in the following summary only to facilitate description of the field relations.

The gneisses exposed on the southern part of Green Head Island (Map B) and southeast of South Bay (Pleasant Point gneisses of Wardle, 1978) consist of chaotically folded orthogneiss ("swirled orthogneiss" of Wardle, 1978). Paragneiss is associated with the orthogneiss along its southern margin and also occurs locally with marble as small xenoliths. An area previously interpreted as paragneiss along the contact with the Fairville pluton (cf. Wardle, 1978) is considered part of the Green Head Group (see Chapter 5). A brittle fault forms the northwestern contact with marbles of the Ashburn Formation; however, large, fractured boudins of paragneiss occur locally in the marble close to the contact. On the southeastern margin, the gneisses were intruded by the Fairville Granite. Gneissic xenoliths are common in the Fairville pluton close to the contact.

The Rockwood Park gneiss (Wardle, 1978) is exposed in a small narrow belt in the Rockwood Park area. It consists of a mixture of paragneiss and orthogneiss with minor thin marble layers. The northeastern contact with marbles of the Ashburn Formation is marked by a linear topographic low and, where exposed, this contact is a brittle fault. Gneissic boudins were not observed in the adjacent marble, although biotite schists have been reported there (Wardle, 1978). The southern margin of the gneiss has been intruded by dioritic and granitic rocks. Within the Rockwood Park gneiss, Wardle (1978) included a belt of gneiss and biotite schist that extends discontinuously from south of Rockwood Park to the Saint John River. This belt of "gneiss and schist" was later mapped as highly deformed zone of granitoid rocks with minor gneiss, amphibolite, quartzite, and marble (White et al., 1990b, and this study). This highly deformed zone is associated with the Caledonia-Clover Hill Fault (Chapter 3).

The Brookville gneiss (as originally defined by Wardle, 1978) is

the largest exposure of gneiss. It forms a belt that widens eastward from Coldbrook to Rothesay and consists dominantly of paragneiss with minor layers of granodioritic to tonalitic orthogneiss, marble, calc-silicate rocks and feldspar-rich quartzite. On its southeastern margin the gneiss is in faulted contact with volcanic rocks of the Caledonia terrane (Caledonia-Clover Hill Fault). The eastern margin has been intruded by the French Village Quartz Diorite and the Duck Lake Gabbro. The northwestern contact with marbles of the Ashburn Formation is well exposed along Highway 1 (MacKay Highway), where a wide northeast-trending ductile shear zone (MacKay Highway shear zone of Nance and Dallmeyer, 1994) juxtaposes the gneiss with marbles of the Ashburn Formation (see Chapter 3).

2.4. DIPPER HARBOUR VOLCANIC UNIT

The Dipper Harbour volcanic unit (McLeod et al., 1994) (previously the Meadow Cove volcanic unit of Rast et al., 1978b) is a suite of volcanic rocks that outcrops in the southwest part of the Brookville terrane in the Dipper Harbour area. Two main areas of volcanic rocks have been delineated and subdivided into three distinct lithological packages (Table 2.1) that are part of a single thrust sheet. This includes: 1) a dominantly rhyolitic unit which consists of rhyolitic ash flows, flow-banded rhyolite, and associated lithic-rich tuff; 2) an andesitic to dacitic lithic-rich tuff unit and, 3) a mixed andesitic to rhyolitic tuff unit with minor sedimentary rocks. A detailed petrographic description of the Dipper Harbour volcanic unit is presented in Chapter 4.

As outlined in Chapter 1, the Dipper Harbour volcanic unit has been interpreted to be interlayered with Carboniferous sedimentary rocks and intruded and metamorphosed by Carboniferous granites, then dissected by a series of thrust sheets (e.g. Rast and Skehan, 1991). Others suggested the volcanic rocks and associated plutons are Precambrian

(Neoproterozoic) and lithologically similar to the Coldbrook Group (e.g. Currie and Nance, 1983).

Detailed mapping during the present study failed to identify any contact metamorphic effects from the granitoid plutons. Clear unconformities were recognized (most overturned) with basal conglomerates that contained fragments of the underlying granite and volcanic units. Volcanic rocks are locally interlayered with minor sedimentary rocks. However, the sedimentary rocks do not resemble any unit in the Carboniferous formations and rare clasts occur in the overlying basal conglomerate suggesting that these sedimentary rocks, and associated volcanic rocks, are older than Carboniferous. Other sedimentary rocks mapped as Green Head Group (e.g. Alcock, 1959; Rast and Grant, 1973b; Rast et al., 1978b; Dickson, 1983; Rast and Skehan, 1991) are also considered to be part of the Dipper Harbour volcanic unit.

These observations are confirmed by recent geochronology. A rhyolite ash flow within the Dipper Harbour volcanic unit in the Dipper Harbour area has yielded a poorly constrained U-Pb age of ca. 555 Ma. (Zain Eldeen et al., 1991; Zain Eldeen, 1991). A U-Pb age of ca. 550 Ma (see Chapter 6) was obtained from the Musquash Harbour pluton (Currie and Hunt, 1991). This appeared to confirm an affinity with the Coldbrook Group in the Caledonia terrane (Currie and Hunt, 1991; Zain Eldeen, 1991) which led Eby and Currie (1993) to correlate the Dipper Harbour volcanic unit and related granite to a Late Proterozoic to Ordovician supracrustal package that included the Saint John Group. This interpretation is not confirmed in this study. The volcanic rocks are clearly associated with the granites; however, these granitic rocks locally intrude Cambrian plutons and marbles interpreted to be equivalent to the Ashburn Formation (see Appendix B). This led White (1994) and White and Barr (in press) to correlate the volcanic and granitic rocks with the Brookville terrane.

2.5. PLUTONIC UNITS

Traditionally all the plutonic units in southern New Brunswick, together with various gneissic rocks, were included in a single assemblage, assumed to be Late Precambrian (Neoproterozoic), termed the Golden Grove Intrusives or Golden Grove Intrusive Complex or Suite (see Appendix A). White et al. (1990b) proposed that the term Golden Grove Intrusive Suite be abandoned because it is not clear that these plutons belong to a single intrusive suite, and suggested the use of individual pluton names following, as closely as possible, the names established by Hayes and Howell (1937). As a result of detailed mapping and petrological studies, many of the previously defined plutonic units and boundaries have been subdivided, redefined, and renamed following as closely as possible the recommendations of the International Subcommission on Stratigraphic Classification (1987). Detailed descriptions of the redefined plutonic units and dykes are presented in Appendix B and detailed petrography in Chapter 4.

These plutonic units range in composition from gabbro to granite (Table 2.2), and have been interpreted to have formed in a continental magmatic arc setting (Dickson, 1983; Deveau, 1989; White et al., 1990b; White and Barr, in press). These igneous units broadly resemble the 610-625 Ma plutons of the Caledonia terrane; however, geochronology (Chapter 6) indicates that most are considerably younger (< ca. 548-537 Ma).

2.6. CAMBRIAN-ORDOVICIAN UNITS

The Cambrian-Ordovician rocks in the Brookville terrane are included in the present study in order to compare their structural and metamorphic style with other units in the terrane. The stratigraphy and lithological descriptions of Hayes and Howell (1937) and Tanoli and Pickerill (1988, 1990) have been only slightly modified (Table 2.3).

Sedimentary rocks of the Cambrian-Ordovician Saint John Group lie conformably on the Coldbrook Group in the Caledonia terrane. However, along the shores of Kennebecasis Bay the Saint John Group occurs as small fault slivers in direct contact with marbles of the Ashburn Formation and granitic rocks of the Renforth and Milkish Head plutons. Exposed on Kennebecasis Island and Milkish Head are fault-bounded slivers of the Middle Cambrian Forest Hills Formation (Tanoli and Pickerill, 1988; previously assigned to the Fossil Brook and Porter Road formations of Hayes and Howell (1937) and Alcock (1938)). This unit consists of highly folded, light to dark grey, laminated siltstone and sandstone, massive mudstone, and minor limestone nodules. It contains numerous brachiopod and trilobite fragments and trace fossils.

The Middle to Upper Cambrian King Square Formation (Tanoli and Pickerill, 1988; previously assigned to the Hastings Cove and Agnostus Cove formations of Hayes and Howell (1937) and Alcock (1938)) outcrops on Long Island and at Sand Point and Hastings Cove. This fault-bounded unit consists of thinly interbedded grey fine-grained sandstone, micaceous shale and siltstone, and minor limestone lenses and nodules. The King Square Formation also outcrops in the Reversing Falls area where it is juxtaposed with the Ashburn Formation along the Caledonia-Clover Hill Fault.

Massive sandstone of the Lower Cambrian Glen Falls Formation was reported to outcrop in the Hastings Cove area (Hayes and Howell, 1937; Alcock, 1938; Wardle, 1978; Tanoli and Pickerill, 1988). However, new exposures of conglomerate associated with this poorly indurated sandstone contain Renforth and Milkish Head granitic clasts and rare plant fragments that led White et al. (1990b; and this study) to exclude these rocks from the Glen Falls Formation and assign them to the Devonian to Carboniferous Kennebecasis Formation. A summary of the field characteristics is given in Table 2.3.

2.7. DEVONIAN TO CARBONIFEROUS UNITS

In the past, the Devonian to Carboniferous stratigraphy in the study area has been very problematic and controversial (see Appendix A and section 1.2). However, recent work by Currie and Nance (1983), Nance (1985, 1986a, 1987b), Caudill and Nance (1986), Caudill (1989), St. Peter (1993) and this study has clarified many of these problems. The Devonian to Carboniferous units in the Brookville terrane can be divided into a zone that extends northeast from Saint John and another zone that extends to the southwest.

2.7.1. Northeastern zone

The northeastern zone consists of red to red-brown conglomerate, sandstone, siltstone, minor limestone, and rare white massive sandstone of the Devonian to Carboniferous Kennebecasis Formation, and is generally restricted to the Kennebecasis Bay area (Table 2.3). This formation was interpreted to be preserved in a half-graben (Wardle, 1978) northwest of Kennebecasis Bay, bounded on the north by the Petitcodiac Fault (van de Poll, 1970) (later renamed the Kennebecasis Fault) and on the south by the Milkish Head Fault (E. Grant, 1972). Bedding orientations dip shallowly to the northwest and the rocks are folded against the Kennebecasis Fault (E. Grant, 1972; O'Brien, 1976; Wardle, 1978). In the Millidgeville area southeast of the half-graben, the Kennebecasis Formation rests unconformably on marbles of the Ashburn Formation and on the Mayflower Lake pluton and is very gently folded. Farther northeast the Memramcook Formation (interpreted to be distal equivalent of Kennebecasis Formation defined by Pickerill et al., 1985) overlies the Renforth and Hammond River plutons and the Ashburn Formation. The southeastern margin of the Hammond River Granite and the Memramcook Formation are in faulted contact (Caledonia-Clover Hill Fault) with red to grey mudstone, sandstone and conglomerate of the

Upper Carboniferous Hopewell Group (St. Peter, 1993; McLeod et al., 1994).

On the west shore of Grand Bay a small body of Kennebecasis Formation (Ruitenbergh et al., 1975, 1979) is in faulted contact with the Kingston Complex to the north and the Henderson Brook Granite to the south; however, locally the conglomerate rests unconformably on the granite. These strata were previously considered to be Eocambrian (Currie 1986a, b, 1987a, 1988a, 1989a; Currie and Hunt, 1991) and related to the Cambrian to Ordovician Saint John Group (McLeod et al., 1994). A small wedge-shaped area of white quartz sandstone and conglomerate that outcrops in the Hastings Cove area is interpreted to be equivalent to the Kennebecasis Formation (section 2.6).

2.7.2. Southwestern zone

Rocks in the southwestern zone (Musquash-Dipper Harbour thrust belt) were traditionally termed the Mispic Group; however, this term has since been abandoned and the area divided into three formations. The oldest unit, the Lower Mississippian Parleeville Formation of the Windsor Group (McCutcheon, 1981, 1984, 1985), consists of grey to red-grey, stromatolitic and thinly bedded limestone (Table 2.3). This formation is best preserved along the west shore of Musquash Harbour where it unconformably rests on the Musquash Harbour Granite. This formation is also reported elsewhere in this zone (e.g. McCutcheon, 1985) but was not confirmed by the present study. Currie (1987a; 1988a) grouped the Parleeville Formation into the basal unit of the Balls Lake Formation.

The Westphalian A to C (Middle to Upper Middle Pennsylvanian) Balls Lake Formation (Caudill and Nance, 1986) consists of locally well cleaved and folded, polymictic, red conglomerate, sandstone, and siltstone with minor slate and rare thin carbonate lenses (Table 2.3). Clasts within the conglomerates appear to be locally derived volcanic

and granitic rocks with rare limestone pebbles (Stringer and Wardle, 1973). The contact with the older Parleeville Formation was not observed. However, several unconformable contacts between the Balls Lake Formation and the Musquash Harbour Granite and Dipper Harbour volcanic unit were observed and these were consistently overturned.

The Westphalian C Lancaster Formation (Caudill and Nance, 1986) is interpreted to gradationally overlie the Balls Lake Formation (Currie, 1986a, b, 1987a, 1988a). Based on field observations these contacts are always tectonic, marked by thrust faults, confirming the interpretation of Zain Eldeen (1991). The Lancaster Formation consists of locally cleaved, grey lithic sandstone and conglomerate with black carbonaceous lenses that are locally coal-bearing (Table 2.3) (Wright and Clements, 1943). This formation is less cleaved and folded than the Balls Lake Formation. Palynomorphs collected from the interpreted base of Lancaster Formation indicate a Westphalian C age for these rocks (Teng, 1978 in Ruitenberg et al., 1979).

Strata similar to the Balls Lake Formation are exposed in a narrow belt that extends from West Branch Reservoir southwestward to Lepreau Harbour. This belt of rocks is faulted (Lepreau Fault of Dickson, 1983) along the northwestern margin with the Lepreau Pluton, whereas the southeastern margin rests unconformably on the Lepreau Harbour Granodiorite. These rocks are moderately folded and display a weak fracture cleavage (Stringer and Wardle, 1973; Sarjeant and Stringer, 1978; Stringer, 1978; Stringer and Burke, 1985). Reptile tracks discovered in sandstone were initially interpreted to be Triassic in age (Sarjeant and Stringer, 1978); however, palynological studies (Barss, 1983 in Stringer and Burke, 1985; p. 4) and the presence of fossiliferous Viséan limestone (written communication, M. McLeod, 1992) indicate a Lower Carboniferous age for this unit and suggest that the tracks were misidentified.

Similar strata are exposed in a discontinuous linear belt along the shores of Spruce Lake to Musquash Harbour. This belt of rocks is

fault-bounded and locally overturned and contains clasts of the underlying lithologies. These strata were previously considered to be part of the Lancaster Formation (Rast and Grant, 1973b; Dickson, 1983), or an Eocambrian sequence (Currie, 1986a, b; 1987a; 1988a; 1989a; Currie and Hunt, 1991), or part of the Lorneville Volcanics (McLeod et al., 1994). The lithologies appear to be identical to those in the Balls Lake Formation and the unit is included here in the Ball Lake Formation.

Carboniferous sedimentary rocks in the Musquash-Dipper Harbour thrust belt were interpreted to reflect deposition that occurred ahead of, and was subsequently overridden by, advancing thrust sheets (Currie and Nance, 1983; Currie, 1984; Nance, 1985; Caudill and Nance, 1986; Caudill, 1989). However, field evidence collected during this study suggests that the Parleeville and Balls Lake formations were deposited prior to the thrusting event (see Chapter 3).

2.8. TRIASSIC UNITS

Rocks of the Middle to Upper Triassic Lepreau Formation occur in the extreme southwestern part of the Brookville terrane, along Macas Bay (Stringer and Wardle, 1973; Sarjeant and Stringer, 1978; Stringer, 1978; Stringer and Burke, 1985). They consist of gently folded, red to red-brown coarse breccia, conglomerate, and sandstone with clasts of adjacent older units (Table 2.3). They are in faulted contact along the northeastern margin with older units. Currie (1987a, 1989a) mapped this contact as an unconformity in this area but that could not be confirmed in this study.

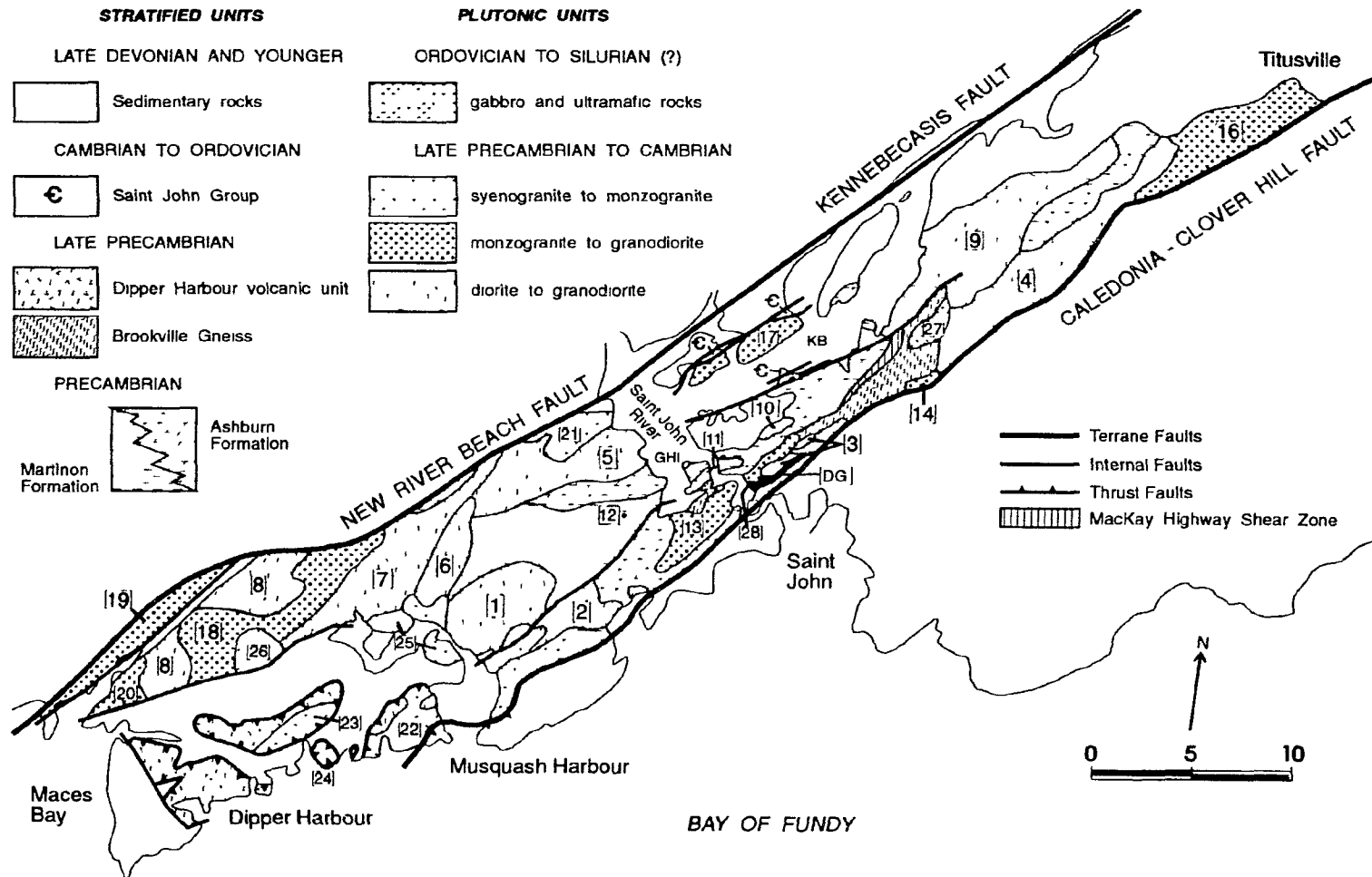


Figure 2.1. Simplified geology map of the Brookville terrane. Boxed numbers refer to individual plutons (see Table 2.2). Abbreviations: KB = Kennebecasis Bay; GHI = Green Head Island; DG = deformed granitoid rocks.

Table 2.1. Summary of main field characteristics of metamorphic and volcanic units.

FORMATION (MAP UNIT) ¹	GENERAL LITHOLOGY	CONTACTS	METAMORPHIC GRADE	OTHER FIELD OBSERVATIONS
ASHBURN FORMATION	calcite marbles (grey to white; f.g. to c.g.); minor dolomite (pink to cream; m.g); minor quartzite, siltstone, and spotted hornfels	dominantly faulted; locally intruded by plutons and dykes; unconformably overlain by Kennebecasis Formation.	albite-epidote to rare pyroxene-hornfels facies; minor regional greenschist facies	rare stromatolites; boudinaged clastic layers and dykes; calcite mylonites; rare mica schist
MARTINON FORMATION	pelitic rocks (grey to black; f.g.); minor calc-silicate, quartzite, conglomerate, and marble	dominantly faulted; locally intruded by plutons and dykes	albite-epidote hornfels facies, locally hornblende-hornfels facies	sedimentary structures preserved; graded and crossbedding, channel and slump structures, olistostromes
BROOKVILLE GNEISS	paragneiss and orthogneiss; locally migmatic; minor amphibolite, marble and calc-silicate rocks	fau'ted; locally intruded by plutons and dykes	upper amphibolite facies	garnet absent; cordierite common; mineral lineation in orthogneiss; rare quartzite
DIPPER HARBOUR VOLCANIC UNIT	rhyolitic ash flows, lithic and crystal-rich tuff; andesitic lithic tuff; minor siltstone and marble	dominantly faulted; intruded by plutons and mafic dykes; unconformably overlain by Parleeville and Balls Lake formations	sub-greenschist facies	quartz and feldspar crystals common in felsic volcanic rocks; siltstone laminated; overturned unconformities; no mafic flows observed

¹ Refer to Figure 2.1 and Map A for unit distribution.

Table 2.2a. Characteristics of the dioritic to granodioritic plutons in the Brookville terrane.

PLUTON ¹ AND AGE ²	GENERAL LITHOLOGY	TEXTURE	CONTACTS	OTHER FIELD OBSERVATIONS
LUDGATE LAKE GRANODIORITE ca. 546 Ma (1)	grey to grey-green granodiorite to tonalite	f.g. to m.g., hypidiomorphic equigranular	intrusive into Martinon Fm. and faulted against Spruce Lake Pluton; locally intruded by Prince of Wales Granite	xenoliths of metasilt- stone; enclaves of f.g. diorite to tonalite; locally foliated; aplite dykes
SPRUCE LAKE PLUTON ca. 546 Ma? (2)	light grey to black quartz diorite to tonalite; minor granodiorite	m.g. to c.g., hypidiomorphic equigranular to inequigranular	generally faulted; intrusive into Ashburn Fm. and intruded by Prince of Wales Granite	xenoliths of metasilt- stone and marble; dioritic enclaves; locally foliated; locally phenocrysts of quartz and plagioclase
ROCKWOOD PARK GRANODIORITE ca. 538 Ma (3)	grey tonalite to granodiorite	m.g. foliated, hypidiomorphic equigranular	poorly exposed; intrusive into Ashburn Fm.	forms two bodies; elongate dioritic to tonalitic enclaves
FRENCH VILLAGE QUARTZ DIORITE and other dioritic plutons ca. 537 Ma (4)	dark grey to black, light grey to white diorite to tonalite	m.g. to c.g., hypidiomorphic equigranular to inequigranular	faulted contacts; intrusive into Brookville Gneiss and Ashburn Fm.	xenoliths of marble, quartzite and gneiss; dioritic enclaves; locally foliated and porphyritic with phenocrysts of quartz
BELMONT TONALITE >ca. 531 Ma (5)	light to dark grey tonalite grada- tional to quartz diorite and granodiorite	m.g., allotri- morphic to hypidiomorphic equigranular; locally inequigranular	intrusive into Martinon Fm.; intruded by Henderson Brook Granite	xenoliths of marble, metasiltstone, quart- zite; locally foliated; f.g. granite/aplite dykes
PERCH LAKE GRANODIORITE >ca. 530 Ma (6)	light to dark grey granodiorite	m.g., hypidio- morphic equi- granular to inequigranular	intrusive into Martinon Fm.; intruded by Prince of Wales Granite	dioritic to tonalitic enclaves; foliated near contacts with Martinon Fm.

Table 2.2a. Continued.

PLUTON ¹ AND AGE ²	GENERAL LITHOLOGY	TEXTURE	CONTACTS	OTHER FIELD OBSERVATIONS
SHADOW LAKE GRANODIORITE >ca. 527 Ma (7)	grey granodiorite to tonalite	m.g. to c.g., hypidiomorphic to allotri- morphic inequi- granular	poorly exposed or faulted; sharp contact with Hanson Stream pluton and intruded by Harvey Hill pluton	varied scaled and elongate dioritic to tonalitic enclaves; magma mixing/mingling textures; locally foliated; f.g. granite/aplite dykes
TALBOT ROAD GRANODIORITE >ca. 521 Ma (8)	grey to pink grano- diorite to tonalite	f.g. to m.g. hypidiomorphic equigranular to locally inequi- granular	poorly exposed; locally faulted	forms two bodies; dioritic to tonalitic enclaves; locally foliated; f.g. granite/aplite dykes
RENFORTH PLUTON (9), MAYFLOWER LAKE (10), NARROWS (11), AND ACAMAC (12) TONALITES >ca. 511 Ma	dark grey to red, quartz diorite to tonalite, locally granodioritic	f.g. to m.g., hypidiomorphic equigranular; locally alotrimorphic inequigranular	generally faulted; intrusive into Ashburn Fm. and French Village Quartz Diorite; uncon- formably overlain by Devonian-Carboniferous sedimentary rocks	dioritic to tonalitic enclaves; locally porphyritic with phenocrysts of plagioclase; locally mineralized along shear zones

¹ Numbers in parenthesis refer to plutons in Figure 1.3 and 2.1. Also refer to Map A for pluton distribution.

² Ages quoted from White et al. (1990), Bevier et al. (1991), Currie and Hunt (1991), Dallmeyer and Nance (1992), and this study.

Table 2.2b. Characteristics of the monzogranitic to granodioritic plutons in the Brookville terrane.

PLUTON ¹ AND AGE ²	GENERAL LITHOLOGY	TEXTURE	CONTACTS	OTHER FIELD OBSERVATIONS
FAIRVILLE GRANITE ca. 548 Ma (13)	pink to orange monzogranite to granodiorite	c.g. hypidio- morphic inequi- granular	strongly deformed southeast contacts; intrusive into Brookville Gneiss and Ashburn Fm.	xenoliths of gneiss and marble; rare dioritic enclaves; megacrysts of K- feldspar
CHALET LAKE GRANITE ca. 548 Ma? (14)	orange monzogranite to granodiorite	c.g. hypidio- morphic inequi- granular	poorly exposed; intrusive into Ashburn Fm.	megacrysts of K- feldspar; tectonic foliation
GAYTON GRANITE ca. 548 Ma? (15)	pink to orange monzogranite to granodiorite	c.g. hypidio- morphic inequi- granular	locally faulted; unconformably overlain by Carboniferous sedimentary rocks	tectonic foliation and brecciated; megacrysts of K-feldspar; flourite common
HAMMOND RIVER GRANITE <ca. 537 Ma? (16)	pink to orange monzogranite to granodiorite	f.g. to c.g. hypidiomorphic equigranular to inequigranular	intrusive into Ashburn Fm. and French Village pluton; unconformably overlain by Devonian to Carboniferous sedimentary rocks	xenoliths of marble, amphibolite, and gneiss; rare elongate dioritic enclaves; locally foliated; similar to Cassidy Lake inlier
MILKISH HEAD PLUTON <ca. 531 Ma? (17)	pink to red monzogranite to granodiorite	c.g. hypidio- morphic inequi- granular monzo- granite; m.g. hypidiomorphic equigranular granodiorite	faulted and locally mylonitic along northern contact	rare dioritic to tonalitic enclaves; large phenocrysts of quartz common; f.g. granite/aplite dykes

Table 2.2b. Continued.

PLUTON¹ AND AGE²	GENERAL LITHOLOGY	TEXTURE	CONTACTS	OTHER FIELD OBSERVATIONS
HANSON STREAM GRANODIORITE >ca. 528 Ma? (18)	grey to light grey granodiorite to monzogranite	c.g. hypidio- morphic ineqi- granular	poorly exposed; intruded by Harvey Hill pluton	small rounded dioritic to tonalitic enclaves; phenocrysts of quartz; interstitial K- feldspar; f.g. granite aplite dykes
LEPREAU PLUTON >ca.528 Ma? (19)	grey to black quartz diorite to monzogranite	m.g. to c.g. hypidiomorphic inequigranular	entirely faulted	magma mingling/mixing textures present.
LEPREAU HARBOUR GRANODIORITE >ca. 528 Ma? (20)	grey to green-grey granodiorite	m.g. hypidio- morphic inequi- granular	poorly exposed; unconformably overlain by Carboniferous sedimentary rocks	rare small rounded dioritic to tonalitic enclaves

¹ Numbers in parenthesis refer to plutons in Figure 1.3 and 2.1. Also refer to Map A for pluton distribution.

² Ages quoted from White et al. (1990), Bevier et al. (1991), Currie and Hunt (1991), Dallmeyer and Nance (1992), and this study.

Table 2.2c. Characteristics of the syenogranitic to monzogranitic plutons in the Brookville terrane.

PLUTON ¹ AND AGE ²	GENERAL LITHOLOGY	TEXTURE	CONTACTS	OTHER FIELD OBSERVATIONS
HENDERSON BROOK GRANITE ca. 537 Ma? (21)	red to orange monzogranite to granodiorite	m.g. to c.g. hypidiomorphic to allotri- morphic equi- granular	northern contact faulted; intrusive into Belmont pluton; unconformably overlain by Carboniferous sedimentary rocks	leucocratic and granophyric; xenoliths of marble and metasiltstone
MUSQUASH HARBOUR GRANITE ca. 537 Ma (22)	pink monzogranite to syenogranite; grey-green grano- diorite to quartz diorite	m.g. to c.g., hypidiomorphic inequigranular to equigranular	faulted contacts; intrusive into Ashburn Fm.; unconformably overlain by Carboniferous limestone	composite pluton; syenogranite granophyric; f.g. granite/aplite dykes in granodiorite to quartz diorite parts
JARVIES LAKE (23) and CRANBERRY HEAD (24) SYENOGRANITE ca. 537 Ma.	pink to maroon to orange syenogranite to monzogranite	m.g. to c.g. hypidiomorphic to allotri- morphic equi- granular to equigranular	thrust faulted; interpreted to be intrusive into Dipper Harbour volcanic unit	locally highly fractured and albitized; leucocratic; granophyric; aplite veins common
PRINCE OF WALES GRANITE ca. 537 Ma? (25)	pink monzogranite to syenogranite	m.g., allotri- morphic to hypidiomorphic equigranular to inequigranular	locally faulted; intrusive into Perch Lake, Ludgate Lake, and Spruce Lake plutons	locally tectonic foliation; leucocratic and granophyric
HARVEY HILL SYENOGRANITE <ca. 527 Ma? (26)	pink to maroon syenogranite	f.g. allotri- morphic to hypidiomorphic inequigranular	faulted; intrusive into Shadow Lake and Hanson Stream plutons	leucocratic and granophyric; locally subporphyritic; minor muscovite and rare garnet

¹ Numbers in parenthesis refer to plutons in Figure 1.3 and 2.1. Also refer to Map A for pluton distribution.

² Ages quoted from White et al. (1990), Bevier et al. (1991), Currie and Hunt (1991), Dallmeyer and Nance (1992), and this study.

Table 2.2d. Characteristics of gabbroic and ultramafic units in the Brookville terrane.

PLUTON ¹ AND AGE ²	GENERAL LITHOLOGY	TEXTURE	CONTACTS	OTHER FIELD OBSERVATIONS
DUCK LAKE (27), INDIANTOWN (28), and COVERDALE (29) PLUTONS ca. 440 Ma?	black to white, varied ultramafic, gabbroic, and anorthositic rocks	varied texture; inequigranular; layered intrusion	poorly exposed; intrusive into French Village pluton and Brookville Gneiss	undeformed; locally pegmatoidal

¹ Numbers in parenthesis refer to plutons in Figure 1.3 and 2.1. Also refer to Map A for pluton distribution.

² Age quoted from White and Barr (in press) and this study.

Table 2.3. Summary of main field characteristics of sedimentary units.

FORMATION (MAP UNIT) ¹	GENERAL LITHOLOGY	CONTACTS	AGE	OTHER FIELD OBSERVATIONS
FOREST HILLS FORMATION	grey, laminated siltstone and sandstone, massive mudstone, and minor limestone	lower and upper contacts faulted	Middle Cambrian	fossiliferous, folded and locally cleaved
KING SQUARE FORMATION	grey, sandstone, silt- stone, minor limestone nodules	lower and upper contacts faulted	Middle to Upper Cambrian	micaceous, mildly folded, fossiliferous
KENNEBECASIS FORMATION	red to red brown, conglomerate, sandstone, siltstone, minor limestone and white sandstone	generally faulted, locally unconformable on older units	Upper Devonian to Lower Carboniferous	mildly folded, found in the Saint John area
MEMRAMCOOK FORMATION	red conglomerate, sandstone, and siltstone	unconformable on older units	Upper Devonian to Lower Carboniferous	folded, found northeast of Saint John
PARLEEVILLE FORMATION	grey, stromatolitic, thin bedded limestone	lower contact unconform- able on Musquash Harbour Syenogranite and Meadow Cove volcanic unit; upper contact not exposed	Lower Carboniferous (Visean)	fossiliferous
BALLS LAKE FORMATION	red to purple conglomerate, siltstone, and shale, rare carbonate lenses	unconform-able on Musquash Harbour Syenogranite and Meadow Cove volcanic unit; upper contact not exposed	Westphalian A to C	folded, cleaved, and typically overtuned
LANCASTER FORMATION	grey, lithic sandstone and conglomerate, minor carbonaceous lenses	lower contact conformable? with Balls Lake Formation; upper contact not exposed	Westphalian C	locally coal- bearing and cleaved
LEPREAU FORMATION	red to red-brown coarse breccia/conglomerate and sandstone	faulted contacts	Triassic	gently folded, clasts of older units

¹ Refer to Figure 2.1. and Map A for unit distribution.

PLATE 1

- 1a. Outcrop showing colour and textural heterogeneity typical of marble in the Ashburn Formation. Alternating grey and white, fine- to medium-grained, subhorizontal layers with numerous small siliciclastic and calc-silicate boudins. Photograph faces northeast. The hammer is 26 cm long. Outcrop located in Rockwood Park.
- 1b. The stromatolite *Archaeozoon acadiense* from relatively undeformed marble in the Ashburn Formation along the northwestern tip of Green Head Island. Looking perpendicular to long axis of columns. Quarter for scale.
- 1c. A rare occurrence of finely laminated siltstone (dark) and small-scale trough cross-bedded sandstone (light) in the Martinon Formation. Note the lack of cleavage and effects of contact metamorphism. Outcrop located north of Menzies Lake. Pen for scale.
- 1d. A poorly sorted quartzite-marble pebble conglomerate interbedded with a thin calcareous sandstone in the Martinon Formation located on the west coast of Green Head Island. Clasts consist dominantly of well-rounded quartzite with minor tabular marble. Larger marble clasts are locally stromatolitic. The chisel is 12 cm long.
- 1e. A poorly sorted carbonate-siliciclastic sedimentary breccia in the Martinon Formation located along Highway 7. Clasts consist dominantly of angular marble and minor rounded siltstone. These deposits are interpreted as olistostromes. The hammer (center of photograph) is 26 cm long.
- 1f. Folded, cordierite-bearing migmatitic paragneiss from the Brookville Gneiss with thin (10 mm wide), white leucosome and thinner (<5 mm wide) black melanosome layers. Located south of Green Head Island. The marker is 12 cm long.

PLATE 1



CHAPTER 3

STRUCTURAL GEOLOGY

3.1 INTRODUCTION

The Brookville terrane has been affected by several periods of deformation and is very structurally complex. Detailed mapping to better define map units and establish field relations (Chapter 2) was critical to the understanding and interpretation of the structural history. This has resulted in the recognition of at least four deformational events (D_1 to D_4) and two metamorphic events (M_1 and M_2) that have affected the rocks of the Brookville terrane.

The first episode of deformation (D_1) can be broadly divided into a pre-Late Neoproterozoic and a Late Neoproterozoic event, although there is no evidence for a considerable time difference. The pre-Late Neoproterozoic deformation resulted in heterogeneous folding in the Martinon and Ashburn formations. The Late Neoproterozoic deformation is directly related to the prolonged juxtaposition of the Brookville Gneiss with the Green Head Group. D_1 locally coincided with a major period of regional metamorphism (M_1) and is responsible for the present internal structural configuration of the Brookville terrane. This occurred prior to Late Neoproterozoic-Cambrian plutonic activity that resulted in broad contact metamorphic effects (M_2) in the Green Head Group. Younger deformations (D_2 , D_3 , D_4), represented by Middle Paleozoic to Early Mesozoic faulting and associated folding, do not appear to have had a significant effect on the overall internal geometry of the area.

The purpose of this chapter is to present the results of the first detailed structural mapping project encompassing the entire Brookville terrane. Most of the previous structural interpretations were based on local areas incorporating what is now considered unreliable radiometric

data and no systematic structural analysis was attempted for the entire terrane.

3.2. CRITERIA FOR DISTINGUISHING STRUCTURAL HISTORY

The identification and classification of structural features were based on overprinting criteria combined with geochronology. However, the well-established method of using intersecting structural features to establish a historical record of deformation in pelitic rocks does not work well with deformed carbonate rocks. Marbles respond to stress by a gradual reshaping of grains, and the reshaping effects may be modified by later recrystallization. Despite this apparent complexity, four superimposed generations of structures have been established on the basis of their mutual geometric relationships, and cross-cutting and overlying relationships with units of known age. These structural features are described in a D_1 - D_2 - D_3 - D_4 framework.

The methods used to deduce the motion of the faults are largely based on oriented thin section observations. Thin sections were cut from oriented samples perpendicular to foliation (inferred plane of shearing) and parallel to mineral lineation (inferred direction of motion). Asymmetric microstructures observed in thin section can be used to determine sense of shear (e.g. Simpson and Schmid, 1983).

3.3. PRE-LATE NEOPROTEROZOIC DEFORMATION (D_1)

Recent structural studies within the Green Head Group and Brookville Gneiss (e.g. Nance, 1992; Nance and Dallmeyer, 1994) demonstrate that the deformation is heterogeneous and structural complexity coincides with higher metamorphic grades. This resulted in a variety of fold patterns and foliations (Table 3.1) that reflect the contrasting behaviour of the gneissic, carbonate, and siliciclastic rocks. This is further complicated by the presence of a major ductile

shear zone (MacKay Highway shear zone of Nance and Dallmeyer, 1994) that separates the Ashburn Formation from the Brookville Gneiss and precludes direct correlation of structural events. The exact age of D_1 structures in the Martinon and Ashburn formation is unknown; however, the age of deformation in the Brookville Gneiss is fairly well constrained by geochronology (section 3.3.7 and Chapter 6). Structures in the Green Head Group and Brookville Gneiss are cross-cut by Late Neoproterozoic to Cambrian plutons which provides a minimum age for regional deformation and metamorphism.

3.3.1. D_{MF1} Structures in the Martinon Formation

Bedding (S_0) in the Martinon Formation is deformed into a series of upright, gently southwest-plunging F_{MF1} folds that range from open to close (Fig. 3.1), with wavelengths on a scale of 100's of metres (Fig. 3.2). Folds of this magnitude are evident along Highway 7 near the southern contact with the Ashburn Formation. Minor folds (on a scale of 10's of metres) are not common.

Folds attributed to soft-sediment deformation are also present in the Martinon Formation. They are small (centimetre scale), variably oriented and often associated with convolute bedding and sedimentary breccias (Chapter 2). These folds were not measured in this study.

S_{MF1} is not well developed. It occurs as northeast-trending, steeply southeast-dipping features (Fig. 3.1) defined by flattened carbonate clasts in conglomerate and rare closely-spaced fractures. S_{MF1} is restricted to contacts near the Ashburn Formation and may be related to deformation along this contact rather than a regional event. As a result rare intersection lineations (L_{MF1}) are evident only as northeast-trending, subhorizontal colour banding on weakly developed fracture cleavages or ridges on bedding planes (Fig. 3.1).

Although the abundant presence of F_{MF1} folds was noted by Leavitt

(1963), his and later structural interpretations (e.g. Wardle, 1978; Nance, 1982; Nance and Dallmeyer, 1994) suggested that the Martinon Formation formed the core of a U-shaped, southwest-plunging syncline (Acamac Syncline) flanked by the older Ashburn Formation and that the Martinon Formation is "totally devoid of F_1 folds" (e.g. Wardle, 1978; Nance, 1982).

3.3.2. D_{AF1} Structures in the Ashburn Formation

Although most of the contacts between the Martinon and Ashburn formations are typically strongly sheared, they are interpreted to have been originally lateral facies equivalents (Chapter 2) deformed during the same D_1 deformation. However, the structural style differs significantly between the two formations, partly due to the lithological contrasts. On the basis of overprinting features the fabrics in the Ashburn Formation are designated as D_{AF1a} and D_{AF1b} . Although D_{AF1b} may record a separate deformational episode, based on field evidence these structures, like those related to D_{AF1a} , occurred prior to intrusion of the Late Neoproterozoic-Cambrian plutons and are here considered to be related.

3.3.2.1. D_{AF1a} Structures

The predominant D_{AF1a} feature is a well developed colour banding in carbonate rocks defined by preferred orientation of carbonate, silicate, and opaque minerals that is typically subparallel to boudinaged siliciclastic/calc-silicate layers. It is not clear if the colour banding is transposed bedding or a secondary layering. However, due to the boudinaged character of associated siliciclastic and dolomitic material with internal bedding orientations locally at a moderate angle to carbonate layering, the carbonate layering is considered to represent

a secondary planar feature, here termed S_{AF1a} and not original sedimentary bedding (Plate 2a, b). S_{AF1a} is northeast-trending, steeply southeast-dipping and is axial planar to rare intrafolial rootless (F_{AF1a}) folds (see below); however, the intersection lineation (L_{AF1a}) between S_0 and S_{AF1a} is poorly preserved and rarely observed in the hinge zones of these folds (Fig 3.1, 3.3).

S_{AF1a} in siliciclastic rocks of the Ashburn Formation is generally absent. However, in areas where metamorphic grade is at greenschist facies (e.g. Saint John River, Drury Cove, and Hammond River areas), the siliciclastic and calc-silicate rocks become increasingly phyllitic to locally schistose. Here S_{AF1a} is a steep northeast-trending fabric defined by a preferred orientation of chlorite, muscovite, and locally biotite and is subparallel S_0 .

Large-scale F_{AF1a} folds have not been identified in the carbonate rocks (cf. Wardle, 1978; Nance, 1982; Nance and Dallmeyer, 1994). However, several small (centimetre scale) upright to steeply-inclined, subhorizontal to steeply northeast to southwest-plunging, F_{AF1a} folds (Fig. 3.1) occur in thinly bedded and laminated calc-silicate and marble layers. They are intrafolial and rootless with strongly attenuated and boudinaged limbs and range from tight to isoclinal. F_{AF1a} folds in siliciclastic units were not observed during the present study, although Wardle (1978, p. 168) recorded the presence of one mesoscopic recumbent fold in quartzite.

Sedimentary layering in large mappable siliciclastic units is typically subparallel to S_{AF1a} in the carbonate rocks, although there is considerable scatter in these data when compared to those from the Martinon Formation (Fig. 3.1). This is likely the result of the anastomosing character of the lens-shaped units and the oblique orientation of some bedding planes to S_{AF1a} . As in the Martinon Formation, these structural features are overprinted by contact metamorphism (Chapter 5).

3.3.3. Northwest to southeast-trending folds in Ashburn Formation

D_{AF1} structures in the Ashburn Formation are locally overprinted by minor upright, moderate to steeply northwest to southeast-plunging folds that range from open to close (Fig. 3.1). Folds of this type are reported from siliciclastic lithologies in the Drury Cove and Howes Lake areas, and northeast of Green Head Island (Leavitt, 1963; Nance, 1982). This was not a fabric-forming event, although Nance (1982) reported an axial fracture cleavage in one of these folds.

Leavitt (1963) attributed these structures to rotational forces during the intrusion of Devonian plutons. Nance (1982) and Nance and Dallmeyer (1994) concluded that they were related to Late Paleozoic dextral faulting whereas Wardle (1978) considered these structures to be the result of sinistral strike-slip motion. The northeast-southwest compression is not recorded in the Devonian to Carboniferous sedimentary rocks that locally overlie these northwest-southeast-trending structures. If they are related to fault movement, it is movement that occurred prior to the deposition of the Kennebecasis Formation. Although these features are minor and of unknown tectonic significance they are overprinted by Late Neoproterozoic to Cambrian contact metamorphic aureoles suggesting they are related to D_{AF1} , but probably late in the history.

3.3.4. MacKay Highway shear zone

The Ashburn Formation is separated from the Brookville Gneiss by a broad northeast-trending, steeply southeast-dipping ductile shear zone (Map C) informally termed the MacKay Highway shear zone by Nance and Dallmeyer (1994). This shear zone is exceptionally well exposed along the MacKay Highway northeast of Saint John and extends from near Renforth in the northeast to Rockwood Park in the southwest (Fig. 3.4). In Rockwood Park and on Green Head Island, this zone is strongly

MacKay Highway shear zone, cross-cut all earlier fabrics, and locally preserve sheath fold geometries.

Kinematic indicators in the shear zone are not common due to recrystallization and are restricted to outcrop-scale features such as asymmetric boudins in marble. These typically yield an inconsistent sense of shear throughout the zone (cf. Nance and Dallmeyer, 1994); however, rare micro-kinematic indicators such as asymmetric porphyroclasts suggest dextral, oblique sense of movement parallel to L_{MHI} and S_{MHI} .

Minor kinks and crenulations trend perpendicular to L_{MHI} and are interpreted to record late-stage movement parallel to the intersection/stretching lineation.

3.3.5. Brookville Gneiss

The Brookville Gneiss was considered to record a complex polyphase deformation, largely based on cross-cutting fold generations (e.g. Wardle, 1978; Nance and Dallmeyer, 1994). However, in gneissic and migmatitic rocks it is not possible to interpret complex structures by simple analogy to structures at lower metamorphic grades. The development of leucosomes and melanosomes during the same melting event will introduce considerable competence contrasts in a layered, partially melted system. This can produce structures that geometrically resemble polyphase deformation (e.g. McLellan, 1983).

A prominent northeast-trending, steeply southeast-dipping gneissic foliation (S_{BG1}) is present in the Brookville Gneiss (Fig. 3.4). Gneissosity in the paragneiss is locally folded into small-scale (10's of centimetres) upright to steeply southeast-inclined, gently to steeply northeast to southwest-plunging F_{BG1} folds (Fig. 3.4) that range from tight to isoclinal. They locally display strongly attenuated limbs and lack an axial planar fabric. F_{BG1} axes in the paragneiss lie in a girdle parallel to axial surfaces and the mean orientation of gneissic

3.3.2.2. D_{AF1b} Structures

Throughout the Ashburn Formation S_{AF1a} in the carbonate rocks is deformed into upright to steeply southeast-inclined, gently to moderately northeast to southwest-plunging F_{AF1b} folds that range from close to tight and everywhere verge to the northwest (Plate 2c). These folds formed at various scales and generally lack an axial planar foliation (cf. Wardle, 1978). However, Nance (1982) noted the presence of minor closely spaced fractures parallel to axial planes and the development of cleavage fans in siliciclastic folds interpreted to be equivalent to F_{AF1b} folds. Generally F_{AF1b} folds in marble become tighter towards the MacKay Highway shear zone and here a northeast-trending, steeply southeast-dipping axial planar S_{AF1b} is developed. As a result, subhorizontal to moderately northeast and southwest-plunging intersection lineations (L_{AF1b}) are developed as colour banding on S_{AF1b} or ridges on S_{AF1a} fold hinges (Fig. 3.3).

The schistose S_{AF1a} in the Drury Cove area is intensely crenulated (S_{AF1b}) and as a result a prominent lineation (L_{AF1b}) is developed. This feature is parallel to L_{AF1b} in the carbonate lithologies.

F_{AF1b} axes define a girdle distribution that dips steeply to the southeast subparallel to S_{AF1a} and S_{AF1b} (Fig. 3.3). The orientation of F_{AF1b} axes suggests a sheath fold geometry, and mesoscopic sheath folds are present locally in the marble (Plate 2d). However, the fact that fold axes of many orientations lie within one common plane is also a reflection of the massive, relatively homogeneous, ductile nature of the marble. Here prolonged deformation involved a progressive modification of pre-existing structures, rather than the intersecting and crosscutting structures commonly observed in pelitic rocks.

overprinted by brittle faults and shear zones but relics of the ductile shear zone are locally preserved.

The shear zone is composed of finely laminated, rectilinear quartzo-feldspathic and carbonate blastomylonite (Plate 3a) and coincides with the area of highest metamorphic grade in the adjacent Ashburn Formation (Chapter 5). The quartzo-feldspathic blastomylonite can be traced into coarse-grained paragneiss and orthogneiss at several localities and large lenticular boudins of gneiss are common in marbles of this zone.

On the northwestern margin of the shear zone in the adjacent Ashburn Formation, S_{AF1b} axial fabrics in F_{AF1b} folds become more prominent (see section 3.3.3) and S_{AF1a} and S_{AF1b} become essentially parallel in the shear zone (S_{MHI}). F_{AF1b} folds become tight to isoclinal and consistently verge to the northwest and are here termed F_{MHI} (Plate 3b). L_{AF1b} intersection lineations also become more prominent and in the shear zone they are progressively rotated towards the northeast (L_{MHI}) (Plate 3c; Fig. 3.4). Asymmetric porphyroclasts, quartz ribbons, and pull-apart garnets define a mineral/stretching lineation in some of the quartzo-feldspathic blastomylonite that is subparallel to L_{MHI} . This suggests that the moderately northeast-plunging L_{MHI} is the slip vector. Minor F_{MHI} axes form a girdle distribution that parallels the average orientation of S_{MHI} and F_{MHI} axial planes (Fig. 3.4).

Boudinaged material, including quartz and pegmatite pods and calc-silicate layers, is common in this zone (Plate 3a) and occurs at all scales. Generally the boudins take on a pancake-like shape, giving the foliation planes a hummocky appearance. Occasionally the quartz pods are elongate and form a weak girdle distribution that parallels the F_{MHI} axes (Fig. 3.4).

Narrow shear zones considered to be related to this major shearing event are locally developed throughout the Ashburn Formation (Plate 3d). These coarse-grained marble mylonites parallel the general trend of the

foliation. As in the marble, this is a reflection of the massive, relatively homogeneous, ductile nature of these gneisses.

Rare isoclinal rootless folds defined by migmatitic leucosomes were interpreted by Nance and Dallmeyer (1994) to be the oldest structures recognized in the Brookville Gneiss. However, these migmatitic folds geometrically resemble those in the gneiss and are here interpreted to be equivalent. These migmatitic folds suggest that deformation accompanied amphibolite-facies metamorphism.

The orthogneiss commonly displays a weak to moderately developed, northeast-plunging, mineral lineation (L_{BGI}) (Fig 3.4) defined by aligned aggregates of quartz and feldspar, and more rarely recrystallized quartz ribbons. Hornblende displays a similar orientation in the paragneiss. In larger bodies of orthogneiss the foliation exhibits a "swirled" appearance (orthogneiss south of Green Head Island) and the associated geometric patterns were interpreted to have no consistent relationship (cf. Wardle, 1978). These types of disharmonic folds in gneiss have been described elsewhere (e.g. McLellan, 1983) and attributed to non-cylindrical folding during melt flowage.

The distribution of asymmetric porphyroblasts in the orthogneiss suggests a dextral sense of movement parallel to the mineral lineation and coplanar with similar structures in the MacKay Highway shear zone.

3.3.6. Timing of D1 deformation

Deformational events in the Martinon and Ashburn formations and Brookville Gneiss cannot be directly correlated; however, structures in all these units are cross-cut by ca. 548-537 Ma plutonic rocks. An upper limit for deformation in the Brookville Gneiss is constrained by the ca. 605 Ma zircon crystallization age for the orthogneiss protolith (Bevier et al., 1990; Dallmeyer et al., 1990). Peak amphibolite facies metamorphism and associated deformation of the Brookville Gneiss likely occurred at ca. 564 Ma /metamorphic titanite age, Bevier et al., 1990;

see Chapter 6). The minimum age for metamorphism and deformation in the Brookville Gneiss is based on abundant $^{40}\text{Ar}/^{39}\text{Ar}$ hornblende cooling ages of ca. 550-540 Ma (Chapter 6). A hornblende age of ca. 548 Ma (Dallmeyer and Nance, 1990) from a strongly lineated paragneiss in the MacKay Highway shear zone is considered to date cooling following the development of S_{MHI} and L_{MHI} related to the juxtaposition of the Brookville Gneiss and the Green Head Group (cf. Nance and Dallmeyer, 1994). By inference, the ca 550-540 Ma thermal event provides an upper age limit for the development of S_{AFib} in the adjacent Ashburn Formation.

The structures preserved in the Brookville Gneiss, MacKay Highway shear zone, and the immediately adjacent Ashburn Formation likely represent phases of a single progressive deformation associated with oblique dextral transpression of the Brookville Gneiss with the Green Head Group. However, structures in the remainder of the Ashburn and Martinon formations have no obvious counterparts in the MacKay Highway shear zone or Brookville Gneiss and are considered to be slightly older.

3.4. PLUTONISM

Late Neoproterozoic to Cambrian plutonic rocks intruded deformed rocks of the Green Head Group and the Brookville Gneiss and on a map scale are generally concordant with the regional structures (Fig. 2.1; Map A). However, in detail (outcrop scale) these plutonic units are discordant and cut all structures related to D_1 .

Many of the plutons are weakly to moderately foliated and it is critical to distinguish whether the foliations result from magmatic flow or later tectonic processes, which will influence the interpretation of the age and significance of these structures and metamorphism in the adjacent country rock.

The main criterion of magmatic flow is the preferred orientation of primary igneous minerals that show no evidence of plastic deformation or recrystallization, either of aligned crystals or of interstitial

minerals (cf. Paterson et al., 1989). This feature is common in Brookville terrane plutons where the foliation is defined by aligned plagioclase and hornblende that are surrounded by anhedral, non-deformed quartz grains. Quartz is a sensitive indicator of solid-state flow and the lack of a shape preferred orientation eliminates this process as a factor. Foliations are also defined by preferred alignment of elongate dioritic enclaves. The enclaves show no evidence of plastic deformation or recrystallization and the orientation is parallel to the enclosing foliated granitoid host. These features also indicate magmatic flow (Paterson et al., 1989).

Although most plutons have quartz with undulose extinction, they do not contain recrystallized subgrain structures or quartz ribbons that indicate solid-state flow (section 3.5.1.1), and the majority of foliations are considered to be igneous in origin.

Dallmeyer and Nance (1992) suggested magmatic activity was locally accompanied by late D_1 ductile shear. This is based on what they interpreted as narrow ductile shear zones in the French Village Quartz Diorite; however, this could not be confirmed. Locally the French Village Quartz Diorite contains thin, fine-grained dioritic enclaves, which gives the rock a striped appearance. This feature may have been misidentified as mylonite.

Because of the primary igneous texture in these plutons the northeasterly-trending fabric is interpreted to reflect intrusion along pre-existing structures, although some of the more foliated plutons may be syn-tectonic (Fig. 3.4).

3.5. FAULTS

In southern New Brunswick, there are a number of major northeast-trending faults which have all been attributed to Late Paleozoic deformation (e.g. Gussow, 1953; Webb, 1963; van de Poll, 1970; E. Grant, 1972; Wardle, 1978; Leger and Williams, 1986; McCutcheon and Robinson,

1987). However, faulting in Saint John area has had a long and complicated history in both the ductile and brittle regimes, and some segments have experienced complex histories of motion. Some of these can be deduced, but many uncertainties remain. Three major episodes of faulting have occurred (Table 3.1). The earliest documented motion, here considered D_2 , occurred some time in the Middle Paleozoic along the Spruce Lake and Long Island shear zones. It has long been recognized that the Late Devonian and Carboniferous sedimentary rocks were variably involved in Late Paleozoic deformation, here termed D_3 , in which two structural styles are recognized, $D_{3,1}$ and $D_{3,2}$. Prominent northeast-trending, steep brittle faults and related folds in Devonian to Carboniferous sedimentary rocks are the result of $D_{3,1}$ and include 1) the major terrane-bounding faults such as the New River Beach-Kennebecasis and Caledonia-Clover Hill faults, and 2) minor internal faults such as the Milkish Head, Ragged Point, Ragged Head, and Lepreau River faults (Fig 3.5). On a local scale these faults record conflicting senses of movement; however, the regional movement is generally considered to be dextral strike-slip (e.g. Leger and Williams, 1986; St. Peter, 1993).

In comparison, $D_{3,2}$ resulted in a slightly younger, narrow, basement-involved, northwest-directed, fold and thrust belt along the present day Bay of Fundy coast (Rast and Grant, 1973a, b; Stringer and Wardle, 1973; Rast et al., 1978a, b; Parker, 1984; Nance 1987b; Zain Eldeen, 1991). This zone extends from Maces Bay to Musquash Harbour and is termed the Musquash-Dipper Harbour thrust belt (Fig. 3.6).

Early Mesozoic faulting (D_3) produced many steep northwest-trending faults that reactivated most of the earlier fault structures, although some segments still preserve the older deformation. Thus detailed structural analysis on different fault segments is used to reconstruct some aspects of the structural and tectonic history of the Brookville terrane.

3.5.1. Middle Paleozoic Faults and Related Fabrics (D₂)

3.5.1.1. Spruce Lake shear zone

The Spruce Lake shear zone is a major, northeast-trending, subvertical shear zone that extends from Musquash Harbour to Green Head Island. Although there is not a prominent topographical expression associated with this shear zone it is marked by a strong linear magnetic low. In the southwest it is a recrystallized (blastomylonite) ductile shear zone that separates the Ludgate Lake Granodiorite from the Spruce Lake Pluton. To the northeast it is a brittle feature that marks the southern boundary between the Martinon and Ashburn formations and probably the northern boundary between the Brookville Gneiss and the Ashburn Formation on Green Head Island (Fig. 3.5). It also offsets contact metamorphic aureoles and associated isograds in the Martinon Formation (Chapter 5). This shear zone is also marked by discontinuous, fault-bounded slivers of sedimentary rocks interpreted to belong to the Carboniferous Balls Lake Formation. The northeast and southwest extensions of this shear zone cannot be traced and may have been modified by later deformation.

In the Spruce Lake area this zone was recognized by Rast and Grant (1973b) and Dickson (1983); however, they interpreted the foliated granitoid rocks as gneisses and grouped them with the Brookville Gneiss. They also suggested that the fault-bounded belt of sedimentary rocks belongs to the Lancaster Formation and was thrust over the Ludgate Lake Granodiorite. Dickson (1983) interpreted this area to represent the terminus of a major northwest-directed thrust package.

The shear zone is defined by strongly foliated rocks of the Ludgate Lake, Spruce Lake and Prince of Wales plutons. Locally these rocks contain a stretching lineation that plunges moderately to the south-southwest (Fig. 3.5). These rocks are recrystallized and the sense of shear is difficult to determine; however, relict asymmetric

porphyroclasts and fractured feldspar grains are preserved that suggest an oblique, dextral strike-slip sense of movement for the present orientation of the shear zone.

Numerous foliated granitoid clasts interpreted to be equivalent to the Ludgate Lake and Prince of Wales plutons are in conglomerates of the overlying(?) Balls Lake Formation.

3.5.1.2. Long Island shear zone

Marbles of the Ashburn Formation on Long Island are strongly deformed and contain large boudins of tonalite, interpreted to be related to the Renforth Pluton. These calcite mylonites are thinly laminated and display fine-grained to aphanitic textures. They define a northeast-trending, moderately northwest-dipping shear zone with a stretching lineations that plunge moderately to the northwest (Fig. 3.5). These lineations are defined by elongate and asymmetric calcite porphyroclasts, mica fish, and elongate titanite.

Small-scale folds are rare and located close to boudins. Kinematic indicators are common; however, they are typically associated with the boudins and give conflicting directions of movement. Structures away from boudins, such as large-scale shear bands, suggest dextral movement, with tops toward the northwest. The contact with the younger Devonian to Carboniferous Kennebecasis Formation was not observed, although it was interpreted to unconformably overlie the marble (cf. Wardle, 1978). However, this zone has many structural features that are similar to those in the Musquash-Dipper Harbour thrust belt (see section 3.5.3).

Mylonitic marble along the southeastern coast of Kennebecasis Bay also contains large boudins of tonalite and these marbles may be related to the Long Island shear zone. However, the southeast coast is strongly overprinted by the younger brittle faults that have obliterated most of the structures related to the earlier deformation (section 3.5.2.4).

Although this shear zone is a major structural feature it has no geophysical expression and its tectonic significance is unknown.

3.5.1.3. Deformed Granitoid Rocks

Narrow zones of intensely deformed granitoid rocks are located along the Caledonia-Clover Hill Fault in the Saint John area. These bound the northwestern margin of the calcite mylonite zone found along this fault (section 3.5.2.2) and locally occur as boudins within the marble. These were originally included with the Brookville Gneiss and the amphibolite portions of the Indiantown Gabbro (Wardle, 1978; Currie et al., 1981). This belt was later recognized as strongly deformed equivalent of the granitic rocks that outcrop in Saint John (White et al., 1990).

The strongly foliated granitoid rocks trend northeast and dip steeply to the southeast (Fig. 3.5), parallel to the trend of the calcite mylonites associated with the Caledonia-Clover Hill Fault. However, due to their recrystallized texture compared to the non-recrystallized texture in calcite mylonites, they are interpreted to reflect earlier movements along the Caledonia-Clover Hill Fault.

3.5.2. Late Paleozoic Faults and Related Fabrics ($D_{3,1}$)

3.5.2.1. New River Beach - Kennebecasis Fault

The New River Beach-Kennebecasis Fault separates the Brookville terrane from rocks of the Kingston Complex to the northeast (Fig. 2.1, Map A). The New River Beach Fault (Rast and Dickson, 1982; Dickson, 1983) extends from Maces Bay in the southwest to the Saint John River in the northeast. It is poorly exposed although it coincides with a prominent northeast-trending topographic lineament reflected by elongate lakes and also characterized as a prominent aeromagnetic low. As a

result, suitable field data to characterize the fault are not available. In the area west of the Saint John River, sedimentary rocks of the Devonian to Carboniferous Kennebecasis Formation are deformed by this fault.

Northeast of the Saint John River, this fault extends along the northwestern shore of the Kennebecasis River and separates the Kingston Complex to the northwest from sedimentary rocks of the Kennebecasis Formation in the southeast. In the past this structure was termed the Petiticodiac or Peekaboo Fault (e.g. Gussow, 1953; Webb, 1963; van de Poll, 1970; E. Grant, 1972), but more recently it has been termed the Kennebecasis Fault (e.g. Ruitenbergh and McCutcheon, 1982; Leger and Williams, 1986; St. Peter, 1993). Still farther northeast the Kennebecasis Fault forms the northwestern margin of the Carboniferous Moncton Sub-basin where it is termed the Berry Mills Fault (St. Peter, 1993). This fault cuts rock units as young as Upper Carboniferous (St. Peter, 1993). There also appears to be no history of pre-Carboniferous movement preserved along the entire length of this fault.

The movement history along the New River Beach-Kennebecasis Faults is complex and controversial and various segments of the faults have been interpreted to range from high-angle reverse to both sinistral and dextral strike-slip (e.g. Gussow, 1953; Webb, 1963; van de Poll, 1970; E. Grant, 1972; Wardle, 1978; Leger and Williams, 1986; St. Peter and Fyffe, 1990). Currie (1987a) suggested the New River Beach Fault did not exist and mapped a gradational contact between the Pocologan mylonite zone and granitoid rocks of the Brookville terrane. However, no mylonitic Brookville terrane granitoid rocks were observed in this zone. Furthermore, recent geochronology in the area (Doig et al., 1990; Dallmeyer and Nance, 1992; Nance and Dallmeyer, 1993) has indicated that the adjacent Pocologan mylonite zone has experienced significant Silurian to Devonian tectonothermal activity that is not recorded in the Brookville terrane and therefore the New River Beach Fault appears to be a significant younger feature.

Due to lack of outcrop, detailed structural and kinematic studies of this fault were not completed during the study. However, the overall sense of movement is interpreted to dextral strike-slip with later (Mesozoic?) normal and reverse movements (cf. Leger and Williams, 1986; St Peter, 1993).

3.5.2.2. Caledonia-Clover Hill Fault

Rocks of the Brookville terrane are separated from the Caledonia terrane (Avalon Zone *sensu stricto*) to the southeast by the Caledonia-Clover Hill Fault. This fault is a regionally extensive, brittle, northeast-trending, steep feature that can be traced by a major topographic lineament from Musquash Harbour in the southwest to south of Moncton over a distance of 150 kilometres. On aeromagnetic maps the Caledonia-Clover Hill Fault is marked by an abrupt change from magnetic highs on the northwest side to magnetic lows on the southeast.

At several localities near Saint John the fault plane is well exposed. It is locally curvilinear with a steep east-southeast dip. In the hanging wall are volcanic and sedimentary rocks of the Coldbrook and Saint John groups (Caledonia terrane) and rocks in the footwall include marble, quartzite, and spotted hornfels of the Ashburn Formation. Deformation increases with proximity to this segment of the fault. Hanging wall rocks exhibit an anastomosing cleavage, defined by sericite and epidote. Cleavage and joint planes contain abundant, variably oriented, slickenside striations, although many are horizontal in places. The quartzite and hornfels in the footwall display the same brittle textures; however, the marbles in this zone are mylonitic. They are fine-grained to aphanitic, finely laminated, and locally strongly lineated. The marbles contain rare boudins of volcanic and sedimentary rocks related to rocks in the hanging wall. All these textures are related to movement along this segment of the fault.

The northeastern segment of the Caledonia-Clover Hill Fault has

been variably interpreted as a post-Middle Devonian feature with movement that ranges from thrust to high-angle reverse and normal to both sinistral and dextral strike-slip (e.g. Gussow, 1953; Webb, 1963; Belt, 1968; Bradley, 1982; Ruitenberg and McCutcheon, 1982; McCutcheon and Robinson, 1987). The presence of fanglomerates in the Horton Group proximal to this segment suggests it was active in the Late Devonian (e.g. St. Peter, 1993).

The southwestern segment of the Caledonia-Clover Hill Fault was considered to be non-existent (Van de Poll, 1970; Gupta, 1975; McCutcheon and Robinson, 1987) or to represent an unconformity (Hayes and Howell, 1937; Currie, 1989b) or faulted (normal dip-slip) unconformity (Wardle, 1978).

Folds in marble adjacent to the fault plane are restricted to small-scale steeply southeast-inclined, gently to steeply northeast to southwest-plunging tight structures and crenulations with axes that define a girdle distribution. Stretching lineations have a moderate to steep southwest plunge (Fig. 3.5). These patterns suggest sheath fold geometries but also reflect the ductile nature of the marble (section 3.3.3).

Farther northeast along this fault, slivers of Ashburn Formation quartzite and rare marble are found. These are overprinted by brittle fractures and lack any structures useful for kinematic studies. Still farther northeast, the Caledonia-Clover Hill Fault juxtaposes the Hammond River pluton with sedimentary rocks of the Upper Carboniferous Hopewell Group. Drill core from vertical holes in the Hammond River pluton has intersected Upper Carboniferous sedimentary rocks at depth. This suggests that the dip of the fault is shallower at depth than its vertical character at surface.

Kinematic indicators along the fault in the Saint John area such as C-S fabrics, rotated porphyroclasts, and microscopic secondary foliations suggest a reverse dip-slip to moderately steep sinistral oblique dip-slip movement along this small segment of the fault. This

zone is further complicated by local normal dip-slip overprinting fabrics. Most slickenside orientations are vertical or plunge steeply to the southeast (cf. Wardle, 1978). Like the New River Beach-Kennebecasis Fault, the overall sense of movement is interpreted to be dextral strike-slip, modified by later (Mesozoic?) normal faults (cf. Leger and Williams, 1986).

The significance of the Caledonia-Clover Hill Fault and the New River Beach-Kennebecasis Fault as major terrane-bounding features with a long and complicated pre-Carboniferous history has only recently been recognized (White et al., 1991). Different senses of movement are documented along these faults and have often been attributed by previous workers to one period of deformation. In reality, these terrane-bounding faults record very complex and prolonged histories; however, evidence of only the last movements are preserved.

3.5.2.3. Milkish Head Fault

A northeast-trending splay off the Kennebecasis Fault on Milkish Head Peninsula, is termed the Milkish Head Fault (E. Grant 1972; Gupta, 1975) (Fig. 3.5). It separates the Kennebecasis Formation from strongly deformed rocks of the Brookville terrane to the southeast. Farther northeast this fault is interpreted to coincide with the Kennebecasis River Fault that merges with the Berry Mills Fault (St. Peter, 1993). It is distinguished on aeromagnetic maps by a linear feature that separates areas of magnetic lows from magnetic highs.

Fanglomerates close to the fault that contain clasts of granite and Saint John Group are interpreted to be talus deposits (E. Grant, 1972). This led O'Brien (1976) and Wardle (1978) to conclude that a period of Devonian to Carboniferous normal faulting resulted in the development of a graben or half graben.

Bedding (S_0) orientations in the Kennebecasis Formation dip moderately to the northwest (Fig. 3.5) and are rarely deformed into

upright subhorizontal folds near the Kennebecasis Fault. Elsewhere the Kennebecasis Formation lies unconformably on older rocks and is not fault-bounded. The fault plane is locally exposed and has variable oriented slickenside striations; its sense of movement is unknown.

3.5.2.4. Ragged Point Fault

A northeast-trending, steep fault can be traced along the southeastern shore of Kennebecasis Bay. It separates the Kennebecasis Formation from the Ashburn Formation in the southwest, although locally it appears to be overlain by the Kennebecasis Formation (Wardle, 1978). Farther northeast the fault separates the Ashburn Formation from the Renforth Pluton and the Brookville Gneiss from the Renforth Pluton. It appears to terminate in the Renforth Pluton. It has no geophysical expression.

First recognized by Hayes and Howell (1937) and briefly described by Wardle (1978), it is herein termed the Ragged Point Fault. Faulted slivers of folded Saint John Group are locally associated with this fault. Large boudins of very fractured tonalite related to the Renforth Pluton and mafic dykes are found in marbles of the Ashburn Formation; however, mafic dykes within the tonalitic boudins are not deformed. The marbles in this zone are typically brecciated.

Structures associated with this fault indicate a steep southeast dip (Fig. 3.5). Folds in unbrecciated marbles are steeply southeast-inclined, gently northeast-plunging and tight. The long axes of boudins are also northeast-trending and sub-horizontal. Based on fold shapes, Wardle (1978) concluded that these structures were related to high-angle reverse movement; however, the kinematics and amount of movement are unknown.

3.5.2.5. Ragged Head Fault

The Ragged Head Fault (Dickson, 1983) is located southwest of Saint John and can be traced by a strong topographic lineament from Maces Bay to Musquash River (Fig. 3.5) and an abrupt change from magnetic highs to lows on aeromagnetic maps. This poorly exposed fault separates the Lancaster Formation from plutonic units to the northwest. Rocks close to this inferred fault are strongly fractured. It was interpreted to represent a fault-modified unconformity with dip-slip movement by Stringer and Wardle (1973) and Dickson (1983); however, there is no sedimentological evidence to support this interpretation. It has also been suggested by Nance (1987b p. 369) to represent a dextral strike-slip fault. Rast and Grant (1973b) and Currie (1987a) considered it to be an unconformity. Due to lack of outcrop the characteristics of this fault are unknown.

3.5.2.6. Lepreau River Fault

The Lepreau River Fault (Dickson, 1983) is a northeast-trending, vertical to steeply southeast-dipping feature along the northwest coast of Lepreau Harbour (Fig. 3.5, 3.6). It separates the Lepreau Pluton to the northwest from the Balls Lake Formation to the southeast and merges with the New River Beach Fault to the northeast. Granitoid rocks of the Lepreau Pluton close to the fault are strongly brecciated. Sedimentary rocks are sheared and locally folded.

The Lepreau River Fault was interpreted to be the northwestern boundary fault of a half-graben by Stringer (1978). The presence of faulted slivers of Lancaster Formation along the fault and the lack of sedimentological evidence for a steep paleoslope suggest that the main movement on the fault post-dated deposition of the Carboniferous Balls Lake Formation. Detailed kinematic analyses by Stringer (1978) suggested that the latest movement was dominantly high-angle reverse.

The sedimentary rocks of the Balls Lake Formation adjacent to the fault are deformed into series of upright, subhorizontal to gently southwest plunging folds. Farther to the southeast, folds are less prominent and the strata dip moderately to the northwest (Fig. 3.6) and rest unconformably on the Lepreau Harbour Granodiorite (Fig. 3.7).

A weak axial planar fabric, locally well developed in the shaly siltstone beds, is defined by a very closely spaced, northeast-trending (Fig. 3.6) anastomosing fracture cleavage (Stringer, 1978). Intersection lineations were not observed.

3.5.3. Musquash-Dipper Harbour thrust belt ($D_{3,2}$)

The Musquash-Dipper Harbour thrust belt lies in a broad area extending from Musquash Harbour in the northeast to Dipper Harbour in the southwest. This area is equivalent to the southwestern portion of the Fundy Coastal Zone of Nance (1987b). These rocks were strongly deformed by Late Carboniferous northwest-directed compression which resulted in a single large thrust sheet tectonically emplaced over the Carboniferous sedimentary rocks. The thrust sheet comprises the Late Neoproterozoic Dipper Harbour volcanic unit (McLeod et al., 1994) and a number of syenogranitic plutons which are locally unconformably overlain by Carboniferous sedimentary rocks of the Parleeville, Balls Lake, and Lancaster formations (Chapter 2).

Structures observed in the field indicate that this thrust zone represents a progressive period of northwest-directed thrusting. Based on cross-cutting and intersecting criteria an older $D_{3,2a}$ and a younger $D_{3,2b}$ are recognized (Table 3.1).

3.5.3.1. $D_{3,2a}$ structures

Field observations suggest that folding in the Late Neoproterozoic Dipper Harbour volcanic unit and Carboniferous Parleeville, Balls Lake,

and Lancaster formations occurred early in the deformation history, as a result of northwest-directed thrusting. These $F_{3,2a}$ folds are best developed in the well layered sedimentary rocks of the Balls Lake and Lancaster formations. The volcanic rocks are largely confined to the overriding thrust block and therefore folds are poorly developed. $F_{3,2a}$ folds in the sedimentary units deform bedding (S_0) into moderately northwest-inclined, subhorizontal to gently southwest-plunging, tight to isoclinal folds that are commonly overturned to the northwest (Fig. 3.6). These folds typically lack an axial planar fabric, although intense fracturing parallel to the axial plane occurs in places. $F_{3,2a}$ folds are not well developed away from the thrust sheets.

Associated with this deformation is a planar subhorizontal fabric ($S_{3,2a}$) that ranges from a weak fracture cleavage to a penetrative foliation (Fig. 3.6). It is found throughout the sedimentary units but is best developed in sedimentary and volcanic rocks proximal to thrust contacts. The fabric is generally a slaty or closely-spaced cleavage defined by sericite, fine-grained chlorite, and rare coarse-grained muscovite. At thrust contacts the rock is typically a fine-grained mica phyllite. In places the cleavage is defined by flattened clasts in the sedimentary and volcanic rocks. $S_{3,2a}$ is subparallel to bedding in the Carboniferous units close to thrust contacts and here minor quartz and calcite veins occur parallel to the cleavage. $L_{3,2a}$ intersection lineations are well developed.

The Balls Lake and Parleeville formations originally were deposited unconformably on the Dipper Harbour volcanic unit and Musquash Harbour syenogranite. These contacts are rarely preserved and where recognized are generally overturned unconformities (Fig. 3.7), confirming earlier interpretations (e.g. Currie, 1986a, b, 1987a, 1988a; Zain Eldeen, 1991).

Any kinematic indicators that may have existed have been overprinted by later deformation. However, asymmetric K-feldspar augen

and S-C fabrics in the basal mylonite under the Cranberry Head Syenogranite (Dallmeyer and Nance, 1990) suggest initial northwest-directed movement.

3.5.3.2. $D_{3,2b}$ structures

As thrusting continued S_0 , $S_{3,2a}$, and quartz and calcite veins are deformed into large (10's of centimetres) gently southwest to southeast-inclined to recumbent, subhorizontal to gently northeast to southwest-plunging $F_{3,2b}$ folds that range from tight to isoclinal. Another dominant structure associated with $D_{3,2b}$ deformation and $F_{3,2b}$ folds is a subhorizontal axial planar cleavage ($S_{3,2b}$) parallel to small scale $S_{3,2b}$ crenulation cleavages (Fig. 3.6). These structures are not regionally significant and are restricted to zones proximal to the thrust planes. These are well developed in the fine-grained lithologies in the sedimentary and volcanic units and are defined by fine-grained muscovite and chlorite.

Fold axes related to the crenulations and folded veins generally plunge shallowly to the northeast and southwest and define a subhorizontal girdle that is subparallel to $S_{3,2b}$. Where both $S_{3,2a}$ and $S_{3,2b}$ are present they commonly look like large scale C-S structures (e.g. Dipper Harbour area).

The intersection of $S_{3,2a}$ and $S_{3,2b}$ produces rare $L_{3,2b}$ lineations defined by colour banding on the $S_{3,2b}$ foliation plane. These structures are parallel to the $F_{3,2b}$ fold axis and are distributed along a subhorizontal girdle (Fig. 3.6).

Calcite mylonites associated with the thrust planes in the Musquash Harbour area display subhorizontal $S_{3,2a}$ foliations that are parallel to $S_{3,2a}$ and $S_{3,2b}$ in the thrust planes to the west (Plate 4a). These rocks have a well developed stretching lineation defined by asymmetric calcite porphyroclasts that plunge shallowly to the southeast

and northwest. Minor recumbent subhorizontal $F_{3.2b}$ folds range from tight to isoclinal and are restricted to zones around boudins. Boudinaged material, common in this zone, consists of granite and diorite, mafic dykes/sills, and quartzite (Plate 4b, c). Long axes of these boudins parallel the average orientation of the fold axes (Fig. 3.6).

Numerous kinematic structures in this zone include shear bands (Plate 4a, d), asymmetric folds and porphyroclasts, and secondary foliations all consistently indicate northwestward emplacement of the thrust sheet.

The thrusting event ($D_{3.2}$) was considered to be responsible for the syntectonic development of northwestward prograding alluvial fans recorded by Balls Lake and Lancaster formations (Plint and van de Poll, 1982; 1984). Further thrusting subsequently caused both formations to become tectonically overridden and was responsible for conjugate folding and southeast directed back-thrusting (Caudill and Nance, 1986; Nance and Warner, 1986; Nance, 1987b; Caudill, 1989). Nance and Warner (1986) and Nance (1987b) suggested that these structural features represent a positive flower structure that developed above a synthetic, convergent wrench fault related to the Cobequid-Chedabucto fault system.

In the Musquash-Dipper Harbour thrust belt, these structures are broadly correlative, but details differ significantly. The southeast-directed back-thrusts and associated conjugate fold structures were not observed. Fold structures all verge to the northwest and all thrusting is northwest-directed (Fig. 3.6, 3.7). Syntectonic alluvial fans were not recognized in the thrust belt and unconformable contacts between the Late Neoproterozoic and Carboniferous rocks are locally preserved on the leading edge of these thrust sheets. These contacts are commonly overturned (Fig 3.7). This suggests that the Parleeville and Balls Lake formations were unconformably deposited upon the Dipper Harbour volcanic unit and associated granitic rocks prior to thrusting. As thrusting was initiated, the sedimentary rocks in the foot wall were strongly folded

and rocks on the thrust sheet (hanging wall) were passively carried along. This post-sedimentation thrusting event is confirmed from field mapping where the Carboniferous sedimentary units can be traced under these thrusts (Fig. 2.1; Map A).

Although the age and structural interpretation differs somewhat from that proposed by Caudill, and Nance (1986), Nance and Warner (1986), Nance, (1987b), and Caudill (1989) for the area southeast of Saint John, their proposed model still applies. The Musquash-Dipper Harbour thrust belt may represent the leading edge of the northwestern flank of the flower structure and record movements that are post-depositional. This would account for the sub-horizontal structures observed. Deformation in this belt intensifies to the southwest and the steeper structures associated with this positive flower structure are probably located just offshore.

A muscovite sample from a mica schist in the basal thrust of the Cranberry Head Syenogranite yielded an $^{40}\text{Ar}/^{39}\text{Ar}$ plateau age of 318 ± 1 Ma (Dallmeyer and Nance, 1990) consistent with a Late Carboniferous age for tectonic emplacement. Based on field evidence, these thrust sheets clearly override the Westphalian C Lancaster Formation. This suggests that this thrusting event was significantly younger than the major dextral movement along the Cobequid-Chedabucto fault system and may record a deformational event not yet recognized elsewhere in the Northern Appalachian orogen.

This northwest-directed thrusting is interpreted to be responsible for folding and faulting in the Balls Lake Formation in the Lepreau Harbour area. This would account for the high-angle reverse movement postulated by Stringer (1978) for the Lepreau River Fault. Because the orientation of the Ragged Head Fault is similar to that of the Lepreau River Fault it is interpreted to have the same sense of movement.

3.5.4. Mesozoic Faults and Related Fabrics (D₄)

Deformation related to the Early Mesozoic opening of the North Atlantic was long considered to be insignificant and, therefore, the effects of extensional faulting during the Triassic have been generally overlooked. Crustal extension has been attributed to listric faulting (Keen et al., 1991; Roberts and Williams, 1993) with northeast-trending thrust faults being reactivated with a normal sense of movement. Many of the thrust faults in the Dipper Harbour area are cut by minor steeply southeast dipping, northeast-trending faults that consistently display a normal sense of movement.

Northwest-trending faults are common in southern New Brunswick and locally offset northeast-trending faults. These show both dextral and sinistral strike-slip movements (Leger and Williams, 1986) and are considered to be transfer faults (Williams and Hy, 1990). In the study area these northwest-trending faults do not generally crop out, but are marked by strong lineaments and elongated lakes and streams. Rock units can generally be correlated across these faults suggesting movement is minimal.

Associated with the faulting was a period of sedimentation. The Middle to Late Triassic Lepreau Formation is in faulted contact with older units along a northwest-trending fault. Conglomerates are proximal to this fault and Stringer (1978) interpreted these to be related to early movements on this fault. The bedding (S₀) is tilted moderately to the northwest (Fig. 3.5). Folds are rare but minor northeast-trending, upright, subhorizontal open folds are recognized northeast of Point Lepreau (Stringer, 1978). These units are not penetratively deformed, placing an upper limit on the age of deformation in southern New Brunswick.

Mesozoic faulting played a greater role in the tectonic development of southern New Brunswick than previously recognized. This event was responsible for significant normal dip-slip movement on some

segments of the Caledonia-Clover Hill Fault as documented by Roberts and Williams (1993). They showed that the Visean Windsor Group was strongly deformed by reactivation of the Caledonia-Clover Hill Fault as a normal fault during the opening of the North Atlantic.

3.6. DYKES AND DEFORMATION

Pre-Late Devonian rocks have been intruded by a variety of mafic dykes (Appendix B). Dyke orientations can be broadly divided into two geometrical domains. One domain includes dykes that intruded competent lithologies such as the plutonic units and the Martinon Formation and the other domain includes dykes that intruded less competent lithologies such as the marbles in the Ashburn Formation.

Dykes in the Ashburn Formation display a weakly bimodal distribution (Fig. 3.6). The dominant orientation strikes northeast, dips southwest, and is sub-parallel to the average orientation of S_0 and S_1 in the marbles. Also a set of southeast-trending, near-vertical dykes is present which is oriented perpendicular to the general northeast trend. This structural pattern suggests that the northeast-trending dykes were intruded along pre-existing structures or transposed into this fabric. Field observations have confirmed that most of these dykes intruded along pre-existing fabrics; however, there appear to be earlier dykes that are boudinaged parallel to S_1 . Based on field evidence, dykes that trend southeast appear to be dominantly (but not exclusively) composed of microdiorite, gabbro, and porphyries.

Dyke orientations in more rigid lithologies, such as the Martinon Formation and the plutonic units, display a broadly conjugate pattern and may have intruded a pre-existing joint set (Fig. 3.6). However, like in the Ashburn Formation, the northeast trend is dominant. These dykes are not penetratively deformed and boudinaged dykes were not observed in the Martinon Formation.

In places, the dykes in all lithologies are offset by minor

northeast-trending cross-fractures. One such north-northeast-trending mafic dyke on Green Head Island has been reported to have had several offsets of 10 metres or more in a dextral sense of movement (Leavitt, 1963).

3.7. SUMMARY

The following section and Table 3.1 summarize the main points of this chapter:

1. Based on field relations and structural analyses four distinct deformational events are recognized in the Brookville terrane (D_1 - D_2 - D_3 - D_4).
- 2a. The oldest deformation (D_1) recognized is pre-Late Neoproterozoic in age and is the main fabric-forming event(s) in the terrane. D_{MPI} deformed bedding in the Martinon Formation into upright, gently southwest-plunging, open to close F_{MPI} folds. An axial planar cleavage with an associated intersection lineation is poorly developed. However, structural style differs significantly in the associated Ashburn Formation and here fabrics are designated as D_{AF1a} and D_{AF1b} .

The most prominent feature in the Ashburn Formation is a well developed northeast-trending, steeply southeast-dipping axial planar fabric (S_{AF1a}). Rare F_{AF1a} folds are upright, to steeply southeast-inclined, gently to moderately northeast to southwest-plunging, close to tight, intrafolial, and rootless. Intersection lineations (L_{AF1b}) are rare. D_{AF1b} did not affect the Martinon Formation; however, it deformed S_{AF1a} in the Ashburn Formation into upright to steeply southeast-inclined, gently to moderately northeast to southwest-plunging, close to tight F_{AF1b} folds. Close to the MacKay Highway shear zone F_{AF1b} folds are locally associated with a northeast-trending, steeply southeast-dipping well developed axial planar fabric (S_{AF1b}) and northeast to southwest-

plunging intersection lineation (L_{AF1b}).

The exact age of deformation in the Martinon and Ashburn formations is unknown but all structures related to D_1 are cross-cut by undeformed Late Neoproterozoic to Cambrian plutonic rocks.

2b. The MacKay Highway shear zone contains a northeast-trending, steeply southeast dipping foliation (S_{MH1}) composed of subparallel S_{AF1a} and S_{AF1b} . This resulted in a moderately northeast-plunging intersection lineation (L_{MH1}) parallel to a prominent stretching lineation in the blastomylonites.

Northeast-trending, steeply southeast-dipping gneissic foliation (S_{BG1}) in the Brookville Gneiss is deformed into upright to steeply southeast-inclined, gently to steeply northeast to southwest-plunging, tight to isoclinal F_{BG1} folds. The orthogneiss displays a weak to moderately developed, northeast-plunging mineral lineation (L_{BG1}) parallel to those in the MacKay Highway shear zone.

These structures are considered to represent several phases of a single progressive period of ca. 564-540 Ma deformation related to the prolonged dextral, transpressional juxtaposition of the Brookville Gneiss with the Green Head Group.

3. The second period of deformation (D_2) occurred in the Middle Paleozoic after the emplacement of plutonic units and is associated with discrete ductile faulting of unknown tectonic significance.

4. The third major period of deformation (D_3) occurred in the Late Devonian to Late Carboniferous and was generally not a fabric-forming event. Instead it produced steep, northeast-trending faults that locally formed calcite mylonites and folded adjacent sedimentary rocks.

5. In the Musquash-Dipper Harbour area, inclined to recumbent, subhorizontal folds with associated calcite mylonites are consistent with sustained or repeated northwest-directed thrusting. This appears to be younger than the major dextral movement associated with the Jobequid-Chedabucto fault system.

6. The fourth period of deformation (D_4) is interpreted to be associated with the development of the Early Mesozoic Fundy Basin, which formed during the rifting leading to the opening of the Atlantic Ocean. This may have reactivated northeast-trending Carboniferous faults so that most of the normal movement on these faults may be related to this event. It also produced a series of steep northwest-trending faults.

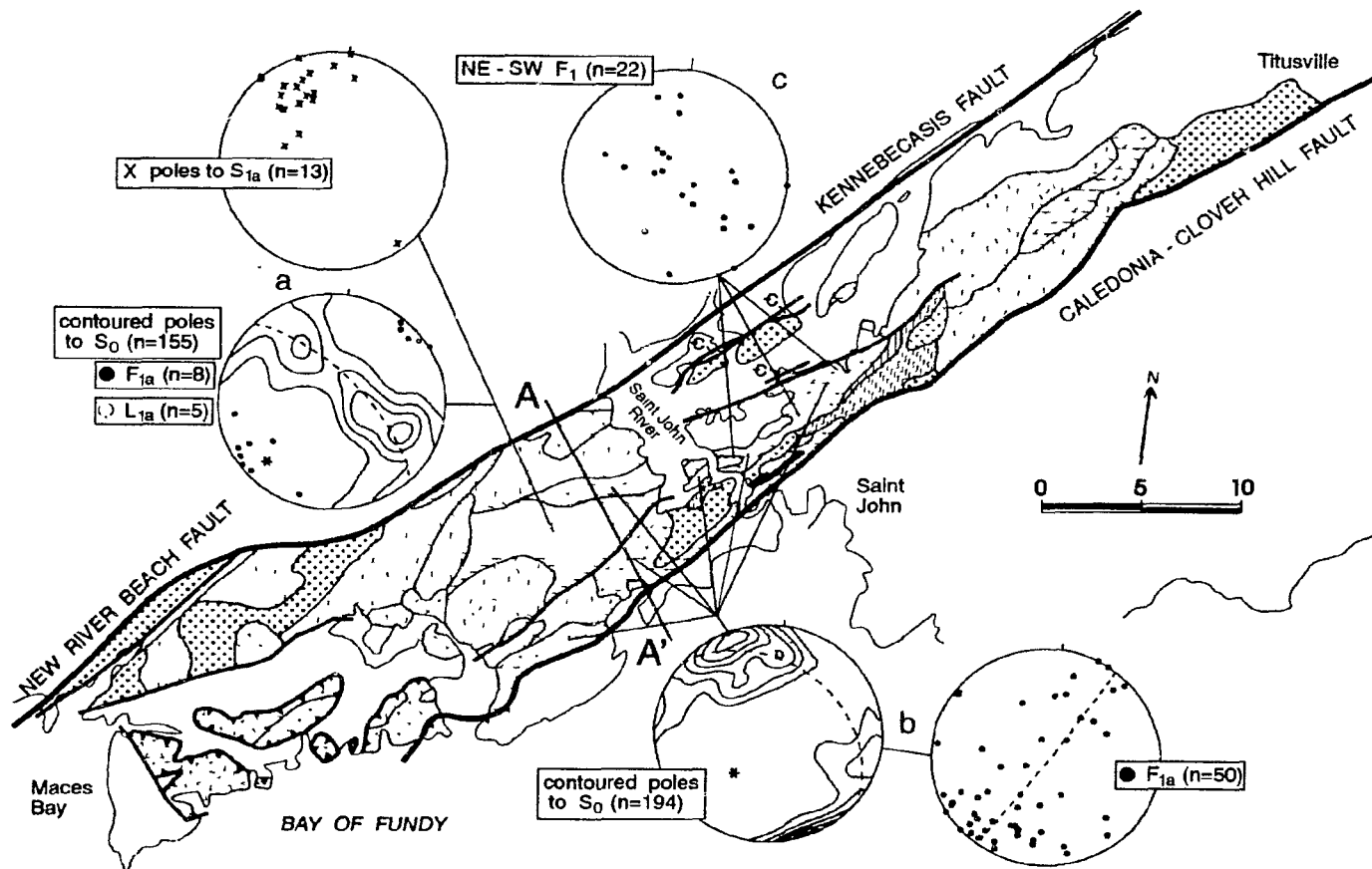


Figure 3.1. Summary of D_{MF1} and D_{AF1a} structural data from the Brookville terrane. Contours on stereonets represent 1, 2, 3 ...n% area; * = calculated fold hinge. Cross section A-A' is shown in Figure 3.2. Legend same as Figure 2.1. a) Martinon Formation; b) siliciclastic units and F_{AF1a} in the Ashburn Formation; c) NW-SE trending F_1 folds.

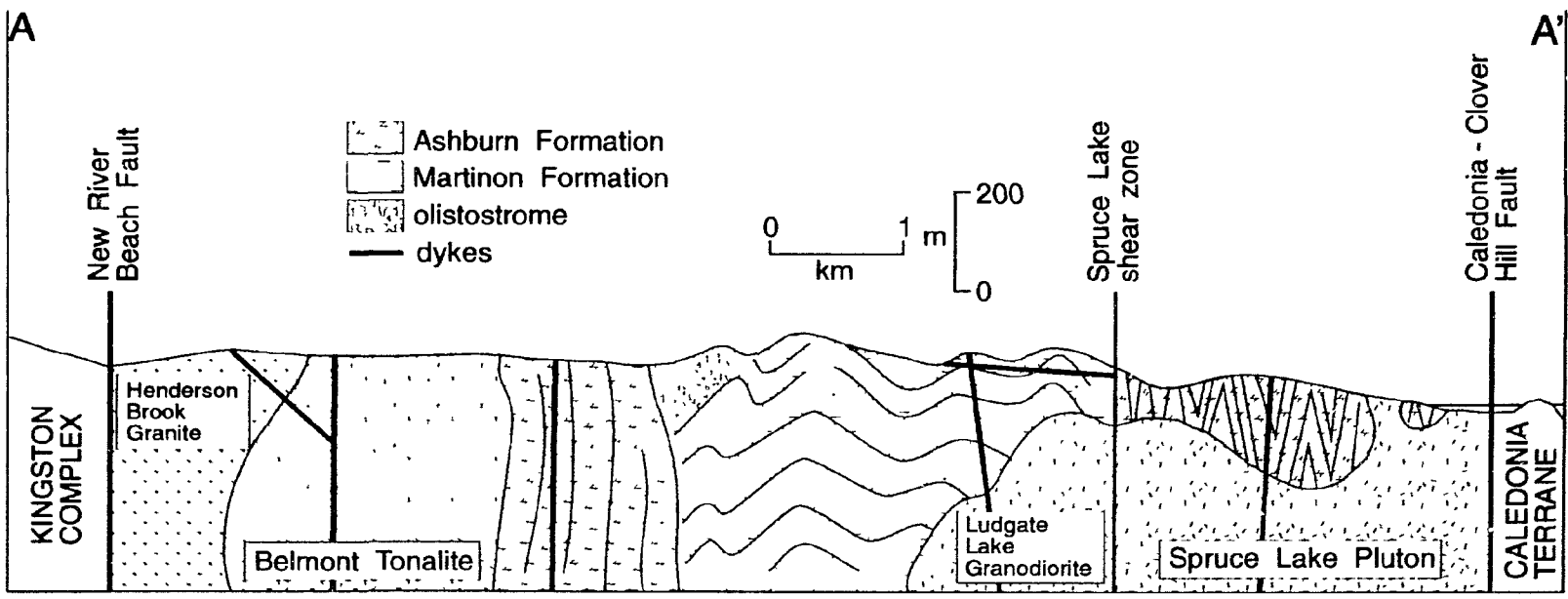


Figure 3.2. Cross section (location shown on Figure 3.1). See Figure 2.1. for Legend.

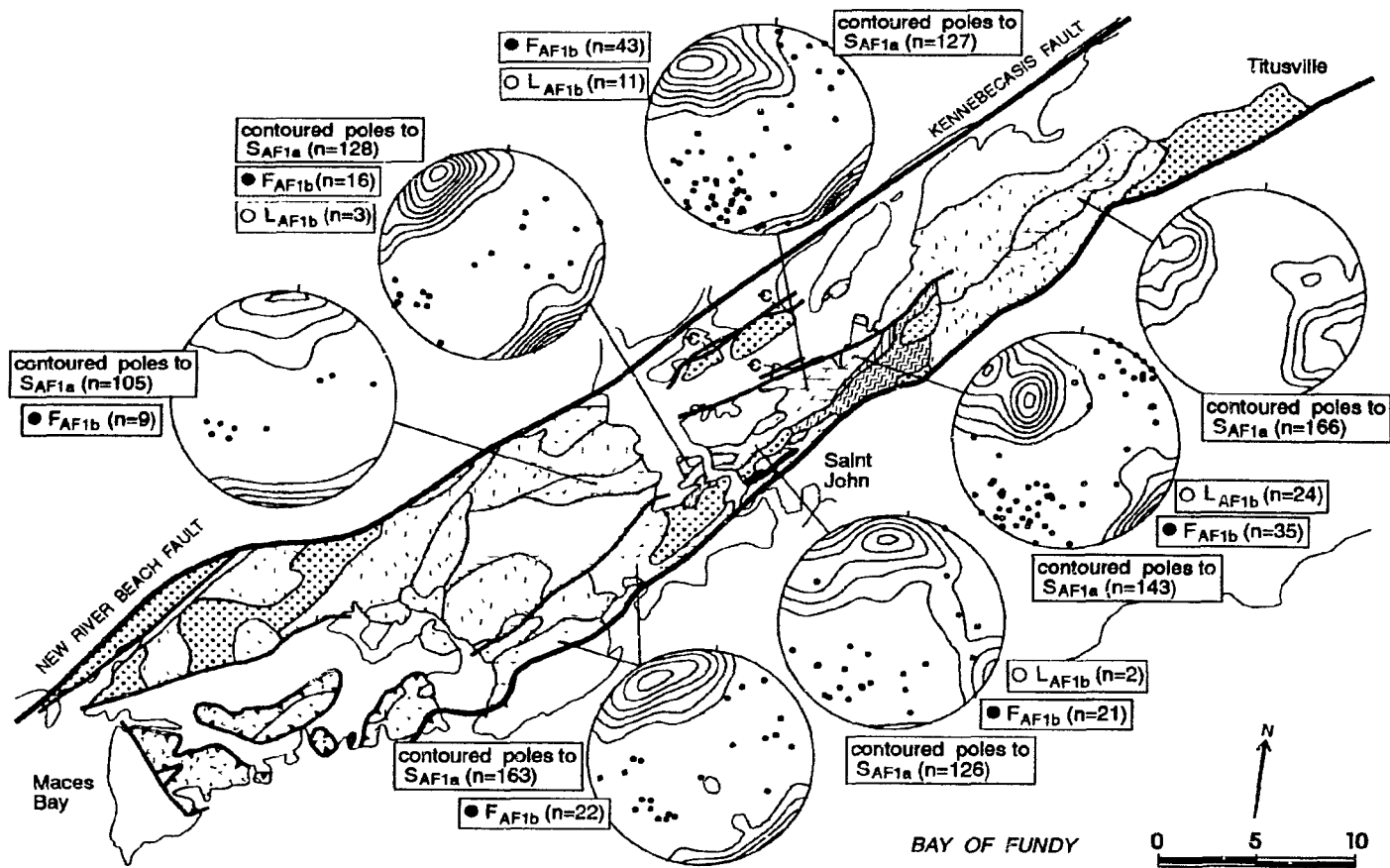


Figure 3.3. Summary of D_{AF1b} structural data from the Ashburn Formation. Contour intervals and symbols same as Figure 3.1 and Legend same as Figure 2.1. Note the increase in L_{AF1b} towards the MacKay Highway shear zone and the Brookville Gneiss.

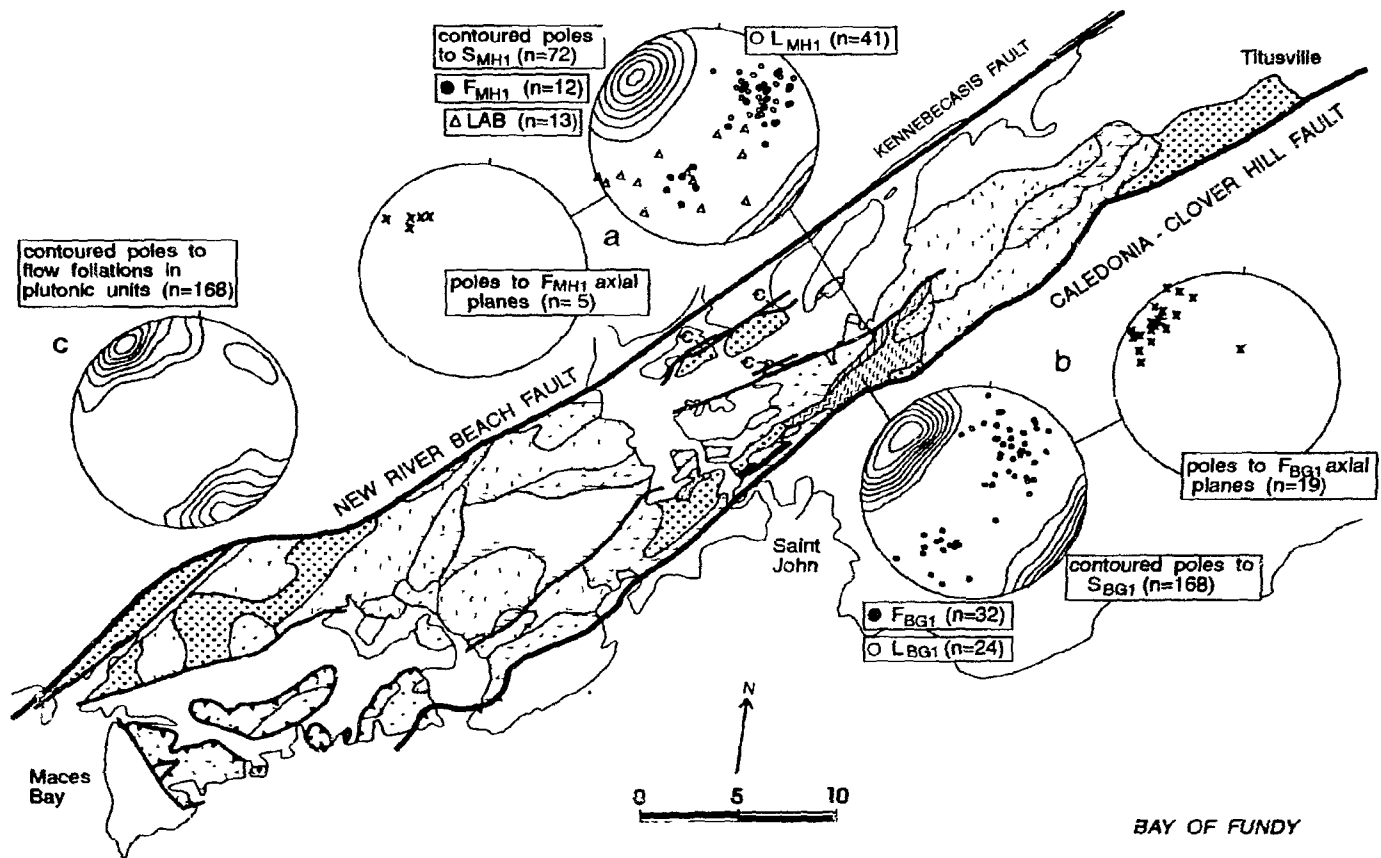


Figure 3.4. Summary of structural data from a) the MacKay Highway shear zone; b) Brookville Gneiss; c) plutonic units. Contour intervals and symbols same as Figure 3.1 and Legend same as Figure 2.1. LAB=long axis of boudins.

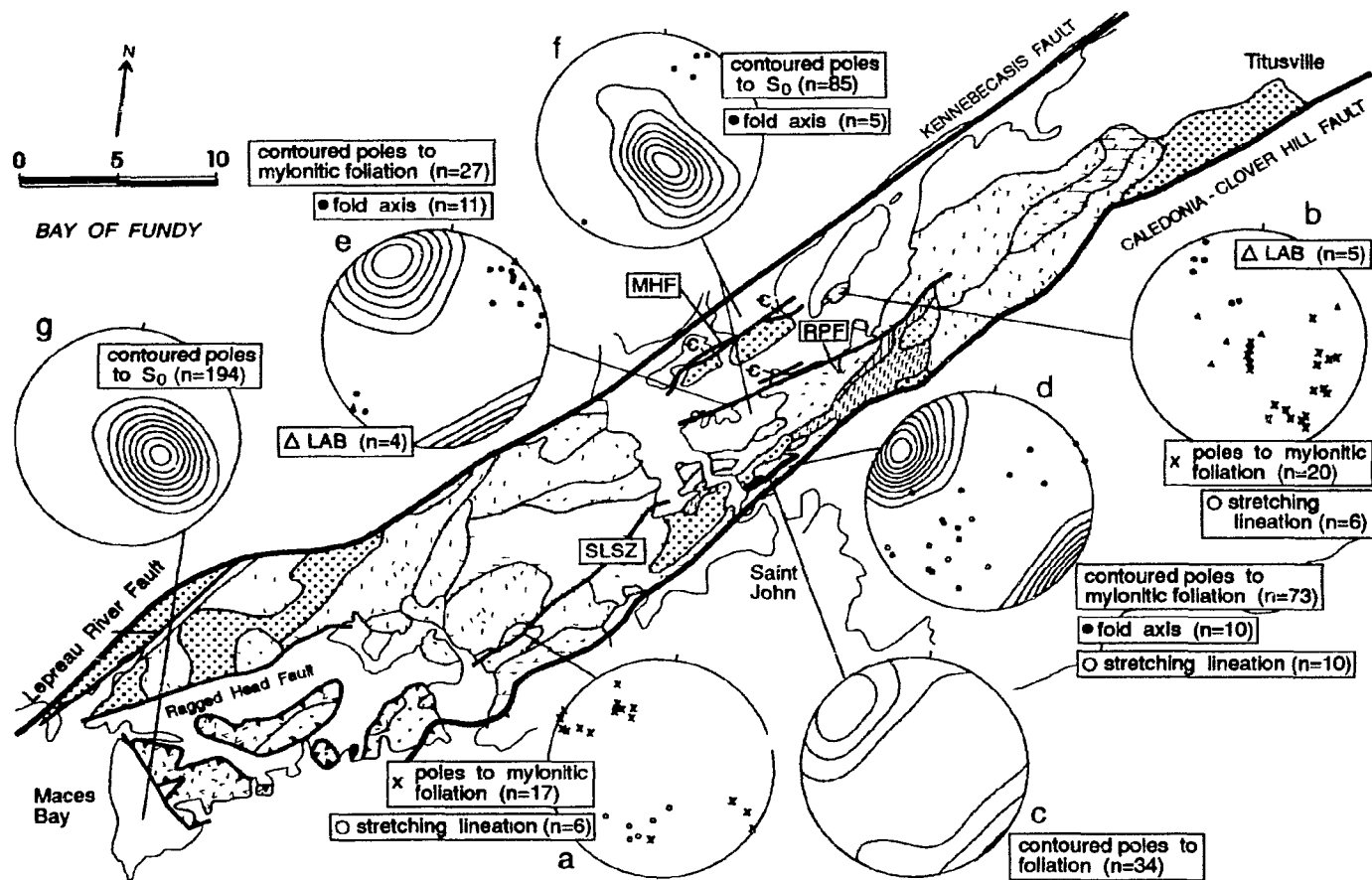


Figure 3.5. Summary of structural data from a) Spruce Lake shear zone; b) Long Island shear zone; c) deformed granitoid unit; d) calcite mylonite in the Caledonia-Clover Hill Fault; e) Ragged Point Fault; f) Kennebecasis Formation; g) Lepreau Formation. Contour intervals and symbols same as Figure 3.1 and Legend same as Figure 2.1. LAB=long axis of boudins; MHF = Milkish Head Fault; RPF = Ragged Point Fault; SLSZ = Spruce Lake shear zone.

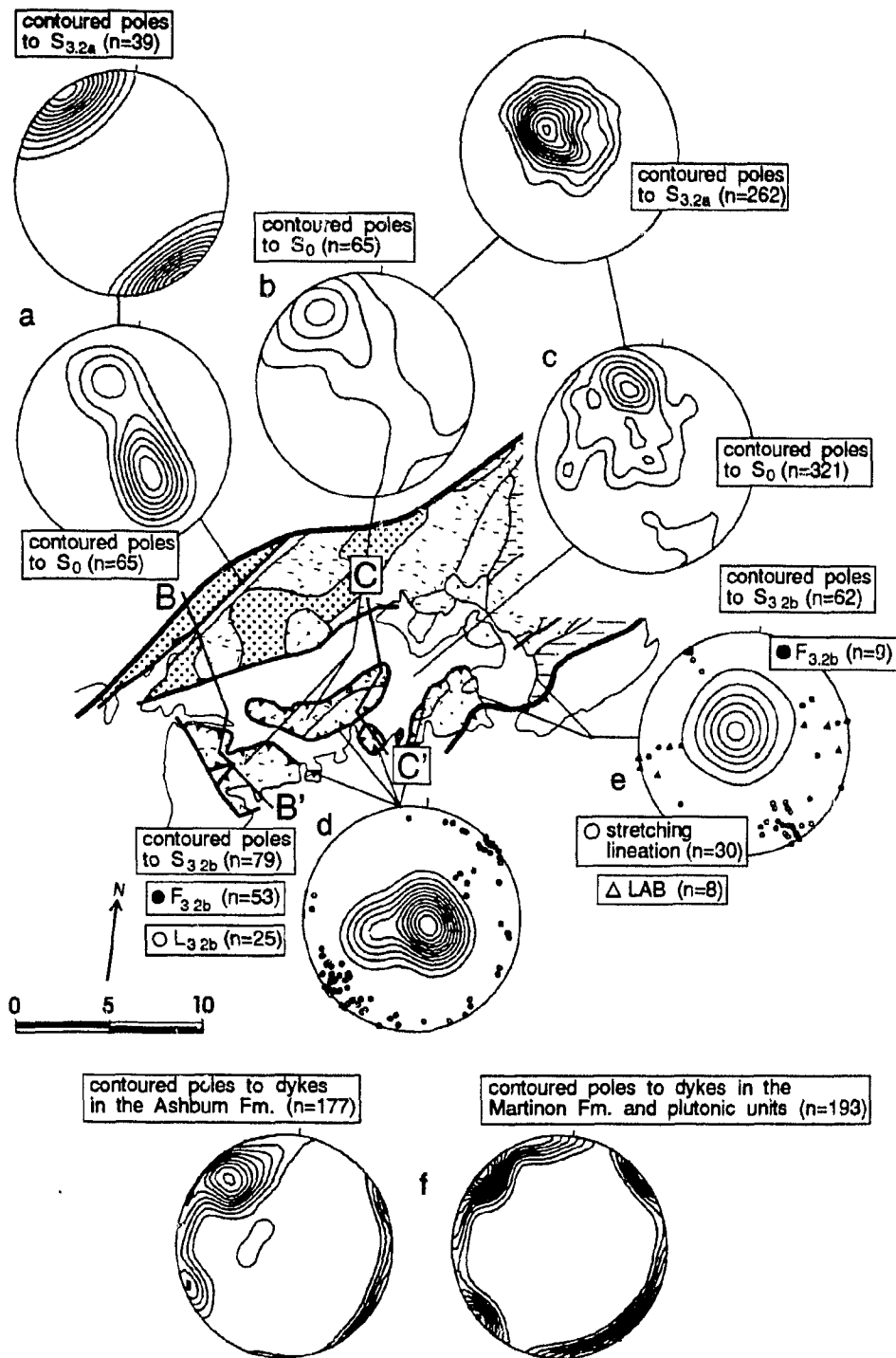


Figure 3.6. Summary of structural data from the Musquash-Dipper Harbour thrust belt. Contour intervals and symbols same as Figure 3.1 and Legend same as Figure 2.1. LAB=long axis of boudins. a) Balls Lake Formation; b) Dipper Harbour volcanic unit; c) Balls Lake and Lancaster formations; d) thrust planes; e) calcite mylonites; f) dykes. Cross section B-B' and C-C' are shown in Figure 3.7.

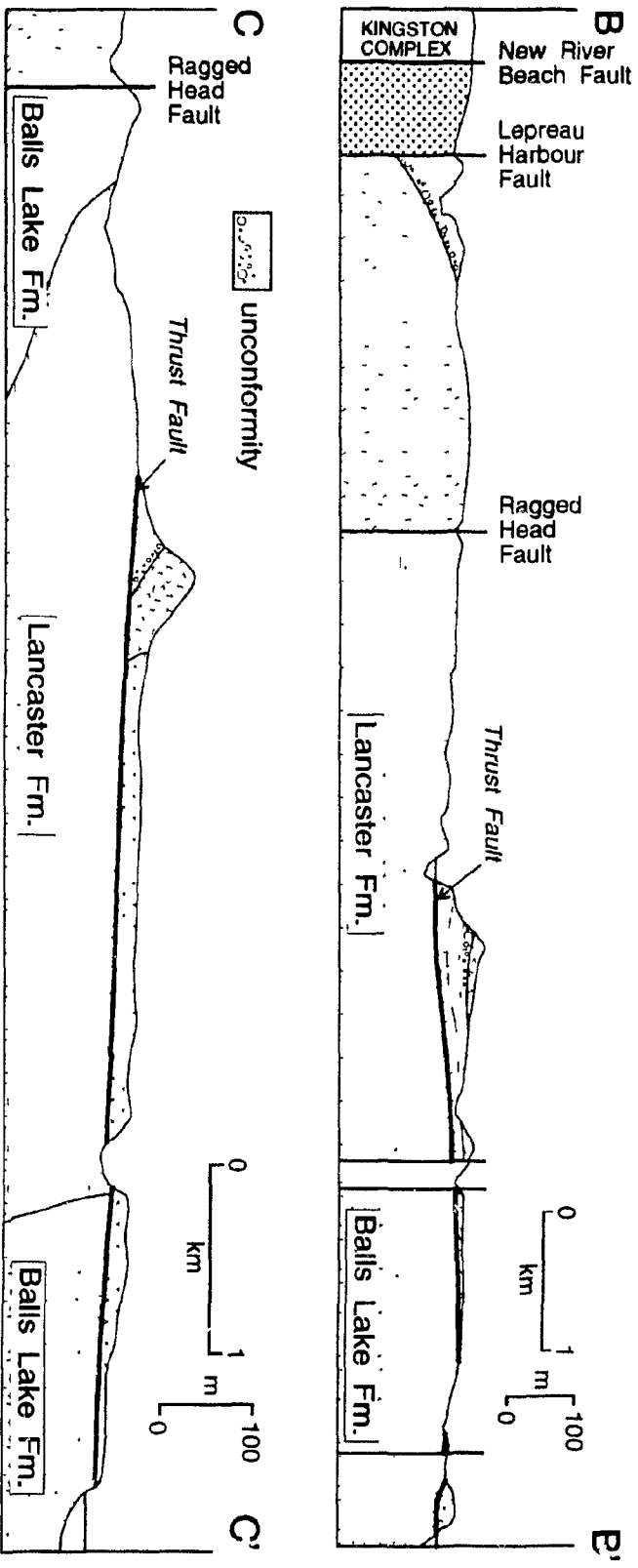


Figure 3.7. Cross sections (location shown on Figure 3.6). See Figure 2.1 for Legend.

Table 3.1. Summary of major deformations and related structures in the Brookville terrane.

DEFORMATION	FORMATION	FOLDS	PLANAR FABRICS	LINEATIONS
pre-D ₁ pre-Late Precambrian	Martinon and Ashburn	soft sediment folds	S ₀	
D _{MP1} pre-Late Precambrian	Martinon	macroscopic, upright, gently SW-plunging, open to close F _{MP1} folds	rare, NE-trending, steeply SE-dipping S _{MP1}	rare, NE-trending, subhorizontal L _{MP1} ; intersection of S ₀ and S _{MP1}
D _{AF1a} pre-Late Precambrian	Ashburn	rare mesoscopic, upright to steeply SE inclined, gently to moderately NE and SW-plunging, close to tight, intrafolial and rootless F _{AF1a} folds	axial planar, NE- trending, steeply SE dipping S _{AF1a}	rare L _{AF1a}
D _{AF1b} pre-Late Precambrian	Ashburn	mesoscopic, upright to steeply SE inclined, gently to moderately NE and SW-plunging, close to tight F _{AF1b} folds	rare to abundant, axial planar, NE- trending, steeply SE dipping S _{AF1b}	minor to abundant, subhorizontal to moderately NE and SW- plunging L _{AF1b} intersection of S _{AF1a} and S _{AF1b} ; crenulation in pelite
D _{MHI} Late Precambrian	MacKay Highway shear zone	mesoscopic, steeply SE inclined, gently to moderately NE and SW- plunging, tight to isoclinal F _{MHI} folds	NE-trending, steeply SE dipping S _{MHI}	moderate NE-plunging L _{MHI} intersection of S _{AF1a} and S _{AF1b} in marble; parallel to mineral stretching lineation in blasto- mylonite
D _{BG1} Late Precambrian	Brookville Gneiss	mesoscopic, upright to steeply SE inclined, gently to moderately NE and SW-plunging, tight to isoclinal F _{BG1} folds	NE-trending, steeply SE- dipping, gneissic S _{BG1}	moderate NE-trending L _{BG1} stretching lineation

Table 3.1. Continued.

DEFORMATION	FORMATION	FOLDS	PLANAR FABRICS	LINEATIONS
D ₂ Middle Paleozoic	Spruce Lake shear zone		NE-trending, steeply SE-dipping, narrow blastomylonite zone	moderately S-SW- plunging stretching lineation
	Long Island shear zone	complex folds near boudins	NE-trending, moderately to shallowly NW-dipping	moderately NW- plunging stretching lineation
	deformed granitoid rocks	related to the Caledonia- Clover Hill Fault	NE-trending, steeply SE-dipping	
D _{3.1} Late Paleozoic	New River Beach- Kennebecasis Fault	NE-trending, upright subhorizontal folds in adjacent sedimentary rocks	NE-trending poorly exposed fault surfaces	
	Caledonia- Clover Hill Fault	steeply SE-inclined, gently to steeply NE and SW-plunging, tight folds in calcite mylonites	NE-trending, vertical to steeply SE-dipping	moderately to steeply SW-plunging stretching lineation; variably oriented slickensides
	Milkish Head Fault		NE-trending and subvertical fault surfaces	
	Ragged Point Fault	steeply SE-inclined, gently NE-plunging, tight folds in calcite mylonites	NE-trending, vertical to steeply SE-dipping	
	Ragged Head Fault		NE-trending, vertical	
	Lepreau River Fault	upright, subhorizontal to gently SW-plunging folds in adjacent sedimentary rocks	NE-trending, vertical to steeply SE-dipping	

Table 3.1. Continued.

DEFORMATION	FORMATIONS	FOLDS	PLANAR FABRICS	LINEATIONS
D _{3.2a} Late Paleozoic	Lancaster Balls Lake Parleeville Dipper Harbour volcanic unit	moderately NW inclined subhorizontal to gently SW-plunging, tight to isoclinal F _{3.2a} folds	minor axial planar fracture cleavage; subhorizontal S _{3.2a} close to thrust planes	L _{3.2a} not well developed
D _{3.2b} Late Paleozoic	thrust planes associated with the Musquash- Dipper Harbour thrust belt	gently SW to SE inclined to recumbent, subhorizontal to gently NE to SW- plunging, tight to isoclinal F _{3.2b} folds	subhorizontal axial planar S _{3.2b}	subhorizontal NE to SW- plunging L _{3.2b} intersection of S _{3.2a} and S _{3.2b} ; subhorizontal to gently SE and NW- plunging stretching lineation in calcite mylonites
D ₄ Early Mesozoic	Lepreau	rare, NE-trending, upright, subhorizontal, open folds	S ₀ tilted moderately to NW	
	faults		reactivated most NE- trending faults; steep NW-trending transfer faults	

PLATE 2

- 2a. Alternating thin dark fine-grained and lighter coarser-grained marble layers in the Ashburn Formation dip steeply to the southeast with a dark grey siliciclastic boudin. Marble layering anastomoses around boudin. This layering is interpreted to be secondary in origin and does not represent original bedding. Photograph faces northeast with the northeast-plunging intersection lineation perpendicular to photograph. Outcrop located in the Brookville Lime Quarry. Quarter for scale.
- 2b. Large white dolomite boudins surrounded by light grey anastomosing calcite layers in the Ashburn Formation. Photograph faces southwest with the southwest-plunging stretching lineation perpendicular to photograph. Outcrop located in the Fort Howe area. The hammer (center of photograph) is 26 cm long.
- 2c. Marble layers in Ashburn Formation deformed into a steeply southeast-inclined, northeast-plunging, tight fold. Photograph faces northeast with the northeast-plunging intersection lineation perpendicular to photograph and subparallel to fold hinge. Outcrop located in the Brookville Lime Quarry. Quarter for scale.
- 2d. Cross section through a complex sheath fold in medium-grained marble of the Ashburn Formation. Photograph faces northeast with the subhorizontal stretching lineation perpendicular to photograph. Outcrop located along the west coast of Green Head Island near the contact with the Martinon Formation. Height of photograph approximately 2 m.

PLATE 2



b



d



a



c

PLATE 3

- 3a. Roadcut along the MacKay Highway showing a portion of the MacKay Highway shear zone. Shear zone composed of finely laminated, rectilinear quartzo-feldspathic (dark) and carbonate (light) blastomylonite. Large brown calc-silicate boudins in center of photograph. Photograph faces northeast with the northeast-plunging intersection lineation plunging away from photograph. Cliff approximately 6 m high.
- 3b. Carbonate blastomylonite in the MacKay Highway shear zone deformed into a steeply southeast-inclined, moderately southwest-plunging, tight folds. Photograph faces east with the northeast-plunging intersection lineation plunging to the left, away from photograph. The marker is 12 cm long.
- 3c. Carbonate blastomylonite in the MacKay Highway shear zone showing a pervasive moderately northeast-plunging intersection lineation that parallels stretching lineation in adjacent orthogneiss. Photograph faces southeast with the intersection lineation plunging to the left. The hammer is 26 cm long.
- 3d. A narrow, northeast-trending, steeply southeast-dipping, coarse-grained marble shear zone cutting folded marbles of the Ashburn Formation. These features are interpreted to be related to the MacKay Highway shear zone. Photograph faces east-northeast. Outcrop located near Snowflake Lime Quarry. The marker is 12 cm long.

PLATE 3



b



d



a



c

PLATE 4

- 4a. Finely laminated, shallowly southeast-dipping calcite ultramylonite associated with the Musquash - Dipper Harbour thrust belt. Photograph faces northeast with the stretching lineation parallel to the picture plane and plunging slightly to the right. Tops to the left. Outcrop located on the east shore of Musquash Harbour near Black Beach. Hand lens for scale.
- 4b. Finely laminated, shallowly southeast-dipping calcite ultramylonite associated with the Musquash - Dipper Harbour thrust belt. Numerous asymmetric quartzite boudins parallel mylonitic layering. Long axis perpendicular to photograph. Photograph faces northeast with the stretching lineation parallel to the picture plane and plunging slightly to the right. Tops to the left. Outcrop located on the east shore of Musquash Harbour near Wallace Cove. The chisel is 12 cm long.
- 4c. Massive to finely laminated, subhorizontal calcite mylonite associated with the Musquash - Dipper Harbour thrust belt. Large dioritic boudin in marble. Photograph faces northeast with the stretching lineation parallel to the picture plane and plunging slightly to the left. Tops to the left. Outcrop located east of Musquash Harbour near Black Beach. Height of cliff approximately 10 m.
- 4d. Photomicrograph of calcite ultramylonite with shear bands associated with the Musquash - Dipper Harbour thrust belt. Section cut parallel to stretching lineation and perpendicular to foliation and faces southwest. Tops to the right. Bar scale is 1 mm. Plane-polarized light.

PLATE 4



CHAPTER 4

VOLCANIC AND PLUTONIC ROCKS OF THE BROOKVILLE TERRANE

4.1. INTRODUCTION

More than 70% of the Brookville terrane is composed of plutonic rocks and minor associated volcanic rocks. These rocks have been recognized since the early part of this century (e.g. Cumming, 1916; Hayes and Howell, 1937; Alcock, 1938). However, a problem that emerged over the last three decades (Chapter 1; Appendix A) was the grouping of all the granitoid rocks into a single suite, considered to be typical of Late Precambrian (Late Neoproterozoic) plutons in southern New Brunswick, and collectively referred to as the Golden Grove Suite (e.g. Currie, 1986a; Nance, 1986b). Together with volcanic rocks of the Coldbrook Group and associated plutons, the plutonic units in the Saint John area were considered to be the result of Late Precambrian (ca. 600 Ma) subduction, characteristic of the Avalon terrane in southern New Brunswick and elsewhere (e.g. Keppie et al., 1991; Nance et al., 1991). However, based on geochronology (Chapter 6) and field relationships (Appendix B), the volcanic and plutonic rocks of the Brookville terrane are now known to be younger (mainly ca. 548 to 537 Ma) than the characteristic Avalonian units (ca. 620 Ma and 560 to 550 Ma) (Barr et al., 1994). Overall, the present study shows that the Brookville terrane includes a complex series of granitoid plutons, the characteristics of which had not been adequately described or interpreted by previous workers.

The purpose of this chapter is to describe the petrography, mineral chemistry, and petrochemistry of the volcanic and plutonic rocks in the Brookville terrane in order to clearly establish the characteristic features of these units. The interpretations presented

in this chapter are based on the examination of over 600 stained rock slabs, 260 thin sections, mineral analyses in 35 samples, and 121 whole-rock chemical analyses (Appendix C).

4.2. VOLCANIC UNITS

Volcanic rocks of the Brookville terrane occur only in the southwest in the Dipper Harbour area (Fig. 2.1, Map A), and have been named the Dipper Harbour volcanic unit (McLeod et al., 1994). In the present study, the volcanic rocks are subdivided into three distinct lithological units: 1) dominantly rhyolitic, 2) andesitic to dacitic and, 3) mixed andesitic to rhyolitic rocks with minor sedimentary rocks.

4.2.1. Rhyolitic unit

The rhyolitic unit consists dominantly of white-weathered, grey to grey-green to maroon, massive to moderately layered (>2 m to <10 cm thick), crystal-rich rhyolitic ash flows. They contain small (<5 mm maximum diameter) phenocrysts of rounded embayed quartz, euhedral anorthoclase, and/or euhedral plagioclase (An₃₅₋₄₀) set in a fine-grained to aphanitic groundmass of microcrystalline quartz and feldspar. Following the classification of Streckeisen (1979) and using the relative modal abundances of phenocrysts (Cas and Wright, 1987, p. 18), these ash flows are termed pheno-rhyolitic to pheno-rhyodactic (Fig. 4.1; Appendix C.1). In massive volcanic layers, flow foliation is defined by thin, up to 15 cm long and 2 cm wide, fiamme-shaped structures that were previously interpreted as flattened pumice fragments (Rast et al., 1978b; Nance et al., 1990; Zain Eideen, 1991). However, these structures are aggregates of extremely fine-grained spherulitic quartz and feldspar and are here considered to be lithophysae. These structures result from spherulitic growth around an expanding vesicle in a hot flow as it moves (Cas and Wright, 1987, p.

84). Pumice fragments were not recognized in any sample.

Associated with the crystal-rich ash flows are minor maroon to purple, or rarely light green, rhyolite flows. Flow banding is defined by alternating aphanitic and fine-grained layers up to 2 mm wide. Phenocrysts of euhedral, moderately saussuritized plagioclase (An₃₀) and subhedral quartz compose less than 5% of the rhyolite and the matrix is generally a cryptocrystalline mass of quartz and feldspar. Within these flows, thin spherulitic lenses are preserved. Due to poor outcrop control, the thickness of the flows is unknown.

Light grey to purple, rhyolitic to dacitic, lithic-rich tuff is commonly associated with the flow-banded rhyolite. Clasts are generally subrounded (<5 cm in diameter) and consist of dacitic to rhyolitic tuff and flow fragments. Basaltic to andesitic fragments occur rarely. Clasts are locally flattened where a tectonic cleavage is present (Chapter 3). Basaltic or andesitic flows were not observed in this unit.

4.2.2. Andesitic to dacitic unit

The andesitic to dacitic unit consists dominantly of cleaved, green to grey-green, locally maroon, lithic-rich tuff. Clasts of andesitic and dacitic tuffs are generally less than 5 cm in diameter and commonly flattened parallel to a subhorizontal cleavage. The matrix is composed of a well foliated mass of fine-grained epidote, chlorite, and sericite. Plagioclase crystals are rare and, where present, are typically broken and intensely altered. Volcanic layering is difficult to recognize because of the strong foliation (Chapter 3). Minor green-grey, well cleaved, laminated siltstone is locally interlayered with the tuff. Volcanic flows were not observed in this unit.

4.2.3. Mixed andesitic to rhyolitic unit

The mixed andesitic to rhyolitic unit consists of green-grey to maroon andesitic lithic-rich tuff and minor purple dacitic to rhyolitic lithic-rich and crystal-rich tuff. Clasts are varied and typically flattened parallel to a subhorizontal cleavage. Associated with the volcanic rocks is well laminated calcareous siltstone that is locally interlayered with maroon lithic-rich tuff. Also associated with the siltstone is grey laminated marble that is locally mylonitic near faults. Because of the presence of marble and siltstone, this unit was previously interpreted to be part of the Green Head Group (e.g. Dickson, 1983).

The more mafic lithologies in the unit are generally altered and deformed similar to those in the andesitic to dacitic unit described above. The rhyolitic lithic-rich tuff is generally composed of subrounded (<2 cm in diameter) dacitic tuff and flow fragments that comprise up to 80% of the rock. The groundmass is typically a mixture of fine-grained quartz and feldspar. The crystal-rich tuffs are phenocrystic and consist of small (<2 mm in diameter) phenocrysts of euhedral plagioclase (An_{10}) and rounded quartz in a groundmass of microcrystalline quartz and feldspar. The sedimentary rocks are recrystallized to a mixture of epidote and chlorite and/or calcite.

4.2.4. Petrochemistry

Five representative samples for major and trace element analyses (Appendix C.2) were collected from rhyolitic ash flows in the Dipper Harbour volcanic unit, from which chemical data have not previously been reported. Sample locations are shown on Map D. Samples from the rhyolite ash flows have a narrow range in silica content from 75 to 77%. On silica variation diagrams, the analyzed samples tend to cluster, with the exception of K_2O and most trace elements which display considerable

scatter (Fig. 4.2, 4.3). The only apparent trend is an increase in Zr with increasing SiO_2 .

All samples are peraluminous with normative corundum values of 2 to 3% and aluminum saturation indices ($A/CNK = \text{molar Al}_2\text{O}_3 / \text{CaO} + \text{Na}_2\text{O} + \text{K}_2\text{O}$) ranging from 1.3 to 1.4 (Appendix C.2, Fig. 4.4). Differentiation indices (Thornton and Tuttle, 1960) are also high, greater than 90 (Appendix C.2).

Based on the $\text{Na}_2\text{O} + \text{K}_2\text{O}$ versus SiO_2 diagram (Fig. 4.5) the samples are subalkaline, and on the AFM diagram (Fig. 4.6) the compositions plot near the $\text{Na}_2\text{O} + \text{K}_2\text{O}$ apex in the calc-alkaline field.

4.3. PLUTONIC UNITS

Plutonic units in the Brookville terrane cover an area greater than 200 km^2 and include numerous lithologies, which, on the basis of systematic mineralogical and/or chemical variations, unique textural and mineralogical features, and age (Chapter 6) are grouped into 29 plutons and 2 orthogneissic units (Map A, Fig. 1.3, 2.1). Each pluton defines a distinct intrusive pulse and may vary in complexity from homogeneous to composite. The apparent size of each pluton (at the present level of erosion) also varies considerably from <1 to >20 km^2 .

Three temporally and lithologically distinct plutonic groups are recognized: 1) ca. 605 Ma orthogneiss associated with the Brookville Gneiss, 2) ca. 548 to 537 Ma set of varied granitoid plutons, and 3) a younger set of gabbroic to ultramafic plutons. Most of these units are cut by numerous younger mafic dyke rocks.

Plutonic units are named following as closely as possible the recommendations of the International Subcommission on Stratigraphic Classification (1987) and the classification scheme of Streckeisen (1976) (Appendix B), as well as the geographic names used by earlier workers (e.g. Hayes and Howell, 1937; Belyea, 1945; Ruitenberg et al.,

1979; Currie, 1987a).

4.3.1. Orthogneiss

Two distinct orthogneissic units are recognized in the Brookville Gneiss and include amphibolite and tonalitic to granodioritic orthogneiss (Fig. 4.1). Modal analysis suggests that the amphibolites are quartz diorite in composition; however, much of the quartz is probably metamorphic in origin and the protolith is interpreted to be gabbroic or dioritic in composition. Based on field evidence the amphibolite and tonalitic to granodioritic orthogneiss are considered to be coeval but it is unclear if they are cogenetic (Chapter 2 and 5). Because the petrography and mineral chemistry reflects an upper amphibolite-facies metamorphic overprint, these features are described in Chapter 5. However, the grade of metamorphism is interpreted to have little effect on the original petrochemical characteristics of the orthogneiss.

4.3.1.1. Petrochemistry

Seven representative samples from the tonalitic to granodioritic orthogneiss and two from hornblende-bearing paragneiss were collected to characterize and classify these units based on major and selected trace elements. Samples from the amphibolite were not analyzed. The geochemical data, CIPW normative mineralogies, and statistical data are tabulated in Appendix C.2. Analyses of samples collected by other workers in the area are integrated with data from this study and noted in Appendix C.2. Sample locations are plotted on Map D.

Although the orthogneiss has a narrow range in silica content (66 to 70%) it still shows a negative correlation with TiO_2 , Al_2O_3 , $\text{Fe}_2\text{O}_3^{\text{T}}$, MnO , MgO , CaO , and P_2O_5 and a weak positive correlation with Na_2O (Fig. 4.2). Most of the trace elements show no correlation with silica (Fig.

4.3). Compared to the ca. 548 to 537 Ma plutons the orthogneiss is slightly enriched in TiO_2 , MgO, CaO, Nb, Ni, Th, and Cr, and depleted in K_2O . The two samples of hornblende-bearing paragneiss have silica contents less than 61% and typically plot on the same trend as the 548 to 537 Ma plutons. They are slightly enriched in TiO_2 , MnO, Nb, Zr, and Cr, and slightly depleted in Ba and Sr. Ni contents are considerably higher.

The orthogneiss is quartz-normative and peraluminous with A/CNK ranging from 0.96 to 1.31 (Appendix C.2, Fig. 4.4). Differentiation indices display a positive correlation with silica and from 69 to 79 (Appendix C.2). The orthogneiss samples are subalkaline and calc-alkaline and are slightly discordant to the main ca. 548 to 537 Ma plutonic trend (Fig. 4.5, 4.6).

4.3.2. Granitoid Plutons

Twenty-six separate granitoid plutons are recognized based on the present study combined with earlier work. The individual plutons are described in Appendix B. They are broadly grouped into three main packages based on lithology, grain size characteristics, and the abundance of mafic minerals: 1) medium-grained, diorite to granodiorite with over 20% biotite and hornblende (see Table 2.2a); 2) generally coarse-grained, locally megacrystic, monzogranite to granodiorite typically containing less than 10% biotite and hornblende (see Table 2.2b); and 3) medium- to fine-grained, locally porphyritic, syenogranite to monzogranite with less than 5% mafic minerals (see Table 2.2c). All three groups are considered to be coeval and cogenetic based on field relations, geochronological data (Chapter 6), and petrochemical continuity. Hence, the petrography, mineral chemistry, and petrochemistry of the three groups of plutons are described together. Significant differences, specific to a set of plutons or individual plutons, are noted as appropriate.

Plutonic rocks assigned to the dioritic to granodioritic group are widespread throughout the terrane but are most abundant southwest of Saint John. They include the Ludgate Lake, Rockwood Park, Perch Lake, Shadow Lake, Talbot Road, Spruce Lake, Belmont, and Renforth plutons, including the smaller Mayflower Lake, Narrows, and Acamac plutons. Most of the plutons are gradational between tonalite and granodiorite, except the Spruce Lake, Belmont, and Renforth plutons which range from quartz diorite to granodiorite and the French Village Quartz Diorite which ranges from diorite to granodiorite (Fig. 4.1; Appendix C.1). They typically form the largest plutons ($>10 \text{ km}^2$) and most are elongate northeast. Flow foliations, where present, are defined by elongate mafic enclaves that are generally oriented parallel to the long axis of plutons. A distinctive characteristic of many of the plutons in this group is the abundance of dioritic to tonalitic enclaves. The majority of these enclaves are interpreted to represent cognate material of earlier consolidated variants of the host (e.g. Pitcher, 1994). However, locally they display minor magma mingling/mixing textures (e.g. Shadow Lake Granodiorite and Lepreau Pluton). Here the dioritic enclaves are interpreted to have crystallized from blebs of immiscible mafic melt within the larger granitoid pluton (e.g. Barbarin and Didier, 1992).

Plutonic units in the monzogranite to granodiorite group are the Fairville, Chalet Lake, Gayton, Milkish Head, Hammond River (and associated Cassidy Lake Inlier), Hanson Stream, Lepreau, and Lepreau Harbour plutons. They are generally smaller ($<10 \text{ km}^2$) and less abundant than the dioritic to granodioritic plutons, and occur scattered throughout the terrane. They typically consist of granodiorite and monzogranite (Fig. 4.1; Appendix C.1). However, a few of the very coarse-grained samples in the Chalet Lake pluton and Cassidy Lake inlier are classified as syenogranite, whereas the Lepreau Harbour pluton is entirely granodioritic in composition. Some parts of the composite Lepreau pluton are tonalitic to quartz dioritic and locally display

magma mingling textures with the monzogranitic portions. In contrast to the dioritic to granodioritic plutons, these units generally lack foliations or abundant enclaves. Granophyric textures are common in these units.

Plutons assigned to the syenogranitic to monzogranitic group are more limited in their geographical distribution than the other two groups and generally occur southwest of Saint John in the Musquash Harbour area. The Jarvies Lake, Cranberry Head, Prince of Wales, and Harvey Hill plutons all show compositional gradations from syenogranite to monzogranite (Fig. 4.1; Appendix C.1); however, some parts of the composite Musquash Harbour Pluton are granodioritic to tonalitic. The Henderson Brook pluton is dominantly monzogranitic, although a few samples are granodioritic. These plutons lack dioritic enclaves, or flow foliations, and are typically leucocratic, granophyric, and highly fractured. Because of intense alteration, no mineral analyses were done for these plutons.

4.3.2.1. Mineralogy

The major mineral phases present in all three groups of plutons are essentially the same, although the relative abundance varies (Appendix C.1). They include plagioclase, potassium feldspar, quartz, hornblende, and biotite. Accessory minerals include titanite, apatite, zircon, magnetite, and rare allanite. Garnet and muscovite were observed only in the Harvey Hill Syenogranite.

Plagioclase in the dioritic to tonalitic plutons (e.g. French Village, Renforth, Belmont, Talbot Road, granodioritic to quartz dioritic units of the Musquash Harbour pluton, and dioritic enclaves) have compositions ranging from An_{31} to An_{53} , with averages greater than An_{40} (Fig. 4.7; Appendix C.3). The more granodioritic plutons in this group (e.g. Rockwood Park, Perch Lake, Shadow Lake, and Ludgate Lake plutons), as well as the granodioritic parts of the Renforth pluton,

have plagioclase with average compositions less than An₄₀. In contrast, average plagioclase compositions in the monzogranitic and syenogranitic plutons are generally less than An₃₀ (Fig. 4.7; Appendix C.3). In some samples plagioclase grains have narrow rims with more albitic compositions (<An₁₀), probably as a result of subsolidus re-equilibration. Normal and oscillatory zoning is common; however, plagioclase in the syenogranitic plutons is not as well zoned as in other units. In the Shadow Lake, Ludgate Lake, and Lepreau plutons, complex plagioclase zoning patterns are more common, and include partly resorbed cores and zones. In addition, some plagioclase grains in the Shadow Lake pluton display reverse zoning. Several processes may result in the formation of complex and reverse zoning at the magmatic stage (e.g. Barbey, 1991); however, the likely mechanism involves increasing the temperature of the magma through mixing of melts of different temperatures (e.g. Hibbard, 1991). The Or component in plagioclase is typically less than 3% but some analyses have K₂O as high as 8%, probably due to incipient sericitic alteration. Myrmekite is common in most plutons, with the exception of the syenogranites, and appears to be a texture that evolved during cooling as opposed to incipient deformation or later alteration.

In most of the plutons, potassium feldspar is typically anhedral, interstitial perthitic microcline; however, in the syenogranitic units, perthitic orthoclase is common and locally forms subhedral phenocrysts. Microcline is generally cryptoperthitic and ranges in composition from Or₉₁ to Or₉₈, with Ab contents <9% and only trace amounts of An (Fig. 4.7). However, some potassium feldspar in the Shadow Lake pluton varies in composition from Or₆₂ to Or₈₅ with Ab contents up to 38%. Sodic lamellae in perthitic grains have only trace amounts of Or and Ab contents up to 98%. Inclusions in the potassium feldspar include plagioclase, hornblende, quartz, and biotite. Granophyric quartz inclusions are common in K-feldspar in the syenogranitic and

monzogranitic plutons.

In all the plutons, quartz typically forms anhedral interstitial grains with small inclusions of plagioclase, biotite, and hornblende. In the Hanson Stream, Milkish Head, and some samples of the Fairville and Chalet Lake plutons, quartz also occurs as single, subhedral rounded subporphyritic grains or aggregates of very fine-grained sutured grains up to 10 mm in diameter. In most of the granitic units, quartz is typically embayed. Rare inclusions of muscovite occur in quartz in the Gayton, Milkish Head, Hammond River, Hanson Stream, and Harvey Hill plutons.

Hornblende, like plagioclase, was mainly an early crystallizing phase in these plutons; however, some grains in the Renforth and French Village plutons, as well as in the dioritic enclaves, are anhedral, poikilitic, and locally interstitial in relation to plagioclase, and appear to have crystallized later. Hornblende commonly displays optical and compositional zoning in the dioritic to granodioritic plutons whereas in the granitic units it is not obviously zoned. Remnant clinopyroxene cores were observed only in some samples from the French Village and Spruce Lake plutons, and from dioritic enclaves in the Shadow Lake pluton. Hornblende is rare in the syenogranite, and is typically chloritized. All the analyzed hornblende grains belong to the calcic amphibole group as defined by Leake (1978), and the majority are magnesio-hornblende (Fig. 4.8). Core to rim variations in Si, Ti, Fe, Na, and K in individual grains are irregular and vary only slightly between samples. However, there is a consistent increase in Al^T , Mn, and Ca and a slight decrease in Mg from core to rim (Appendix C.3). Some hornblende cores in the French Village pluton are compositionally distinct from their rims and the other hornblende compositions. These cores have significantly higher Al^T , Ti, and Na and lower Si, Mn, and K and are ferroan paragonite (Fig. 4.8). High-Al and low-Si hornblende cores have been described elsewhere (e.g. Hammarstrom and Zen, 1986) and attributed to hornblende crystallizing prior to quartz in the melt.

However, the presence of vermicular quartz in the cores of these hornblende grains, interpreted to be the result of early symplectic growth, combined with the high-Ti contents indicates higher temperatures and/or pressures during early crystallization of the melt (Anderson, 1980). Hornblendes from the Fairville and Chalet Lake plutons are distinctly different from compositions in the dioritic to granodioritic plutons. They typically contain high Fe and low Mg, similar to associated biotite compositions (see below), and are ferro-edinitic in composition (Fig. 4.8). This is consistent with the whole rock compositions for these samples.

Biotite typically occurs as subhedral intergranular grains, commonly poikilitic and partially altered to chlorite. Biotite in the syenogranitic plutons is commonly entirely altered to chlorite. Biotite compositions (Appendix C.3) from most of the plutons are generally very restricted in terms of $Mg/(Mg+Fe)$ and Al^{VI} and plot approximately midway between phlogopite and annite (Fig. 4.9). Average FeO/MgO is about 1.5 and consistent with a calc-alkaline host rock (Abdel-Rahman, 1994). In contrast, biotite compositions from the Fairville and Chalet Lake plutons have lower $Mg/(Mg+Fe)$ and FeO/MgO greater than 5.0 which suggests an alkaline host according to the criteria of Abdel-Rahman (1994). However, they lack other mineralogical characteristics such as alkali amphibole to confirm this interpretation.

Magnetite is the most common accessory mineral in the plutonic units and ilmenite was not observed (Appendix C.1, C.3).

4.3.2.2. Petrochemistry

Representative samples from most of the plutons were collected to characterize and classify these units based on major, selected trace, and rare earth elements. Ninety-six samples were analyzed, 51 samples from dioritic to granodioritic plutons, 24 samples from monzogranitic to granodioritic plutons, and 21 samples from syenogranitic to

monzogranitic plutons. Twelve of these samples were also analyzed for rare earth elements. The geochemical data, CIPW normative mineralogies, and statistical data are tabulated in Appendix C.2. Analyses of samples collected by other workers in the area are integrated with data from this study and also noted in Appendix C.2. Sample locations are plotted on Map D.

The plutons range in silica content from a low of 47% in dioritic rocks (e.g. French Village pluton) to 78% in the syenogranitic rocks (e.g. Harvey Hill pluton). Silica content shows a negative correlation with TiO_2 , Al_2O_3 , $\text{Fe}_2\text{O}_3^{\text{T}}$, MnO , MgO , CaO , and P_2O_5 and a positive correlation with Na_2O and K_2O (Fig. 4.2). These trends are consistent with decreasing abundances of hornblende, biotite, and calcic plagioclase and increasing proportions of quartz and potassium feldspar in the more silicic samples. Systematic chemical and mineralogical variations of this type are commonly attributed to fractional crystallization processes (e.g. Tindle and Pearce, 1981). However, Chappell and White (1991) suggest that similar compositional trends may result from different degrees of partial melting of the crust "restite hypothesis". In addition, similar trends have been noted from mafic and felsic magma mixing (e.g. Pitcher, 1994), a model favoured by Whalen et al. (1994) for the origin of plutonic units in the Brookville terrane.

Major and trace element variations in the syenogranitic plutons (e.g. Jarvies Lake and Musquash Harbour) are generally parallel to those in the rhyolitic samples from the Dipper Harbour Volcanic unit, with the exception of considerably lower Na_2O and higher Ba in the rhyolite (Fig. 4.2, 4.3).

Variations in major oxide concentrations in some of the plutons in the monzogranitic to granodioritic group (e.g. Fairville, Chalet Lake, and Gayton plutons) display trends distinctly different from other plutons of similar silica content. These plutons are slightly enriched in TiO_2 , $\text{Fe}_2\text{O}_3^{\text{T}}$, MnO , and P_2O_5 and have steeper slopes on the silica variations diagrams relative to the other plutons. They are also

slightly depleted in Al_2O_3 and MgO .

All of the samples are quartz-normative and, with the exception of the more mafic samples, most are corundum-normative. The aluminum saturation index generally increases from 0.75 to greater than 1.5 with increasing silica content (Fig. 4.4) but the majority are greater than 1.0. The increase in A/CNK from the metaluminous to peraluminous rocks is interpreted to be the result of progressive decrease in CaO due primarily to the removal of hornblende (Cawthorn et al., 1976). The differentiation index also displays a positive correlation with silica and increases from 29 in the dioritic enclaves to 96 in the syenogranites.

The granitoid plutons are dominantly subalkaline (Fig. 4.5) and display a typical calc-alkaline trend (Fig. 4.6). The chemical dissimilarity between many of the monzogranitic to granodioritic units and the other plutons is clear on this diagram. Samples from the Fairville, Chalet Lake, Gayton, Hammond River, and Milkish Head plutons parallel the $\text{Na}_2\text{O}+\text{K}_2\text{O}-\text{FeO}^{\text{T}}$ join. Similarly, the QAP diagram of normative mineral contents (not shown) displays the same pattern, with the Fairville and Chalet Lake more orthoclase-rich.

Most of the trace elements show "normal" variations with SiO_2 , generally attributable to fractional crystallization processes; however these variations are not as smooth as those in the major oxides. With increasing SiO_2 in the granitoid plutons, abundances of Rb and Ba increase and Sr decreases. Rubidium, and to a lesser extent Ba, mimic the variations in K_2O due to their similar chemical characteristics. This is also the case for the similar trends in Sr and CaO which suggests fractional crystallization of alkali feldspar and plagioclase. Barium contents are enriched in the Fairville and Chalet Lake plutons, possibly due to the presence of Ba-rich megacrystic potassium feldspar.

The Y and Zr contents in the low silica units (<65%) display a moderate positive correlation with SiO_2 . In samples with silica

contents greater than 65%, both Y and Zr contents are quite varied and show no systematic trend with silica. This scatter may be the result of preferential fractionation of zircon in certain plutons and not others. Because Nb values are generally low and close to the detection limit of 10 ppm, the abundance patterns are not considered significant.

Zinc and V contents display good negative correlations with SiO_2 . Zinc is attributed to the fractionation of hornblende and/or biotite which can both host Zn (Gill, 1981). Hornblende and biotite can also host V; however, the negative trend is probably due mainly to magnetite fractionation. Nickel, Cr, and Ga contents have weak negative correlations that probably reflect the fractionation of mafic mineral phases, mainly hornblende.

Chondrite-normalized rare earth element (REE) distribution patterns have moderate light rare earth element (LREE) enrichment, slight negative or no Eu anomalies, and relatively flat heavy rare earth element (HREE) patterns (Fig. 4.10). However, granodiorite from the Renforth Pluton is more enriched in LREE and granite from the Hammond River pluton is depleted in HREE. The lack of a Eu anomaly and flat HREE suggests minimal feldspar fractionation or, more likely, simultaneous fractionation of subequal amounts of plagioclase and hornblende, as indicated by the major and trace element patterns (Hanson, 1980). Total REE contents generally increase with increasing silica content. The syenogranitic and monzogranitic plutons have the highest total REE values with the most prominent negative Eu anomalies. The syenogranite sample has a slightly lower total REE content than the monzogranite, probably due to the fractional crystallization of small amounts of titanite, allanite, or apatite.

4.3.3. Gabbroic to Ultramafic Plutons

Three layered gabbroic to ultramafic plutons occur in the Brookville terrane: Duck Lake, Indiantown, and Coverdale (see Table

2.2d; Appendix B). The Duck Lake pluton is a small, irregular-shaped body that outcrops about 10 km northeast of the centre of the city of Saint John. It consists of gabbro, orthopyroxene gabbro, gabbronorite to olivine gabbronorite, and anorthosite, with minor ultramafic rocks such as dunite and wehrlite (Fig. 4.11; Appendix C.1). Numerous small gabbroic bodies in and around the French Village Quartz Diorite to the northeast are interpreted to be related to the Duck Lake pluton. The poorly exposed Indiantown pluton outcrops in the Indiantown area of Saint John. It is essentially composed of anorthosite and orthopyroxene gabbro (Fig. 4.11; Appendix C.1). The Coverdale pluton is located 2 km south of Moncton and is interpreted to be the largest (30 km² in area) gabbroic pluton in the terrane. However, this pluton does not crop out and is covered by Carboniferous sedimentary rocks. Based on limited drill core data it is lithologically similar to the Duck Lake pluton; however, it contains more anorthosite and the ultramafic rocks are oxide-apatite-clinopyroxenites (Fig. 4.11; Appendix C.1).

The gabbroic and ultramafic rocks in the Duck Lake and Coverdale plutons are favourable hosts for nickel sulphides, titanium, and platinum-group elements and have been staked and prospected in detail (e.g. PGE Resource Corp. and Noranda).

4.3.3.1. Mineralogy

The Duck Lake, Indiantown, and Coverdale plutons are dominantly medium- to coarse-grained, inequigranular, and hypidiomorphic to allotriomorphic and commonly display cumulate textures. Mineral chemistry was obtained only from the Duck Lake pluton and not from the Indiantown or Coverdale plutons.

Subhedral, generally unzoned and unaltered plagioclase is the main cumulate phase in all the plutons. In the Duck Lake pluton plagioclase compositions range from bytownite (An₃₅) to almost pure anorthite (An₉₈) in the olivine gabbronorite and labradorite (An₅₈) to bytownite (An₇₄) in

the gabbroic lithologies (Deveau, 1989; Grammatikopoulos, 1992). Plagioclase in anorthosite from the Duck Lake pluton ranges from An₆₅₋₇₀ (Carlsbad-albite combined twin method) where it forms adcumulate textures. Based on optical determinations, plagioclase compositions from similar lithologies in the Indiantown and Coverdale plutons are similar to those in the Duck Lake pluton. Plagioclase grains are typically inclusion-free and clearly crystallized prior to other phases. However, plagioclase from orthopyroxene-bearing gabbro in the Duck Lake pluton displays moderately developed reverse zoning (Grammatikopoulos, 1992), and here the plagioclase contains small laths of clinopyroxene and apatite which suggests co-crystallization. In the Coverdale pluton, plagioclase in the gabbroic samples is typically altered to saussurite and minor carbonate minerals.

Like plagioclase, olivine is a dominant cumulate phase. It generally occurs as discrete euhedral to subhedral grains in the Duck Lake gabbro and the Coverdale clinopyroxenite; however, in dunite and wehrlite samples from the Duck Lake pluton it forms massive, interlocking grains. Olivine is typically highly fractured and completely replaced by serpentine with minor amounts of chlorite and opaque minerals. Compositions obtained from one sample of gabbro in the Duck Lake pluton show little variation (Fo₇₆₋₇₇) (Grammatikopoulos, 1992). Olivine in some gabbro samples from the Duck Lake pluton displays kelyphitic textures with overgrowths of clinopyroxene and amphibole.

In all plutons clinopyroxene is generally anhedral and intercumulate, although locally in a few gabbroic samples from the Duck Lake pluton it is subhedral and suggests that it crystallized with associated subhedral plagioclase. Clinopyroxene is commonly rimmed by amphibole and/or chlorite or is entirely replaced by amphibole or a mixture of chlorite, fibrous actinolite, epidote, and calcite. Clinopyroxenes in the orthopyroxene-bearing gabbro and olivine gabbro from the Duck Lake pluton are salitic to augitic in

composition (Deveau, 1989; Grammatikopoulos, 1992) and similar to clinopyroxene compositions in the Coverdale pluton (D.R. Boyle personal communication, 1994).

Orthopyroxene is less common than clinopyroxene and is typically anhedral and interstitial. Locally in the Indiantown pluton it is subhedral and poikilitic. It displays the same alteration patterns as clinopyroxene. Orthopyroxene in unaltered samples of orthopyroxene-bearing gabbro and olivine gabbro from the Duck Lake pluton are bronzite to hypersthene (Grammatikopoulos, 1992).

Amphibole appears to be secondary in most of the samples, commonly replacing the rims of some pyroxenes. Primary amphibole is rare and is restricted to one sample of olivine gabbro from the Duck Lake pluton where it is intercumulate to clinopyroxene, plagioclase, and olivine. In this sample the composition ranges from magnesio-hornblende to tschermakite (Fig. 4.8). Secondary amphibole from the Duck Lake orthopyroxene-bearing gabbro is magnesio-hornblende with higher $Mg/(Mg+Fe)$ compared to hornblende compositions in the dioritic to monzogranitic plutons (Fig. 4.8). Because the secondary amphibole is not actinolitic in composition it is not interpreted to be the result of greenschist facies metamorphism but probably the result of subsolidus equilibration.

In the Duck Lake and Indiantown plutons, fine-grained opaque minerals are anhedral, locally exhibit skeletal texture, and are commonly associated with chlorite and titanite, suggesting that some of the opaque minerals are secondary in origin. In the Coverdale pluton, larger opaque minerals are also anhedral but commonly occur as discrete amoeboid shapes or complex intercumulate grains. Mineral analyses indicates that magnetite is the dominant phase in the Duck Lake pluton (Deveau, 1989; Grammatikopoulos, 1992) and both magnetite and ilmenite are present in the Coverdale pluton (Boyle and Stirling, 1994).

Euhedral grains of apatite tend to be concentrated within the oxide phases of the Coverdale pluton and a small volume of apatite is

enclosed in clinopyroxene. Samples of olivine gabbronorite from the Duck Lake pluton contain subhedral spinel as inclusions in clinopyroxene.

4.3.3.2. Petrochemistry

A total of 10 samples from gabbro, gabbronorite, olivine gabbronorite, orthopyroxene gabbro, and anorthosite in the Duck Lake and Indiantown plutons were analyzed for major and trace elements. In addition, four samples were analyzed for rare earth elements (Appendix C.2). Sample locations are plotted on Map D. The Coverdale pluton was not sampled for chemistry because of the lack of surface outcrop and limited access to available drill core.

Gabbroic rocks range from 34.9 to 47.0% SiO_2 . Positive correlations with SiO_2 are shown by TiO_2 , Al_2O_3 , CaO , and Na_2O and negative correlations by $\text{Fe}_2\text{O}_3^{\text{T}}$, MnO , and MgO . K_2O and P_2O_5 have very low values and display weak negative correlations with SiO_2 (Fig. 4.2). Most of the trace elements show no correlation with silica; however, Sr is the exception, and increases with increasing silica to about 45% SiO_2 and then sharply decreases (Fig. 4.3). The olivine gabbronorite samples have the highest $\text{Fe}_2\text{O}_3^{\text{T}}$, MgO , Ni, and Cr contents due to the apparent accumulation of olivine and pyroxene.

Most of the analyzed samples are diopside-normative with the exception of four of the more silica-poor samples which are slightly corundum-normative (Appendix C.2). A/CNK values range from 0.6 to 1.1 and are independent of lithology but display a weak negative correlation with silica (Fig. 4.4). Differentiation indices are typically less than 26.

The gabbroic rocks are generally subalkaline, with the exception of a few samples that appear alkaline (Fig. 4.5). The Zr/ TiO_2 vs. Nb/Y diagram of Winchester and Floyd (1977) (not shown) also indicates

subalkaline affinity. Clinopyroxene compositions plotted on the discrimination diagrams of Leterrier et al. (1982) (not shown) also suggests they are subalkaline, but transitional to alkalic (Deveau, 1989; Grammatikopoulos, 1992) and formed in an orogenic setting. On the AFM diagram the gabbroic rocks display tholeiitic affinity (Fig. 4.6).

Chondrite-normalized rare earth element (REE) distribution patterns for samples from the Duck Lake pluton have total REE values considerably lower than samples from the dioritic to syenogranitic plutons and are largely controlled by the cumulus phase present. Two distinct REE patterns are present (Fig. 4.10). Two samples of olivine gabbro-norite have nearly parallel, relatively steep LREE enrichment, a moderate positive Eu anomaly, and a depleted HREE pattern. The other two samples of Indiantown anorthosite and Duck Lake gabbro-norite have a flat LREE pattern with little or no Eu anomaly and slightly depleted, relatively flat HREE. The positive Eu anomalies suggest that plagioclase is an important cumulate phase which is supported by the presence of abundant anorthosite. LREE enrichment with Ce <10 ppm in the Duck Lake and Indiantown plutons is typical in rocks which lack cumulus apatite (e.g. Hanson, 1980).

4.4. DYKES

Although a minor component in the Brookville terrane, dykes have long been recognized in the Saint John area and were first described in detail by W.D. Matthew (1895); later workers expanded on his observations (Cumming, 1916; Hayes and Howell, 1937; Alcock, 1938; Wardle, 1978; Dickson, 1983). The dykes were generally considered to be Late Precambrian (Late Neoproterozoic) in age and used to imply a coeval relationship with the adjacent Caledonia terrane (e.g. Currie, 1983; Dickson, 1983). Therefore a thorough description is warranted here (Appendix B).

Because of their subvolcanic character, the dykes are named

following the volcanic rock classification of Streckeisen (1979), with amendments from Cas and Wright (1987). More than 90% of the dykes are basaltic to andesitic in composition. Dacitic to rhyodacitic dykes are rare. Aplitic and pegmatitic dykes are only slightly more common and because of their granitoid composition are named following the plutonic rock classification scheme of Streckeisen (1976).

The age(s) of the dykes are poorly constrained. All the dykes appear to be younger than the plutonic rocks because they intrude both the plutons and their associated contact aureoles. The youngest pluton dated at ca. 537 Ma (French Village pluton; U-Pb zircon) (Chapter 5) provides a maximum age for dyke emplacement and the lack of dykes in the Devonian to Carboniferous sedimentary rocks provides a minimum age. Muscovite extracted from a pegmatite dyke has yielded an $^{40}\text{Ar}/^{39}\text{Ar}$ cooling age of ca. 510 Ma (Dallmeyer and Nance, 1992) which gives a minimum age for pegmatite and associated aplite dyke emplacement. Similar pegmatite and aplite dykes are locally cut by basaltic and andesitic dykes which suggests that many of the mafic dykes are younger than ca. 510 Ma.

4.4.1. Basaltic to andesitic dykes

The basaltic to andesitic dykes are typically 1 to 2 m wide, fine- to medium-grained and equigranular to locally inequigranular and porphyritic, with well developed chilled margins. They consist of plagioclase and amphibole, with varying, but minor, amounts of quartz, potassium feldspar, clinopyroxene, titanite, apatite, and opaque minerals (Fig. 4.12; Appendix B).

Plagioclase laths commonly display pilotaxitic texture, although trachyoidal textures are locally developed near the interiors of larger dykes. Saussuritization and sericitization of plagioclase is locally intense, although some of the coarser grained samples display unaltered, normally zoned, acicular laths with compositions that range from An_{25-35} .

Amphibole locally occurs as a secondary replacement on the rims of clinopyroxene, but more commonly it forms randomly oriented, weakly zoned, prismatic grains interstitial to plagioclase, with no obvious igneous precursor. Clinopyroxene occurs as subhedral to anhedral, poikilitic grains with inclusions of altered plagioclase. Amphibole and clinopyroxene are commonly partially to entirely altered to biotite and/or chlorite.

Anhedral quartz and potassium feldspar are rare and tend to be restricted to interstices and appear to be the last minerals to have crystallized in these dykes. Euhedral apatite laths are common inclusions in the plagioclase, quartz, and potassium feldspar. Orthopyroxene and olivine were not observed in any samples.

The secondary mineral assemblage (amphibole, biotite, and chlorite) is probably the result of deuteric alteration as opposed to the regional metamorphism suggested by Dickson (1983). Igneous textures are well preserved in all samples as well as primary igneous zoning in plagioclase.

4.4.2. Petrochemistry

Ten samples for major and trace element analyses were collected from the basaltic and andesitic dykes (Appendix C.2). Sample locations are plotted on Map D. The samples range in silica content from 46.2 to 52.3% and the major and trace element contents show considerable scatter. The narrow range in silica contents and relatively low LOI values (generally less than 3%) suggest that the scatter is not a product of alteration. Some trends appear to be present in the data, although the range in silica is small. With increasing silica, MgO, CaO, Sr, and Ni decrease, and Na₂O, P₂O₅, and Ga increase (Fig. 4.2, 4.3). These trends are similar to those obtained by Dickson (1983) for mafic dykes in the Musquash area. He attributed these patterns to pyroxene and olivine fractionation.

The mafic dykes contain normative quartz and corundum and are metaluminous (Fig. 4.4). Differentiation indices range from 21 to 43 (Appendix C). They are dominantly subalkaline (Fig. 4.5) and the iron enrichment trend along the MgO-FeO^T join indicates a tholeiitic affinity (Fig. 4.6).

4.4.3. Dacitic to rhyodactic dykes

Dacitic to rhyodactic dykes are typically aphanitic and inequigranular with subhedral to euhedral phenocrysts of plagioclase and quartz set in a matrix of anhedral quartz, plagioclase, microcline, and euhedral muscovite (Fig. 4.12; Appendix C.1). These dykes are generally less altered than the basaltic to andesitic dykes and show little textural or mineralogical variation from margins to interiors. Plagioclase phenocrysts are locally altered to sericite; however, composition determined on unaltered grains is about An₁₅₋₂₀. Plagioclase in the groundmass has sericitized cores and clear albitic(?) rims. Quartz phenocrysts commonly display embayed boundaries and weak undulose extinction. Rare phenocrysts of biotite are partially altered to chlorite and calcite. Microcline is restricted to the groundmass.

4.4.4. Pegmatite and aplite dykes

Pegmatite dykes are typically coarse-grained, allotriomorphic, and inequigranular, whereas aplite dykes are aphanitic to fine-grained and locally subporphyritic. Both contain the same minerals as the syenogranite plutons but in different proportions. However, based on their ca. 510 Ma muscovite age, many are not considered to be cogenetic with the plutons.

Microcline is the most prominent mineral (Fig. 4.12; Appendix C.1) and is typically anhedral, finely to coarsely perthitic, and generally occurs in interstitial granophyre or as separate grains. It commonly

has serrated margins with numerous angular and rounded inclusions of quartz and plagioclase.

Plagioclase occurs as weakly zoned, moderately sericitized, anhedral grains with compositions of An₁₀₋₂₀. Grain boundaries are typically strongly serrated; however, phenocrysts in the aplite dykes are subhedral to euhedral. Plagioclase may contain inclusions of rounded quartz and microcline and are partially enclosed by larger microcline grains.

Anhedral quartz displays the same serrated boundaries and occurs as interstitial grains in the granophyre and, rarely, as large (up to 1 cm) subhedral grains in pegmatite. The serrated quartz and plagioclase grain boundaries appear to be a primary crystallization textures as opposed to a deformational feature.

Muscovite and biotite form large, locally kinked single grains or "books" with minor alteration to chlorite along cleavage traces. Accessory minerals include rosettes of pleochroic blue euhedral tourmaline with apatite, titanite, zircon, and rare garnet.

4.5. CONDITIONS OF CRYSTALLIZATION IN THE ca. 548 TO 537 Ma PLUTONS

Understanding the evolution of granitoid plutons requires knowledge of the depth at which the various minerals crystallized. Estimation of crystallization pressures in the ca. 548 to 537 Ma plutons was based on the empirical calibrations of Hammarstrom and Zen (1986) and Hollister et al. (1987) using the Al content of hornblende coexisting with quartz, plagioclase, K-feldspar, biotite, titanite, and magnetite. Estimation of crystallization temperatures was largely based on the plagioclase geothermometer of Blundy and Holland (1990). Complicating factors such as iron substitution in amphibole, effects of oxygen fugacity, and volatile and magma compositions (e.g. Hammarstrom and Zen, 1986; Hollister et al., 1987; Rutherford et al., 1989; Holland and Blundy, 1994; Anderson and Smith, 1995) are important considerations

in the crystallization of magma; however, as a first approximation these factors are considered negligible.

Calculation of rim and core crystallization pressures for an average of spots in individual hornblende samples using the calibrations of Hammarstrom and Zen (1986) (P1) and Hollister et al. (1987) (P2) are similar and typically within error (Table 4.2). However, calculated pressures obtain from the equation of Hammarstrom and Zen (1986) are typically lower and more compatible with inferred P-T conditions from associated contact aureoles (Chapter 5).

The application of the amphibole-plagioclase geothermometer is complicated by zoning in plagioclase and hornblende and uncertainties as to which part of the plagioclase crystallized in equilibrium with the co-existing amphibole. For the most part amphibole and plagioclase that share a common grain boundary were selected and here it is assumed that the cores of both minerals constitute a pair, as does the rims.

There is a positive correlation between the calculated rim pressure and temperature estimates with the highest values from the dioritic to tonalitic plutons (Fig. 4.13; Table 4.2). The exceptions are the Fairville and Chalet Lake granites and French Village Quartz Diorite that yield relatively higher pressures (3.5 to 5.3 kbar) and temperatures (734 to 800°C). Calculated core pressure and temperature estimates subparallel this trend; however, compared to their respective rim P-T estimates there is considerable scatter (Table 4.2). However, some hornblende cores are compositionally distinct from their rims (e.g. sample CW88-246; section 4.3.2.1) and are attributed to early crystallization of hornblende cores in the melt under higher pressure and temperature conditions.

Many of these plutons crystallized under relatively vapour-undersaturated conditions where P_{H_2O} was on the order of 0.75 to 2.0 kbar (Fig. 4.13). However, the abundance of local pegmatites in some of the plutons requires that some portions of the magma became water-saturated during the final stages of crystallization. However, from

field evidence dyke emplacement occurred after many of the plutons had solidified and may not be related to the main magmatic event.

The positive correlation (Fig. 4.13) is likely a cooling trend (cf. Blundy and Holland, 1990) which represents near and sub-solidus re-equilibration of amphibole and plagioclase, and is consistent with an upper mesozonal to epizonal depth of emplacement. This is confirmed by field relations where the associated country rocks are typically contact metamorphosed to hornblende-hornfels facies (Chapter 5) and geochronology which indicates rapid cooling and crystallization of most igneous units (Chapter 6). However, the calculated pressures and temperatures are the highest for samples from the French Village, Chalet Lake, and Fairville plutons which is broadly consistent with pyroxene-hornfels facies metamorphism in the adjacent Green Head Group (Chapter 5) and indicates a deeper level of emplacement.

4.6. TECTONIC SETTING

A detailed investigation of the petrogenesis of the various igneous units is beyond the scope of this study; however, some inferences can be made with regard to genetic classification and tectonic setting. The close spatial and temporal characteristics between the dioritic to syenogranitic plutons and the rhyolite of the Dipper Harbour volcanic unit suggest a genetic relationship between them. The petrochemical trends in the major and trace elements and normal variations in the A/CNK and differentiation indices suggest chemical continuity between these groups. This, combined with geochronology (Chapter 6), indicates that these plutonic and volcanic units were emplaced during the same magmatic event, and provides compelling evidence that they are genetically related.

The systematic chemical variations in these units can be explained by plagioclase and hornblende fractionation. The progressive removal of hornblende with increasing silica explains the systematic decrease in

TiO₂, Fe₂O₃^T, MnO, and V and the relative absence of hornblende in the syenogranitic plutons. Plagioclase fractionation is indicated by the negative Eu anomaly and the decrease in CaO and Sr and the marked increase in Rb and Ba. Although magma mixing is evident in a few plutons, it is a minor, outcrop-scale feature that is not regionally extensive and therefore can not account for the all the systematic chemical variations.

All the dioritic plutons have Ni contents significantly lower than 40 ppm and are therefore unlikely to have been derived from a mantle peridotite (Gill, 1981). The relatively undepleted, flat HREE patterns suggest that the source was dominantly amphibole-bearing and not garnet-bearing (Nicholls and Harris, 1980).

The major differences in major, trace, and rare earth elements abundances between the dioritic to syenogranitic plutons and the gabbroic plutons are not compatible with an origin from the same source. The presence of spinel and anorthosite layers, low total REE abundances, and positive Eu anomalies suggests that these gabbroic rocks may represent cumulates possibly derived from fractional crystallization of magma derived from a mantle (ultramafic) source.

The basaltic and andesitic dykes have major and trace element compositions that are distinctly different, and combined with field relations, it is clear that they lack a comagmatic relationship with the other mafic intrusions in the Brookville terrane. The consistently high Ni content suggests derivation from a mantle peridotite (Gill, 1981).

It is obvious from the modal QAP plots (Fig. 4.1) that the dioritic to syenogranitic plutons, mafic enclaves, rhyolitic units, and to a lesser extent the orthogneiss define a compositionally expanded, calc-alkaline distribution (Lameyre and Bowden, 1982) typical of I-type granitoid rocks.

On the discrimination diagrams of Whalen et al. (1987) using the concentration of high field strength elements, samples from the orthogneiss, and cogenetic plutonic and volcanic rocks plot mostly

within the fields for I-type and fractionated felsic granite types. However, samples from the Fairville, Chalet Lake, and Gayton plutons tend to overlap with the A-type field. An example of this is shown on the FeO^T/MgO versus $\text{Zr}+\text{Nb}+\text{Ce}+\text{Y}$ plot (Fig. 4.14). The Fairville, Chalet Lake, and Gayton plutons could on their own be classified as having an A-type affinity, but their association with the dioritic to granodioritic plutons that display a trend back towards "normal" granite compositions suggests they are more likely to be fractionated I-type granites. The distinctive S-shaped trend, and slight overlap into the A-type field is interpreted to be the result of late fractionation of zircon from the melt.

On the widely used Rb versus Nb+Y tectonic setting discrimination diagram of Pearce et al. (1984) for felsic samples ($\text{SiO}_2 > 65\%$) the orthogneiss and a majority of the plutons lie within the field occupied by granitoid rocks formed in volcanic arcs (Fig. 4.15). Some samples from the Fairville, Chalet Lake, Gayton, and syenogranite plutons plot in the volcanic arc field but most plot in the within plate field with the rhyolite samples. The trend from volcanic arc to within plate granites simply reflects the relatively incompatible character of the elements concerned (Rb, Y, Nb) and such behaviour is typical of fractionated I-type granites emplaced above a subduction zone along an active continental margin (Pearce et al., 1984).

The orthogneiss, and cogenetic granitoid plutons and associated volcanic rocks are marginally metaluminous to dominantly peraluminous (Fig. 4.4) which is in contrast to chemical criteria that I-type granitoid rocks are metaluminous with $\text{A}/\text{CNK} < 1.1$ (e.g. Chappell and White, 1974). However, peraluminous granitoid rocks can form by a variety of mechanisms (e.g. Halliday et al., 1981) and in I-type granitoid rocks fractional crystallization of amphibole can result in peraluminous chemical characteristics (Cawthorn et al., 1976).

Determining tectonic setting and geochemical signature for gabbroic rocks is difficult and has been questioned by many authors

(e.g. Arculus, 1987). This is a particular problem when dealing with layered intrusions where the usual tectonic setting discrimination diagrams for mafic rocks are not intended for cumulates (e.g. Shervais, 1977; Pearce and Cann, 1973; Meschede, 1986). Grammatikopoulos (1992) used these diagrams to indicate a volcanic arc tectonic setting for the Duck Lake pluton; however, it is unclear if all the gabbroic to ultramafic rocks in the Brookville terrane formed this way.

The basaltic to andesitic dykes are mainly subalkaline and display a tholeiitic trend. On the Ti-Zr-Y tectonic setting diagram of Pearce and Cann (1973) they dominantly plot in the volcanic-arc tholeiites (VAT)-mid-ocean-ridge basalts (MORB) with some overlap in the calc-alkaline basalt field (CAB) (Fig. 4.16). This indicates that many of these dykes formed in a volcanic arc setting. However, the emplacement age(s) of these dykes, a key element in deciphering their tectonic significance, is unknown.

4.7. SUMMARY

1. Detailed systematic pluton mapping, combined with geochronology, petrography, and petrochemistry has resulted in the subdivision of the Brookville terrane into geologically meaningful units. The plutonic and volcanic rocks are subdivided into 4 distinct groups: a) an older (ca. 605 Ma) tonalitic to granodioritic orthogneiss and amphibolite interlayered with paragneissic rocks of the Brookville Gneiss; b) a set of 26 relatively undeformed granitoid plutons that are grouped into dioritic to granodioritic plutons, monzogranitic to granodioritic plutons, and syenogranitic to monzogranitic plutons; c) the Dipper Harbour volcanic unit which is subdivided into a dominantly rhyolitic unit, an andesitic to dacitic unit, and a mixed andesitic to rhyolitic unit with minor sedimentary rocks; d) a younger set gabbroic to ultramafic rocks that comprise 3 plutons. An extensive set of dykes intrude all these units and are subdivided into basaltic to andesitic

dykes, dacitic to rhyodactic dykes, and pegmatite and aplite dykes.

2. The tonalitic to granodioritic orthogneiss exhibit petrographic (Chapter 5) and chemical characteristics typical of I-type granitoid rocks. They define a tight cluster on all variation diagrams, indicating they are probably part of a single petrogenetic suite.

3. The geological setting and age of the dioritic to syenogranitic plutons and associated volcanic rocks indicate that they may represent a single continuum (or punctuated episodes) of calc-alkaline, subduction-related magmatism in the latest Neoproterozoic to Cambrian. Chemical characteristics indicate that hornblende and plagioclase were the dominant fractionating phases. The apparent A-type affinity of the Fairville, Chalet Lake, and Gayton plutons may be the result of accessory phases (e.g. zircon) not fractionating from the melt. Many of the silica-rich granitoid rocks have Alumina Saturation Indices >1 and are peraluminous with quartz in the norm. The silica-poor rocks have Alumina Saturation Indices <1 and are metaluminous with diopside in the norm.

The I-type chemistry in the granitoid rocks is reflected by the I-type mineralogy. Most of the plutons contain hornblende and rare relict clinopyroxene and lack diagnostic S-type minerals such as cordierite, muscovite, and garnet (except for the Harvey Hill pluton). The occurrence of abundant mafic enclaves in many of the plutons is also typical of I-type plutons.

Based on geothermobarometry and field relations many of these plutons crystallized under upper mesozonal to epizonal conditions.

4. The tholeiitic layered gabbroic to ultramafic plutons are younger, not related to the main period of plutonism, and are of unknown age and tectonic affinity.

5. Although minor, the dykes are the youngest igneous rocks in the Brookville terrane and appear to be of two ages. Pegmatite and aplite dykes are older than ca. 510 Ma but younger than ca. 537 Ma and are of unknown tectonic setting. Tholeiitic basaltic to andesitic dykes

appear to be younger than ca. 510 Ma and older than Devonian and formed in a volcanic arc setting.

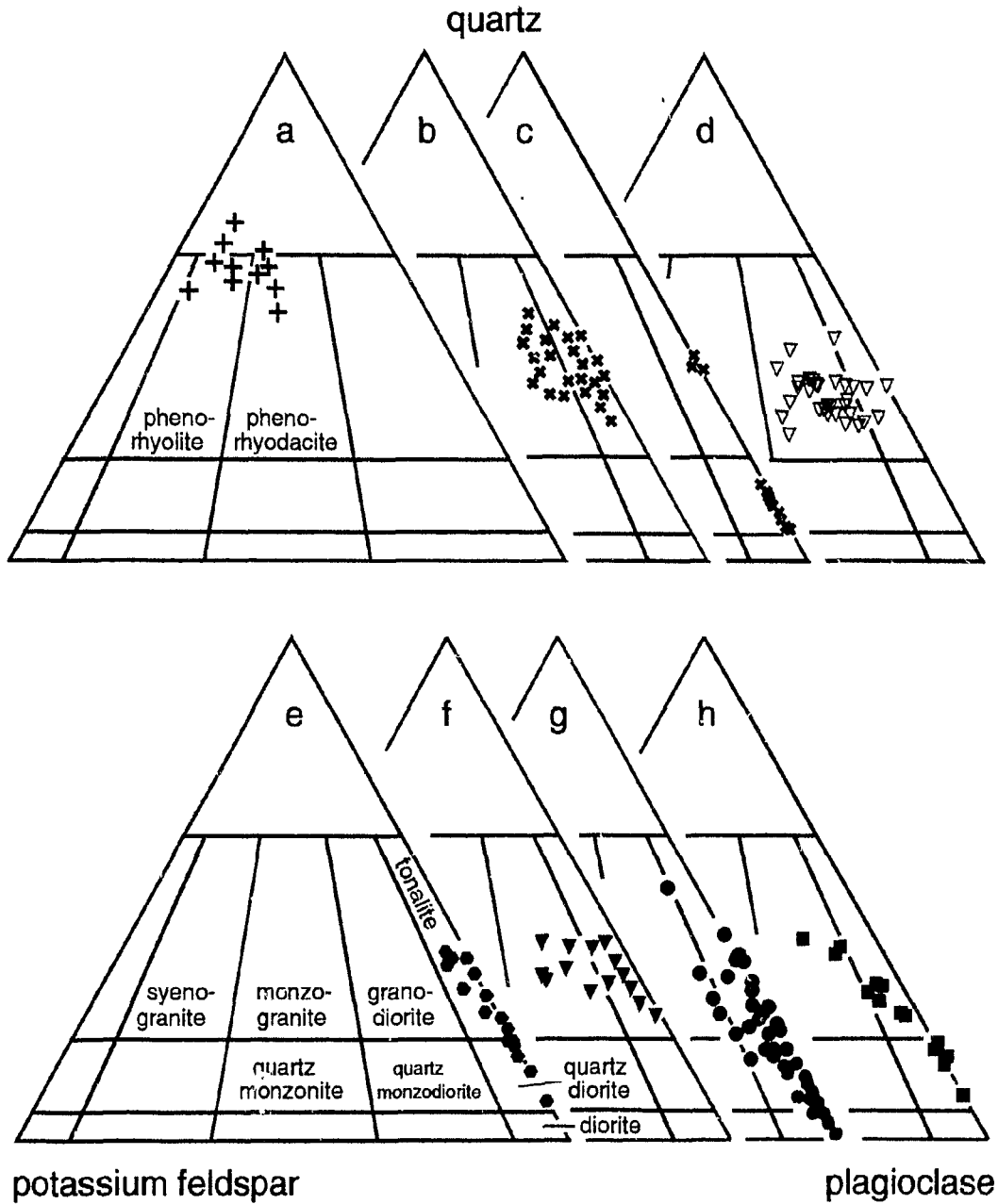


Figure 4.1. Ternary plots of modal quartz-plagioclase-potassium feldspar compositions of samples from the volcanic and plutonic units in the Brookville terrane. Fields and nomenclature from Streckeison (1976). a) Dipper Harbour rhyolite; b) Brookville Gneiss orthogneiss; c) Brookville Gneiss amphibolite and associated tonalitic dykelets; d) Ludgate Lake Granodiorite; e) Spruce Lake Pluton; f) Rockwood Park Granodiorite; g) French Village Quartz Diorite and related dioritic plutons; h) Belmont Tonalite.

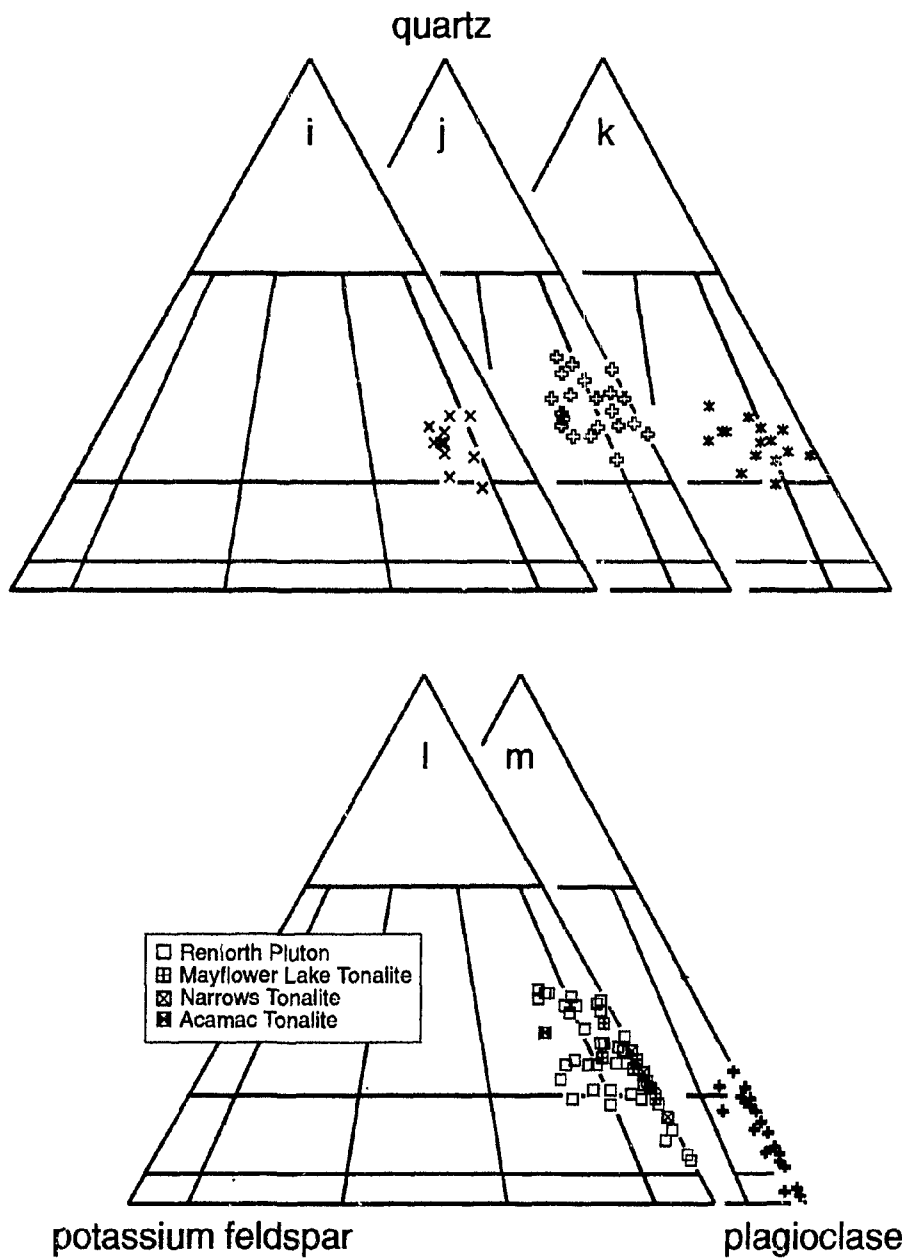


Figure 4.1. Continued. i) Perch Lake Granodiorite; j) Shadow Lake Granodiorite; k) Talbot Road Granodiorite; l) Renforth Pluton and Mayflower Lake, Narrows, and Acamac tonalites; m) mafic enclaves.

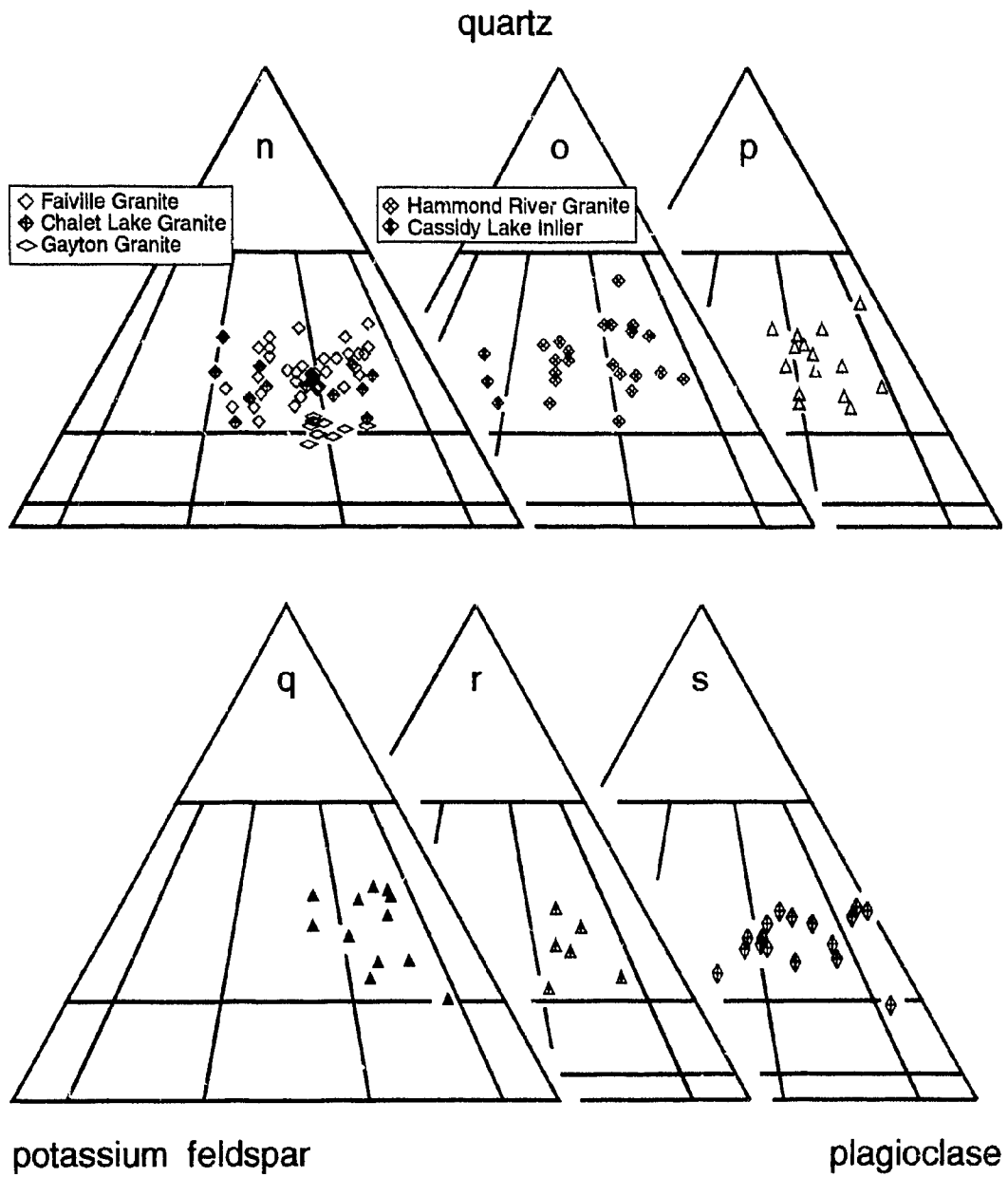


Figure 4.1. Continued. n) Fairville, Chalet Lake, and Gayton granites; o) Hammond River Granite and Cassidy Lake Inlier; p) Milkish Head Pluton; q) Hanson Stream Granodiorite; r) Lepreau Granodiorite; s) Lepreau Pluton.

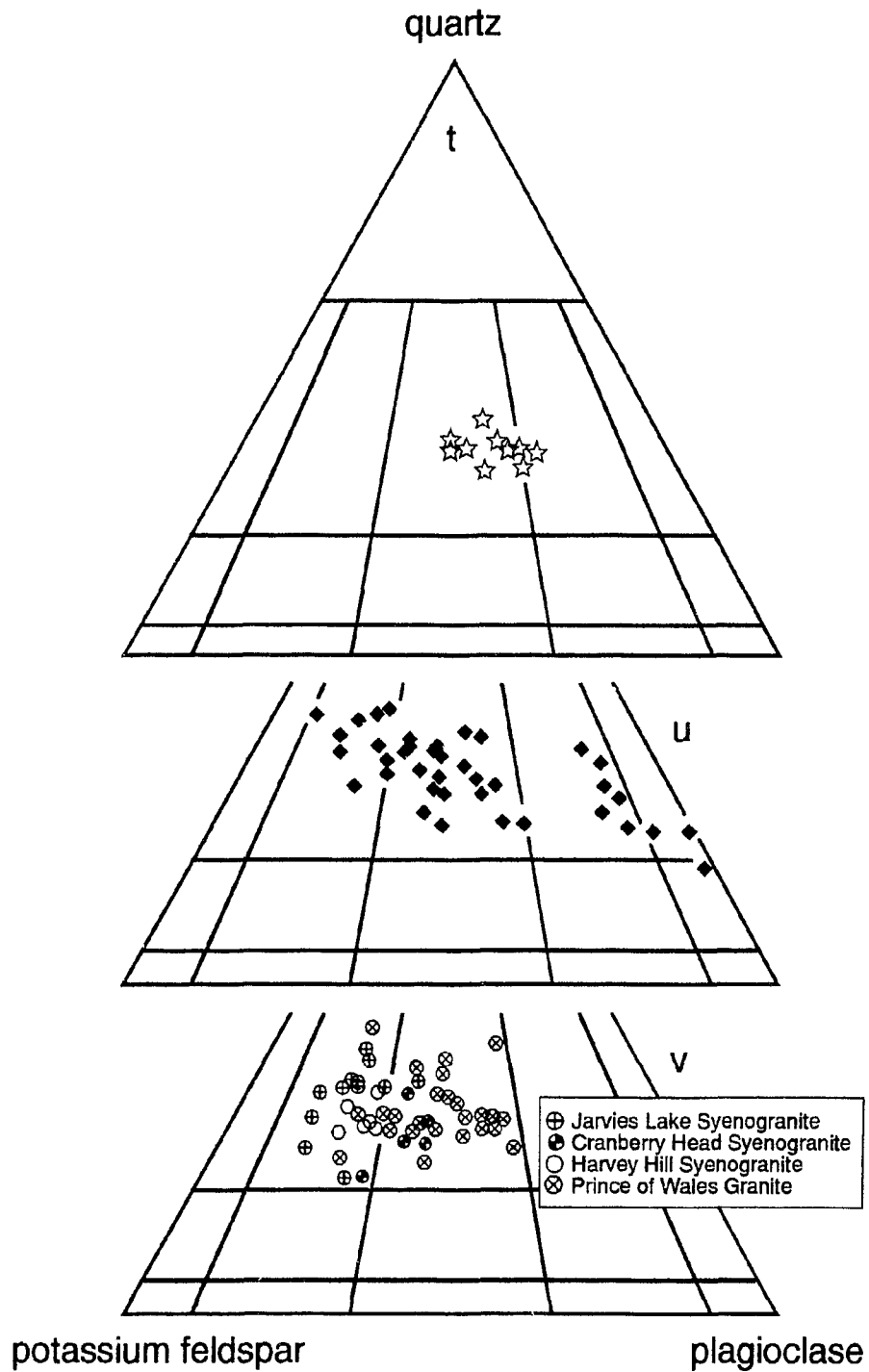


Figure 4.1. Continued. t) Henderson Brook Granite; u) Musquash Harbour Granite; v) Jarvis Lake, Cranberry Head, and Harvey Hill syenogranites, and Prince of Wales Granite.

List of symbols used in figures 4.2 and 4.3.

Dioritic to Granodioritic Plutons

- | | | | |
|---|-------------------------------|---|--------------------------|
| ▽ | Ludgate Lake Granodiorite | ⊕ | Shadow Lake Granodiorite |
| ○ | Spruce Lake Pluton | ⊕ | Shadow Lake enclave |
| ▼ | Rockwood Park Granodiorite | * | Talbot Road Granodiorite |
| ● | French Village Quartz Diorite | □ | Renforth Pluton |
| ■ | Belmont Tonalite | ▣ | Mayflower Lake Tonalite |
| × | Perch Lake Granodiorite | ⊠ | Narrows Tonalite |

Monzogranitic to Granodioritic Plutons

- ◇ Fairville Granite
- ⊠ Chalet Lake Granite
- ◇ Gayton Granite
- ⊠ Hammond River Granite
- △ Milkish Head Pluton
- ▲ Hanson Stream Granodiorite
- ⊠ Lepreau Harbour Granodiorite
- ⊠ Lepreau Pluton
- ◆ Deformed Granitoid Rocks

Syenogranitic to Monzogranitic Plutons and related volcanic rocks

- ☆ Henderson Brook Granite
- ◆ Musquash Harbour Pluton
- ⊕ Jarvies Lake Syenogranite
- Cranberry Head Syenogranite
- ⊗ Prince of Wales Granite
- Harvey Hill Syenogranite
- + Dipper Harbour rhyolitic units

Gabbroic to Ultramafic Plutons

- ◇ Duck Lake Pluton
- ◆ Indiantown Pluton
- ◆ Coverdale Pluton

Brookville Gneiss

- * Orthogneiss
- ⊗ Hornblende-bearing gneiss

Dykes

- ★ Basalt to andesite
- ◇ Pegmatite and aplite

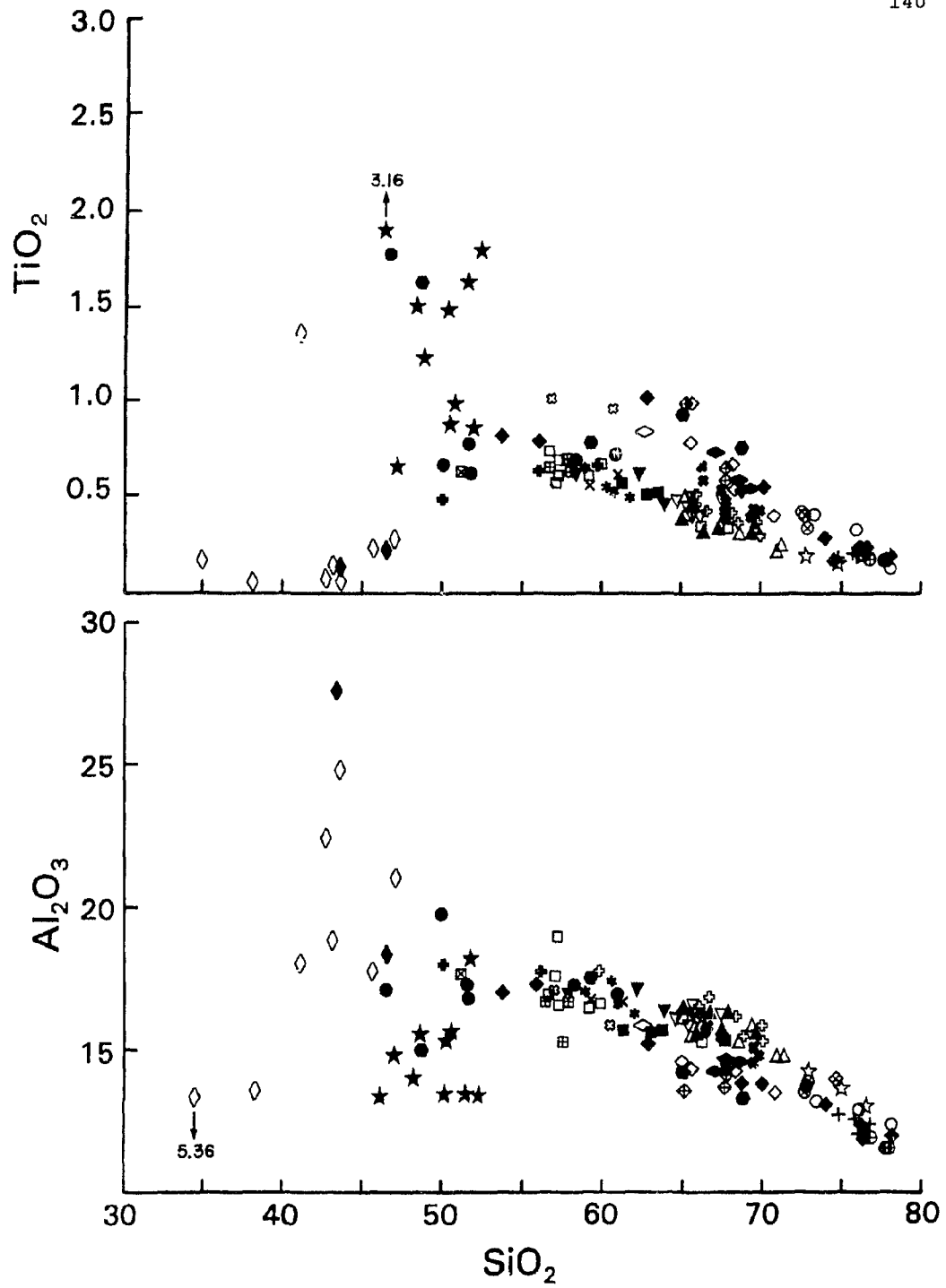


Figure 4.2a. Major element silica variation diagrams for analyzed samples from the study area. Plots of TiO_2 and Al_2O_3 against SiO_2 .

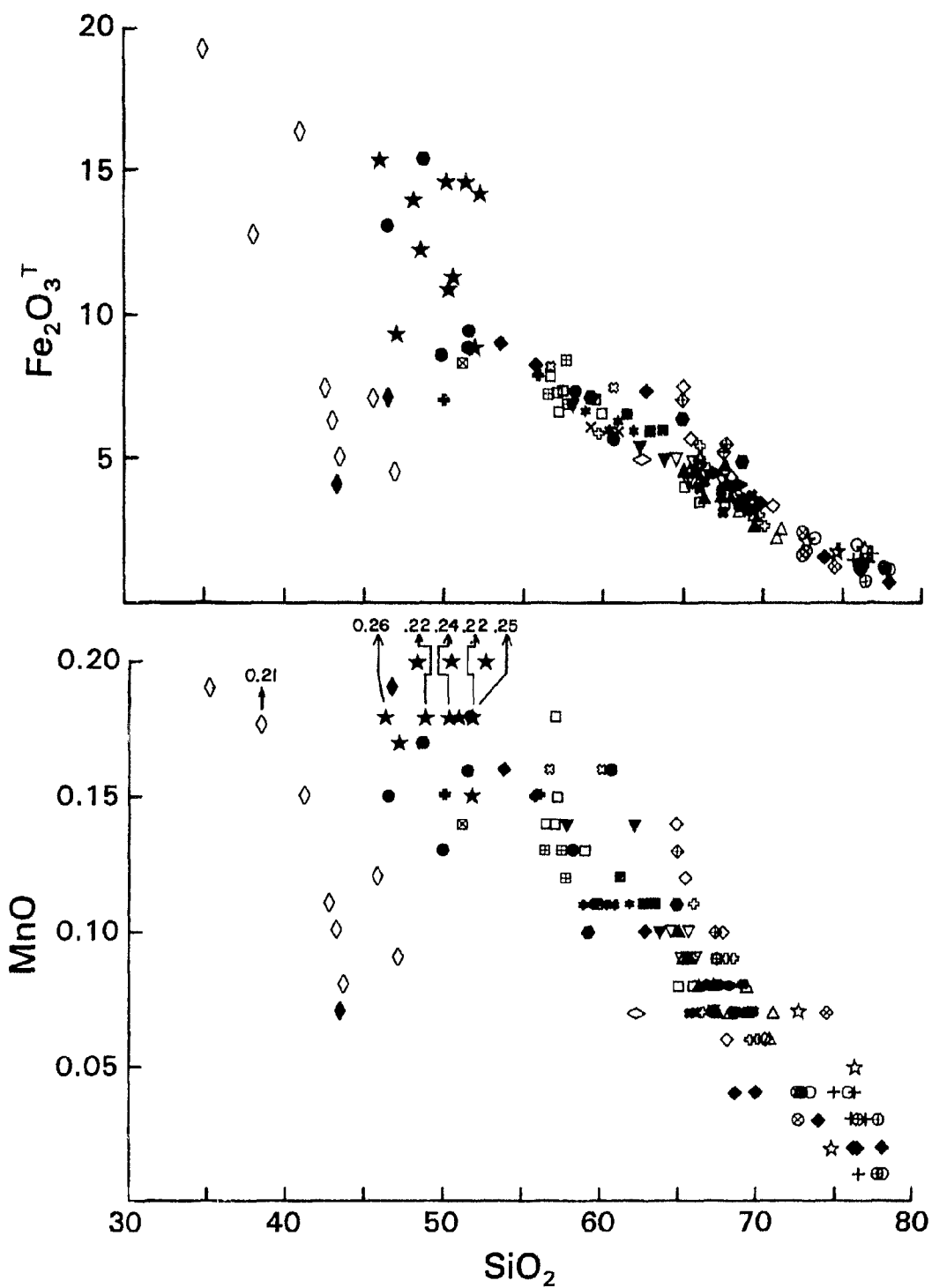


Figure 4.2b. Continued. Plots of Fe_2O_3^T and MnO against SiO_2 .

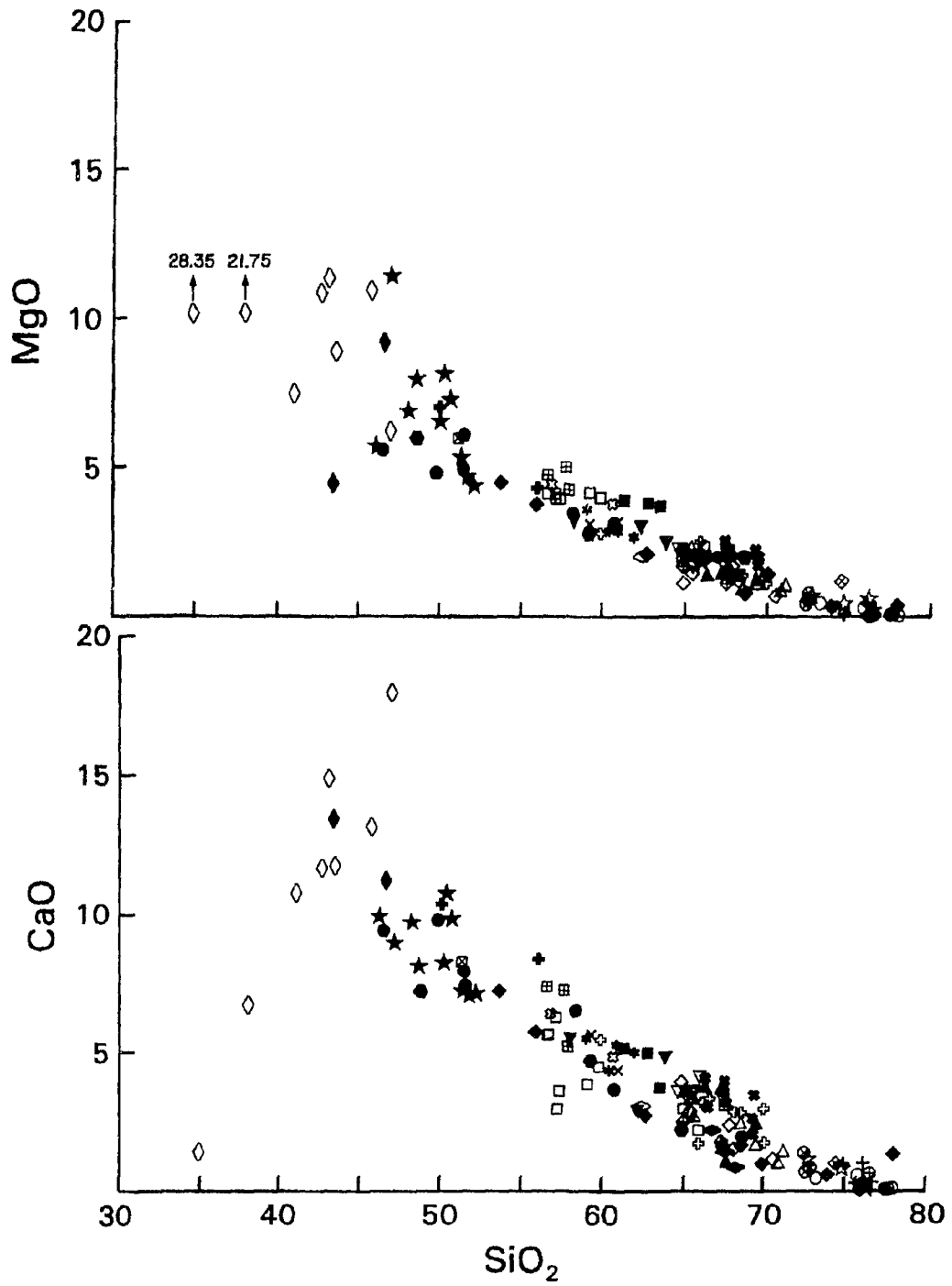


Figure 4.2c. Continued. Plots of MgO and CaO against SiO_2 .

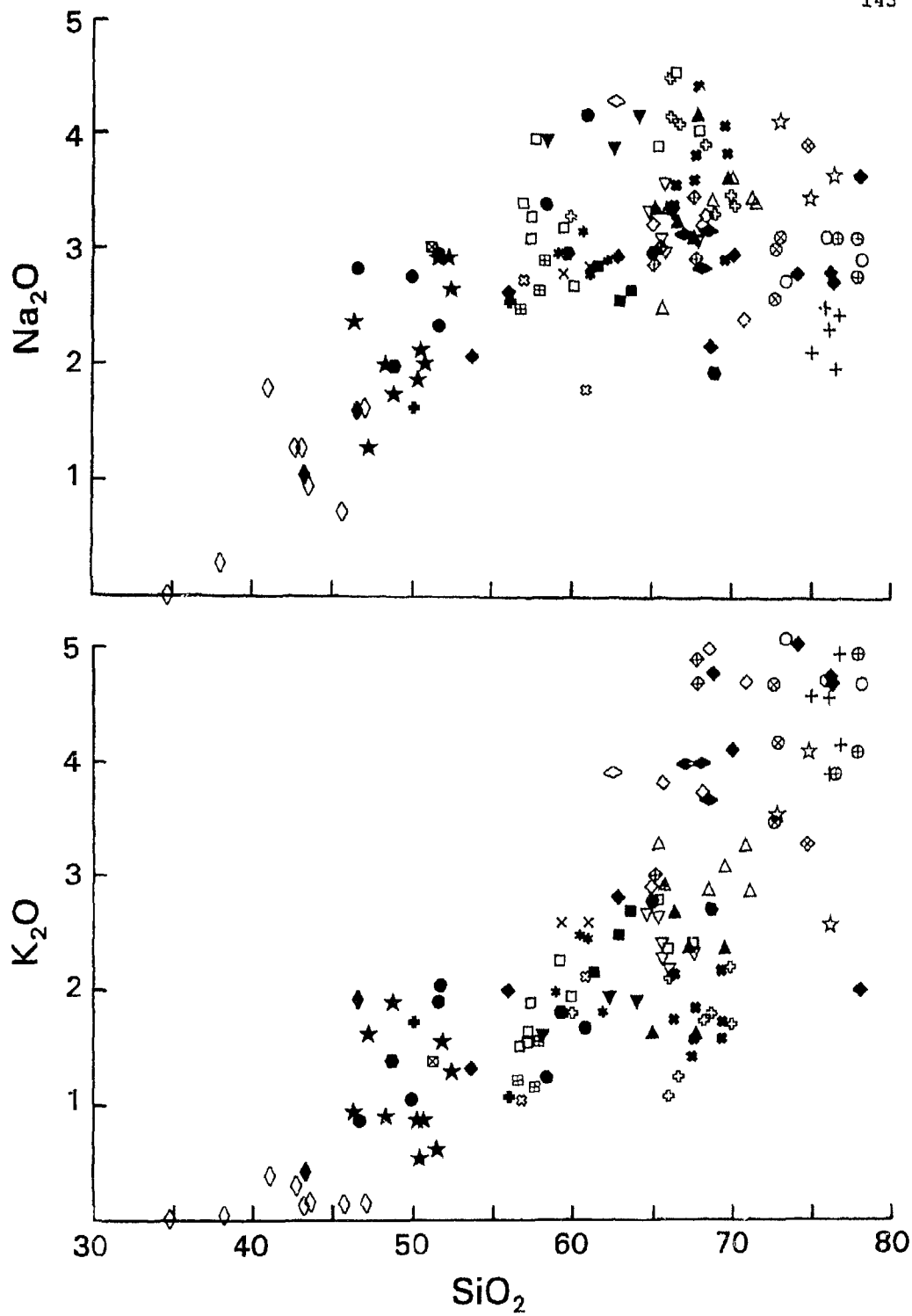


Figure 4.2d. Continued. Plots of Na_2O and K_2O against SiO_2 .

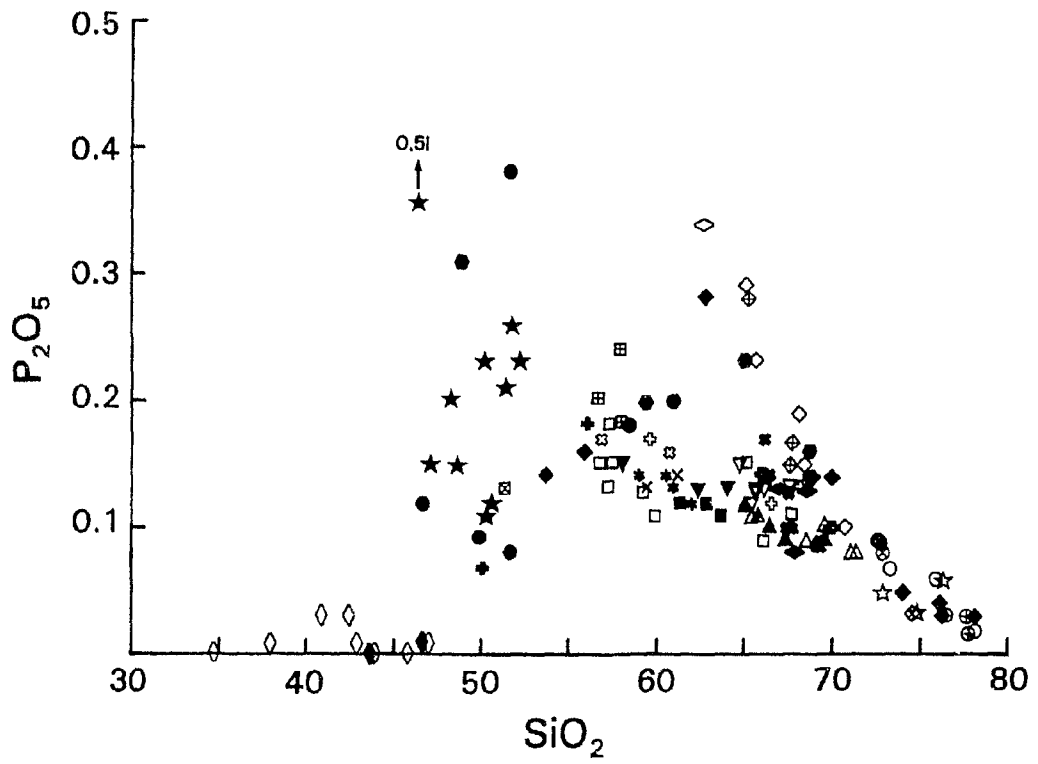


Figure 4.2e. Continued. Plot of P_2O_5 against SiO_2 .

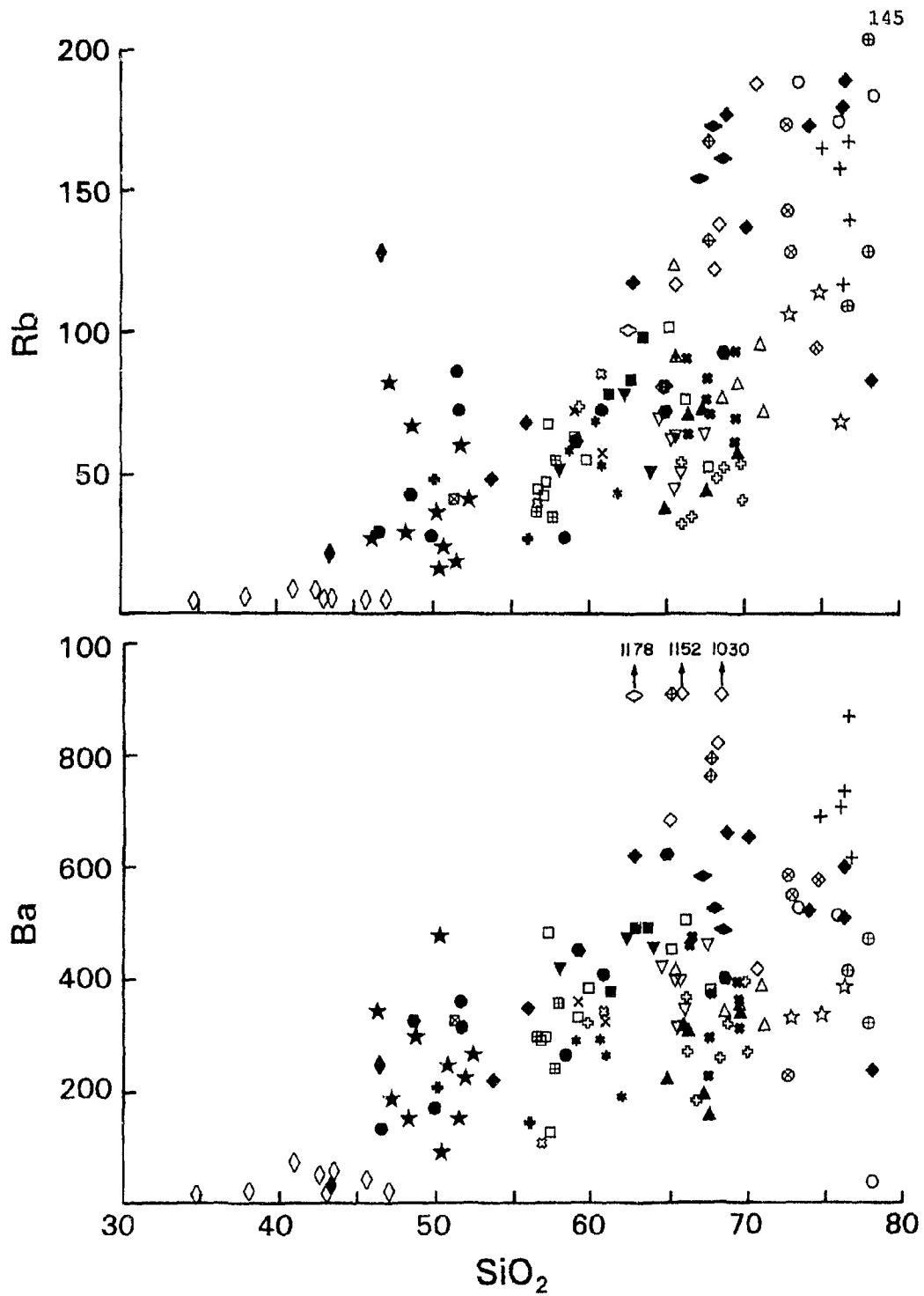


Figure 4.3a. Trace element silica variation diagrams for analyzed samples from the study area. Plots of Rb and Ba against SiO_2 .

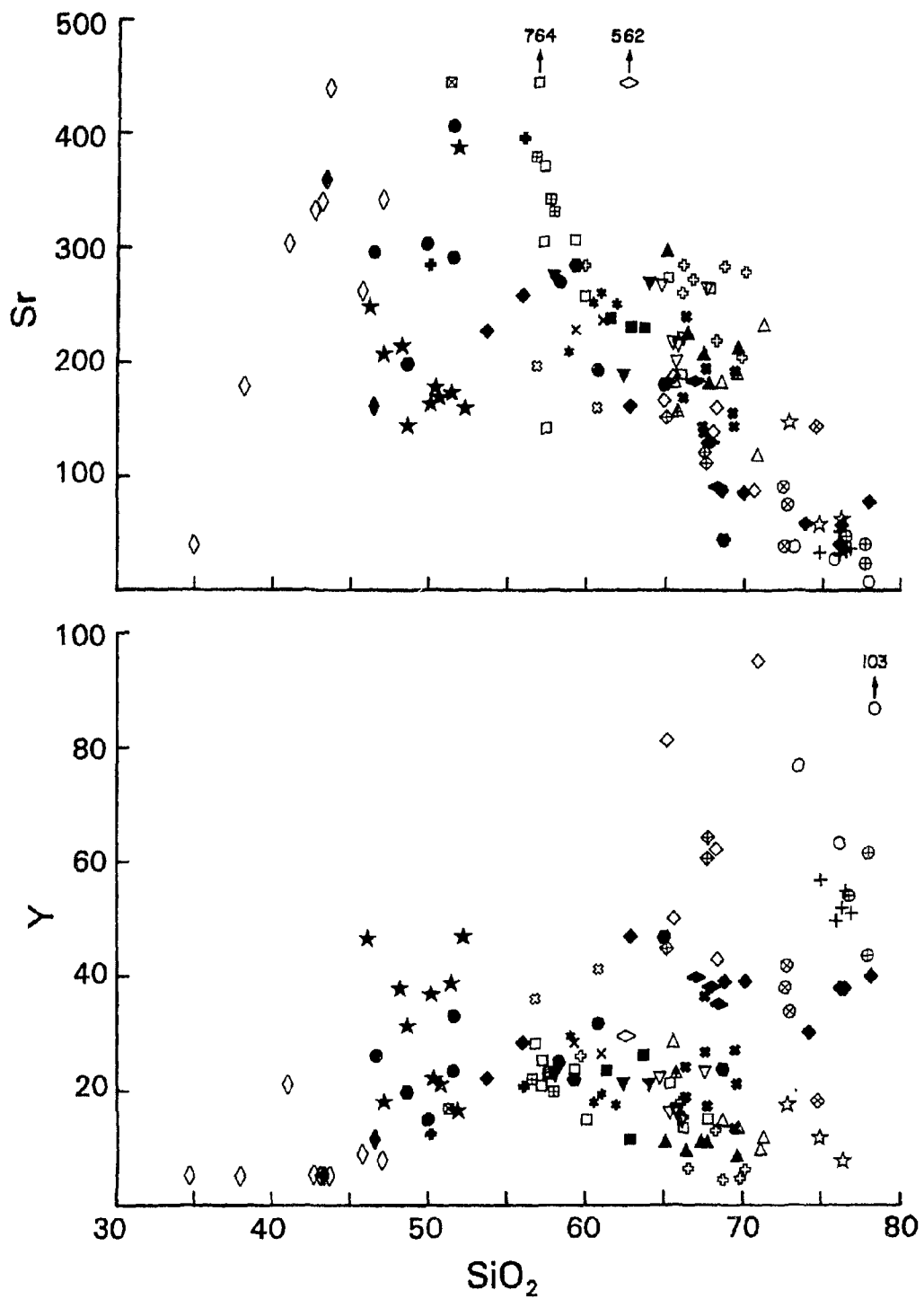


Figure 4.3b. Continued. Plots of Sr and Y against SiO_2 .

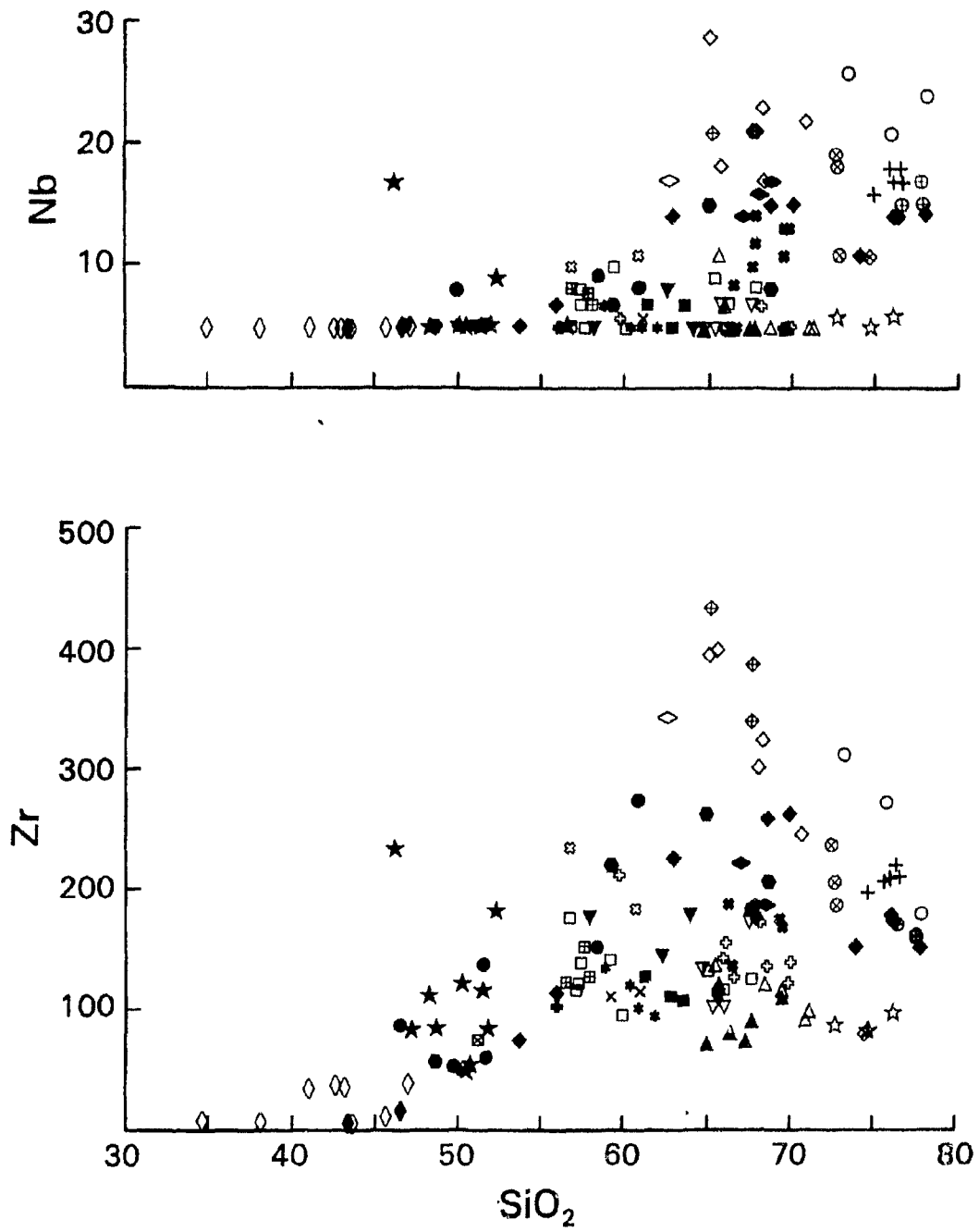


Figure 4.3c. Continued. Plots of Nb and Zr against SiO₂.

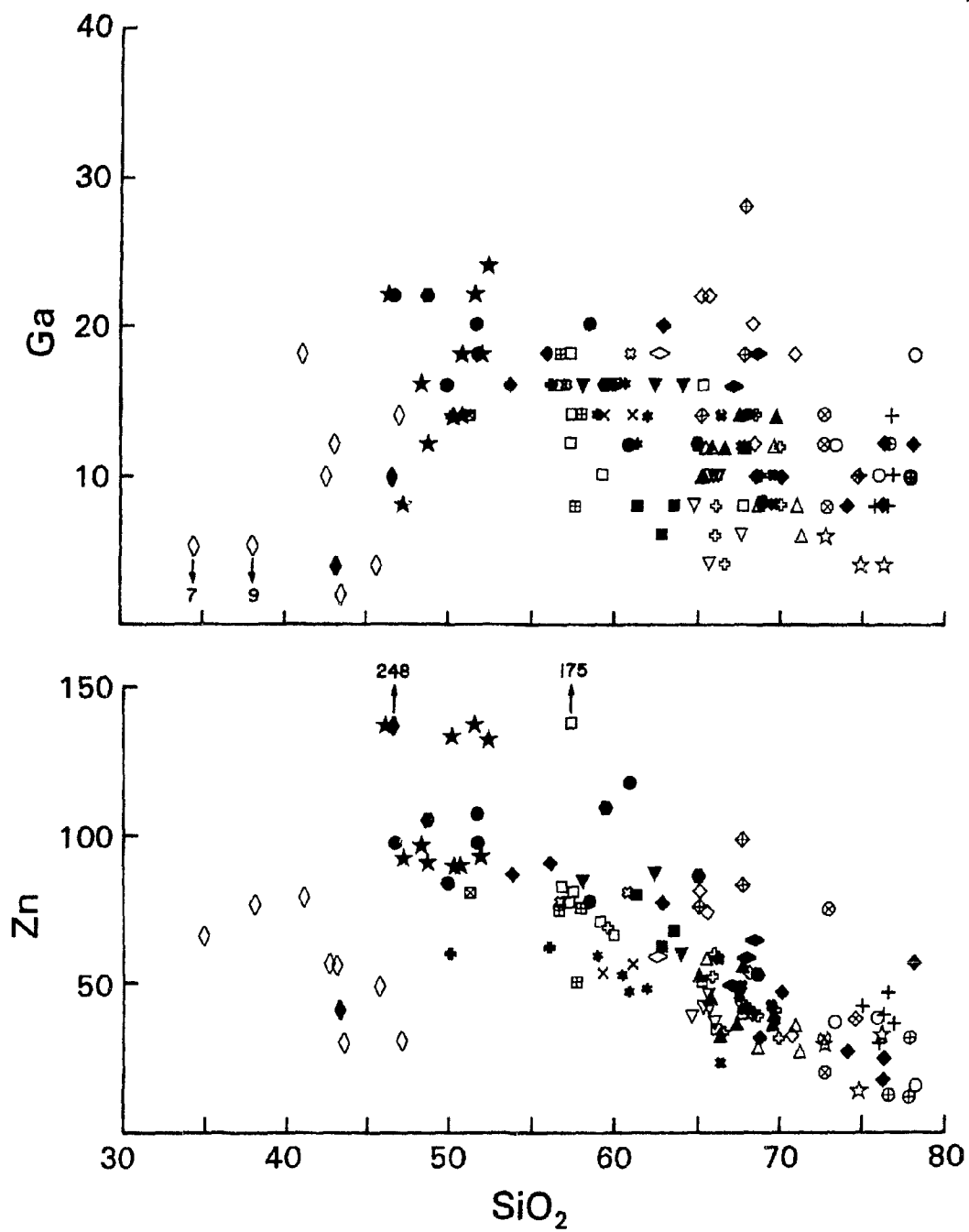


Figure 4.3d. Continued. Plots of Ga and Zn against SiO_2 .

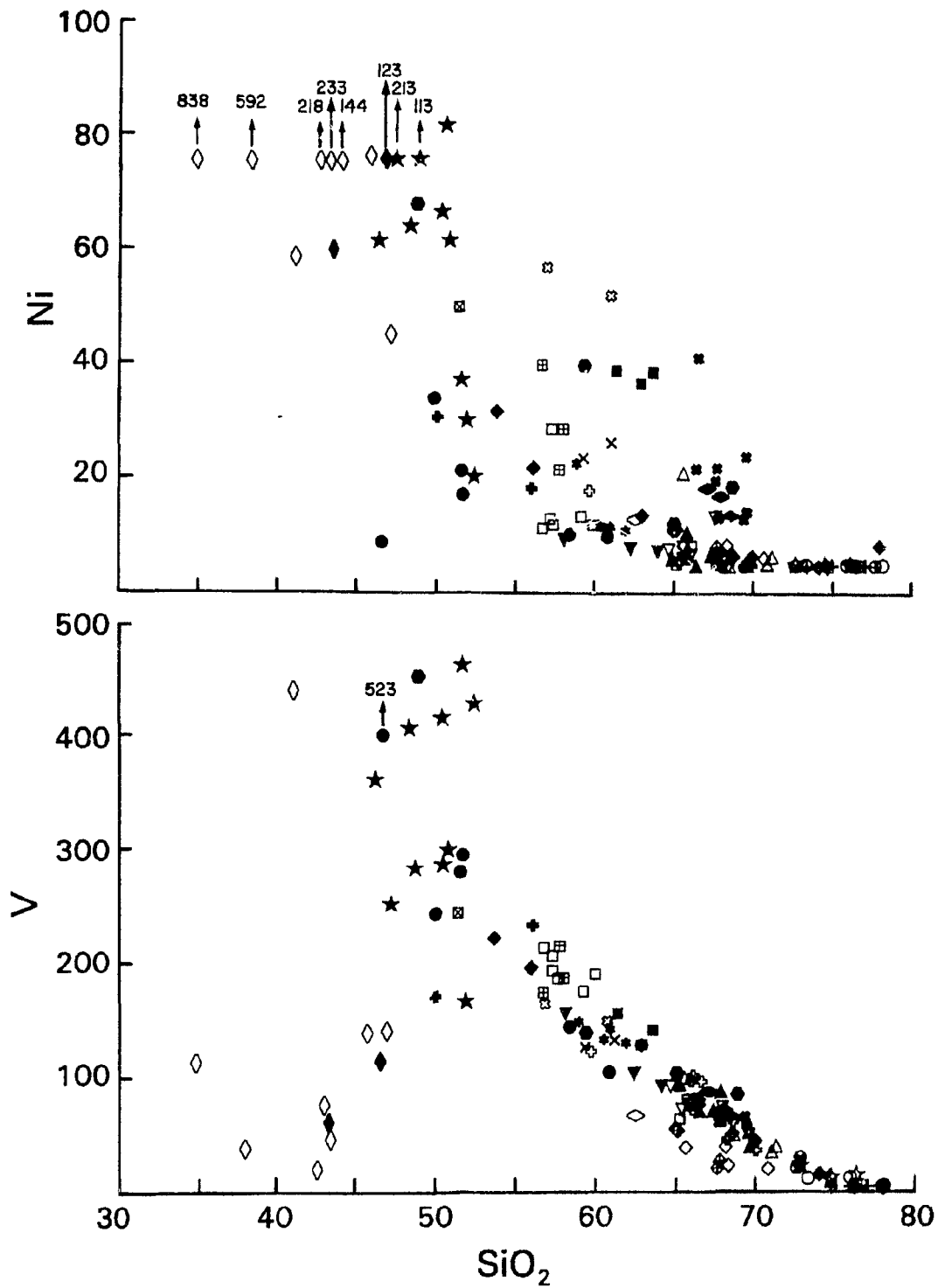


Figure 4.3e. Continued. Plots of Ni and V against SiO_2 .

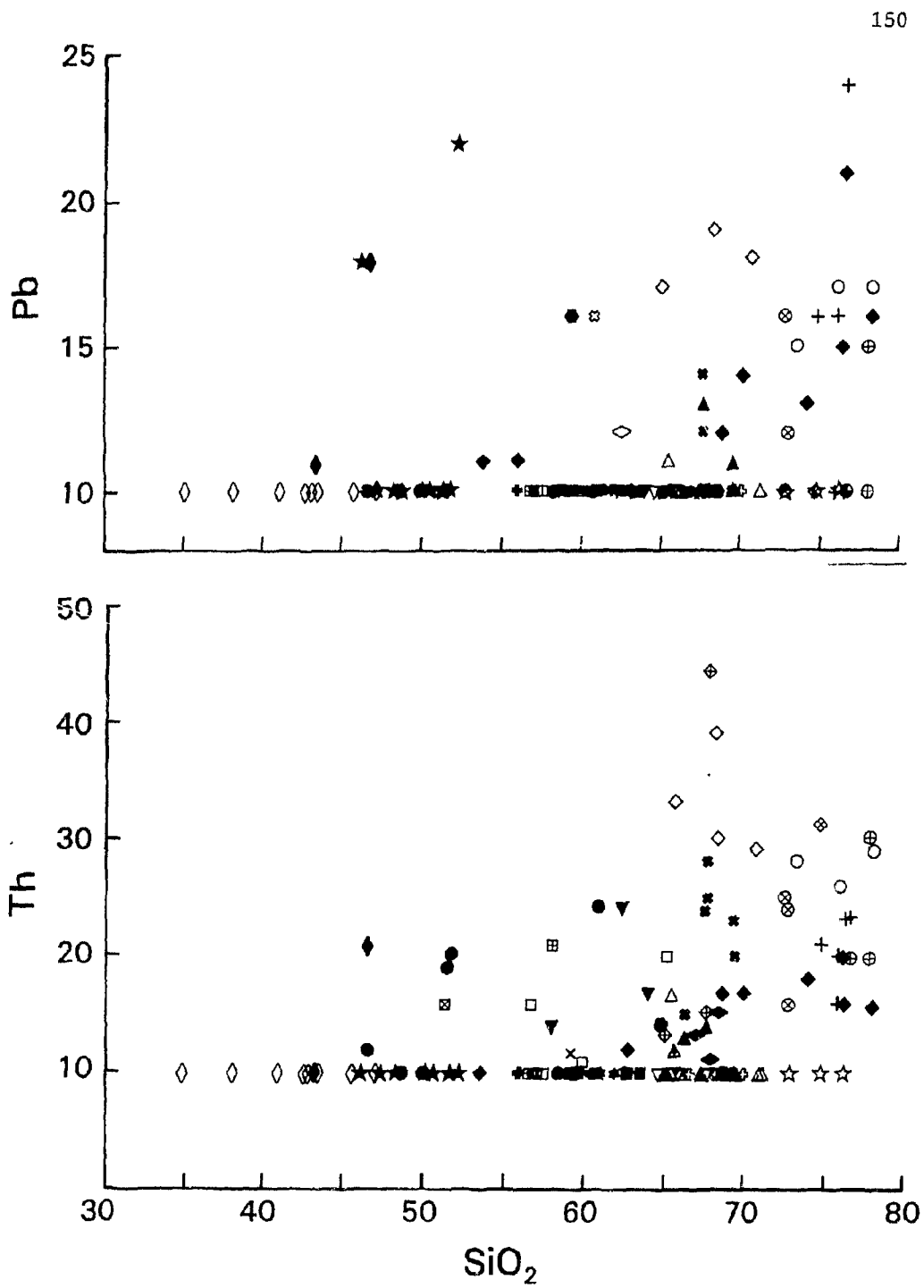


Figure 4.3f. Continued. Plots of Pb and Th against SiO₂.

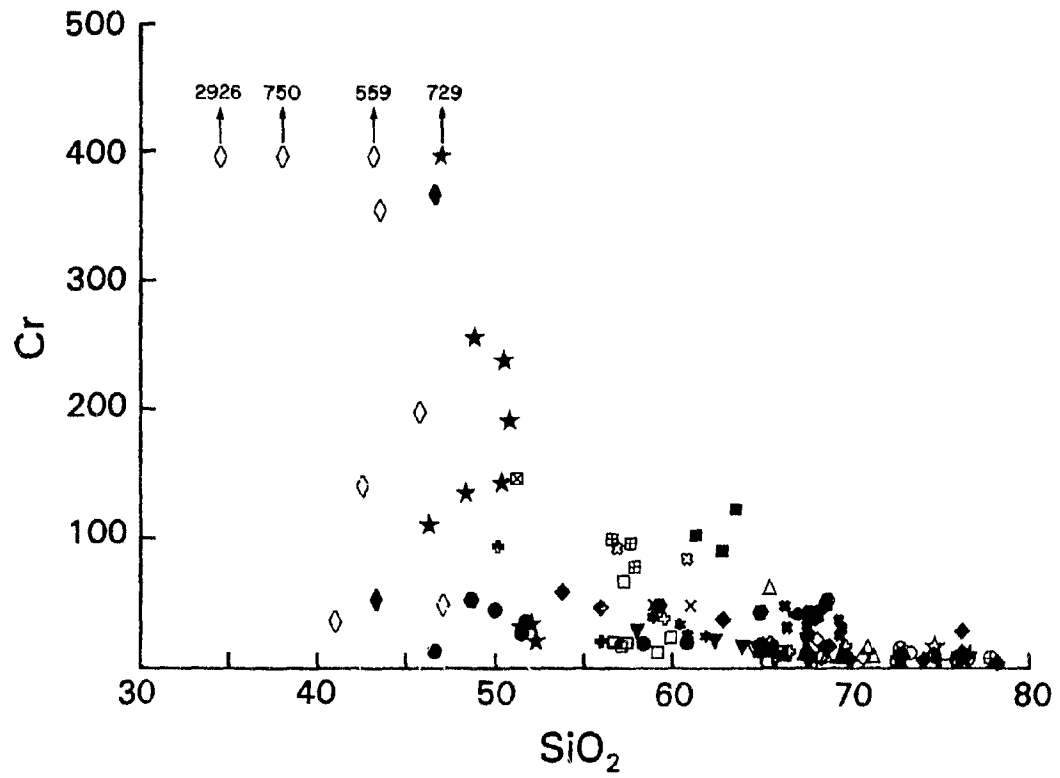
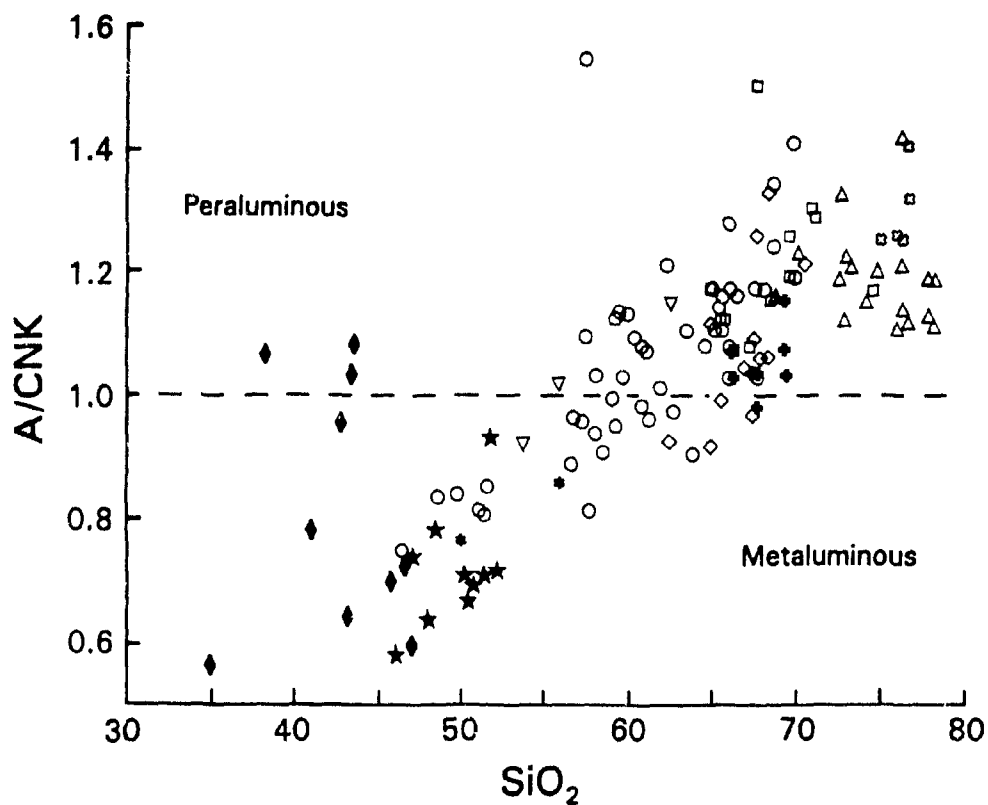


Figure 4.3g. Continued. Plot of Cr against SiO₂.



- diontic to granodioritic plutons
- * diontic to tonalitic enclaves
- monzogranitic to granodioritic plutons
- ◇ Fairville, Chalet Lake, and Gayton plutons
- △ syenogranitic to granitic plutons
- ▽ mafic units in Musquash Harbour Pluton
- ⊗ Dipper Harbour rhyolite
- ◆ Gabbroic plutons
- ⊕ orthogneiss
- ★ basaltic and andesitic dykes

Figure 4.4. A/CNK against SiO₂ variation diagram for analyzed samples from the study area. A/CNK = molar Al₂O₃/(CaO + K₂O + Na₂O). Line separating peraluminous and metaluminous fields from Shand (1947).

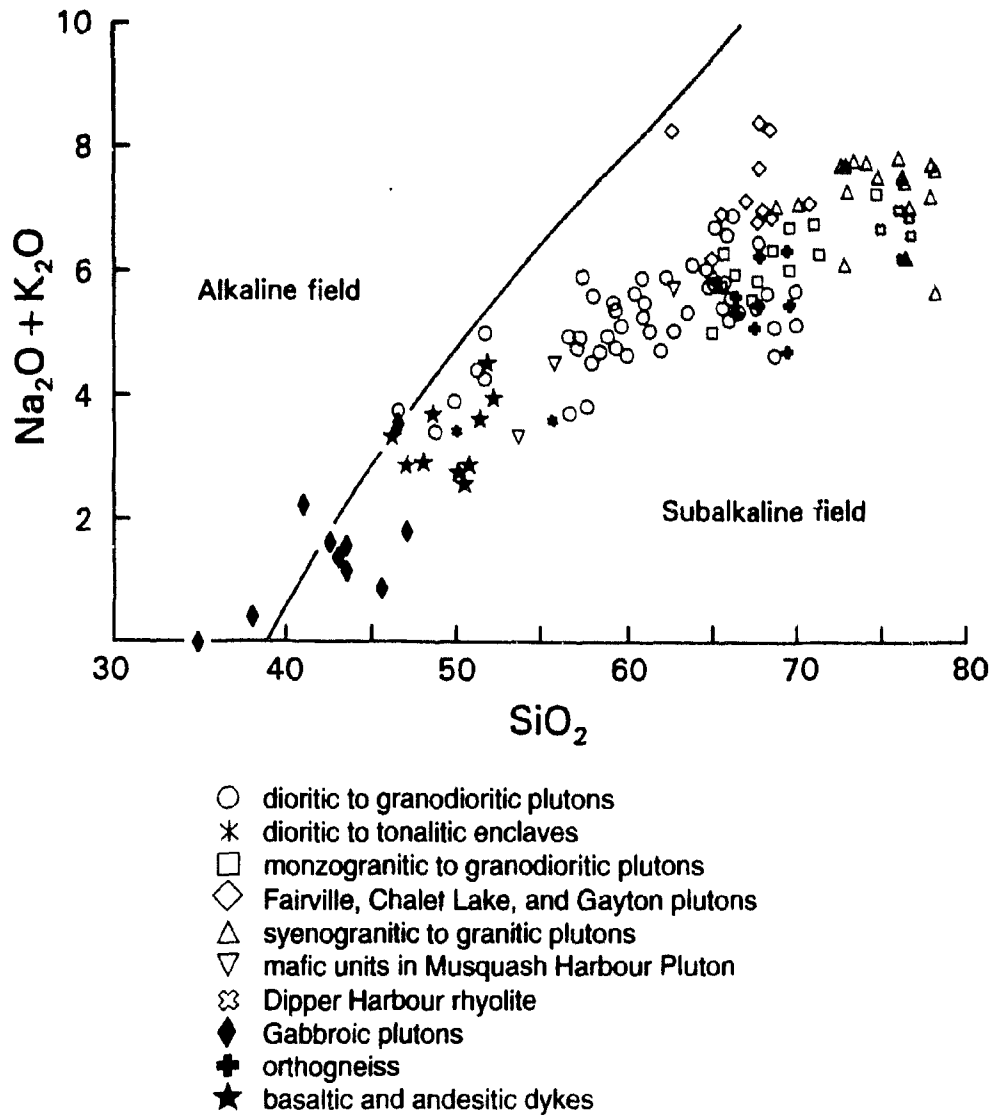


Figure 4.5. Na₂O + K₂O against SiO₂ variation diagram for analyzed samples from the study area. Line separating alkaline from subalkaline fields is from Irvine and Baragar (1971).

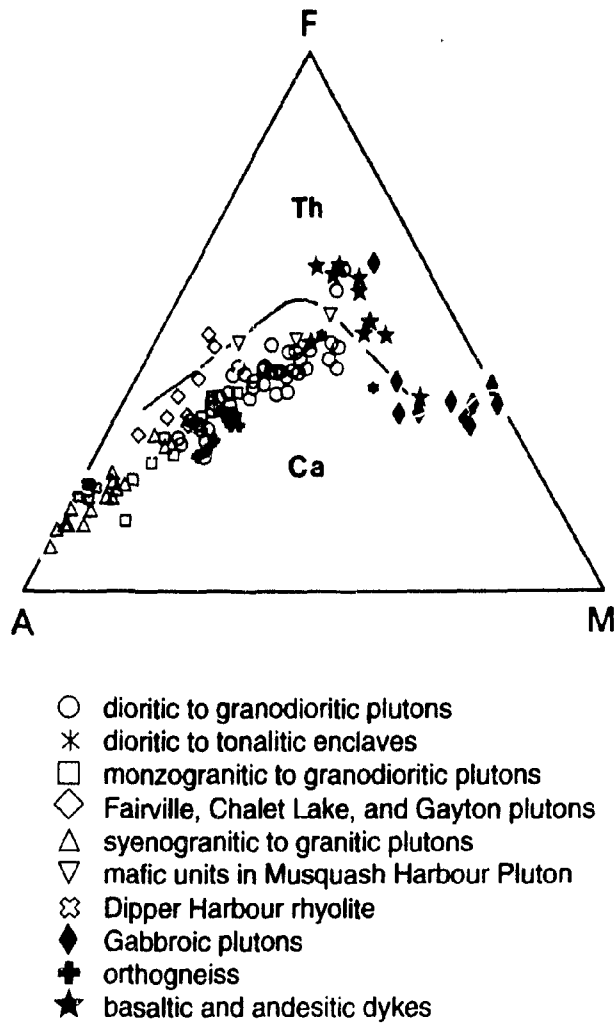


Figure 4.6. A $(\text{Na}_2\text{O} + \text{K}_2\text{O}) - \text{F} (\text{FeO}^{\text{T}}) - \text{M} (\text{MgO})$ ternary plot for analyzed samples in the study area. Tholeiitic (TH) and calc-alkaline dividing line from Irvine and Baragar (1971).

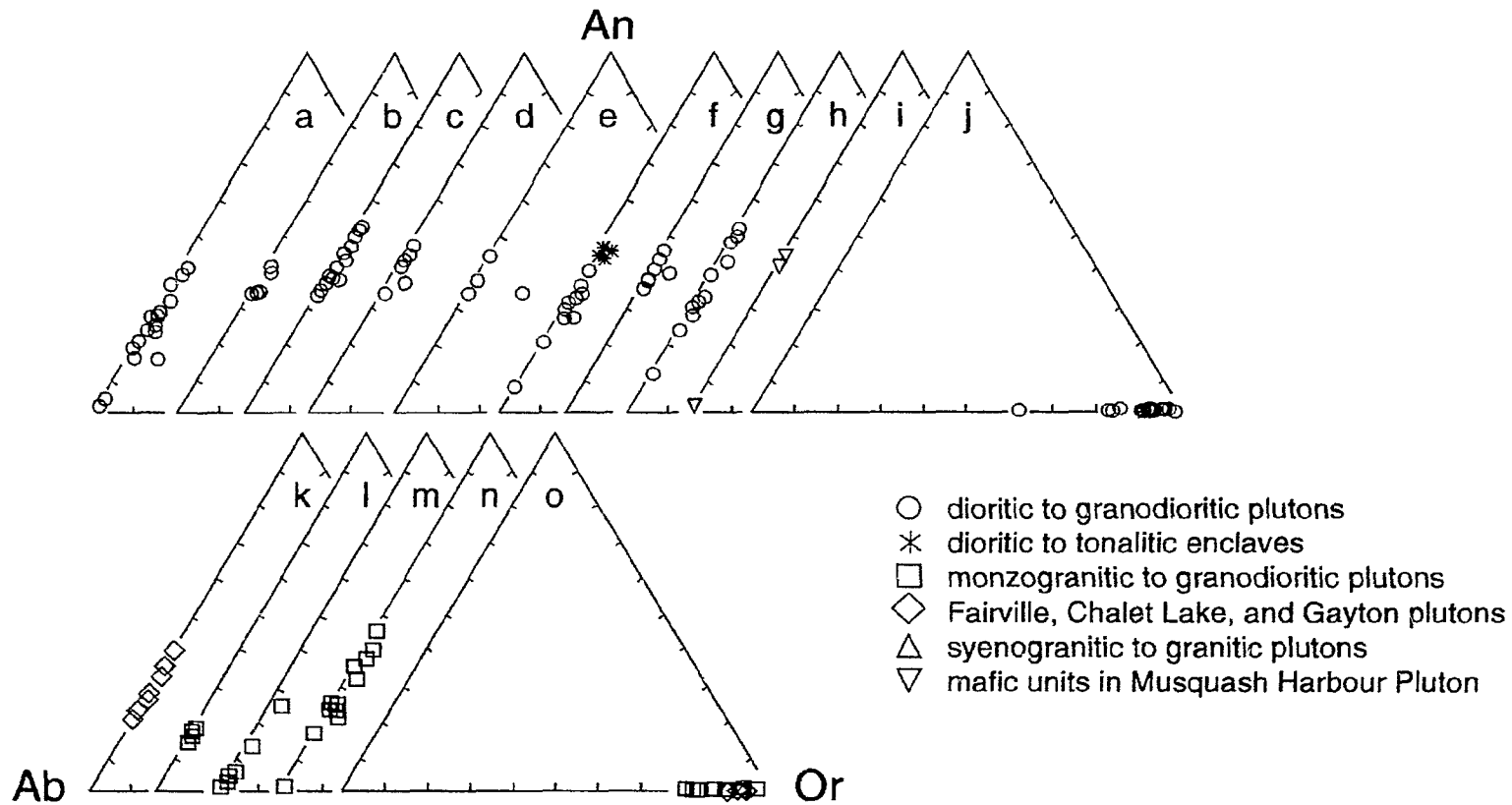
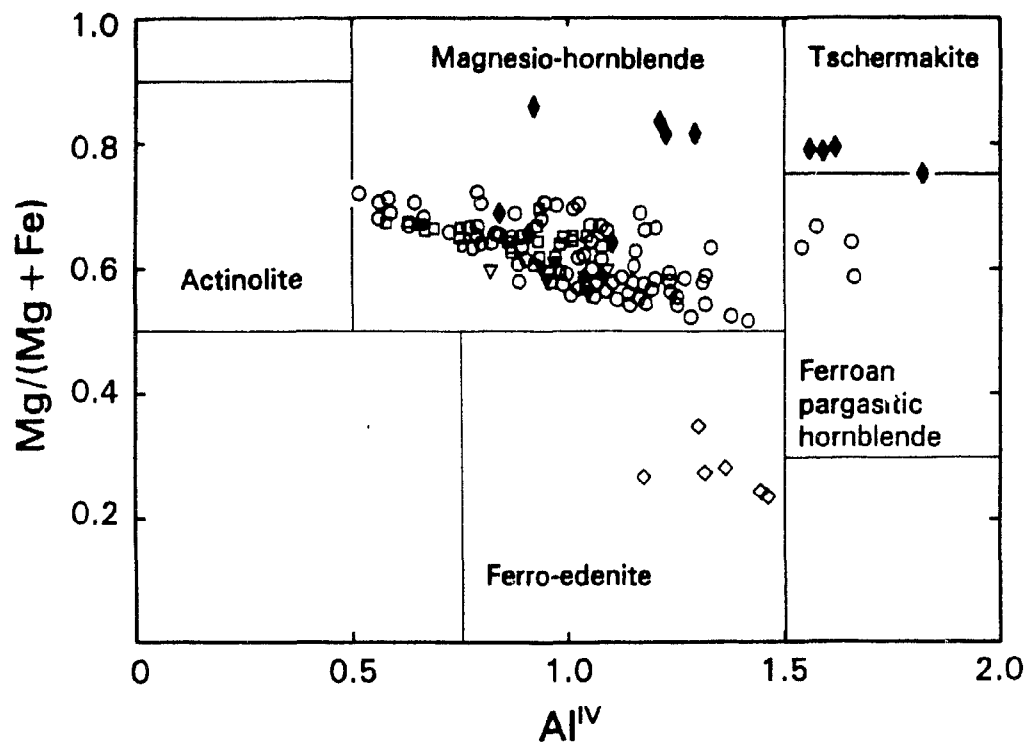


Figure 4.7. Plagioclase and K-feldspar compositions plotted in terms of Ab - An - Or. a) Ludgate Lake Granodiorite; b) Rockwood Park Granodiorite; c) French Village Quartz Diorite; d) Belmont Tonalite; e) Perch Lake Granodiorite; f) Shadow Lake Granodiorite and enclaves; g) Talbot Road Granodiorite; h) Renforth and Narrows plutons; i) Musquash Harbour pluton; j) K-feldspar in dioritic to granodioritic plutons; k) Fairville and Chalet Lake plutons; l) Hammond River Granite; m) Milkish Head Pluton; n) Hanson Stream Granodiorite; o) K-feldspar in monzogranitic to granodioritic plutons.



- dioritic to granodioritic plutons
- * dioritic to tonalitic enclaves
- monzogranitic to granodioritic plutons
- ◇ Fairville, Chalet Lake, and Gayton plutons
- △ syenogranitic to granitic plutons
- ▽ mafic units in Musquash Harbour Pluton
- ⊗ Dipper Harbour rhyolite
- ◆ Gabbroic plutons
- ⊕ orthogneiss
- ★ basaltic and andesitic dykes

Figure 4.8. Modified version of the International Mineralogical Association nomenclature for calcic amphiboles (after Hammarstrom and Zen, 1986) for analyzed samples from the study area.

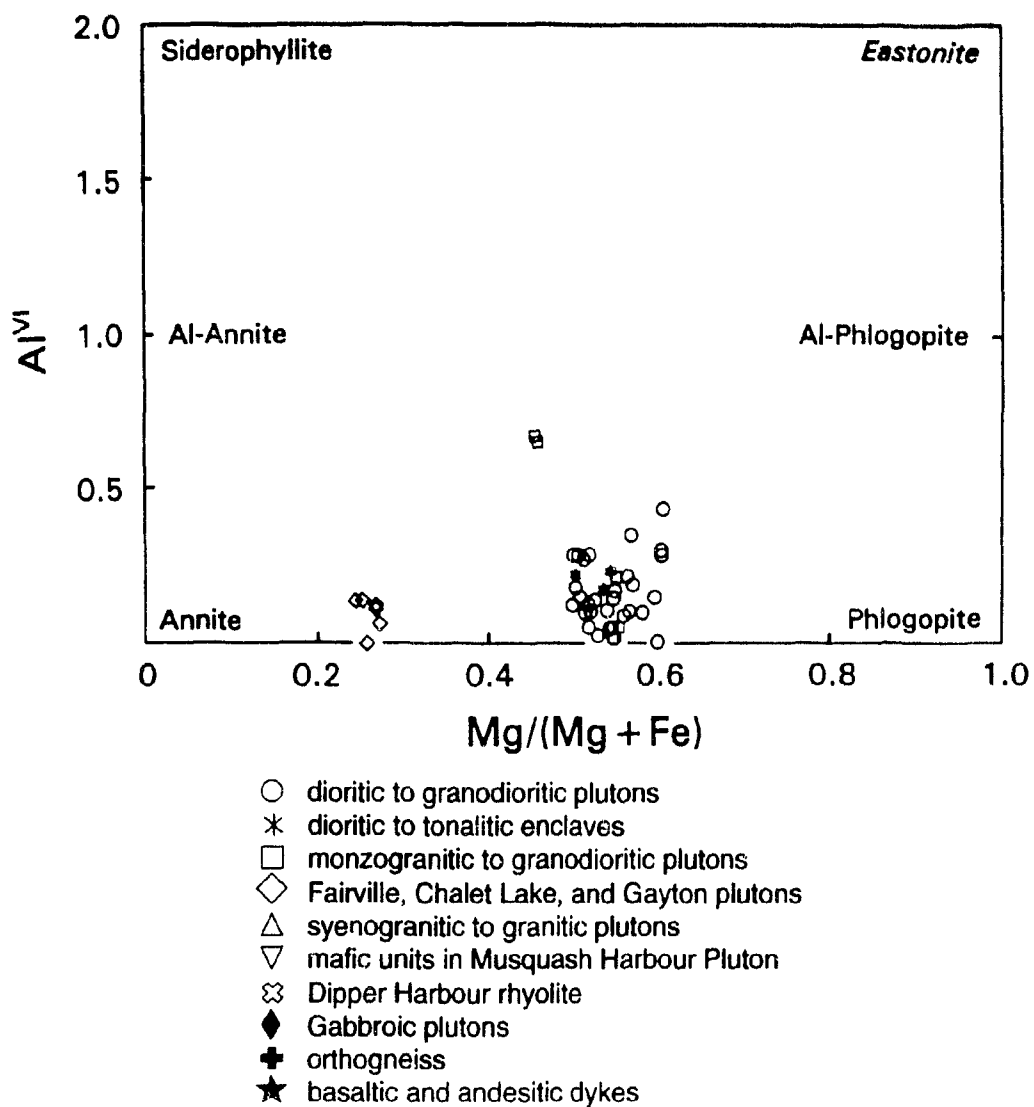


Figure 4.9. Classification of biotite compositions (after Guidotti, 1984) for analyzed samples from the study area.

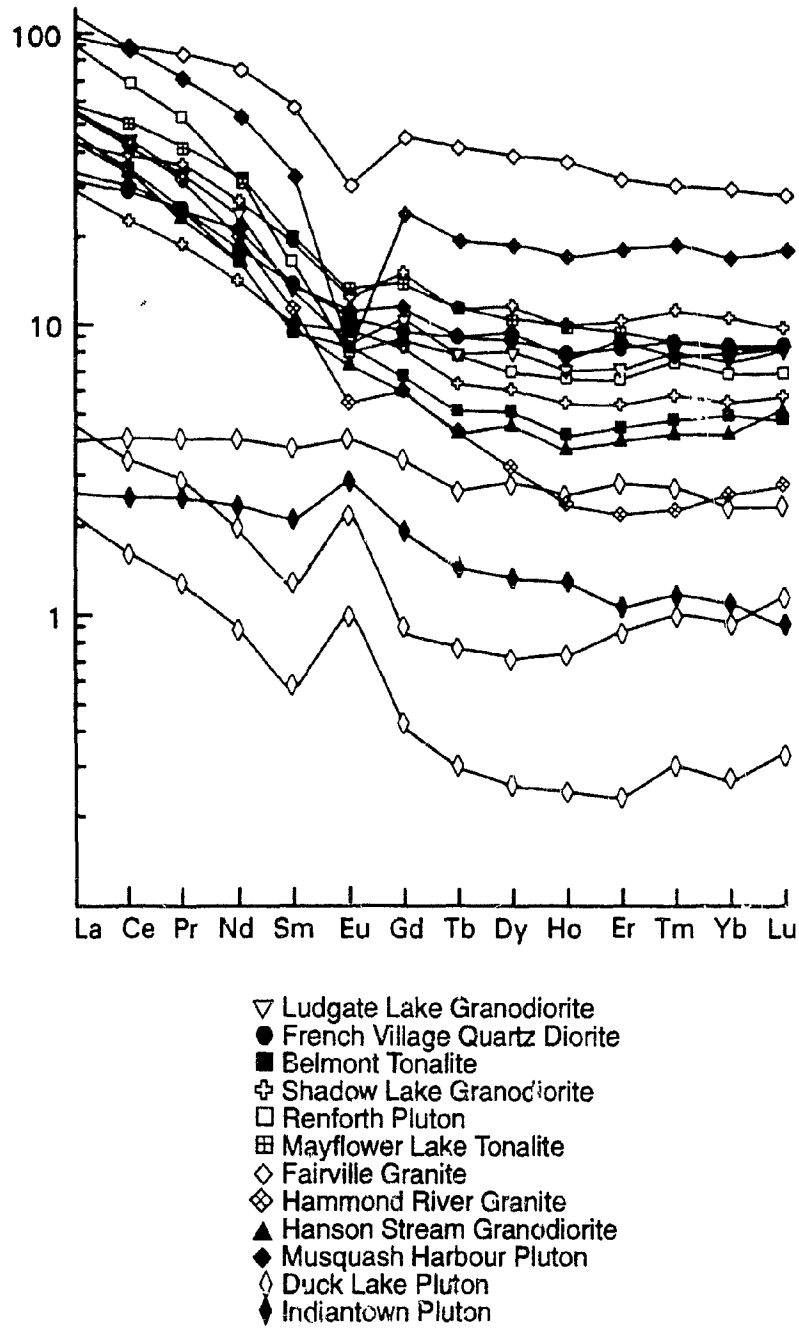


Figure 4.10. Chondrite-normalized REE patterns for analyzed samples from the study area.

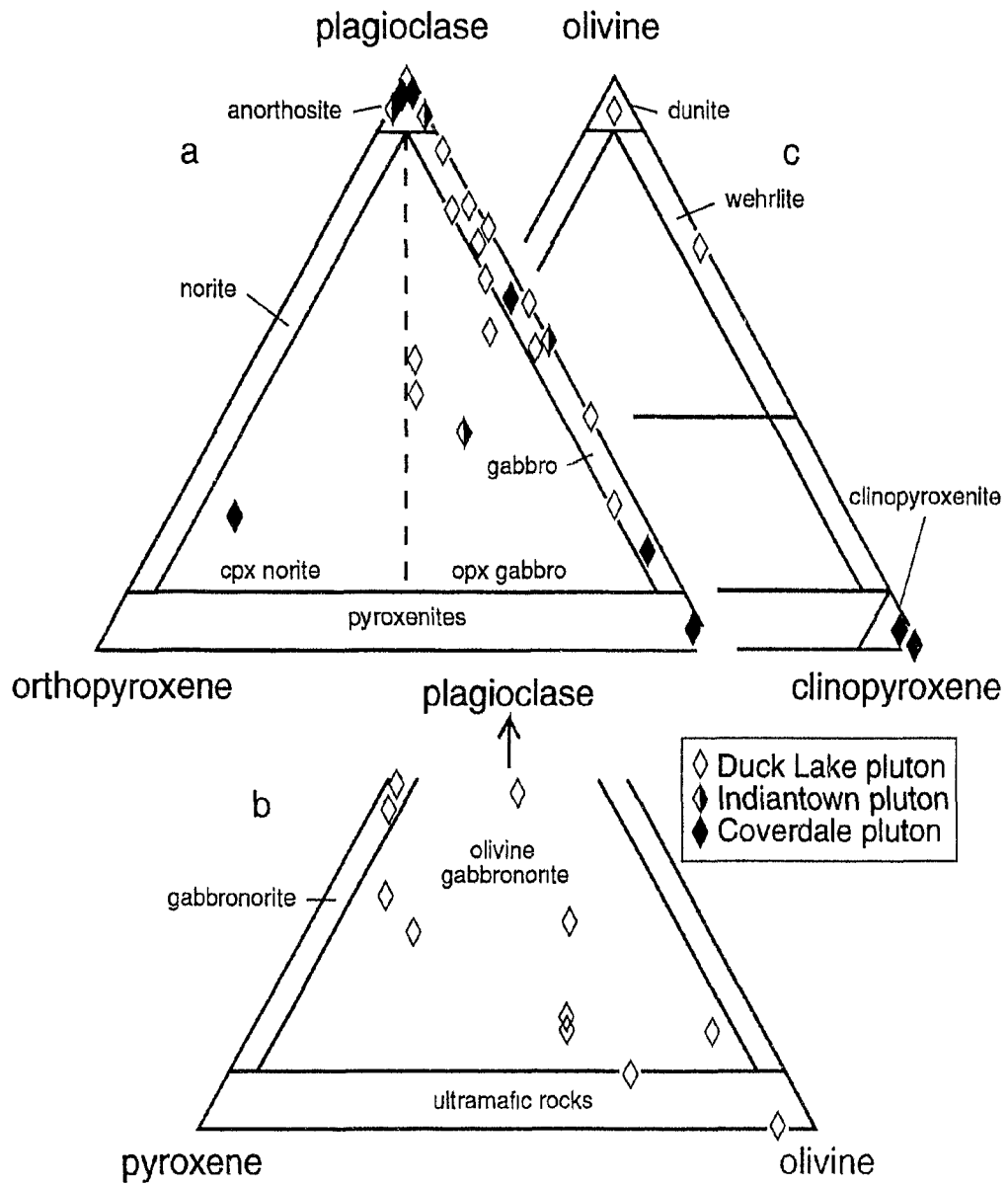


Figure 4.11. Ternary plots, classification, and nomenclature of gabbroic and ultramafic rocks from the Duck Lake, Indiantown, and Coverdale plutons.

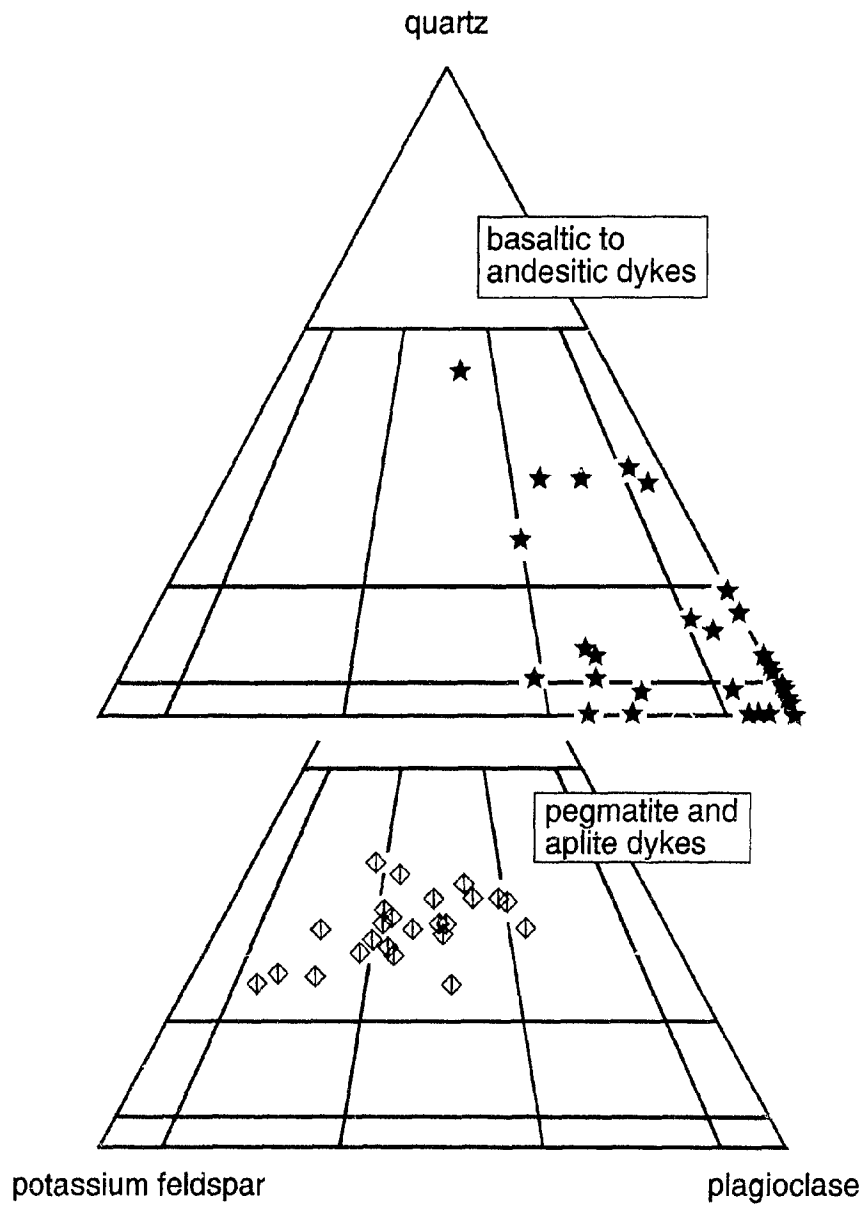


Figure 4.12. Ternary plots of modal quartz - plagioclase - potassium feldspar compositions of samples from dykes.

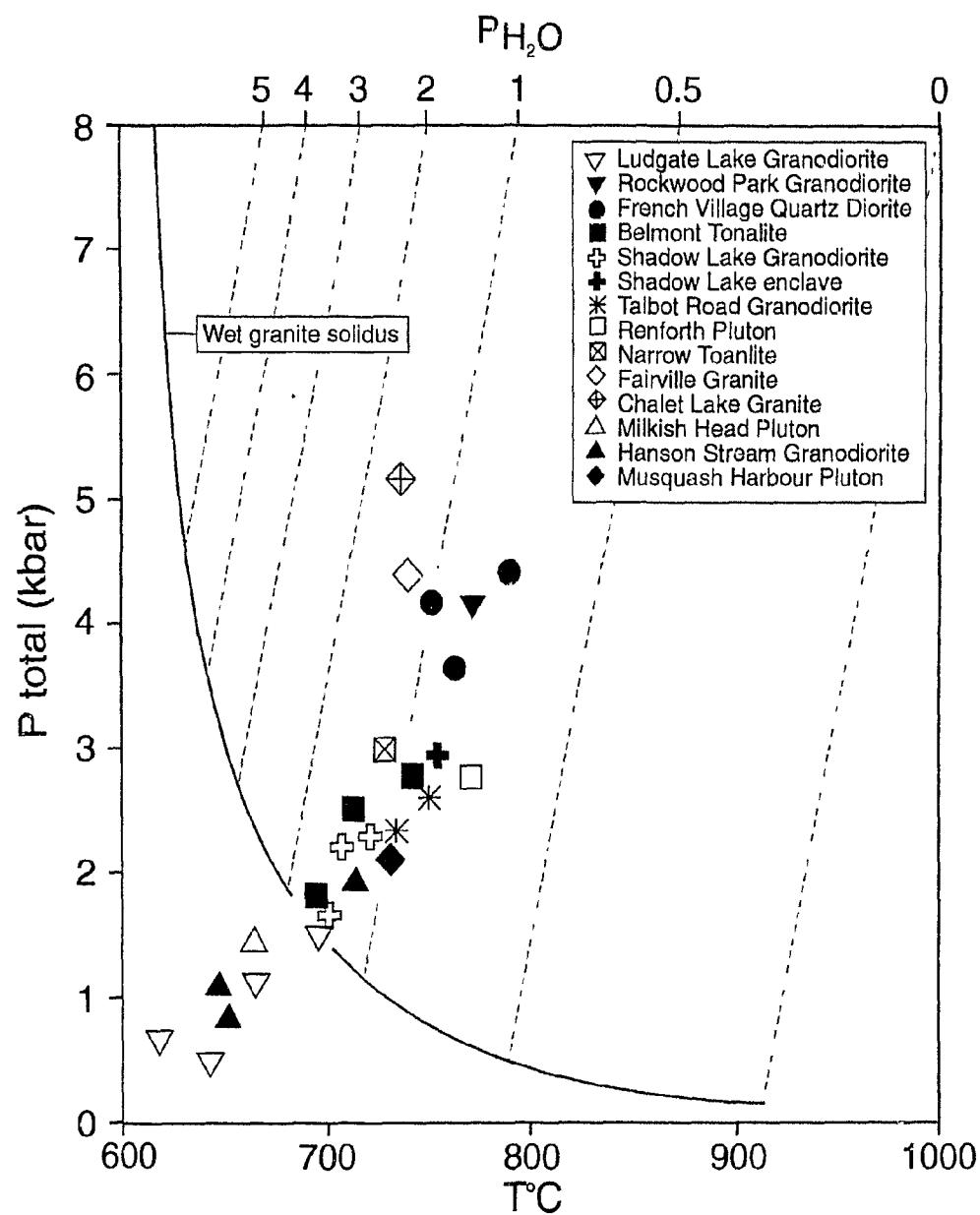


Figure 4.13. Emplacement thermobarometry for the Ca. 548 to 537 Ma plutons. Wet granite solidus and schematic P_{H2O} isobars from Cullers et al. (1992).

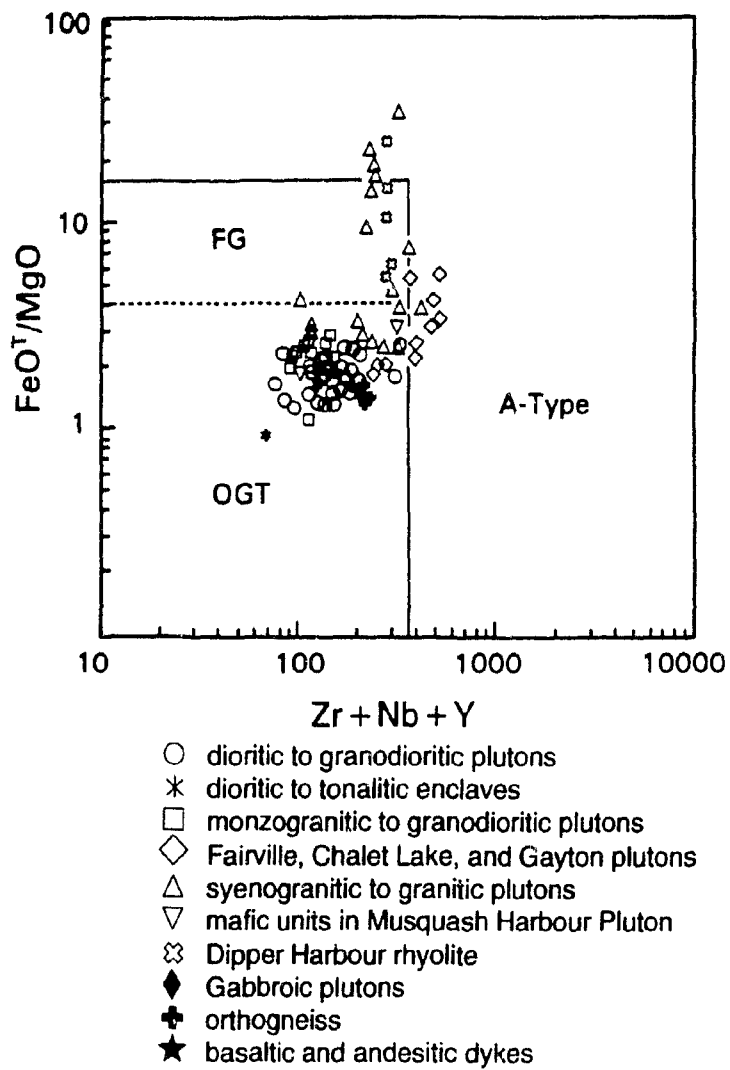
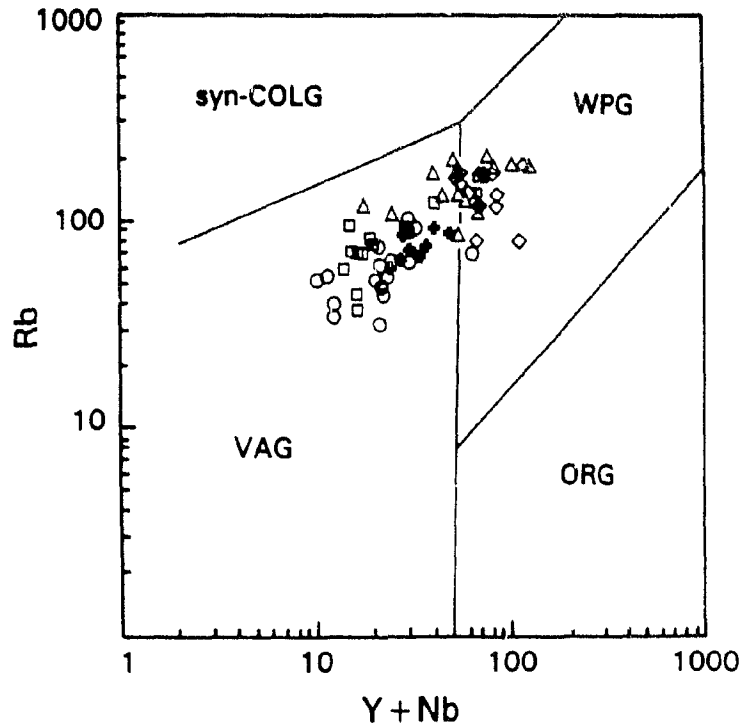


Figure 4.14. FeO^T/MgO against $\text{Zr} + \text{Nb} + \text{Y}$ discrimination diagram for analyzed samples from the study area after Whalen et al. (1987). FG and OGT are fields for fractionated felsic granites and unfractionated M-, I-, and S-type granites.



- dioritic to granodioritic plutons
- * dioritic to tonalitic enclaves
- monzogranitic to granodioritic plutons
- ◇ Fairville, Chalet Lake, and Gayton plutons
- △ syenogranitic to granitic plutons
- ▽ mafic units in Musquash Harbour Pluton
- ⊗ Dipper Harbour rhyolite
- ◆ Gabbroic plutons
- orthogneiss
- ★ basaltic and andesitic dykes

Figure 4.15. Rb against Y + Nb tectonic discrimination diagram for analyzed samples from the study area. Fields from Pearce et al. (1984): syn-COLG = syn-collision Granites; WPG = Within-Plate Granites; ORG = Ocean Ridge Granites; VAG = Volcanic Arc Granites.

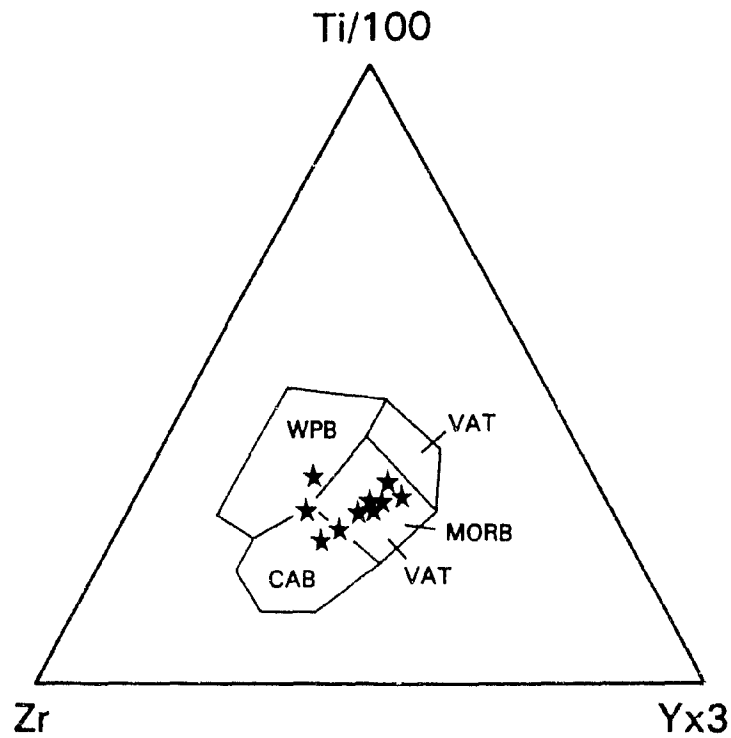


Figure 4.16. Ternary Ti - Zr - Y tectonic discrimination diagram for analyzed mafic dykes in the study area. Fields from Pearce and Cann (1973): VAT = Volcanic-Arc Tholeiites; MORB = Mid-Ocean-Ridge Basalts; CAB = Calc-Alkalic Basalts; WPB = Within-Plate Basalts.

Table 4.1. Estimation of pressure and temperature of crystallization in the ca. 548 to 537 Ma plutonic units based on the hornblende geobarometer and amphibole-plagioclase geothermometer. Pressure in kbar and temperature in °C. N = number of samples; C = core; R = rim; P1 = calibration of Hammarstrom and Zen (1986); P2 = calibration of Hollister et al. (1987); T = calibration of Blundy and Holland (1990).

Pluton	Sample		N	P1	P2	T
Ludgate Lake	NB91-8590	R	4	1.03 ± 0.75	0.89 ± 0.68	663 ± 39
	NB91-8622	R	4	1.46 ± 0.33	1.27 ± 0.38	694 ± 19
	NB92-9195-B	C	3	0.81 ± 0.99	0.66 ± 0.98	632 ± 38
		R	3	0.64 ± 0.85	0.48 ± 0.84	623 ± 37
	NB92-9251	R	4	0.44 ± 0.52	0.32 ± 0.38	642 ± 20
Rockwood Park	CW89-509-A	C	4	3.16 ± 0.73	3.18 ± 0.82	739 ± 35
		R	2	4.21	4.35	764
French Village	CW88-144	C	2	2.80	2.77	814
		R	2	4.46	4.63	777
	CW88-153	C	4	4.43 ± 0.18	4.60 ± 0.20	760 ± 34
		R	4	4.20 ± 0.70	4.35 ± 0.78	748 ± 30
	CW88-246	C	4	6.57 ± 0.69	7.01 ± 0.78	831 ± 23
		R	6	3.64 ± 0.67	3.72 ± 0.75	760 ± 11
Belmont	NB91-8513	R	5	2.36 ± 0.53	2.28 ± 0.55	712 ± 15
	NB91-8522	R	4	1.75 ± 0.26	1.60 ± 0.29	694 ± 24
	NB92-9027	C	4	2.80 ± 0.31	2.77 ± 0.34	743 ± 17
		R	4	2.60 ± 0.40	2.59 ± 0.38	738 ± 12
Shadow Lake enclave	NB91-8565	R	4	2.13 ± 0.64	2.02 ± 0.71	706 ± 16
	NB91-8599-B	R	4	2.27 ± 0.18	2.18 ± 0.21	720 ± 14
	NB92-9033	R	3	1.63 ± 0.46	1.46 ± 0.51	699 ± 10
	NB91-8597	C	2	1.92	1.81	740
		R	2	2.85	2.83	747
Talbot Road	NB92-9045	C	5	2.27 ± 0.54	2.18 ± 0.61	740 ± 22
		R	3	2.62 ± 0.10	2.57 ± 0.11	749 ± 47
	NB92-9153	C	2	1.59	1.42	701
		R	3	2.29 ± 0.13	2.20 ± 0.15	737 ± 21
Renforth	CW88-169	C	3	2.84 ± 0.43	2.81 ± 0.49	768 ± 29
		R	3	3.07 ± 0.09	3.08 ± 0.10	781 ± 28
Narrows	CW89-616	C	4	1.84 ± 0.72	1.70 ± 0.81	707 ± 35
		R	6	2.96 ± 0.64	2.96 ± 0.71	728 ± 27
Fairville	CW89-611	R	4	4.32 ± 0.32	4.48 ± 0.36	743 ± 19
Chalet Lake	CW88-254	C	2	5.19	5.45	726
		R	1	5.13	5.39	734
Milkish Head	NB92-9144	R	4	1.30 ± 0.81	1.14 ± 0.82	661 ± 44
Hanson Stream	NB92-9039	C	2	1.82	1.67	711
		R	4	1.99 ± 0.22	1.87 ± 0.25	712 ± 11
	NB92-9050	C	3	0.65 ± 1.09	0.59 ± 1.03	625 ± 52
		R	5	1.07 ± 0.94	0.95 ± 0.90	646 ± 41
	NB92-9154	C	2	1.87	1.73	675
	R	4	0.91 ± 0.38	0.66 ± 0.43	650 ± 24	
Musquash Harbour	NB92-9202	R	6	2.21 ± 0.60	2.11 ± 0.67	725 ± 21

CHAPTER 5

METAMORPHIC ROCKS OF THE BROOKVILLE TERRANE

5.1. INTRODUCTION

The most characteristic units of the Brookville terrane, the metasedimentary rocks of the Green Head Group, gneissic rocks of the Brookville Gneiss, and associated blastomylonitic rocks of the MacKay Highway shear zone show evidence of a complex geological history that included episodes of metamorphism. Despite the potential importance of these metamorphic events, the current published knowledge of the metamorphic history in these units is limited to the petrological descriptions of Leavitt (1963) and Wardle (1978) and the age determinations of Bevier et al. (1990), Dallmeyer et al. (1990), and Nance and Dallmeyer (1994). In addition, a separate area of high-grade metamorphic rocks, termed the Hammondvale metamorphic unit, was interpreted to be a metamorphic equivalent to the Green Head Group (e.g. Ruitenberg et al., 1979; McLeod et al., 1994); however, this area also lacks detailed petrological studies. Therefore, the purpose of this chapter is to provide detailed description and interpretation of 1) mineral textures and assemblages, 2) the spatial distribution of mineral assemblages, and 3) mineral chemistry, to better constrain the conditions under which they were metamorphosed. Constraints on the timing of these metamorphic events are presented in detail in Chapter 6.

The data presented here are based on more than 500 samples collected from representative lithologies in the Brookville Gneiss, Green Head Group, MacKay Highway shear zone, and Hammondvale metamorphic unit. Two hundred and seventy five thin sections were examined and mineral analyses were done in 27 samples.

5.2. PETROGRAPHY AND MINERAL ASSEMBLAGES

A wide variety of rock types is present in the metamorphic units of the study area, largely due to the heterogeneous character of the original sedimentary protoliths. Therefore, each of these different rock types has a diagnostic mineral assemblage reflecting its particular chemical system. The pelitic lithologies are the most informative in describing the metamorphic evolution of the area, whereas the metacarbonate rocks are extremely sensitive to bulk rock composition and variations in H₂O and CO₂ and are therefore less reliable indicators of metamorphic grade. However, some inferences can be made about the mineralogical and textural development of the metacarbonate assemblages by examination of associated pelitic rocks and vice versa. Mineral assemblages in orthogneissic lithologies are less diagnostic in indicating metamorphic grade.

5.2.1. Brookville Gneiss

The Brookville Gneiss displays a uniformly high-grade amphibolite-facies metamorphism throughout. However, based on field and petrological criteria, several distinct lithologies with characteristic mineral assemblages are recognized: biotite paragneiss, biotite-cordierite paragneiss, hornblende paragneiss, arkosic paragneiss, cordierite-sillimanite migmatite, granodioritic to tonalitic orthogneiss, and amphibolite. Marble and calc-silicate rocks are also present, although less common and interlayered with the paragneiss and migmatitic paragneiss. Field relationships of these various lithologies were outlined in section 2.3.

5.2.1.1. Paragneiss

The most common paragneissic lithology is semi-pelitic biotite

gneiss which contains the assemblage plagioclase-quartz-biotite-K-feldspar (as also noted by Wardle, 1978). Andalusite and sillimanite are locally developed. The second most common lithology is pelitic biotite-cordierite gneiss with the assemblage plagioclase-quartz-biotite-cordierite-K-feldspar ± andalusite ± sillimanite (Plate 5a). Minor lithologies include hornblende gneiss with the assemblage plagioclase-quartz-biotite-hornblende (Plate 5b) and feldspar-rich quartzite with the assemblage quartz-K-feldspar-plagioclase-biotite ± hornblende. Associated with these assemblages are accessory apatite, Fe-Ti oxides, tourmaline, zircon, titanite, and rare rutile (Table 5.1). Garnet was not observed in the paragneissic component of the Brookville Gneiss, although Wardle (1978) reported its occurrence in what he interpreted as paragneiss from the Pleasant Point area. Although the rocks in the Pleasant Point area have a gneissic appearance, based on lithological association and thin section petrography they are here interpreted to represent a high-grade portion of a contact metamorphic aureole around the Fairville Granite (see below).

Gneissic banding in the paragneiss is defined by well foliated biotite-rich layers alternating with granular quartz and feldspar-rich layers. Granoblastic textures are not well developed. Most of the grains are elongate and have sutured boundaries, with local development of recrystallized subgrains. This texture was noted by Wardle (1978; p. 140) in migmatitic leucosomes and attributed to ductile shear during cooling of the gneiss. However, the lack of deformation in the biotite suggests that this deformation may have been relatively synchronous with metamorphism. The foliation is defined by subidioblastic biotite that typically displays moderately to well developed uniform crystallographic orientation. The rims and cleavage planes of some biotite grains are chloritized.

Plagioclase is generally subidioblastic to xenoblastic and concentrated in the leucocratic layers where it is strongly twinned and weakly zoned. Unlike biotite, plagioclase appears to have random

distribution, although it is rarely elongate parallel to the regional stretching lineation. The grain margins are commonly myrmekitic and contain small inclusions of rounded quartz. Plagioclase may occur as aggregates of small granoblastic grains associated with quartz in asymmetric augen. These may represent original pebbles in the sedimentary rock or metamorphic segregations that were later deformed. Sericite and/or saussurite commonly have replaced plagioclase cores and/or twin-planes and locally grains are entirely replaced by sericite.

Xenoblastic microcline and perthitic microcline are less common than plagioclase but are also associated with the leucocratic layers. Grain boundaries are more irregular than in plagioclase and the grains typically have numerous rounded quartz inclusions. Both plagioclase and microcline are less common in biotite-rich layers. Microcline is relatively fresh in appearance, although patches of sericite are locally developed.

Quartz is xenoblastic and generally elongate parallel to layering and the regional stretching lineation. It also occurs as small rounded grains in all other minerals. Like the other felsic minerals, quartz has irregular boundaries and inclusions of small subgrains.

Cordierite is present in the pelitic paragneisses. It is typically ovoid and poikiloblastic with inclusions of rounded quartz, biotite, minor Fe-Ti oxides, and rare andalusite. Cordierite is restricted to the biotite-rich layers where the biotite inclusions display the same crystallographic orientation as biotite outside the grain. Twinning is not common. The cordierite is commonly entirely to partially altered to pinite or a combination of pinite on the rim and coarse-grained muscovite in the core.

Andalusite and sillimanite are not abundant in the pelitic gneiss. Andalusite occurs in some biotite-rich layers as small distinctive square idioblastic grains that are typically entirely altered to sericite or muscovite. More rarely andalusite occurs as small, unaltered, embayed grains associated with cordierite or clusters of

biotite. Sillimanite occurs as small fibrolitic knots in biotite or minute needles in the cores of quartz and plagioclase. Sillimanite and andalusite rarely occur together, although both are locally associated with cordierite.

Hornblende is relatively uncommon and restricted to the hornblende gneiss and feldspar-rich quartzite. It typically occurs as large idioblastic poikiloblasts with inclusions of prismatic apatite and rutile with xenoblastic biotite, quartz, plagioclase, and Fe-Ti oxides. The rims are locally replaced by chlorite. The hornblende defines a moderate to strong lineation parallel to the regional stretching lineation. Hornblende also occurs as smaller, unoriented, inclusion-free, lobe-shaped grains in the matrix. In contrast to the other paragneisses, the hornblende-bearing gneiss typically displays well developed granoblastic texture.

Fe-Ti oxides occur throughout the felsic and mafic layers but are concentrated in the biotite-rich layers. They are typically xenoblastic lobe-shaped grains that are locally inclusion-rich and appear to be elongate parallel to the stretching lineation. Microprobe analysis indicates that magnetite is the dominant phase, with minor ilmenite.

Muscovite is common in the paragneiss. It typically occurs as large, subidioblastic, relatively inclusion-free grains that are uniformly oriented at high angles to compositional banding. It partially to entirely pseudomorphs plagioclase, K-feldspar, andalusite, sillimanite, and cordierite and is interpreted to be a product of retrograde metamorphism.

5.2.1.2. Migmatitic Paragneiss

The nomenclature used here for describing migmatites is that of Johannes (1988). The mesosome is the mesocratic lithology of a migmatitic suite that is metamorphic in appearance and resembles paragneiss. The leucosome is the leucocratic layer formed during

migmatization and typically has an igneous appearance, and the melanosome is the dark-coloured selvage between the leucosome and mesosome.

Mineralogically, the migmatitic paragneiss is similar to the paragneiss; however, there is an increase in modal sillimanite and decrease in modal andalusite. The common assemblage is plagioclase-quartz-biotite-cordierite-K-feldspar \pm sillimanite \pm andalusite \pm spinel (Table 5.1). However, texturally the migmatitic paragneiss is distinct from the other paragneissic lithologies. Other than the mesosome, the texturally homogeneous original gneissic banding is replaced by well developed, commonly contorted and folded leucosomes that are in places bordered by narrow discontinuous rims of melanosome. In places, melanosomes occur as wispy lenses within the leucosome.

The melanosome consists dominantly of foliated, brown to green-brown biotite, with minor plagioclase, quartz, cordierite, and rare microcline and sillimanite. Accessory minerals include titanite, apatite, Fe-Ti oxides, zircon, and rare tourmaline. Locally the melanosome is almost entirely composed of biotite. Biotite is subidioblastic, well aligned, weakly chloritized, and displays a uniform crystallographic orientation similar to biotite in the paragneiss. Plagioclase and quartz are both subidioblastic to xenoblastic and elongate parallel to the foliation. Microcline, where present, typically occurs as small xenoblastic, evenly distributed grains or as large grains concentrated along the melanosome-leucosome contact. Feldspar grains are moderately altered to sericite and/or saussurite. Cordierite occurs as xenoblastic elongate grains throughout the melanosome but in a few samples it is concentrated along the contact with the leucosome. Although generally altered to muscovite and pinite, it has fewer inclusions of biotite, quartz, and Fe-Ti oxides compared to cordierite in the paragneissic rocks. Sillimanite, where present, is idioblastic and appears to be concentrated toward the centre of the melanosome where it is generally inclusion-free and randomly oriented.

Andalusite is rare and occurs as minute embayed grains typically intergranular to biotite. It is interpreted to be relict from lower temperature metamorphic conditions.

The contact between melanosome and leucosome is typically sharp and marked by an abrupt change in grain size and modal mineralogy. The leucosome is mineralogically inhomogeneous. It commonly consists of varying amounts of plagioclase and quartz; however, some leucosomes have a high concentration of microcline. The leucosome can display a substantial difference in modal composition (Fig. 5.1) over very short distances from tonalitic to more syenogranitic varieties. This type of compositional variation has been attributed to inhomogeneous chemical composition of the host rock, with the high microcline content probably due to a high content of K-feldspar in the parent rock (c.f. Maaloe, 1992). However, these differences can also be attributed to fluid infiltration and/or migration of minerals during metamorphism.

The leucosome generally displays granoblastic texture, although in detail most grain boundaries are serrated with the development of subgrains similar to those in the leucocratic layers in the paragneiss. Compared to the other gneissic lithologies, myrmekitic intergrowths are not as well developed. Plagioclase in the leucosome is typically subidioblastic to rarely idioblastic. Quartz and microcline are xenoblastic and elongated parallel to the foliation. Microcline also occurs as large, highly poikilitic grains with rounded inclusions of plagioclase, quartz, biotite, and cordierite. Feldspar grains are less altered than those in the melanosome and paragneissic samples. Biotite is less common and is generally xenoblastic; however, it still displays the same uniform crystallographic orientation as in the melanosome.

Cordierite is not common in the leucosome; however, locally it is quite abundant and occurs as lobe-shaped or clusters of grains with rare inclusions of biotite, Fe-Ti oxides, and spinel. This is in marked contrast to their poikiloblastic habit in the paragneiss and melanosome. The lack of abundant inclusions in leucosome cordierites suggests they

grew from the melt (cf. Ellis and Obata, 1992). Cordierite is commonly altered to muscovite and pinitite.

Sillimanite is also not common in the leucosomes, and compared to the melanosome typically form swarms of tiny fibrolite needles in the cores of plagioclase and quartz and more rarely microcline and cordierite. Andalusite was not observed in the leucosome.

As in the paragneissic lithologies, muscovite is common and for the same reasons is also interpreted to be a product of retrograde metamorphism.

5.2.1.3. Marble and Calc-silicate Gneiss

Associated with the Brookville Gneiss are coarse-grained, granoblastic, massive to moderately layered marble and fine- to medium grained, thinly layered calc-silicate boudins. The typical mineral assemblage in the marble is calcite/dolomite-phlogopite-plagioclase-tremolite/actinolite-diopside-forsterite \pm K-feldspar-plagioclase, whereas the assemblage in the calc-silicate rocks is diopside-calcite/dolomite-quartz-K-feldspar-plagioclase \pm tremolite \pm phlogopite \pm forsterite. Accessory minerals common to both assemblages include titanite, apatite, magnetite, rutile, and rare tourmaline (uvite) (Table 5.1). A rare occurrence of chondrodite was reported by Wardle (1978) associated with forsterite from a calc-silicate band. Monomineralic calcite marbles are rare.

Marbles are typically medium- to coarse-grained with granoblastic calcite comprising >75% of the rock (Plate 5c). Dolomite is less common and typically occurs as small rounded to lobe-shaped inclusions in calcite or more rarely as separate grains. Many of the silicate minerals are concentrated in discrete layers. Idioblastic to subidioblastic tremolite is the dominant silicate mineral and occurs as randomly oriented grains parallel to compositional banding. Locally tremolite occurs as radiating fibrous clusters associated with diopside.

Phlogopite is typically idioblastic, inclusion-free, and parallel to layering, but unlike the biotite in the paragneissic host, does not display uniform crystallographic orientation. Tremolite and phlogopite rims are locally replaced by chlorite. Untwined and inclusion-free plagioclase (anorthite) occurs as small, unaltered, rounded grains throughout the marble. Microcline is more abundant than plagioclase and also occurs as small, unaltered, rounded inclusion-free grains. However, locally in some silicate-rich layers it forms large poikilitic grains with inclusions of Fe-Ti oxides, tremolite, titanite and apatite. Diopside occurs as subidioblastic grains concentrated along the compositional banding. It is locally partially replaced by serpentine, actinolite, and chlorite.

Forsterite occurs as small scattered grains throughout the marble and is rarely concentrated in the silicate-rich bands. It is typically partially to entirely pseudomorphed by serpentine or a mixture of serpentine and dolomite. The larger forsterite grains locally contain inclusions of tremolite and diopside.

Prograde actinolite is rare, and like tremolite, typically forms well developed prismatic grains that parallel compositional banding. Prograde actinolite was not observed with tremolite.

Titanite and magnetite are typically minor accessory minerals in the marble, comprising less than 1%. Idioblastic apatite is abundant and forms large randomly oriented grains throughout the marble.

Calc-silicate rocks are less common than marble. Calcite typically comprises <5% of the rock and diopside is the dominant silicate mineral phase. It typically forms massive, polygonal granular textures. The other less abundant mineral phases form randomly oriented subidioblastic grains. However, microcline is xenoblastic and highly poikilitic. Plagioclase (An₃₀₋₃₅) is subidioblastic, strongly twinned, and partially altered to sericite and/or saussurite. Titanite is typically quite abundant with local concentrations up to about 5%.

5.2.1.4. Orthogneiss

Orthogneissic rocks, interlayered with paragneiss and migmatitic paragneiss, include two distinct lithologies: homogeneous tonalitic to granodioritic orthogneiss and relatively heterogeneous amphibolite. The tonalitic to granodioritic orthogneiss contains the assemblage plagioclase-quartz-biotite \pm K-feldspar with accessory apatite, titanite, zircon, and Fe-Ti oxides (Table 5.1). Although hornblende has been reported from the Pleasant Point area (e.g. Wardle, 1978; Nance and Dallmeyer, 1994) it was not recognized in rocks herein defined as orthogneiss. The orthogneiss is mineralogically and texturally very similar to the biotite paragneiss, with elongate quartz grains with numerous rounded quartz inclusions, and well developed mymerkitic textures. However, compared to the paragneiss the orthogneiss is typically more leucocratic and compositional banding is typically less than mm-scale, giving the orthogneiss a texturally homogeneous appearance. As in the paragneiss, biotite displays a uniform crystallographic orientation. With the exception of some orthogneisses at Pleasant Point, most of the samples display a moderately to strongly developed stretching lineation comprising elongated quartz and asymmetric lens-shaped aggregates of quartz and plagioclase.

The orthogneiss lacks significant migmatite; however, it is locally intruded by both concordant and cross-cutting syenogranitic dykelets that may represent partial melts from the orthogneiss or adjacent migmatitic paragneiss. The orthogneiss lacks melanosomes.

Compared to the paragneissic lithologies, the orthogneiss is more altered, with most feldspar grains totally replaced by sericite and/or saussurite, and biotite pseudomorphed by chlorite. Secondary muscovite is generally lacking.

The other major orthogneissic lithology in the Brookville Gneiss is amphibolite with the assemblage hornblende + plagioclase + biotite + quartz \pm clinopyroxene with accessory titanite, apatite, and Fe-Ti

oxides (Plate 5d). In some samples titanite forms discrete layers (0.2 mm wide) comprising up to 5% of the rock. The amphibolites are texturally heterogeneous. Layering ranges from less than 1 cm to greater than 10 cm and consists of alternating hornblende/biotite-rich and plagioclase-rich layers. Hornblende is the dominant mineral phase and forms subidioblastic to xenoblastic, inclusion-rich grains that locally preserve a uniform crystallographic orientation. Inclusions in the hornblende typically include idioblastic to xenoblastic plagioclase, biotite, quartz, titanite, apatite, and Fe-Ti oxides. Where the cores are actinolitic, inclusions of vermicular quartz and rutile are common suggesting retrogression.

Subidioblastic biotite is commonly associated with the hornblende. It is the dominant phase in some layers associated with minor plagioclase and quartz and may also form small clusters. It locally displays preferred crystallographic orientation. Hornblende and biotite are locally partially replaced by chlorite.

Plagioclase (An_{35-40}) is typically unaltered, subidioblastic to granoblastic and is weakly zoned. Quartz is a minor phase and occurs as small intergranular or elongated grains with serrated margins. Clinopyroxene is rare. It is xenoblastic, inclusion-rich, and variably replaced by hornblende. Inclusions are rounded plagioclase, quartz, and Fe-Ti oxides. The amphibolite generally lacks K-feldspar.

5.2.2. MacKay Highway shear zone

The northwest boundary between the Brookville Gneiss and Green Head Group is marked by the recrystallized MacKay Highway ductile shear zone (Chapter 3). This zone was also referred to as the MacKay Highway salient by Wardle (1978). The shear zone brings amphibolite-facies rocks of the Brookville Gneiss over greenschist-facies lithologies of the Green Head Group. This results in a regional zone of high strain that affects the entire Brookville Gneiss and about 500 metres of the

structurally lower Green Head Group in the Brookville area (Chapter 3; Map A). Toward the southwest the shear zone thins and is cut out by younger faults. The ductile deformation is inhomogeneously distributed in the footwall rocks of the Green Head Group and is characterized by large tectonic blocks or megaboudins of paragneiss and orthogneiss of the Brookville Gneiss that grade into finer grained, flaggy blastomylonitic schists. The boudins are enclosed in coarse-grained carbonate blastomylonites that are interpreted to have originated as carbonate rocks of the Green Head Group. The term blastomylonite is typically used to denote a mylonitic rock that has undergone syntectonic recrystallization (e.g. Yardley, 1989). However, here the term is used to describe a mylonitic rock that has been late syn- to post-tectonically recrystallized.

5.2.2.1. Gneissic Boudins

The paragneissic and orthogneissic boudins generally have mineralogical and textural characteristics similar to those in the Brookville Gneiss. However, the presence of abundant sillimanite and andalusite and the general lack of muscovite distinguishes the paragneissic boudins from paragneiss in the Brookville Gneiss. The diagnostic mineral assemblage in the paragneiss is plagioclase-quartz-K-feldspar-biotite-cordierite \pm sillimanite \pm andalusite with accessory tourmaline, apatite, titanite, zircon, rutile, and Fe-Ti oxides (Plate 6a) (Table 5.1).

Sillimanite typically occurs in the biotite-rich layers as wispy fibrous knots and as small acicular grains in K-feldspar, quartz, and plagioclase. Fibrolite locally forms thin monomineralic layers bordered by biotite and andalusite. Andalusite associated with sillimanite is commonly embayed and xenoblastic and separated from the sillimanite by thin quartz rims. However, in the absence of sillimanite, andalusite forms stubby moderately poikilitic grains with rounded inclusions of

quartz and microcline. Andalusite and sillimanite grains define a preferred orientation parallel to the regional stretching lineation observed in the Brookville Gneiss. Cordierite is also associated with the biotite-rich layers and is typically xenoblastic with minor biotite, Fe-Ti oxide, and sillimanite inclusions. It is commonly replaced by pinitite. Biotite is typically unaltered and displays the same uniform crystallographic orientation as in the Brookville Gneiss. Muscovite, where present, typically pseudomorphs sillimanite and cordierite, and is interpreted to be secondary.

5.2.2.2. Pelitic Blastomylonitic Schists

The gneissic layering can be traced from the interior of the boudins into blastomylonitic rocks that bound the boudins, indicating that mineral assemblages in the sheared rocks were derived from recrystallization of pre-existing assemblages in the interior of the gneissic boudins. The blastomylonitic foliation generally parallels the gneissic layering in the boudin interiors. The mylonite zone is characterized by grain size reduction, extreme thinning and attenuation of gneissic layering, and recrystallization of textural and mineral assemblages (Plate 6b). This results in a fine-grained, well laminated, granoblastic phyllonite, herein termed blastomylonite, with a mineral assemblage similar to that in the gneissic boudins (plagioclase-quartz-K-feldspar-biotite \pm sillimanite \pm cordierite \pm andalusite). However, it differs from the boudins in that it contains rare garnet and prograde muscovite. Titanite, apatite, tourmaline, clinozoisite, rutile, and Fe-Ti oxides are accessory minerals (Table 5.1).

Sillimanite is not abundant and occurs as fine-grained, uniformly oriented needles intergrown in biotite-rich layers or as discrete grains in quartz and K-feldspar. Cordierite occurs as small elongate, grains enclosed in sillimanite or as xenoblastic, highly poikilitic, intergranular grains that are partially to entirely altered to sericite

and pinitite. Garnet, where present, occurs as xenoblastic broken grains parallel to foliation (as noted by Wardle, 1978, p. 217), but they are also elongate parallel to the regional stretching lineation. Inclusions in the garnet include elongate quartz, Fe-Ti oxide, and biotite. Compared to the Brookville Gneiss, biotite is typically red to orange, probably due to relatively high Fe contents (e.g. Lalonde and Bernard, 1993) and displays a well developed uniform crystallographic orientation. Andalusite is not common and typically occurs as small lobate grains intergrown with biotite. As in the boudins, muscovite is not common and generally replaces cordierite; however, locally it is intergrown with biotite and appears to be prograde. Fe-Ti oxides and titanite are commonly broken and elongate parallel to foliation.

Due to the recrystallized texture of the blastomylonite, any previous geometric evidence of the high strain related to this shear zone has been obliterated. However, the orientation of elongate, broken garnet parallel to the regional stretching lineation and the presence of quartz ribbons, now recrystallized, are features that resulted from high strain prior to recrystallization.

The pelitic blastomylonite schists are generally unaltered. Secondary muscovite is not common, some biotite grains are slightly chloritized, and a few feldspars are sericitized.

5.2.2.3. Calc-silicate Blastomylonites

Associated with the pelitic blastomylonites are numerous thin, commonly boudinaged, calc-silicate layers. The typical assemblage is actinolite/tremolite-biotite/phlogopite-quartz-K-feldspar-plagioclase-diopside \pm calcite/dolomite with accessory tourmaline, titanite, apatite, zircon, clinozoisite, and Fe-Ti oxides (Plate 6c) (Table 5.1). Like the pelitic blastomylonites, these rocks are fine-grained, granoblastic, well laminated, and relatively unaltered. However, recrystallized porphyroclasts of actinolite/tremolite are generally

coarser grained than the matrix and occur as elongate poikiloblasts with numerous randomly oriented inclusions of rounded quartz and biotite. The foliation is draped around these features. The matrix actinolite/tremolite is idioblastic and typically lineated and parallel to foliation. Here the actinolite/tremolite displays a preferred crystallographic orientation. Diopside is typically fine-grained and subidioblastic but also occurs as large broken porphyroclasts in boudins. As in the pelitic blastomylonite, biotite is idioblastic, red to orange, and typically displays a strong preferred crystallographic orientation. Recrystallized quartz ribbons are common as are monomineralic laminations of idioblastic tourmaline and titanite. Some Fe-Ti oxides are broken and parallel to foliation.

5.2.2.4. Marble Blastomylonites

In contrast to the pelitic and calc-silicate blastomylonites, the associated carbonate rocks are typically coarse-grained and granoblastic. The only evidence of their earlier mylonitic history is the presence of numerous boudinaged clastic/calc-silicate layers with "pull-apart" features and sheath folds. Two mineral assemblages are present: 1) calcite/dolomite-diopside-garnet \pm K-feldspar \pm quartz \pm plagioclase (Plate 6d) and 2) calcite/dolomite-diopside-phlogopite-K-feldspar-quartz-plagioclase \pm tremolite, both with accessory titanite, apatite, and Fe-Ti oxides. Carbonate blastomylonites are generally layered on a centimetre-scale with alternating carbonate-rich and silicate-rich layers. Diopside is typically subidioblastic to xenoblastic, relatively inclusion-free, and randomly oriented in some layers. Garnet (grossular?) poikiloblasts are generally idioblastic with numerous inclusions of rounded diopside and calcite/dolomite. In one sample, inclusions of fibrous tremolite were identified. Garnet is locally xenoblastic, highly fractured, and apparently stretched along compositional layering. Phlogopite is subidioblastic to xenoblastic

near tremolite and displays a uniform preferred crystallographic orientation. Tremolite occurs as subidioblastic to xenoblastic grains that are weakly oriented parallel to compositional banding. Phlogopite and tremolite are locally replaced by chlorite along cleavage planes. Craterite was not observed.

5.2.3. Green Head Group

The intrusion of numerous plutons into the Ashburn and Martinon formations produced extensive contact aureoles that are locally superimposed on regional greenschist-facies mineral assemblages and textures. In the absence of pelitic rock, it is difficult to distinguish regional from contact metamorphism in carbonate lithologies. However, scattered throughout the Ashburn Formation are minor pelitic rocks that locally contain a strong foliation interpreted to be the result of regional greenschist-facies metamorphism. The presence or absence of this fabric was used here to delineate the extent of regional and contact metamorphism. The main area of regional metamorphism is in the Ashburn Formation that borders the MacKay Highway shear zone and extends northwest to Drury Cove (Fig. 5.2). A second area of regional metamorphism is located in the Hammond River area (Fig. 5.3) where strongly cleaved mica schists are locally associated with carbonate rocks. Phyllites and mica schists are also present near the Caledonia-Clover Hill Fault in the Saint John River area (Fig. 5.2). Evidence of extensive regional greenschist-facies metamorphism was not observed in the Martinon Formation.

Contact metamorphism is generally characterized by hornblende-hornfels-facies mineral assemblages, although peak metamorphic grades locally reached pyroxene hornfels conditions. Contact metamorphic assemblages are divided into three main groups: low-grade, medium-grade, and high-grade assemblages.

Because there are minor marble and calc-silicate lithologies in the

mainly clastic Martinon Formation and minor pelitic lithologies in the mainly carbonate Ashburn Formation, they are described together in the following sections.

5.2.3.1. Regional metamorphic rocks

Pelitic metasedimentary rocks that do not appear to be modified by contact metamorphism have the mineral assemblage muscovite-chlorite-quartz-K-feldspar-plagioclase \pm biotite \pm clinozoisite with accessory tourmaline, titanite, apatite, zircon, and Fe-Ti oxides (Table 5.1). These rocks are fine-grained and have a moderate to well developed, near-vertical schistosity defined by alignment of subidioblastic muscovite, chlorite, and rarely biotite. Schistosity is typically subparallel to bedding and this results in a moderately developed, relatively shallow intersection lineation (Chapter 3). Metapelitic rocks with a high proportion of sheet silicates are coarse-grained, the schistosity is intensely crenulated, and the original sedimentary structures are mainly obliterated (Plate 7a). Quartz-rich rocks have large amounts of angular quartz with minor K-feldspar, and are weakly foliated.

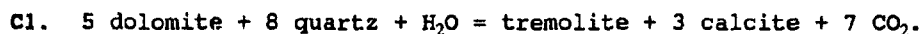
The main mineral assemblage in carbonate rocks is calcite/dolomite-phlogopite \pm tremolite \pm quartz \pm plagioclase \pm K-feldspar with accessory titanite, apatite, and Fe-Ti oxides (Table 5.1). These rocks are typically coarse- to medium-grained, granoblastic, and moderately layered. Compositional layering is defined by variations in carbonate grain size and abundance of silicate minerals. Locally the marble displays a weakly developed foliation defined by dimensionally preferred calcite/dolomite grains that is subparallel to colour banding and results in shallow intersection lineations similar to those in the associated pelitic rocks. The granoblastic texture is probably the result of contact metamorphism (see below); however, the intersection lineation is still preserved.

5.2.3.2a. Low-grade rocks (Zone A)

The first evidence of contact metamorphism in the pelitic rocks is the development of small (<1.0 mm diameter) randomly oriented clinozoisite, chlorite and muscovite porphyroblasts. In addition, the associated calc-silicate lithologies generally have randomly oriented tremolite porphyroblasts (Table 5.1.).

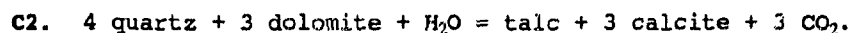
Original sedimentary structures are still well preserved in the pelitic and calc-silicate lithologies and in thin section relatively coarse-grained, angular to rounded quartz, K-feldspar (typically microcline), and plagioclase (albite and labradorite) are set in a very fine-grained chlorite and clinozoisite matrix. Xenoblastic to subidioblastic clinozoisite, muscovite, and tremolite poikiloblasts generally form intergrowths with many of the matrix minerals. Inclusions are generally randomly oriented, although chlorite in the matrix is commonly aligned parallel to bedding. Tremolite is associated with quartz-rich layers. The range in size and shape of many of the quartz and microcline grains, together with the range in plagioclase compositions suggest that their origin is detrital, and that they have survived contact metamorphism. Based on textural evidence, these low-grade rocks did not have a penetrative cleavage prior to contact metamorphism.

The mineral assemblage clinozoisite-chlorite-muscovite probably formed from the conversion of clay minerals of diagenetic origin. However, the presence of tremolite in calc-silicate rocks of this metamorphic grade is not common (e.g. Turner, 1980). The growth of tremolite is inferred to have formed by the hydration-decarbonation reaction (e.g. Yardley, 1989):



The associated marbles typically display well developed

granoblastic texture with 120° triple-point junctions, although locally they are strongly deformed and mylonitic in the Saint John area (Chapter 3). Exsolution lamellae were not observed. The marble typically consists entirely of dolomite or calcite or a mixture of both, with trace amounts of detrital quartz, feldspar, and Fe-Ti oxides (Table 5.1). Minute clusters of idioblastic chlorite and muscovite are not common, but occur in marbles with relatively abundant detrital minerals. Cubes of pyrite are commonly concentrated along fractures. Talc is not abundant and was only observed near the contact with the Acamac pluton; however, other occurrences have been documented (e.g. Wardle, 1978) in the contact aureole of the Narrows Pluton and a small dioritic intrusion east of Green Head Island (Indiantown Gabbro contact aureole of Wardle, 1978). Talc is associated with quartz and inferred to have formed by the reaction (e.g. Holness, 1992):



5.2.3.2b. Low-grade rocks (Zone B)

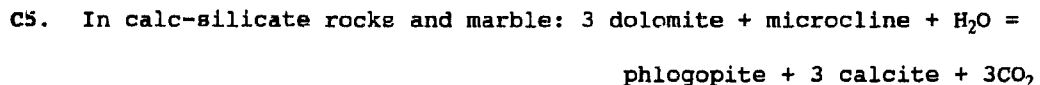
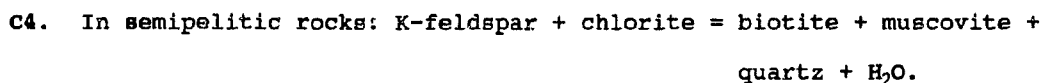
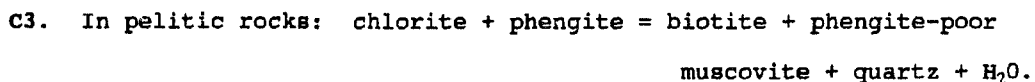
With an increase in temperature in this zone, biotite/phlogopite developed and there is a general increase in matrix grain size, although sedimentary structures are still preserved. The transition from lower grade (Zone A) rocks is evident in small and fewer inclusions and the sharper porphyroblast boundaries. The fine-grained matrix of quartz and feldspar in pelitic and calc-silicate rocks is typically granoblastic, although larger fragments still preserve angular to rounded boundaries (Plate 7b). Biotite, muscovite, and chlorite typically occur as small decussate grains or aggregates of grains in the matrix. However, muscovite and chlorite also occur as larger subidioblastic poikiloblasts. In this zone clinozoisite is less abundant and is mainly fine-grained, xenoblastic, and associated with biotite in the matrix.

Biotite/phlogopite in calc-silicate lithologies is typically

subidioblastic and inclusion-free, and occurs as weakly oriented grains parallel to compositional layering. Idioblastic tremolite is more abundant but remains randomly oriented and inclusion-rich.

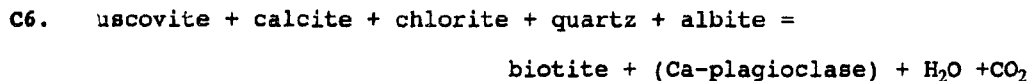
Marbles are texturally and mineralogically similar to those in the lower-grade rocks; however, the major difference is the occurrence of idioblastic phlogopite and a general decrease in the amount of chlorite. Phlogopite is typically concentrated in quartz and feldspar-rich layers and oriented parallel to compositional layering.

A number of reactions may lead to the generation of biotite (e.g. Mather, 1970) and some common reactions (Thompson, 1979) that could apply to these rocks are:



Reaction (C4) can also be applied to some calc-silicate rocks.

At this metamorphic grade, marbles lack muscovite and are depleted in chlorite possibly through the reaction proposed by Ferry (1983):



However, the absence of muscovite and chlorite can be interpreted in two ways; both may have been completely consumed by the continuous reactions cited above or may be absent due to whole rock compositions.

The mineral assemblages in zones A and B are typical of the chlorite and biotite zones in many regionally metamorphosed greenschist facies rocks (c.f. Turner, 1980; Yardley, 1989). However, the lack of well developed cleavage and the random orientation of many of the poikiloblasts suggests that mineral growth was the result of contact metamorphism. The pelitic, calc-silicate, and carbonate mineral assemblages in this zone are characteristic of the albite-epidote hornfels facies (e.g. Yardley, 1989).

5.2.3.3. Medium-grade rocks

The medium-grade assemblages are generally developed in the inner part of the contact aureole within a zone approximately 1000 m from the exposed plutonic contacts. They are characterized by the first appearance of cordierite in pelitic rocks (Plate 7c). The grain size is slightly coarser than in the low-grade rocks but many of the sedimentary structures are still preserved.

Cordierite first appears concentrated in mica-rich layers as small ovoid, highly poikilitic, randomly oriented grains with numerous small inclusions of muscovite, quartz, Fe-Ti oxides, biotite, and matrix accessories. In the cores of some cordierite grains are small, poikilitic spinel grains on which the cordierite appears to have nucleated. Cordierite is partially to entirely replaced by sericite.

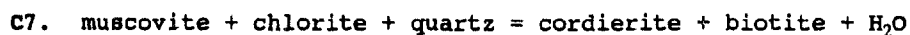
The matrix is typically granoblastic; however, where fine-grained muscovite and biotite are abundant, a moderately developed, bedding-parallel foliation exists which is commonly draped around the porphyroblasts. This foliation is not common in these hornfels. Shelley (1993) reported similar features in contact aureoles and suggested that they are a result of strain associated with the emplacement of the adjacent pluton, rather than some earlier (or later), separate regional metamorphic event.

However, in areas of regional greenschist facies metamorphism

(e.g. Drury Cove area) large ovoid patches of sericite, interpreted to have been cordierite grains, are locally abundant close to contacts with the tonalitic parts of the Renforth Pluton (Map A; Fig. 5.2). They commonly have crenulated inclusion trails similar in orientation to those outside the cordierite. Cordierite in this area is locally associated with large xenoblastic, randomly oriented biotite that also overgrows the crenulated foliation. The cordierite and associated biotite are interpreted to be the result of contact metamorphism by the Renforth Pluton.

In hornfels, chlorite and muscovite are still present as small grains associated with biotite in the matrix; however, locally they occur as subidioblastic, randomly oriented poikiloblasts.

The inferred reaction that introduced cordierite is similar to that proposed by Pattison and Harte (1985):

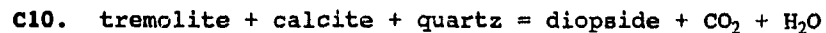
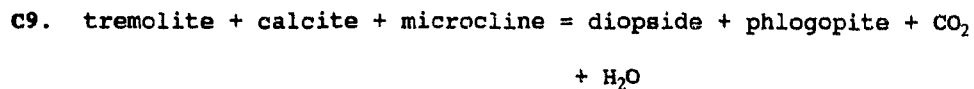
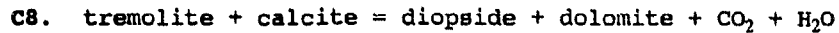


This reaction continues as temperature increases until chlorite is consumed and the resulting assemblage muscovite-biotite-quartz-cordierite becomes abundant. This assemblage exists over a wide area. Reactions involving spinel and cordierite at this grade of metamorphism are unclear.

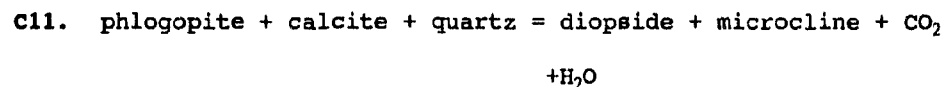
In calc-silicates and marbles, medium-grade metamorphism is marked by the appearance of diopside, although many of the marbles in the Green Head Group are monomineralic and are difficult to characterize in terms of metamorphic grade.

Subidioblastic to idioblastic diopside and tremolite are typically concentrated in thin discrete layers associated with rounded microcline, quartz, and minor plagioclase. In some calc-silicate rocks diopside may form large coarse clusters. The rims of tremolite and diopside are locally replaced by chlorite. Phlogopite is common in these layers. Idioblastic titanite and apatite are also concentrated in these layers.

From thin section observations, the presence of diopside in the metacarbonate rocks involved reactions with tremolite similar to those outlined by Peters and Wickham (1994):



Although phlogopite is generally in textural equilibrium with diopside, it is responsible for some diopside production by the reaction (Peters and Wickham, 1994):



The mineral assemblages in the medium-grade part of the contact aureole are characteristic of the hornblende-hornfels facies (e.g. Yardley, 1989). This facies forms the greater part of the outcrop width of the contact aureole and continues up to many of the plutonic contacts (Fig. 5.2 and 5.3). A typical feature of many hornblende-hornfels facies contact aureoles is the presence of andalusite (e.g. Turner, 1980). Abundant andalusite was reported by Wardle (1978, p.218 and Fig. 30) in many of the pelitic rocks of the Green Head Group; however, based on petrography these occurrences are now known to be cordierite. Prismatic rectangular grains occur in the contact aureole around the Acemac Pluton but due to abundant sericite replacement, they were not clearly identifiable as andalusite. The lack of andalusite may be the result of Al-poor bulk rock compositions.

5.2.3.4. High-grade rocks

Within a narrow (<100 metres wide), discontinuous zone around some plutons (e.g. Fairville, Spruce Lake, and French Village), all minerals have been totally recrystallized and most primary sedimentary textures have been obliterated. The pelitic and semi-pelitic rocks are generally characterized by coarse-grained texture, a lack of chlorite, a general depletion of muscovite, and an increase in K-feldspar. These rocks are typically composed of alternating granoblastic quartzo-feldspathic and biotite-rich layers which, in outcrop, give the rock a gneissic appearance (e.g. Pleasant Point Paragneiss of Wardle, 1978).

Distinctive mineral assemblages involving cordierite and hornblende in the semi-pelitic rocks and sillimanite-cordierite ± garnet in the pelitic rocks are present in this zone (Table 5.1.). Cordierite in the semi-pelitic rocks is typically subidioblastic to xenoblastic, moderately to strongly pinitized, and associated with the quartzo-feldspathic layers (Plate 7d). It locally appears to be intergranular and contains fewer matrix inclusions than in the medium-grade rocks. Cordierite grains in the pelitic rocks are relatively unaltered and larger than those in the semi-pelites. They occur as subidioblastic poikiloblasts with inclusions of biotite, K-feldspar, Fe-Ti oxides, and rare chlorite. Biotite inclusions are coarser in the rims of most cordierite grains compared to the cores and similar in size to those in the matrix. Spinel is locally associated with unaltered cordierite in pelitic and semi-pelitic rocks.

Sillimanite is rare and occurs only in the pelitic rocks. It forms fine, needle-like grains in biotite and in the cores or rims of some cordierite and quartz grains. Garnet is also rare and only observed in one sample from the pelitic rocks. It occurs as small, relatively inclusion-free, xenoblastic porphyroblasts.

Blue-green hornblende is present in the relatively biotite-depleted semi-pelitic lithologies, where it occurs as subidioblastic,

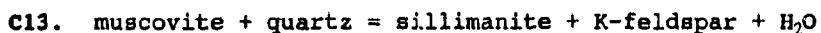
moderately poikilitic grains. Cordierite and hornblende were not observed together in the same sample. Granoblastic microcline to perthitic microcline commonly has small rounded inclusions of quartz and plagioclase and, when in contact with plagioclase and quartz, myrmekite is well developed.

Biotite in this zone is typically coarser grained than in lower-grade compositionally equivalent rocks and generally concentrated in distinct layers. Although these rocks appear to have a gneissic texture (e.g. Pleasant Point Paragneiss of Wardle, 1978), biotite is randomly oriented and does not have a uniform crystallographic orientation as it does in Brookville Gneiss biotite.

The reaction that accounts for the depletion of mica and the incoming of K-feldspar with cordierite in the semi-pelitic rocks may have been (e.g. Pattison and Harte, 1985) :



The appearance of sillimanite with K-feldspar in pelitic rocks is inferred to be similar to the reaction of Pattison and Harte (1985):



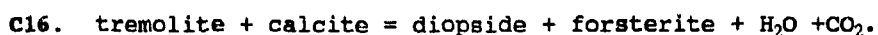
and the inferred reaction that accounts for the presence of spinel and cordierite in these high-grade rocks is (e.g. Xu et al., 1994):



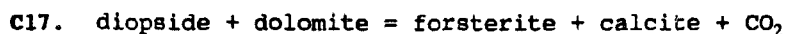
The formation of garnet is restricted to pelitic rocks and the inferred reaction is similar to that of Pattison and Harte (1985):



Marbles and calc-silicate lithologies within this high-grade zone are typically very coarse-grained and characterised by the development of forsterite, followed by garnet, and periclase (Table 5.1.). Forsterite appears to have formed first and typically occurs as isolated rounded grains or clusters associated with diopside and typically rimmed or completely replaced by serpentine. Tremolite is not commonly associated with forsterite. Forsterite appears to be in textural equilibrium with diopside in the calc-silicate rocks and probably formed by the reaction (e.g. Yardley, 1989):



In marble, forsterite is associated with calcite and appears to have formed from the breakdown of diopside by the reaction (e.g. Yardley, 1989):



Garnet grains (grossular?) are subidioblastic to xenoblastic and typically highly poikiloblastic with inclusions of diopside, calcite/dolomite, anorthite, and rare quartz. Forsterite is rarely associated with garnet, but where present occurs as inclusions in garnet rims. Locally garnet is associated with copper mineralization and abundant Fe-Ti oxides. Here the assemblage can be extremely altered with most minerals partially to entirely pseudomorphed by actinolite, serpentine, chlorite, and other indistinguishable minerals. These skarns are extremely limited in their distribution and significant only within 2-5 m of the contact with portions of the Renforth Pluton in the Kennebecasis Bay area (e.g. Leavitt, 1963). The reactions that formed garnet in non-skarn marbles is not clear but its close association with diopside, forsterite, anorthite, and calcite/dolomite suggests that these minerals might be involved (see section 5.4.2).

Periclase is rare and commonly completely pseudomorphed by of brucite. It has been observed in marble xenoliths in the French Village Quartz Diorite and was also documented in contact aureoles around plutons in the Saint John area (Leavitt, 1963). Periclase is locally associated with serpentinized forsterite and minute diopside grains. As in garnet, the reaction(s) that formed periclase are not clear (see section 5.4.2).

The mineral assemblages in this zone are characteristic of the pyroxene-hornfels facies (e.g. Turner, 1980). However, the first appearance of forsterite in carbonate rocks coincides with cordierite (prior to the development of sillimanite) in the pelitic rocks and could therefore be assigned to the upper hornblende-hornfels facies or transitional pyroxene-hornfels facies. Although temperatures were high enough to produce new K-feldspar and some rocks have a gneissic appearance, there is no evidence of partial melting (e.g. leucosome development) in the pelitic hornfels.

5.2.4. Hammondvale metamorphic unit

The Hammondvale metamorphic unit is a fault-bounded block located along the northwestern margin of the Caledonian Highlands in the Hammondvale area (Chapter 2). It was previously considered part of the Ashburn Formation of the Green Head Group (e.g. Ruitenberg et al., 1979; McLeod et al., 1994). This unit has been interpreted to provided a direct link between the Caledonia and Brookville terranes (e.g. Ruitenberg et al., 1979). However, a detailed petrological description of this unit has not been conducted to evaluate this correlation.

The Hammondvale metamorphic unit consists dominantly of albite and garnet porphyroblastic mica schist with minor marble and amphibolite. The main mineral assemblage in the mica schist is quartz-muscovite-albite ± garnet ± biotite ± calcite ± K-feldspar with abundant apatite, titanite, tourmaline, Fe-Ti oxides, epidote, and a small amount of

zircon and rare rutile as accessory minerals (Table 5.1). These rocks have a well developed schistosity and a local stretching lineation. The foliation is defined by alignment of muscovite and minor biotite and is draped around porphyroblasts, whereas the lineation is defined by recrystallized quartz ribbons and asymmetric albite and garnet porphyroblasts. Asymmetric quartz-rich pressure shadows are common on the margins of many of the porphyroblasts.

Albite porphyroblasts are small (<5 mm in diameter), subidioblastic, and highly poikilitic (Plate 8a, b). They contain well developed sigmoidal and straight inclusion trails defined by idioblastic epidote, titanite, tourmaline and xenoblastic to subidioblastic muscovite, quartz, Fe-Ti oxides, and rare biotite, chlorite, and rutile. Quartz inclusions are coarser grained toward the rims compared to the cores. Albite is usually unaltered and has well developed simple twins. Rare oligoclase patches occur in the albite grains. These are typically well twinned and partially altered to sericite. The internal foliation is subparallel to, or commonly truncated against the main external foliation. K-feldspar is not common. It occurs in the pressure shadows of some albite porphyroblasts or more rarely as altered patches in the albite with oligoclase. Only two samples had asymmetric K-feldspar porphyroblasts with the same inclusion trails as in the albite. Subidioblastic, highly poikilitic garnet porphyroblasts display the same type of inclusion trail as the albite; however, they are defined by quartz, titanite, and Fe-Ti oxides. In addition, tiny, idioblastic, inclusion-free garnet occurs as inclusions in albite poikiloblasts and in the matrix.

Marble associated with the mica schist is well banded with thin (1-2 mm wide) alternating calcite-rich and muscovite-rich layers (Plate 8c). Prismatic apatite, titanite, tourmaline, epidote, and Fe-Ti oxides are associated with the muscovite layers. Locally, fine-grained chlorite develops along muscovite rims and cleavage planes. Apatite is typically zoned with dark cores and clear rims.

Amphibolite is also well layered, alternating between plagioclase-rich and hornblende-rich layers (Plate 8d). Albite porphyroblasts are not common in the amphibolite, but where present are elongate parallel to banding. They typically contain straight inclusion trails defined by elongated quartz and titanite parallel to the external foliation. Blue-green hornblende is elongate parallel to banding and is inclusion-free. It is typically partially to entirely replaced by actinolite and chlorite. Quartz is not present.

Limited detailed structural studies indicate that all the porphyroblasts overgrew an earlier crenulation cleavage and continued to grow after a coarsening of the matrix minerals. The main episode of deformation occurred after porphyroblast growth which resulted in the local development of mylonitic textures such as quartz ribbons and asymmetric porphyroclasts. Based on lithological differences alone, correlation between the Ashburn Formation in the Green Head Group and the Hammondvale metamorphic unit appears unlikely.

5.3. MINERAL CHEMISTRY

Mineral compositions were determined by electron microprobe in representative samples from: 1) paragneissic, orthogneissic, and marble lithologies in the Brookville Gneiss, 2) gneissic boudins and blastomylonites in the MacKay Highway shear zone, 3) marble and pelitic lithologies in the Ashburn Formation of the Green Head Group, and 4) mica schist in the Hammondvale metamorphic unit. These data are used here to assess variations in mineral chemistry and chemical equilibrium, and for pressure-temperature estimates. Analytical data are presented in Appendix D.

In the following section mineral compositions from the Brookville Gneiss and the MacKay Highway shear zone are described together because of their inferred similar protoliths.

5.3.1. Brockville Gneiss and MacKay Highway shear zone

5.3.1.1. Biotite

In general, the range of biotite compositions in samples of paragneiss, melanosomes in the migmatitic paragneiss, orthogneiss, and associated marble is typical of those in amphibolite facies rocks (e.g. Guidotti, 1984), with paragneiss and orthogneiss samples having Mg/Mg+Fe of about 0.50 and relatively enriched Ti contents (Fig. 5.4a). Orthogneiss samples typically have Al contents that are considerably lower.

A negative correlation between Al^{VI} and Mg/Mg+Fe contents for biotite in the orthogneiss (Fig. 5.4a) may be due to more variable degrees of retrograde resorption by chlorite, during which the biotite became more enriched in Fe and Mg. This is consistent with patterns predicted by Xu et al. (1994) where lower-temperature re-equilibration results in MgO enrichment, whereas bulk rock compositional differences generally cause variations in both Mg/(Mg+Fe+Mn) and Tschermak's substitution. However, biotite in the pelitic samples is less chloritized and does not display this trend. Instead the compositions show a positive correlation between Al^{VI} and Mg/Mg+Fe contents. Biotite samples from the migmatitic melanosome are enriched in Al and Mg and depleted in Fe compared to the biotite from paragneissic samples, and both are significantly enriched in Al^{VI} compared to orthogneissic biotite (Fig. 5.4 and 5.5; Appendix D). Similar trends are reported from the experimental results on biotite involved in partial melting reactions where biotite samples from melanosome are depleted in Fe and biotite from leucosome samples is enriched (Patiño Douce and Johnston, 1991).

Biotite compositions from pelitic blastomylonite and gneissic boudin samples from the MacKay Highway shear zone are similar; however, they are distinct from other gneissic biotite compositions, being

relatively high in Al and low in Mg/Mg+Fe contents (Fig. 5.4a). This may be due to bulk composition and Al-saturation which can be confirmed by the relatively high abundance of sillimanite in the boudins. However, sillimanite is a minor phase in the pelitic blastomylonites and therefore the high Al^{VI} contents may possibly be attributed to higher grades of metamorphism (e.g. Guidotti, 1984).

Mica in the marbles is typically phlogopite (Fig. 5.4a).

5.3.1.2. Cordierite

Most of the analyzed cordierite samples appear to be relatively unaltered, with pinitized rims and pale yellow cores; however, microprobe data indicate that they are moderately to intensely altered. The altered cordierite is similar in composition to those analyzed by Jamieson (1984). The altered cordierites have K₂O values up to 8 wt.% and are relatively depleted in FeO and MgO (Fig. 5.5; Appendix D) and are similar to some clay minerals described by Deer et al. (1992). Pinitization is more widespread in samples from the blastomylonite zone, paragneiss and melanosome than from the leucosome. Cordierite from an unaltered migmatitic paragneiss contains a uniform composition from leucosome to melanosome with the approximate formula $Al_3Mg_{1.4}Fe_{0.6}AlSi_5O_{18}$ and Fe/Fe+Mg values of about 0.30. Relatively unaltered cordierite grains from paragneissic samples have distinctly higher Fe/Fe+Mg values of greater than 0.50.

5.3.1.3. Feldspar

Plagioclase grains in samples of paragneiss and orthogneiss display a relatively narrow range in composition from about An₃₀ to An₄₀, with identical averages of 34% (Fig 5.6; Appendix D). They are typically unzoned, and contain only minor K₂O. Analyses from leucosome samples show a similar, although slightly higher, range in An

compositions with an average of 39% (Fig. 5.6). Potassium feldspar (microcline) from paragneiss, leucosome, and orthogneiss samples also displays a narrow range in compositions with average Or contents greater than 90%. The relative uniformity of feldspar compositions (e.g. An_{34-39}) suggests that these grains probably grew/recrystallized during amphibolite grade metamorphism.

Plagioclase in marble is nearly pure anorthite, with An contents greater than 99% and only trace amounts of Ab (Fig 5.6; Appendix D). Potassium feldspar (microcline) in marble has compositions of Or_{96} with minor amounts of Ab (Fig. 5.6).

Plagioclases in the MacKay Highway shear zone are more albite-rich than those from the gneiss with an average of about An_{18} . Plagioclase compositions from gneissic boudins have trace amounts of Or, whereas compositions from the associated pelitic blastomylonite are moderately enriched in Or (Fig. 5.6; Appendix D). Potassium feldspar (microcline) compositions are similar to those in the gneiss with a slightly lower average of Or_{88} . Lower An contents in shear zone plagioclase compositions compared to their host rocks have been observed by numerous workers (e.g. Kneller and Leslie, 1984) and commonly attributed to re-equilibration of the shear zone during a lower-grade ambient metamorphism.

5.3.1.4. Garnet

Garnet in the blastomylonite is dominantly an Fe-Mg solid solution (Appendix D). The relatively inclusion-rich garnet cores are higher in Mg, whereas the inclusion-free rims are high in Fe (Fig. 5.5). The Ca and Mn contents show a slight increase from core to rim. This is also true for garnet fragments in the matrix which suggests that each fragment probably behaved as an individual grain during re-equilibration. Average analyses give $(Fe_{2.52}Mg_{0.36}Ca_{0.11})Al_{1.96}Si_{2.97}O_{12}$

and $(\text{Fe}_{2.58}\text{Mn}_{0.02}\text{Mg}_{0.28}\text{Ca}_{0.12})\text{Al}_{1.99}\text{Si}_{2.98}\text{O}_{12}$ for cores and rims. Relative enrichment of Fe and the depletion of Mg from garnet cores to rims are commonly assumed to be the result of some type of retrograde modification (e.g. Tracy, 1982; Spear, 1991), probably Fe-Mg exchange of garnet rims with adjacent biotite.

5.3.1.5. Clinopyroxene

Clinopyroxene in samples of marble from the Brookville Gneiss is nearly pure diopside (Fig. 5.7a). However, some of the pyroxene grains appear to be more complex than the three component Ca-Fe-Mg series and are significantly more aluminous. Clinopyroxenes from marble samples with amphibole as a major mineral phase have higher proportions of Al_2O_3 (>5 wt.%) and TiO_2 (>1.5 wt.%) than clinopyroxenes from samples with minor amphibole. These relations probably reflect bulk compositional differences.

5.3.1.6. Amphibole

Ca-amphibole is one of the most abundant silicate minerals in the marbles of the Brookville Gneiss. The composition ranges from tremolite to magnesio-hornblende, although some are actinolitic in composition (Fig. 5.8; Appendix D). The close spatial relationship of these marbles in the uniformly high-grade gneiss suggests that metamorphic grade (P-T) was not an important factor in the formation of different amphibole compositions. The variation in compositions is probably a result of differences in bulk rock chemistry and/or metamorphic fluid composition; however, in some samples it appears to be the result of retrograde metamorphism.

5.3.1.7. Muscovite

Based on textural evidence muscovite is interpreted to have formed as a result of retrograde metamorphism. The composition is essentially that of the muscovite (*sensu stricto*) end member, but also contains minor paragonite component (Fig. 5.9a; Appendix D). Muscovite generally displays uniform composition from sample to sample; however, Fe varies considerably between 0.10 to 0.38 (for 22 oxygen). Large muscovite grains that are the product of cordierite retrogression are generally high in Fe, whereas muscovite replacing sillimanite has much lower Fe content. No zoning was detected within individual grains. Sericite after cordierite and feldspar was not analyzed.

5.3.1.8. Other phases

Calcite has low Fe (<0.02) and Mg (<0.10) contents (for 6 oxygen); however, in samples with coexisting dolomite, Mg contents are typically higher (>0.10). In dolomite-free marbles, some calcite is nearly pure CaCO_3 with $\text{Fe}+\text{Mg} \leq 0.04$ (Appendix D). Andalusite samples from the MacKay Highway shear zone and gneissic boudins are greater than 99% pure end-member compositions with minor FeO, MgO, and CaO. Tourmaline in the paragneiss is magnesium-rich and approaches dravite compositions whereas those in marble samples are dominantly uvite. Apatite in the marble is greater than 99% pure end-member with minor NiO and ZnO. The dominant opaque phase in the paragneiss, migmatitic paragneiss, orthogneiss, and marble is magnetite which is greater than 98% pure end-member composition. Ilmenite occurs only in the paragneiss and is generally 98% pure end-member with minor hematite component.

5.3.2. Ashburn Formation

5.3.2.1. Mica

Muscovite compositions are very similar to those in the Brookville Gneiss (Fig. 5.9b). Muscovite from a sample of spotted cordierite schist generally has relatively constant Al^T values, with Fe+Mg varying between 0.23 and 0.31 (for 22 oxygen). The composition is essentially that of muscovite (*sensu stricto*), but also contains minor paragonite (Appendix D). The one analyzed sample with a higher Fe+Mg value (0.47) is in contact with altered cordierite and is probably affected by this sericitic retrogression.

Biotite from marble in the Ashburn Formation has high Mg contents and, like that in the Brookville Gneiss marbles, is of phlogopite composition (Fig. 5.4b).

5.3.2.2. Amphibole

As in marble in the Brookville Gneiss, Ca-amphibole is one of the most abundant silicate minerals in the Ashburn Formation. It has constant Mg/Mg+Fe values with Al^{IV} varying between 0.08 and 0.69 and therefore composition ranges from tremolite to magnesio-hornblende (Fig. 5.8). Compared to marble in the Brookville Gneiss, these amphiboles are more restricted in their compositional range; however, within individual samples there is wide variation in composition (Appendix D), which may reflect alteration.

5.3.2.3. Clinopyroxene

Clinopyroxene analyzed in two samples of marble is very close to pure diopside (Fig. 5.7b). It has a more "normal" composition compared to diopside in the Brookville Gneiss with only trace amounts of Al and

Ti, and higher Na (Appendix D). The compositional variability within individual samples is negligible.

5.3.2.4. Plagioclase

Plagioclase compositions from the spotted schist are spread from albite (An_0) to oligoclase (An_{25}) (Fig. 5.6). These compositions are considerably different from those in the Brookville Gneiss and are typical of lower grade rocks. However, the relatively large range for this grade of metamorphism probably reflects a diverse provenance of detrital grains that were only partially modified during regional and/or contact metamorphism. The wide variations in grain size and shape of plagioclase also suggests that their origin is detrital, and that they have survived textural modification. Plagioclase is not present in the analyzed marble samples.

5.3.2.5. Other phases

Calcite and dolomite in marble samples have variable Fe contents from 0 to 0.05 (for 6 oxygen). Dolomites in dolomite-rich marbles have considerably higher Mg contents (>3.02) than those coexisting in calcite-rich samples (<2.95), although calcite with or without dolomite has similar Mg values (Appendix D). In calcite-free marbles, the dolomite is nearly pure $MgCO_3$ (Appendix D).

Tourmaline in the schist is near end-member dravite whereas that in the marble is close to uvite composition. Apatite is also near end-member composition with minor Cl values (<0.7 wt.%). The dominant opaque phase in the schist and marble is magnetite which is greater than 98% pure.

5.3.3. Hammondvale metamorphic unit

5.3.3.1. Mica

White mica from the Hammondvale metamorphic unit contains relatively high, although variable, Fe+Mg values between 0.52 and 0.98 (for 22 oxygen) and is typically phengitic in composition (Fig. 5.9c). Muscovite coexisting with garnet has the highest and most constant Fe+Mg values, whereas that not associated with garnet has lower and more variable Fe+Mg values. It also has Na/(Na+K+Ca) values that are consistently low (Appendix D). Muscovite is subject to electron beam damage which will result in some elements "burning-off" and therefore remain undetected (e.g. McMullin, 1991). Sodium is especially susceptible to this, resulting in unusually low paragonite contents. It is necessary to use large beam diameters (about 10 μm) to obtain muscovite compositions. However, the spot size used for muscovite analysis in this study was considerably narrower (about 2 μm) and therefore the Na contents are considered minimum values. This assumption is significant when using TWEEQU calculations for this unit (section 5.4.3).

The muscovite differs significantly from that in the low-grade Green Head Group in increased Fe+Mg values and lower XNa. The higher Fe+Mg values could reflect bulk rock compositions (e.g. Guidotti, 1984); however, phengitic muscovites are common in high pressure - low temperature metamorphic environments (e.g. Shelly, 1980).

Biotite is not common in the Hammondvale metamorphic unit, and where present, is typically partially altered to chlorite or replaced by muscovite. Two fresh biotite grains yielded "normal" compositions (Fe/Fe+Mg = 0.53; Al^{VI} = 0.69, for 22 oxygen) (Fig. 5.4a).

5.3.3.2. Garnet

Small, idioblastic, inclusion-free garnet grains that occur as inclusions in albite porphyroblasts (CW88-115A) have an average composition of $(\text{Fe}_{1.75}\text{Mn}_{0.55}\text{Mg}_{0.21}\text{Ca}_{0.50})\text{Al}_{1.96}\text{Si}_3\text{O}_{12}$. Other larger, subidioblastic, relatively inclusion-rich garnet (NBS7-4090) have similar core-rim compositions of $(\text{Fe}_{1.77}\text{Mn}_{0.34}\text{Mg}_{0.11}\text{Ca}_{0.79})\text{Al}_{2.04}\text{Si}_{2.95}\text{O}_{12}$ and $(\text{Fe}_{1.75}\text{Mn}_{0.21}\text{Mg}_{0.11}\text{Ca}_{0.96})\text{Al}_{2.01}\text{Si}_{2.95}\text{O}_{12}$, respectively, although they display a decrease in spessartine and pyrope contents and increase in andradite content compared with the garnet inclusions.

5.3.3.3. Plagioclase

Highly poikiloblastic plagioclase porphyroblasts typically display a very restricted range in composition, from An_0 to An_2 with trace Or components, and are generally unzoned. However, rare patches of twinned, partially sericitized plagioclase occur in some albite porphyroblasts. These patches typically have compositions of An_{29} (Fig. 5.6; Appendix D). Similar observations were noted by Jamieson and O'Beirne-Ryan (1991) in albite schists of the Fleur de Lys Supergroup. Here the growth of oligoclase was attributed to retrogression and the breakdown of garnet. Based on textural evidence it is unclear if oligoclase formed during prograde or retrograde metamorphism in the Hammondvale metamorphic unit.

5.3.3.4. Other phases

Epidote inclusions do not differ significantly from those in the matrix and have similar average composition of $\text{Ca}_{1.95}\text{Fe}_{0.65}\text{Al}_{2.30}\text{O}(\text{SiO}_4)(\text{Si}_2\text{O}_7)(\text{OH})$ (Appendix D). They do not appear to be zoned. Calcite is nearly pure CaCO_3 with negligible amounts of Fe, Mn,

and Mg (Appendix D). Tourmaline is dravite.

5.4. METAMORPHIC CONDITIONS

5.4.1. Introduction

In spite of the textural evidence for extensive retrograde metamorphism in the metamorphic units of the Brookville terrane, the limited amount of chemical variation in most minerals on the scale of a thin section indicates that at some time all samples had approached relatively homogeneous intergrain mineral compositions, presumably during peak metamorphic conditions. Most of the major compositional variations observed between samples appear to be controlled by bulk rock compositions; however, variations on a millimetre scale are interpreted to be the result of post-peak retrograde re-equilibration.

Pressure and temperature can be estimated using the TWEEQU software (version 1.02) of Berman (1991). This program calculates the location of reaction equilibria in P-T space using the internally consistent thermodynamic data set of Berman (1988; 1991) for end-member phases. Ideal solution models were used for pyroxene and amphibole and the solution models of Berman (1990), Fuhrman and Lindsley (1988), and McMullin et al. (1991) for garnet, plagioclase, and biotite, respectively.

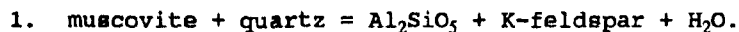
5.4.2. Brookville Gneiss and MacKay Highway shear zone

5.4.2.1. Paragneiss and migmatitic paragneiss

The pelitic mineral assemblages in the paragneiss and migmatitic paragneiss are not well suited to treatment by TWEEQU, largely due to poorly calibrated thermodynamic properties of Fe-rich cordierite. This results in unstable cordierite reactions (negative pressures) on the P-T

grid. However, information about the relative orientation in P-T space can be obtained from the KFMASH petrogenetic grid of Spear and Cheney (1989) which is largely based on the same database as TWEEQU. For the purpose of this study, cordierite-producing reactions of Holdaway and Lee (1977) and Hoffer (1976) are incorporated to account for the presence of Fe-rich cordierite. The location of the Al_2SiO_5 triple point is similar to that of Holdaway (1971).

The absence of primary muscovite in the paragneiss and migmatitic paragneiss can be used to constrain the minimum P-T conditions in the Brookville Gneiss based on the reaction:

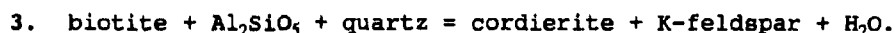


This reaction also accounts for the production of andalusite in assemblages containing plagioclase-quartz-biotite-K-feldspar-andalusite (without sillimanite). This assemblage constrains the pressure estimates (≤ 2.2 kbar) at relatively low temperatures (Fig. 5.10).

The occurrence of minor assemblages of andalusite-sillimanite-K-feldspar-biotite in the paragneiss indicates that metamorphic conditions were near those of the andalusite-sillimanite phase boundary:



Cordierite in the assemblage containing inclusions of biotite probably formed by the reaction calibrated by Holdaway and Lee (1977):



Metamorphic conditions for this assemblage are close to the intersection of reaction (2) and reaction (3) at approximately 625°C and 1.9 kbar (Fig. 5.10). This assumes the Fe content of cordierite in the paragneiss is 100%, although analyzed cordierite in this assemblage

typically has Fe contents greater than 50%, none are 100% (Appendix D). For this assemblage to plot on the P-T grid, Fe contents should be at least 75%, therefore assuming Fe at 100% results in minimum pressure estimates. The absence of andalusite and the presence of sillimanite in this assemblage implies that metamorphic conditions were above the Al_2SiO_5 phase boundary and parallel to reaction (3).

Partial melting of the paragneiss typically resulted in the formation of leucosome and melanosome with quartz-K-feldspar-cordierite-sillimanite-biotite-bearing assemblages, although cordierite is not present in all samples. The composition (similar Fe contents of 30%) and texture of cordierite co-existing in the leucosome and melanosome suggest that they are in equilibrium (c.f. sample CW88-218). Andalusite forms rare, small, embayed grains in the melanosome and, based on this textural evidence, it is considered relict from lower temperature conditions. This assemblage indicates peak metamorphic conditions close to the intersection of the minimum temperature hydrous melting curve and reaction (3) at approximately 675°C and 4.0 kbar, using the reaction of Holdaway and Lee (1977) (Fig. 5.10). The cordierite reaction of Hoffer (1976) for Fe contents of 30% increases the temperature to 685°C and lowers the pressure to 3.1 kbar.

Fluid composition and pressure will affect the position of these reactions. The activity of H_2O in metamorphic rocks largely depends on the composition of the fluid, whether or not H_2O exists as a free fluid phase, and the CO_2 component. Although marble and calc-silicate rocks occur in the Brookville Gneiss, carbonate minerals were not observed in the pelitic assemblages which may argue against significant CO_2 in the metamorphic fluid. However, it is likely that activity of H_2O was locally quite variable.

5.4.2.2. Marble

Given appropriate activity-corrected T-XCO₂ diagrams using actual mineral chemistry, the observed mineral assemblages in the marble can be used to constrain temperature and fluid composition in the Brookville Gneiss. The analyzed calc-silicate minerals developed in the marbles are very close to pure end-member compositions (section 5.3.1.). Activity models are those used in TWEQU for diopside and amphibole (see above). Calcite, dolomite, and titanite were assumed to be pure end-member compositions. A pressure of 3.1 kbar is assumed in all calculated reactions (see section 5.4.1.1). Phlogopite, K-feldspar, and quartz were eliminated from the calculations for clarity.

The typical mineral assemblage in the marble is calcite-dolomite-phlogopite-tremolite-diopside-K-feldspar ± forsterite ± plagioclase ± quartz. Some assemblages include actinolite instead of tremolite. Two separate samples with tremolite-bearing assemblages and one with actinolite were used in the calculation. Mineral chemistry of this assemblage requires the use of the 10-component system SiO₂-TiO₂-Al₂O₃-FeO-MgO-CaO-Na₂O-K₂O-CO₂-H₂O to describe the reactions involving these phases. There are 16 possible activity-corrected reactions (Table 5.3) for the selected end-member phases (diopside, tremolite-actinolite, forsterite, rutile, titanite, calcite, dolomite, H₂O, and CO₂) assuming activities for rutile and H₂O at about 0.94 and 0.96, respectively. The intersections of these reactions yield similar results and constrain the T-XCO₂ conditions experienced by the tremolite-bearing assemblages between 638-642°C and 0.54-0.58 XCO₂ at 3.1 kbar (Fig. 5.11a, b).

The assemblage containing actinolite is defined by similar activity-corrected reactions, assuming the activity of rutile at 0.99 and H₂O at 0.65. The results are slightly high than the tremolite-bearing assemblages at 654°C and 0.66 XCO₂ at 3.1 kbar (Fig. 5.11c).

5.4.2.3. Pelitic blastomylonite

The mineral assemblage in the paragneissic boudins is similar to that in the Brookville Gneiss, although modal abundances may vary. The diagnostic mineral assemblage in the boudins is quartz-K-feldspar-sillimanite-biotite-cordierite-andalusite. This assemblage indicates metamorphic conditions above the muscovite breakdown curve at the intersection of reactions (2) and (3) at approximately 625°C and 1.9 kbar (Fig. 5.10). This is identical to metamorphic conditions inferred from samples of the Brookville Gneiss.

The mineral assemblage in the pelitic blastomylonite that best represents peak recrystallized metamorphic conditions is similar to the mineralogy in the boudins, except that it locally contains garnet and prograde muscovite. The most notable feature of the shear zone is the general lack of retrograde metamorphism and many of the minerals appear unaltered. These features, together with the mineral assemblage, are consistent with re-equilibration under amphibolite facies conditions. The peak recrystallized mineral assemblage (excluding garnet) lies on the andalusite-sillimanite phase boundary between reaction (1) and (3) (Fig. 5.10).

The presence of garnet in the shear zone and the lack of garnet in the host gneiss require explanation. Variations in mineral assemblages in shear zones compared to the surrounding rocks are commonly attributed to increased fluid flow in an open system (e.g. Beach, 1980) or re-equilibration under high-grade conditions in a closed system (e.g. White and Clarke, 1994). However, in each case, the resulting minerals are typically neoblastic and undeformed, whereas garnet from the MacKay Highway shear zone preserves broken and stretched textures that parallel the regional stretching lineation. This suggests that the garnet existed in the host rock prior to deformation. However, due to the recrystallized textures, it is not clear what reaction(s) initially produced garnet in the gneiss. If those of Holdaway and Lee (1977) are

used, then minimum metamorphic conditions for the production of garnet in the gneiss and/or migmatitic paragneiss could be about 740°C and < 3.0 kbar (Fig. 5.10). This would imply that higher grade rocks were exhumed along the shear zone but this is highly speculative.

5.4.2.4. Geothermobarometry

Lithologies in the Brookville Gneiss do not contain many assemblages suitable for quantitative geothermobarometry. The solubility of Mg in calcite in the assemblage calcite + dolomite has been calibrated as a geothermometer (e.g. Powell et al., 1984; Anovitz and Essene, 1987) and applied to a sample of marble from the Brookville Gneiss (Table 5.2). Calcite with dolomite exsolution lamellae were not used and only those with granoblastic (120° triple-point junctions) were intergrated in the calculation (e.g. Anovitz and Essene, 1987). Temperatures obtained from the calibration of Anovitz and Essene (1987) are consistently low with an average of $382 \pm 26^\circ\text{C}$. Applying their Fe-correction only raises the average temperature by 2°C. The low temperatures are the direct result of low Mg values (section 5.3.1h). Retrograde equilibration produces calcite grains with Mg contents lower than those defined at peak metamorphic temperatures (cf. Cook and Bowman, 1994).

The two-feldspar geothermometer is based on the partitioning of $\text{NaAlSi}_3\text{O}_8$ between plagioclase and alkali feldspar (e.g. Stormer, 1975; Haselton et al., 1983). This method was applied to paragneiss, migmatitic paragneiss, gneissic boudins, and orthogneiss. Temperature estimates obtained from both two-feldspar calibrations give comparable results from sample to sample; however, like the calcite-dolomite geothermometer the results are consistently low (Table 5.2). The calibration of Stormer (1975) yields on average temperature of $422 \pm 69^\circ\text{C}$ and that of Haselton et al. (1983) gives $397 \pm 87^\circ\text{C}$. This suggests

significant subsolidus re-equilibration, likely due to retrograde metamorphism or cooling.

Three calibrations of the garnet-biotite Fe-Mg exchange thermometer have been applied to determine the temperatures during metamorphism. This includes the empirical calibration of Thompson (1976), the experimentally calibrated, ideal ionic model of Ferry and Spear (1978), and the model of Hodges and Spear (1982) which incorporates an empirical correction factor for the effects of Ca in garnet. These results are compared to temperatures calculated with TWEEQU employing the activity models of Berman (1990) and McMullin et al. (1991).

Five coexisting garnet-biotite pairs were analyzed in a sample from the pelitic blastomylonite. Where possible both garnet core and rim were analyzed, together with adjacent biotite and one inclusion of biotite. Temperature estimates obtained using the different calibrations yield comparable results within 30°C, although estimates from TWEEQU are generally slightly higher. Temperatures from garnet cores and adjacent biotite or inclusions of biotite are systematically higher (up to 170°C) than estimates from the rims of adjacent minerals (Table 5.2). The average temperature obtained by TWEEQU using garnet core compositions is $668 \pm 19^\circ\text{C}$ at 3.0 kbar.

Pressure estimates based on calibrations of the anorthite breakdown reaction (e.g. Ghent et al., 1979; Newton and Haselton, 1981; Koziol and Newton, 1988; TWEEQU) were used in an attempt to evaluate pressure conditions during metamorphism. However, the only suitable assemblage (garnet-plagioclase-andalusite/sillimanite-quartz) is restricted to lithologies in the shear zone. Pressure estimates obtained by these methods are inconsistent with the observed petrography and result in overestimation of pressures (e.g. 5 to >10 kbar). Applying an Mn correction to garnet activity (e.g. Ganguly and Saxena, 1984) lowers many of the pressure estimates (lowest at 4.2 kbar) but they still appear to be too high. It appears that the garnet is not in

equilibrium with other minerals in this sample. This is not surprising given the recrystallized character of many of the minerals in the shear zone. There does not appear to be a way to quantify the pressure conditions.

5.4.2.5. Summary of metamorphic conditions

The absence of prograde muscovite and the presence of andalusite paragneiss and cordierite-bearing migmatitic paragneiss limits the P-T conditions for the mineral assemblages developed in the Brookville Gneiss (Fig. 5.10). At lower temperatures the P-T trajectory accounts for the disappearance of muscovite and the presence of andalusite before the andalusite-sillimanite phase boundary was reached. With an increase in temperature, cordierite co-exists with andalusite and sillimanite in the paragneiss near the Al_2SiO_5 and cordierite-in reactions. From this point two trajectories are possible. Based on the cordierite-forming reactions of Holdaway and Lee (1977) and the decrease in Fe contents in migmatitic cordierite, peak metamorphic conditions could be 675°C and 4.0 kbar. However, a more realistic estimate, consistent with the observation that anatexis is closely associated with cordierite, is 685°C and 3.1 kbar based on the reaction of Hoffer (1976).

Equilibration temperatures of 638-654°C for the tremolite and actinolite-bearing assemblages in carbonate rocks represent peak metamorphic conditions that are consistent with estimates based on paragneiss and migmatitic paragneiss phase equilibria (Fig. 5.10).

The results of thermobarometric calculations are generally incompatible with peak metamorphic temperature and pressure estimates on the basis of the petrogenetic grid. However, calibrations of the calcite-dolomite (Anovitz and Essene, 1987) and two feldspar geothermometer (Stormer, 1975; Haselton et al., 1983) yielded similar results of about 400°C. The low temperature suggests significant re-equilibration under greenschist facies conditions following the peak

of metamorphism.

Temperatures determined by applying TWEEQU calibration of the garnet-biotite geothermometer to garnet core and biotite grains in the shear zone yielded results that are compatible with peak metamorphic conditions (ca. 670°C). However, garnet rim temperatures are lower (ca. 550°C) and consistent with retrograde garnet zoning during post-peak re-equilibration. The high temperature results from garnet core analyses are surprising given the highly recrystallized textures in the shear zone. It is unclear if the garnet and biotite preserve their pre-deformation peak metamorphic geochemical signature or are partially "reset". Given these uncertainties the interpretation of this temperature should be treated with caution.

Taking into account all available data, the preferred peak metamorphic conditions in the Brookville Gneiss are between 585-700°C and 1.5-3.5 kbar.

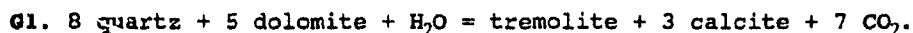
5.4.3. Green Head Group

No systematic chemical data were obtained from the various mineral assemblages related to contact metamorphism in pelitic lithologies of the Green Head Group. This is largely due to the fine-grained textures and variable degrees of retrograde metamorphism. However, mineral chemistry was obtained from some relatively unaltered carbonate assemblages in this zone. Here a T-XCO₂ phase diagram can be constructed using TWEEQU to characterize the metamorphic history of the aureole(s), but several assumptions must be made. The first is that bulk rock compositions are similar from low- to high-grade, the second is that they are in chemical equilibrium at all times (cf. Holness, 1992), and the third is that the system is closed to infiltration of fluids (c.f. Peters and Wickham, 1994), especially those rich in F and/or NaCl from the intruding pluton(s). Evidence for chemical

equilibration is the presence of concentric zones with mineral assemblages appropriate to the inferred P-T conditions and the general presence of both reactants and products, which suggests that reactions were internally buffered (except for the garnet and periclase assemblages). With these assumptions in mind, the equilibrium approach can be useful as a first approximation of metamorphic conditions (Fig. 5.12). A pressure of 1 kbar is assumed in the construction of the T-XCO₂ phase diagram. A pressure estimate of 2 kbar increases the temperature of the invariant points by about 50°C.

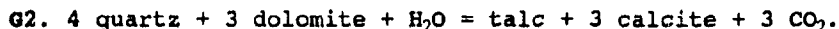
Two reaction paths exist in the contact aureoles: marbles develop the sequence talc-phlogopite-tremolite-diopside-forsterite ± periclase (Fig. 5.12a) whereas the calc-silicate rocks show the sequence tremolite-phlogopite-diopside-forsterite ± garnet (Fig. 5.12b).

In calc-silicate lithologies reaction begins with the growth of subidioblastic tremolite associated with quartz in phlogopite-free rocks by the reaction:



At low grades, K-feldspar grains are scattered through the metasedimentary rocks and these react in the temperature range 300-400°C to form phlogopite (Holness, 1992). The lack of phlogopite in this assemblage suggests temperatures below the range 300-400°C for the formation of tremolite and associated muscovite and clinozoisite (section 5.2.4.1.) and indicates that the associated fluids were extremely CO₂-depleted (Fig. 5.12).

The reaction for the formation of talc in marble is uncertain (5.2.4.1.) but is commonly attributed to the breakdown of quartz and dolomite by the reaction:



The lack of phlogopite in the talc-bearing assemblages (Wardle, 1978) suggests that the associated fluids, as in the tremolite assemblages, were CO₂-depleted (Fig. 5.12).

The two reaction paths meet at the invariant point A (T=412°C and XCO₂=0.63). The nature of the reaction after this point is related to the amount of quartz and talc remaining in the rock. If talc is present further reaction can only take place by:

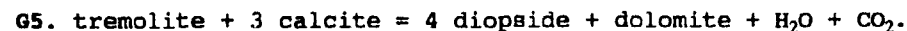


Talc is not common (e.g. Wardle, 1978) and this reaction probably does not occur; however, quartz is relatively abundant and reaction will continue take place by reaction (G1). By invariant point A phlogopite and biotite have probably developed in the carbonate and clastic rocks, respectively.

After an increase in temperature, invariant point B (T=466°C and XCO₂=0.98) is reached and diopside appears. If quartz is still present, as in most calc-silicate rocks, the reaction will proceed:



In most marbles quartz is exhausted and further reaction will continue by:

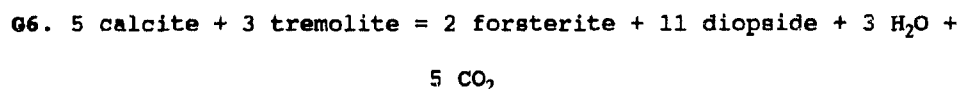


After quartz is eliminated from calc-silicate lithologies via reaction (G4), they undergo no further reaction until the temperature reaches that of reaction (G5). This relatively long period of annealing can result in large coarse clusters of diopside.

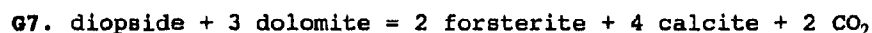
Point B also coincides with the appearance of small voids of

cordierite in pelitic lithologies associated with the carbonate rocks and marks an important isograd (cordierite and diopside-in).

Both calc-silicates and marbles appear to form forsterite at invariant point C ($T=553^{\circ}\text{C}$ and $X_{\text{CO}_2}=0.69$). If calcite and tremolite remain in calc-silicate rocks, forsterite forms by the reaction:

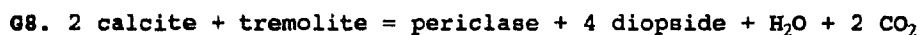


and to account for the co-existence of forsterite and calcite in marble, forsterite forms by the reaction:



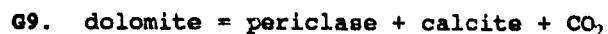
These are common assemblages in the carbonate rocks of the Ashburn Formation adjacent to many plutons and therefore appears to record peak metamorphic conditions. The equivalent mineral assemblages in the pelitic units contain cordierite and rare hornblende, but sillimanite and garnet are not present. This suggests that the minimum contact temperature in many of the plutonic units was about 570°C (Fig. 5.12), although samples in direct contact with plutonic units were not sampled.

Minor areas in the contact aureole(s) preserve the highest grade assemblages as shown by the presence of periclase in marble and garnet in calc-silicate lithologies. With increasing temperature invariant point D ($T=575^{\circ}\text{C}$ and $X_{\text{CO}_2}=0.99$) is reached which accounts for the mineral assemblage periclase-forsterite-diopside-calcite. Periclase forms from the reaction:



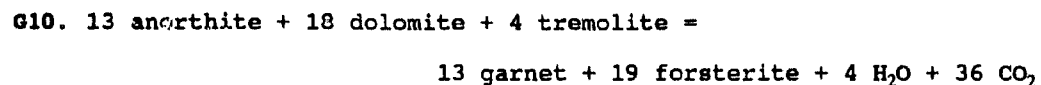
until calcite is gone. The maximum temperature reached by this reaction

is 645°C with X_{CO_2} at 0.67. It is unclear if periclase formed by the dissociation of dolomite by the reaction:

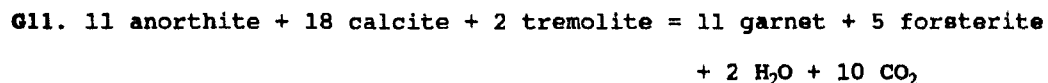


because there is no direct evidence for this reaction. If this reaction took place it was apparently not buffered along a univariant curve but was subject to control by externally derived fluids.

Based on limited textural evidence garnet probably initially formed by the reaction:



and with an increase in temperature after the consumption of dolomite garnet is interpreted to form by the reaction:



Garnet and periclase were not observed in the same rock, although there reactions cross in T- X_{CO_2} space (invariant point E on Fig. 5.12).

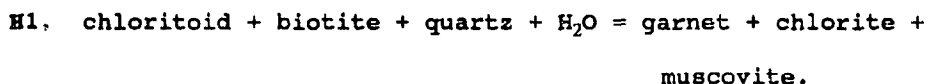
The peak metamorphic assemblages containing garnet and periclase probably formed in the temperature range 575-650°C; although temperatures may have locally exceeded 750°C (Fig. 5.12). The associated pelitic units contain cordierite, sillimanite, and rare garnet and, based on carbonate phase equilibria, formed at equivalent temperatures. This broadly coincides with temperature estimates from associated plutonic units (Chapter 4).

5.4.4. Hammondvale metamorphic unit

Microprobe analyses of mineral assemblages in this unit were conducted at a reconnaissance scale and therefore conclusions based on these data are considered preliminary.

The mineral assemblages in the albite and garnet schist (Table 5.1) are similar to those described by Jamieson (1990) and Jamieson and O'Beirne-Ryan (1991) from the Fleur de Lys Supergroup in western Newfoundland. However, the Hammondvale metamorphic unit has a restricted mineral assemblage that lacks chloritoid and staurolite, and biotite and chlorite are not common. Most of the minerals appear to be in textural and chemical disequilibrium which makes qualitative P-T estimates difficult. Also, the lack of biotite, Al_2SiO_5 , and the extremely low An-content of albite porphyroblasts makes most geothermobarometers unreliable. However, some constraints on the P-T conditions can be obtained by comparison with other areas with similar assemblages and inferred metamorphic conditions (e.g. Jamieson, 1990) and using reaction boundaries calculated using TWEEQU.

Assuming similarity with the Fleur de Lys Supergroup, the lack of chloritoid and the general absence of biotite could be consistent with the reaction of Spear and Cheney (1989):



This reaction occurs over a wide pressure range with peak temperatures consistently less than 510°C. This reaction places a lower temperature limit on the Hammondvale metamorphic unit.

A TWEEQU P-T plot can be constructed for sample NB87-4090 with mineral compositions using the end-member phases: albite-anorthite, grossular-almandine, muscovite-paragonite, annite, clinozoisite, quartz, and H_2O . There are 14 possible equilibria resulting in 3 independent

reactions (Fig. 5.13) that can be written for the selected end-member phases (Table 5.4). However, several assumptions must first be made to construct the P-T plot. The first assumption concerns the analytical problems associated with muscovite analysis already noted (section 5.3.3.). Sodium contents in analyzed muscovite grains are considered minimum values and therefore the most Na-rich muscovite composition were used in the TWEEQU calculations.

A second problem is that the TWEEQU data base lacks essential thermochemical information for epidote. Therefore, as a substitute, the clinozoisite end-member was used, assuming an activity of epidote based on the equation [activity = $(Al^I/Al^T + Fe)^3$ (e.g. 0.47)].

A third assumption deals with the activity of H₂O. Assuming an ideal activity of 1 increases the pressure and temperature constraints of the assemblage. Although F and Cl were not analyzed, the presence of carbonate minerals in this assemblage will lower the activity and therefore a value of 0.93 is considered a reasonable estimate for these rocks.

Based on these assumptions, and using average garnet, biotite, and epidote compositions and the most oligoclase-rich plagioclase, the assemblage in sample NB87-4090 yields an extremely tight temperature and pressure intersection at 586°C and 8.9 kbar, respectively (Fig. 5.13). Using the less Na-rich muscovite results in a difference in pressure up to 5 kbar and temperature in excess of 600°C. Using albite yields less constrained intersections with temperature ranging from 200-600°C and pressure from 6-15 kbar. The elimination of H₂O from the calculations results in four activity corrected equations and 2 independent reactions that yield identical results.

Whether or not H₂O is used in the TWEEQU calculations does not significantly change the resulting pressure and temperature estimates and indicates that oligoclase was in equilibrium with co-existing garnet-biotite-muscovite-epidote-quartz at about 586°C and 9.0 kbar.

Jamieson and O'Beirne-Ryan (1991) interpreted the growth of oligoclase on albite in similar rocks in the Fleur de Lys Supergroup as a product of retrogression. If the oligoclase-bearing assemblages in the Hammondvale metamorphic unit are similar in origin then the P-T estimates do not represent peak metamorphic conditions but likely re-equilibration after the peak of metamorphism.

5.5. SUMMARY

With varying degrees of confidence, the metamorphic P-T conditions for the Brookville Gneiss, Green Head Group, and the Hammondvale metamorphic unit have been estimated.

The low-pressure/high-temperature mineral assemblages developed in various lithologies of the Brookville Gneiss indicate peak metamorphic conditions of $645 \pm 50^\circ\text{C}$ and 2.5 ± 1 kbar, within the upper amphibolite facies. This resulted in the formation of sillimanite-cordierite-bearing migmatitic paragneiss and forsterite-diopside-bearing marbles.

In contrast, most of the Green Head Group underwent contact metamorphism generally ranging from albite-epidote to hornblende-hornfels facies which is locally superimposed on regional greenschist facies metamorphic textural and mineral assemblages. Contact metamorphism resulted in cordierite-bearing hornfels in the pelitic rocks and diopside-tremolite-bearing assemblages in the carbonate rocks. Locally peak metamorphic temperatures and pressures reached pyroxene-hornfels facies conditions which are broadly similar to peak conditions in the Brookville Gneiss. However, cordierite-sillimanite-bearing hornfels of the Green Head Group is not migmatitic, and in contrast to the Brookville Gneiss, locally contains garnet. Also the carbonate rocks contain garnet and periclase-bearing assemblages that are not present in the Brookville Gneiss.

The Green Head Group and Brookville Gneiss are tectonically separated by a major ductile shear zone (MacKay Highway shear zone) that

coincides with an area of greenschist facies metamorphism in the Green Head Group. This zone is extensively recrystallized and overprinted by lower amphibolite facies metamorphism that resulted in the development of carbonate and pelitic blastomylonites with sillimanite, cordierite, andalusite, and local garnet-bearing assemblages.

The Hammondvale metamorphic unit was considered to be a metamorphic equivalent of portions of the Green Head Group (Ruitenberg et al., 1979; McLeod et al., 1994). However, this unit displays a higher pressure metamorphism distinct from that in the Green Head Group and Brookville Gneiss. This metamorphism resulted in muscovite-garnet-albite-bearing assemblages that developed at conditions of about 9.0 kbar.

The Brookville Gneiss records pressures and temperatures that indicate extremely high, near-surface geotherms which requires metamorphism to be driven by an extremely large magmatic heat flux (cf. Wickham and Oxburgh, 1987; Lux et al., 1986; Golderg and Leyreloup, 1990). In contrast, data from the Hammondvale metamorphic unit are incompatible with a high-heat flow type of metamorphism. It is consistent with high-pressure/low-temperature metamorphism typically associated with major tectonic boundaries (cf. Jamieson, 1990).

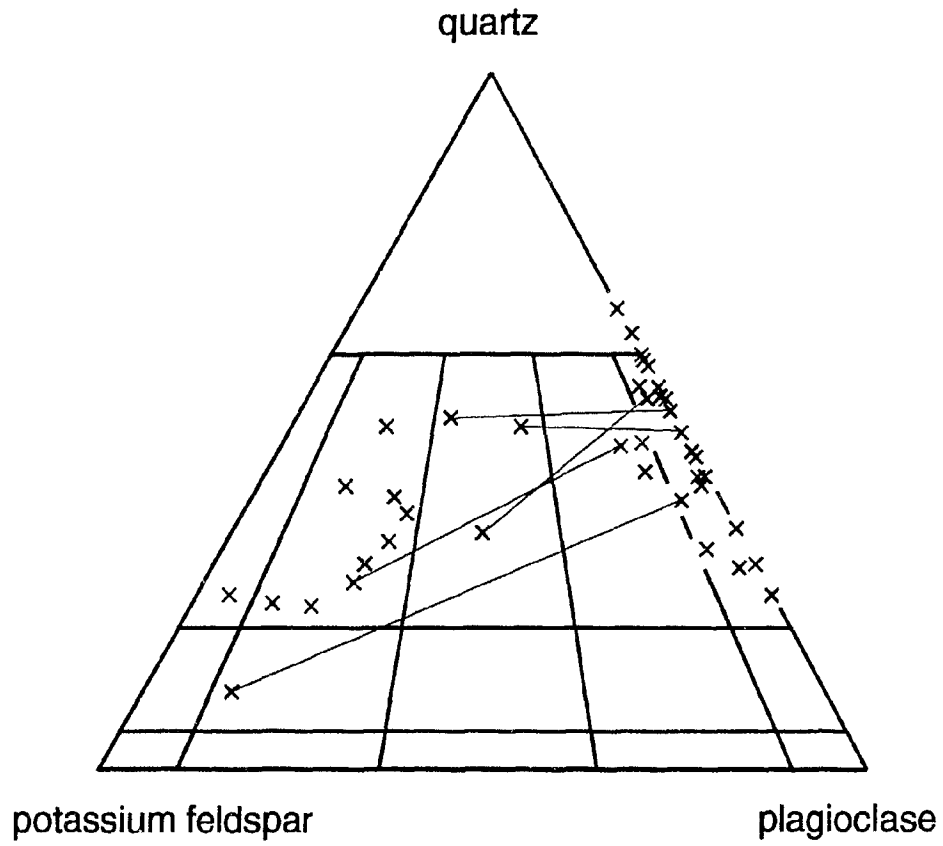


Figure 5.1. Modal mineralogy of leucosome samples in the Brookville Gneiss. Tie-lines (dashed) connect two most extreme modal mineralogies in the same leucosome sample (n=40).

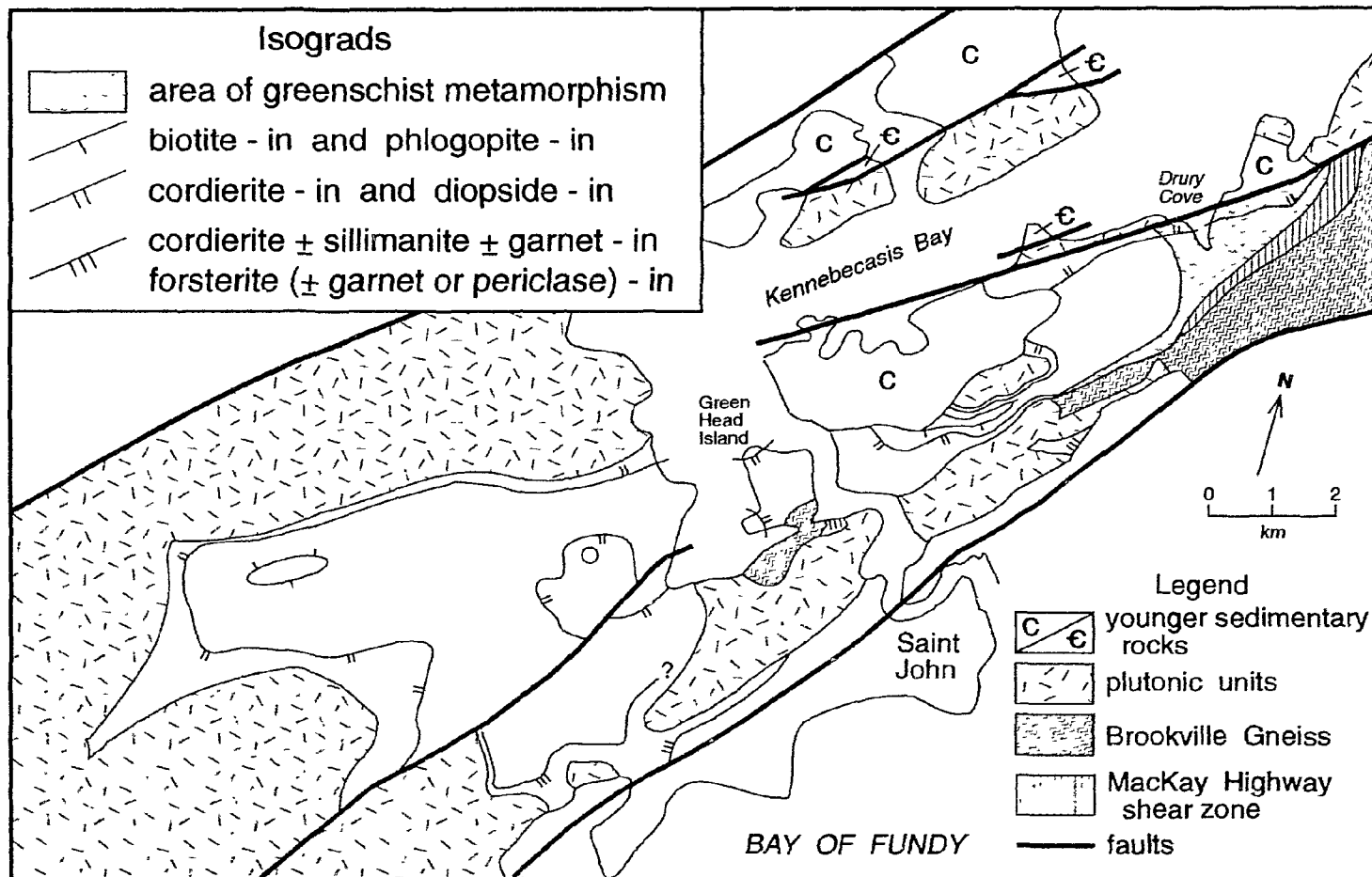


Figure 5.2. A simplified geological map of the Saint John area showing the distribution of isograds in the Green Head Group surrounding plutonic units.

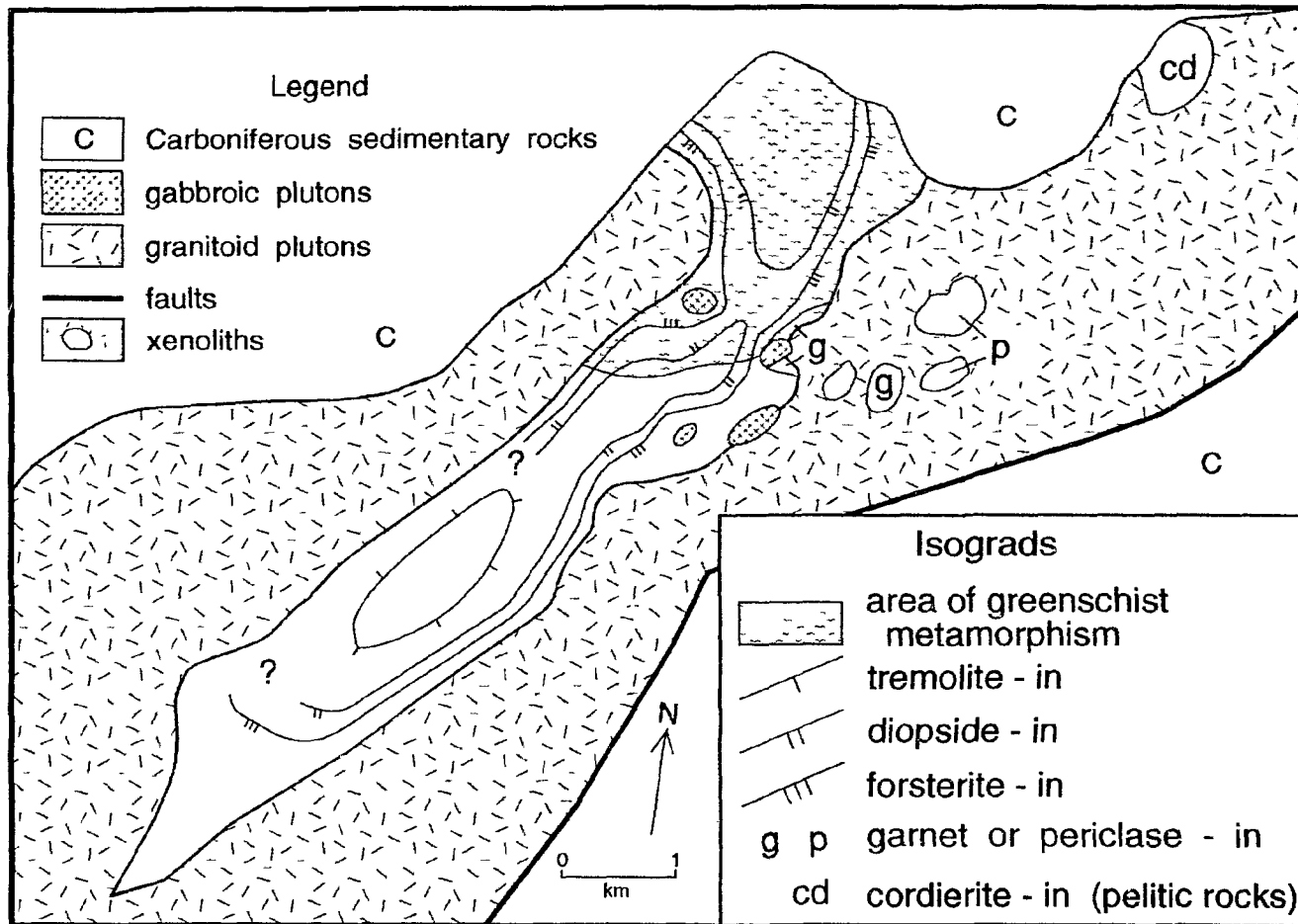


Figure 5.3. A simplified geological map of the Hammond River area showing the distribution of isograds in marbles (pelitic rocks are not common) of the Ashburn Formation surrounding plutonic units. Note the lack of continuity of the garnet isograd.

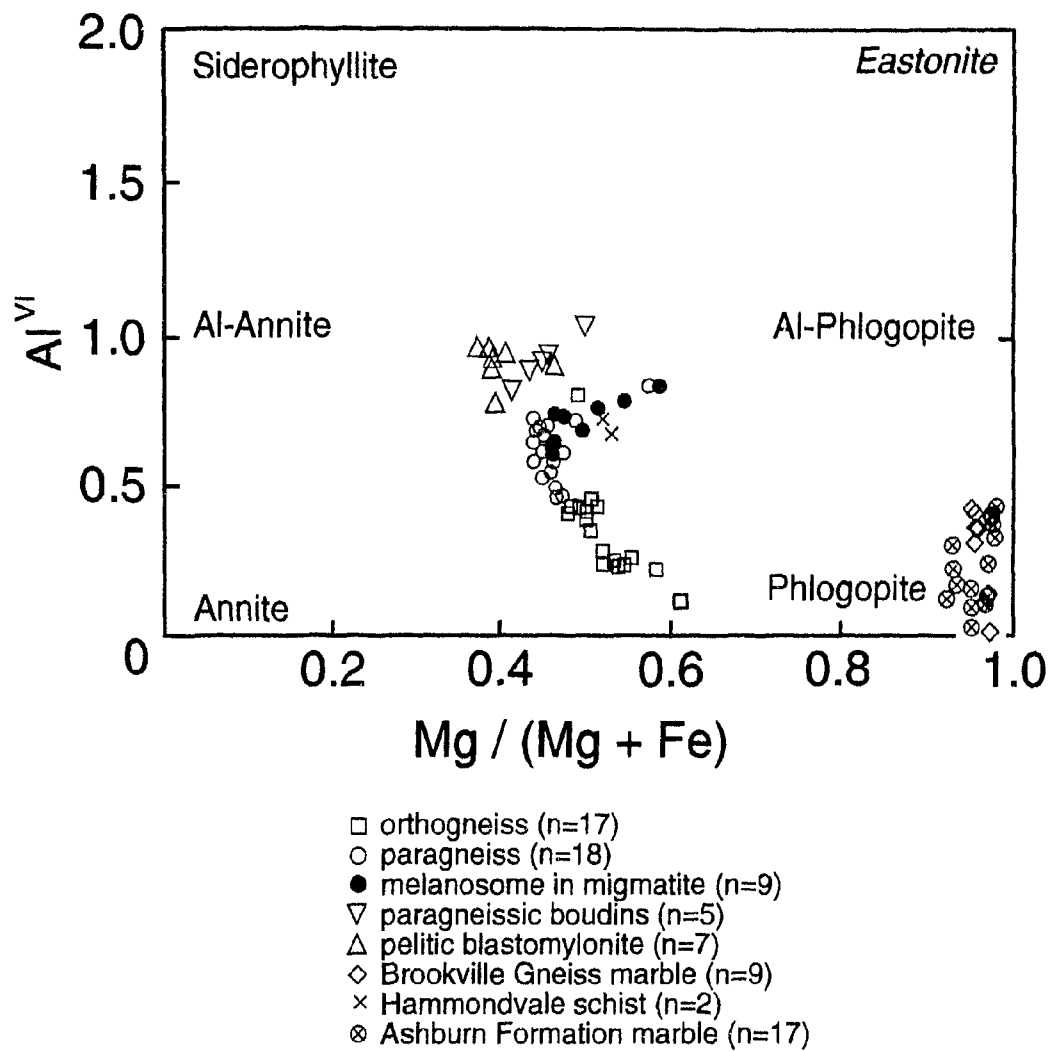


Figure 5.4. Plot of biotite compositions on an "ideal biotite plane" (after Guidotti, 1984).

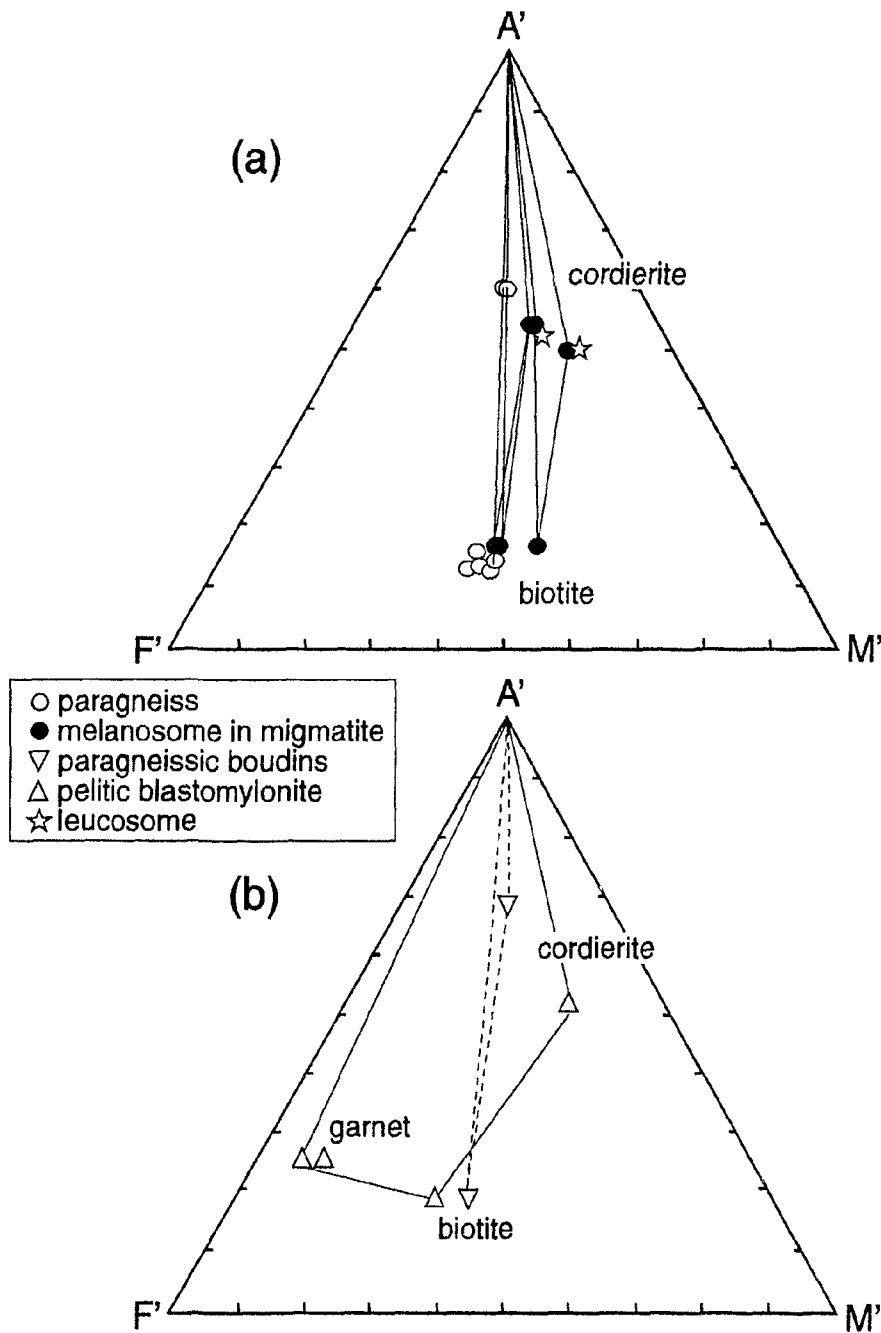


Figure 5.5. A'F'M' projections of co-existing phases (projection point from K-feldspar). a) Prograde phases in the Brookville Gneiss. Note overlap of leucosome and melanosome cordierite compositions. b). Prograde phases in the MacKay Highway shear zone. Solid tie-lines for gneissic boudin samples. (Note: cordierite present but not analyzed, therefore assumed ideal composition. Dashed tie-lines for samples from pelitic blastomylonite.

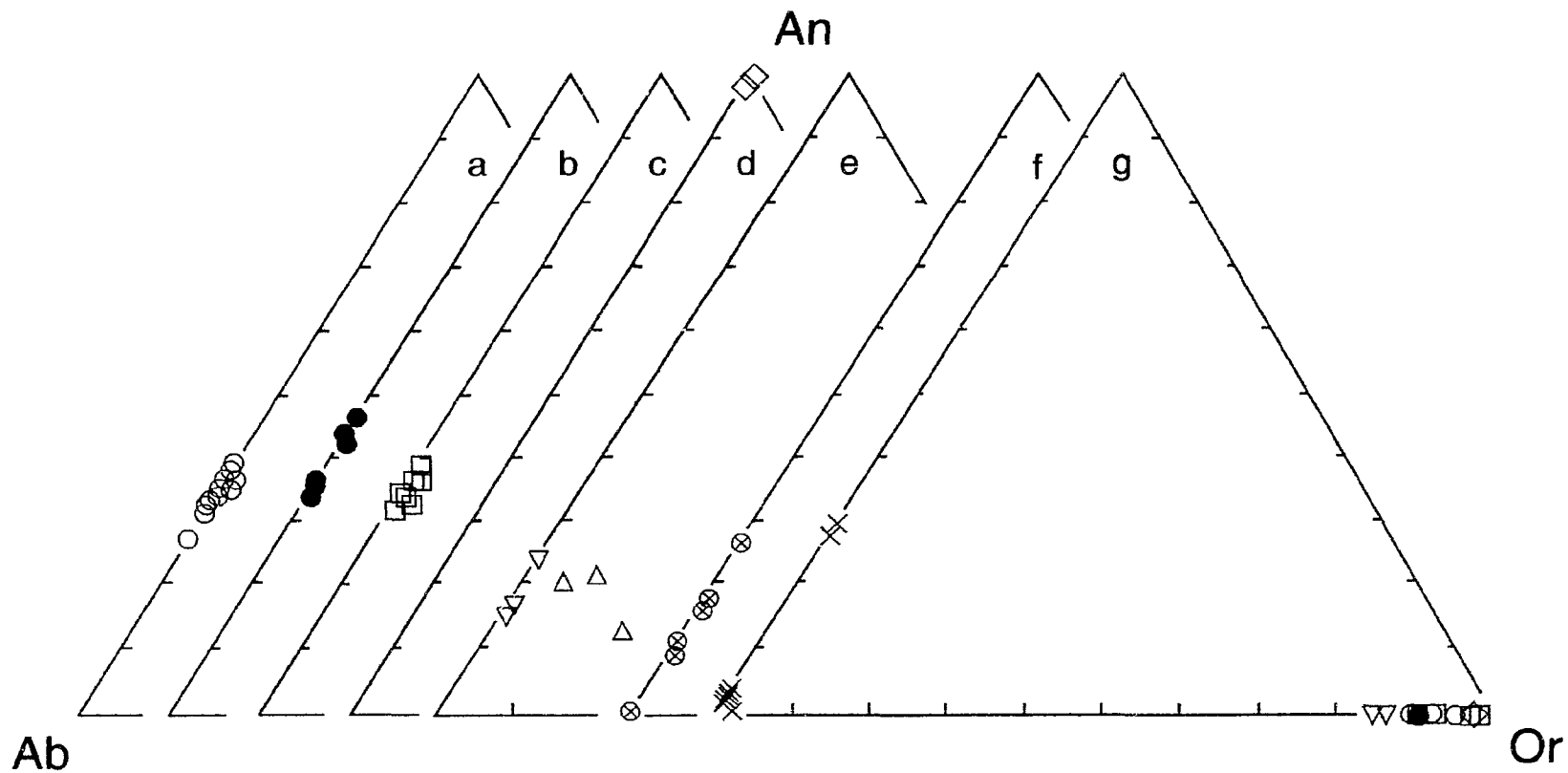


Figure 5.6. Variations in the composition of feldspar in the metamorphic rocks of the Brookville terrane. a) paragneiss; b) leucosome; c) orthogneiss; d) marble in Brookville Gneiss; e) gneissic boudins and pelitic blastomylonite; f) schist in the Ashburn Formation; g) Hammondvale metamorphic unit.

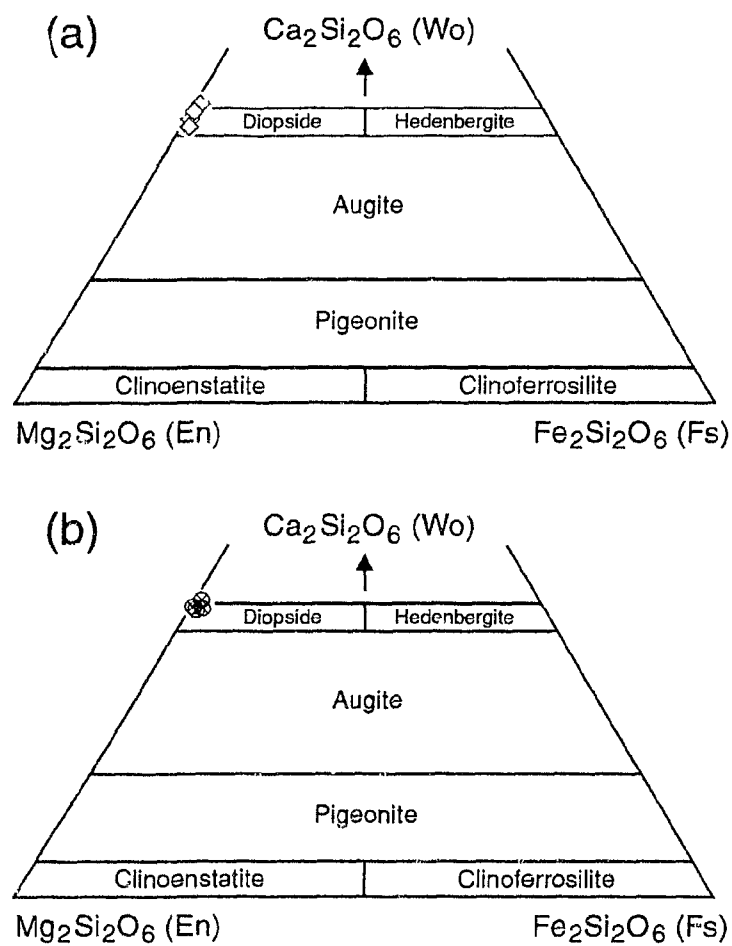


Figure 5.7. Compositional ranges and nomenclature of clinopyroxenes (after Deer et al., 1992). a) pyroxene samples from marble in the Brookville Gneiss; b) pyroxene samples from marble in the Ashburn Formation.

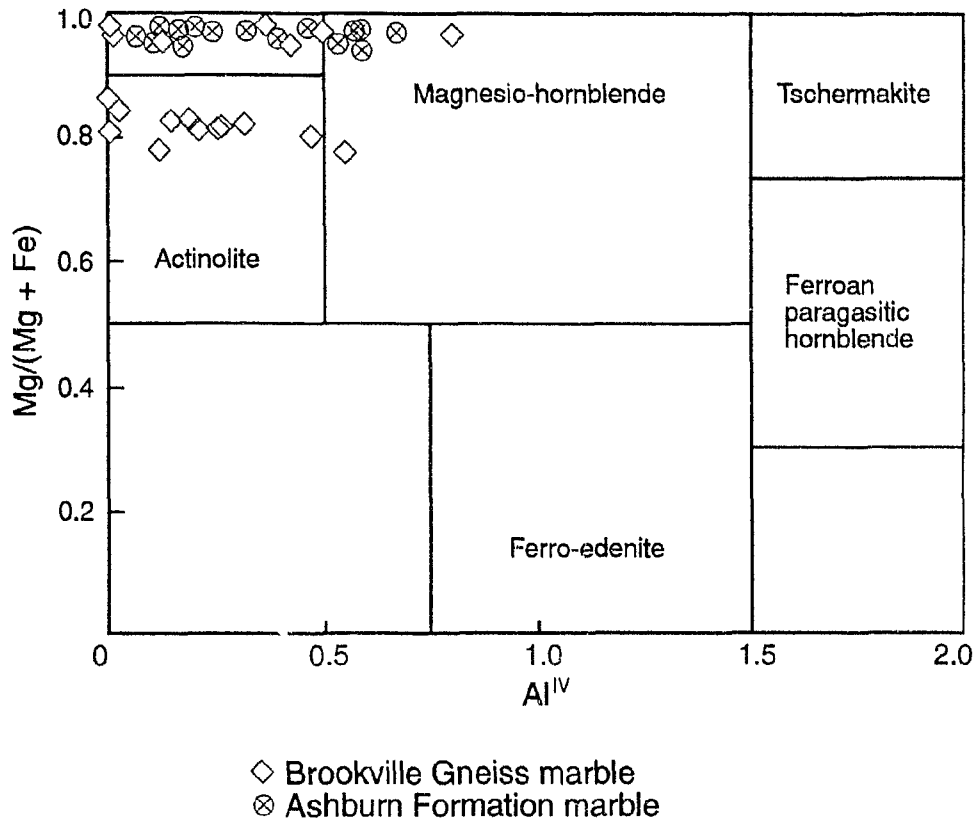


Figure 5.8. Modified version of the recommended plot for naming calcic amphiboles (after Hammarstrom and Zen, 1986).

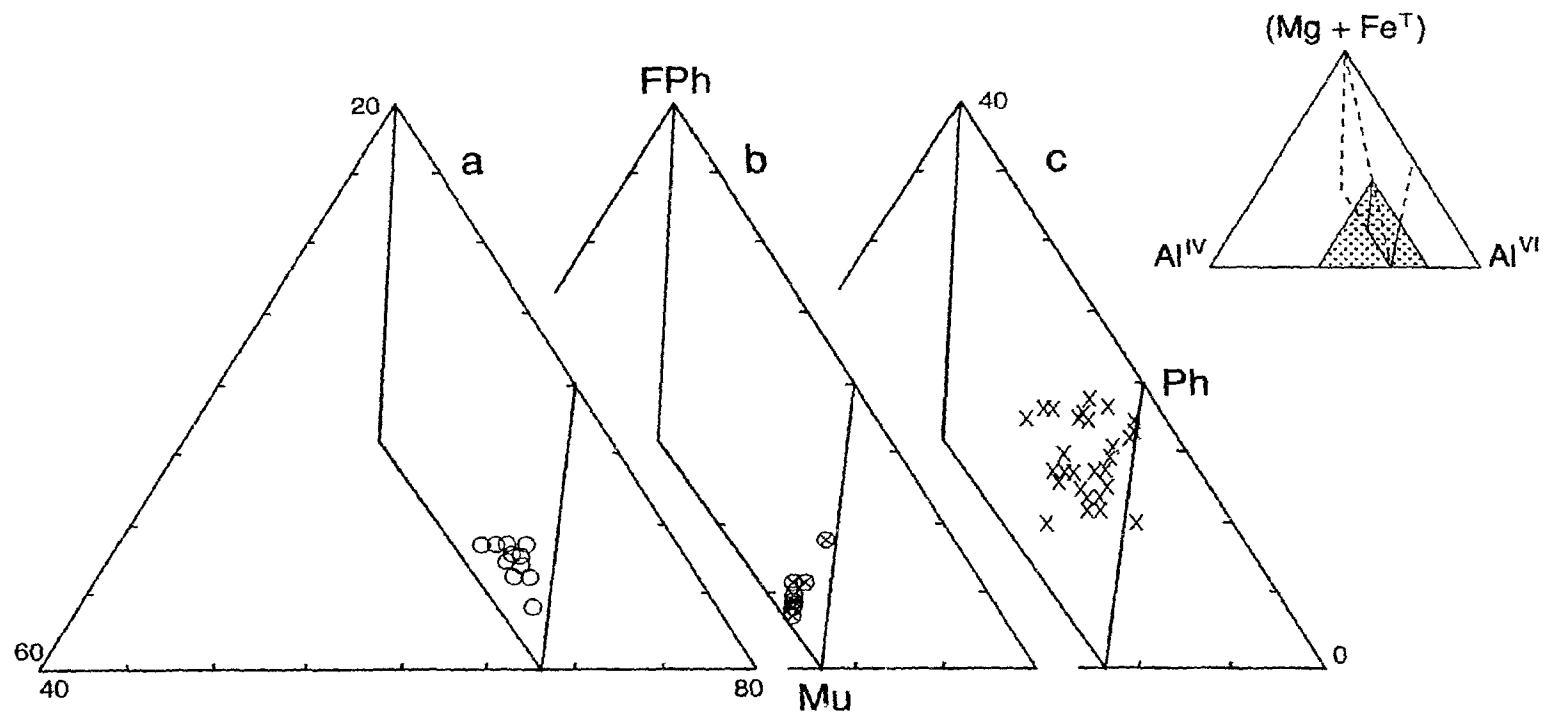


Figure 5.9. Plot of white mica compositions (after Guidotti, 1984) for a) Brookville Gneiss; b) schist in the Ashburn Formation; c) Hammondvale metamorphic unit. FPh = ferriphengite; FMu = ferri-muscovite; Ph = phengite; Mu = muscovite.

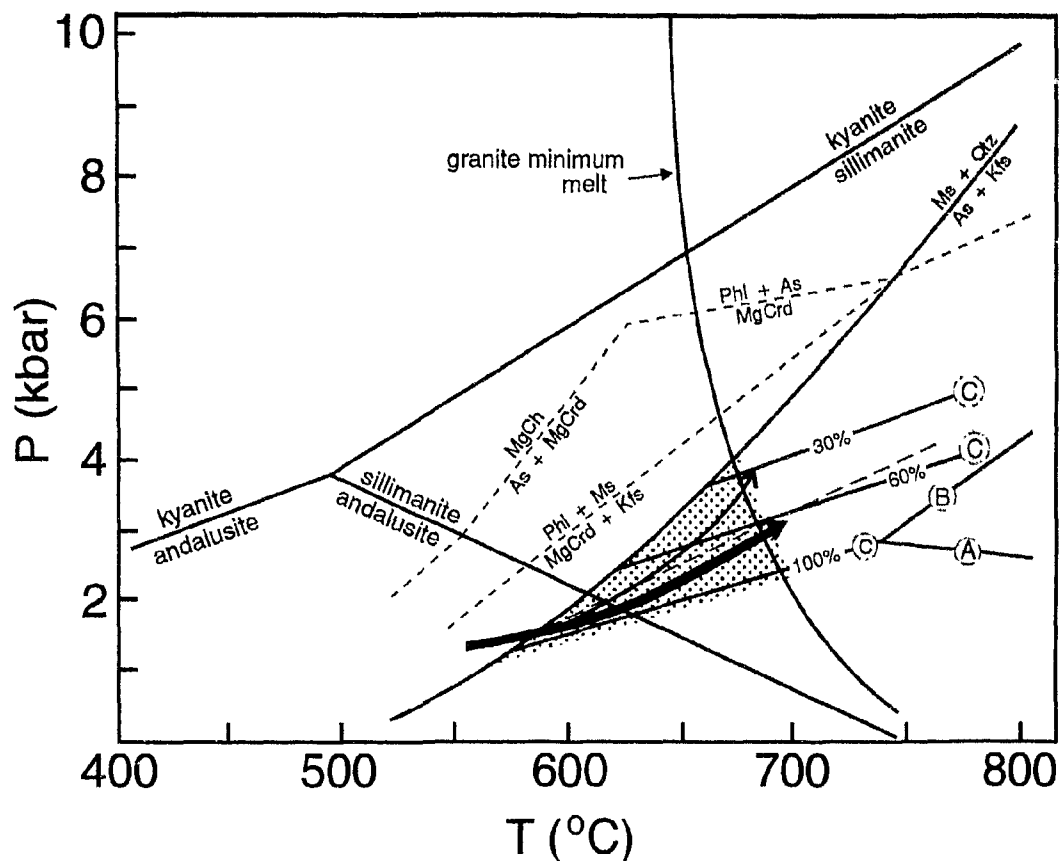


Figure 5.10. Simplified petrogenetic grid for the system KFMASH after Spear and Cheney (1989) with addition of "granite minimum melt" curve from Johannes (1984) (using plagioclase composition from the leucosomes of An39%). Small dashed lines indicate the upper stability of cordierite (Spear and Cheney, 1989). High temperature products written on right-hand side of equation. Reaction A: Fe-cordierite = garnet + sillimanite + quartz + water (Holdaway and Lee, 1977). Reaction B: biotite + sillimanite + quartz = cordierite + garnet + K-feldspar + water (Holdaway and Lee, 1977). Reaction C: biotite + aluminum silicate + quartz = Fe-cordierite + K-feldspar + water (at 100%, 60%, and 30% mol % Fe) (Holdaway and Lee, 1977). Long dashed lines is reaction of Hoffer (1976): biotite + sillimanite + quartz = cordierite (34 mol % Fe) + K-feldspar + water. Inferred peak metamorphic conditions estimated on the basis of phase relations are indicated by shaded area. Arrows indicate possible prograde P-T trajectories (see text).

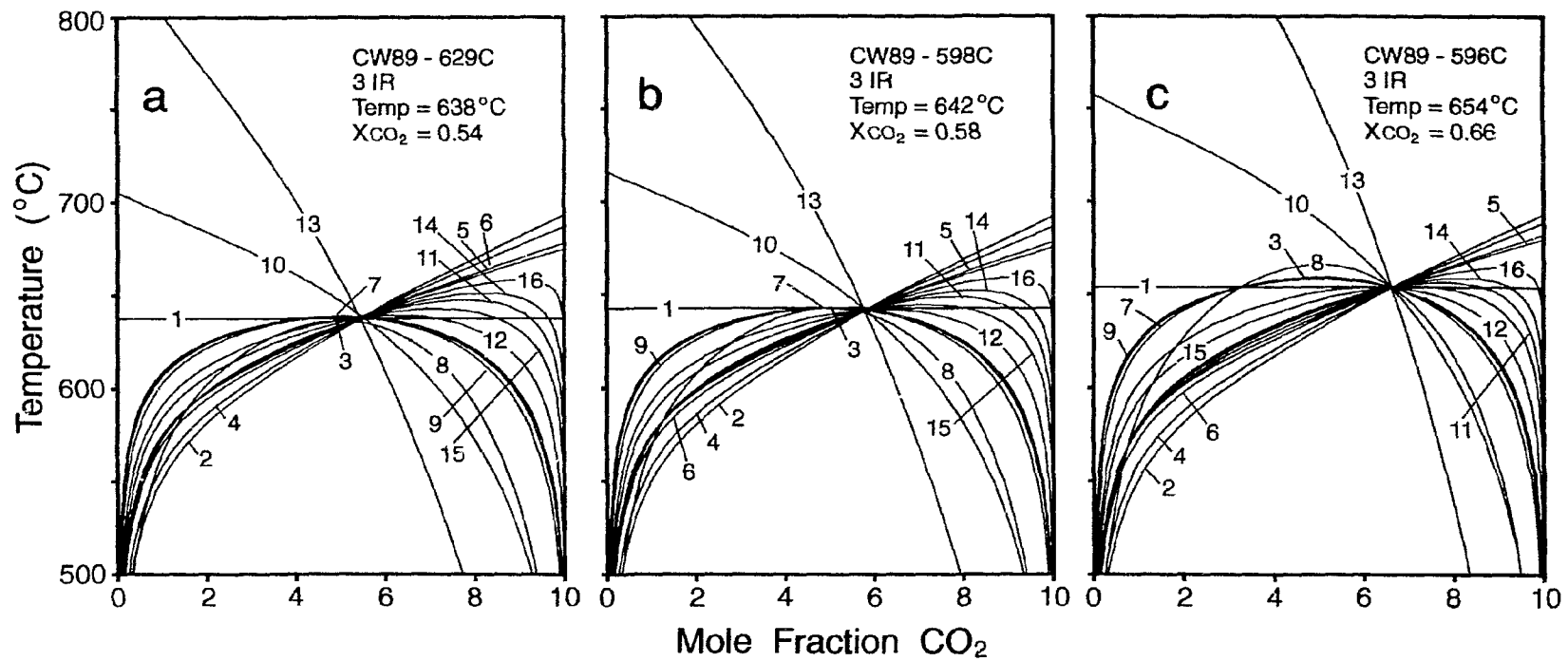


Figure 5.11. T-X diagrams with activity corrected curves (TWEEQU) which constrain conditions recorded by marble assemblages in the Brookville Gneiss at 3.1 kbar (see text). Reactions listed in Table 5.3. IR = number of independent reactions.

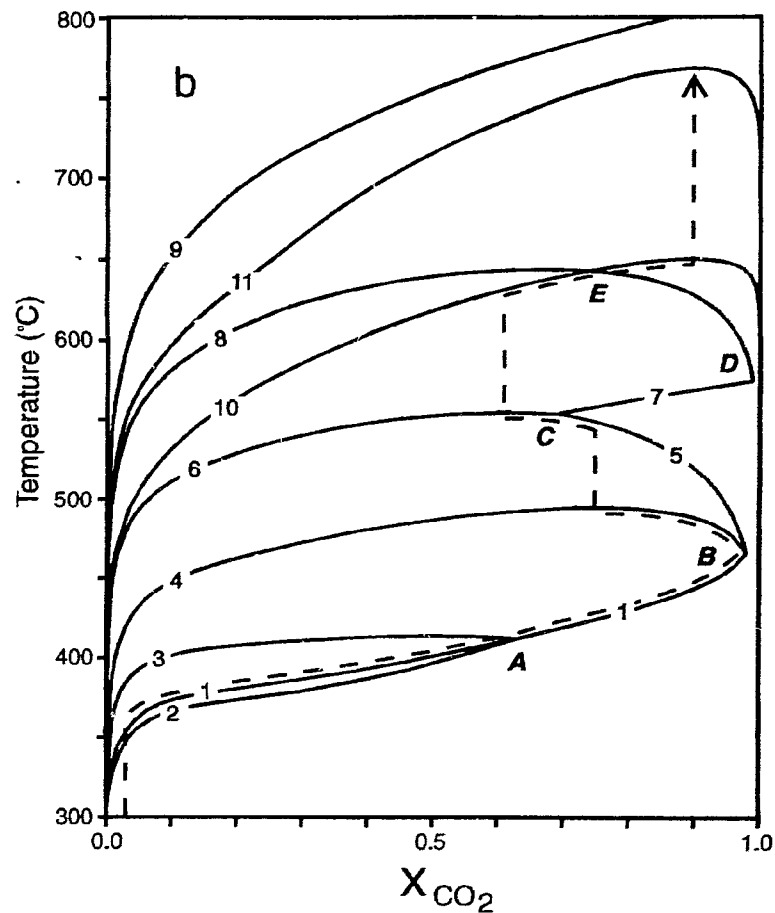
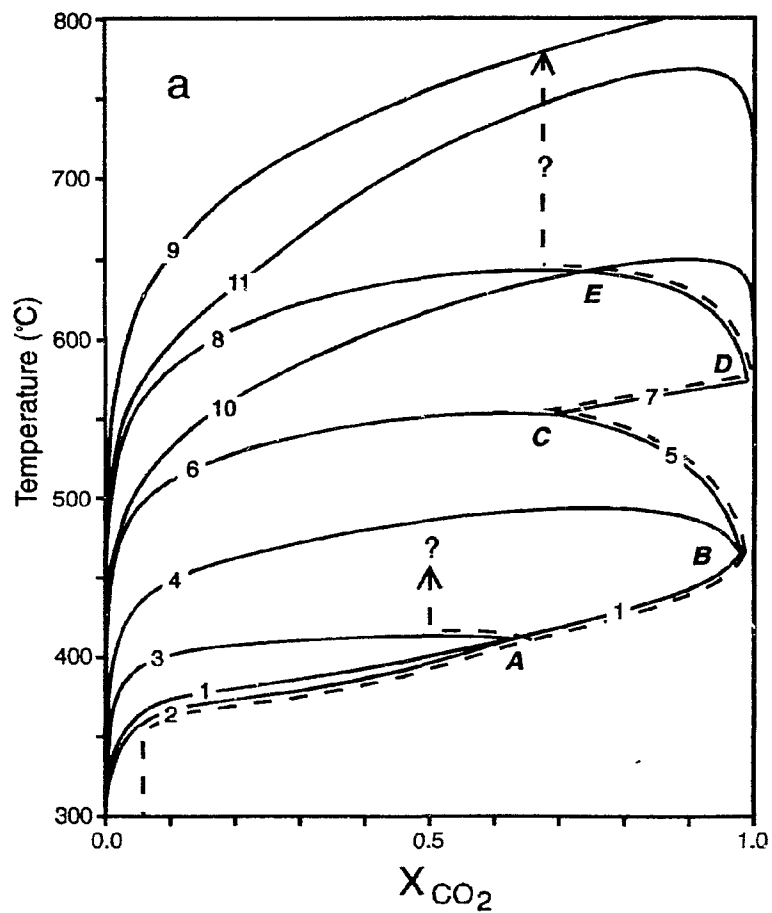


Figure 5.12. T- X_{CO_2} diagrams with activity-corrected curves (TWEEQU) which constrain conditions recorded by (a) marble and (b) calc-silicate assemblages in the metamorphic contact zones in the Green Head Group at 1 kbar (see text). The reactions are denoted by the reference numbers used in text. A to E represent invariant point reactions cited in text.

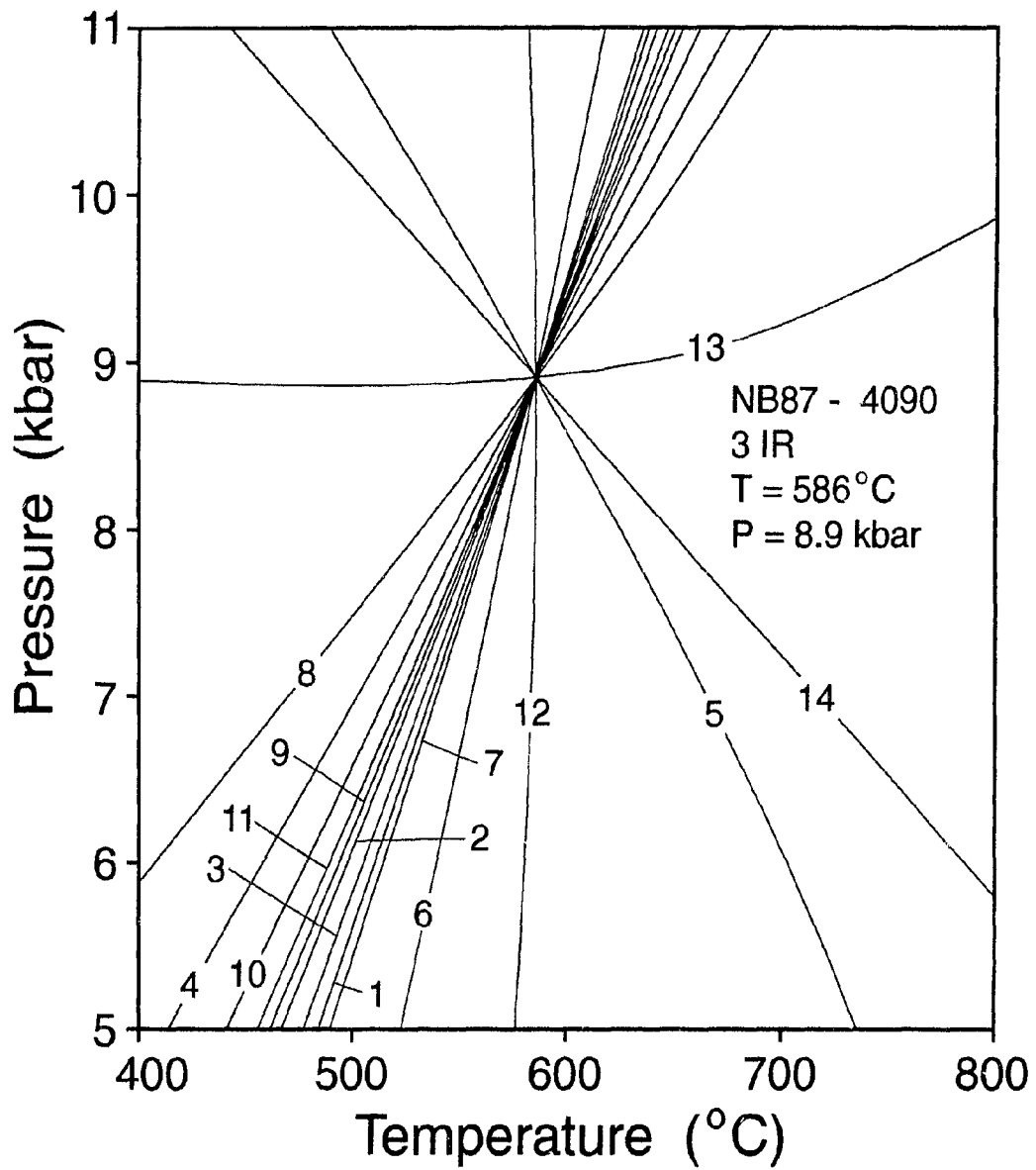


Figure 5.13. Petrogenetic grid for the Hammondvale metamorphic unit using the TWEEQU program applying the assumptions cited in the text. The reactions are listed in Table 5.4. IR = number of independent reactions.

Table 5.1. Observed mineral assemblages in metamorphic rocks of the Brookville terrane.

BROOKVILLE GNEISS

Semi-pelitic to pelitic paragneiss

- B1. plagioclase + quartz + biotite + K-feldspar
 B2. plagioclase + quartz + biotite + K-feldspar + andalusite
 B3. plagioclase + quartz + biotite + K-feldspar + sillimanite
 B4. plagioclase + quartz + biotite + K-feldspar + andalusite + sillimanite

Pelitic paragneiss

- B5. plagioclase + quartz + biotite + cordierite + K-feldspar
 B6. plagioclase + quartz + biotite + cordierite + K-feldspar + andalusite
 B7. plagioclase + quartz + biotite + cordierite + K-feldspar + sillimanite
 B8. plagioclase + quartz + biotite + cordierite + K-feldspar + andalusite + sillimanite

Hornblende paragneiss

- B9. plagioclase + quartz + biotite + hornblende

Arkosic paragneiss

- B10. quartz + K-feldspar + plagioclase + biotite ± hornblende

Migmatitic paragneiss

- B11. plagioclase + quartz + biotite + cordierite + K-feldspar + sillimanite ± andalusite (melanosome)
 B12. plagioclase + quartz + biotite + cordierite + K-feldspar + sillimanite ± spinel (leucosome)

Marble

- B13. calcite/dolomite + phlogopite + tremolite + diopside + forsterite ± plagioclase ± K-feldspar
 B14. calcite/dolomite + phlogopite + actinolite + diopside + forsterite ± plagioclase ± K-feldspar

Calc-silicate rocks

- B15. diopside + calcite/dolomite + quartz + K-feldspar + plagioclase ± tremolite ± phlogopite ± forsterite ± chondrodite(?)

Orthogneiss

- B16. plagioclase + quartz + biotite ± K-feldspar

MACKEY HIGHWAY SHEAR ZONE

Paragneissic boudins

- M1. plagioclase + quartz + biotite + K-feldspar + cordierite ± andalusite
 M2. plagioclase + quartz + biotite + K-feldspar + cordierite ± sillimanite
 M3. plagioclase + quartz + biotite + K-feldspar + cordierite ± sillimanite ± andalusite

Pelitic blastomylonite

- M4. plagioclase + quartz + biotite + K-feldspar + cordierite + sillimanite + andalusite + muscovite ± clinozoisite
 M5. plagioclase + quartz + biotite + K-feldspar + cordierite + sillimanite ± muscovite ± garnet (rare)

Calc-silicate blastomylonite

- M6. actinolite/tremolite + biotite/phlogopite + quartz + K-feldspar + plagioclase + diopside ± calcite/dolomite

Marble blastomylonite

- M7. calcite/dolomite + diopside + garnet ± K-feldspar ± quartz ± plagioclase
 M8. calcite/dolomite + diopside + phlogopite + K-feldspar + quartz + plagioclase ± tremolite

Table 5.1. Continued.

GREENSCHIST FACIES ROCKSPelitic schist

G1. muscovite + chlorite + [quartz + K-feldspar + plagioclase] ± biotite
 ± clinozoisite

Carbonate rocks

G2. calcite/dolomite + phlogopite ± tremolite ± [quartz + K-feldspar +
 plagioclase]

CONTACT AUREOLE ASSEMBLAGES**Low-grade (Zone A)**Pelitic hornfels

C1. muscovite + chlorite + clinozoisite + [quartz + K-feldspar +
 plagioclase]

Calc-silicate hornfels

C2. muscovite + chlorite + clinozoisite + tremolite ± calcite/dolomite +
 [quartz + K-feldspar + plagioclase]

Marble

C3. calcite/dolomite ± muscovite ± chlorite ± talc ± [quartz +
 K-feldspar + plagioclase]

Low-grade (Zone B)Pelitic hornfels

C4. muscovite + chlorite + biotite ± clinozoisite + [quartz + K-feldspar
 + plagioclase]

Calc-silicate hornfels

C5. muscovite + chlorite + biotite/phlogopite + clinozoisite + tremolite
 ± calcite/dolomite + [quartz + K-feldspar + plagioclase]

Marble

C6. calcite/dolomite + phlogopite + [quartz + K-feldspar + plagioclase]

Medium-gradePelitic hornfels

C7. muscovite + biotite + chlorite + cordierite ± spinel + [quartz +
 K-feldspar + plagioclase]

C8. muscovite + biotite + cordierite ± spinel ± andalusite(?) + [quartz
 + K-feldspar + plagioclase]

Carbonate hornfels

C9. calcite/dolomite + diopside + tremolite + phlogopite ± [quartz +
 K-feldspar + plagioclase]

High-gradeSemi-pelitic hornfels

C10. biotite + cordierite + K-feldspar + plagioclase + quartz ±
 muscovite ± spinel

C11. hornblende + biotite + K-feldspar + plagioclase + quartz

Pelitic hornfels

C12. biotite + cordierite + K-feldspar + plagioclase + quartz ± spinel ±
 sillimanite ± garnet (rare)

Calc-silicate hornfels and marble

C13. calcite/dolomite + diopside + forsterite ± tremolite ± phlogopite ±
 K-feldspar ± plagioclase ± quartz

C14. diopside + garnet ± plagioclase ± K-feldspar ± quartz ± calcite/
 dolomite ± forsterite

C15. calcite/dolomite + periclase ± forsterite ± diopside

Table 5.1. Continued.

HAMMONDVALE METAMORPHIC UNITPelitic schist

H1. quartz + muscovite + plagioclase ± biotite ± epidote ± K-feldspar ± chlorite ± calcite

H2. quartz + muscovite + plagioclase + garnet ± biotite ± epidote ± K-feldspar ± chlorite ± calcite

Marble

H3. calcite + muscovite + [quartz]

Amphibolite

H4. hornblende + plagioclase ± quartz

All assemblages contain variable amounts of accessory titanite, apatite, tourmaline, Fe-Ti oxides, zircon, and rutile. Minerals in parentheses are detrital minerals and appear not to be part of the equilibrium assemblage.

Table 5.2. Estimates of temperature in the Brookville Gneiss based on calcite-dolomite, two-feldspar, and garnet-biotite geothermometers. Temperature in °C.

Calcite-dolomite CW89-596C

	T1	T2	
Pair 1	400	402	
2	398	400	T1 = Anovitz and Essene (1987)
3	337	339	T2 = with Fe-correction
4	384	385	
5	391	393	
Average	382 ± 26	384 ± 26	

Two-feldspar

	T1	T2	
<u>Paragneiss</u>			
CW88-181C	422	398	
CW89-569	475	463	T1 = Stormer (1975)
CW89-622A	469	453	T2 = Haselton et al. (1983)
<u>Orthogneiss</u>			
CW88-132A	459	444	
CW88-178	281	220	
CW88-181A	427	402	
CW89-629A	430	409	
Average	423 ± 66	398 ± 83	

Garnet-biotite NB92-9097B

	T1	T2	T3	T4
garnet core-1	638	642	662	669
garnet core-2	650	659	674	680
garnet core-3	647	654	667	660
garnet core-4	622	621	638	641
garnet core-5	672	689	705	689
Average	646 ± 18	653 ± 25	669 ± 24	668 ± 19
garnet rim-4	576	561	576	577
garnet rim-5	518	489	501	518
Average	547	525	539	548

T1 = Thompson (1976), T2 = Ferry and Spear (1978),
 T3 = Hodges and Spear (1982), T4 = TWEEQU
 Temperature and pressure estimates calculated at 650°C and 3 kbar,
 respectively.

Table 5.3. Reactions used in the TWEEQU intersection diagrams (Fig. 5.11) for marbles in the Brookville Gneiss. Assemblages on the left are stable on the high side of the Y-axis or the high side of the X-axis for vertical reactions.

1. 2 rutile + diopside + 2 calcite = dolomite + 2 titanite
2. forsterite + 3 titanite + CO₂ = 3 rutile + 2 diopside + calcite
3. 2 rutile + 5 diopside + H₂O + CO₂ = calcite + 2 titanite + tremolite
4. 2 forsterite + 4 titanite + 2 CO₂ = 4 rutile + dolomite + 3 diopside
5. rutile + forsterite + 3 calcite + CO₂ = 2 dolomite + titanite
6. 4 calcite + 2 forsterite + 2 CO₂ = 3 dolomite + diopside
7. 6 rutile + 11 diopside + 2 H₂O + 2 CO₂ = dolomite + 6 titanite +
2 tremolite
8. 8 titanite + 5 dolomite + H₂O + CO₂ = 11 calcite + 8 rutile +
tremolite
9. dolomite + 4 diopside + H₂O + CO₂ = 3 calcite + tremolite
10. 7 diopside + 5 rutile + H₂O = tremolite + 5 titanite + forsterite
11. 5 forsterite + 11 titanite + 7 CO₂ + 2 H₂O = 2 tremolite + 11 rutile
+ 7 calcite
12. 2 forsterite + 11 diopside + 3 H₂O + 5 CO₂ = 5 calcite + 3 tremolite
13. 9 diopside + 5 dolomite = 2 H₂O = 2 tremolite + 2 forsterite +
10 calcite
14. 11 forsterite + 1 titanite + 14 CO₂ + 3 H₂O = 3 tremolite +
13 rutile + 7 dolomite
15. 6 forsterite + 13 diopside + 4 H₂O = 10 CO₂ = 5 dolomite +
4 tremolite
16. 13 calcite + 8 forsterite + 9 CO₂ + H₂O = tremolite + 11 dolomite

Table 5.4. Reactions used in the TWEQU intersection diagrams (Fig. 5.13) for an albite+garnet-bearing schist in the Hammondvale metamorphic unit. Assemblages on the left are stable on the high side of the Y-axis or the high side of the X-axis for vertical reactions.

1. 4 clinozoisite + quartz = 5 anorthite + grossular + 2 H₂O
2. 4 clinozoisite + quartz + muscovite + almandine = annite +
8 anorthite + 2 H₂O
3. 2 clinozoisite + 2 quartz + paragonite = albite + 4 anorthite + 2 H₂O
4. almandine + grossular + muscovite = 3 anorthite + annite
5. 5 muscovite + 8 grossular + 5 almandine + 6 H₂O = 5 annite + 3 quartz
+ 12 clinozoisite
6. albite + 2 clinozoisite = quartz + paragonite + grossular + anorthite
7. albite + 6 clinozoisite = paragonite + 2 grossular + 6 anorthite +
2 H₂O
8. 4 grossular + 5 paragonite + 6 quartz = 6 clinozoisite + 5 albite +
2 H₂O
9. 3 quartz + 2 paragonite + grossular = 2 albite + 3 anorthite + 2 H₂O
10. albite + almandine + muscovite + 2 clinozoisite = quartz
+ paragonite + 4 anorthite + annite
11. albite + 2 almandine + 2 muscovite + 6 clinozoisite = paragonite +
12 anorthite + 2 annite + 2 H₂O
12. 3 quartz + 2 paragonite + annite = 2 albite + almandine + muscovite
+ 2 H₂O
13. 3 quartz + 3 paragonite + muscovite + 4 grossular + almandine =
3 albite + annite + 6 clinozoisite
14. paragonite + 2 muscovite + 4 grossular + 2 almandine + 2 H₂O =
albite + 2 annite + 6 clinozoisite

PLATE 5

Photomicrographs taken from thin sections cut perpendicular to foliation and, where present, parallel to mineral lineation. Bar scale for all photomicrographs is in the lower left corner of 5a and is 1 mm in length.

- 5a. Typical quartzo-feldspathic and biotite-rich layers in paragneiss of the Brookville Gneiss. Xenoblastic cordierite (c) is partially to entirely altered to pinitite and/or sericite and is associated with the biotite (b). Larger cordierite grains along the biotite/quartzo-feldspathic contact. Cross-polarized light. Sample CW88-220.
- 5b. Typical mineralogy of hornblende-bearing paragneiss in the Brookville Gneiss. Light green subidioblastic hornblende (h) is typically inclusion-rich, associated with biotite (b), and strongly lineated. Quartzo-feldspathic layers are coarser. Note relatively uniform crystallographic orientation of biotite. Plane-polarized light. Sample CW89-667.
- 5c. Medium-grained marble from the Brookville Gneiss consists of granoblastic calcite with randomly oriented subidioblastic phlogopite (p) and diopside (d). Forsterite not in field of view. Plane-polarized light. Sample CW89-658.
- 5d. Medium-grained amphibolite from the Brookville Gneiss consists dominantly of subidioblastic hornblende (h) with minor xenoblastic clinopyroxene (cp) and biotite (b). Biotite is entirely replaced by chlorite. Idioblastic titanite (t) is associated with hornblende-rich layers. Plane-polarized light. Sample CW88-223.

PLATE 5



b



d



a



c

PLATE 6

Photomicrographs taken from thin sections cut perpendicular to foliation and, where present, parallel to mineral lineation. Bar scale for all photomicrographs is in the lower left corner of 6a and is 1 mm in length.

- 6a. Medium-grained, foliated, paragneissic boudin in MacKay Highway shear zone. Xenoblastic cordierite (c) is partially replaced by pinite. Subidioblastic andalusite (a) is associated with biotite (b) and the rims of cordierite. Fine sillimanite needles in the cores of biotite. Note the orange colour of biotite compared to those in the Brookville Gneiss (Plate 5a and b). Plane-polarized light. Sample NB93-9303.
- 6b. Fine-grained, strongly foliated, granoblastic pelitic blastomylonite from the margin of a gneissic boudin in the MacKay Highway shear zone. Note the strong crystallographic orientation of orange biotite. Plane-polarized light. Sample CW89-662C.
- 6c. Medium-grained calc-silicate blastomylonite from the MacKay Highway shear zone that consists dominantly of subidioblastic diopside (d) with minor granoblastic calcite (low relief minerals) and idioblastic phlogopite (p). Cross-polarized light. Sample CW88-160B.
- 6d. Medium-grained marble blastomylonite that consists dominantly of granoblastic calcite (low relief minerals) with minor subidioblastic diopside (d), garnet (g), and rounded quartz (q). Subidioblastic garnet contains inclusions of diopside. Cross-polarized light. Sample CW89-581.



PLATE 6

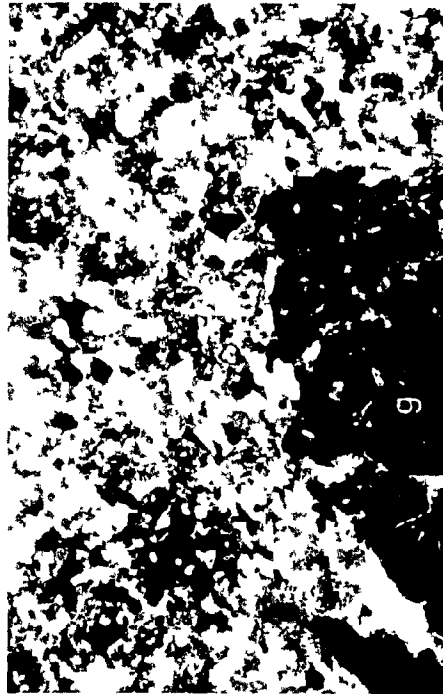
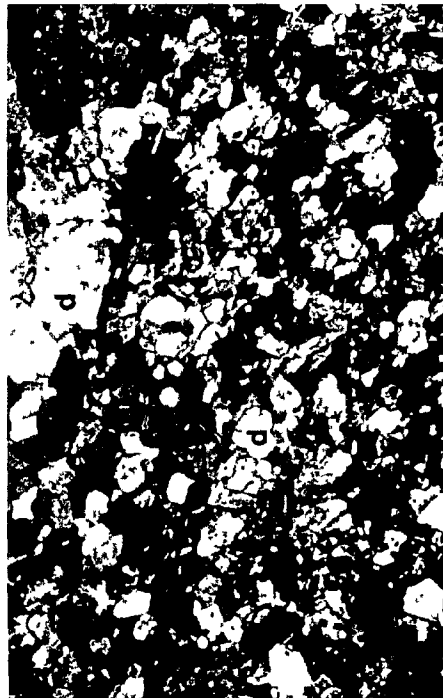
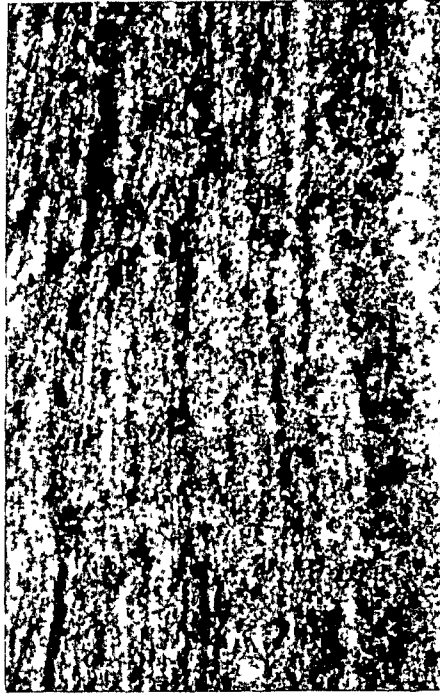


PLATE 7

Photomicrographs taken from thin sections cut perpendicular to foliation or bedding. Bar scale for all photomicrographs is in the lower left corner of 7a and is 1 mm in length.

- 7a. Medium-grained, strongly foliated and crenulated mica schist from the Ashburn Formation in the Drury Cove area. Foliation defined by subidioblastic muscovite and elongate quartz and feldspar. Xenoblastic cordierite (c) is totally replaced by sericite and appears to be associated with the muscovite-rich layers. It is interpreted to be the product of contact metamorphism. Biotite is not well preserved in this sample. Cross-polarized light. Sample NB92-9107.
- 7b. Fine-grained, well laminated siltstone from Zone B in the Ashburn Formation. Fine-grained biotite and minor chlorite throughout the sample displays a decussate texture. Note the lack of a pre-existing foliation. Plane-polarized light. Sample CW90-797.
- 7c. Spotted hornfels from the Martinon Formation. Cordierite forms rounded, inclusion-rich porphyroblasts in a matrix of fine-grained quartzo-feldspathic minerals and decussate biotite and rare chlorite. Note the lack of a pre-existing foliation. Cross-polarized light. Sample NB91-8548.
- 7d. Medium-grained, cordierite-bearing schist from the Ashburn Formation close to the contact with the Fairville Granite. Xenoblastic cordierite (c) is partially replaced by pinite. Biotite (b) is sparse and randomly oriented compared to those in paragneissic samples from the Brookville Gneiss. Fibrolite is present in some biotite but not obvious in this section. Cross-polarized light. Sample CW89-542B.

PLATE 7



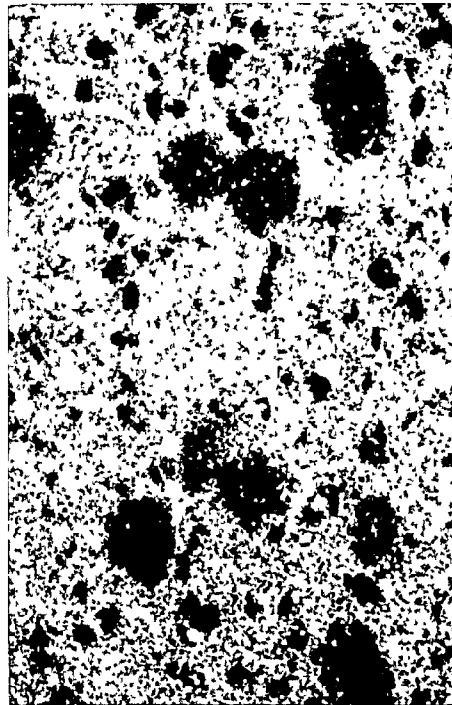
b



d



a



c

PLATE 8

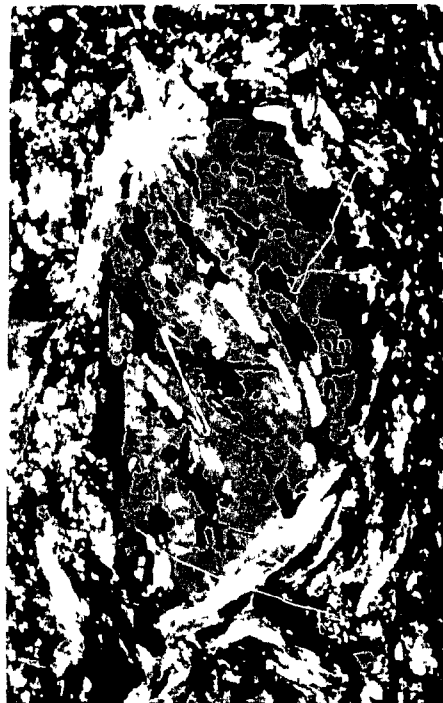
Photomicrographs taken from thin sections cut perpendicular to foliation and, where present, parallel to mineral lineation in samples from the Hammondvale metamorphic unit. Bar scale for all photomicrographs is in the lower left corner of 8a and is 1 mm in length.

- 8a. Large albite porphyroblast with inclusions of elongate quartz, biotite, opaque minerals, epidote, and muscovite that define a straight inclusion trail. Small idioblastic garnet also occurs as inclusions. Cross-polarized light. Sample NB87-4090.
- 8b. Smaller albite porphyroblast with curved inclusion trail defined by elongate quartz and epidote. External foliation of subidioblastic muscovite and minor biotite at a high angle to internal foliation. Cross-polarized light. Sample CW88-115A.
- 8c. Medium-grained muscovite-rich marble with randomly oriented subidioblastic muscovite. Apatite is common but not obvious in this sample.
- 8d. Strongly foliated amphibolite defined by alternating hornblende- and plagioclase-rich layers. Titanite is common.

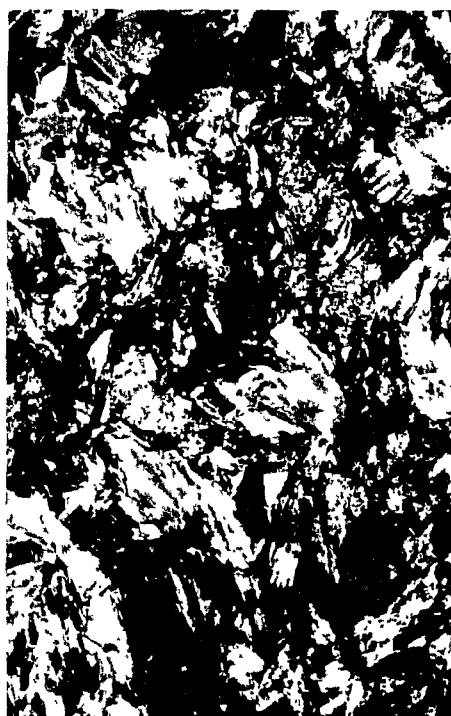
PLATE 8



a



b



c



d

CHAPTER 6

GEOCHRONOLOGY

6.1. INTRODUCTION

A detailed geochronological study was undertaken using U-Pb dating techniques on zircon and titanite in conjunction with $^{40}\text{Ar}/^{39}\text{Ar}$ dating on hornblende and mica from units in the Brookville terrane. These data are used to place constraints on the timing of key events in the evolution of the Brookville terrane including plutonism, volcanism, metamorphism, and deformation. These data also provide the first direct evidence for the age of the Brookville terrane and has regional implications for the configuration of the Avalon Zone in southern New Brunswick.

Geochronological investigation in the study area began in the early 1960's using K-Ar and Rb-Sr, and later U-Pb techniques. Although most of these early data are considered unreliable by today's analytical standards, the interpretations that developed from these dates remain firmly entrenched in the literature. The early geochronological data are summarized and reassessed in this chapter and compared to the results from more precise analytical techniques used during the present study and concurrent studies on the same rock units.

Parallel geochronological study by other workers (e.g. Dallmeyer et al., 1990; Dallmeyer and Nance, 1992; Nance and Dallmeyer, 1994) complement the present study. Much of the U-Pb data from this study has been published by the author (e.g. White et al., 1990a, b, c; Bevier et al., 1990, 1991) and noted throughout the Chapter; however, the details of additional U-Pb and $^{40}\text{Ar}/^{39}\text{Ar}$ data are presented here.

6.2. PREVIOUS GEOCHRONOLOGY

Results of previous geochronological studies are summarized in Table 6.1. The early attempts to interpret these ages were largely based on the assumption that a continuous stratigraphic succession exists in southern New Brunswick. Most of the resulting "ages" were considered to be inconsistent with the assumed field relations and led to conflicting geological interpretations (see section 1.2). All the early data have large errors associated with them and because of this have limited geological significance.

6.2.1. K-Ar Data

Ruitenbergh et al. (1973a, b, 1975, 1977, 1979) and Giles and Ruitenbergh (1977) used K-Ar dates (Table 6.1) exclusively to subdivide the plutonic and gneissic units into four groups; Precambrian and younger, Ordovician and older, upper Silurian and younger, and Carboniferous and older.

The complexity of interpretations surrounding these dates is obvious from the literature. Many contemporary workers in the area argued that these K-Ar ages were much too young based on the absence of plutonic material in the Cambrian to Ordovician Saint John Group and the lack of any evidence for contact metamorphism. Others (e.g. Rast et al., 1976b; Schenk, 1978) did not include the available K-Ar dates in their interpretation of the study area.

Poole et al. (1964) suggested that the anomalously young ages are the result of radiogenic argon loss during the Devonian Acadian Orogeny. Poole (1967) later regarded these K-Ar ages as reliable and postulated a Middle Ordovician age for the plutonic units. However, based on field relations Poole and others concluded that the plutons are middle to late Devonian (Poole et al., 1970) or Cambrian to Ordovician (Poole and Rodgers, 1972). Poole (1980) later suggested that the young ages are

probably cooling ages following an intrusive event at the Hadrynian - Cambrian boundary (or earlier).

Wardle (1978) suggested that the Ordovician K-Ar ages could be related to depth of intrusion. He argued that granites that intruded the Green Head Group at depth may never have reached the crustal levels where deposition of the Cambrian to Ordovician Saint John Group was occurring. Based on geological field evidence he proposed that the plutonic units are Precambrian in age.

6.2.2. Rb-Sr Data

By the late 1970's to early 1980's, the Rb-Sr whole rock method of dating plutonic rocks became the technique of choice of many geologists in southern New Brunswick. The K-Ar method was considered to be too restrictive and unreliable, and the resulting ages too young and uninterpretable. The Rb-Sr method allowed for collection and analyses of several samples from geographically separate plutons that were assumed to be cogenetic. If the samples did not define an isochron the plutons were assumed to be of different ages (Table 6.1).

It was generally believed that the absence of plutonic units in the Cambrian to Ordovician Saint John Group clearly indicated a Precambrian age for the igneous event. The Precambrian age was also confirmed by earlier Rb-Sr work by Fairbairn et al. (1966) and Cormier (1969) based on numerous volcanic and plutonic rock analyses from southern New Brunswick. This late Precambrian age also appeared to confirm the reliability of the Rb-Sr technique.

Poole (1980) collected samples from several plutonic units southwest of Saint John for Rb-Sr analyses which yielded 4, 6, and 7 point isochron ages of ca 546 Ma, 526 Ma, and 439 Ma, respectively. These ages were younger than the Rb-Sr age of 615 ± 37 Ma obtained on the Ludgate Lake pluton by Olszewski and Gaudette (in Poole, 1980, p. 171). Poole (1980) argued that some of his dated plutons are

Precambrian; however, he also concluded that they may be cogenetic with Cambrian volcanic rocks found elsewhere in the Avalon Zone [e.g. Bourinot Group in Cape Breton Island (Hutchinson, 1952)].

Olszewski and Gaudette (1982) produced a series of Rb-Sr ages from the Brookville Gneiss which yielded a combined isochron age of ca. 771 Ma, considerably older than previous Rb-Sr ages. This was interpreted to represent a major early period of high grade metamorphism and deformation in the gneiss. The Musquash Harbour Granite yielded a Rb-Sr age of ca. 392 Ma which was considered to represent a second igneous and/or deformational event (Olszewski and Gaudette, 1982).

6.2.3. Early U-Pb Data

The U-Pb method of dating was first applied in southern New Brunswick by Olszewski and Gaudette (1982) as a means of correlation with similar rock types elsewhere in the Avalon terrane (Table 6.1). They restricted their work to analyses of the Brookville Gneiss. U-Pb detrital zircon analyses on multi-grain samples from the paragneiss did not plot on a single discordia and a curved line was fitted interpreted to represent two Pb-loss events at ca. 783 and 369 Ma (Olszewski and Gaudette, 1982; Fig. 3, p. 2163). The upper intercept of this curved line is ca. 1641 Ma and based on detrital zircon morphology, was interpreted to date the source area. A single concordant zircon yielded an age of ca. 814 Ma and was interpreted to be metamorphic in origin. U-Pb results from the orthogneiss defined a two point discordia with an upper intercept of ca. 827 Ma and a lower intercept of ca. 333 Ma.

Olszewski and Gaudette (1982) collectively interpreted the U-Pb and Rb-Sr data to indicate that the maximum age for the Brookville Gneiss and the Green Head Group is about ca. 1640 Ma. These data also suggested a major period of metamorphism and deformation at ca. 880 Ma to form the Brookville Gneiss either by metamorphism of the Green Head Group (Wardle, 1978) or by complex remobilization of a tonalitic

basement gneiss and subsequent intrusion into the Green Head Group (e.g. Currie et al., 1981; Currie, 1983).

Unfortunately, the early analytical techniques associated with the unrefined U-Pb method are considered primitive by today's standards (e.g. unabraded zircon samples and relatively high Pb-blanks) and as a result the significance of these ages, if any, is uncertain.

6.3. PRESENT GEOCHRONOLOGY

This study represents the first attempt to decipher the complex geochronology as described by previous workers, by applying more precise analytical techniques combined with essential detailed field control. Concurrently with this study, additional dates have been obtained by other workers (e.g. Dallmeyer et al., 1990; Zain Eldeen, 1991; Currie and Hunt, 1991; Dallmeyer and Nance, 1992; Nance and Dallmeyer, 1994) and this chapter integrates all available data (Table 6.2).

In this study U-Pb and $^{40}\text{Ar}/^{39}\text{Ar}$ isotopic dating was undertaken to help constrain: 1) the protolith age and subsequent metamorphic age of the Brookville Gneiss and Green Head Group, and 2) the original crystallization and cooling ages for many of the plutonic units. The ages can be used to place constraints on geological events in the terrane. A significant amount of data have already been published and only new data are presented in detail here.

U-Pb and $^{40}\text{Ar}/^{39}\text{Ar}$ geochronological analytical techniques employed in the study are summarized in Appendices E.1 and E.2, respectively; also described there are criteria for sample selection, and location and description of samples.

6.3.1. U-Pb Data from Plutonic Units

As part of this study several U-Pb ages from the Brookville terrane were obtained by Dr. M.L. Bevier using the Geochronology

Laboratory at the Geological Survey of Canada (Ottawa). They include a detailed zircon and titanite study on: 1) the paragneissic and orthogneissic components from the Brookville Gneiss (Bevier et al., 1990; White et al., 1990, b, c), and 2) the Rockwood Park and French Village plutons (White et al., 1990; Bevier et al., 1991). An independent U-Pb study on the orthogneissic parts of the Brookville Gneiss was undertaken by Dallmeyer et al. (1990). The following sections summarize new U-Pb data from this study on the Fairville and Ludgate Lake plutons obtained using the Geochronology Laboratory at Memorial University of Newfoundland, St. John's, Newfoundland, under the supervision of Dr. G. Dunning.

6.3.1.1. Fairville Granite

Sample NB92-9012 from the Fairville Granite (Fig. 6.1, 6.2) contains one morphologically heterogeneous population of zircon. These are colourless to very pale yellow with a minor rust-brown coating on some tips, euhedral simple prisms with a dipyrmaid, having an average length/breadth (L/B) ratio of 3.3 (Plate 9a, b). These grains have good to excellent clarity with rare translucent fractures near tips. Clear tubes and bubbles are the only types of inclusions present, and there is no visible evidence for inherited core material. No titanite was present in this sample.

Two abraded zircon fractions (Z1, Z3) were hand picked avoiding any obvious inclusions and one fraction (Z2) contained minor inclusions. Analyses Z1 and Z2 are slightly discordant (< 3.3 %) with $^{207}\text{Pb}/^{206}\text{Pb}$ ages of ca. 570 Ma and 560 Ma, respectively (Appendix E.1.3). One other analysis (Z3) is 11.4% discordant and has a significantly older $^{207}\text{Pb}/^{206}\text{Pb}$ age of ca. 631 Ma (Appendix E.1.3). These fractions define a simple discordia line with lower and upper intercept ages of 548 ± 2 and $1997 +280/-215$ Ma, respectively (Fig. 6.3). The lower intercept age is the best estimate of the emplacement age of the Fairville Granite, and

the upper intercept indicates the presence of a significant component of inherited zircon with an Palaeoproterozoic average age.

6.3.1.2. Ludgate Lake Granodiorite

Sample NB91-9010 from the Ludgate Lake Granodiorite (Fig. 6.1) contains two morphologically distinct zircon populations. The most abundant grains (>60% by volume) include colourless, euhedral, needle-shaped simple prisms with a dipyrmaid, and an average L/B ratio of 6.2. (Plate 9c). They exhibit excellent clarity with minor clear tubes and bubbles as inclusions. No visible cores were observed.

The other 40% of the zircons are stubby to slightly elongate, euhedral, colourless with rare brown staining on tips, multifaceted dipyrramids with short to only incipiently formed prisms, with an average L/B ratio of 2.2 (Plate 9d). These grains have good to excellent clarity with rare cloudy cross-fractures. Clear tubes and bubbles are the only types of inclusions present, and there is no visible core material.

Titanite in this sample forms light amber to dark brown, clear to slightly cloudy, anhedral to subhedral grains (Plate 9e, f). No visible inclusions or cores were detected in these grains.

Three fractions of zircon were analyzed (Appendix E.1.3), one from the needle-shaped population (Z1) and two from the stubby set (Z2 and Z3). Isotopic ratios are strongly clustered, slightly discordant (< 2%) and yield $^{207}\text{Pb}/^{206}\text{Pb}$ ages of ca. 548 Ma to 544 Ma. Two fractions of titanite were analyzed (Appendix E.1.3); one fraction (T1) was more abraded than the second fraction (T2). The zircon and titanite fractions define a discordia line with an upper intercept age of 546 ± 2 Ma considered to be the age of crystallization for the Ludgate Lake Granodiorite (Fig. 6.3). The lower intercept, at ca. 30 Ma, is very uncertain due to the length of the projection but probably reflects recent Pb loss.

Both fractions of titanite are slightly discordant; however T1 yields a $^{207}\text{Pb}/^{206}\text{Pb}$ age of ca. 545 Ma, in agreement with the upper intercept age, suggesting relatively rapid cooling, at least through the closure temperature of titanite.

6.3.2. $^{40}\text{Ar}/^{39}\text{Ar}$ Data from Plutonic Units

The following sections summarize new $^{40}\text{Ar}/^{39}\text{Ar}$ data from this study obtained from the argon laboratory in the Earth Sciences Department at Dalhousie University, Halifax, Nova Scotia. Six hornblende fractions and one biotite fraction were analyzed from the Fairville, French Village, Rockwood Park, Renforth, and Shadow Lake plutons. The $^{40}\text{Ar}/^{39}\text{Ar}$ analytical data for six hornblende fractions from the plutonic units are listed in Appendix E.2.3. and ages are summarized in Table 6.2. The data are presented as incremental release age spectra with $^{37}\text{Ar}/^{39}\text{Ar}$ ratios (Fig. 6.4).

Most of the six hornblende fractions display slightly discordant $^{40}\text{Ar}/^{39}\text{Ar}$ age spectra of variable complexity which probably result from intrasample variations as reflected in the $^{37}\text{Ar}/^{39}\text{Ar}$ ratios. Most of the age spectra display considerable variation in apparent ages at lower temperatures which are matched by irregularities in $^{37}\text{Ar}/^{39}\text{Ar}$ ratios. These variations have been attributed to slight impurities, sample contamination, ^{39}Ar recoil effects, or a combination of all three factors (e.g. McDougall and Harrison, 1988), which result in the expulsion of argon from relatively non-retentive phases. Turner (1968) suggested that the apparent low ages at the low temperature portions of the spectra develop as a result of partial, intracrystalline, diffusive loss of radiogenic ^{40}Ar during a superimposed thermal event. Rex et al. (1993) suggested that initial low-age steps, typical of hornblende spectra, are due to degassing of minor, submicroscopic biotite contaminant rather than diffusive argon loss (see Section 6.4.9.).

Intermediate and high temperature steps generally display less variation in the age spectra and $^{37}\text{Ar}/^{39}\text{Ar}$ ratios. This suggests that the experimental evolution of gas occurred from compositionally uniform intracrystalline sites.

In the high temperature steps some hornblende concentrates display anomalously narrow low apparent age increments (mini saddle-shaped). Larger saddle-shaped spectra have been reported from biotite analyses (e.g. Lo and Onstott, 1989) and rarely from hornblende (e.g. Plint and Ross, 1993) but they have never been satisfactorily explained. Small saddle shapes are commonly attributed to ^{39}Ar recoil (Faure, 1986; McDougall and Harrison, 1988), probably into intergrown chlorite during irradiation (Lo and Onstott, 1989), or have been attributed to experimentally induced fractionation (Dalrymple and Lanphere, 1974). In any case, the amount of argon gas involved is very small and these "burps" are considered geologically insignificant.

6.3.2.1. Fairville Granite

A hornblende concentrate (sample CW89-611) from the Fairville Granite (Fig. 6.2) yields a total gas age of ca. 527 Ma with a slightly disturbed age spectrum (Fig. 6.4a). The first three low-temperature increments cover a wide range of ages and constitute <5% of the total gas released. This wide variation in age is also indicated in the $^{37}\text{Ar}/^{39}\text{Ar}$ ratio. The intermediate and high temperature portion of the age spectrum do not display a wide variation except the temperature increments at 1025°C and 1050°C which define a small saddle. This variation is also reflected in the $^{37}\text{Ar}/^{39}\text{Ar}$ ratio.

The apparent age based on the intermediate to high temperature increments (950°C to 1100°C), the most Ar-retentive steps, is 536 ± 3 Ma. The average $^{37}\text{Ar}/^{39}\text{Ar}$ ratio for the segment used in the age calculation is 4.2 ± 0.4 which agrees (within error) with the ratio of 4.7 ± 0.9

(Appendix E.3) calculated from electron microprobe data on the same hornblendes. Excluding the saddle temperature increments (1025°C and 1050°C; <8% of ^{39}Ar released) an integrated age of 540 ± 3 Ma is obtained which is not significantly different from the intermediate to high-temperature age. The best estimate of the maximum cooling age of this sample is 536 ± 3 Ma.

6.3.2.2. French Village Quartz Diorite

A hornblende concentrate (sample CW88-246) from the French Village Quartz Diorite (Fig. 6.5) yields a relatively flat age spectrum which generally conforms to the shape expected for a relatively undisturbed sample with no significant excess Ar effects (Fig. 6.4b). However, the $^{37}\text{Ar}/^{39}\text{Ar}$ ratios display an internally discordant spectrum which is also observed in the large error (13.8 ± 3.2) associated with the Ca/K ratio measured from microprobe data. The total gas age for this sample is ca. 527 Ma. The stepped shape of the early part of the spectrum is closely matched by the irregularities in the $^{37}\text{Ar}/^{39}\text{Ar}$ ratio. This sample does not strictly define a plateau (cf. Fleck et al. 1977) but based on intermediate to high temperature steps (975°C to 1375°C; 86% of ^{39}Ar released) it defines a "near plateau" at 540 ± 5 Ma which is interpreted as the cooling age of this sample.

6.3.2.3. Rockwood Park Granodiorite

A hornblende concentrate (sample CW89-509A) from the Rockwood Park Granodiorite (Fig. 6.2) yields an age spectrum very similar in shape to that for the Fairville Granite, including the same small saddle-shape in the high temperature steps (Fig. 6.4c). Total gas age for this sample is ca. 527 Ma. The intermediate to high temperature steps (975°C to 1400°C; 90% of ^{39}Ar released) yield an average age of 538 ± 5 Ma, which is considered the best estimate of the cooling age. The average $^{37}\text{Ar}/^{39}\text{Ar}$

ratio for these steps is 8.2 ± 1.4 , which is higher but within error of the value (5.9 ± 1.4) inferred from Ca/K measurements. Exclusion of the saddle temperature steps (1100°C, 1125°C, and 1150°C; <8% of ^{39}Ar released) yields an integrated age of 540 ± 5 Ma, which is not significantly different from the intermediate to high-temperature age.

In addition to the hornblende sample, a biotite concentrate (sample CW89-509A) was prepared from the same sample of Rockwood Park Granodiorite. The sample displays an age spectrum that is typical of a biotite in an undisturbed geological environment, although there is a slight internal discordance in the low-temperature steps (Fig. 6.4d). This sample has a total-gas age of ca. 496 Ma. The age spectrum is fairly flat and defines a plateau (750°C to 950°C; 51% of ^{39}Ar released) of 511 ± 3 Ma; however, a "near plateau" age of 509 ± 3 Ma is defined by intermediate to high temperature increments (700°C to 1050°C; 86% of ^{39}Ar released). This age does not differ significantly from the plateau age. The best estimate of the cooling age for this sample is 511 ± 3 Ma.

6.3.2.4. Renforth Pluton

A hornblende concentrate (sample CW88-169) from the tonalitic portion of the Renforth Pluton (Fig. 6.5) yields an age spectrum very similar to hornblende from the Fairville and Rockwood Park plutons, although portions of the high temperature increments (1100°C and 1125°C; 7% of ^{39}Ar released) define a much more pronounced saddle (Fig. 6.4e). The total gas age for this sample is ca. 502 Ma. The intermediate to high temperature increments (1000°C to 1300°C; 85% of ^{39}Ar released) yields an average age of 511 ± 5 Ma. The $^{37}\text{Ar}/^{39}\text{Ar}$ ratio, 6.4 ± 0.9 , is similar to that deduced from Ca/K microprobe data of 6.2 ± 0.7 for these steps. Excluding the saddle temperature steps (1100°C and 1125°C; <8% of ^{39}Ar released) an integrated age of 516 ± 5 Ma is obtained. The preferred estimate of the cooling age is 511 ± 5 Ma.

6.3.2.5. Shadow Lake Granodiorite

Hornblende concentrates were prepared from two samples of the Shadow Lake Granodiorite (Fig. 6.1): sample NB91-8599, from a medium-grained granodiorite, and sample NB91-8597, from a tonalitic enclave near the same exposure. Sample NB91-8599 yields a disturbed, U-shaped spectrum (Fig. 6.4f). The first four steps have high ages constituting about 20% of gas released. Apparent ages drop to a minimum and level off, then rise again. This form of spectrum is attributed to the presence of excess Ar, and the apparent age minimum is generally assumed to be the maximum age of the sample (Harrison and McDougall, 1981). However, recent workers (e.g. Faure, 1986; McDougall and Harrison, 1988) suggest that ages calculated from these types of profiles overestimate the age of the sample and are therefore not geologically valid. The four lowest apparent age increments (1025°C to 1090°C; 63% of ^{39}Ar released) define a plateau age of 543 ± 5 Ma. The absolute minimum in the age spectrum (increment 1050°C) is 542 ± 3 Ma. The $^{37}\text{Ar}/^{39}\text{Ar}$ ratio, 7.0 ± 0.1 , is similar to that deduced from Ca/K microprobe data of 7.4 ± 0.5 for these steps. This suggests that the excess Ar was probably evenly distributed throughout the sample.

Due to the presence of excess Ar in this sample the steps that define the plateau age are plotted on an isotope correlation diagram (McDougall and Harrison, 1988). The resulting isochron yields an age of 544 ± 5 Ma which is identical to the plateau age. The geological significance of this age is uncertain and interpreted with caution because other $^{40}\text{Ar}/^{39}\text{Ar}$ dates in the immediate area are considerably younger (see Table 6.2).

Sample NB91-8597 displays an internally discordant age spectrum defining a total-gas age of ca. 523 Ma (Fig. 6.4g). Intermediate and high temperature increments (1000°C to 1350°C; 92% of ^{39}Ar released) record a similar apparent age of 527 ± 5 Ma corresponding to a flat $^{37}\text{Ar}/^{39}\text{Ar}$ spectrum. A "near plateau" age is defined from temperature

increments 1000°C to 1100°C (51% of ^{39}Ar released) of 529 ± 5 Ma which is not significantly different from the intermediate to high temperature age. The average $^{37}\text{Ar}/^{39}\text{Ar}$ ratio for these steps is 7.5 ± 0.5 , which is lower but within error of the value (9.4 ± 1.9) inferred from Ca/K microprobe measurements. The best estimate of the cooling age for this sample is 527 ± 5 Ma.

6.3.3. $^{40}\text{Ar}/^{39}\text{Ar}$ Data from the Brookville Gneiss

Phlogopite concentrates were prepared from two separate coarse-grained marble layers within the paragneiss of the Brookville Gneiss (Fig. 6.6). $^{40}\text{Ar}/^{39}\text{Ar}$ analytical data, locations, and descriptions of samples are listed in Appendix E.2 and are portrayed as incremental release spectra in Figure 6.7.

The phlogopite concentrates display similar, internally discordant, $^{40}\text{Ar}/^{39}\text{Ar}$ age spectra corresponding to total-gas ages of ca. 513 Ma (CW89-598C) and ca. 530 Ma (CW89-629). The character of the age spectrum discordance is identical for the low-temperature portions of each analysis (<10% of ^{39}Ar released) with very low initial ages that rise abruptly to very high ages and back down to geologically reasonable ages. The intermediate and high temperature increments for sample CW89-598C gradually step up from about 512 Ma to 544 Ma. Due to this age gradient (see Appendix E.2.1), the most Ar-retentive steps (1020°C to 1200°C) are interpreted to record the minimum age of this sample. These high temperature steps yield an age of 541 ± 5 Ma.

Intermediate to high temperature increments for sample CW89-629 (830°C to 1300°C; 95% of ^{39}Ar released) yield an age of 536 ± 5 Ma; however, the higher temperature steps (1070°C to 1300°C; 75% of ^{39}Ar released) define a plateau age of 534 ± 5 Ma which is interpreted to be the minimum age for this sample. These two ages do not differ significantly and agree well with the total gas age.

The high temperature ages recorded by these two phlogopite samples are within error and are interpreted to record the minimum time since cooling through phlogopite closure temperatures of ca. 390 Ma.

6.3.4. $^{40}\text{Ar}/^{39}\text{Ar}$ Data from the Green Head Group

Phlogopite concentrates have been prepared from coarse-grained marbles at three locations in the Green Head Group and in addition, a muscovite concentrate was prepared from a mica schist (Fig. 6.6, 6.8). $^{40}\text{Ar}/^{39}\text{Ar}$ analytical data, locations, and descriptions of the mica concentrates are listed in Appendix E.2 and are shown as incremental release spectra in Figure 6.9.

Two of the phlogopite concentrates (CW90-764 and CW90-812) display internally discordant $^{40}\text{Ar}/^{39}\text{Ar}$ age spectra corresponding to total-gas ages of ca. 515 Ma and ca. 511 Ma, respectively. However, the characteristics of the age spectra are identical to phlogopite analyzed from the marble in the Brookville Gneiss. The relatively small volume low-temperature gas fractions (<7% of ^{39}Ar released) display the same variation in apparent age, with very low initial values followed by a high apparent age peak which lowers and levels off. Although little work has been done on phlogopite systematics (e.g. Kaneoka and Aoki, 1978; Harrison et al., 1985) the spectra associated with these micas appear to be characteristic.

The intermediate and high temperature steps (860°C to 1300°C; <93% of ^{39}Ar released) for sample CW90-764 display an age gradient with an average apparent age of 525 ± 5 Ma; however, the higher temperature steps (980°C to 1300°C; 65% of ^{39}Ar released) define a "near-plateau" age of 530 ± 5 Ma. Both apparent ages are slightly older than the total-gas age; however, 530 ± 5 Ma is considered the minimum cooling age for this sample (Fig. 6.9a).

Similar intermediate to high temperature increments for sample CW90-812 (830°C to 1200°C; 94% of ^{39}Ar released) yield an average apparent

age similar to the total-gas age of 518 ± 5 Ma. The higher temperature steps (1040°C to 1200°C; 54% of ^{39}Ar released) define a "near-plateau" age of 515 ± 5 Ma (Fig. 6.9b). This is considered to be the best estimate of the minimum cooling age.

The third phlogopite sample (CW88-204) displays a very internally discordant $^{40}\text{Ar}/^{39}\text{Ar}$ age spectrum with a total-gas age of ca. 547 Ma (Fig. 6.9c). No plateau is observed in this sample, but the intermediate to high temperature increments (870°C to 1200°C; <89% of ^{39}Ar released) yield an average apparent age of 556 ± 6 Ma similar to the total gas age. This age is incompatible with other $^{40}\text{Ar}/^{39}\text{Ar}$ hornblende and U-Pb zircon ages from the area. The character of this phlogopite age spectrum, weakly convex upwards, does not conform to the pattern acquired from other phlogopite analyses. The relatively high age and the overall shape of the spectrum suggest excess Ar is probably present (McDougall and Harrison, 1988, p.116-117). However, the higher temperature steps (1120°C to 1200°C; 16% of ^{39}Ar released) yield an age of 538 ± 6 Ma which is compatible with other $^{40}\text{Ar}/^{39}\text{Ar}$ hornblende and U-Pb zircon ages from the area. 538 ± 6 Ma is interpreted to be the minimum cooling age of this sample (Fig. 6.9c).

A concentrate of coarse-grained muscovite (CW90-767) from a muscovite-biotite schist of the Green Head Group displays an internally discordant $^{40}\text{Ar}/^{39}\text{Ar}$ age spectrum with a slight age gradient (Fig. 6.9d). The intermediate to high temperature increments (750°C to 1130°C; 92% of ^{39}Ar released) record an average apparent age of 505 ± 5 Ma, corresponding very well to the total-gas age of ca. 503 Ma. The high temperature increments (870°C to 1130°C; 64% of ^{39}Ar released) yield a plateau age of 507 ± 5 Ma interpreted to be the minimum cooling age.

6.3.5. $^{40}\text{Ar}/^{39}\text{Ar}$ Data from the Hammondvale metamorphic unit

Muscovite concentrates have been analyzed from mica schists

collected at three locations in the Hammondvale metamorphic unit (Fig. 1.3, 6.10). The Hammondvale metamorphic unit was previously considered to be a metamorphic equivalent of the Ashburn Formation of the Green Head Group (McCutcheon, 1978; Ruitenberg et al., 1975, 1979; McLeod et al., 1994). However, based on field relations and petrography (Chapter 5) this unit is considered to be part of the Caledonia terrane. To test this interpretation muscovite concentrates were analyzed to determine their Brookville or Caledonia terrane affinity. $^{40}\text{Ar}/^{39}\text{Ar}$ analytical data are listed in Appendix E.2 and the resulting incremental release spectra are shown in Figure 6.11.

The three muscovite concentrates display very similar internally discordant $^{40}\text{Ar}/^{39}\text{Ar}$ age spectra corresponding to total-gas ages of ca. 613 Ma (sample NB87-4090), ca. 598 Ma (sample CW88-101), and ca. 590 Ma (sample CW88-115A). The shape of the age spectra discordance is marked by ages that systematically increase throughout the low-temperature portion of each analysis. In the intermediate to high temperature steps the sharp increase in ages is less dramatic although an age gradient is still present.

Intermediate and high temperature increments (835°C to 1120°C; <87% of ^{39}Ar released) in the muscovite concentrate from sample NB87-4090 yield an average apparent age of 611 ± 6 Ma similar to the total-gas age (Fig. 6.11a). The muscovite also defines two similar plateau ages of 609 ± 6 Ma and 611 ± 6 Ma (835°C to 950°C; 67% of ^{39}Ar released and 860°C to 980°C; 63% of ^{39}Ar released, respectively). The high temperature increments (980°C to 1070°C; <19% of ^{39}Ar released) yields an age of 617 ± 6 Ma which is within error of the plateau ages and is interpreted to represent the minimum cooling age of this sample.

Sample CW88-101 yields an intermediate to high temperature (825°C to 1120°C; 77% of ^{39}Ar released) average apparent age of 608 ± 6 Ma but also defines a plateau age (825°C to 960°C; 50% of ^{39}Ar released) of 605 ± 6 Ma (Fig. 6.11b). The high temperature increments (960°C to 1120°C;

<37% of ^{39}Ar released) yields an age of 613 ± 6 Ma which is interpreted to represent the minimum cooling age of this sample.

Muscovite from sample CW88-115A yields a nearly flat spectrum but does not define a plateau (Fig. 6.11c). The high temperature increments (950°C to 1400; 47% of ^{39}Ar released) define an average apparent age of 603 ± 6 Ma. This age is considered to represent the minimum cooling age for this sample.

6.4. INTERPRETATION

6.4.1. Previous Age Determinations

Much of the Rb-Sr work undertaken in this region is now considered to have uncertain geological significance. This was first noted by Stukas (1977) who regrouped and recalculated the Rb-Sr data of Fairbairn et al. (1966) and Cormier (1969) as a result of his reinterpretation of the geology in southern New Brunswick. He divided the large Rb-Sr data set, which included units of various ages, into more restricted geographic locations which locally corresponded to specific map units (Table 6.1.) and suggested that the Rb-Sr systematics are highly disturbed. Subsequent workers (e.g. Poole, 1980; Olszewski and Gaudette, 1982; Dickson, 1983) largely ignored this new data set because it was difficult to interpret many of these "new" Ordovician to Devonian dates in light of the assumed stratigraphic succession in southern New Brunswick.

In addition, Poole (1980) and Olszewski and Gaudette (1982) produced analytically precise Rb-Sr isochron ages of 526 ± 13 Ma (MSWD = 0.5), 771 ± 55 Ma (MSWD = 0.4), and 392 ± 55 Ma (MSWD = 0.01) for plutonic units southwest of Saint John. They suggested that the low MSWD added credibility to these ages and the Rb-Sr method. However, Rb-Sr isotopic systems have been demonstrated to have been disturbed elsewhere within similar units of the Northern Appalachian Orogen

(Reynolds et al., 1989; Barr et al., 1990) and based on present geochronology, it is considered that these generally young isochron ages may result from disturbances in the isotopic systems, and do not record the true age of emplacement.

The U-Pb data of Olszewski and Gaudette (1982) on the Brookville Gneiss were collected using what are now considered outdated techniques and therefore most of their data are considered unreliable. There have been major advances in U-Pb microchemistry, mass spectrometry, and sample preparation that have resulted in increasingly more precise analyses of smaller samples (e.g. Parrish et al. 1987) and many of these analytical techniques were unavailable to Olszewski and Gaudette (1982).

K-Ar age determinations on mica, hornblende and whole rock samples from granitic and gneissic rocks in the Brookville terrane range from 340 Ma to 531 Ma, recalculated using the decay constants of Steiger and Jager (1977). However, with a few exceptions, ca. 473 Ma to 508 Ma ages predominate (Table 6.1). In the past these K-Ar ages were interpreted to measure the time since emplacement of plutons or to date peak metamorphism; however, these ages yield information more relevant to the cooling rather than the emplacement history.

However, even as cooling ages the results appear to be too young, with the exception of the ca. 531 Ma on biotite from the Brookville Gneiss (Table 6.1). It has long been recognized (e.g. Roddick et al., 1992) that incorrect K-Ar ages are a reflection of low K contents in the sample. Obradovich and Cobban (1975) showed that altered biotites with K contents below 5% yielded K-Ar ages that are usually too young. Clearly radiogenic Ar and to a lesser degree K has been lost from these samples, probably the result of reactions during chloritization of biotite (Lo and Onstott, 1989) and hornblende.

Where $^{40}\text{Ar}/^{39}\text{Ar}$ methods have been applied to the same rock units dated by K-Ar, the $^{40}\text{Ar}/^{39}\text{Ar}$ ages are consistently older. This is evident from the pre-1975 K-Ar analyses; however, analyses after this date are within error of many of the $^{40}\text{Ar}/^{39}\text{Ar}$ ages (cf. Table 6.1 and 6.2) and are

probably due to better sample preparation resulting in less chlorite contamination. However, the very large errors associated with many of these K-Ar ages renders them useless for constraining detailed thermal histories.

6.4.2. Closure Temperatures

The age calculated for a mineral from an accumulated radioactive decay product is the time when the chemical system of that mineral became effectively closed to diffusion of that particular radioactive decay product. Diffusion is dominantly controlled by temperature (cf. Heaman and Parrish, 1991) and to a lesser extent by cooling rates (Dodson, 1973), chemical composition (cf. Harrison et al., 1985; Scaillet et al., 1992; Dahl, 1994) and strain history (cf. Gromet, 1991; Getty and Gromet, 1992). Specifically, each mineral has a characteristic closure temperature for diffusion of a given element and its apparent age measures the time when the mineral cooled through this temperature. The closure temperature is higher for relatively fast cooling (e.g. 100°C/Ma) and is lower if cooling is slow (e.g. 1°C/Ma) (cf. Onstott and Peacock, 1987). Closure temperatures adopted in this study are compiled in Table 6.3.

Closure temperatures for minerals dated using the U-Pb method are discussed and summarized by Heaman and Parrish (1991). In their study on U-bearing accessory minerals, they concluded that the best estimate of the closure temperature in zircon is in excess of 800°C. Tucker et al. (1987) and Heaman and Parrish (1991) considered 600°C a reasonable estimate for the maximum closure temperature for titanite. This differs slightly from the closure temperature used by Ghent et al. (1988) quoted in Bevier et al. (1990) at 550°C. A value of $600 \pm 25^\circ\text{C}$ is used in the present study.

An isothermal-hydrothermal diffusion study by Harrison (1981) suggested a closure temperature of 500-550°C (McDougall and Harrison,

1988) for argon in hornblende at a geologically fast cooling rate (100°C/Ma). Many of the hornblendes dated in this study are from igneous units, that based on field evidence and petrography, cooled rapidly after emplacement. If significant exsolution (e.g. cummingtonite from hornblende) is present in the sample, the closure temperature may be lower (Harrison and Fitz Gerald, 1986). A detailed petrological examination of the hornblende samples used in this study indicates that exsolution is not present and the closure temperature for these hornblende is assumed to be $525 \pm 25^\circ\text{C}$.

The closure temperature of biotite may be strongly dependent on composition (Harrison et al., 1985), with a tendency for Mg-rich biotite (phlogopite) to be more Ar-retentive than Fe-rich biotite (annite). Phlogopites used in this study have Mg/(Mg+Fe) ratios of 0.96 ± 0.02 and annite has Mg/(Mg+Fe) ratios of 0.51 ± 0.01 . Assuming a cooling rate of 10°C/Ma (and other parameters established by Yu and Morse, 1992) the estimated closure temperatures for phlogopite [with Mg/(Mg+Fe) = 0.77] are from 355°C to 365°C. Because the Mg# is much higher in phlogopite used in this study an estimate of 380°C to 400°C has been adopted for the closure temperature. The composition of the annite is similar to that used by Harrison et al. (1985) and Yu and Morse (1992), and therefore a closure temperature of 300°C to 320°C is assigned.

The closure temperature for argon diffusion in muscovite is not well known. It has been quoted as high as 375-400°C (Dallmeyer and Nance, 1990; 1992) or as low as 270-285°C (Snee et al., 1988). Based on literature research Snee (1982) estimated muscovite closure temperature to be $320^\circ \pm 40^\circ\text{C}$. Harrison and McDougall (1980) suggested that the closure temperature is similar to strontium diffusion in biotite at approximately 320°C. Using temperatures estimated from fluid inclusion studies, Snee et al. (1988) suggested that muscovite closed to diffusion of argon at approximately 325°C. A value of $325 \pm 10^\circ\text{C}$ is adopted in this study.

6.4.3. Brookville Gneiss

A detailed U-Pb geochronologic study on various morphological populations of zircon from the Brookville Gneiss was undertaken by Bevier et al. (1990). Based on single grain analysis of detrital zircons from the paragneiss, a maximum depositional age of ca. 641 Ma is suggested (youngest zircon analyzed). Other detrital zircons from the paragneiss cluster in the ranges 640-1640 Ma and 2260-2700 Ma (Fig 6.12a, b). Olszewski and Gaudette (1982) were correct in their interpretation that their upper intercept age of ca. 1641 Ma (average age of several bulk zircon fractions) represents the age of source area for the paragneiss.

Zircons from the orthogneiss (Fig. 6.6) yielded an igneous crystallization age of ca. 605 Ma (Bevier et al. 1990; Dallmeyer et al. 1990) and a metamorphic titanite age of ca. 564 Ma (Bevier et al., 1990). The latter is interpreted to date cooling after peak amphibolite-facies metamorphism (Fig. 6.12c).

Hornblende concentrates extracted from orthogneiss, hornblende paragneiss, and amphibolite in the Brookville Gneiss (Dallmeyer and Nance, 1989; Dallmeyer et al., 1990; Nance and Dallmeyer, 1994) (Fig. 6.2, 6.6) have yielded $^{40}\text{Ar}/^{39}\text{Ar}$ plateau and "near-plateau" ages of ca. 543-552 Ma (Table 6.2) with an average age of ca. 547 Ma. However, these workers considered the younger, corresponding isotopic correlation ages of ca. 538-542 Ma to be more geologically significant because the age calculation does not require assumption of a present-day $^{40}\text{Ar}/^{36}\text{Ar}$ ratio. Their calculations showed that $^{40}\text{Ar}/^{36}\text{Ar}$ ratios did not differ significantly from present-day atmosphere which suggests little or no intracrystalline contamination with extraneous argon. Based on this, the plateau and "near-plateau" hornblende ages are herein considered to better represent the last cooling (525°C) following amphibolite facies metamorphism in the Brookville Gneiss.

The phlogopite concentrates from marble layers within the gneiss

(Fig. 6.6) yield slightly younger $^{40}\text{Ar}/^{39}\text{Ar}$ ages of 541 ± 5 Ma (CW89-598C) and 534 ± 5 Ma (CW89-629). The phlogopite data are simply interpreted as cooling ages post-dating thermal peak conditions and indicates that the gneiss cooled relatively quickly to 390°C . These ages are slightly older than a K-Ar biotite age of 531 ± 17 Ma obtained by Stevens et al. (1982) from a paragneiss at the same location that yielded the $^{40}\text{Ar}/^{39}\text{Ar}$ phlogopite age of 541 ± 5 Ma. The low chloritic alteration (<9%) of the biotite in this sample probably rendered the resulting K-Ar age geologically significant. Another biotite from a paragneiss in the Brookville Gneiss defined a K-Ar age of ca. 508 Ma; however, this concentrate contained 22% chlorite (Leach et al., 1963) and is considered to be unreliable.

One muscovite concentrate from a paragneiss (Fig. 6.6) yielded a plateau age of ca. 516 Ma (Nance and Dallmeyer, 1994). Based on petrography much of the muscovite present defines the gneissic foliation; however, randomly oriented large flakes of muscovite commonly pseudomorph feldspar and may be secondary in origin (Nance and Dallmeyer, 1994; Chapter 5). If the muscovite age does not represent a reset age (see Section 6.5) then the data suggest that the last cooling of the Brookville Gneiss through 325°C following amphibolite facies metamorphism (and associated retrograde metamorphism) occurred at ca. 516 Ma.

The U-Pb and $^{40}\text{Ar}/^{39}\text{Ar}$ data indicate that the Brookville Gneiss is much younger than previously interpreted and does not represent remobilized Grenvillian (or older) continental basement as interpreted by Currie et al. (1981). Furthermore, the gneisses appear to be younger than the Green Head Group and cannot be considered "basement" to the Green Head Group (cf. Currie, 1983; Olszewski and Gaudett, 1982; Nance, et al., 1991) or its higher grade equivalent (cf. Alcock, 1938; O'Brien, 1976; Wardle, 1978).

6.4.4. Plutonic Units

Based on available geochronological data there appear to be several episodes of plutonic activity in the Brookville terrane. The oldest dated pluton is the granodioritic to tonalitic orthogneiss in the Brookville Gneiss which has yielded U-Pb zircon crystallization ages of ca. 605 Ma (Bevier et al., 1990; Dallmeyer et al., 1990); this was subsequently metamorphosed at ca. 564 Ma (see Section 6.4.3.).

The Brookville Gneiss and Green Head Group were intruded by numerous lithologically varied plutonic units (Chapter 4). The ca. 605 Ma igneous age and the ca. 564 Ma metamorphic age of the Brookville Gneiss suggest that the other plutons intruding the gneiss are younger.

The oldest dated pluton that intrudes the Brookville Gneiss is the Fairville Granite (Fig. 6.2) which yields a U-Pb crystallization age for zircon at 548 ± 2 Ma (NB92-9012), similar to a $^{40}\text{Ar}/^{39}\text{Ar}$ isotope correlation hornblende age of ca. 547 Ma obtained by Dallmeyer and Nance (1992) (Table 6.2). This date is much older than the $^{40}\text{Ar}/^{39}\text{Ar}$ hornblende age of 536 ± 3 Ma (CW89-611) obtained from this study (Table 6.2). Based on petrography and hornblende geobarometry (Chapter 4) the Fairville Granite appears to have cooled slowly and the ca. 536 Ma hornblende age is considered to better date the cooling of this pluton through the closure temperature of hornblende (525°C). K-Ar biotite and hornblende ages are considerably younger (Table 6.1) (Wanless et al., 1970, 1972, 1973).

The Ludgate Lake Granodiorite (Fig. 6.1) has yielded a U-Pb upper intercept age of 546 ± 2 Ma (NB92-9010) for the crystallization of the zircon and titanite and, by inference, the emplacement of the pluton (Table 6.2). This age is identical to the age of the Fairville Granite. No minerals suitable for $^{40}\text{Ar}/^{39}\text{Ar}$ analyses were obtained from this pluton. Previous K-Ar whole-rock and biotite analyses (Table 6.1) are significantly younger at ca. 473 - 493 Ma; however, there are no published data on the sample quality to appraise these dates. The

Ludgate Lake Granodiorite formed a broad high temperature-low pressure contact metamorphic aureole in the adjacent Martinon Formation and the similarity in the zircon and titanite ages suggests that the pluton initially cooled very rapidly. A ca. 530 Ma hornblende plateau age (Dallmeyer and Nance, 1992) from the adjacent Perch Lake Granodiorite suggests the pluton cooled more slowly from 600°C to 525°C (Table 6.2).

The major period of plutonism in the Brookville terrane appears to have occurred from ca. 527 Ma to 538 Ma. A concordant zircon and titanite age of ca. 538 from the Rockwood Park Granodiorite (Fig. 6.2, 6.13a) is interpreted to date the crystallization of this pluton (White et al., 1990). This age is identical to a $^{40}\text{Ar}/^{39}\text{Ar}$ hornblende age of 538 \pm 5 Ma (CW89-509A) obtained in this study. The similarity of these ages (Table 6.2) indicates that the pluton cooled extremely fast from 800°C to 525°C. A $^{40}\text{Ar}/^{39}\text{Ar}$ biotite plateau age of 511 \pm 3 Ma may suggest that the pluton cooled slowly through the range 525°C to 310°C or is reset by a younger thermal event (see Section 6.5). Previous $^{40}\text{Ar}/^{39}\text{Ar}$ analyses of hornblende concentrates from this pluton (Table 6.2) yielded plateau ages of ca. 550 Ma with corresponding isotope correlation ages of ca. 523 Ma and 529 Ma (Dallmeyer and Nance, 1992). They interpreted the isotope correlation ages to date the last cooling through hornblende argon retention temperatures. The spectra associated with these analyses are highly discordant and display a decreasing age gradient, therefore the quoted "ages" are interpreted with caution. However, the high temperature increments of these spectra yield consistent ages of ca. 538 Ma, identical to $^{40}\text{Ar}/^{39}\text{Ar}$ hornblende age obtained in this study.

The French Village Quartz Diorite (Fig. 6.5) has yielded a U-Pb zircon age of ca. 537 Ma (Fig. 6.13b; Appendix E.1.3) (Bevier et al., 1991), essentially identical to the U-Pb age from the Rockwood Park Granodiorite. $^{40}\text{Ar}/^{39}\text{Ar}$ hornblende analyses by Dallmeyer and Nance (1992) have yielded plateau ages of ca. 537 Ma (sample 1) and ca. 532 Ma (sample 3) with similar corresponding isotope correlation ages of ca. 537 Ma and 530 Ma, respectively. These are similar to a "near-plateau"

hornblende age of 540 ± 5 Ma (CW88-246) obtained in this study. A third hornblende concentrate (sample 2 of Dallmeyer and Nance, 1992) displays a spectrum typical of excess argon with a plateau age of ca. 564 Ma. The isotope correlation yields an age of ca. 539 Ma and is considered to be more reliable. The youngest age (ca. 532 Ma) was interpreted to date the cooling of a narrow syn-plutonic mylonite zone (Dallmeyer and Nance, 1992). This age is slightly younger than the other analyses and may be due to argon loss during mylonitization (cf. Gromet, 1991; Getty and Gromet, 1992) and thus underestimate the true age. The zircon and hornblende ages suggest that the French Village Quartz Diorite cooled quickly through the range 800°C to 525°C (Table 6.2).

The only other pluton dated by U-Pb methods is the Musquash Harbour Granite (Fig. 6.1). This pluton yielded a $^{207}\text{Pb}/^{206}\text{Pb}$ age of 550 ± 15 Ma (Table 6.2) which was considered by Currie and Hunt (1991) to be the best estimate of the time of emplacement. However, the large associated error and the abundance of inherited zircon grains makes the interpretation of this age uncertain and the age is also incompatible with $^{40}\text{Ar}/^{39}\text{Ar}$ analyses from the area. It is considered a maximum age.

The other plutonic units in the Brookville terrane do not have U-Pb data to constrain their emplacement age(s). $^{40}\text{Ar}/^{39}\text{Ar}$ results from the Belmont, Shadow Lake, and Hanson Stream plutons southwest of Saint John (Fig. 6.1, Table 6.2), all yield hornblende plateau or "near-plateau" ages of ca. 527 Ma to 531 Ma (Dallmeyer and Nance, 1989, 1992; this study). The corresponding isotope correlation ages are considerably younger than the plateau ages (Table 6.2) and are not used in this interpretation. It is clear that many of the $^{40}\text{Ar}/^{39}\text{Ar}$ ages obtained from the Brookville terrane are identical to, or slightly younger than, their corresponding U-Pb ages. This suggests that all of the plutons were emplaced at relatively shallow levels in the crust and experienced rapid cooling. This is evident from the mineral assemblages in the contact metamorphic aureoles around these plutons. The hornblende cooling ages obtained could then be interpreted to approximate the time of pluton

emplacement.

The exceptions to the main period of igneous activity in the Brookville terrane may be the younger Talbot Road and Renforth plutons (Table 6.2). $^{40}\text{Ar}/^{39}\text{Ar}$ results from the Talbot Road pluton yield a hornblende plateau and isotopic correlation age of ca. 520 Ma. The Renforth Pluton yielded a $^{40}\text{Ar}/^{39}\text{Ar}$ hornblende cooling age of 511 ± 5 Ma (CW88-169). This appears to confirm field evidence (Appendix A) that it intruded the French Village Quartz Diorite. If this hornblende age represents the time of emplacement, the Renforth Pluton is the youngest dated pluton in the terrane. The significance of these younger plutons is discussed in section 6.4.6.

Pegmatites are common in most plutonic units and the Brookville Gneiss but also occur in the Ashburn Formation. Muscovite concentrate from a pegmatite that intruded the Brookville Gneiss (Fig. 6.6) yielded a plateau age of ca. 510 Ma, interpreted to date the pegmatite emplacement (Dallmeyer and Nance, 1992).

6.4.5. Dipper Harbour volcanic unit

Previous interpretations of the age of the Dipper Harbour volcanic unit included this unit with the Carboniferous Mispec Group based on field relations (Appendix A; Section 1.2). The first radiometric age determination of this volcanic unit was conducted by Stukas (1977) using regrouped and recalculated Rb-Sr data of Cormier (1969). The resulting isochron yielded an age of 443 ± 6 Ma (Table 6.1). However, subsequent workers (e.g. McCutcheon, 1984, 1985; Currie, 1986a, b; 1987a, b; Nance, 1986a, 1987b) mapped the volcanic unit as Precambrian; although, Rast and Skehan (1991) continued to map the volcanic and associated plutonic rocks as Carboniferous.

A rhyolite ash flow in the Dipper Harbour volcanic unit (Fig. 6.1) has yielded two discordant $^{207}\text{Pb}/^{206}\text{Pb}$ zircon ages of ca. 554 Ma and 556 Ma (Zain Eldeen et al., 1991; Zain Eldeen, 1991) which suggests a

correlation with the younger volcanic units in the Caledonia terrane (Zain Eldeen, 1991; Dallmeyer and Nance, 1992). However, the ca. 555 Ma age (Table 6.2) is only based on two analyses and is therefore considered to be of dubious quality and is not used in the interpretation. Furthermore, based on field evidence, these volcanic units are interpreted to represent the extrusive equivalents of the Musquash Harbour Granite that locally intrudes the Ashburn Formation.

6.4.6. Green Head Group

The Green Head Group is interpreted to be the oldest unit exposed in the Brookville terrane, based on the presence of the stromatolite *Archaeozoon acadense* in marbles of the Ashburn Formation to which Hofmann (1974) assigned a mid-Riphean (Mesoproterozoic) age. This is considered to be the maximum age of the Green Head Group; the only assessment of the minimum age is based on the oldest U-Pb dated pluton that clearly intruded the unit (Fairville Granite at 548 ± 2 Ma and Ludgate Lake Granodiorite at 547 ± 2 Ma). Recent U-Pb analysis on detrital zircons from quartzite in the Ashburn Formation yielded several single concordant zircon grains. The youngest at ca. 1230 Ma (D. Davis, personal communication, 1995) appears to confirm the stromatolite age (Table 6.2).

The Green Head Group is locally metamorphosed to greenschist facies near the Saint John River, east of Drury Cove, and in the Hammond River area (Fig. 5.2, 5.3). However, the Green Head Group is dominantly contact metamorphosed to albite-epidote hornfels facies and grade increases to hornblende-hornfels facies and locally pyroxene-hornfels facies in proximity to intrusive bodies (Chapter 5). This contact metamorphism locally overprints the cleaved greenschist facies rocks.

Several $^{40}\text{Ar}/^{39}\text{Ar}$ muscovite and phlogopite ages have been obtained from pelite and marble in the Ashburn Formation of the Green Head Group (Table 6.2). The three $^{40}\text{Ar}/^{39}\text{Ar}$ muscovite plateau ages obtained by Nance

and Dallmeyer (1994) of ca. 509 Ma, 509 Ma, and 519 Ma were interpreted to provide cooling ages for regional metamorphism in the Green Head Group. These muscovite samples yielded analytically precise dates; however, field and petrological studies related to this study suggest that the significance of these dates is unclear.

Samples 2 and 3 of Nance and Dallmeyer (1994) are from a cleaved, well crenulated spotted schist that preserves two or three major foliations in the Drury Cove area (Fig. 6.6). Thin section examination indicates two generations of muscovite growth. Smaller muscovite grains define an earlier foliation whereas the larger grains define the major foliation. Some larger grains of muscovite appear to pseudomorph cordierite. However, the age spectra acquired from these two samples do not show the typical pattern of mixed mica ages (cf. Hanes, 1991) and define identical plateau ages of ca. 509 Ma. This suggests that the different populations of muscovite cooled together from some temperature higher than their argon closure temperature, or that they were affected by a thermal overprint that was intense enough to reset their plateau ages totally. Although the ca. 511 Ma Renforth Pluton is in faulted contact to the northeast with these spotted schists, it may have originally been responsible for the source of the thermal overprint. In contrast to the interpretation of Nance and Dallmeyer (1994) the ca. 509 Ma ages probably reflect resetting of the greenschist facies muscovite and subsequent cooling following contact metamorphism.

A muscovite concentrate from a sparsely spotted, cordierite-bearing schist (CW90-767) from the Ashburn Formation northeast of Hammond River (Fig. 6.8) yielded an age of 507 ± 5 Ma. The ca. 511 Ma Renforth Pluton outcrops to the west and may project under the Ashburn Formation in this area. The ca. 507 Ma age is similar to the ca. 509 Ma ages from the Drury Cove area. Both are interpreted to reflect resetting of the greenschist facies muscovite and subsequent cooling following contact metamorphism by the Renforth Pluton.

A phlogopite concentrate from a greenschist grade Ashburn

Formation marble (CW90-812) just east of Drury Cove (Fig. 6.6) yielded an age of 515 ± 5 Ma, similar to the ca. 519 Ma muscovite age obtained by Nance and Dallmeyer (1994) from the Saint John River area (Fig. 6.2). These are interpreted to reflect resetting following contact metamorphism in the Ashburn Formation by the ca. 511 Ma Renforth Pluton. These ages are also identical to a 516 ± 1 Ma muscovite age from the Brookville Gneiss (Nance and Dallmeyer, 1994) which suggests that muscovite ages from both the Ashburn Formation and Brookville Gneiss may have been reset.

Two phlogopite samples (CW90-764 and CW88-204) are from the Ashburn Formation marble in the contact metamorphic aureole of the ca. 537 Ma French Village Quartz Diorite (Fig. 6.8). They yielded ages of 530 ± 5 Ma and 538 ± 6 Ma, respectively and are interpreted to date the cooling of the contact zone through the phlogopite argon retention temperature (390°C).

6.4.7. MacKay Highway Shear Zone

The MacKay Highway shear zone (Map C) separates the Green Head Group from the Brookville Gneiss (Fig. 6.19). A $^{40}\text{Ar}/^{39}\text{Ar}$ hornblende age obtained from strongly deformed and lineated gneisses in the margin of this zone (Dallmeyer and Nance, 1989; Dallmeyer et al., 1990) suggests that the gneiss was juxtaposed with the Green Head Group prior to ca. 548 Ma. The Fairville Granite intruded both the Green Head Group and the Brookville Gneiss at ca. 548 Ma which confirms the minimum age on the time of juxtaposition.

The presence of deformed and boudinaged pegmatite dykes interpreted to be equivalent to the ca. 510 Ma ($^{40}\text{Ar}/^{39}\text{Ar}$ muscovite) pegmatite was interpreted by Nance and Dallmeyer (1994) to indicate that the MacKay Highway shear zone was locally reactivated subsequent to ca. 510 Ma (assuming the pegmatite crystallized at ca. 510 Ma). However, the muscovite age is interpreted here to be a cooling age which suggests

that the pegmatite may have crystallized and been locally deformed prior to cooling through 325°C at ca. 510 Ma. A muscovite age of ca. 502 Ma was obtained from the mylonitic margins of a large gneiss boudin in the MacKay Highway shear zone (mylonitic meta-psammite of Nance and Dallmeyer, 1994). This age is interpreted to date the time since amphibolite facies recrystallization of the mylonite zone and may provide a minimum age for the MacKay Highway shear zone. However, muscovite from the pegmatite and gneissic boudin may also represent a reset age from the intrusion of younger plutons (see Section 6.5).

6.4.8. Hammondvale Metamorphic Unit

The $^{40}\text{Ar}/^{39}\text{Ar}$ muscovite ages of ca. 617 Ma, 613 Ma, and 603 Ma from the Hammondvale metamorphic unit (Fig. 6.10) are interpreted to date post-metamorphic cooling through the closure temperature of muscovite. They provide minimum ages for regional high-pressure/low-temperature metamorphism in this unit. The ages, field relations, and metamorphic petrology indicate that this unit is part of the Caledonia terrane, not the Brookville terrane.

This correlation is further substantiated by $^{40}\text{Ar}/^{39}\text{Ar}$ ages of detrital muscovite from the late Precambrian to early Paleozoic cover sequence (Saint John Group) on the Caledonia terrane.

In an attempt to better define the sediment source of this cover sequence Dallmeyer and Nance (1990) dated several detrital muscovite concentrates from the Precambrian-Cambrian units of the Saint John Group exposed in southern New Brunswick. The detrital muscovite concentrates yielded plateau ages ranging from ca. 600 to 620 Ma (Dallmeyer and Nance, 1990; Nance, personal communication, 1994). These muscovites were considered to be derived from muscovite-bearing schists within the Green Head Group and Brookville Gneiss (cf. Wardle, 1978) and the age range was interpreted to date a period of late Precambrian metamorphism in the Green Head Group and Brookville Gneiss.

The $^{40}\text{Ar}/^{39}\text{Ar}$ results of this study and Nance and Dallmeyer (1994) clearly show that muscovites within the Green Head Group and Brookville Gneiss are younger than ca. 520 Ma. The muscovite ages in the Saint John Group are consistent with derivation from the Hammondvale metamorphic unit and are not consistent with derivation from the Brookville terrane.

6.4.9. Partial Argon Loss from $^{40}\text{Ar}/^{39}\text{Ar}$ Minerals

The muscovite and phlogopite age spectra increase in age upward from low-temperature extraction increments to intermediate temperature extraction increments. The increasing age with increasing temperature closely mimics the pattern predicted by Turner (1968) to result from partial, intracrystalline, diffusive loss of radiogenic ^{40}Ar during a superimposed thermal event. This type of phenomenon was also observed in hornblende spectra (Harrison, 1981). This led many workers (e.g. Dallmeyer and Nance, 1990, 1992, 1994; Nance and Dallmeyer, 1994) to speculate that meaningful ages of geological events or conditions could be obtained from these low-temperature release spectra.

Taken together, the muscovite and hornblende low-temperature increments record several age groups: 325 Ma to 329 Ma; 400 Ma to 426 Ma; and 476 Ma to 512 Ma. However, several low-temperature hornblende ages are considerably older than ca. 500 Ma. The younger age range was interpreted to be related to nearby faults (Nance and Dallmeyer, 1994). However, these faults have long movement histories which are not just confined to the Carboniferous (Leger and Williams, 1986; Chapter 3) and can hardly be considered major thermal events. Late Paleozoic overprint ages documented in muscovite from the basal Saint John Group in the Caledonia terrane (Dallmeyer and Nance, 1990) are consistent with results from the Brookville terrane.

The slightly older low-temperature overprint is similar to the range (ca. 390 Ma to 416 Ma) recorded by $^{40}\text{Ar}/^{39}\text{Ar}$ ages associated with

the mylonite zones in the Kingston Complex (Nance and Dallmeyer, 1993). This range is also broadly coincident with ca. 400 Ma low-temperature overprint ages on muscovite from metatuff in the Broad River Group of the Caledonia terrane (Dallmeyer and Nance, 1994). These similar Late Silurian to Early Devonian ages, common to the Kingston Complex and Brookville and Caledonia terranes, suggest that these units have been affected by the same middle Paleozoic event. This may record the accretion of terranes to the northern Appalachian Orogen.

The significance of the older 476 Ma to 512 Ma overprint range in the Brookville terrane is unknown. This range is identical to the low-temperature muscovite age range (477 Ma to 519 Ma) from the Hammondvale metamorphic unit.

Low-temperature age increments from phlogopite samples are consistently younger than all other low-temperature increments at about 50 Ma. There are no known thermal events in southern New Brunswick that correspond to this age and the reason for the low age compared to the biotite is unknown. The 50 Ma age therefore appears to have no geological significance.

The geological significance of these low-temperature "ages" is unclear. Southern New Brunswick has experienced several geological events since the Cambrian and the fact that the low age data coincide approximately with these events may be just coincidental. Caution should be used when interpreting the low temperature increments as representing younger "overprinting ages" due to diffusive Ar loss as predicted by Turner et al. (1966) and Harrison and McDougall (1980). The "step-up" lower temperature spectra can be controlled by many factors including excess Ar (e.g. Heizler and Harrison, 1988), ^{39}Ar recoil artifacts (e.g. Lo and Onstott, 1989) or expulsion of ^{39}Ar in nonretentive sites (e.g. Scaillet et al., 1992). One of the major factors controlling the pattern in the low temperature release increments may be contamination. Berger (1975) and Rex et al. (1993) have shown that amphiboles displaying "diffusive loss profiles" are

actually contaminated by biotite or other phases which release Ar at low extraction temperatures. They argued that steps below 900°C should be discarded from a hornblende age calculation.

It is clear that all samples should be examined under the SEM, especially if any conclusions are to be drawn from the low-temperature steps of the age spectrum.

6.5. THERMAL HISTORY

The radiometric data presented in this chapter are used to date the plutonic activity and development of metamorphic minerals associated with specific structures and events which provide important new constraints on the thermal history of the Brookville terrane.

Many of the individual age spectra appear to be complex; however, a pattern of similar ages within and among the group of samples has emerged from this study and related work. U-Pb and $^{40}\text{Ar}/^{39}\text{Ar}$ ages constrain the timing of at least two major tectonothermal events in the Brookville terrane at ca. 564-527 Ma and ca. 521-502 Ma (Table 6.2, Fig. 6.14).

The oldest documented events in the Brookville terrane are recorded in samples from the Brookville Gneiss. The tonalitic to granodioritic orthogneiss has a igneous protolith ages of ca. 605 Ma (Bevier et al., 1990; Dallmeyer et al., 1990). The ca. 564 Ma metamorphic titanite age (Bevier et al., 1990) from the orthogneiss is interpreted to date cooling (<600°C) following peak upper amphibolite facies metamorphism of the unit. Based on mineral assemblage and geothermometry, peak metamorphic conditions likely exceeded 650°C at a pressure of 3 kbar. $^{40}\text{Ar}/^{39}\text{Ar}$ hornblende results (543-552 Ma) from the Brookville Gneiss indicate that cooling following amphibolite facies metamorphism (525°C) occurred at ca. 547 Ma (Fig. 6.15). This indicates a slow cooling rate of 4°C/Ma over a span of 17 Ma (564-547 Ma).

The ca. 547 Ma is also broadly synchronous with a major period of

ductile deformation associated with the juxtaposition of the high-grade Brookville Gneiss over the relatively cool Green Head Group along the MacKay Highway shear zone. By inference, the ca. 547 Ma hornblende ages indicate the minimum age for local amphibolite facies metamorphism in the MacKay Highway shear zone and the approximate age for greenschist facies metamorphism in the adjacent Ashburn Formation.

Intrusion of the undeformed Fairville Granite (ca. 548 Ma) and Ludgate Lake Granodiorite (ca. 546 Ma) appears to be broadly coeval with the average hornblende cooling age (ca. 547 Ma) in the Brookville Gneiss. The age and undeformed character of these plutons suggest that major deformation associated with the MacKay Highway shear zone had ceased at this time.

U-Pb zircon and titanite results from other plutonic units in the Brookville terrane suggest that many of the plutons are slightly younger than ca. 547 Ma and were emplaced after ca. 538 Ma. $^{40}\text{Ar}/^{39}\text{Ar}$ hornblende ages of ca. 527 Ma to 538 Ma indicate that many of these plutons cooled very rapidly to 525°C (Fig. 6.15). $^{40}\text{Ar}/^{39}\text{Ar}$ phlogopite ages of ca. 530 Ma and 538 Ma from contact metamorphic aureoles of these plutons also indicate that they cooled relatively rapidly from hornblende to phlogopite closure temperatures.

The ca. 534 Ma and 541 Ma $^{40}\text{Ar}/^{39}\text{Ar}$ phlogopite ages from the Brookville Gneiss coincide with phlogopite ages from the contact aureoles in the Ashburn Formation. This suggests that the country rocks were relatively cool during this period of igneous activity contributing to the rapid cooling of the ca. 527 Ma to 538 Ma plutonic units.

A second intrusive event and associated metamorphism appears to have occurred at ca. 502-521 Ma (Fig. 6.14). Younger ca. 515 Ma to 519 Ma $^{40}\text{Ar}/^{39}\text{Ar}$ phlogopite and muscovite ages from the Brookville Gneiss and Ashburn Formation may represent uniform cooling in these two units following the earlier peak metamorphism and plutonism. However, the Talbot Road Granodiorite yielded a $^{40}\text{Ar}/^{39}\text{Ar}$ hornblende age of ca. 520 Ma interpreted by Dallmeyer and Nance (1992) to closely date the

crystallization age of this pluton. If this interpretation is correct the younger ca. 515 Ma to 519 Ma $^{40}\text{Ar}/^{39}\text{Ar}$ ages likely record cooling following emplacement of ca. 520 Ma plutons rather than a cooling from earlier thermal events. The similarity of the ages indicate that these later plutons also cooled rapidly.

The youngest plutonic event is recorded in a $^{40}\text{Ar}/^{39}\text{Ar}$ hornblende analysis from the Renforth Pluton which suggests emplacement occurred at ca. 511 Ma. $^{40}\text{Ar}/^{39}\text{Ar}$ muscovite ages of ca. 507 Ma to 509 Ma from the Ashburn Formation close to the contact suggests that this pluton cooled extremely quickly and strengthens the evidence for a younger thermal event in the Brookville terrane. A $^{40}\text{Ar}/^{39}\text{Ar}$ biotite age of ca. 509 Ma from the ca. 538 Ma Rockwood Park Granodiorite is probably a reset age following the intrusion of the Renforth Pluton. The ca. 502 $^{40}\text{Ar}/^{39}\text{Ar}$ muscovite age from the MacKay Highway shear zone can also be interpreted as a cooling age related to this younger intrusion.

The intrusion of the Renforth Pluton may record the final period of magmatic activity in the Brookville terrane.

Based on the present distribution of radiometric ages (Fig. 6.14) several discrete tectonothermal events can be distinguished in the Brookville terrane. However, additional radiometric analyses are required to rule out the possibility that nearly continuous tectonothermal activity from ca. 500 Ma to 550 Ma affected the region.

6.6. SUMMARY

1. Based on geochronology, fossil control, and cross cutting relationships, the Green Head Group is interpreted to be the oldest unit in the Brookville terrane.
2. U-Pb and $^{40}\text{Ar}/^{39}\text{Ar}$ data indicate that the Brookville Gneiss is much younger (<ca. 641 Ma) than the Green Head Group and clearly does not represent basement to the Avalon terrane or a higher grade equivalent of

the Green Head Group.

3. Amphibolite facies metamorphism in the Brookville Gneiss occurred shortly before ca. 564 Ma at temperatures in excess of 600°C and did not cool to 390°C (phlogopite closure temperature) until ca. 534 Ma.

4. Present U-Pb and $^{40}\text{Ar}/^{39}\text{Ar}$ results indicate that the plutonic units and associated contact metamorphism can be divided into distinct tectonothermal events at ca. 605 Ma, ca. 550-525 Ma, and ca. 520-500 Ma. It also indicates that many of the plutons cooled extremely quickly.

5. On the basis of field relations, metamorphic petrology, and ca. 603-617 Ma muscovite cooling ages, the Hammondvale metamorphic unit is not a metamorphosed equivalent of the Ashburn Formation but may have affinities to the Caledonia terrane.

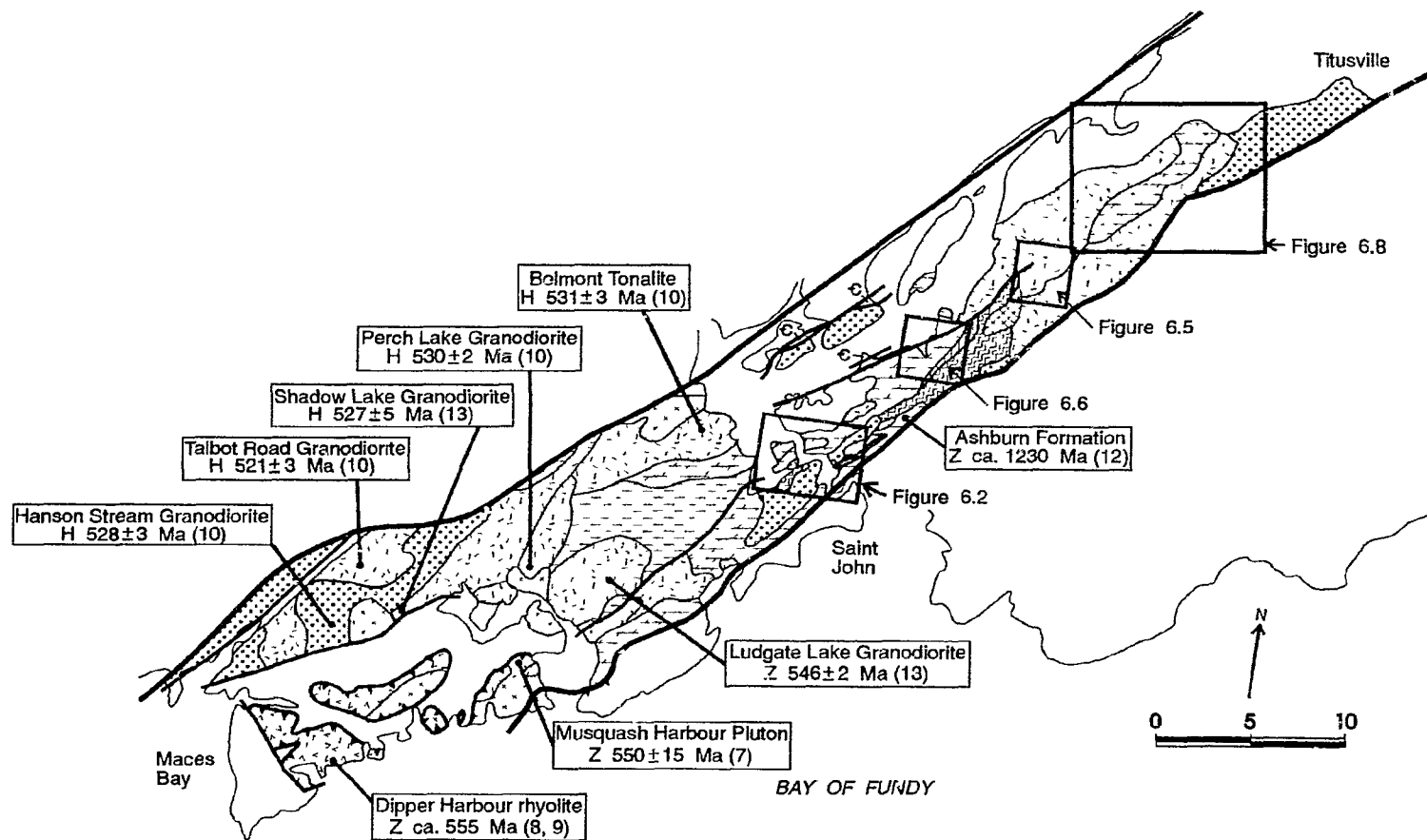


Figure 6.1. Geological map of the Brookville terrane showing locations of figures used in this chapter and geochronology samples. Legend as in Figure 2.1. Numbers in brackets after age refers to reference cited in Table 6.2. Z = zircon; T = titanite; H = hornblende; P = phlogopite; B = biotite; M = muscovite.

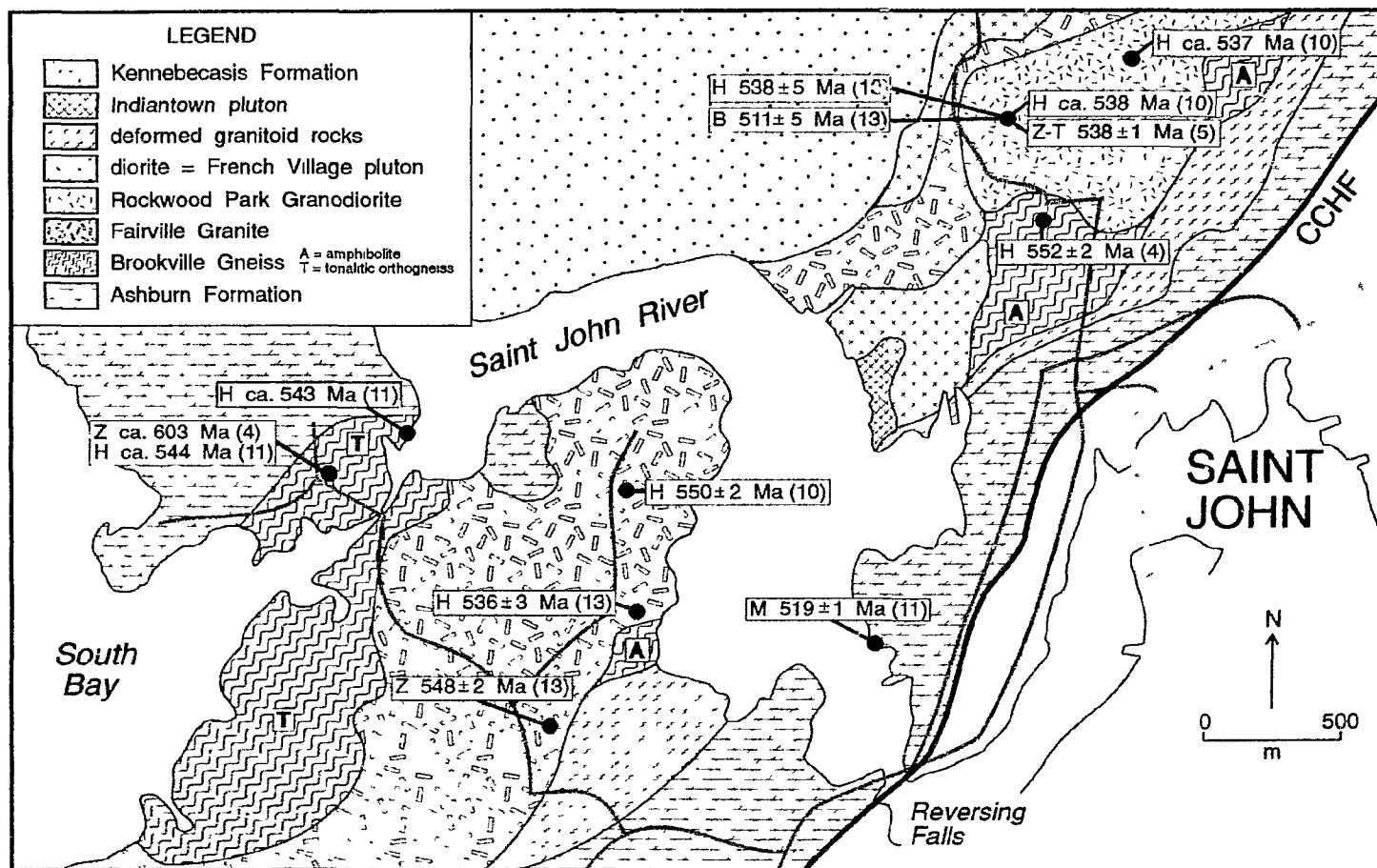


Figure 6.2. Detailed geological map of the Saint John River area showing sample locations and corresponding ages. Abbreviations as in Figure 6.1.

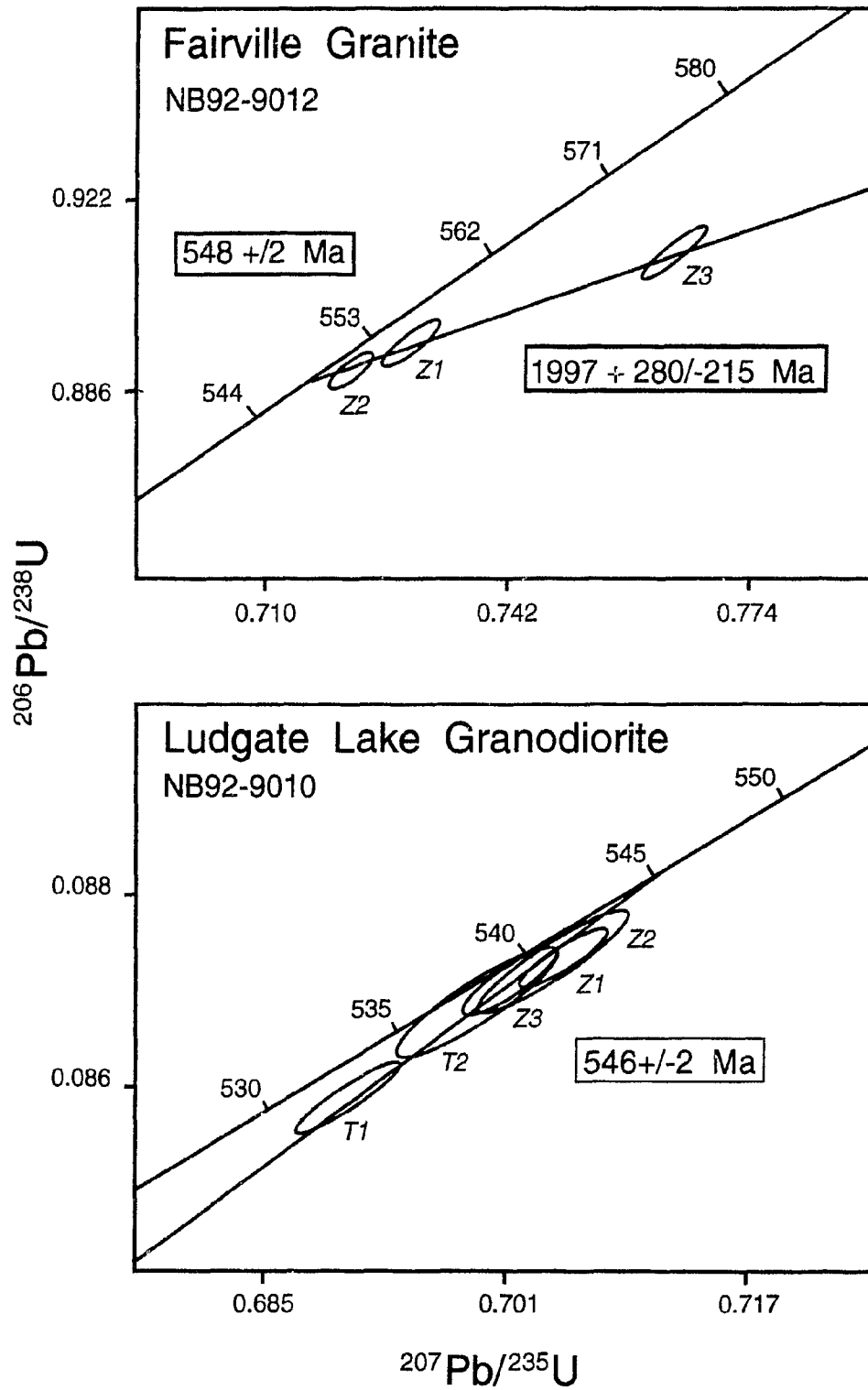


Figure 6.3. U-Pb isochron plot for Fairville Granite and Ludgate Lake Granodiorite.

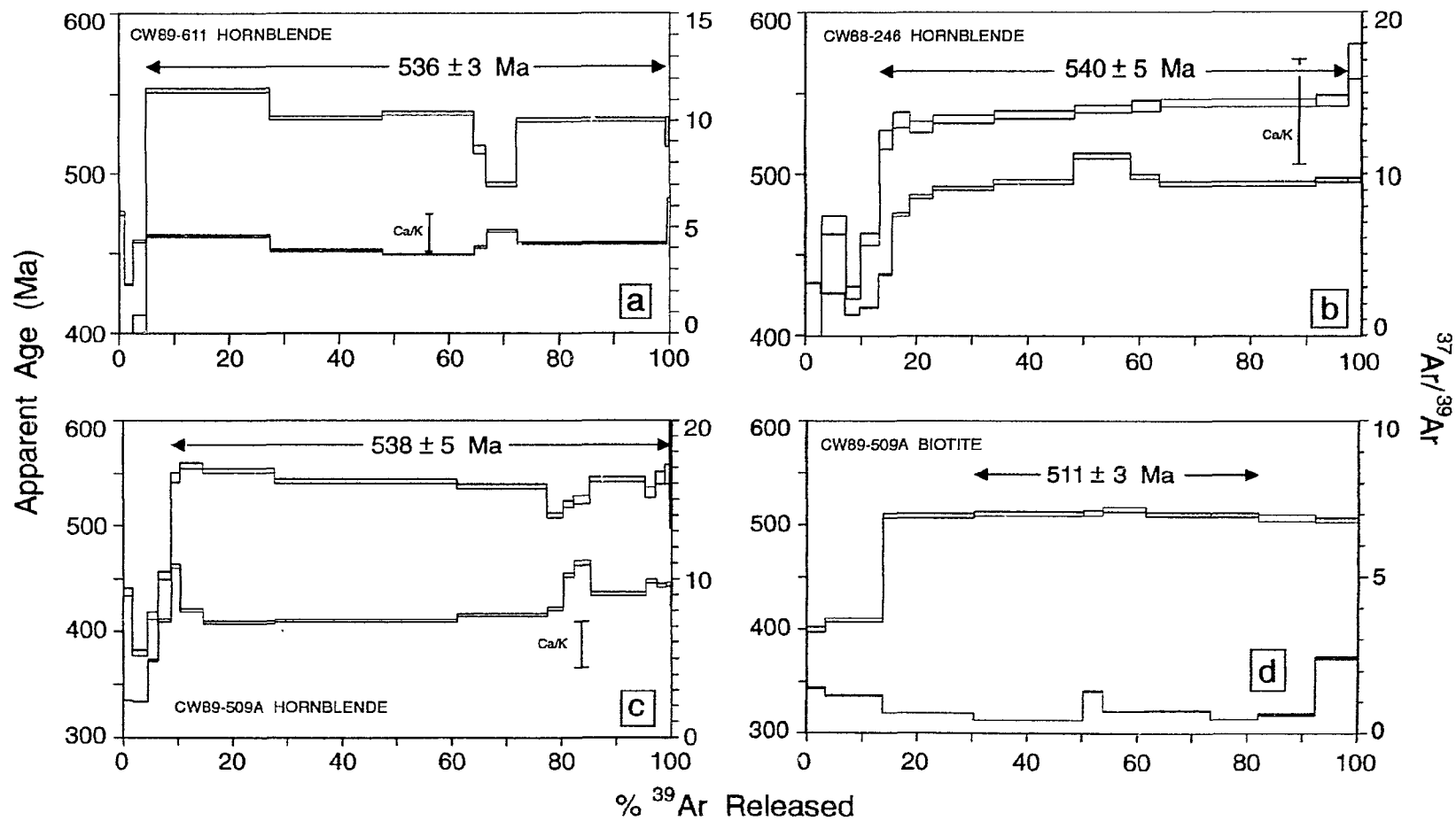


Figure 6.4. $^{40}\text{Ar}/^{39}\text{Ar}$ age spectra from: a) hornblende in the Fairville Granite; b) hornblende in the French Village Quartz Diorite; c) hornblende in the Rockwood Park Granodiorite; d) biotite in the Rockwood Park Granodiorite.

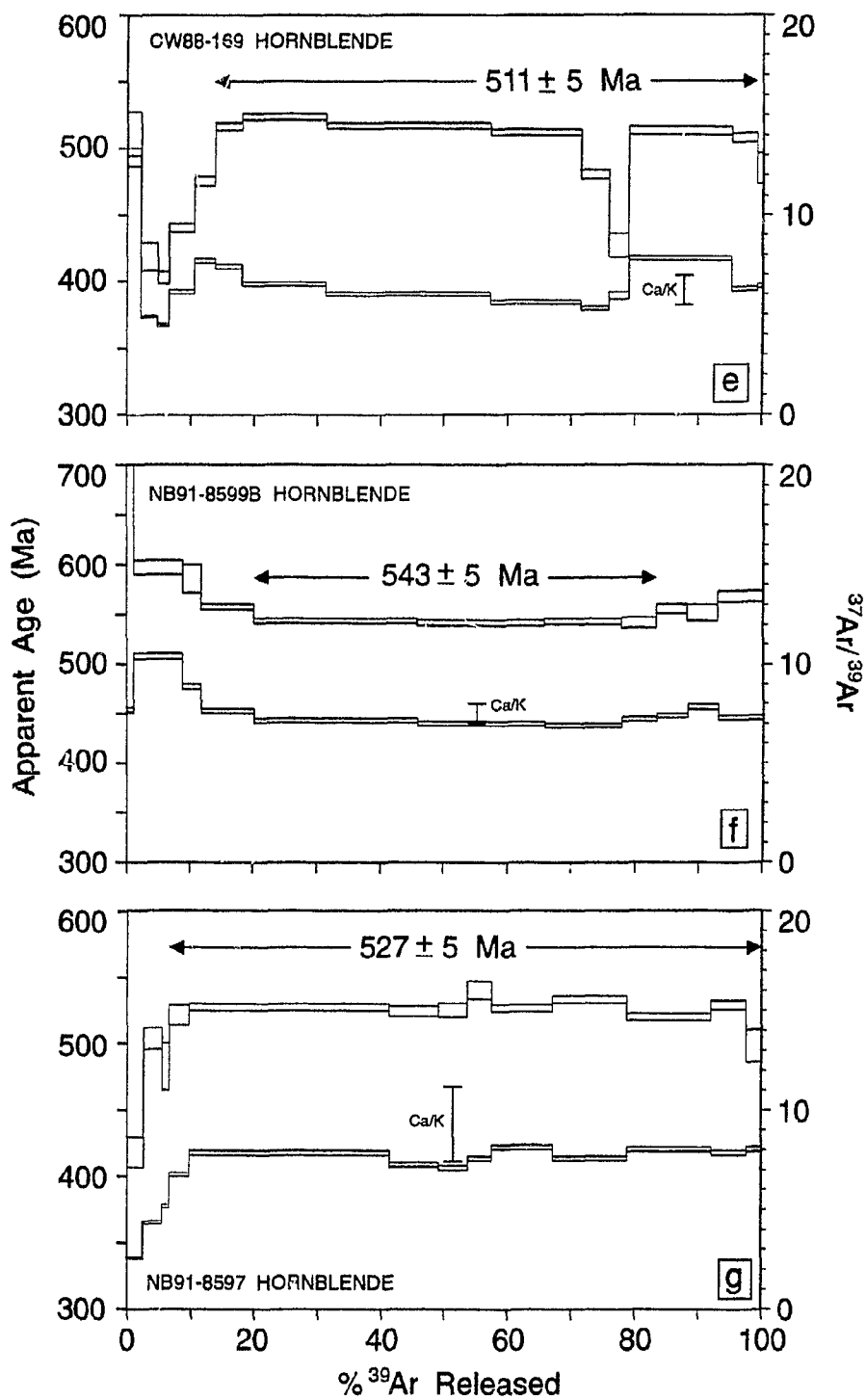


Figure 6.4. Continued. e) hornblende in the Renforth Pluton; f) hornblende in the Shadow Lake Granodiorite; g) hornblende in a tonalitic enclave in the Shadow Lake Granodiorite.

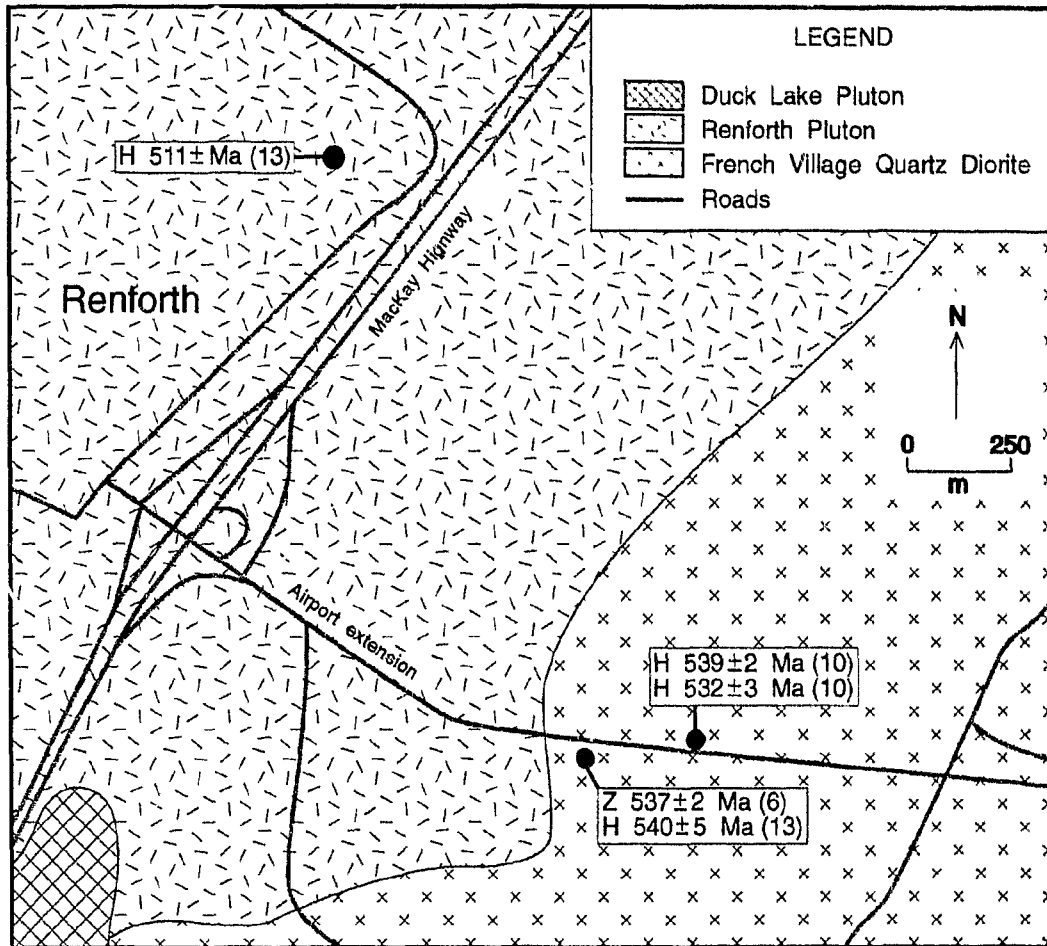


Figure 6.5. Detailed geological map of the Renforth area showing sample locations and corresponding ages. Abbreviations as in Figure 6.1.

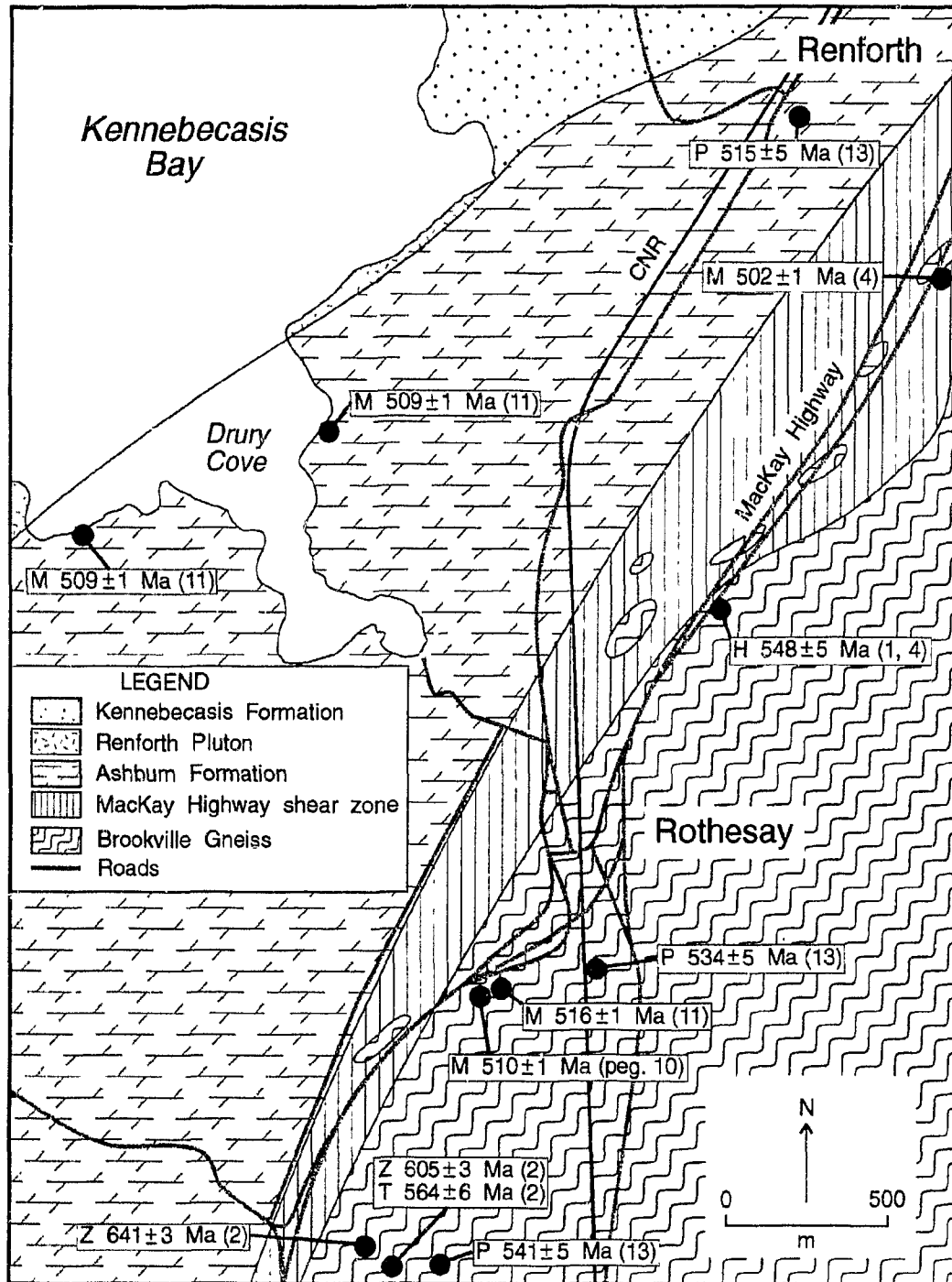


Figure 6.6. Detailed geological map of the Drury Cove area showing sample locations and corresponding ages. Abbreviations as in Figure 6.1.

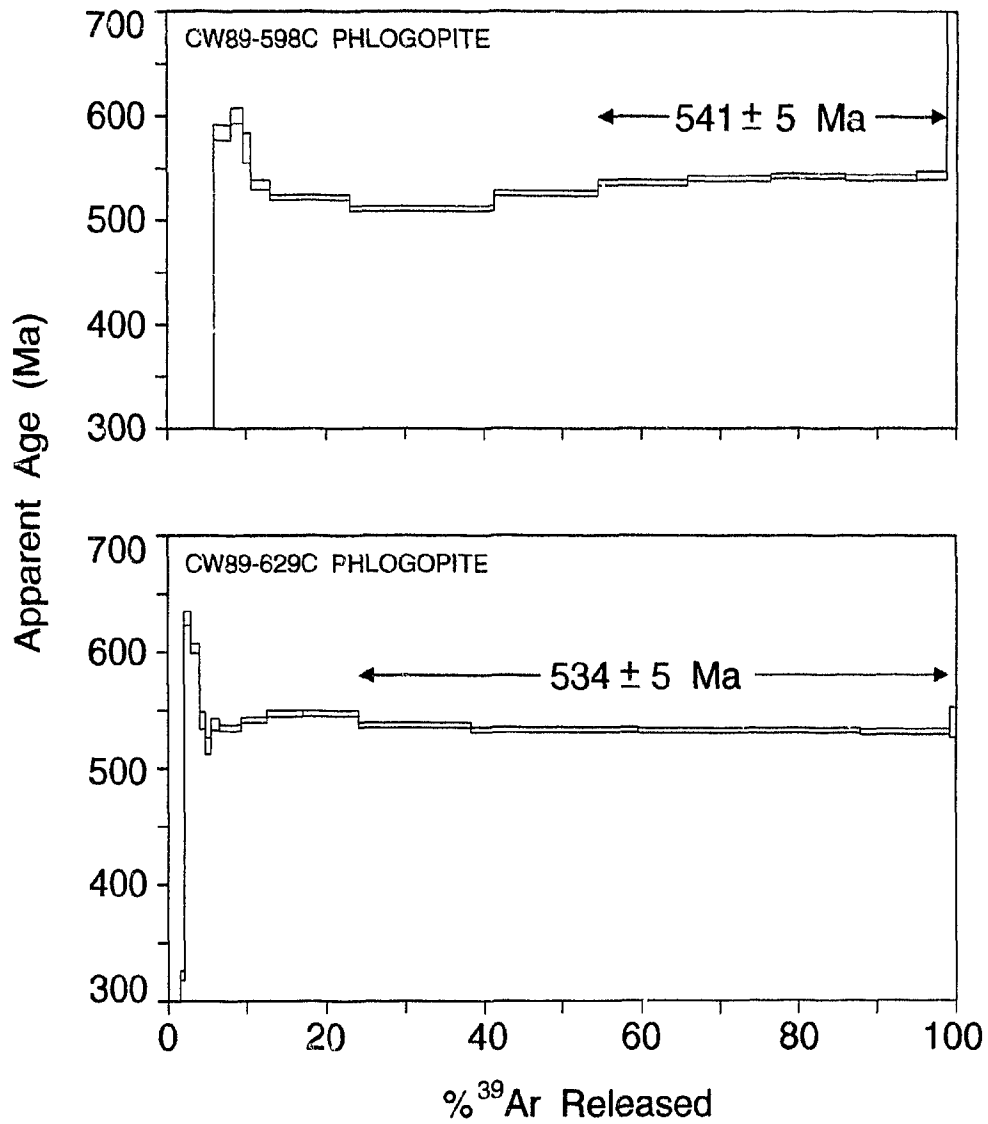


Figure 6.7. $^{40}\text{Ar}/^{39}\text{Ar}$ age spectra from phlogopite in marble samples from the Brookville Gneiss.

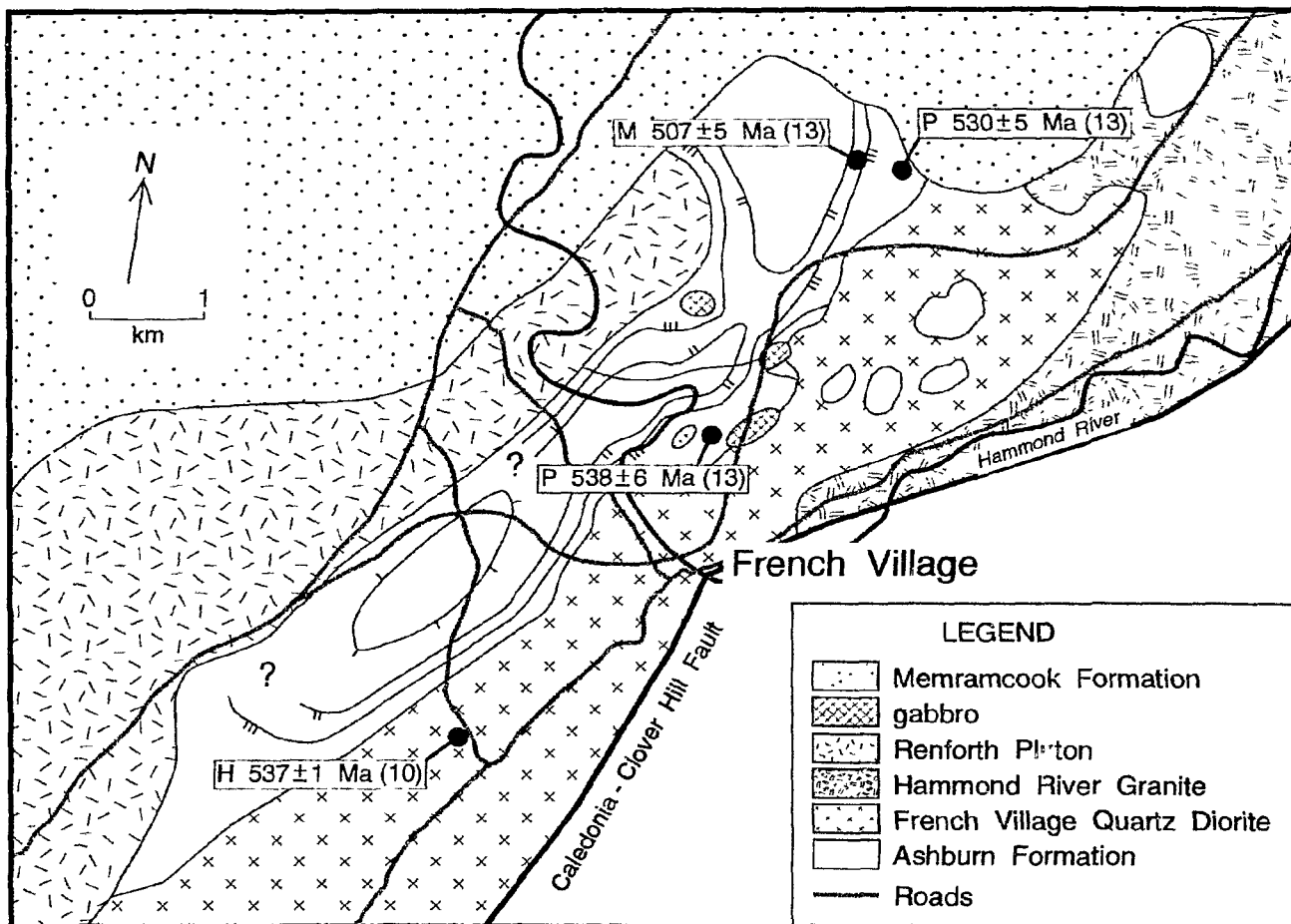


Figure 6.8. Detailed geological map of the Hammond River area showing locations, corresponding ages, and metamorphic isograds from Figure 5.3. Abbreviations as in Figure 6.1.

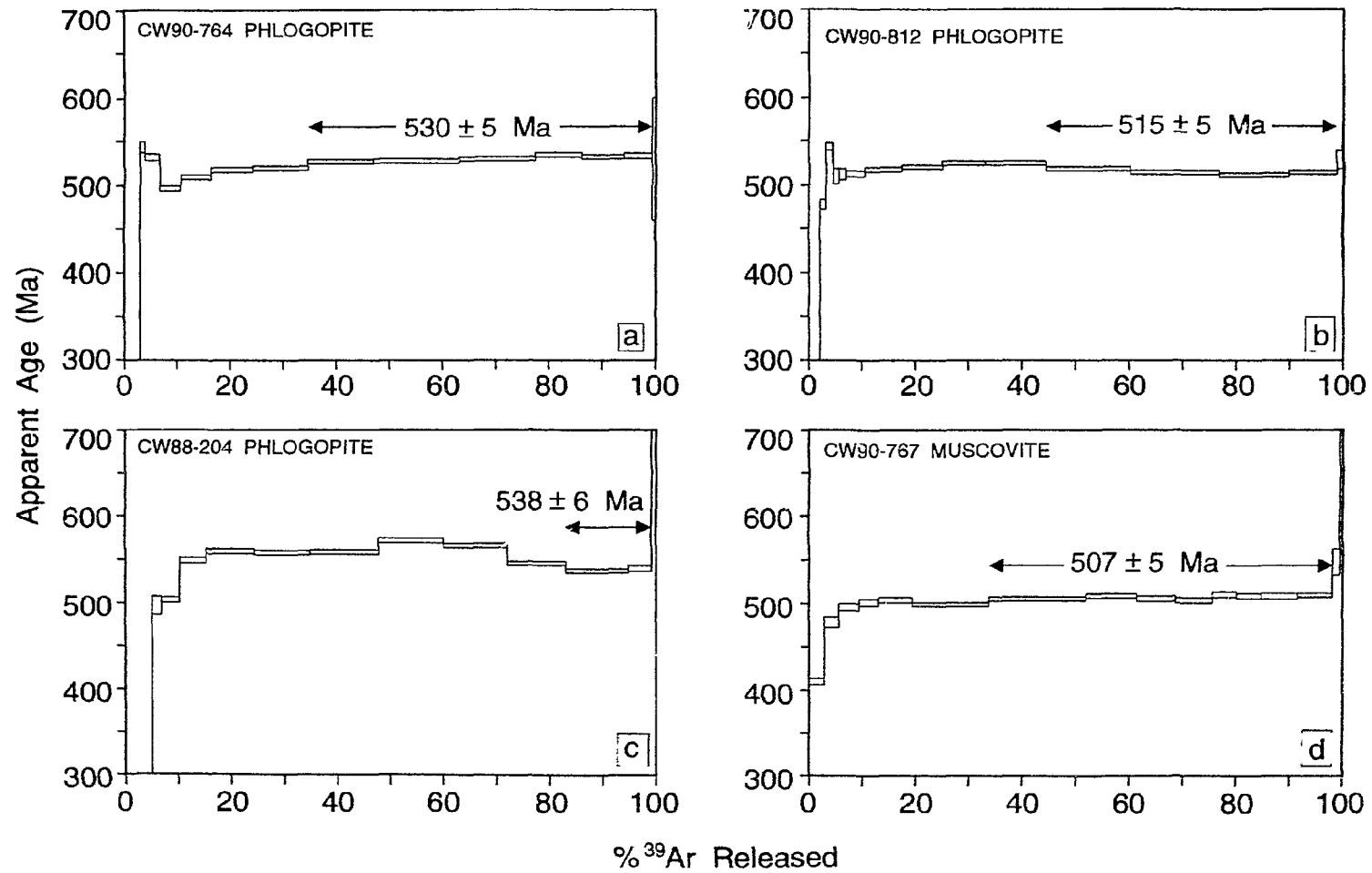


Figure 6.9. $^{40}\text{Ar}/^{39}\text{Ar}$ age spectra from samples in the Ashburn Formation: a) phlogopite in marble; b and c) phlogopite in marble; d) muscovite in pelitic schist.

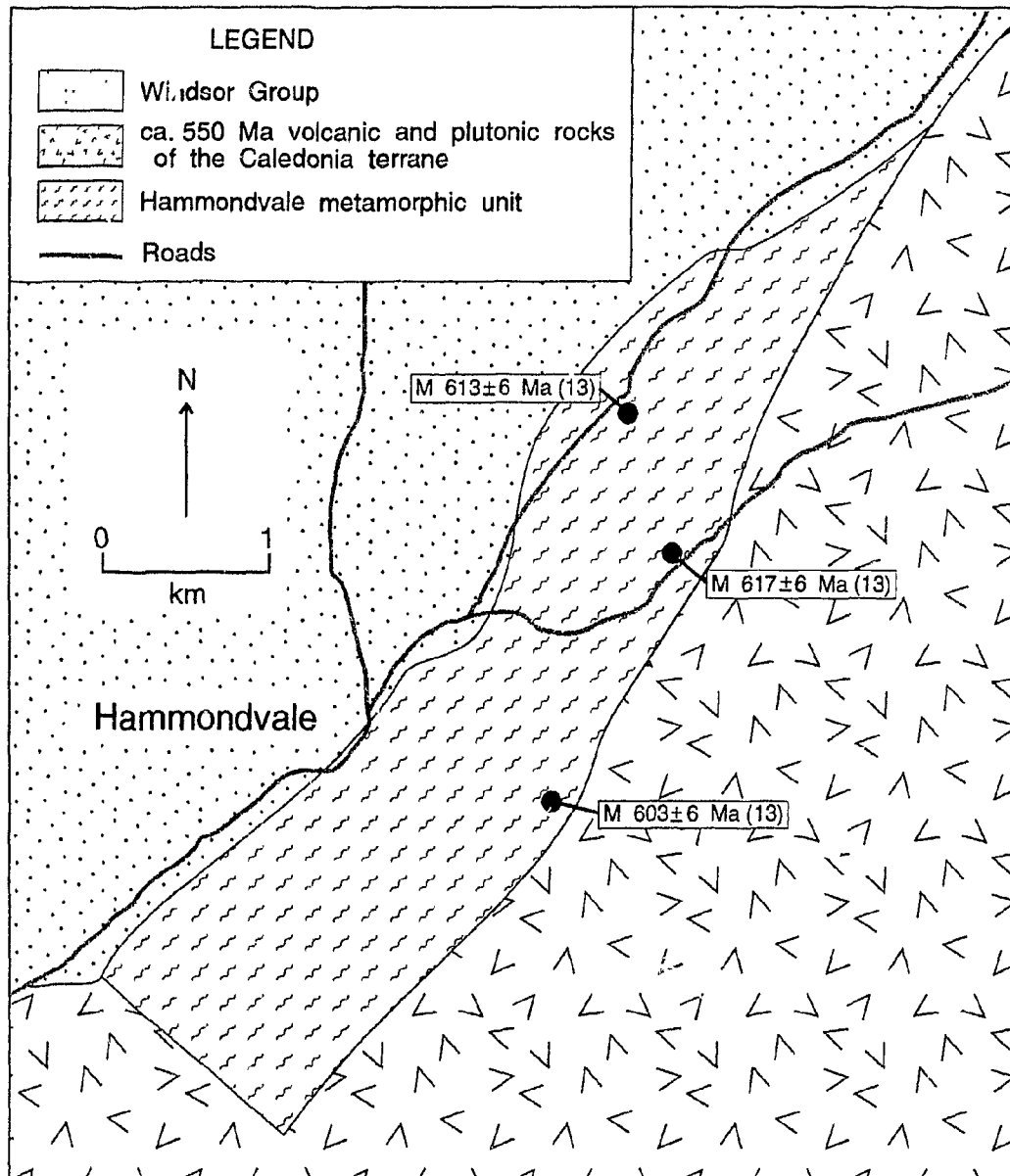


Figure 6.10. Detailed geological map of the Hammondvale area showing sample locations and corresponding ages. See Figure 1.3 for location. Abbreviations as in Figure 5.1.

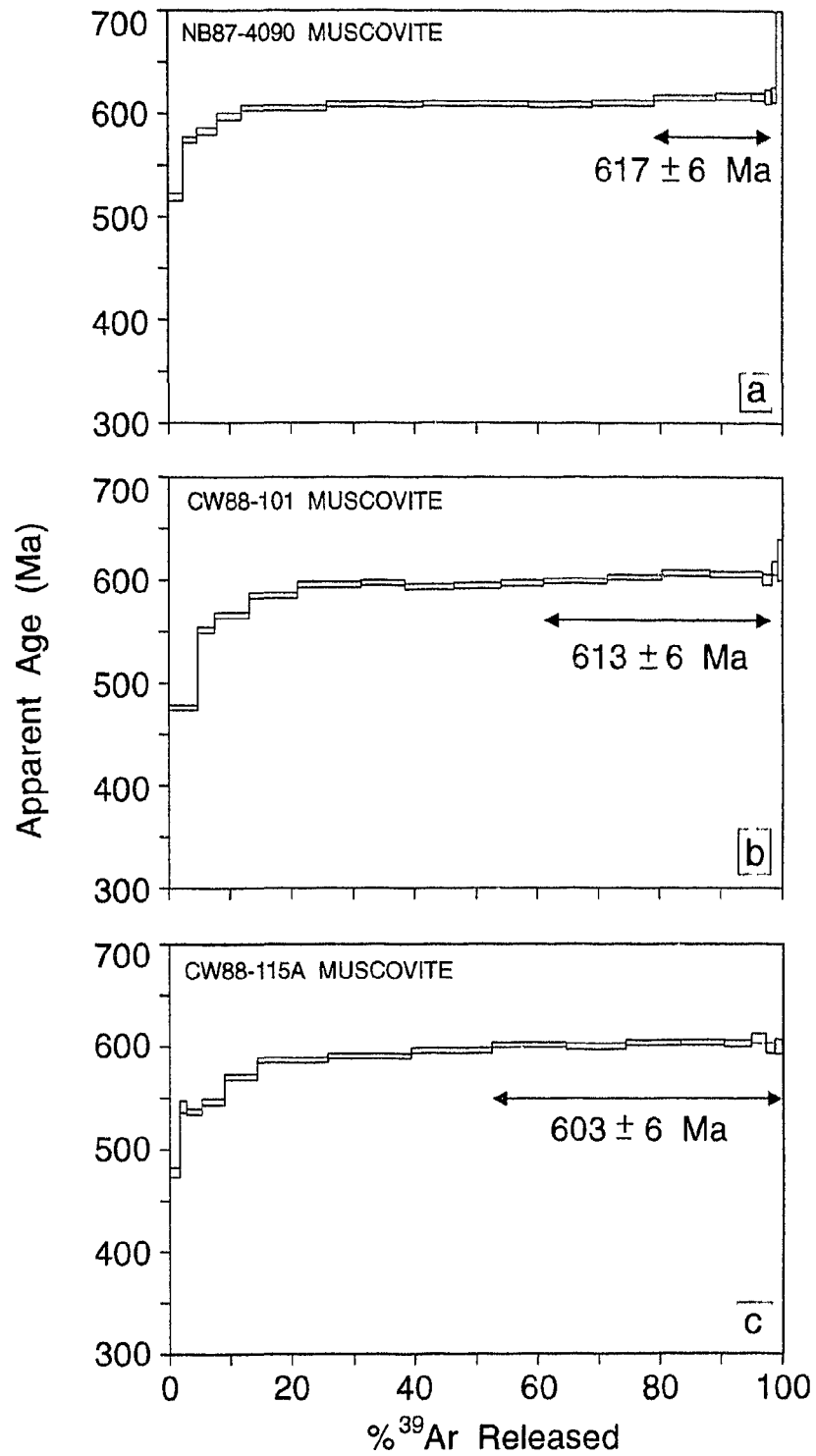


Figure 6.11. $^{40}\text{Ar}/^{39}\text{Ar}$ age spectra from muscovite samples in the Hammondvale metamorphic unit.

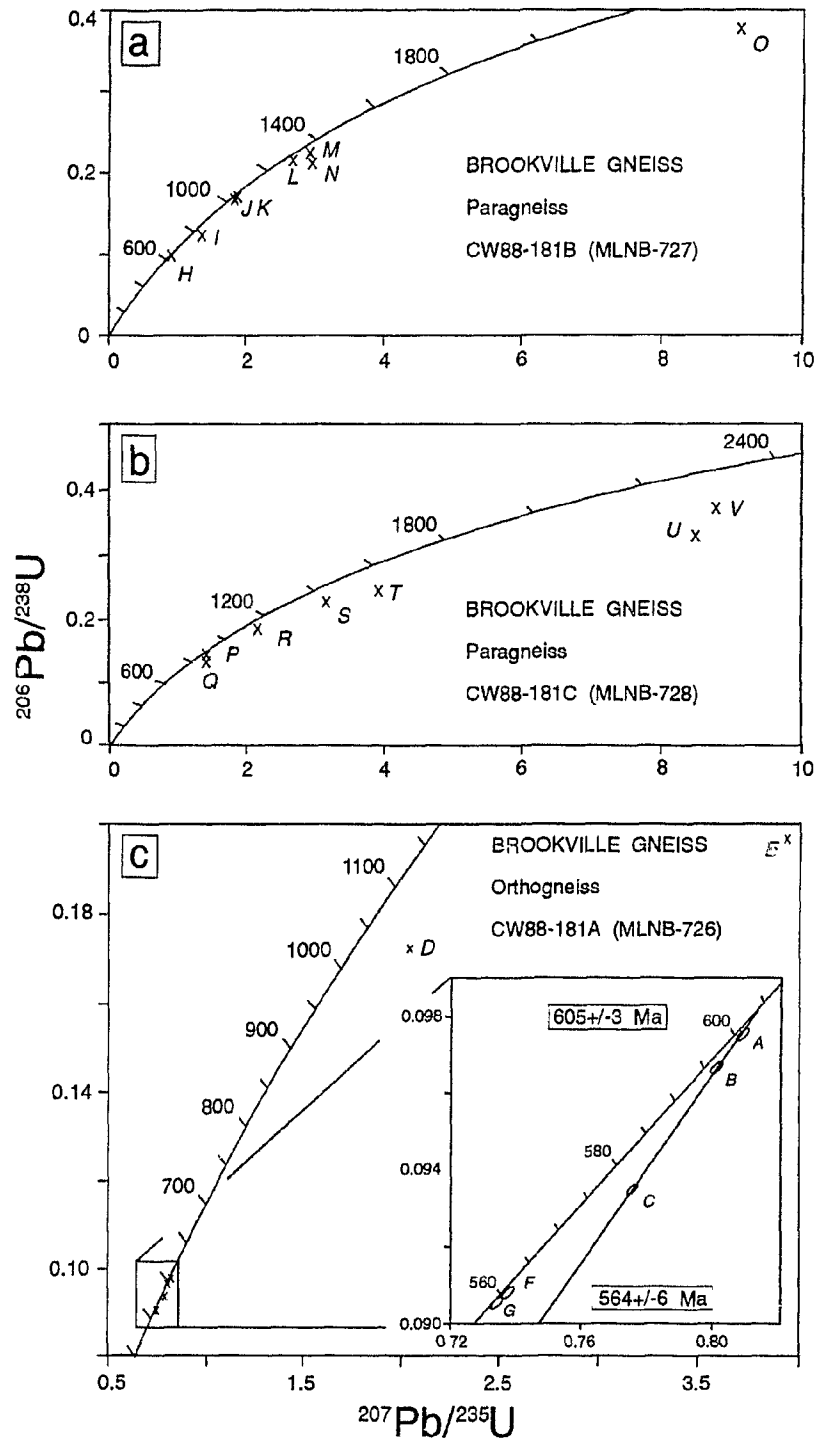


Figure 6.12. U-Pb concordia plots for samples from the Brookville Gneiss. Letters A to E and H to V refer to zircons and letters F and G to titanite. a) biotite-cordierite migmatitic paragneiss; b) cordierite paragneiss; c) orthogneiss. Inset shows igneous zircon and metamorphic titanite (after Bevier et al., 1990).

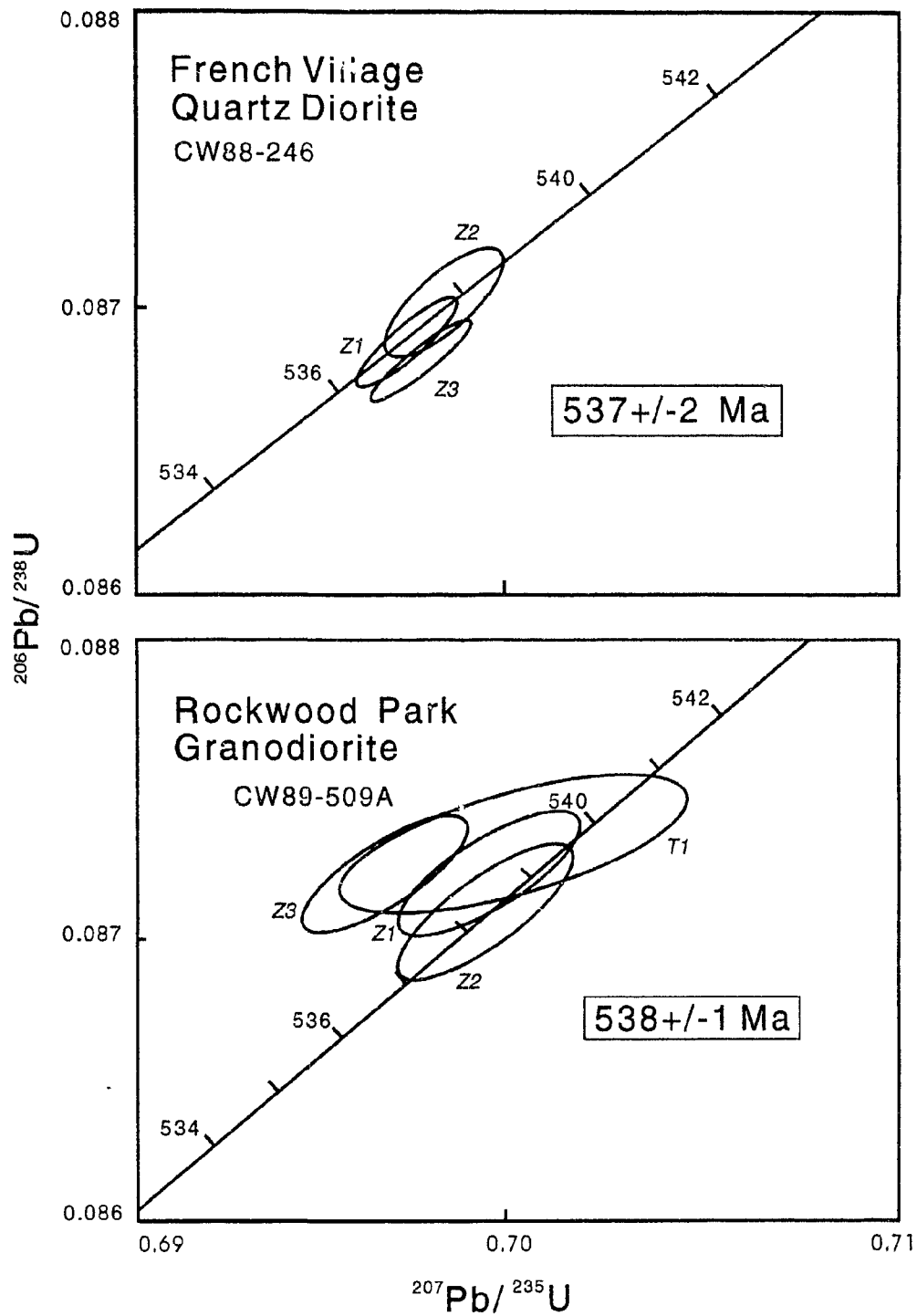


Figure 6.13. U-Pb concordia plots for a) French Village Quartz Diorite and b) Rockwood Park Granodiorite. Error ellipses are 2 sigma.

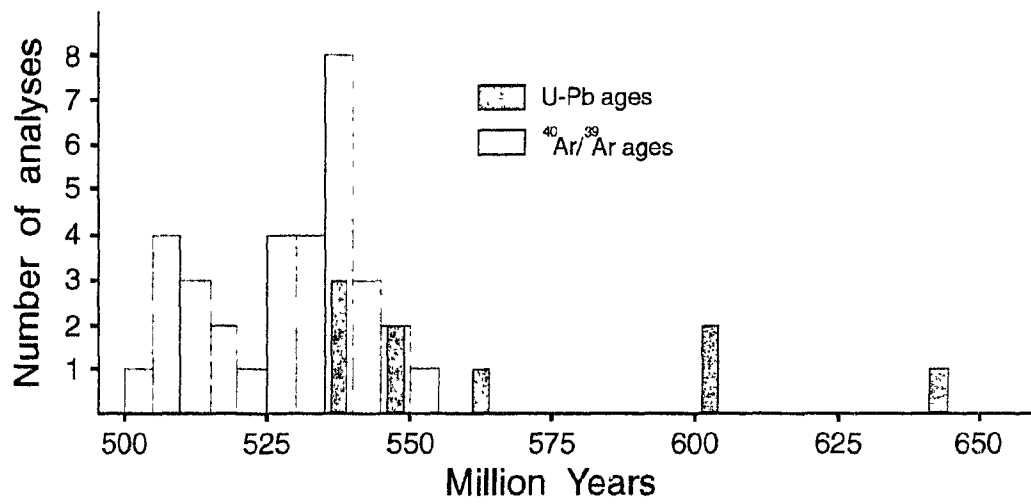


Figure 6.14. Histogram of ages against number of analyses.

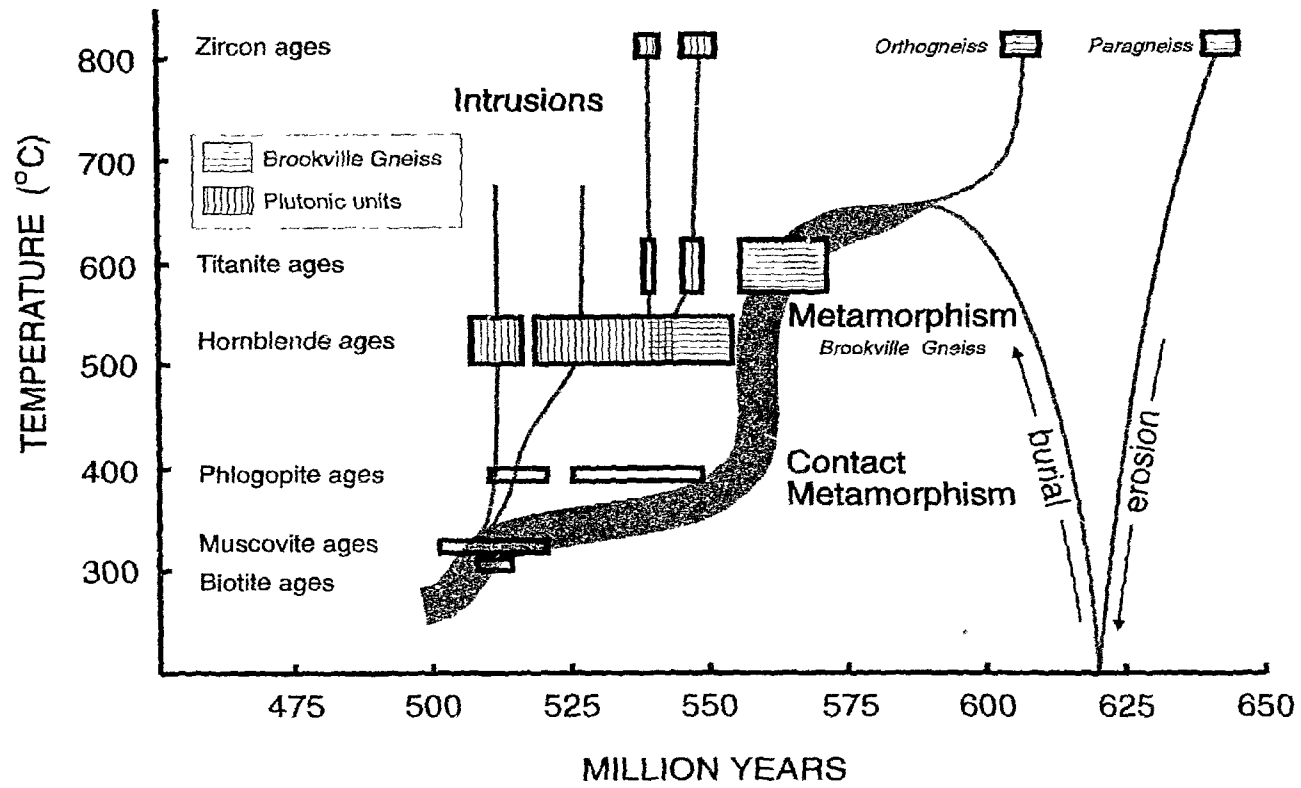


Figure 6.15. Temperature against time diagram showing proposed thermal evolution of the Brookville terrane. Ages from Table 6.2.

Table 6.1. Summary of early age determinations for units within the Brookville terrane.

ROCK UNIT	AGE (Ma) ^a	METHOD	SOURCE
ASHBURN FORMATION marble	Aphebian - Hadrynian	stromatolite morphology	8
BROOKVILLE GNEISS			
paragneiss	508 [*]	K-Ar biotite	1
orthogneiss	804 ± 97	Rb-Sr whole rock	15
paragneiss	767 ± 55	whole rock	15
both gneisses	771 ± 55	whole rock	14,15
orthogneiss	827 ± 40	U-Pb zircon (UI)	14,15
	333 ± 40	(LI)	14,15
paragneiss	1641 ± 60	U-Pb zircon (UI)	14,15
	783 ± 40	(LI)	14,15
	369 ± 45	(LI)	14,15
	814	(SG)	14,15
pegmatite	466	U-Pb zircon (UI)	14
	485 ± 30	U-Pb zircon (UI)	16
paragneiss	531 ± 17	K-Ar biotite	17
ALL PLUTONIC AND VOLCANIC UNITS	776 ± 80 ^b	Rb-Sr whole rock	3
PLUTONIC UNITS SOUTHWEST of SAINT JOHN	546 ± 75 526 ± 13 ca. 439 ca. 525 ^b	Rb-Sr whole rock Rb-Sr whole rock Rb-Sr whole rock Rb-Sr whole rock	12 12 12 12
FAIRVILLE GRANITE	479 ± 20 [*] 486 ± 20 [*] 482 ± 20 [*] 508 ± 20 [*]	K-Ar biotite K-Ar biotite K-Ar biotite K-Ar hornblende	4 5,6 6 6
FRENCH VILLAGE QUARTZ DIORITE	443 ± 6	Rb-Sr whole rock	10
ROCKWOOD PARK GRANODIORITE	395 ± 30	Rb-Sr whole rock	10
LUDGATE LAKE GRANODIORITE	473 ± 26 474 ± 27 493 ± 15 615 ± 37	K-Ar whole rock K-Ar whole rock K-Ar whole rock/biotite Rb-Sr whole rock	7 7 9,11 13
MUSQUASH HARBOUR GRANITE	392 ± 55	Rb-Sr whole rock	15
dyke of HARVEY HILL SYENOGNANITE in Shadow Lk Gd	340 ± 18	K-Ar biotite	11
MEADOW COVE VOLCANIC UNIT	443 ± 6	Rb-Sr whole rock	10
WOLVES ISLAND GRANITE	411 [*]	K-Ar biotite	1
DRILL CORE: WESTMORELAND 1	376 ± 17 [*]	K-Ar mica	2

^a Locations of samples used in age determinations are re-evaluated based on rock units in this study. In most cases, this unit name will differ from the source (see Table A2.1).

^b Recalculated age based on the omission of samples outside of present study area.

^c Recalculated with decay constants employed by Steiger and Jager (1977).

(UI) = Upper intercept age

(LI) = Lower intercept age

(SG) = Single Grain

Sources:

1. Leach et al. (1963)
2. Wanless et al. (1966)
3. Cormier (1969)
4. Wanless et al. (1970)
5. Wanless et al. (1972)
6. Wanless et al. (1973)
7. Shafiquallah in Ruitenberg et al. (1973a)
8. Hofmann (1974)
9. Shafiquallah in Giles and Ruitenberg (1977)
10. data from Cormier (1969) regroup and recalculated by Stukas (1977)
11. Shafiquallah in Ruitenberg et al. (1979)
12. Poole (1980)
13. Olszewski and Gaudette in Poole (1980)
14. Olszewski et al. (1980)
15. Olszewski and Gaudette (1982)
16. Currie in Stevens et al. (1982)
17. Stevens et al. (1982)

Table 6.2. Recent age determinations for units in the Brookville terrane.

ROCK UNIT	AGE (Ma)	METHOD	SOURCE
ASHBURN FORMATION			
mica schist	<u>519 ± 1</u>	Ar/Ar muscovite (PD)	11
mica schist	<u>509 ± 1</u>	Ar/Ar muscovite (PD)	11
mica schist	<u>509 ± 1</u>	Ar/Ar muscovite (PD)	11
marble	<u>538 ± 6</u>	Ar/Ar phlogopite (H)	13
marble	<u>530 ± 5</u>	Ar/Ar phlogopite (IH)	13
marble	<u>515 ± 5</u>	Ar/Ar phlogopite (H)	13
mica schist	<u>507 ± 5</u>	Ar/Ar muscovite (PF)	13
quartzite	<u>ca. 1230</u>	U-Pb zircon (SG)	12
MacKAY HIGHWAY SHEAR ZONE	<u>502 ± 1</u>	Ar/Ar muscovite (PD)	4
BROOKVILLE GNEISS			
paragneiss	<u>548 ± 5</u>	Ar/Ar hornblende (PD)	1
orthogneiss	<u>605 ± 3</u>	U-Pb zircon (UI)	2
	<u>564 ± 6</u>	U-Pb titanite	2
paragneiss	<u>641 ± 3</u>	U-Pb zircon (SG)	2
paragneiss	<u>542 ± 4</u>	Ar/Ar hornblende (IC)	4
	<u>548 ± 5</u>	Ar/Ar hornblende (PD)	4
amphibolite	<u>538 ± 2</u>	Ar/Ar hornblende (IC)	4
	<u>552 ± 2</u>	Ar/Ar hornblende (PD)	4
orthogneiss	<u>ca. 603</u>	U-Pb zircon	4
paragneiss	<u>516 ± 1</u>	Ar/Ar muscovite (PD)	11
orthogneiss	<u>540 ± 1</u>	Ar/Ar hornblende (IC)	11
	<u>ca. 543</u>	Ar/Ar hornblende (IH)	11
orthogneiss	<u>540 ± 1</u>	Ar/Ar hornblende (IC)	11
	<u>ca. 544</u>	Ar/Ar hornblende (IH)	11
marble	<u>541 ± 5</u>	Ar/Ar phlogopite (H)	13
marble	<u>534 ± 5</u>	Ar/Ar phlogopite (PF)	13
pegmatite	<u>510 ± 1</u>	Ar/Ar muscovite (PD)	10
FAIRVILLE GRANITE	<u>547 ± 1</u>	Ar/Ar hornblende (IC)	10
	<u>550 ± 2</u>	Ar/Ar hornblende (PD)	10
	<u>548 ± 2</u>	U-Pb zircon (LI)	13
	<u>1997+280/ -215</u>	U-Pb zircon (UI)	13
	<u>536 ± 3</u>	Ar/Ar hornblende (IH)	13
FRENCH VILLAGE QUARTZ DIORITE	<u>537 ± 2</u>	U-Pb zircon	6
	<u>537 ± 1</u>	Ar/Ar hornblende (IC)	10
	<u>537 ± 2</u>	Ar/Ar hornblende (PD)	10
	<u>539 ± 2</u>	Ar/Ar hornblende (IC)	10
	<u>561 ± 4</u>	Ar/Ar hornblende (PD)	10
	<u>530 ± 2</u>	Ar/Ar hornblende (IC)	10
	<u>532 ± 3</u>	Ar/Ar hornblende (PD)	10
	<u>540 ± 5</u>	Ar/Ar hornblende (IH)	13
ROCKWOOD PARK GRANODIORITE	<u>538 ± 1</u>	U-Pb zircon and titanite	5
	<u>523 ± 4</u>	Ar/Ar hornblende (IC)	10
	<u>551 ± 2</u>	Ar/Ar hornblende (PD)	10
	<u>ca. 538</u>	Ar/Ar hornblende (H)	10
	<u>529 ± 2</u>	Ar/Ar hornblende (IC)	10
	<u>547 ± 2</u>	Ar/Ar hornblende (PD)	10
	<u>ca. 538</u>	Ar/Ar hornblende (H)	10
	<u>538 ± 5</u>	Ar/Ar hornblende (IH)	13
	<u>511 ± 3</u>	Ar/Ar biotite (IH)	13
RENFORTH PLUTON	<u>511 ± 5</u>	Ar/Ar hornblende (IH)	13

Table 6.2. Continued.

ROCK UNIT	AGE (Ma)	METHOD	SOURCE
BELMONT TONALITE	520 ± 2	Ar/Ar hornblende (IC)	10
	<u>531 ± 3</u>	Ar/Ar hornblende (PD)	10
LUDGATE LAKE GRANODIORITE	<u>546 ± 2</u>	U-Pb zircon and titanite (UI)	13
PERCH LAKE GRANODIORITE	526 ± 2	Ar/Ar hornblende (IC)	10
	<u>530 ± 2</u>	Ar/Ar hornblende (PD)	10
SHADOW LAKE GRANODIORITE tonalitic enclave	543 ± 5	Ar/Ar hornblende (PF)	13
	544 ± 5	Ar/Ar hornblende (IC)	13
	<u>527 ± 5</u>	Ar/Ar hornblende (IH)	13
HANSON STREAM GRANODIORITE	518 ± 2	Ar/Ar hornblende (IC)	10
	<u>528 ± 3</u>	Ar/Ar hornblende (PD)	10
TALBOT ROAD GRANODIORITE	520 ± 3	Ar/Ar hornblende (PD)	1
	519 ± 2	Ar/Ar hornblende (IC)	10
	<u>521 ± 3</u>	Ar/Ar hornblende (PD)	10
MUSQUASH HARBOUR GRANITE	550 ± 15	U-Pb zircon	7
	<u>ca. 537</u>		7
DIPPER HARBOUR VOLCANIC UNIT	ca. 555	U-Pb zircon	8,9
HAMMONDVALE METAMORPHIC UNIT	<u>617 ± 6</u>	Ar/Ar muscovite (H)	13
	<u>612 ± 6</u>	Ar/Ar muscovite (PF)	13
	<u>613 ± 6</u>	Ar/Ar muscovite (H)	13
	<u>605 ± 6</u>	Ar/Ar muscovite (PF)	13
	<u>603 ± 6</u>	Ar/Ar muscovite (H)	13

Sources:

1. Dallmeyer and Nance (1989)
2. Bevier et al. (1990)
3. Dallmeyer and Nance (1990)
4. Dallmeyer et al. (1990)
5. White et al. (1990)
6. Bevier et al. (1991)
7. Currie and Hunt (1991)
8. Zain Eldeen (1991)
9. Zain Eldeen et al. (1991)
10. Dallmeyer and Nance (1992)
11. Nance and Dallmeyer (1994)
12. D. Davis (personal communication, 1995)
13. This study

Abbreviations:

Ar/Ar = $^{40}\text{Ar}/^{39}\text{Ar}$

- (IH) = Intermediate to high temperature age
(H) = High temperature age
(PF) = Plateau age as defined by Fleck et al. (1977)
(PD) = Plateau age as defined by Dallmeyer et al. (1990)
(IC) = Isotope correlation age
(UI) = Upper intercept age
(LI) = Lower intercept age
(SG) = Single grain analysis

Underlined ages are used in interpretations (see text).

Table 6.3. Closure temperatures used in this study.

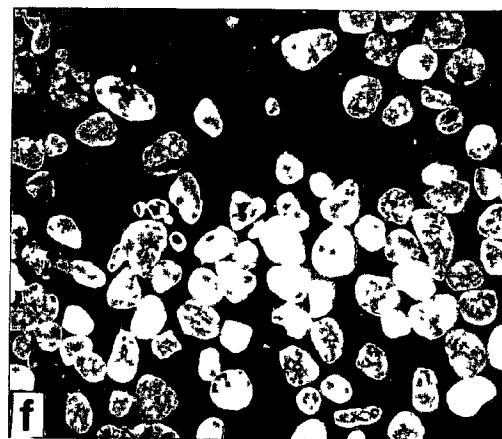
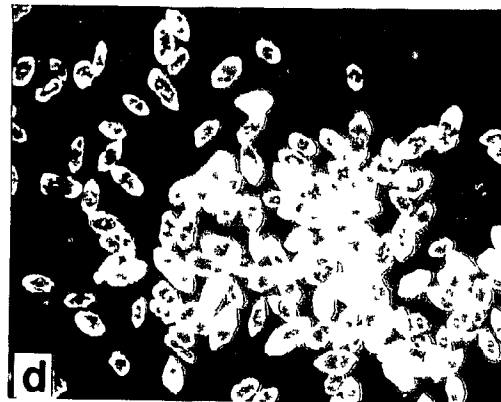
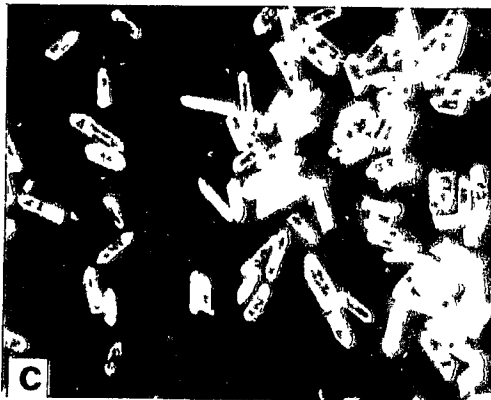
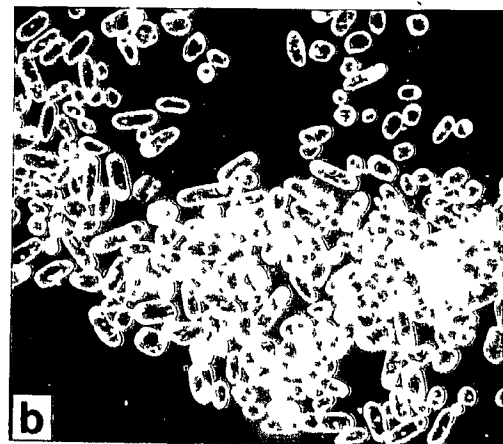
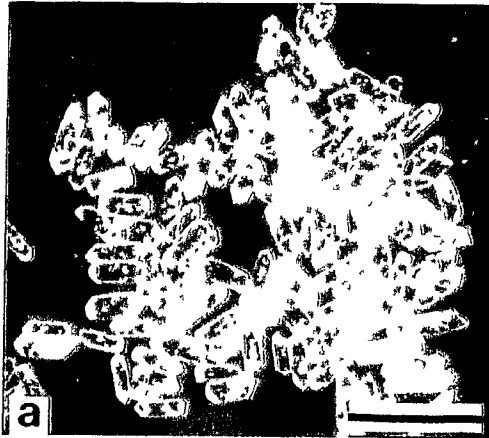
MINERAL	CLOSURE TEMPERATURE	METHOD
zircon	> 800°C	U-Pb (e.g. Heaman and Parrish, 1991)
titanite	600 ± 25°C	U-Pb (e.g. Heaman and Parrish, 1991)
hornblende	525 ± 25°C	⁴⁰ Ar/ ³⁹ Ar (e.g. McDougall and Harrison, 1988)
phlogopite	390 ± 10°C	⁴⁰ Ar/ ³⁹ Ar (e.g. Yu and Morse, 1992)
muscovite	325 ± 10°C	⁴⁰ Ar/ ³⁹ Ar (Snee et al., 1988)
biotite (annite)	310 ± 10°C	⁴⁰ Ar/ ³⁹ Ar (e.g. Yu and Morse, 1992)

PLATE 9

Photomicrographs of picked aliquots of zircon and titanite from U-Pb dated plutons in this study. Bar scale for all photomicrographs is in the lower right corner of 9a and is 0.5 mm in length.

- 9a. A typical aliquot of unabraded, acicular zircons (Z2) from the Fairville Granite (Sample NB92-9012). Most zircons contain rounded and tubular transparent inclusions.
- 9b. Same aliquot of zircon abraded about 80%.
- 9c. An aliquot of unabraded, acicular zircons (Z1) from the Ludgate Lake Granodiorite (Sample NB92-9010). Most zircons contain rounded and tubular transparent inclusions.
- 9d. An aliquot of much less abundant, unabraded, equant zircons (Z2) from the Ludgate Lake Granodiorite (Sample NB92-9010). Like Z1, most zircons contain rounded and tubular transparent inclusions.
- 9e. An aliquot of unabraded titanite (T1) from the Ludgate Lake Granodiorite (Sample NB92-9010).
- 9f. Same aliquot of titanite abraded about 80%.

PLATE 9



CHAPTER 7

DISCUSSION

7.1. COMPARISONS WITH PREVIOUS INTERPRETATIONS

Conflicting and often controversial models have been previously proposed to explain the tectonic evolution of rocks in the Saint John area of southern New Brunswick. Discrepancies can be attributed to lack of detailed field mapping, structural analysis, and reliable radiometric ages of critical units, combined with the assumption that a continuous stratigraphic relationship exists among units in the area. The purpose of this section is to summarize previous interpretations and compare them to a tectono-stratigraphic model that is more consistent with the observed field relationships and present structural, geochronological, and geochemical data.

7.1.1. GREEN HEAD GROUP

One of the most important results of this study is the recognition of the widespread, highly mobile (mylonitic) nature of carbonate rocks in the Ashburn Formation of the Green Head Group. In contrast, previous workers interpreted many of the features in these rocks in terms of processes related to primary deposition (e.g. Leavitt, 1963; Wardle, 1978; O'Brien et al., 1983). The inferred "sedimentary" origin of these features led to the subdivision of the Ashburn Formation into lithostratigraphic units (e.g. Hamilton, 1968) and finally replacement of the Ashburn Formation by three formations: 1) a lower clastic sequence (Lily Lake Formation); 2) a middle limestone and dolomite sequence (Drury Cove Formation); 3) an upper interbedded clastic and carbonate sequence (Narrows Formation) (Wardle, 1978). However, this study has demonstrated that the ductility of the marble and associated

structural complexity precludes the establishment of these formations, although some of the siliciclastic divisions established by Leavitt (1963) and Wardle (1978) locally exist as mappable units. Hence, the original subdivision of the Green Head Group into the Martinon and Ashburn formations (Leavitt, 1963) is retained.

Previous workers (e.g. Leavitt 1963; Wardle, 1978; Currie, 1991) restricted the Martinon Formation to the west side of the Saint John River, and included siliciclastic rocks east of the river in the Ashburn Formation. However, the siliciclastic rocks east of the river are identical to lithologies in the Martinon Formation, and hence the Martinon Formation is here extended east of the river to include large areas of these rocks (Map A). Smaller siliciclastic units in the Ashburn Formation are typically lens-shaped on a scale of a few metres to about 1 kilometre and are interpreted to represent megaboudins, although locally they are not deformed and are clearly interlayered with marble along their margins.

New road cuts along New Brunswick Highway 7 have better exposed the northern and southern contacts between the Ashburn and Martinon formations. The contacts are mainly tectonic with zones of tightly folded marble and large boudins of siliciclastic and mafic dyke material in the Ashburn Formation. However, the original relationship between the two formations is preserved locally along the northeasternmost contact, where lithologies similar to the Martinon Formation are interlayered with the Ashburn Formation. Sedimentary siliciclastic and carbonate conglomerate and breccia occur throughout the Martinon Formation but are best exposed at the northern contact with the Ashburn Formation along Highway 7, where they are associated with complexly folded siltstone and large blocks of marble. These chaotic deposits are olistostromes and associated turbidite deposits within the Martinon Formation, previously recognized as submarine slide breccias by Wardle (1978). These relationships suggest that the Ashburn and Martinon formations may have originally been interlayered, and could represent

lateral facies equivalents (Fig. 7.1a).

In contrast, Leavitt (1963) and Hamilton (1965, 1968) interpreted the olistostrome to be a basal conglomerate in the Martinon Formation, which they considered to overlie the Ashburn Formation. However, the Martinon Formation was not considered to be significantly younger than the Ashburn Formation (e.g. Leavitt, 1963). Wardle (1978) and O'Brien et al. (1983) interpreted the contact to be gradational, with the upward transition from carbonate-rich to siliciclastic-rich representing a transgressive sequence.

Currie (1984, 1986a, 1987a, 1991) agreed with the interpretation of Leavitt (1963) and Hamilton (1965, 1968) that a carbonate conglomerate forms the base of the Martinon Formation. He suggested that the Ashburn Formation is considerably older than the Martinon Formation based on what he interpreted as: 1) deformed Ashburn Formation clasts in the conglomerate and 2) volcanic flows in the Martinon Formation that were lacking in the Ashburn Formation. Based on this interpretation, Currie (1984) and subsequent workers (e.g. Nance and Dallmeyer, 1994) excluded the Martinon Formation from the Green Head Group (Fig. 7.1b) and concluded that this formation was deposited in an active volcanic arc setting like some units in the Coldbrook Group (e.g. Currie, 1991). However, this study failed to identify any volcanic flows in the Martinon Formation.

The presence of abundant carbonate rocks and local stromatolite fossils indicates that the Ashburn Formation was deposited in shallow water. The presence of olistostrome and turbidite deposits in the Martinon Formation suggests deposition in deeper water, probably penecontemporaneously with the Ashburn Formation. The lack of associated volcanic units or detritus indicates that both formations were deposited at a passive stable continental margin.

Although the absolute age of the Green Head Group is not well constrained, it is interpreted to be the oldest unit in the Brookville terrane (Fig. 7a). Hofmann (1974) originally assigned a Neohelikian

(Mesoproterozoic) age based on stromatolite fossils in the Ashburn Formation; however, later he suggested they could be as young as 750-880 Ma (written communication, 1991). The youngest detrital zircon extracted from a quartzite in the Ashburn Formation yielded a concordant age of 1230 Ma (D. Davis personal communication, 1995) which provides a maximum age for the deposition of the Green Head Group.

Pre-Late Neoproterozoic deformation produced a series of large-scale, upright, gently plunging, open to close folds in the Martinon Formation. In contrast, smaller scale, upright to steeply inclined, gently to steeply plunging, close to isoclinal folds were developed in the Ashburn Formation. Thus, the structural styles differ in the two formations, which precludes a direct correlation of specific structures and tectonic events. Parts of the Ashburn Formation, closest to the Brookville Gneiss, were later deformed by Late Neoproterozoic ductile juxtaposition of these two units along the MacKay Highway shear zone. Structures in Green Head Group are cross-cut by ca. 548-537 Ma plutonic rocks which constrains the minimum age for their deformation.

Previous structural interpretations of the Green Head Group (Leavitt, 1963; Wardle, 1978; Nance, 1982; Currie, 1984) suggested that the distribution of the Martinon and most of the Ashburn formation was controlled by a major syncline (Acamac Syncline of Wardle, 1978). The Martinon Formation was interpreted to form the core of a U-shaped, southwest-plunging syncline flanked by older carbonate rocks (e.g. Leavitt, 1963). Although Wardle (1978) noted the presence of folds in the Martinon Formation, based on facing directions, he considered the Acamac Syncline to be a multiply hinged fold with a U-shaped profile. Based on detailed structural examination, the Martinon and Ashburn formations are folded into a series of folds that do not define a simple syncline (e.g. Fig. 3.2).

The main period of deformation was considered to be post-intrusion and Late Palaeozoic, not Neoproterozoic. This was largely based on comparisons with structures in the Cambrian to Ordovician Saint John

Group, which were interpreted to overlie the Green Head Group (Richards, 1971; Leavitt, 1963; Wardle, 1978), an interpretation no longer considered valid (see section 7.2). However, Wardle (1978) and Nance (1982) suggested that some deformation in the carbonate rocks may be as old as Neohelikian (Mesoproterozoic).

Metamorphism in the Green Head Group is largely the result of contact metamorphism by the ca. 548-537 Ma plutonic units; in contrast to the suggestion by Currie (1984) that basaltic sills were responsible for much of the metamorphism. This widespread contact metamorphism ranges from albite-epidote to hornblende-hornfels facies, with local areas of pyroxene-hornfels facies. Contrary to the interpretations of Leavitt (1963), Wardle (1978), Nance (1982), and Nance and Dallmeyer (1994), evidence of an older, regionally extensive greenschist-facies metamorphism is lacking. The Martinon Formation and most of the Ashburn Formation are hornfelsic and unfoliated. The only areas that preserve evidence of greenschist facies metamorphism are apparently deeper parts of the terrane near the MacKay Highway shear zone (Drury Cove area) and the Hammond River area; however, the mica schists in these areas are also overprinted by younger contact metamorphism and yield $^{40}\text{Ar}/^{39}\text{Ar}$ muscovite ages of ca. 510 Ma.

Although the principal exposure of the Green Head Group is in the Saint John area, Wardle (1978) extended the group to include a small fault-bounded sliver of marble and mica schist in the Hammondvale area 70 km to the northeast. This sliver was considered to be a higher metamorphic grade equivalent of the Ashburn Formation (McCutcheon, 1978; Ruitenberg et al., 1979; McLeod et al., 1994), and was named the Hammondvale metamorphic unit by Barr and White (1991a). This study has shown that the lithological assemblage in the Hammondvale metamorphic unit is distinct from that in the Ashburn Formation, and that the unit experienced high-pressure/low-temperature metamorphism at ca. 600 Ma ($^{40}\text{Ar}/^{39}\text{Ar}$ muscovite ages) that is not present in the Green Head Group. These differences, combined with the presence of syenogranite dykes

related to the Bonnell Brook Pluton, suggest that this unit is part of the Caledonia terrane (see section 7.2).

7.1.2. BROOKVILLE GNEISS

The Brookville Gneiss is a locally migmatitic, cordierite-sillimanite-biotite-K-feldspar-bearing paragneiss with granodioritic to tonalitic orthogneiss and amphibolite. To categorize all these lithologies as tonalitic (cf. Currie et al., 1981 to Currie, 1991) is an over-simplification. The Brookville paragneiss contains detrital zircons ranging in age from Neoproterozoic to Mesoproterozoic. The youngest zircon (ca. 641 Ma) is interpreted to constrain the maximum age for the sedimentary protolith (Bevier et al., 1990). Zircon from the orthogneiss indicates an igneous crystallization age of ca. 605 Ma (Bevier et al., 1990; Dallmeyer et al., 1990). The orthogneiss and associated amphibolite are interpreted to represent pre-metamorphic intrusions in the protolith of the paragneiss. Amphibolite-facies metamorphism in the gneiss was of a low-pressure/high-temperature type with an anomalously steep geothermal gradient on the order of 75°C/km. Metamorphism and deformation were initiated in the Late Neoproterozoic (ca. 564 Ma) and continued up to juxtaposition with the Ashburn Formation along the MacKay Highway shear zone at ca. 548 Ma. Although the MacKay Highway shear zone has locally conflicting shear-sense indicators, the gneiss is strongly deformed with locally well developed mineral lineations and asymmetric porphyroclasts, suggesting an overall dextral transpressional sense of movement for this zone. This event may have been broadly synchronous with regional greenschist-facies metamorphism in the immediately adjacent Ashburn Formation (Fig. 7.1a).

The relationship between the Brookville Gneiss and the Green Head Group prior to ca. 548 Ma is still unknown; however, many interpretations have been proposed. Cumming (1916), Hayes and Howell (1937), Belyea (1939, 1944, 1945), and Ruitenberg et al. (1975, 1979)

considered the Brookville gneiss to be entirely igneous in origin and intrusive into the Green Head Group. Alcock (1938) and Leavitt (1963) recognized both orthogneissic and paragneissic components; they considered the orthogneiss to be intrusive into the Green Head Group and the paragneiss to be metamorphosed Green Head Group. Leavitt (1963) also suggested that some of the paragneiss may represent basement on which the Green Head Group accumulated. O'Brien (1976), Rast et al. (1976a, b), and Wardle (1978) also recognized orthogneiss and paragneiss; however, Wardle (1978) further suggested that the orthogneiss originated as a metamorphic segregation from a "mobilized basement" that intruded syn-metamorphically into paragneiss of the Green Head Group during the Grenville Orogeny. He also suggested that this event amphibolitized the margins of the Indiantown Gabbro. The tectonic character of the MacKay Highway shear zone was noted by Wardle (1978) but he interpreted it as a "gneiss front", where gneisses exhibit a rather abrupt change to weakly metamorphosed biotite schist over a very short distance.

The paragneiss and orthogneiss were both interpreted to represent a remobilized Aphebian to Grenvillian "tonalitic" basement unconformably overlain by the Green Head Group (Currie et al., 1981; Currie, 1983, 1984, 1986a, 1987a, b, c, 1988a, b; Olszewski and Gaudette, 1982; Nance, 1986, 1987a, 1988, 1990; Nance et al., 1990, 1991). These authors suggested that "remobilization" occurred several times corresponding to intrusion of plutonic units. This resulted in "mutually intrusive contacts" between the Green Head Group and Brookville Gneiss (Fig. 7.1).

Superficially, the Brookville Gneiss and Green Head Group appear to have a basement-cover relationship (e.g. Wardle, 1978). The Brookville Gneiss was considered to have an older, more complex structural history than the Green Head Group and the metamorphic grade contrasts sharply between the two units. However, the "complex" structural history in the Brookville Gneiss is interpreted here to be the result of several phases of a single progressive period of ca. 564-

540 Ma deformation with associated amphibolite facies metamorphism, related to the juxtaposition of the Brookville Gneiss with the Green Head Group along the MacKay Highway shear zone. In addition, if the Neohelikian (Mesoproterozoic) stromatolite age of Hofmann (1974) is correct, then the Green Head Group is older than the Brookville Gneiss, which precludes a basement-cover relationship (Fig. 7.1a).

The presence of marble and feldspar-rich quartzite is consistent with a sedimentary protolith for the paragneiss in the Brookville Gneiss. Although the gneiss contains abundant pelite and minor marble suggesting a depositional environment similar to that of the Martinon Formation, the age difference demonstrated during the present study is inconsistent with the interpretation that the paragneiss is a high-grade metamorphic equivalent of parts of the Green Head Group.

The tectonic setting for low-pressure/high-temperature metamorphism of the Brookville Gneiss is unclear but is attributed to regional high heat flow that may be the result of mafic intrusions at shallow depths (e.g. Wickham and Oxburgh, 1987; Lux et al. 1986; Rothstein and Hoisch, 1994) or extreme crustal attenuation (e.g. Golderg and Leyreloup, 1990). The spatially limited outcrop exposure of the Brookville Gneiss and the lack of igneous material similar in age to the amphibolite-facies metamorphism preclude identification of any one of these above processes. However, the narrow time span between inferred peak amphibolite-facies metamorphism (ca. 564 Ma) and cooling (<ca. 548 Ma) is consistent with an intrusive model.

7.1.3. PLUTONIC AND VOLCANIC UNITS

The main magmatic event in the Brookville terrane occurred in the Late Neoproterozoic to Cambrian. It involved emplacement of numerous calc-alkaline plutons and associated pegmatite/aplite dykes. Systematic examination of the plutons on the basis of mineralogical and chemical variations, unique textural and mineralogical features, and age led to

the recognition of 29 distinct plutonic units (Map A). These are broadly grouped into four main packages: 1) medium-grained diorite to granodiorite; 2) coarse-grained monzogranite to granodiorite; 3) medium-grained syenogranite to monzogranite; 4) coarse-grained gabbro and ultramafic rocks. The expanded I-type character of these plutonic units is consistent with generation at a continental margin subduction zone.

The Dipper Harbour volcanic unit is interpreted to be an eruptive equivalent of syenogranitic plutons in the terrane, and together they are interpreted to represent a chemically evolved part of this Late Neoproterozoic to Early Cambrian volcanic arc. Evidence from $^{40}\text{Ar}/^{39}\text{Ar}$ data and the restriction of volcanic and syenogranitic rocks to the southwestern part of the Brookville terrane suggests that this area represents a higher level of exposure compared to the rest of the terrane. However, radiometric data from across the terrane suggest that many of the plutons were emplaced at relatively high crustal levels and cooled rapidly.

It is not clear if magmatic activity was continuous between ca. 550–500 Ma or if two discrete episodes occurred at ca. 550–525 Ma and ca. 520–500 Ma (Fig. 7.1a). Even though the plutons cooled rapidly, they were responsible for widespread contact metamorphism in the Green Head Group.

Traditionally, all of the plutonic units in southern New Brunswick, together with the Brookville Gneiss, were included in a single assemblage, termed the Golden Grove Intrusives or Golden Grove Intrusive Complex (e.g. Hayes and Howell, 1937). The age(s) of these plutons were variably considered to be Late Proterozoic, Ordovician, or Carboniferous, based largely on what is now considered unreliable radiometric data (e.g. Ruitenberg et al., 1979; Olszewski and Gaudette, 1982), and their tectonic significance was not known. Sufficient detailed mapping, and related geochronological, chemical, and petrological studies have now been completed (e.g. Barr and White, 1988, 1996; White et al., 1990b; Barr et al., 1994; and this study) to enable

a clear understanding of the relationships among many of the plutonic units in southern New Brunswick.

Plutonic units in the Brookville terrane were previously correlated with a similar compositionally expanded, calc-alkalic, I-type plutons of the Caledonia terrane (e.g. Deveau, 1989). However, plutons in the Caledonia terrane are typically deformed and metamorphosed to greenschist facies (White and Barr, 1991). In addition U-Pb dates show that they were emplaced at ca. 625-615 Ma (Barr et al., 1994), and hence are considerably older than Brookville terrane plutons. Younger ca. 560-550 Ma plutons in the Caledonia terrane, although more similar in age to plutons of the Brookville terrane, are bimodal syenogranite-gabbro/diorite suites that are related to a major rifting event, and hence not petrochemically similar to the Brookville terrane plutons.

The Dipper Harbour volcanic unit was previously interpreted to be Carboniferous in age, interlayered with fossiliferous sedimentary rocks, regionally metamorphosed, intruded by Carboniferous granite, and subsequently deformed by a major Carboniferous thrusting event (Rast and Grant, 1973a, b; Ruitenberg et al., 1979; Dickson, 1983; Rast and Skehan, 1991). Other workers (McCutcheon, 1984, 1985; Currie, 1986a, b; 1987a, b; Currie and Hunt, 1991; Nance, 1986a, 1987b; Eby and Currie, 1993) considered the volcanic and associated plutonic rocks to be Precambrian (NeoProterozoic) in age, but correlated them with the Coldbrook Group of Barr and White (1988).

Detailed examination of this area during this study confirms a Late Neoproterozoic age for the volcanic and plutonic units and a Carboniferous age for the fossiliferous sedimentary rocks, but failed to confirm the existence of a regional metamorphic event. The Dipper Harbour volcanic unit and associated syenogranite plutons form a large single thrust sheet that was thrust over Carboniferous sedimentary rocks in the Late Carboniferous. Present U-Pb dates are not sufficiently precise to resolve any age differences between the Dipper Harbour volcanic unit and associated syenogranite plutons and the Coldbrook

Group. However, chemical data suggest that the former have affinity with the Brookville terrane and not with the distinctly bimodal Coldbrook Group and related plutons that formed in an extensional environment (e.g. Barr and White, 1988, 1996; Barr et al., 1994).

7.2. RELATIONSHIP OF THE BROOKVILLE TERRANE TO ADJACENT AREAS

In addition to the Brookville terrane, three other distinct tectonostratigraphic terranes or belts have been recognized in southern New Brunswick, all of which have been traditionally included in the Avalon Zone or Terrane (compare Fig 1.1 to 1.3). These include the Caledonia terrane (Barr and White, 1989, 1991), the Kingston Complex (Currie, 1984), and the New River belt (Johnson and McLeod, 1994) (Fig. 1.3, 7.2).

7.2.1. Caledonia terrane

The Caledonia terrane comprises rocks of two main ages (Bevier and Barr, 1990; Barr et al. 1994; Barr and White, 1996, in press) (Fig. 7.2). The older (ca. 635-600 Ma) volcanic and sedimentary rocks have been regionally metamorphosed to greenschist facies and contain epidote, chlorite, and muscovite-bearing mineral assemblages. The associated plutonic units (ca. 625-615 Ma) are calc-alkaline and formed during subduction at a continental margin (Barr and White, 1988). The younger volcanic-sedimentary group (ca. 560-550 Ma) is unmetamorphosed and intruded by a ca. 560-550 Ma suite of bimodal plutons typical of post-orogenic extension (Barr and White, 1988). These units are overlain by shallow to deep-water sedimentary rocks of the Cambrian to Ordovician Saint John Group that contain an Acado-Baltic fauna (Tanoli and Pickerill, 1988, 1990). On the basis of character and age of rock units, the Caledonia terrane is considered part of the Avalon terrane *sensu stricto*, like the area east of the Dover-Hermitage Bay fault

system in Newfoundland (e.g. O'Brien et al., 1983). The Caledonia terrane is separated from the Brookville terrane by the Caledonia-Clover Hill Fault (Fig. 1.3).

The Brookville terrane experienced ca. 564-548 Ma low-pressure/high-temperature amphibolite-facies metamorphism that is not present in the Caledonia terrane. Although the calc-alkaline plutons in the Brookville terrane are compositionally similar to ca. 625-615 Ma plutons in the Caledonia terrane, they have yielded considerably younger crystallization and cooling ages (ca. 550-510 Ma).

The radiometric data from the Brookville terrane indicate that temperatures remained elevated ($>300^{\circ}\text{C}$) from 550 to 500 Ma, coincident with the tectonic juxtaposition of the high-grade Brookville Gneiss with the low-grade Green Head Group, and with emplacement of numerous calc-alkaline plutons. This age range coincides with passive platformal conditions in the Caledonia terrane and the deposition of the Saint John Group.

The existence of separate Brookville and Caledonia terranes in southern New Brunswick was not supported by Dallmeyer and Nance (1992) and Nance and Dallmeyer (1994). They agreed that the Brookville and Caledonia "assemblages" had separate tectonothermal histories in the latest Neoproterozoic through Late Paleozoic but argued that they were proximal tectonic elements prior to ca. 550 Ma. This assumption was based on magmatism of similar age and composition in the Brookville terrane (referring to the ca. 605 Ma orthogneiss in the Brookville Gneiss) and regional metamorphism of broadly similar age in both the Brookville and Caledonia "assemblages". They suggested that the Brookville and Caledonia "assemblages" were subsequently separated by extension or strike-slip movements prior to 550 Ma. Magmatic activity ceased in the Caledonia "assemblage" and was followed by the deposition of shallow to deep-water marine strata (Saint John Group), whereas subduction in the Brookville "assemblage" continued well into the Cambrian.

Although the age and chemical affinity of ca. 605 Ma orthogneiss in the Brookville Gneiss is similar to that of the older igneous units in the Caledonia terrane, it is spatially and compositionally much more restricted. The orthogneissic protoliths are tonalitic to granodioritic or gabbroic in composition, whereas tonalitic to granodioritic plutons in the Caledonia terrane have ages of ca. 625-615 Ma. The host rocks to the ca. 605 Ma orthogneiss in the Brookville terrane are also significantly different from those that host the ca. 625-615 Ma plutons in the Caledonia terrane. The Brookville Gneiss consists predominantly of a pelitic protolith with minor calc-silicate, carbonate, and quartzite, whereas the units in the Caledonia terrane are dominantly volcanic tuffs with subordinate slate and arkosic rocks (Barr and White, 1988, 1996, in press).

The minimum age of regional metamorphism in the Hammondvale metamorphic unit is established by $^{40}\text{Ar}/^{39}\text{Ar}$ muscovite ages of ca. 600 Ma. By comparison, regional metamorphism in the 635-600 Ma part of the Caledonia terrane may be of similar age. This metamorphism is both older and different in style from the ca. 564-548 Ma low-pressure/high-temperature metamorphism in the Brookville Gneiss and associated greenschist-facies metamorphism in the Green Head Group. The younger ca. 560-550 Ma units in the Caledonia terrane have not been metamorphosed.

7.2.2. Kingston Complex

The Kingston Complex (Currie, 1984; Nance and Dallmeyer, 1993) is a northeast-trending belt of volcanic and plutonic rocks intruded by a suite of mafic and felsic dykes that display varying degrees of metamorphism and mylonitization (e.g. Pocologan mylonite zone). Geochronological and geochemical data indicate that the plutonic-volcanic units and associated dykes were emplaced in an Early Silurian sinistral transtensional setting (Doig et al. 1990; Eby and Currie,

1993; McLeod et al. 1994). Most of the complex in the southwest was subsequently metamorphosed to lower amphibolite facies and deformed during Late Silurian to Early Devonian dextral transpression (Fig. 7.2) (e.g. Leger and Williams, 1986; Nance and Dallmeyer, 1993). The Kingston Complex has been interpreted to reflect either accretion of the Avalon terrane to cratonic North America (e.g. Nance and Dallmeyer, 1993) or magmatic activity along a major transcurrent fault near the edge of the Avalon terrane (Eby and Currie, 1993). The Kingston Complex is separated from the Brookville terrane by the New River Beach-Kennebecasis fault (Fig. 1.3).

In contrast to the Kingston Complex, no Silurian to Early Devonian units have been recognized in the Brookville terrane, although the abundant mafic dykes have been correlated with those in the Kingston Complex (e.g. Nance et al., 1990). The age of dyke emplacement in the Brookville terrane is poorly constrained between ca. 510 Ma and 370 Ma, so a Silurian age is possible. However, they are not bimodal or metamorphosed (even those close to the Kingston Complex), and they typically display a volcanic arc affinity in contrast to the extensional affinity of the Kingston Complex dykes (cf. Eby and Currie, 1993).

Currie (1987a), McLeod et al. (1994), and Park et al. (1994) considered the Pocologan mylonite zone in the southwest to be the ductile equivalent of the Kennebecasis Fault to the northeast, and interpreted it to affect plutonic rocks of the Brookville terrane. Eby and Currie (1993) further argued that some truncated plutons appear on opposite sides of the complex without significant displacement. However, mylonites were not observed in units adjacent to this fault in the Brookville terrane, and the Kingston Complex and associated Pocologan mylonite zone are separated from the Brookville terrane by the brittle New River Beach-Kennebecasis fault along their entire boundary. Furthermore, contrary to the interpretation of Dallmeyer and Nance (1990) and Nance and Dallmeyer (1994), there is no evidence in the Brookville terrane for a thermal event younger than ca. 500 Ma.

7.2.3. New River Belt

The New River Belt or terrane (Johnson and McLeod, 1994; Barr et al., 1995) includes a suite of calc-alkaline Late Neoproterozoic plutons and minor cogenetic felsic volcanic rocks overlain by Early Cambrian to Late Ordovician volcanic and sedimentary units that locally contain Acado-Baltic fauna (Greenough et al., 1985). Minor Silurian sedimentary and volcanic rocks are associated with these units (McLeod et al. 1994). Units in the New River Belt are locally contact metamorphosed by Late Devonian plutons (Fig. 7.2). The New River Belt is in faulted contact against the Kingston Complex along its southeastern margin (Belleisle Fault) and against the Annidale belt (McLeod et al., 1992) along its northwestern margin (Wheaton Brook Fault) (Fig. 1.3).

Based on present data the New River Belt displays some similarities to both the Caledonia and Brookville terranes. The Cambrian sedimentary units in the New River Belt are equivalent in age to sedimentary rocks of the Saint John Group and contain similar Acado-Baltic fauna. However, abundant rift-related volcanic rocks are associated with the sedimentary units in the New River Belt whereas Cambrian sedimentary units in the Caledonia terrane lack volcanic rocks and were deposited in a passive margin setting. Compared to the Brookville terrane, the New River Belt displays similar Late Neoproterozoic to Cambrian magmatic/volcanic activity and hence may contain the extrusive equivalents of many plutonic units in this terrane (Fig. 7.2). If correct, this implies that the New River Belt may be part of the Brookville terrane, physically separated from it by Silurian transtension and magmatism represented by the Kingston Complex.

Volcanism and sedimentation continued sporadically in the New River Belt well into the Silurian, in contrast to the Brookville and Caledonia terranes where magmatism, volcanism, and sedimentation generally ceased by Early Ordovician time. However, in the Caledonia terrane there is evidence of minor Ordovician and Devonian volcanism

(Barr et al., 1994) (Fig. 7.1).

7.2.4. Timing of Terrane Amalgamation

The timing of initial juxtaposition of the Brookville terrane with the Caledonia terrane is poorly constrained by the available data. It clearly post-dated the deposition of the Cambrian to Ordovician Saint John Group in the Caledonia terrane. Dallmeyer and Nance (1990) and Nance and Dallmeyer (1994) suggested that the low-temperature $^{40}\text{Ar}/^{39}\text{Ar}$ release steps from muscovite defined a major thermal event at ca. 400 Ma in the Brookville terrane and Saint John Group. They speculated that this recorded the initial juxtaposition of the Brookville and Caledonia terranes in the middle Paleozoic. This appeared to be further substantiated by ca. 420 Ma $^{40}\text{Ar}/^{39}\text{Ar}$ whole-rock phyllite ages from low-grade metavolcanic units in Caledonia terrane (Dallmeyer and Nance, 1994). A major tectonothermal event of similar Silurian-Devonian age has been documented in the Kingston Complex (Nance and Dallmeyer, 1993). Dallmeyer and Nance (1990) and Nance and Dallmeyer (1994) suggested that the development of the Kingston Complex during the early Silurian, and its deformation and metamorphism during the Late Silurian to Early Devonian, may be related to the initial juxtaposition of terranes in southern New Brunswick with the outboard Meguma terrane.

Although the Caledonia terrane and Kingston Complex may have shared a thermal event at ca. 400 Ma, this event is not evident in the Brookville terrane. The only stratigraphic unit that unequivocally links these terranes is the Late Devonian to Carboniferous Horton Group (Fig. 7.2) (St. Peter, 1993; McLeod et al. 1994). Late Carboniferous thrust faults in the southwestern Brookville terrane are related to the Cobequid-Chedabucto fault system and the juxtaposition of the Meguma terrane with the Caledonia and Brookville terranes in southern New Brunswick. All the northeast-trending, terrane-bounding faults deform these Late Devonian to Late Carboniferous sedimentary strata suggesting

that movements may have continued well into the Mesozoic (e.g. Roberts and Williams, 1993).

7.3. REGIONAL CORRELATIONS

Rocks of the Brookville terrane are lithologically similar to assemblages documented in the Bras d'Or terrane of central Cape Breton Island (Barr and Raeside, 1986, 1989; Raeside and Barr, 1990). The Bras d'Or terrane is in faulted contact on the southeast with the Mira terrane, a series of volcanic and sedimentary belts similar to the Caledonia terrane (Barr and White, in press). The Bras d'Or terrane is characterized by a suite of low-pressure/high-temperature cordierite-bearing gneiss and migmatite (e.g. Jamieson, 1984) collectively termed the Bras d'Or metamorphic suite (Raeside and Barr, 1990). The protolith age(s) for the Bras d'Or gneiss is unknown; however, limited geochronological data indicate that amphibolite-facies metamorphism occurred at ca. 550-540 Ma (Keppie et al., 1990; Sangster et al., 1990; Davis, 1994) and ca. 500 Ma (Keppie and Dallmeyer, 1989; Dunning et al., 1990). The gneiss is typically in faulted contact with mainly low-grade (locally medium- to high-grade) siliciclastic, carbonate, and volcanic rocks that have been interpreted to be equivalent to the Green Head Group (e.g. Poole, 1967). The depositional age of these units is uncertain, although the youngest detrital zircon extracted from a quartzite in the Creignish Hills yielded an age similar to that from the Green Head Group at ca. 1200 Ma (Davis, 1994). Armitage (1989) and Campbell (1990) suggested that an unconformable relationship originally existed between the Bras d'Or metamorphic suite and the low-grade rocks.

Both the Bras d'Or metamorphic suite and the stratified units are intruded by a compositionally expanded suite of Late Neoproterozoic (ca. 565-555 Ma) calc-alkaline plutons, slightly older than comparable plutons in the Brookville terrane (Dunning et al., 1990; Farrow and Barr, 1992; Dallmeyer and Keppie, 1993).

The Bras d'Or terrane is also intruded by a younger suite of ca. 500 Ma granitic plutons, the result of crustal melting during post-orogenic uplift (e.g. Barr, 1990) or localized extension (White et al., 1994). In the southeastern part of the Bras d'Or terrane, these 500 Ma plutonic units are associated with a fault-bounded belt of Middle Cambrian to Early Ordovician sedimentary and volcanic rocks (Bourinot belt of White et al., 1994) that contain an Acado-Baltic fauna (Hutchinson, 1952). Similar Middle Cambrian to Early Ordovician sedimentary and volcanic rocks exist in the New River Belt and hence may provide an early Paleozoic link between this belt and the Brookville and Bras d'Or terranes. In the Brookville terrane, ca. 500 Ma plutonic units have not been recognized, although $^{40}\text{Ar}/^{39}\text{Ar}$ data indicate a 510-500 Ma tectonothermal event that may have been related to plutonism.

Lithologies like those of the Brookville terrane also occur in the Hermitage Flexure of southern Newfoundland. The most characteristic elements in this zone are Late Neoproterozoic (ca. 578-563 Ma) plutonic units that intruded undated amphibolite-facies gneiss (Cinq Cerf Gneiss) and a greenschist-facies sedimentary and volcanic succession (Whittle Hill Sandstone-Third Pond Tuff) (Dunning and O'Brien, 1989; O'Brien et al., 1991; O'Brien et al., 1993). Orthogneiss(?) of the Grey River Gneiss, interpreted to be equivalent to the Cinq Cerf Gneiss, yielded a crystallization age of ca. 686 Ma and a metamorphic age of ca. 579 Ma (Dunning and O'Brien, 1989). Although these ages have relatively high errors associated with them, they are still considerably older than equivalent ages from the Brookville Gneiss. Associated with the Grey River Gneiss is a narrow zone of low-grade ca. 544 Ma volcanic and sedimentary rocks (Dunning and O'Brien, 1989). This unit is similar in age to older parts of the New River Belt; however, Acado-Baltic fauna have not been reported in the Newfoundland sequence which makes this correlation speculative. The Whittle Hill-Third Pond succession, although apparently lacking carbonate rocks, contains quartzite, sandstone, turbidite, olistostrome, and tuff lithologies similar to some

low-grade units in the Bras d'Or terrane and to the Martinon Formation of the Brookville terrane. Although these units are in faulted contact with the Cinq Cerf Gneiss, O'Brien et al. (1993) suggested that they were originally deposited on the gneiss. All of these units experienced high-grade Early Cambrian (ca. 543 Ma) regional metamorphism of as yet undefined character (O'Brien et al., 1993), and were intruded by ca. 500 Ma plutons (Dunning and O'Brien, 1989; O'Brien et al., 1991). The rocks in the Hermitage Flexure have had a long and complex geological history; however, the broad similarities in lithologies, style of plutonism and metamorphism, and age to the Brookville and Bras d'Or terranes suggest that all of these areas may be correlative.

7.4. IMPLICATIONS FOR PALINSPASTIC RESTORATION

The Avalon terrane in Atlantic Canada is characterized by Late Neoproterozoic (ca. 620 Ma) calc-alkalic volcanic and plutonic units and varied younger (ca. 575-550 Ma) tholeiitic to calc-alkalic to alkaline and peralkaline bimodal volcanic and plutonic rocks (e.g. Barr and White, in press; Barr and Kerr, in press). These units are overlain by latest Neoproterozoic to Early Paleozoic sequences that contain an Acado-Baltic fauna considered to be distinct from the Laurentian fauna (e.g. Neuman, 1994).

Based on regional similarities (section 7.3), the Brookville and Bras d'Or terranes, and parts of the Hermitage Flexure have been correlated and collectively referred to as Bras d'Oria (e.g. Barr and White, in press). In the Late Neoproterozoic and Early Late Paleozoic, most of Bras d'Oria was experiencing deformation, subduction-related plutonism and associated thermal overprinting, and uplift, whereas sedimentary rocks were being deposited in tectonically quiet basins in the Avalon terrane. However, the presence of volcanic and sedimentary rocks containing Acado-Baltic fauna in the Bras d'Or terrane (Bourinot belt of White et al., 1994) and the New River Belt appears to provide a

link in the Late Neoproterozoic and Early Palaeozoic between Bras d'Oria and other areas with such fauna, including the Avalon terrane *sensu stricto* (e.g. Landing, 1991a, b, 1994). The significance of this link is controversial (White et al., 1994). The presence of Acado-Baltic fauna in the New River belt has been used to provide evidence of a direct, contiguous link with the Avalon terrane (e.g. Greenough et al., 1985); however, it may also be interpreted to mean that both of these terranes, although separate, were formed on the non-Laurentian margin of the Iapetus Ocean.

Although many of the detrital and xenocrystic zircon ages have large errors associated with them, they can be used as a first approximation in broad comparisons between terranes in the Northern Appalachian orogen. Many of the plutonic and volcanic units in the Avalon terrane contain abundant xenocrystic zircons that range in $^{207}\text{Pb}/^{206}\text{Pb}$ and upper intercept ages from ca. 700 to 3500 Ma (Bevier and Barr, 1990; Bevier et al., 1993; Barr et al., 1994; Samson, in press); however, many cluster at ca. 925, 1025, 1500, and 2500 Ma. Detrital zircons from the Georgeville Group in the Avalon terrane around Antigonish range from ca. 600 to 2606 Ma and cluster at ca. 625, 1200, and 1525 Ma (Keppie and Krogh, 1990; Davis, 1993, 1994). Detrital zircons from the Brookville Gneiss and Green Head Group and correlative units in the Creignish Hills of the Bras d'Or terrane have a similar range in ages to those of the Avalon terrane (ca. 641 to 2830 Ma; Bevier et al., 1990; Davis, 1993, 1994; D. Davis personal communication, 1995), but cluster at ca. 675, 1200, 1625, 1850, and 2700 Ma. Orthogneissic units in the Brookville Gneiss and the Lime Hill Gneiss in the Bras d'Or terrane contain a minor component of xenocrystic zircons which have ages that range from ca. 1329 to 2330 Ma; however, most are older than 1.9 Ga (Bevier et al., 1990; Sangster et al., 1990). In contrast, the Late Neoproterozoic to Cambrian plutonic units in Bras d'Oria contain even less xenocrystic zircon and are typically devoid of inheritance (e.g. Barr et al., 1990b; Dunning et al., 1990; White et al., 1990; Bevier et

al., 1991). However, where present (e.g. Fairville Granite), upper intercept ages are greater than 1.9 Ga. It is possible that the lack of abundant ancient zircon inheritance in Bras d'Oria indicates a fundamental difference between the two terranes and is evidence against a direct link.

The distinction between Bras d'Oria and the Avalon terrane is further supported by isotopic data which suggest that they evolved on crust with significantly different isotopic signatures (e.g. Barr and Hegner, 1992; Fryer et al., 1992; Whalen et al., 1994; Ayuso et al., in press). Lithologies in the Brookville terrane all have negative ϵ_{Nd} and elevated ^{18}O suggesting involvement of more ancient and weathered crustal material than those in the Avalon terrane (cf. Whalen et al., 1994).

Because the detrital zircon dates from Bras d'Oria and the Avalon terrane are similar to cratonic provinces in the Amazonian craton, not the West African Craton (e.g. Nance and Murphy, 1994) a peri-Amazonian (or peri-Gondwana) (Murphy and Nance, 1991) position has been inferred for these terranes during the Neoproterozoic. Nd isotopic data and xenocrystic zircon dates support this interpretation for the Avalon terrane because the crustal material that fulfills the isotopic requirements is exposed in the Amazonian Craton (Pimental and Fuck, 1992). However, Nd isotopic data and xenocrystic zircon dates (>1.9 Ga) for Bras d'Oria suggest that this terrane formed on ancient crust similar in age and isotopic composition to that exposed in the West African Craton (Nance and Murphy, 1994). It is proposed that Bras d'Oria formed on crust typical of the West African Craton but it was close enough to derive sediments from the exposed ancient crust of the Amazonian Craton. This interpretation suggests considerable palinspastic separation between the Brookville and Caledonia terranes until the Late Paleozoic.

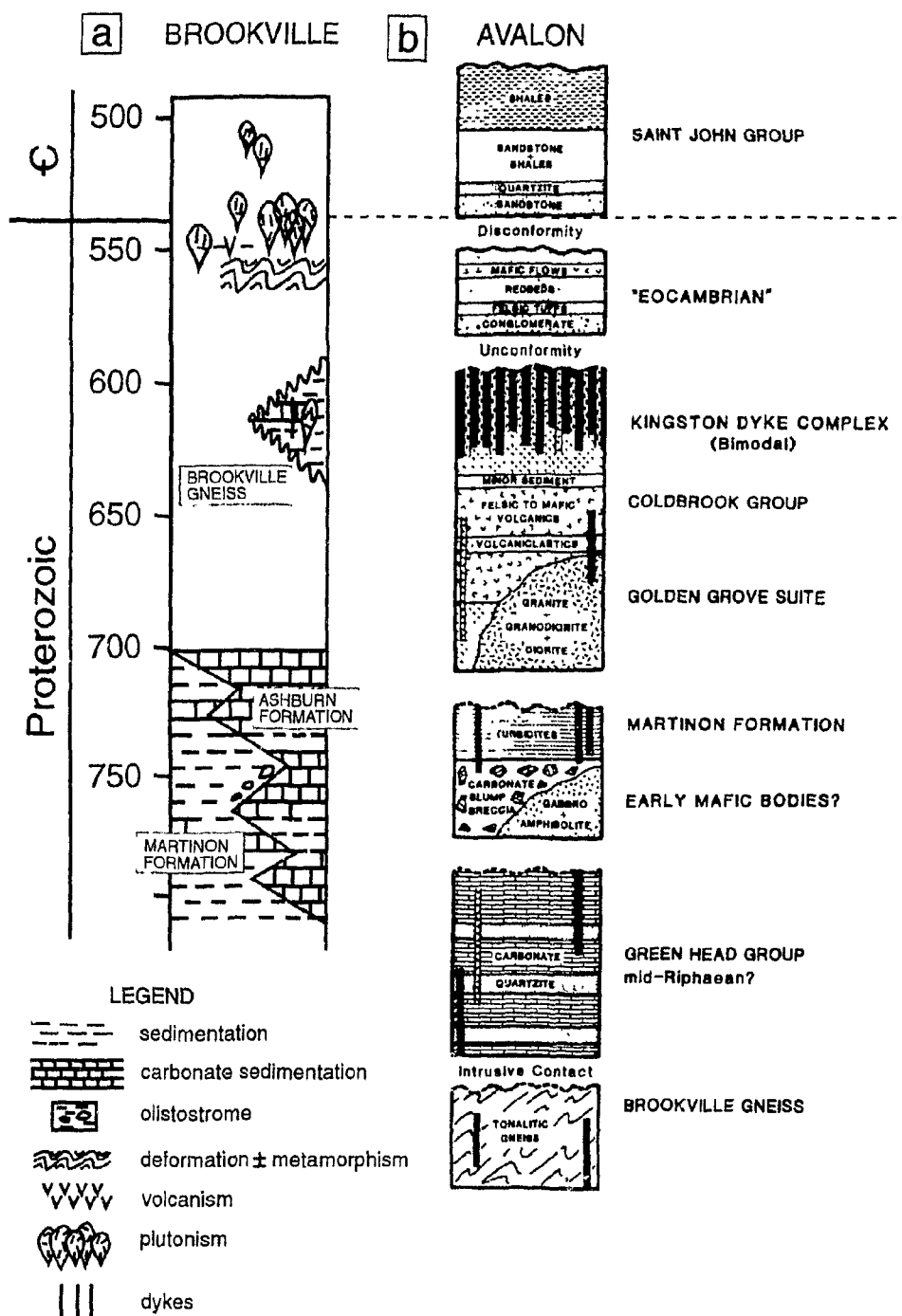


Figure 7.1. Schematic comparative stratigraphic columns for present versus previous interpretations for the geology in the Saint John area. Avalon stratigraphy from Nance (1990).

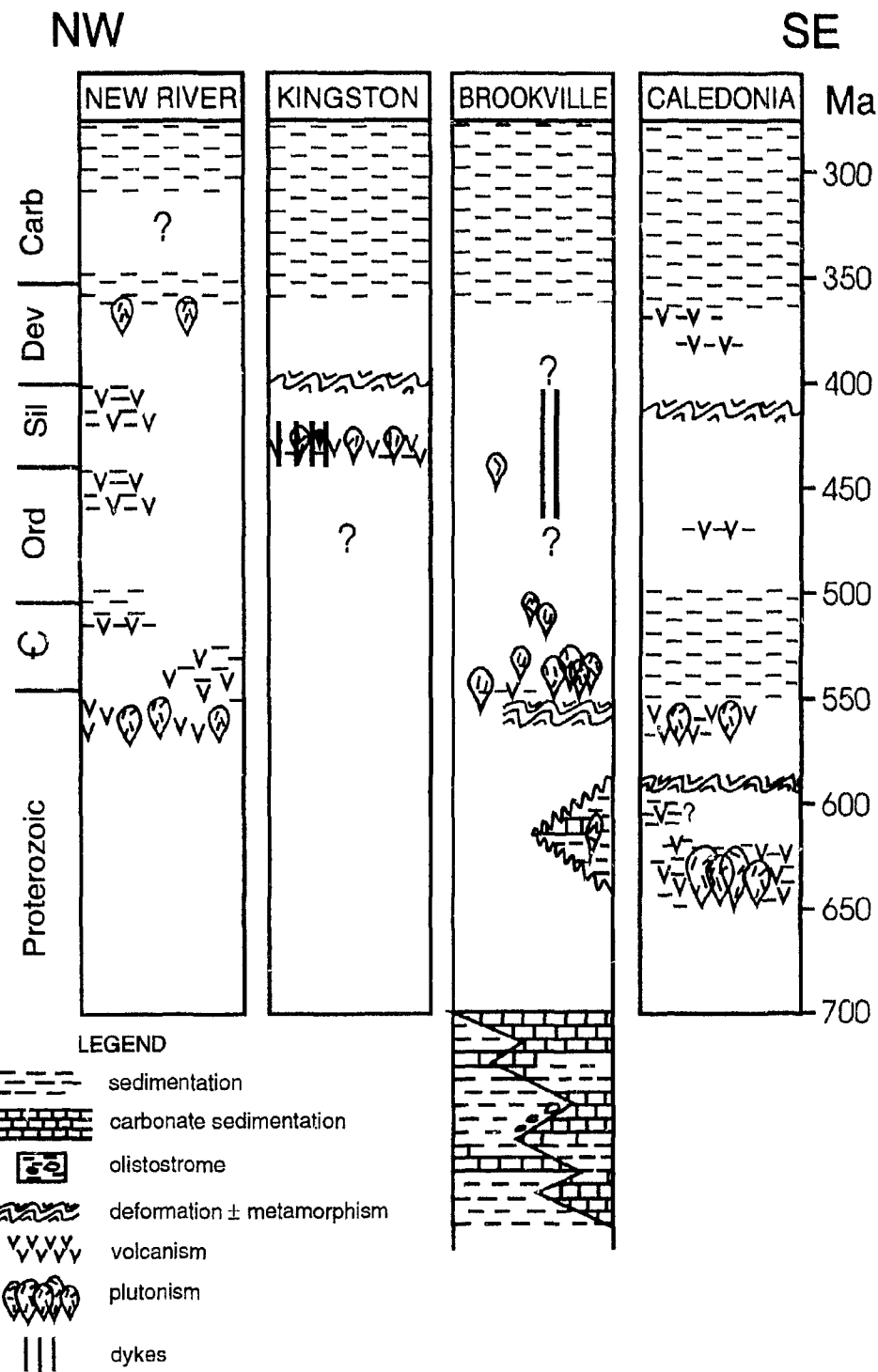


Figure 7.2. Schematic comparative stratigraphic columns for various terranes and belts in southern New Brunswick.

CHAPTER 8

CONCLUSIONS

1. The Brookville terrane of southern New Brunswick consists of the Green Head Group, Brookville Gneiss, Dipper Harbour volcanic unit, and associated plutonic units.
2. The Green Head Group is the oldest unit in the Brookville terrane and consists of the Ashburn Formation, a dominantly carbonate sequence, and the Martinon Formation, a siliciclastic sequence. These formations represent lateral facies equivalents that were deposited at a passive stable continental margin. Based on stromatolite fossils and detrital zircon ages, the depositional age of the Green Head Group is interpreted to be Mesoproterozoic with a maximum age of 1230 Ma. The Green Head Group was moderately to intensely folded after deposition and prior to contact metamorphism by ca. 548-537 Ma plutonic units. Contact metamorphism ranges from albite-epidote to hornblende-hornfels facies, with local areas of pyroxene-hornfels facies. Older greenschist-facies regional metamorphism is present only in the northeast where deeper parts of the Ashburn Formation are exposed.
3. The Brookville Gneiss is a locally migmatitic, cordierite-sillimanite-biotite-K-feldspar-bearing paragneiss with granodioritic to tonalitic orthogneiss and amphibolite. Based on detrital zircon, the maximum age for the sedimentary protolith of the paragneiss is ca. 641 Ma. The orthogneiss has an igneous crystallization age of ca. 605 Ma. Amphibolite-facies metamorphism in the gneiss was of low-pressure (2.5 ± 1 kbar)/high-temperature ($645 \pm 50^\circ\text{C}$) type that was initiated at ca. 564 Ma.

4. The Brookville Gneiss is not basement to the Green Head Group. The two units were juxtaposed along the Late Neoproterozoic MacKay Highway shear zone, which records a significant dextral transpressional sense of movement. This movement was responsible for intense deformation in the Brookville Gneiss and overprinted structural features in the adjacent Ashburn Formation of the Green Head Group.

5. The main plutonic event and associated volcanism (Dipper Harbour volcanic unit) occurred in the Late Neoproterozoic to Early Cambrian. The plutons are compositionally expanded, calc-alkalic, and I-type, emplaced in a continental margin subduction zone. They are broadly grouped into four main packages: 1) medium-grained diorite to granodiorite; 2) coarse-grained monzogranite to granodiorite; 3) medium-grained syenogranite to monzogranite; and 4) coarse-grained gabbro and ultramafic rocks. They are exposed at more shallow crustal levels in the southeast, where they are associated with the Dipper Harbour volcanic unit, compared to the northeast, where they intruded the Brookville Gneiss and Green Head Group. Even though the plutons cooled quickly, they were responsible for wide-spread contact metamorphism in the Green Head Group.

6. The Brookville terrane was deformed by steep, northeast-trending, dextral strike-slip faults and associated folds in the Middle to Late Paleozoic. The two prominent faults include the terrane-bounding Caledonia-Clover Hill Fault on the southeast and the New River Beach-Kennebecasis Fault on the northeast.

7. The southwestern part of the terrane was strongly deformed by Late Carboniferous northwest-directed compression which thrust a single large sheet of Brookville terrane volcanic and plutonic rocks over Carboniferous sedimentary rocks. This thrusting is interpreted to have occurred after dextral transpression associated with the Cobequid-

Chedabucto fault system and the juxtaposition of the Meguma terrane. Many of the northeast-trending Carboniferous faults were reactivated with a normal sense of movement during the development of the Early Mesozoic Fundy Basin. This event also produced a series of steep, northwest-trending faults.

8. The Brookville terrane is considered to be closely related to the New River Belt to the northeast, from which it is now separated by the Silurian Kingston Complex. Together these areas are correlated with the Bras d'Or terrane of Cape Breton Island and parts of the Hermitage Flexure of southern Newfoundland. These elements have a tectonostratigraphic assemblage that is separate and distinct from that in the Avalon terrane *sensu stricto*, as represented in southern New Brunswick by the Caledonia terrane. However, like the Avalon terrane *sensu stricto*, the Brookville terrane and related areas formed on the periphery of Gondwana in the Late Neoproterozoic to Early Cambrian.

APPENDIX A**A.1. HISTORICAL PERSPECTIVE (pre-1966)**

The following historical review provides the geological background for more recent interpretations (see section 1.2). As one reviews the voluminous literature pertaining to southern New Brunswick it is clear that the geology in this area is extremely complex and difficult to decipher and that the geological complexity may have been inadvertently compounded by the numerous geologists who have worked in the area. This review compiles numerous stratigraphic interpretations and classification hierarchies devised by early workers in southern New Brunswick as outlined in Table A1.1 (in back pocket). The age terminology used here is based on the time scale of that era and has not been upgraded to today's terminology.

Geological investigations in southern New Brunswick began with the appointment of Dr. Abraham Gesner as the first Provincial Geologist. He published five annual reports from 1839 to 1843 that included geological studies from most areas of the province. In his first report Gesner (1839) divided southern New Brunswick (and this study area) into three simple classes: 1) granite and other crystalline rocks referred to as the "Primary Series"; 2) Carboniferous and Triassic sandstones and conglomerates termed the "Secondary Formations" and 3) the remainder of the rocks in southern New Brunswick called the "Transition Series" or "Greywacke System".

In his second and third reports, Gesner (1840, 1841) subdivided the Primary Series into granite, syenite (felsic volcanic rocks) and trap (basalt and gabbro) and described these as the oldest rocks exposed in New Brunswick. He also made important fossil discoveries in the Transition Series enabling him to divide this unit into an Older Greywacke Group consisting of unfossiliferous schists and an overlying Newer Greywacke Group consisting of a basal limestone, trap and

fossiliferous slates of Lower Silurian age. The Carboniferous Secondary Formations were divided into the Old Red Sandstone (Kennebecasis Formation), the Coal Measures (Lancaster Formation), and the New Red Sandstone (Triassic Lepreau Formation). Gesner (1841) provided the first geological map of New Brunswick (reproduced by Matthew in 1897). Robb (1841) used the terminology established by Gesner to describe the geological features along the Saint John River.

In his fourth and fifth reports, Gesner (1842, 1843) concluded that the fossil assemblages in the Newer Greywacke System are Cambrian in age and placed the granite, syenite and trap of the "Primary Series" in an older unit termed "Unstratified Rocks".

After his dismissal from the provincial government, Gesner continued independent geological work in New Brunswick. Gesner (1847) further subdivided the distribution of the granites, syenite and trap and referred to the Older Greywacke Group as "Metamorphic Rocks". He also discovered plant fossils in the Secondary Formation and suggested that portions of this formation are Devonian in age.

The task of geological investigation fell to Robb who in 1850 produced the second geological map of New Brunswick. Although Robb's map is based partly on Gesner's data he discounts much of the earlier work as "unwarrantable exaggerations". Robb mapped Gesner's "trap" as "slates altered and disturbed by igneous action" and divided the Primary Formations into trap, syenite, feldspar rocks and porphyry. He also placed the Metamorphic Rocks and Greywacke Group in the Lower and Upper Silurian, respectively.

Dawson (1855) was the next to work in southern New Brunswick and based much of his work on Robb's earlier interpretations. Dawson was concerned with the age of the crystalline limestone in the Greywacke Group. He suggested that it could represent metamorphosed Lower Carboniferous beds or may belong to an older Precambrian formation. However, on his geological map he assigned an Upper Silurian to Devonian age to this crystalline limestone and included it as part of the Coast

Metamorphic belt. Dawson suggested that the igneous rocks are older than Devonian and possibly Laurentian (Precambrian) in age, but could be as young as Lower Silurian. He grouped these rocks into the Granite Metamorphic District because of their similarities with igneous rocks in Nova Scotia.

Dawson (1861) made detailed subdivisions of the pre-Carboniferous rocks in Saint John and mapped conformable contacts among the marble, granitoid and volcanic rocks and shales. He grouped these rocks into one stratigraphic package termed the Devonian Saint John group. In 1862 Dawson further subdivided the Saint John group into eight numerical packages and suggested that the age of the lower members (No. 7 and 8) may be Silurian. He grouped the plutonic rocks with the lower gneissic member.

Matthew (1863) substituted local names for the numerical divisions of Dawson and provided a geological map showing the distribution of formations. He agreed with Dawson and did not separate the crystalline limestones and gneisses from the fossiliferous "Devonian". He named the lowest unit of limestone and gneiss the Portland Series and assigned this horizon to the upper part of the Silurian. He placed the Coldbrook Group (a lower Devonian sequence of green and red volcanic rocks and conglomerates) above this series. The Coldbrook Group was interpreted to be overlain by fossiliferous shales of the Saint John Group, followed by the Bloomsbury Group, largely of volcanic origin with an upper section of unfossiliferous sedimentary rocks. Overlying this are the Little River and Mispec groups, largely comprising sedimentary rocks with abundant plant and rare insect fossils. The red conglomerates of the Lower Carboniferous overlie these units. Red conglomerates of the Triassic age were not recognized as such but included with the Devonian Mispec Group.

Bailey (1865), Bailey et al. (1865) and Matthew (1865, 1868) did reconnaissance mapping east of Saint John and found a much wider distribution of the Portland, Coldbrook and Saint John groups. A very

important result of their work was the discovery of distinctive fauna near the base of the Saint John Group that Hartt (1865) placed in the Lower Silurian. (Note: the Ordovician System was not established until 1879 by Lapworth). They assigned a Laurentian or Azoic age (early Precambrian) to the Portland Group based on stratigraphic position (below the Saint John Group) and similarity of rock types to the Laurentian (Grenville) in Ontario (Logan, 1858a, b). The presence of graphite in the crystalline limestone of the Portland Group was regarded as evidence of life. The Coldbrook Group was interpreted to lie unconformably on the Portland Group and stratigraphically below the Saint John Group and was assigned a Huronian age (late Precambrian). Matthew (1865) split the Coldbrook Group into a lower, mainly volcanic division and an upper, dominantly sedimentary division. Volcanic and sedimentary rocks of the Devonian Bloomsbury Group were placed above the Saint John Group. Bailey et al. (1865) mapped a belt of gneiss, felsite, slates and "interstratified" diorite on the Kingston Peninsula that extended eastward toward Sussex and southwest to Beaver Harbour. This belt of rocks was described under the provisional name of the Kingston Series (Kingston complex) and was interpreted as Upper Silurian based on fossils. Granites associated with this belt were interpreted to be Devonian, whereas the granites in the Saint John area were considered Laurentian in age. The youngest rocks in the present study area were considered to be the coarse conglomerate and sandstone of the Carboniferous Kennebecasis Conglomerate.

Dawson (1868) summarized the previous work in southern New Brunswick and provided more detailed descriptions of rock units along with a geological map of the Maritime Provinces. He also renamed the Saint John Group the Acadian Group and considered all granites in southern New Brunswick to be Devonian.

Matthew and Bailey (1869a, b, 1870) compared the metamorphic rocks in the Saint John area to those in Maine and concluded that the upper part of the Laurentian Series, containing "feldspar rock", should be

referred to as the Labrador Series, and that the Huronian Series may be Cambrian in age. Based on metasedimentary xenoliths, granitic rocks were interpreted to be altered sediments and were mapped as gradational into fossiliferous Upper Silurian and/or Devonian strata.

After Confederation (1867), the Geological Survey of Canada systematically mapped the province and produced a series of annual reports and maps. The first reports dealing with the geology of southern New Brunswick were by Bailey (1872) and Bailey and Matthew (1872). They subdivided the Portland Group into a lower, dominantly gneiss and syenite series with associated diorite, and an overlying crystalline limestone and quartzite series with minor beds of gneiss. The Lower Coldbrook Group was confirmed to rest upon the Portland Group; however, the Upper Coldbrook Group was thought to represent an unfossiliferous portion of the lower Saint John Group. Upon a more detailed examination of the Mispic and Bloomsbury groups they recognized that the volcanic rocks were lithologically similar to the Huronian in the Saint John area. This led to the removal of the volcanic units from the Devonian system and their placement in the Huronian under the title of Coastal Group. Based on stratigraphy and lithology, the Kingston Group was placed in the Huronian System, equivalent to the Coldbrook Group. The Coldbrook Group was considered to be the oldest member in the Huronian system, and the Coastal Group the youngest. The Kingston Group was considered to be transitional in age between the two. Igneous rocks in the area were considered to be of two ages: 1) Devonian granites associated with the Kingston Group and 2) Laurentian granites in the Saint John area. Matthew (1878) extended the Coastal and Kingston groups to the southwestern portion of the present study area. However, he suggested that the Coastal Group in this area may be related to the Laurentian system.

Dawson (1878) and Ellis (1879) generally agreed with the previous geological work done in southern New Brunswick. However, Dawson suggested that the Saint John Group (Acadian Series) is Cambrian in age,

based on the fossil assemblage. He also discovered stromatolites (previously interpreted as fossilized tree trunks) in the Upper Portland Group that appeared to confirm a Laurentian age.

Bailey (1879, 1881) and Bailey et al. (1880) attempted to define more precisely the contact relationships between units in the area. They dropped the formal names of each group because these names were applied to a variety of rocks not originally included under that name and substituted numerical and lithological nomenclature. They also dropped the Laurentian and Huronian designation for age and used the term Precambrian. They placed the Precambrian Coastal and Bloomsbury groups into one division. However, Bailey (1881) divided the Kingston Group into a lower, dominantly volcanic division of Huronian age and an upper, sedimentary unit of Lower Silurian age. They agreed with Dawson that the Saint John Group was Cambrian or Primordial Silurian (Ordovician). They regrouped the Devonian System into their previous divisions of 1865. Bailey (1881) considered the granitic rocks to be intrusive or "exotic" in origin, whereas the dioritic and syenitic rocks are "highly altered forms of sedimentary beds". He also concluded that the intrusive rocks of New Brunswick and Maine are Laurentian in age or older.

Subsequent workers throughout the late 1880's continued to use the established local names for unit nomenclature in the study area, although most of the work was centred around the "Silurian", Devonian and Carboniferous formations. The rocks of the Devonian System were divided into five groups (Ells, 1886; Bailey, 1890a, b). The Bloomsbury Group (at the base) consists of conglomerate sandstone and shale associated with great masses of "diabase". These pass upward into plant-rich grey sandstone and shales of the Dadoxylon Sandstone. Overlying this unit are green to purple shales and sandstones of the Corlate Shale and the overlying purple-tinted conglomerates of the Mispic Group. The Perry Group is the youngest in the system and consists of red-brown conglomerate and sandstone and included what was

previously the Lower Carboniferous Kennebecasis Conglomerate and the present-day Triassic Lepreau Formation.

Matthew (1890a,b) mapped stromatolite localities and discovered what he interpreted as fossil sponge spicules (later discredited) within the Upper Portland Group that enabled him to subdivide this package into three horizons. The Lower Division consisted of unfossiliferous limestone and gneiss, overlain by sponge spicule-bearing quartzites and siliceous schists of the Middle Division. The Upper Division consisted of a series of argillite, limestone and graphitic shales containing stromatolites and spicules.

Dawson (1891) briefly summarized recent work in southern New Brunswick and correlated pre-Devonian rocks of New Brunswick and Nova Scotia with those in New England, Newfoundland and Western Europe.

Van Hise (1892), in a review of the literature on southern New Brunswick geology, inferred that many of the supposed conclusions and facts were open to doubt and pointed out numerous inconsistencies. He suggested that there was no evidence for correlating the Portland and Coldbrook groups with the Laurentian and Huronian of Upper Canada. He noted that the Lower Portland Group more closely resembles the Archean of western Canada and suggested that this unit may also represent younger intrusive rocks, metamorphosed equivalents of the Upper Portland Group or an older basement complex. He placed a major unconformity between the Coldbrook and Portland groups. This unconformity represented a considerable epoch of time during which the Portland Group was deformed and eroded prior to the deposition of the Coldbrook Group.

Detailed petrographic studies were carried out by W.D. Matthew (1894a, b; 1895; 1896) on the Precambrian rocks in the Saint John area. He determined that much of the Lower Portland Group is igneous in origin and intrusive into the Upper Portland Group. He divided the igneous unit into an older gabbro and a younger granite-diorite series and suggested that they are Precambrian in age, although the granite-diorite may be as young as Devonian. The volcanic rocks of the Coldbrook Group

were interpreted to represent the surface equivalents of these intrusive rocks; however, Matthew still considered them to be Huronian in age. He also determined that great portions of the Huronian System in southern New Brunswick are igneous in character instead of sedimentary as previously thought.

G.F. Matthew (1896) mapped the Lepreau Basin in the southwestern portion of the study area. The northern boundary of the basin coincided with quartz diorites and gneisses of the Lower Laurentian whereas the southern boundary consisted of quartzite and limestone of the Upper Series rocks. The basin consists of sandstones of the Little River and Mispec groups overlain by conglomerates and sandstones considered to be lower Carboniferous (Triassic Lepreau Formation).

Ami (1900), referring to unpublished work of Matthew, and Bailey (1899) described the geology throughout the city of Saint John. They agreed with previous workers and placed the Lower Portland Group in the Laurentian system of Archean age (Bailey, 1899); however, because of a "marked discordance of stratification", Ami (1900) suggested that the overlying Upper Portland Group be assigned a Grenvillian age. Ami agreed with Matthew (1899) on the term "Etcheminian" to describe a redbed succession above the Coldbrook Group and beneath the Cambrian (previously the Upper Coldbrook Group of Matthew, 1865). Ami (1900), Bailey (1904) and Ells (1905) placed this unit in the Precambrian; however, they describe the fauna as essentially Cambrian.

Ells (1906, 1907) remapped much of southern New Brunswick, including the present study area, and provided a complete review of the literature to date (Ells, 1907). He concluded that the Upper Portland Group is conformable with the overlying Saint John Group and should be placed in the Lower Cambrian system due to similarities between the quartzites and slates. He observed that granites and gneisses of the Lower Portland Group intruded the Saint John Group, and are therefore younger than Laurentian (i.e. Cambrian or possibly Devonian in age). Ells (1907, 1908) also considered the Coastal Group, east and west of

Saint John, to be Carboniferous in age and placed it with the Mispic Group. Parts of the Kingston Group were considered to be igneous in origin and therefore post-Huronian in age, whereas the Coldbrook Group still retained a Huronian age.

Matthew (1908a, b) believed that rocks of the Portland Group represented an ancient (Archean) metamorphic terrane, locally intruded by syenite, gneiss and diorite, upon which the Coldbrook and Saint John groups accumulated. The Coldbrook Group was previously thought to be Huronian in age, however, equivalent rocks in Cape Breton Island are associated with fossiliferous Lower Cambrian strata (Matthew, 1903). In southern New Brunswick the Coldbrook Group was therefore placed at the base of the Cambrian, below the Saint John Group. Matthew considered the Kingston Group to be Upper Huronian in age. He assigned all the Devonian sedimentary rocks with plant fossils to the Upper Silurian, whereas Ellis (1907, 1908) agreed with Dawson (1891) on a Devonian age. Matthew considered the conglomerates related to the Upper Devonian Perry Group (Kennebecasis Formation) to be the youngest rocks exposed in the area. In 1911, Matthew suggested that the gneisses of the Laurentian Series are the result of chemical changes in ancient clay and mud and are not intrusive in character.

Young (1913) suggested that the Precambrian Portland and Coldbrook groups are of greatly differing ages but both were deformed, intruded and eroded prior to deposition of the Cambrian Saint John Group. He agreed with Stopes (1914) that most of the plant-bearing sedimentary rocks in the area are Carboniferous in age, including a red conglomerate with marble and granite clasts that he termed the Red Head formation (Kennebecasis Formation).

Hayes (1914) proposed a numerical classification for rock units in the area and suggested a tentative stratigraphic succession. Series 1 through 5 included plutonic units considered to be pre-Carboniferous and post-Precambrian. Series 1 and 2 (gabbro and granite-diorite of Matthew 1894b) intruded the limestone series only, and therefore were considered

the oldest plutonic rocks. Series 6 included non-plutonic(?) gneisses of the Portland Group (gneissic rocks of Matthew, 1911) and Series 7 included the sedimentary portion. Series 8 (Kingston Group) was considered Precambrian in age whereas Series 9, the Coldbrook Group, was placed in the Lower Cambrian in agreement with Matthew (1908a). Series 10 included the Cambro-Ordovician Saint John Group. Hayes (1914) considered Series 11, the Bloomsbury and Little River groups (previously the Cordate and Dadoxylan units), to be Carboniferous. Overlying this unit is Series 12 (Mispec Group) and Series 13 (Kennebecasis and Red Head formations)

Cumming (1916), working as Hayes' assistant, considered that the limestones and quartzites in the Portland Group were deformed and eroded prior to the eruption of the Coldbrook and Kingston groups. He disagreed with Hayes (1914) that the Coldbrook Group was Cambrian and concluded that the volcanic rocks were folded and eroded before deposition of the Lower Cambrian sedimentary rocks.

Cumming (1916) also performed the first "modern" petrological and geochemical study in the Saint John area. Based on this work he subdivided and named eight individual plutonic and gneissic units and considered them to be the result of "primary differentiation" in the Devonian to Early Carboniferous. This included Granite and Biotite gneiss, Indiantown gabbro, Fairville granite, Rockwood Park granodiorite, Duck Lake gabbro, Mayflower Lake quartz diorite and the Kennebecasis granite and granodiorite.

Bailey and Matthew (1919) and Matthew (1921) made only minor changes in the stratigraphy of the Saint John area from Matthew (1908). They removed the volcanic rocks from the Mispec Group and placed them in the Precambrian Coastal Group. They also suggested that major unconformities exist between each package of rocks. They remained unconvinced of a Carboniferous age for plant-bearing units (e.g. Young, 1913; Hayes, 1914; Stopes, 1914) and used the degree of metamorphism and development of slaty cleavage to define a Silurian age for these

sedimentary rocks.

Hayes and Howell (1937) produced a map and report on the geology of the Saint John area based predominantly on the stratified units. Descriptions of the igneous rocks were incorporated from Cumming (1916). They proposed the term Green Head formation for the sedimentary portion of the Portland Group and concluded that the Green Head formation was Early Proterozoic in age and severely deformed prior to the intrusion of the Golden Grove Intrusives. They believed that the lower portion of the Kingston Group was the same age as the upper portion of the Coldbrook Group and proposed the term Saint John Volcanics for these Late Proterozoic units (in full agreement with the unpublished work of Cumming 1916). The Golden Grove Intrusives were interpreted to have been emplaced during two separate events in the Precambrian. The Green Head formation and Golden Grove Intrusives were eroded prior to the deposition of the Saint John Volcanics. The oldest Cambrian beds lie unconformably on these eroded volcanic rocks with a basal conglomerate containing volcanic detritus. Syenites that intrude the Saint John Volcanics on Hayes and Howell's map are described in their text as granophyric flows, presumably the same age as the volcanic rocks. Hayes and Howell dropped the formal name Saint John Group for the Cambro-Ordovician sedimentary rocks and established a number of new unit names. They completely revised the Carboniferous stratigraphy of the area and concluded that no Devonian sedimentary rocks were present. They considered the Lower Carboniferous to include the Kennebecasis, Boars Head and Red Head formations. The Mispec Series was interpreted to overlie these units and included the sedimentary rocks of the Little River and Balls Lake formations, sandstones and volcanic rocks of the Cranberry Point Formation and volcanic rocks of the Partridge Island Formation. The Courtenay Bay Formation consisted of intrusive and extrusive diabase and was interpreted to overlie the Mispec Series. Hayes and Howell (1937) agreed with Ellis (1908) and placed volcanic rocks of the Coastal Group back into the Mispec Series.

Alcock (1938) produced a geological map and report that did not differ greatly from Hayes and Howell (1937). He upgraded the Green Head formation to group status and suggested an Archean age. He used the term Coldbrook Group to refer to all volcanic rocks in the area and because of its unconformable relations with the Green Head Group, it was considered to be Early Precambrian. He restored the term Saint John Group for the Cambro-Ordovician strata and revised Carboniferous stratigraphic terminology. He referred to the Lower Carboniferous conglomerates as the Horton Series which included the Kennebecasis and Boars Head formations. The Mispic Series, above the Horton Series, included the Balls Lake Formation and West Beach Formation (Red Head, Cranberry Point, Courtenay Bay and Partridge Island formations of Hayes and Howell, 1937). Resting on these units was the Little River Series which included the Lancaster Formation (Little River Formation of Hayes and Howell). He dropped the Golden Grove intrusive designation and used local names established by Cumming (1916) and Hayes and Howell (1937) for the plutons. Alcock (1938) suggested that granite and gneiss pebbles in a conglomerate within the Coldbrook Group suggested plutonism during deformation of the Green Head Group in the early Precambrian. He also suggested that plutonism was associated with volcanism related to the Coldbrook Group. In addition, he considered that the Coldbrook Group was intruded by granites of Middle Devonian age and the West Beach Formation by Carboniferous granites. Alcock (1941) later concluded that the Kingston Group was Silurian in age, based on fossils, and excluded it from the Coldbrook Group.

Belyea (1939, 1944, 1945) mapped and divided the plutonic rocks southwest of Saint John into five units and considered them to be an extension of the Golden Grove intrusives. The oldest unit was considered to be the Lepreau Diorite which is intruded by the Milkish Head granitic rocks and cut by the Musquash Granite. The Chance Harbour Granite, the fourth unit, was considered to be Carboniferous based on its inferred intrusive contact with mid-Carboniferous sedimentary rocks.

The fifth unit, a gneiss of unknown age and origin (Pocologan Mylonite), was correlated with the Lepreau and Milkish Head granitoids. She agreed with Cumming (1916) on a mid-Devonian age for the majority of the plutons. Belyea (1939) considered the sedimentary and volcanic rocks in the area to be pre- and post-plutonic; however, she was the first to recognize Triassic sedimentary rocks in the Point Lepreau area and termed them the Point Lepreau Formation (previously considered to be Horton Series by Alcock in 1938). Lepreau Formation was introduced to replace Point Lepreau Formation by Wright and Clements (1943). They subdivided the Carboniferous rocks in the Lepreau-Musquash area into a younger (Pennsylvanian) sedimentary sequence, containing coal deposits termed the Lancaster Formation and an older pre-Lancaster Formation (Mississippian) sequence of sedimentary and volcanic rocks.

Alcock (1948) summarized the major problems earlier workers faced in the Saint John area and provided only limited updated stratigraphic data from his previous work in 1938. On lithological and structural evidence he correlated the Green Head Group with the Grenville rocks of eastern Ontario and western Quebec; however, he continued to consider the Green Head Group as Archean in age. Alcock (1948) also reported the presence of minor volcanic rocks in the Green Head Group. He suggested that the Coldbrook Group, including the Kingston Group, may be early Lower Cambrian in age, but concluded that they should be referred to as Proterozoic. He suggested that the Coldbrook and Green Head group supplied various types of detritus to the Saint John Group; however, he never succeeded in finding a single granite pebble in the conglomerates. Alcock (1948) supported the interpretation of Hayes and Howell (1937) and Alcock (1938) of two igneous events in the Precambrian. He excluded the Red Head Formation from the Carboniferous and placed it in the Triassic, equivalent to the Lepreau Formation. He reinstated the old name "Little River Group" for the Lancaster Formation.

Weeks (1957) described the geology of the Appalachian region including rocks in the study area. He considered the Green Head Group

to be Archean in age and overlain, with angular unconformity, by the Proterozoic volcanic rocks of the Coldbrook Group. The gneiss of Belyea (1939, 1944, 1945) was considered by Weeks (1957) to more closely resemble the Green Head Group than the volcanic rocks of the Coldbrook Group. The Saint John Group was interpreted to rest conformably on the Coldbrook Group with a basal conglomerate that consisted of volcanic Coldbrook Group pebbles and boulders and minor granitic clasts. Weeks (1957) agreed with Alcock (1938, 1948) on a Carboniferous age for the sedimentary and volcanic rocks of the Mispick Group and a Triassic age for red conglomerates at Red Head and Point Lepreau. Based on radiometric determinations, the majority of granitic rocks in southern New Brunswick are considered to be Devonian. Based on field evidence, the only Carboniferous granites in the area intruded the Mispick Group. Weeks (1957) suggested that the granitic clasts in the Saint John Group indicated a Precambrian intrusive event, possibly Archean.

Alcock (1959) mapped the same area as Belyea and concluded that the granites are Silurian or older. He grouped the associated volcanic rocks (previously the Coastal Group of Bailey and Matthew, 1872 and the Mississippian rocks of Wright and Clements, 1943) with the Carboniferous Mispick Group and considered the Green Head Group to be Archean in age. Alcock (1959) and Alcock and Perry (1960) considered the gneiss of Belyea (1939, 1944, 1945) to be acid and basic volcanic rocks related to the Coldbrook Group as opposed to Weeks (1957) interpretation.

Feale et al. (1961) produced the first tectonic map of the Canadian Appalachian region based on age of folding. They considered the Green Head Group to represent Grenvillian basement that was involved in subsequent Paleozoic orogenies. Based on K-Ar and Rb-Sr dates they concluded that most of the granites in southern New Brunswick are Devonian. No granitic rocks of Carboniferous age were positively identified, except those that intruded the Mispick Group.

The Green Head Group was mapped in considerable detail by Leavitt and Hamilton (1962) and divided into the Ashburn Formation and a younger

Martinon Formation. Both Leavitt (1963) and Hamilton (1965, 1968) suggested that structural complexity in the Ashburn Formation and the lack of marker beds have precluded the establishment of formal stratigraphic members. Hamilton (1965, 1968) later subdivided the Ashburn Formation into three informal units: 1) the lower part - predominantly clastic rocks; 2) the upper part - limestone and dolomite; 3) the middle part - a transition zone of clastic and calcareous rocks. The Martinon Formation consisted of various quartzites, argillite, minor schist and gneiss with a basal conglomerate and was interpreted to overlie the Ashburn Formation with an angular unconformity or disconformity (Leavitt, 1963; Hamilton, 1965). The Green Head Group is complexly folded and was interpreted to form a broad southwesterly plunging synclinorium. The age of the Golden Grove Intrusives, including the gneiss, were considered to be post-Green Head Group and pre-Carboniferous although Leavitt (1963) and Poole et al. (1964) believed that some of the plutons were late Precambrian and the gneisses might represent an older basement. The Coldbrook-Green Head group contact was mapped by Leavitt and Hamilton (1962) and Leavitt (1963) as partly faulted and they suggested that an original unconformable relationship existed. The Cambro-Ordovician Saint John Group was consistently faulted against the Green Head Group; however, it is reported by Leavitt (1963) to rest unconformably on the Coldbrook Group.

MacKenzie (1951, 1964) mapped the area northwest of Saint John. He considered the dykes that intrude the Milkish Head granite were related to the Precambrian Coldbrook Group and therefore the granite was pre-Coldbrook Group in age. He suggested that the remainder of the Golden Grove Intrusives are Devonian based on the lack of cross-cutting dykes.

Smith (1966) agreed with earlier workers that the Green Head Group is Precambrian; however, he suggested that it is Archean and hence considerably older than the Proterozoic Coldbrook Group. He also suggested that the age of the Kingston Group had not been satisfactorily

resolved and therefore assigned a Precambrian to Silurian age. He interpreted the Cambrian-Ordovician Saint John Group to conformably overlies the Coldbrook Group, and considered plutonic rocks that intruded the Green Head and Coldbrook groups to range in age from late Precambrian to Devonian. He agreed with the Carboniferous subdivisions established by Alcock (1938, 1959). By the late 1960's, the stratigraphy of the Saint John area appeared to be firmly established (Table A1.1). The Green Head Group represented a metamorphosed basement complex, overlain by the Coldbrook and Saint John groups. The age of the plutonic rocks was variably considered to be late Precambrian or Paleozoic.

This historical perspective illustrates the immaturity of geology as a science during this period. These early geologists were trained before many of the basic geological concepts and principles were formulated. As the science evolved so did the ability to understand and interpret the geology of southern New Brunswick; however, this also added to the complexity of geological interpretations in the area. As aptly stated by G.F. Matthew in 1897 on previous geological work in the area "We are not to expect from a geologist living in that early period, the exact methods of the modern trained specialist".

APPENDIX B**PLUTONS AND THEIR FIELD RELATIONSHIPS****B.1. INTRODUCTION**

Plutons are described below in order of oldest to youngest, inferred from intrusive relationships observed in the field and geochronology (Chapter 6). The geographic distribution of individual plutons is shown in Figure 2.1 and Map A. Granitoid nomenclature follows Streckeisen (1976) and the recommendations of the International Subcommittee on Stratigraphic Classification (1987). Previous names used for plutonic units are listed in Table B.1.

B.2. DIORITIC TO GRANODIORITIC PLUTONS**B.2.1. Ludgate Lake Granodiorite**

The Ludgate Lake Granodiorite (Currie, 1986b) is located south of the Martinon Formation and outcrops around the shore of Ludgate Lake and along numerous powerlines and roads to the west. It extends as far southwest as the Musquash River and has an estimated surface area of approximately 11 km². It is characterized by grey to grey-green, fine- to medium-grained granodiorite to tonalite with numerous rounded dioritic xenoliths. It is intrusive into the Martinon Formation along its northern margin, based on the presence of a wide contact metamorphic aureole and numerous metasedimentary xenoliths. Along its southwestern margin it appears to be intruded by pink granite of the Prince of Wales pluton. Fine-grained red granite/aplite dykes are throughout the granodiorite. The Ludgate Lake Granodiorite becomes increasingly more foliated and tonalitic toward the southeastern margin where it is in faulted contact with the Spruce Lake Tonalite and Prince of Wales

Granite. This shear zone is marked by a discontinuous, narrow belt of red conglomerate and siltstone (Devonian-Carboniferous Kennebecasis Formation(?)) that extends from Spruce Lake to Musquash Harbour. The granodiorite has yielded a zircon and titanite crystallization age of ca. 548 Ma. (see Chapter 6).

B.2.2. Spruce Lake Pluton

The Spruce Lake Pluton (Wardle, 1978) occurs in a narrow northeast-trending belt southeast of Spruce Lake and extends to Lorneville Harbour. It also occurs as a small body to the northeast in Manawagonish Cove and has a total surface area of approximately 5 km². It is a texturally and compositionally varied unit that ranges from diorite to tonalite to granodiorite. The wide range in the abundance of mafic minerals results in a variation in the colour from black to white. The texture also varies considerably from medium-grained and equigranular to porphyritic with large quartz and plagioclase phenocrysts. The southeastern margin of this pluton is in faulted contact with the Ashburn Formation; however, to the northeast a broad contact metamorphic aureole is preserved with marble and rare meta-siltstone xenoliths common in the pluton close to contacts. The southwestern margin appears to be intruded by pink granite of the Prince of Wales pluton. Granodiorite within the Spruce Lake Pluton is identical to the Ludgate Lake Granodiorite and are therefore the plutons are considered coeval and cogenetic.

B.2.3. Rockwood Park Granodiorite

The Rockwood Park Granodiorite (White et al., 1990) forms two bodies separated by a band of marble in the vicinity of Rockwood Park, north of Saint John. As defined by White et al. (1990) and this study, the pluton is much more geographically restricted than previous.

defined (see Table B.1) and covers an area slightly greater than 1 km². It consists of grey, medium-grained granodiorite gradational to tonalite and is characterized by the presence of a moderate to strongly developed foliation defined by aligned euhedral hornblende grains and ellipsoidal dioritic enclaves. Contacts with adjacent units were not observed. However, the sliver of marble dividing the pluton is coarse-grained, suggesting a contact metamorphic effect from the pluton. An intrusive contact is also supported by U-Pb zircon and titanite crystallization ages of ca. 538 Ma (White et al., 1990). Hornblende and biotite fractions have yielded ⁴⁰Ar/³⁹Ar ages of ca. 538 Ma and ca. 511 Ma, respectively (see Chapter 6). Dallmeyer and Nance (1992) also obtained two hornblende ⁴⁰Ar/³⁹Ar ages of ca. 538 Ma (see Chapter 6).

B.2.4. French Village Quartz Diorite and other dioritic plutons

The French Village Quartz Diorite (White et al., 1990) occurs in the northeastern part of the terrane and consists of diorite gradational to quartz diorite and tonalite with a surface area of approximately 20 km². The wide range in the abundance of mafic minerals results in a variation in the colour from black to white. The texture also varies considerably from medium-grained and equigranular to porphyritic with large quartz and plagioclase phenocrysts. In the northeast the tonalitic portions of the pluton contain numerous small fine-grained dioritic enclaves. Smaller dioritic bodies (<1 km²) occur throughout the study area and are interpreted to be correlative. This includes rocks previously included in the Indiantown Gabbro and Rockwood Park amphibolite (Hayes and Howell, 1937; Wardle, 1978) (Table B.1).

The southeastern margin of the pluton is strongly sheared and is in faulted contact (Caledonia-Clover Hill Fault) with the Caledonia terrane. The northwestern margin of the pluton has an intrusive contact with the Ashburn Formation. This is based on a well developed contact

metamorphic aureole in the French Village area and the presence of numerous marble and quartzite xenoliths of Ashburn Formation affinity. The pluton probably also has intrusive contacts with the Brookville Gneiss, based on the presence of a small dioritic intrusion (Chalet Lake Gabbro of Wardle, 1978) and dioritic dykes in the gneiss, probably related to the French Village Quartz Diorite. The pluton is in contact with the Duck Lake Pluton which is inferred to be younger because gabbroic and anorthositic dykes and plugs, interpreted to be related to the Duck Lake Gabbro, have intruded the pluton. The Renforth Pluton to the northwest intruded the French Village Quartz Diorite and this contact is well exposed in roadcuts on Highway 111.

The French Village Quartz Diorite has yielded a U-Pb zircon crystallization age of ca. 537 Ma (Bevier et al., 1991) and a $^{40}\text{Ar}/^{39}\text{Ar}$ hornblende age of ca. 540 Ma. (see Chapter 6). These ages agree well with $^{40}\text{Ar}/^{39}\text{Ar}$ hornblende ages of ca. 532-539 Ma obtained by Dallmeyer and Nance (1992).

Contacts of the smaller dioritic intrusions in Saint John are generally strongly sheared and the relative age is not known from field evidence. However, locally the Fairville Granite is intruded by dioritic rocks that are interpreted to be correlative with the French Village Quartz Diorite.

B.2.5. Belmont Tonalite

The pluton is herein termed the Belmont Tonalite (previously Red Bridge Pluton of Currie, 1987b; Table B.1) after its principle area of outcrop. It occurs north of the Martinon Formation and extends from Belmont, on the west coast of Grand Bay, westward to just past Henderson Lake with a surface area of about 13 km². It consists of relatively homogeneous, light to dark grey, medium-grained tonalite gradational to granodiorite and quartz diorite and is locally porphyritic and foliated. The southern contact with the Martinon Formation is generally faulted;

however, in the Belmont area it is clearly intrusive because a contact metamorphic aureole is well developed. In addition, numerous marble and metasedimentary xenoliths are common in the pluton close to the contact. Fine-grained red granite dykelets are common within the tonalite near the northern contact with the Henderson Brook Granite (see below). The Belmont Tonalite has yielded an $^{40}\text{Ar}/^{39}\text{Ar}$ hornblende age of ca. 531 Ma (Dallmeyer and Nance, 1992) (see Chapter 6).

B.2.6. Perch Lake Granodiorite

The name Perch Lake Granodiorite is proposed for pluton that occurs in a north-trending belt and outcrops in the Perch Lake area west of the Martinon Formation and extends southward to Musquash River. Its exposed surface area is approximately 8 km². It is intruded by red granite of the Prince of Wales pluton. It is dominantly a light to dark grey, medium-grained (rarely coarse-grained) granodiorite with fine- to coarse-grained dioritic enclaves of varied size (10 cm to 20 m). The Perch Lake Granodiorite is intrusive into the Martinon Formation along its eastern margin where a foliation is locally developed. Its southern margin is not exposed but is inferred to be separated from Carboniferous sedimentary rocks by the Ragged Head Fault (Dickson, 1983). The western contact with the Shadow Lake Granodiorite is not exposed and therefore the relative ages are not known. Mineralogically the Perch Lake Granodiorite is very similar to the Ludgate Lake Granodiorite; however, texturally it is quite distinct. The Perch Lake Granodiorite has yielded an $^{40}\text{Ar}/^{39}\text{Ar}$ hornblende age of ca. 530 Ma (Dallmeyer and Nance, 1992) (see Chapter 6).

B.2.7. Shadow Lake Granodiorite

The Shadow Lake Granodiorite is a new name proposed for one of the largest plutons west of Saint John with a surface area of approximately

15 km². It occurs in a northeast-trending unit from East Branch Musquash River in the south to northeast of East Branch Reservoir in the northeast and is best exposed in the Shadow Lake area. It is characterized by grey, medium- to locally coarse-grained, granodiorite to tonalite with large subhedral quartz grains. It is locally foliated and contains numerous elongated, varied-scaled dioritic to tonalitic enclaves. It also locally displays magma mingling textures. It is in faulted contact (Ragged Head Fault) with Carboniferous sedimentary rocks along the southern boundary. Also in this area fine-grained red syenogranite of the Harvey Hill pluton is clearly intrusive into the pluton. This is based on numerous dykes related to this granite that occur near the contact. Small bodies of pink granite porphyry occur throughout the pluton and may be related to the Musquash Harbour and Harvey Hill plutons. The northern margin is in contact with strongly deformed Green Head Group lithologies along the New River Beach Fault (Rast and Dickson, 1982; Dickson, 1983). The western contact with the Hanson Stream Granodiorite appears to be sharp and in places it is faulted. The Shadow Lake Granodiorite has yielded a ⁴⁰Ar/³⁹Ar hornblende age of ca. 527 Ma. (see Chapter 6).

B.2.8. Talbot Road Granodiorite

The name "Talbot Road" (Currie, 1987a) is a local name and not a geographic location on the 1:50,000 NTS map and therefore contravenes codes of stratigraphic nomenclature; however, there is no other geographic location that can be used satisfactorily and the name "Talbot Road" is retained. The Talbot Road Granodiorite consists of grey to pink, fine- to medium-grained granodiorite gradational to tonalite. It is locally foliated and inequigranular with large plagioclase grains. It also contains small rounded to elongated dioritic xenoliths. This pluton differs from other granodioritic units in its relatively high mafic mineral content. It outcrops in the central part of the West

Branch Reservoir northwest of the Hanson Stream Granodiorite, where it is separated from the Pocologan mylonite zone to the north by the New River Beach Fault. Currie (1987a) mapped a gradational contact between the Pocologan Mylonite Zone and the Talbot Road Granodiorite, but this could not be confirmed. The tonalite is inferred to be unconformably overlain by Carboniferous Balls Lake Formation(?) on its northwestern margin. A second body of granodiorite to tonalite exposed along Highway 790, southwest of the Hanson Stream Granodiorite, is interpreted to be correlative. The Talbot Road Granodiorite has a total area of approximately 10 km². Contacts with the Hanson Stream Granodiorite were not observed.

Like the Hanson Stream Granodiorite, this pluton is cut by pink syenogranite dykes presumably related to the Harvey Hill pluton. The pluton has yielded a ⁴⁰Ar/³⁹Ar hornblende age of ca. 521 Ma. (Dallmeyer and Nance, 1992) (see Chapter 6).

B.2.9. Renforth Pluton

The Renforth Pluton (Currie et al., 1981) is the largest pluton in the Brookville terrane with a surface area of approximately 25 km². It is best exposed in the area southeast of Kennebecasis Bay and extends northeastward to the lower reaches of the Hammond River. It consists of dark grey to red, medium-grained quartz diorite and tonalite that locally contain fine-grained diorite xenoliths. It appears to grade into grey to grey-pink, medium- to coarse-grained granodiorite along its northwest margin in the Quispamsis area. Three smaller intrusions to the southwest, the Mayflower Lake, Narrows, and Acamac plutons (Hayes and Howell, 1937; Wardle, 1978) are considered to be related because of their similar mineralogy and texture to the more mafic portions of the Renforth Pluton (Deveau, 1989; White et al., 1990). Although the Acamac Pluton is poorly exposed, it appears to be finer grained and inequigranular.

Contacts between the Renforth pluton and adjacent units are generally faulted; however, an intrusive contact with the French Village Quartz Diorite is exposed along Highway 111. At this contact dioritic xenoliths, inferred to be related to the French Village Quartz Diorite, are more numerous and tonalitic dykes of the Renforth Pluton cut the pluton. In Drury Cove, the Renforth Pluton is faulted against foliated spotted mica schist of the Ashburn Formation. Contacts between the three smaller intrusions and the country rocks were not observed but Wardle (1978) reported the presence of contact metamorphic aureoles in the Green Head Group around these plutons. Locally Devonian-Carboniferous conglomerate of the Memramcook and/or Kennebecasis formations unconformably overlies the Renforth and Mayflower Lake plutons (McLeod et al., 1994).

Small deformed bodies of tonalite are tectonically interlayered with marble on Long Island and other small islands in the Kennebecasis Bay. These are interpreted to be correlative with the Renforth Pluton. The Renforth Pluton has yielded an $^{40}\text{Ar}/^{39}\text{Ar}$ hornblende age of ca. 511 Ma (see Chapter 6).

B.2.10. Enclaves

Many of the dioritic to granodioritic plutons contain mafic enclaves that generally consist of black to grey, fine- to coarse-grained diorite to tonalite. Locally quartz phenocrysts are common. The size of the enclaves vary from a few centimetres to several 100's of metres. The morphology of the enclaves are also variable, from small, well rounded shapes to lenticular shapes.

Enclave contacts are commonly straight and sharp; however, lobate and cusped contacts were only observed in the Lepreau Pluton. Rarely the enclaves are bordered by thin (<1 cm) biotite-rich rims but chill margins were not observed. Locally lenticular banded structures (<5 cm) over 10's of metres occur in contact zones, especially in the Shadow

Lake pluton.

B.3. MONOGRANITIC TO GRANODIORITIC PLUTONS

B.3.1. Fairville Granite

The Fairville Granite (Cumming, 1916; Hayes and Howell, 1937) is a pink to orange, generally coarse-grained monzogranite gradational to granodiorite that typically displays megacrysts (<3 cm) of potassium feldspar. Locally phenocrysts include quartz and plagioclase. The pluton is best exposed south of Green Head Island in the Pleasant Point area and can be traced southwest to the Manawagonish Cove area and northeastward as far as Rockwood Park and has a total surface area of approximately 4 km². It includes portions of the Rockwood Park Pluton of Hayes and Howell (1937) and Wardle (1978) and the poorly-defined Fisher Lakes Pluton of Currie et al. (1981) (see Table B.1). Although most exposed contacts are faulted, it locally contains elongated xenoliths of amphibolite, gneiss, and marble and is therefore interpreted to be intrusive into the Brookville Gneisses and Ashburn Formation. The pluton also contains rare elongate enclaves of fine grained dioritic rocks. The Fairville Granite is locally intruded by dioritic rocks assumed to be related to the French Village Quartz Diorite. The Fairville granite has yielded a U-Pb zircon crystallization age of ca. 548 Ma and an ⁴⁰Ar/³⁹Ar hornblende age of ca. 536 Ma. These ages are discussed in more detail in Chapter 6.

B.3.2. Chalet Lake Granite

The Chalet Lake Granite (Deveau, 1989; White et al., 1990) forms two small bodies in the Golden Grove Mountain area near Chalet Lake with a total surface area of about 1 km². It is mineralogically and texturally similar to the Fairville Granite and is therefore interpreted

to be correlative. Contacts with the surrounding rocks are poorly exposed and the relationship is therefore not clear; however, the southwesterly body intrudes calc-silicate lithologies of the Ashburn Formation. Locally the southwest body is strongly foliated due to its proximity to the Caledonia-Clover Hill Fault.

B.3.3. Gayton Granite

The Gayton Granite is a new name proposed for a small granitic pluton (<4 km² in area) located approximately 30 km east of Moncton. This pluton is interpreted to represent the most northeasterly exposure of pre-Carboniferous rocks related to the Brookville terrane. It is pink to orange and coarse-grained with large megacrysts (< 6 cm) of K-feldspar with minor phenocrysts of plagioclase. It is texturally similar to the Fairville and Chalet Lake granites; however, it generally has less quartz and locally more foliated. It is intruded by pink aplite and fine-grained granitic dykes. Fluorite is common along fracture surfaces and forms the matrix to many brecciated zones in the granite.

The granite is unconformably overlain by conglomerate and sandstone of the Upper Carboniferous Cumberland Group; however, it is faulted along its southern contact against conglomerates of the Devonian to Lower Carboniferous Horton Group (St. Peter, 1993). Lithologies similar to the Gayton pluton have been intersected in drill core south of Moncton (D. Boyle, personal communication, 1994) which indicates that this pluton is much more extensive than its outcrop distribution suggests.

B.3.4. Hammond River Granite

The Hammond River Granite (Deveau, 1989; White et al., 1990) outcrops in the extreme northeastern part of the terrane and covers an

area of approximately 13 km². It is similar to portions of the Fairville Granite; however, the grain size varies from medium- to coarse-grained. The pluton appears to be granodioritic in the southwestern portions and grades to more monzogranitic varieties towards the northeast. The southeastern margin the granite is in fault contact (Caledonia-Clover Hill Fault) with conglomerate and sandstone of the Upper Carboniferous Hopewell Group (St. Peter, 1987, 1993) and Lower Carboniferous Windsor Group (McLeod et al., 1994). This faulted contact is also observed in drill core, which suggests that the fault dips steeply northwest, under the granite. Along its northeastern margin the granite is unconformably overlain by conglomerate and sandstone of the Devonian-Carboniferous Memramcook and Kennebecasis formation (St. Peter, 1987; McLeod et al., 1994). The presence of numerous dioritic xenoliths along the southwestern margin suggests an intrusive contact with the French Village Quartz Diorite. The Hammond River Granite is interpreted to have intruded the Ashburn Formation and the Brookville Gneiss, based on the presence of gneiss, marble, amphibolite, and quartzite xenoliths. The Hammond River Granite is interpreted to be younger than the Fairville Granite because of the intrusive contact with the ca. 537 Ma French Village Quartz Diorite to the southwest.

Small inliers of coarse-grained syenogranite to monzogranite occur to the northeast along the Caledonia-Clover Hill Fault. A small inlier (<3 km² in area) located approximately 15 km to the northeast of the Hammond River Granite (herein termed the Cassidy Lake inlier) is interpreted to be related to the Hammond River Granite. It is unconformably overlain by the Devonian to Carboniferous Memramcook Formation on its northwestern margin (St. Peter, 1987) that contain clasts of the granite, although McLeod et al. (1994) and St. Peter (1993) later mapped a faulted contact. The southeastern margin the granite is in fault contact (Caledonia-Clover Hill Fault) with conglomerate and sandstone of the Upper Carboniferous Hopewell Group (St. Peter, 1987, 1993; McLeod et al., 1994).

A second poorly exposed inlier of granite is located approximately 10 km to the northeast of the Cassidy Lake inlier in the Jeffrey Corner area (McCutcheon, 1978; McCutcheon personal communication 1994). Contact relationships with the Devonian to Carboniferous Memramcook Formation are not exposed and the granite is highly fractured due to its proximity to the Caledonia-Clover Hill Fault. This granite is interpreted to be related to the Hammond River Granite and Cassidy Lake Inlier.

B.3.5. Milkish Head Pluton

The name "Milkish Head" is a local name and not a geographic location on the 1:50,000 NTS map and therefore contravenes codes of stratigraphic nomenclature. However, the name "Milkish Head Pluton" is entrenched in the literature and hence the name is retained. The Milkish Head Pluton, as herein defined, is confined to the Kennebecasis Island and Summerville area northwest of Kennebecasis Bay and has a surface area of approximate 5 km². It consists of pink-green to red, coarse-grained monzogranite with large quartz grains that grades into medium-grained granodiorite to the southwest. Locally the pluton contains small elongate dioritic enclaves. Commonly associated with the Milkish Head Pluton are numerous pink to red fine-grained to aplitic granite dykes. Previous workers included the K-feldspar-poor plutonic rocks to the southeast (Renforth Pluton of Currie et al., 1981; and this study) in the Milkish Head Pluton (e.g. Hayes and Howell, 1937; Wardle, 1978; Deveau, 1989; White et al., 1990). However, detailed mapping suggests that, although the Renforth Pluton locally grades into granodiorite, it is texturally distinct from the Milkish Head Pluton.

Contacts between the pluton and adjacent units to the southeast are not exposed; however, a northeast-trending fault is inferred to exist in Kennebecasis Bay. On Kennebecasis Island the pluton is in faulted contact on the northwest with marble of the Ashburn Formation

and sedimentary rocks of the Saint John Group. Rocks similar to the Milkish Head Pluton also occurs as tectonic slivers within the marble. Near Summerville the northwestern margin of the pluton is in tectonic contact with the Saint John Group and sedimentary rocks of the Kennebecasis Formation along the Milkish Head Fault (Grant, 1972); however, clasts of granodiorite in the conglomerate attest to an originally unconformable contact. Locally the pluton exhibits a mylonitic texture near the contact with the Kennebecasis Formation.

B.3.6. Hanson Stream Granodiorite

The Hanson Stream Granodiorite (Currie, 1987a) is a large (15 km² in area) northeast-trending pluton that consists of a distinctive grey to light grey, coarse-grained granodiorite to monzogranite with distinctive large quartz grains. It differs from the Fairville Granite and related plutons in that the K-feldspar is interstitial and not megacrystic. The pluton contains numerous small dioritic xenoliths in contrast to the larger map-scale ones in the Shadow Lake Granodiorite (see below). The northern contact is faulted against rocks of the Pocologan mylonite zone and Kingston Complex along the New River Beach Fault. The southern contact is faulted along the Ragged Head Fault against Carboniferous sedimentary rocks. Also along the southern margin red syenogranite dykes related to the Harvey Hill Granite are abundant. Small granite porphyry bodies are common throughout the pluton but the relationship to the coarse-grained granodiorite is unknown. The contact with the Talbot Road Granodiorite to the west is not exposed. This pluton has yielded an ⁴⁰Ar/³⁹Ar hornblende age of ca. 518 Ma. (Dallmeyer and Nance, 1992).

B.3.7. Lepreau Pluton

The Lepreau Pluton (Belyea, 1939, 1944, 1945), as herein defined,

is much more geographically restricted than previously defined (see Table B.1). It is confined to a narrow, northeast-trending, faulted-bounded area northwest of Lepreau Harbour with a surface area of about 5 km². It is a texturally and mineralogically varied unit that ranges in composition from quartz diorite and tonalite to monzogranite and is considered to be a composite pluton. The granodioritic varieties are medium- to coarse-grained and closely resemble rock types in the Hanson Stream and Milkish Head plutons whereas the dioritic to tonalitic rocks are grey to black, medium-grained, with plagioclase and/or quartz phenocrysts. The Lepreau Pluton commonly exhibit magma mixing/mingling textures between the granodioritic and tonalitic lithologies.

B.3.8. Lepreau Harbour Granodiorite

The Lepreau Harbour Granodiorite is a new name proposed for a small (3 km² in area) granodioritic body in the extreme southwestern part of the terrane exposed on the southeastern shore of Lepreau Harbour. It consists of grey-green, medium-grained granodiorite that is locally weakly foliated. Texturally it appears identical to the medium-grained granodiorite parts of the Milkish Head Pluton. Its eastern contact with the Talbot Road Granodiorite is not exposed and it is in faulted contact (New River Beach Fault) with the Carboniferous Lancaster Formation to the south. It is unconformably overlain by the Carboniferous Balls Lake Formation along its northwestern margin.

B.4. SYENOGRANITIC TO MONZOGRANITIC PLUTONS

B.4.1. Henderson Brook Granite

The Henderson Brook Granite is a new name proposed for a relatively small body (3 km² in area) exposed in the Martinon area and along the west coast of Grand Bay. It consists of red to orange,

unfoliated, medium- to coarse-grained monzogranite to granodiorite. It is interpreted to be intrusive into the Ashburn Formation based on the presence of rare quartzite xenoliths. Along its southern margin the pluton appears to be locally chilled against the Belmont Tonalite and numerous fine-grained dykes related to this granite occur in the tonalite close to the contact. The northern margin is faulted along the New River Beach Fault with volcanic rocks of the Kingston Complex. It is also in faulted contact with sedimentary rocks of the Devonian to Carboniferous Kennebecasis Formation; however, locally the conglomerate unconformably overlies the granite. The Henderson Brook Granite differs from the coarse-grained granite in the Milkish Head Pluton in its low abundance of mafic minerals and its equigranular texture.

**B.4.2. Musquash Harbour, Jarvis Lakes, Cranberry Head,
Prince of Wales, and Harvey Hill granites**

The Musquash Harbour Granite (Olszewski and Gaudette, 1982) outcrops principally around Musquash Harbour and extends to the southwest beyond Little Musquash Cove along the Bay of Fundy. It has a surface area of about 9 km². It dominantly consists of pink to grey-green, medium- to coarse-grained monzogranite gradational to syenogranite. Distinct from the granite are large areas of grey-green to dark grey, medium-grained granodiorite to tonalite. This pluton is considered to be composite; however, based on the presence of syenogranite dykelets, these more mafic granitoid rocks are interpreted to be slightly older.

Locally the Musquash Harbour pluton is intrusive into marbles of the Ashburn Formation; however, this contact is generally modified by thrust faults as evident along the east and southwest coast of Musquash Harbour. Along the northern margin the Musquash Harbour pluton it is locally unconformably overlain by the Balls Lake Formation and is in thrust contact with both the Balls lake and Lancaster formations.

Locally stromatolitic limestone of the Carboniferous Parleeville Formation unconformably overlies the pluton (e.g. Hepburn Basin area). The Musquash Harbour Granite has yielded a somewhat poorly constrained U/Pb zircon age of ca. 550 Ma. that is interpreted by Currie and Hunt (1991) to date the time of intrusion. However, this is here considered to be a maximum age for the emplacement of this pluton (see Chapter 6).

A small, thrust-bound body of fine- to medium-grained granodiorite outcrops to the west of the Musquash Harbour pluton and is correlated with the more granodioritic portions of the pluton.

The Jarvies Lakes Syenogranite is a new name proposed for a homogeneous, pink to maroon, unfoliated, medium- to coarse-grained syenogranite that outcrops in a northeast-trending body north of Chance Harbour in the Jarvies Lakes area with a surface area of about 6 km². Locally the granite is highly fractured and sheared and albitized. Aplitic pods and veins are common. The southern margin is marked by a major thrust zone where it overrides Carboniferous sedimentary rocks. Although the eastern contact with Carboniferous sedimentary rocks is not exposed it is interpreted to be a steep, north-trending fault. The northwestern contact with the Meadow Cove volcanic unit does not appear to exhibit a chill margin and the granite is highly fractured and characterized by numerous zones of quartz veins. Although this contact may have originally been intrusive, it is now a faulted contact. Currie and Hunt (1991) suggested a gradational contact between the granite and volcanic rocks but this could not be confirmed. A small isolated body of granite outcrops within the volcanic rocks to the west and is texturally similar to the Jarvies Lakes Granite.

The Cranberry Head Syenogranite (Dickson, 1983) outcrops east of Chance Harbour and consists of highly-fractured, pink to pale orange, medium-grained syenogranite identical to the Jarvies Lakes Granite. It is a small pluton with a surface area of about 1 km². The Cranberry Head Granite is bounded by a thrust fault along its contacts with Carboniferous sedimentary rocks, except on the northwestern margin where

it is in contact with a small thrust-bound sliver of volcanic rocks. Similar red granite is found in the Lepreau Harbour area but its relationship to the surrounding units is not known.

A large (5 km² in area), red granite body appears to intrude the Perch Lake and the Ludgate Lake plutons and is herein named the Prince of Wales Granite after its principle area of outcrop. The southeastern contact is strongly foliated in proximity to the Spruce Lake shear zone. It consists of pink, medium-grained monzogranite gradational to syenogranite and locally contains tonalitic enclaves. This pluton resembles portions of the Musquash Harbour pluton and is interpreted to be correlative.

The Harvey Hill Syenogranite (Currie, 1987a) outcrops southwest of West Branch Reservoir north of the Ragged Head Fault and a surface area of about 3 km². It consists dominantly of pink to maroon, fine-grained subporphyritic syenogranite along its contacts that becomes increasing medium-grained away from these zones. Microplitic cavities are present. Although this pluton resembles portions of the other syenogranite to monzogranite plutons in the area, it differs in that it locally contains garnet and muscovite. It is clearly intrusive into the Shadow Lake and Hanson Stream plutons where numerous syenogranite dykes occur close to the contact and can be from the pluton. Its southern margin is inferred to be faulted against Carboniferous Lancaster Formation.

B.5. DEFORMED GRANITOID ROCKS

A belt of pervasively deformed granitoid rocks extends from the Saint John River south of the Fairville Granite to the southeastern margin of the Rockwood Park Granodiorite, and also along the southern margin of the Brookville Gneiss southwest of the Chalet Lake area. It consists dominantly of strongly deformed grey, fine- to medium-grained monzogranite to granodiorite that locally preserve large lense-shaped grains of feldspar and quartz. This belt probably represents strongly

deformed equivalents of the Fairville Granite and to a lesser extent the Rockwood Park Granodiorite; however, due to the extent of deformation it is difficult to assign them with certainty to one pluton. Locally it appears to have strongly deformed paragneiss intercalated with it and these may represent original xenoliths in the granite. In the Saint John River area this belt of rocks appears to be intruded by the undeformed Indiantown Gabbro (see below).

These strongly foliated granitoid rocks occur in close proximity to the terrane-bounding Caledonia-Clover Hill Fault and also occur as small boudins within marbles of the Ashburn Formation (see Structure Chapter). In the past these rocks were included with the Brookville Gneiss and the amphibolitic portions of the Indiantown Gabbro (Wardle, 1978; Currie et al., 1981).

B.6. GABBROIC TO ULTRAMAFIC PLUTONS

Three gabbroic to ultramafic plutons are recognized in the Brookville Terrane and include the Duck Lake, Indiantown, and Coverdale plutons. The Duck Lake pluton is a small (1.5 km² in area), undeformed, layered intrusion located southeast of Rothesay. It is mainly within the Brookville Gneiss, except on its eastern margin where it has an inferred intrusive contact with the French Village and Renforth plutons. The gabbros are medium- to coarse-grained, and range in composition from gabbroic to ultramafic (Deveau, 1989; Grammatikopoulos, 1992). Small gabbroic bodies to the northeast within the Ashburn Formation and French Village pluton are interpreted to be related to the Duck Lake pluton.

A small body (<0.5 km² in area) of pyroxene-bearing gabbro and anorthosite outcrops near the Saint John River and was previously included into a much larger unit termed the Indiantown Gabbro (Hayes and Howell, 1937; Wardle, 1978). Detailed mapping during this study shows that most of the rocks included in the Indiantown Gabbro are dioritic and are here correlated with the French Village Quartz Diorite. Also

previously included in the Indiantown Gabbro were foliated amphibolite rocks which are interpreted to be part of the Brookville Gneiss. It intrudes the strongly deformed granitoid unit and is considered to be equivalent in age to the Duck Lake pluton. In this study the name Indiantown pluton is restricted to the undeformed gabbro and anorthosite body on the Saint John River.

The Coverdale pluton or the Coverdale Basic Intrusive Complex of Boyle and Stirling (1994) is located 2 km south of Moncton, under 50 to 100 m of Upper Carboniferous sedimentary rock cover. Based on aeromagnetic and drill core data the pluton has an inferred area of approximately 30 km² and is lithologically and texturally similar to the Duck Lake pluton. Contacts with the surrounding host rocks are not exposed and the relationship is therefore not clear.

Based on field relationships the gabbroic and ultramafic rocks are interpreted to be the youngest plutonic units in the terrane and based on comparisons with similar mafic plutons elsewhere in southern New Brunswick and Maine (e.g. West et al., 1992) and in the Bras d'Or terrane of Cape Breton Island (D. Davis, personal communication, 1994) it is interpreted to be Ordovician to Silurian in age.

B.7. DYKE ROCKS

B.7.1. Basaltic to andesitic dykes

Mafic dykes in the Saint John area intrude the Green Head Group, Brookville Gneiss, and all plutonic units; however, they have not been observed in units younger than Early Devonian. Based on modal mineralogy (Appendix C) and texture mafic dykes in the area can be subdivided into three groups: 1) basaltic to quartz basalts; 2) quartz basalts and; 3) quartz andesites to andesites. Basaltic to quartz basaltic dykes are the most abundant and are typically fine-to medium-grained, equigranular, and range in colour from green to grey-green to

light rusty-brown on weathered surface. Locally these dykes are porphyritic with phenocrysts of plagioclase and/or hornblende (replaced clinopyroxene) and display a weak flow foliation. These dykes vary in thickness from about 2 centimetres to over 10 metres but are commonly 1 to 2 metres wide. Dyke contacts are generally parallel with well developed chill margins and a direct correlation between crystal size and dyke width is often evident. In places, dykes are bifurcated and thin (<2 cm) offshoots are common. Most of the basaltic dykes trend northeast, with a subordinate set trending northwest (see Chapter 6).

Basaltic dykes that intruded marbles of the Ashburn Formation are commonly fractured with polished and slickensided joint planes, and are generally conformable with carbonate layering. Locally the dykes are extremely sheared and boudinaged parallel to marble layering. Some of the porphyritic varieties crosscut the non-boudinaged diabase dykes but are interpreted to be of similar age.

Basaltic dykes that intruded the Martinon Formation are generally dark grey to green and in places are difficult to distinguish from the massive dark grey siltstone on fresh surfaces. They are undeformed and generally have well developed chill margins. Basaltic dykes in the plutonic units are similar.

Andesitic dykes are light grey-green, fine-grained, and very difficult to distinguish from the fine-grained basaltic dykes in the field. Their relationship to the basaltic dykes is unknown but are interpreted to be of similar age.

Quartz basaltic dykes are generally light to dark grey, fine- to medium-grained and equigranular and were informally termed microdiorite dykes in the field. These dykes are less than 5 metres wide and are texturally very homogeneous with thin chilled margins. Locally they contain hornblende phenocrysts (replaced clinopyroxene) and may display a flow texture. These are less common than the basaltic and andesitic dykes and are more pristine. Local crosscutting relationships indicate that these dykes cut the older basaltic and andesitic dykes.

B.7.2. Dacitic to rhyodacitic dykes

Dyke rocks that are intermediate (dacitic to rhyodacitic) in composition are rare and have been observed only in the Green Head Group and the Henderson Brook and Perch Lake plutons. These are typically aphanitic, light grey to light green-grey, and less than 5 metres in width with well developed chill-margins. They are locally porphyritic with phenocrysts of feldspar, quartz, and rarely biotite and may display a weak flow texture. Like the basaltic and andesitic dykes in the marbles they are highly fractured and are therefore interpreted to be of similar age.

B.7.3. Pegmatites and aplites

Pegmatites and aplites are associated with all of the plutonic units and Brookville Gneiss. They also occur in the Green Head Group but have only be observed close to plutonic contacts. The dykes are fine- to coarse-grained, and range in colour from pink to brick red to white. Aplite dykes are commonly associated with and locally grade into pegmatite dykes. They typically have a granitic composition and may contain rosettes of tourmaline and patches of muscovite and/or biotite. Garnet is rarely present. Pegmatites associated with the Brookville Gneiss are both concordant and discordant to the gneissosity and are locally foliated. The pegmatites in the MacKay Highway shear zone are similar; however, these are locally deformed into boudins. Aplite lenses are common throughout the gneiss. In the igneous units the pegmatites and aplites form discrete dykes and veins. These pegmatites and aplites are locally cut by mafic dykes.

Muscovite extracted from a pegmatite dyke in the Brookville Gneiss yielded an $^{40}\text{Ar}/^{39}\text{Ar}$ cooling age of ca. 510 Ma (Dallmeyer and Nance, 1992). Based on this age the pegmatites and aplites are interpreted to be younger than the main plutonic event.

Table B.1. Previous names used for plutonic units in the present study.

PLUTONIC UNIT	PREVIOUS PLUTONIC UNIT NAMES	SOURCE
FAIRVILLE GRANITE	-Fairville Granite and part of Rockwood Park Granodiorite -Fairville Granite and part of Rockwood Park Granite -Fairville Granite and part of Rockwood Park Granite and Granodiorite -Fairville Pluton -Fairville Pluton, part of Rockwood Park Pluton, Fisher Lake Pluton -Rockwood Park Pluton -Fairville Granite	1,2,18 3,7,11 9,10 17 19 32 26,34,36,37
CHALET LAKE GRANITE	-Fairville Granite -undivided gneiss and granite -Chalet Lake Pluton -Chalet Lake Granite	1,2 3,18,19 32 34,36
HAMMOND RIVER GRANITE	-undivided Golden Grove Intrusives -undivided gneiss and granite -granodiorite (Golden Grove Suite) -Hammond River Pluton -Hammond River Granite	2 3,18 23,24,26 32,37 34,36
FRENCH VILLAGE QUARTZ DIORITE	-Indiantown Gabbro, Fairville Granite, Rockwood Park Granodiorite -undivided gneiss and granite -Brookville Gneiss -French Village Pluton -French Village Quartz Diorite	1,2 3,18,19 23,24,26,27,31 32 34,36,37
ROCKWOOD PARK GRANODIORITE	-Rockwood Park Granodiorite -Rockwood Park Granite -Rockwood Park Granite and Granodiorite -Rockwood Park Pluton	1,2,18,26,34,36,37 3,7,11 9,10 17,19
RENFORTH PLUTON	-Kennebecasis Granodiorite -Milkish Head Granodiorite -Milkish Head Granite -Milkish Head Granite and Granodiorite -East Milkish Head Pluton -Milkish Head Pluton -Renforth Pluton -Fairville-Renforth Pluton	1 2,25 3,7,11 9,10 17 18,32,34,36,37 26,19 31
MAYFLOWER LAKE TONALITE	-Mayflower Lake Quartz Diorite -Quartz Diorite -Mayflower Lake Pluton -Milkish Head Pluton -Mayflower Lake Tonalite	1,2,9,10,18,25 26,37 3,7,11 17,19 32 34,36
NARROWS TONALITE	-Mayflower Lake Quartz Diorite -Quartz Diorite -Narrows Pluton -Narrows Tonalite	1,2,9,10,18 3,11 17 34,36

Table B.1. Continued.

PLUTONIC UNIT	PREVIOUS PLUTONIC UNIT NAMES	SOURCE
ACAMAC TONALITE	-Milkish Head Granite and Granodiorite -Acamac Pluton	9,10 17
MILKISH HEAD PLUTON	-Kennebecasis Granite -Milkish Head Granodiorite -Milkish Head Granite -Milkish Head Granite and Granodiorite -East Milkish Head Pluton -Milkish Head Pluton -Fairville-Renforth Pluton -Milkish Head Quartz Diorite	1 2,25 3,7,11,13,14 26 9,10 17 18,19,34,36 31 37
DUCK LAKE PLUTON	-Duck Lake Gabbro -Gabbro and Hornblende Schist -Duck Lake Pluton	1,2,3,9,10, 18,26,34,36 7,11 32,37
INDIANTOWN PLUTON	-Indiantown Gabbro -Gabbro and Hornblende Schist	1,2,3,9,10, 17,19,26 7,11
BELMONT TONALITE	-Kennebecasis Granodiorite -Milkish Head Granodiorite -Milkish Head Granite -Milkish Head Granite and Granodiorite -West Milkish Head Pluton -Milkish Head Pluton -diorite (Golden Grove Suite) -Renforth Pluton -Musquash Pluton -Red Bridge Pluton -Milkish Head Quartz Diorite	1 2,25 3,7,11 9,10 17 18 23,24 26 28 29,30,35 37
LUDGATE LAKE GRANODIORITE	-Milkish Head Granitics -granite, diorite, and allied rocks -Rockwood Park Granite and Granodiorite -Spruce Lake Pluton -Musquash Pluton -undivided Milkish Head Complex -granodiorite (Golden Grove Suite) -Ludgate Lake Pluton	4,5,6 8 9,10 17 18 21 23,24 28,29,30,31, 36,37
SPRUCE LAKE TONALITE	-Rockwood Park Granodiorite -Milkish Head Granitics -granite, diorite, and allied rocks -Granite Complex -Spruce Lake Pluton -Musquash Pluton -undivided Milkish Head Complex -Spruce Lake Plutonic Complex -granodiorite (Golden Grove Suite) -Ludgate Lake Pluton	1,2,3 4,5,6 8 15 17 18 21 22 23,24 27

Table B.1. Continued.

PLUTONIC UNIT	PREVIOUS PLUTONIC UNIT NAMES	SOURCE
PERCH LAKE GRANODIORITE	-Milkish Head Granitics -granite, diorite, and allied rocks -Milkish Head Granite and Granodiorite -Granite Complex -Musquash Pluton -undivided Milkish Head Complex -east part of Prince of Wales Pluton and East Musquash Pluton -east part of Prince of Wales Pluton and East Branch Pluton -east part of Prince of Wales Pluton	4,5,6 8 9,10 15 18,26,28 21 29,35 30 31,37
SHADOW LAKE GRANODIORITE	-Milkish Head Granitics and Lepreau Diorite -granite, diorite, and allied rocks -Granite Complex -Musquash Stock -Lepreau Pluton -undivided Milkish Head Complex -Musquash Pluton -Prince of Wales Pluton -Prince of Wales Pluton and Musquash Reservoir Pluton	4,5,6 8 15 16 18,26 21 28 29,30,35 31,37
HANSON STREAM GRANODIORITE	-Milkish Head Granitics -granite, diorite, and allied rocks -Granite Complex -Lepreau Pluton -undivided Milkish Head Complex -Musquash Pluton -Hansen Stream Pluton	4,5,6 8 15 18 21 28 29,30,31,35 37
TALBOT ROAD GRANODIORITE	-Milkish Head Granitics -granite, diorite, and allied rocks -Granite Complex -Lepreau Pluton -undivided Milkish Head Complex -Musquash Pluton -Talbot Road Pluton and Lepreau Pluton	4,5,6 8 15 18 21 28 29,30,31,35 37
LEPREAU HARBOUR GRANODIORITE	-Milkish Head Granitics -granite, diorite, and allied rocks -Lepreau Pluton -undivided Milkish Head Complex -Hansen Stream Pluton	4,5,6 8 18 21 29,30,31,35 37
LEPREAU PLUTON	-Lepreau Diorite -granite, diorite, and allied rocks -Red Head Pluton -undivided Milkish Head Complex -Musquash Pluton -Talbot Road Pluton	4,5,6,26 8 18,37 21 28 29,30,31,35

Table B.1. Continued.

PLUTONIC UNIT	PREVIOUS PLUTONIC UNIT NAMES	SOURCE
HENDERSON BROOK GRANITE	-Kennebecasis Granite -Milkish Head Granite -Milkish Head Granite and Granodiorite -Martinon Pluton -Grand Bay Pluton -granodiorite (Golden Grove Suite) -Milkish Head Granodiorite -Ludgate Lake Pluton(?) -Henderson Lake Pluton -Milkish Head Quartz Diorite	1 2,3,7,11,26 9,10 17 18 23,24 25 28 29,30,35 37
MUSQUASH HARBOUR GRANITE	-Musquash Granite -granite, diorite, and allied rocks -Chance Harbour Intrusion -Musquash Harbour Granite -Hepburn Basin Granite -Ludgate Lake Pluton(?) -Musquash Pluton	4,5,6,12,26 8 18 20,22 21 28 29,30,31,35 37
JARVIES LAKE SYENOGANITE	-Musquash Granite -granite, diorite, and allied rocks -Chance Harbour Intrusion -Chance Harbour Granite -Musquash Pluton	4,5,6,26 8 18 21 29,30,35
CRANBERRY HEAD SYENOGANITE	-Chance Harbour Granite -granite, diorite, and allied rocks -Cranberry Granite -Chance Harbour Intrusion -Cranberry Head Granite -Musquash Pluton	4,5,6,37 8 12 18 21,33 30
HARVEY HILL SYENOGANITE	-Musquash Granite -granite, diorite, and allied rocks -Chance Harbour Intrusion -foliated granite in Milkish Head Complex -Harvey Hill Pluton -Harvey Hill Granite	4,5,6 8 18 21 29,30,31,35 37
PRINCE OF WALES GRANITE	-Milkish Head Granitics -granite, diorite, and allied rocks -Milkish Head Granite -Granite Complex -Chance Harbour Intrusion and part of the Musquash Pluton -Milkish Head Complex -parts of Ludgate Lake and Musquash plutons -part of Ludgate Lake and Prince of Wales plutons	4,5,6 8 12 15 18 21 28 29,30,31,35 37

Source:

1. Cumming (1916)
2. Hayes and Howell (1937)
3. Alcock (1938)
4. Belyea (1939)
5. Belyea (1944)
6. Belyea (1945)
7. MacKenzie (1951)
8. Alcock (1959)
9. Leavitt and Hamilton (1962)
10. Leavitt (1963)
11. MacKenzie (1964)
12. Subhas (1970)
13. Richards (1971)
14. Grant E. (1972)
15. Grant R. (1972)
16. Butt (1976)
17. Wardle (1978)
18. Ruitenberg et al. (1979)
19. Currie et al. (1991)
20. Olszewski and Gaudette (1982)
21. Dickson (1983)
22. Parker (1984)
23. Currie (1984)
24. Currie (1985)
25. McCutcheon and Ruitenberg (1985)
26. Williams et al. (1985)
27. Currie (1986a)
28. Currie (1986b)
29. Currie (1987a)
30. Currie (1987b)
31. Currie (1989a)
32. Deveau (1989)
33. Dallmeyer and Nance (1990)
34. White et al. (1990)
35. Currie and Hunt (1991)
36. White and Barr (1991)
37. McLeod et al. (1994)

APPENDIX C.1

MODAL ANALYSES

Means (Mean), standard deviations (Std.), maxima (Max.), minima (Min.), and number of sample (n) for modal analyses from the rhyolitic and plutonic units and dikes in the Brookville terrane.

	Mean	Std.	Max.	Min.	Mean	Std.	Max.	Min.
DIPPER HARBOUR RHYOLITIC UNIT (n=11)				ORTHOgneiss (n=26)				
plagioclase	3.2	1.6	5.3	1.5	49.4	8.2	62.9	34.5
quartz	13.8	4.0	20.8	9.0	34.6	6.2	51.8	22.9
K-feldspar	6.7	2.2	11.5	4.1	6.1	4.2	15.8	0.2
groundmass	75.2	6.1	80.8	63.6	-	-	-	-
biotite	-	-	-	-	9.5	4.8	18.7	0.0
opaque minerals	-	-	-	-	0.3	0.4	1.2	0.0

DICRITIC TO GRANODIORITIC PLUTONS

	Mean	Std.	Max.	Min.	Mean	Std.	Max.	Min.
Ludgate Lake Granodiorite (n=29)				Spruce Lake Pluton (n=22)				
plagioclase	48.5	4.4	56.2	40.1	59.0	8.5	78.6	44.7
quartz	28.5	4.5	37.1	18.0	19.4	10.1	34.8	0.1
K-feldspar	10.1	4.9	25.0	3.7	1.6	3.6	16.6	0.0
hornblende	6.2	4.5	16.3	0.0	13.1	11.6	41.7	0.0
biotite	6.3	4.7	21.0	0.0	5.5	3.5	12.4	0.0
titanite	0.0	0.0	0.0	0.0	0.1	0.2	0.9	0.0
opaque minerals	0.3	0.5	1.6	0.0	1.1	1.9	7.8	0.0
Rockwood Park Granodiorite (n=14)				French Village Pluton (n=55)				
plagioclase	49.9	6.4	62.7	42.9	53.0	10.3	72.2	18.9
quartz	27.1	4.7	35.9	20.5	11.1	9.3	34.8	0.0
K-feldspar	6.7	5.1	14.7	0.9	1.4	2.9	18.3	0.0
hornblende	9.1	5.9	21.4	0.0	29.0	17.1	67.3	0.0
biotite	6.9	4.6	21.5	2.0	4.0	4.8	15.5	0.0
clinopyroxene	0.0	0.0	0.0	0.0	6.0	2.2	11.3	0.0
titanite	0.1	0.1	0.4	0.0	0.0	0.0	0.0	0.0
opaque minerals	0.3	0.7	2.7	0.0	1.0	1.6	10.1	0.0
Belmont Tonalite (n=15)				Perch Lake Granodiorite (n=11)				
plagioclase	52.3	10.4	66.9	32.7	51.1	4.4	59.1	44.1
quartz	18.9	6.7	28.9	5.9	23.2	4.3	30.7	16.2
K-feldspar	3.7	3.0	9.4	0.0	9.7	2.4	12.5	4.6
hornblende	16.8	6.3	29.6	8.7	8.0	7.5	23.7	0.0
biotite	7.7	4.2	17.0	0.0	7.4	4.5	16.6	0.0
titanite	0.0	0.0	0.0	0.0	0.2	0.4	1.1	0.0
opaque minerals	0.4	0.6	1.7	0.0	0.4	0.6	1.9	0.0
Shadow Lake Granodiorite (n=22)				Talbot Road Granodiorite (n=15)				
plagioclase	50.6	5.6	58.3	35.7	49.8	4.5	56.5	41.1
quartz	29.2	6.8	40.8	12.2	21.7	3.3	28.1	16.0
K-feldspar	6.5	4.1	12.2	0.0	8.0	4.0	15.2	1.2
hornblende	6.0	4.1	19.3	1.0	12.4	4.9	26.1	6.1
biotite	7.2	7.0	35.7	2.6	7.1	4.1	15.8	1.6
titanite	0.1	0.1	0.6	0.0	0.1	0.2	0.7	0.0
opaque minerals	0.6	0.5	1.6	0.0	0.9	1.7	6.5	0.0
Renforth Pluton (n=48)				Mayflower Lake Tonalite (n=7)				
plagioclase	55.4	7.7	75.0	42.6	53.5	5.0	62.0	46.6
quartz	21.8	7.7	34.1	10.8	18.2	3.6	24.1	13.1
K-feldspar	4.6	5.3	26.2	0.0	1.1	1.8	4.7	0.0
hornblende	10.5	8.1	40.0	0.0	17.8	4.1	23.2	11.1
biotite	6.2	3.9	18.8	0.0	7.8	1.5	10.0	5.0
opaque minerals	1.1	1.6	3.3	0.0	1.5	1.0	3.1	0.0

Appendix C.1. Continued.

	Mean	Std.	Max.	Min.	Mean	Std.	Max.	Min.
Narrows and Acamac tonalites (n=5)					Dioritic Enclaves (n=20)			
plagioclase	54.2	4.7	59.8	48.2	52.3	9.6	68.8	29.2
quartz	18.5	6.8	28.0	9.8	7.5	5.8	18.5	0.0
K-feldspar	0.0	0.0	0.0	0.0	0.3	0.6	2.1	0.0
hornblende	15.0	12.1	33.6	0.0	34.7	14.8	69.9	13.6
biotite	8.6	2.3	10.7	4.8	4.6	3.8	11.3	0.0
titanite	0.0	0.0	0.0	0.0	0.1	0.2	0.7	0.0
opaque minerals	1.2	0.5	1.9	0.4	0.6	0.6	2.2	0.0

MONZOGRANITIC TO GRANODIORITIC PLUTONS

Fairville Granite (n=35)					Chalet Lake Granite (n=12)				
plagioclase	37.2	6.4	49.1	28.0	33.6	9.1	46.5	18.0	
quartz	29.8	4.8	40.3	22.0	26.9	4.9	35.0	18.6	
K-feldspar	22.8	8.3	38.5	10.8	25.7	11.1	40.0	9.8	
hornblende	1.9	3.2	12.7	0.0	7.0	6.9	24.5	0.6	
biotite	7.6	5.9	15.2	0.0	6.1	5.4	15.3	1.0	
titanite	0.2	0.5	1.6	0.0	0.0	0.0	0.0	0.0	
opaque minerals	0.6	0.8	3.0	0.0	0.8	0.9	3.0	0.0	
Gaytor Granite (n=9)					Hammond River Granite (n=21)				
plagioclase	45.0	3.7	50.7	39.6	36.8	6.5	51.1	26.9	
quartz	18.3	2.4	21.0	14.6	33.7	6.4	41.6	17.7	
K-feldspar	24.5	4.2	30.4	15.4	21.9	9.4	38.5	8.7	
hornblende	3.6	1.6	5.9	1.6	2.8	4.4	17.2	0.0	
biotite	6.4	4.1	16.7	3.3	4.3	3.4	11.5	0.0	
titanite	0.8	0.7	2.2	0.2	0.1	0.3	1.2	0.0	
apatite	0.6	0.4	1.5	0.2	0.0	0.0	0.0	0.0	
opaque minerals	0.9	0.9	2.3	0.0	0.5	0.6	1.9	0.0	
Cassidy Lake Inlier (n=3)					Milkish Head Pluton (n=15)				
plagioclase	20.4	4.4	24.6	15.9	41.0	7.9	56.8	28.5	
quartz	30.6	4.6	35.1	30.9	31.8	6.5	44.6	22.1	
K-feldspar	46.7	2.1	48.3	44.4	16.3	5.3	23.2	3.7	
hornblende	1.3	1.1	2.0	0.0	3.9	3.1	10.0	0.0	
biotite	0.6	0.8	2.0	0.0	6.3	3.0	13.4	1.4	
titanite	0.0	0.0	0.0	0.0	0.1	0.3	1.2	0.0	
opaque minerals	0.0	0.0	0.0	0.0	0.6	0.5	1.8	0.0	
Hanson Stream Granodiorite (n=14)					Lepreau Pluton (n=15)				
plagioclase	43.2	6.9	59.0	32.0	45.7	7.1	55.6	31.0	
quartz	32.2	6.9	40.0	18.1	29.4	5.7	36.6	13.5	
K-feldspar	16.6	6.1	27.5	8.8	14.5	9.9	33.9	0.2	
hornblende	3.7	2.8	10.6	0.0	3.5	3.9	12.6	0.0	
biotite	4.0	2.5	9.1	0.9	6.8	6.8	26.4	1.4	
titanite	0.0	0.0	0.0	0.0	0.1	0.4	1.6	0.0	
opaque minerals	0.4	0.5	1.2	0.0	0.1	0.1	0.3	0.0	
Lepreau Harbour Granodiorite (n=6)									
plagioclase	45.9	5.5	55.7	39.0					
quartz	26.6	5.3	33.7	20.2					
K-feldspar	15.8	4.6	23.4	10.4					
hornblende	7.8	2.0	10.8	5.0					
biotite	3.2	2.0	6.7	1.5					
titanite	0.3	0.5	1.2	0.0					
opaque minerals	0.5	0.4	1.2	0.0					

Appendix C.1. Continued.

SYENOGRANITIC TO MONZOGANITIC PLUTONS

	Mean	Std.	Max.	Min.	Mean	Std.	Max.	Min.
Henderson Brook Granite (n=8)					Musquash Harbour Granite (n=28)			
plagioclase	36.1	4.0	40.9	30.2	24.5	8.5	39.7	6.0
quartz	34.5	2.7	40.0	31.4	36.4	5.8	45.4	26.8
K-feldspar	26.4	5.1	32.6	18.6	36.1	7.0	49.0	24.9
hornblende	1.2	1.4	3.7	0.0	0.5	1.1	4.4	0.0
biotite	1.4	1.6	4.7	0.0	2.0	2.3	8.0	0.0
titanite	0.0	0.0	0.0	0.0	0.1	0.2	0.9	0.0
opaque minerals	0.2	0.3	0.9	0.0	0.4	0.6	2.0	0.0

	Mean	Std.	Max.	Min.	Mean	Std.	Max.	Min.
Musquash Harbour Granite tonalite (n=11)					Jarvis Lake Granite (n=11)			
plagioclase	51.1	6.3	64.8	42.2	15.6	4.4	23.4	10.1
quartz	25.0	6.4	36.0	14.9	39.9	5.8	47.1	24.6
K-feldspar	8.7	6.5	23.7	0.6	43.7	6.1	52.7	33.4
hornblende	9.6	6.7	19.9	1.6	0.0	0.0	0.0	0.0
biotite	6.2	3.0	11.3	2.2	0.6	1.0	2.9	0.0
titanite	0.1	0.2	0.6	0.0	0.0	0.0	0.0	0.0
opaque minerals	0.7	1.2	3.9	0.0	0.0	0.0	0.0	0.0

	Mean	Std.	Max.	Min.	Mean	Std.	Max.	Min.
Cranberry Head Granite (n=5)					Harvey Hill Granite (n=6)			
plagioclase	25.6	2.2	28.6	23.5	18.4	2.6	20.4	15.0
quartz	31.3	5.7	39.7	24.4	35.8	1.9	39.0	33.6
K-feldspar	38.7	6.8	50.8	34.3	44.6	2.9	49.4	40.4
biotite	4.2	4.4	9.1	0.0	0.5	0.6	1.1	0.0
titanite	0.0	0.0	0.0	0.0	0.2	0.3	0.7	0.0
opaque minerals	0.0	0.0	0.0	0.0	0.5	0.8	2.0	0.0

	Mean	Std.	Max.	Min.
Prince of Wales Granite (n=27)				
plagioclase	27.7	7.3	40.5	11.7
quartz	35.7	5.7	50.7	27.7
K-feldspar	32.6	8.2	51.4	17.6
hornblende	0.9	1.3	5.8	0.0
biotite	2.9	2.1	8.9	0.0
titanite	0.1	0.4	1.7	0.0
opaque minerals	0.3	0.4	1.4	0.0

GABBROIC TO ULTRAMAFIC PLUTONS

	Mean	Std.	Max.	Min.	Mean	Std.	Max.	Min.
Duck Lake Pluton (n=25)					Indiantown Pluton (n=4)			
plagioclase	41.7	21.1	74.8	1.0	63.7	23.7	90.0	37.5
quartz	0.2	0.5	2.0	0.0	2.1	2.6	5.2	0.0
olivine	17.0	27.9	94.0	0.0	0.0	0.0	0.0	0.0
hornblende	1.6	21.7	67.6	0.0	0.3	2.9	6.1	0.0
biotite	0.5	1.1	4.4	0.0	1.1	2.2	4.3	0.0
orthopyroxene	5.8	8.0	2.5	0.0	5.6	11.1	22.2	0.0
clinopyroxene	31.8	10.7	36.0	0.0	24.7	22.4	43.7	0.0
titanite	0.2	0.9	4.8	0.0	0.0	0.0	0.0	0.0
spinel	0.4	0.9	3.0	0.0	0.0	0.0	0.0	0.0
opaque minerals	0.8	1.1	4.4	0.0	2.6	5.2	10.4	0.0

	Mean	Std.	Max.	Min.
Coverdale Pluton (n=6)				
plagioclase	45.2	46.3	100.0	0.0
quartz	0.4	0.6	1.2	0.0
orthopyroxene	0.5	1.3	3.3	0.0
clinopyroxene	35.3	32.7	73.6	0.0
apatite	7.9	9.2	40.1	0.0
ilmenite	10.7	12.1	40.0	0.0

Appendix C.1. Continued.

DYKES

	Mean	Std.	Max.	Min.
Basaltic to andesitic dykes (n=30)				
plagioclase	51.4	10.6	65.8	29.0
quartz	3.6	3.9	12.7	0.0
K-feldspar	4.5	8.2	33.7	0.0
hornblende	36.1	15.8	66.1	0.0
titanite	0.2	0.7	2.5	0.0
clinopyroxene	1.6	6.8	3.2	0.0
opaque minerals	2.5	2.7	8.2	0.0

Dacitic to rhyodacitic dykes (n=8)				
plagioclase	42.0	15.6	61.5	18.8
quartz	31.2	8.5	45.5	20.3
K-feldspar	11.8	7.3	23.6	2.8
hornblende	13.9	14.3	45.1	0.0
biotite	1.0	2.4	6.8	0.0

Pegmatite and aplite dykes (n=25)				
plagioclase	25.8	8.8	42.3	10.1
quartz	33.7	4.5	42.5	25.1
K-feldspar	38.0	11.8	63.1	20.0
biotite	2.1	1.9	5.8	0.0
muscovite	0.2	0.5	2.1	0.0

APPENDIX C.2

GEOCHEMICAL DATA

Table C.2.1. Geochemical data from igneous and metamorphic units in the study area.

Pluton	Dioritic to Granodioritic Plutons						Spruce Lake Pluton		
	Ludgate Lake Granodiorite								
Sample	NB91-8590	NB91-8622	NB91-8624	NB91-8634	NB92-9195b	NB92-9251	NB91-8629	NB92-9111	NB91-8588
Major elements (wt. %)									
SiO ₂	64.75	66.15	65.71	67.65	65.74	65.51	68.79	65.07	59.42
TiO ₂	0.49	0.44	0.48	0.49	0.44	0.45	0.77	0.94	0.78
Al ₂ O ₃	16.17	16.09	16.29	16.27	16.34	15.93	13.33	14.19	17.52
Fe ₂ O ₃ ^T	5.00	4.74	4.83	4.27	4.25	4.28	5.02	6.32	7.18
MnO	0.10	0.09	0.10	0.07	0.09	0.09	0.07	0.11	0.10
MgO	2.30	1.93	2.01	1.66	1.81	1.80	2.05	2.22	2.91
CaO	3.58	4.08	3.57	3.41	3.53	3.26	2.06	2.24	4.71
Na ₂ O	3.33	3.34	3.55	3.10	3.00	3.10	1.93	3.00	2.98
K ₂ O	2.65	2.17	2.22	2.31	2.39	2.64	2.70	2.76	1.78
P ₂ O ₅	0.15	0.13	0.13	0.13	0.13	0.12	0.16	0.23	0.20
LOI	1.50	1.20	1.60	1.60	1.20	1.70	3.80	1.80	2.30
TOTAL	100.02	100.36	100.49	100.96	98.92	98.88	100.68	98.88	99.88
CIPW Normative Mineralogy (0.5 Fe ratio)									
Q	24.33	26.82	26.01	31.14	29.44	28.37	41.18	30.00	21.15
C	1.70	1.15	1.89	2.81	2.78	2.41	4.01	2.84	2.68
Or	15.93	12.96	13.30	13.77	14.48	16.09	16.51	16.85	10.82
Ab	28.67	28.57	30.45	26.45	26.03	27.05	16.90	26.23	25.93
An	17.07	19.60	17.09	16.21	17.09	15.87	9.49	9.93	22.69
Di	0.00	0.00	0.00	0.00	0.00	0.00	0.00	0.00	0.00
Hy	7.30	6.27	6.48	5.26	5.85	5.85	6.25	7.02	9.37
Mt	3.69	3.47	3.55	3.12	3.16	3.20	3.77	4.74	5.35
Il	0.95	0.85	0.92	0.94	0.86	0.88	1.51	1.85	1.52
Ap	0.35	0.30	0.31	0.30	0.31	0.29	0.38	0.55	0.48
Trace elements (ppm)									
Ba	419	345	393	458	311	394	398	617	448
Rb	69	50	44	64	62	61	92	70	60
Sr	266	220	212	261	200	216	45	180	281
Y	22	15	17	23	17	16	24	47	22
Zr	135	103	113	175	116	104	210	267	222
Nb	5	5	5	7	7	5	8	15	7
Th	10	10	10	10	10	10	10	14	10
Pb	10	10	10	10	10	10	10	10	16
Ga	14	15	12	13	15	15	14	16	18
Zn	40	38	46	43	42	42	52	86	109
Cu	78	5	5	8	8	5	5	17	25
Ni	8	7	6	14	9	5	19	12	40
V	95	81	80	75	78	76	89	102	138
Cr	15	9	14	22	15	13	54	43	51

Note: KC samples from K. Currie (written communication, 1995); DL samples from Grammatikopoulos (1992); samples in bold from Deveau (1989).

Table C.2.1. Continued.

Pluton	Dioritic to Granodioritic Plutons								
	Spruce Lake	Rockwood Park Granodiorite			French Village Quartz Diorite				
	NB91-8644	CW89-509A	CW89-552	CW89-654	CW88-144	CW88-153	CW88-246	CW89-503A	CW89-506
Major elements (wt. %)									
SiO ₂	48.75	64.02	62.40	58.10	58.51	49.96	46.60	60.89	51.60
TiO ₂	1.64	0.49	0.63	0.66	0.69	0.67	1.78	0.73	0.79
Al ₂ O ₃	15.01	16.32	17.13	17.03	17.23	19.74	17.10	16.66	17.31
Fe ₂ O ₃ ^T	15.48	5.00	5.49	6.95	7.35	8.67	13.14	6.02	8.98
MnO	0.17	0.10	0.14	0.14	0.13	0.13	0.15	0.16	0.16
MgO	6.04	2.51	2.99	3.53	3.55	4.78	5.65	3.02	4.96
CaO	7.24	4.92	3.05	5.36	6.55	9.72	9.43	3.63	7.85
Na ₂ O	2.01	4.18	3.91	3.98	3.42	2.79	2.84	4.20	2.98
K ₂ O	1.38	1.90	1.94	1.60	1.24	1.06	0.86	1.69	2.02
P ₂ O ₅	0.31	0.13	0.13	0.15	0.18	0.09	0.12	0.20	0.38
LOI	2.40	0.90	2.20	2.50	0.70	1.60	1.50	1.90	2.00
TOTAL	100.43	100.47	100.01	100.00	99.55	99.21	99.17	99.10	99.03
CIPW Normative Mineralogy (0.5 Fe ratio)									
Q	7.83	18.73	21.46	12.30	15.03	2.86	0.41	18.12	4.16
C	0.00	0.00	3.45	0.00	0.00	0.00	0.00	1.86	0.00
Or	8.38	11.30	11.75	9.73	7.44	6.45	5.24	10.31	12.36
Ab	17.49	35.61	33.92	34.66	29.38	24.29	24.77	36.67	26.11
An	28.64	20.29	14.64	24.58	28.43	39.32	32.34	17.24	28.88
Di	4.95	2.72	0.00	1.42	2.68	7.71	11.96	0.00	7.05
Hy	17.23	6.45	9.16	10.48	9.87	11.38	11.69	9.39	12.24
Mt	11.54	3.65	4.08	5.19	5.41	6.47	9.82	4.50	6.74
Il	3.20	0.94	1.23	1.29	1.33	1.31	3.49	1.43	1.55
Ap	0.74	0.30	0.31	0.36	0.42	0.22	0.29	0.48	0.91
Trace elements (ppm)									
Ba	325	454	478	416	267	169	132	406	355
Rb	41	51	79	53	28	27	29	73	86
Sr	196	269	189	272	269	304	297	193	406
Y	20	21	21	23	25	15	26	32	33
Zr	60	177	145	177	153	54	86	275	141
Nb	5	5	8	5	9	8	5	8	5
Th	10	17	24	14	10	10	12	24	19
Pb	10	10	10	10	10	10	10	10	10
Ga	21	18	18	18	20	18	21	16	20
Zn	105	60	88	85	77	84	96	118	106
Cu	164	17	22	50	5	70	103	39	68
Ni	68	8	8	10	10	34	9	10	21
V	451	93	104	159	144	243	523	104	277
Cr	53	16	23	29	19	43	12	18	25

Table C.2.1. Continued.

Pluton	Dioritic to Granodioritic Plutons								
	FVQD	Belmont Tonalite			Perch Lake Granodiorite		Shadow Lake Granodiorite		
	CW89- 571	NB91- 8513A	NB91- 8522	NB91- 8530	NB92- 9025	NB92- 9027	NB91- 8564	NB91- 8565	NB91- 8569

Major elements (wt.%)

SiO ₂	51.71	61.39	62.88	63.60	61.11	59.36	66.65	66.14	66.04
TiO ₂	0.64	0.59	0.53	0.52	0.62	0.59	0.43	0.52	0.46
Al ₂ O ₃	16.83	15.71	15.62	15.64	16.68	16.76	16.71	16.28	16.53
Fe ₂ O ₃ ^T	9.55	6.52	5.90	5.86	6.10	6.09	4.60	5.36	5.01
MnO	0.18	0.12	0.11	0.11	0.11	0.11	0.07	0.11	0.09
MgO	6.12	3.73	3.79	3.65	3.14	3.11	2.01	1.95	2.32
CaO	7.55	5.11	5.00	3.78	4.41	5.59	3.39	3.19	1.72
Na ₂ O	2.34	2.83	2.53	2.62	2.84	2.79	4.10	4.15	4.50
K ₂ O	1.91	2.14	2.46	2.70	2.58	2.60	1.22	1.06	2.08
P ₂ O ₅	0.08	0.12	0.12	0.11	0.14	0.13	0.12	0.14	0.14
LOI	1.80	2.70	1.60	2.10	1.50	1.00	1.70	1.70	2.20
TOTAL	98.71	100.96	100.54	100.69	99.23	98.13	101.00	100.60	101.09

CIPW Normative Mineralogy (0.5 Fe ratio)

Q	6.01	20.26	22.23	24.41	20.75	16.97	27.87	28.28	24.83
C	0.00	0.00	0.00	1.83	1.57	0.00	2.80	2.88	4.14
Or	11.70	12.91	14.74	16.23	15.65	15.87	7.28	6.35	12.46
Ab	20.53	24.45	21.70	22.55	24.66	24.38	35.02	35.60	38.60
An	30.88	24.35	24.33	18.35	21.52	26.37	16.18	15.12	7.72
Di	5.89	0.59	0.02	0.00	0.00	1.11	0.00	0.00	0.00
Hy	16.35	11.19	11.35	11.04	9.77	9.28	6.39	6.51	7.36
Mt	7.18	4.83	4.34	4.32	4.54	4.56	3.37	3.94	3.68
Il	1.26	1.14	1.02	1.01	1.21	1.16	0.82	1.00	0.89
Ap	0.19	0.28	0.28	0.26	0.33	0.31	0.28	0.33	0.33

Trace elements (ppm)

Ba	315	378	487	490	328	356	184	269	362
Rb	72	77	83	98	58	71	34	31	52
Sr	291	239	228	227	235	224	271	282	258
Y	24	24	12	27	26	29	7	16	18
Zr	58	125	109	105	120	114	124	152	145
Nb	5	7	5	7	6	7	5	5	5
Th	20	10	10	10	10	12	10	10	10
Pb	10	10	10	10	10	10	10	10	10
Ga	19	14	13	14	17	17	12	14	13
Zn	98	80	63	68	56	54	32	60	52
Cu	92	34	73	51	12	33	34	16	46
Ni	17	39	37	39	26	24	5	6	8
V	295	156	127	141	133	129	96	99	97
Cr	32	102	90	124	49	49	13	10	9

Table C.2.1. Continued.

Pluton	Dioritic to Granodioritic Plutons Shadow Lake Granodiorite					enclaves		Talbot Road Granodiorite	
	NB91- 8599B	NB92- 9033	NB92- 9096	NB92- 9258A	NB92- 9260	NB91- 8597	NB92- 9095	NB92- 9045	NB92- 9115
Sample									
Major elements (wt.%)									
SiO ₂	59.74	68.27	69.83	68.73	70.05	56.05	50.09	61.00	60.52
TiO ₂	0.68	0.42	0.38	0.38	0.32	0.63	0.48	0.55	0.56
Al ₂ O ₃	17.72	16.07	15.92	15.49	15.35	17.58	17.94	16.66	17.32
Fe ₂ O ₃ ^T	6.06	3.59	3.02	3.37	2.74	7.82	7.03	6.25	5.96
MnO	0.11	0.09	0.06	0.09	0.06	0.15	0.15	0.11	0.11
MgO	2.87	1.32	1.22	1.37	1.07	4.20	6.99	2.92	2.90
CaO	5.34	2.93	1.72	2.78	2.95	8.38	10.32	5.30	4.35
Na ₂ O	3.30	3.91	3.48	3.31	3.41	2.54	1.62	2.78	3.16
K ₂ O	1.78	1.73	2.20	1.78	1.69	1.05	1.73	2.45	2.47
P ₂ O ₅	0.17	0.13	0.10	0.14	0.10	0.18	0.07	0.13	0.14
LOI	1.50	0.90	1.40	1.40	0.90	0.70	2.50	1.20	1.60
TOTAL	99.27	99.36	99.33	98.84	98.64	99.28	98.92	99.35	99.09
CIPW Normative Mineralogy (0.5 Fe ratio)									
Q	18.24	31.13	36.43	35.61	36.67	14.18	3.84	19.69	19.19
C	1.09	2.80	5.04	3.50	2.86	0.00	0.00	0.11	1.93
Or	10.79	10.40	13.29	10.81	10.23	6.32	10.64	14.80	15.02
Ab	28.65	33.66	30.11	28.79	29.56	21.89	14.27	24.04	27.51
An	26.04	13.93	8.06	13.24	14.32	34.08	38.07	26.01	21.26
Di	0.00	0.00	0.00	0.00	0.00	5.62	11.64	0.00	0.00
Hy	8.96	4.32	3.86	4.47	3.46	10.50	15.13	9.35	9.22
Mt	4.51	2.65	2.24	2.51	2.04	5.77	5.31	4.63	4.45
Il	1.23	0.81	0.74	0.74	0.62	1.22	0.95	1.07	1.09
Ap	0.10	0.31	0.24	0.33	0.24	0.43	0.17	0.31	0.33
Trace elements (ppm)									
Ba	327	256	392	316	269	146	209	264	292
Rb	72	48	52	51	40	26	47	52	67
Sr	280	219	202	282	278	393	283	260	249
Y	26	14	6	5	7	21	13	20	19
Zr	209	172	120	135	139	100	51	99	118
Nb	6	7	5	5	5	5	5	5	5
Th	10	10	10	10	10	10	10	10	10
Pb	10	10	10	10	10	10	10	10	10
Ga	18	17	16	15	14	18	17	16	18
Zn	71	41	40	39	31	62	60	47	52
Cu	29	5	5	5	5	23	6	16	16
Ni	19	5	5	5	5	18	31	12	12
V	124	46	53	62	36	233	173	143	133
Cr	40	9	15	15	10	22	94	25	35

Table C.2.1. Continued.

Pluton	Dioritic to Granodioritic Plutons								
	Talbot Road		Renforth Pluton						
	Granodiorite								
Sample	NB92-9153	NB92-9082	CW88-152	CW88-169	CW88-183	CW88-267	CW88-268	CW89-648	NB92-9131
Major elements (wt.%)									
SiO ₂	62.00	59.06	57.25	60.00	59.29	57.49	66.17	56.79	57.36
TiO ₂	0.50	0.65	0.59	0.68	0.62	0.70	0.35	0.73	0.61
Al ₂ O ₃	16.23	17.06	17.46	16.67	16.44	16.59	15.43	16.91	18.97
Fe ₂ O ₃ ^T	5.87	6.59	7.37	6.61	7.06	7.42	3.47	7.93	6.74
MnO	0.11	0.11	0.14	0.11	0.13	0.15	0.08	0.14	0.18
MgO	2.69	3.47	4.12	3.96	4.11	3.94	2.32	4.07	4.00
CaO	5.05	5.54	6.20	4.48	3.82	3.57	2.30	5.64	2.84
Na ₂ O	2.91	2.97	3.09	2.68	3.18	3.96	4.52	3.41	3.28
K ₂ O	1.80	1.97	1.63	1.93	2.25	1.89	2.33	1.50	1.57
P ₂ O ₅	0.12	0.14	0.13	0.11	0.13	0.15	0.09	0.15	0.18
LOI	1.60	1.40	1.70	2.30	2.70	5.20	3.20	1.80	3.30
TOTAL	98.88	98.96	99.68	99.53	99.73	101.06	100.26	99.07	99.03
CIPW Normative Mineralogy (0.5 Fe ratio)									
Q	23.59	17.23	13.45	21.68	17.86	13.75	23.09	12.96	20.73
C	0.62	0.31	0.00	2.36	2.21	1.99	1.56	0.00	7.49
Or	10.97	11.97	9.87	11.77	13.75	11.70	14.21	9.15	9.73
Ab	25.39	25.84	26.78	23.40	27.83	35.09	39.47	29.72	29.09
An	25.02	27.32	29.67	22.19	18.72	17.52	11.17	27.26	13.54
Di	0.00	0.00	0.78	0.00	0.00	0.00	0.00	0.49	0.00
Hy	8.77	10.79	12.53	12.05	12.80	12.57	7.00	12.64	12.66
Mt	4.39	4.91	5.47	4.95	5.29	5.63	2.60	5.93	5.12
Il	0.98	1.27	1.15	1.33	1.22	1.39	0.69	1.43	1.22
Ap	0.29	0.33	0.31	0.26	0.31	0.36	0.22	0.36	0.44
Trace elements (ppm)									
Ba	194	289	292	379	333	123	504	288	479
Rb	42	57	43	55	62	68	76	45	48
Sr	251	210	302	255	306	142	187	764	370
Y	18	30	21	15	23	24	14	28	25
Zr	95	133	117	94	138	137	116	174	119
Nb	5	7	8	5	10	5	7	5	7
Th	10	10	10	11	10	10	10	16	10
Pb	10	10	10	10	10	10	10	10	52
Ga	17	17	19	18	15	17	15	18	16
Zn	49	60	78	69	72	80	35	83	175
Cu	17	49	33	35	30	19	28	76	25
Ni	11	23	13	12	13	12	8	11	29
V	132	150	194	191	176	187	72	214	206
Cr	26	42	16	21	11	18	11	19	66

Table C.2.1. Continued.

Pluton	Dioritic to Granodioritic Plutons					Narrows Tonalite CW89- 616
	Renforth Pluton		Mayflower Lake Tonalite			
	CW88- 189	CW88- 191	CW88- 266	CW89- 664	KC79- 044	
Sample						
Major elements (wt.%)						
SiO ₂	67.83	65.27	56.66	58.06	57.75	51.33
TiO ₂	0.35	0.40	0.64	0.66	0.69	0.64
Al ₂ O ₃	15.54	16.25	16.81	16.74	15.40	17.57
Fe ₂ O ₃ ^T	3.65	4.16	7.19	6.95	8.46	8.34
MnO	0.09	0.08	0.13	0.12	0.13	0.14
MgO	2.09	2.09	4.75	4.27	5.00	6.00
CaO	3.12	2.91	7.40	5.25	7.24	8.30
Na ₂ O	4.04	3.90	2.50	2.91	2.65	3.00
K ₂ O	2.38	2.76	1.21	1.56	1.16	1.39
P ₂ O ₅	0.11	0.15	0.20	0.18	0.24	0.13
LOI	1.10	1.50	1.70	2.70	2.00	2.70
TOTAL	100.30	99.47	99.19	99.40	100.72	99.54
CIPW Normative Mineralogy (0.5 Fe ratio)						
Q	25.49	23.07	15.52	17.80	16.36	3.26
C	0.92	1.96	0.00	1.19	0.00	0.00
Or	14.20	16.68	7.36	9.57	6.97	8.52
Ab	34.52	33.75	21.78	25.55	22.81	26.32
An	14.91	13.76	31.99	25.81	27.16	31.50
Di	0.00	0.00	3.53	0.00	6.18	8.18
Hy	6.37	6.56	12.73	13.12	12.38	14.38
Mt	2.67	3.09	5.37	5.23	6.24	6.27
Il	0.67	0.78	1.25	1.30	1.33	1.26
Ap	0.26	0.36	0.48	0.43	0.57	0.31
Trace elements (ppm)						
Ba	383	449	291	356	237	324
Rb	53	102	36	55	35	41
Sr	263	273	378	330	341	444
Y	15	21	22	20	23	17
Zr	124	132	123	127	152	75
Nb	8	9	8	7	7.8	5
Th	10	20	10	21	3.8	16
Pb	10	10	10	10	5	10
Ga	14	18	19	17	14	17
Zn	40	51	75	76	51	81
Cu	5	16	37	76	28	171
Ni	5	5	40	29	22	50
V	61	61	174	188	215	246
Cr	5	5	104	77	96	148

Table C.2.1. Continued.

Pluton	Monzogranitic to Granodioritic Plutons							
	Fairville							
	Granite							
Sample	CW88-	CW89-	CW89-	CW89-	CW89-	CW89-	NB92-	KC79-
	272	523	525	543A	589	611	9215A	069
Major Elements (wt.%)								
SiO ₂	68.46	68.00	68.57	68.21	67.12	65.62	70.85	65.10
TiO ₂	0.56	0.60	0.58	0.67	0.74	0.80	0.41	0.99
Al ₂ O ₃	14.36	14.58	14.62	14.53	14.27	14.35	13.47	14.45
Fe ₂ O ₃ ^T	4.02	4.27	4.13	4.55	4.63	5.75	3.41	7.47
MnO	0.06	0.08	0.08	0.10	0.08	0.12	0.06	0.14
MgO	1.42	1.96	2.06	1.57	2.05	1.60	0.58	1.20
CaO	1.45	1.43	0.93	2.37	2.27	2.82	1.08	3.92
Na ₂ O	3.30	2.86	3.19	3.22	3.18	3.04	2.42	3.25
K ₂ O	4.96	3.97	3.66	3.72	3.96	3.82	4.68	2.93
P ₂ O ₅	0.15	0.08	0.13	0.19	0.13	0.23	0.10	0.29
LOI	1.20	1.70	2.00	1.00	1.60	1.00	1.40	0.75
TOTAL	99.94	99.53	99.95	100.13	100.03	99.16	98.46	100.49
CIPW Normative Mineralogy (0.5 Fe ratio)								
Q	25.47	30.73	31.62	28.24	26.00	25.48	36.73	25.29
C	1.31	3.25	4.12	1.37	0.95	0.62	2.79	0.00
Or	29.74	24.03	22.13	22.22	23.83	23.06	28.54	17.42
Ab	28.33	24.79	27.61	27.55	27.40	26.28	21.13	27.67
An	6.31	6.73	3.85	10.63	10.60	12.81	4.86	16.29
Di	0.00	0.00	0.00	0.00	0.00	0.00	0.00	1.12
Hy	4.45	5.95	6.17	4.92	6.05	5.38	2.36	4.19
Kt	2.96	3.17	3.06	3.34	3.42	4.26	2.55	5.45
Il	1.08	1.17	1.13	1.29	1.43	1.55	0.80	1.89
Ap	0.35	0.19	0.31	0.45	0.31	0.54	0.24	0.68
Trace Elements (ppm)								
Ba	1030	522	485	820	579	1152	418	683
Rb	139	174	161	123	155	118	187	81
Sr	158	131	91	138	184	187	89	166
Y	43	38	35	61	40	50	95	81
Zr	326	189	187	303	225	400	246	397
Nb	17	16	17	23	14	18	22	28.6
Th	30	11	15	39	13	33	29	6.2
Pb	19	10	10	10	10	10	18	17
Ga	16	17	19	20	18	21	19	21
Zn	40	59	65	54	50	74	32	81
Cu	5	14	17	20	14	16	15	0
Ni	8	17	14	7	19	8	6	0
V	23	72	66	37	89	37	19	53
Cr	5	42	46	21	42	18	7	0

Table C.2.1. Continued.

Pluton Sample	Monzogranitic to Granodioritic Plutons								
	Chalet Lake Granite			Gayton Granite	Hammond River	Milkish Head Pluton			
	CW88- 243	CW88- 254	CW88- 263	NB91- 8108A	CW88- 200	NB90- 7012	NB92- 9107B	NB92- 9104A	
Major Elements (wt.%)									
SiO ₂	67.80	67.71	65.19	62.61	74.84	68.70	71.17	71.36	
TiO ₂	0.66	0.60	1.00	0.85	0.16	0.34	0.22	0.25	
Al ₂ O ₃	14.06	13.79	13.73	15.71	13.91	15.43	14.90	14.93	
Fe ₂ O ₃ ^T	5.52	5.14	7.13	5.00	1.33	3.19	2.22	2.47	
MnO	0.09	0.10	0.13	0.07	0.07	0.07	0.06	0.07	
MgO	1.22	1.22	1.91	1.96	1.08	1.05	0.82	0.98	
CaO	1.59	1.75	2.35	3.08	0.97	2.48	1.17	1.50	
Na ₂ O	2.93	3.46	2.90	4.30	3.95	3.44	3.47	3.43	
K ₂ O	4.70	4.89	3.00	3.92	3.27	2.88	3.25	2.84	
P ₂ O ₅	0.17	0.15	0.28	0.34	0.03	0.09	0.08	0.08	
LOI	1.00	0.80	2.00	2.90	0.40	1.20	1.50	1.20	
TOTAL	99.74	99.61	99.62	100.74	100.01	98.87	98.86	99.11	
CIPW Normative Mineralogy (0.5 Fe ratio)									
Q	27.84	23.48	29.87	14.25	35.72	31.43	35.73	36.57	
C	1.70	0.00	2.17	0.00	2.19	2.42	3.84	3.76	
Or	28.20	29.32	18.22	23.73	19.41	17.45	19.75	17.16	
Ab	25.18	29.70	25.23	37.28	33.57	29.85	30.19	29.68	
An	6.88	7.77	10.10	12.28	4.64	12.01	5.43	7.08	
Di	0.00	0.04	0.00	0.87	0.00	0.00	0.00	0.00	
Hy	4.46	4.40	6.47	5.40	3.12	3.59	2.78	3.25	
Mt	4.06	3.78	5.31	3.71	0.97	2.37	1.66	1.83	
Il	0.27	1.16	1.95	1.65	0.31	0.66	0.43	0.49	
Ap	0.40	0.35	0.67	0.81	0.07	0.21	0.19	0.19	
Trace Elements (ppm)									
Ba	794	764	909	1178	576	339	389	320	
Rb	133	168	81	101	95	78	98	72	
Sr	114	118	151	562	144	180	119	230	
Y	64	60	45	30	18	15	10	12	
Zr	388	340	433	344	84	122	90	98	
Nb	21	21	21	17	11	5	5	5	
Th	44	15	13	10	31	10	10	10	
Pb	10	10	10	12	10	10	36	10	
Ga	24	19	17	19	15	14	14	13	
Zn	83	99	76	59	38	29	36	27	
Cu	5	5	9	6	5	38	6	7	
Ni	7	8	11	13	5	5	5	6	
V	24	21	52	66	13	50	38	41	
Cr	5	14	17	23	8	8	17	12	

Table C.2.1. Continued.

Pluton	Monzogranitic to Granodioritic Plutons							Lepreau Har. Granodiorite
	Milkish Head Pluton		Hanson Stream Granodiorite					
	NB92-	NB92-	NB92	NB92-	NB92-	NB92-	NB92-	
Sample	9144	9149	9039	9044	9050	9154	9218	9084
Major Elements (wt.%)								
SiO ₂	65.60	69.73	65.13	67.82	66.48	67.43	69.73	65.81
TiO ₂	0.46	0.33	0.41	0.39	0.34	0.35	0.33	0.46
Al ₂ O ₃	15.49	15.75	16.40	16.19	16.31	15.72	15.65	15.59
Fe ₂ O ₃ ^T	4.43	3.14	4.63	4.86	3.73	3.80	2.79	4.50
MnO	0.09	0.08	0.10	0.07	0.08	0.08	0.07	0.09
MgO	2.29	1.10	2.14	1.64	1.49	1.55	1.30	1.96
CaO	3.34	1.73	3.65	1.12	3.76	3.69	2.48	2.81
Na ₂ O	2.49	3.62	3.36	4.19	3.25	3.12	3.66	3.37
K ₂ O	3.28	3.07	1.64	1.63	2.68	2.39	2.36	2.90
P ₂ O ₅	0.11	0.10	0.12	0.10	0.10	0.09	0.09	0.11
LOI	1.90	1.30	1.60	1.80	1.20	0.30	1.00	1.40
TOTAL	99.48	99.95	99.18	99.81	99.42	98.52	99.46	99.00
CIPW Normative Mineralogy (0.5 Fe ratio)								
Q	28.50	31.93	28.76	32.70	27.35	30.25	32.63	26.60
C	2.09	3.62	2.82	5.87	1.50	1.54	2.83	2.12
Or	19.91	18.42	9.95	9.85	16.15	14.41	14.18	17.60
Ab	21.64	31.10	29.20	36.26	28.05	26.93	31.50	29.28
An	16.28	8.05	17.79	5.02	18.36	18.07	11.91	13.58
Di	0.00	0.00	0.00	0.00	0.00	0.00	0.00	0.00
Hy	7.13	3.70	6.94	5.71	4.94	5.10	4.04	6.31
Mt	3.30	2.31	3.45	3.60	2.76	2.81	2.06	3.35
Il	0.90	0.64	0.80	0.76	0.66	0.68	0.64	0.90
Ap	0.25	0.24	0.29	0.24	0.24	0.21	0.21	0.26
Trace elements (ppm)								
Ba	414	347	222	156	306	193	341	315
Rb	125	83	38	45	71	73	57	91
Sr	183	190	297	180	222	207	209	156
Y	29	14	11	11	10	11	9	23
Zr	133	117	74	94	82	76	111	120
Nb	11	5	5	5	5	5	5	7
Th	17	10	10	14	13	10	10	12
Pb	11	10	10	13	10	10	11	10
Ga	16	16	15	16	16	17	17	16
Zn	59	40	52	57	32	37	37	45
Cu	40	5	5	5	6	6	5	23
Ni	21	5	6	6	5	7	5	10
V	101	53	93	86	72	72	42	79
Cr	61	10	16	12	11	13	10	18

Table C.2.1. Continued.

Pluton	Syenogranitic to Monzogranitic Plutons								
	Henderson Brook Granite			Musquash Harbour Pluton					
	NB91-8517	NE91-8532B	NB92-9141B	NB92-9158	NB92-9160	NB92-9200	NB92-9203	NB92-9156B	KC85-021
Major elements (wt. %)									
SiO ₂	74.89	72.93	76.37	70.12	68.82	76.45	76.33	74.15	78.20
TiO ₂	0.16	0.20	0.21	0.57	0.59	0.25	0.24	0.30	0.19
Al ₂ O ₃	13.72	14.23	13.02	13.74	13.80	11.82	12.26	13.03	12.00
Fe ₂ O ₃ ^T	1.62	1.95	1.77	3.38	3.51	1.50	1.39	1.58	0.92
MnO	0.02	0.07	0.05	0.04	0.04	0.02	0.02	0.03	0.02
MgO	0.35	0.57	0.54	1.25	0.82	0.06	0.09	0.43	0.30
CaO	0.70	1.09	0.14	0.97	1.72	0.35	0.16	0.66	1.33
Na ₂ O	3.43	4.16	3.67	2.97	2.17	2.76	2.80	2.78	3.65
K ₂ O	4.05	3.53	2.57	4.08	4.74	4.70	4.73	5.00	2.00
P ₂ O ₅	0.03	0.05	0.06	0.14	0.14	0.03	0.04	0.05	0.03
LOI	1.40	1.20	0.70	1.90	3.00	0.50	0.30	0.80	1.90
TOTAL	100.37	99.98	99.10	99.16	99.35	98.44	98.36	98.81	100.54
CIPW Normative Mineralogy (0.5 Fe ratio)									
Q	37.72	32.33	44.79	34.45	34.62	42.45	42.33	37.61	46.72
C	2.52	1.73	4.16	3.10	2.40	1.66	2.39	2.01	1.51
Or	24.20	21.14	15.45	24.83	29.12	28.38	28.52	30.17	11.99
Ab	29.35	35.67	31.58	25.88	19.09	23.86	24.18	24.02	31.32
An	3.31	5.15	0.31	4.01	7.92	1.57	0.54	3.01	6.49
Di	0.00	0.00	0.00	0.00	0.00	0.00	0.00	0.00	0.00
Hy	1.33	2.05	1.85	3.75	2.70	0.40	0.45	1.31	0.86
Mt	1.19	1.43	1.31	2.52	2.65	1.11	1.03	1.17	0.68
Il	0.31	0.39	0.41	1.12	1.17	0.49	0.47	0.58	0.37
Ap	0.07	0.12	0.14	0.33	0.34	0.07	0.10	0.12	0.07
Trace elements (ppm)									
Ba	336	332	390	653	664	603	507	518	240
Rb	114	106	68	137	176	190	180	173	84
Sr	58	148	61	84	86	56	42	57	79
Y	13	19	9	39	39	38	38	30	40
Zr	81	88	97	263	259	174	178	153	153
Nb	5	6	6	15	15	14	14	11	14.4
Th	10	10	10	17	17	20	16	18	15.5
Pb	10	10	10	14	12	21	15	13	16
Ga	12	13	12	15	15	16	14	14	0
Zn	14	30	33	48	33	25	19	27	57
Cu	5	5	5	8	5	5	5	5	1
Ni	5	5	5	6	6	5	5	5	8
V	13	21	15	44	51	5	5	16	4
Cr	17	5	7	9	16	9	28	7	4

Table C.2.1. Continued.

Pluton	Syenogranitic to Monzogranitic Plutons								
	Musquash Harbour Pluton			Jarvies Lake Syenogranite			Prince of Wales Granite		
	NB92-9162B	NB92-9202A	NB92-9204	NB91-8643A	NB92-9065A	NB92-9222	NB92-9177	NB92-9196	NB92-9199A
Major elements (wt. %)									
SiO ₂	62.91	53.79	55.95	76.70	77.95	77.95	72.81	72.70	73.02
TiO ₂	1.04	0.82	0.79	0.23	0.18	0.20	0.41	0.44	0.36
Al ₂ O ₃	15.22	17.00	17.36	11.97	11.51	11.51	13.72	13.64	13.71
Fe ₂ O ₃ ^T	7.37	9.17	8.12	0.76	1.23	1.16	1.79	2.49	1.85
MnO	0.10	0.16	0.15	0.03	0.03	0.01	0.03	0.04	0.04
MgO	2.13	4.56	3.84	0.04	0.06	0.11	0.65	0.48	0.64
CaO	2.85	7.29	5.72	0.67	0.12	0.05	1.23	0.77	0.84
Na ₂ O	2.95	2.06	2.58	3.13	2.77	3.11	2.59	3.02	3.11
K ₂ O	2.80	1.30	2.00	3.88	4.92	4.05	0.47	4.65	4.17
P ₂ O ₅	0.28	0.14	0.16	0.03	0.02	0.03	0.09	0.09	0.08
LOI	2.20	3.00	2.50	1.00	0.30	0.50	2.30	0.70	1.50
TOTAL	99.85	99.29	99.17	98.44	99.09	98.68	99.09	99.02	99.32
CIPW Normative Mineralogy (0.5 Fe ratio)									
Q	26.58	14.60	15.27	43.36	43.15	44.95	42.46	35.70	37.18
C	2.90	0.00	0.97	1.51	1.48	2.03	3.81	2.50	2.81
Or	17.01	8.02	12.28	23.54	29.45	24.39	21.20	27.98	25.21
Ab	25.66	18.19	22.68	27.19	23.74	26.82	22.66	26.02	26.93
An	12.65	34.75	28.39	3.21	0.47	0.05	5.70	3.29	3.73
Di	0.00	1.62	0.00	0.00	0.00	0.00	0.00	0.00	0.00
Hy	7.01	13.93	12.35	0.10	0.42	0.45	1.80	1.60	1.88
Mt	5.49	6.94	6.12	0.55	0.90	0.86	1.34	1.84	1.37
Il	2.03	1.63	1.56	0.45	0.35	0.39	0.81	0.85	0.70
Ap	0.67	0.34	0.39	0.07	0.05	0.07	0.22	0.21	0.19
Trace elements (ppm)									
Ba	619	218	353	414	325	473	222	582	550
Rb	118	47	67	109	205	129	143	174	129
Sr	159	224	255	48	26	41	37	92	74
Y	47	22	28	54	61	44	42	38	34
Zr	227	75	113	171	158	159	207	236	187
Nb	14	5	7	15	17	15	18	19	11
Th	12	10	10	20	30	20	24	25	16
Pb	10	11	11	10	15	10	10	16	12
Ga	20	18	19	16	15	15	16	17	14
Zn	77	88	91	12	32	13	20	31	75
Cu	28	68	52	5	5	5	5	5	10
Ni	14	31	22	5	5	5	5	5	5
V	129	222	196	7	5	5	29	23	28
Cr	36	59	48	10	8	5	14	6	13

Table C.2.1. Continued.

Pluton	Dipper Harbour Volcanic Unit							
	Harvey Hill Syenogranite			rhyolite ash flows				
	NB92- 9041	NB92- 9042	NB92- 9217	NB91- 9073	NB92- 9190	NB92- 9191C	NB92- 9243A	NB92- 9248
Major elements (wt. %)								
SiO ₂	76.05	78.24	73.43	76.81	74.98	76.22	76.70	76.08
TiO ₂	0.34	0.15	0.42	0.20	0.19	0.20	0.21	0.20
Al ₂ O ₃	12.74	12.20	13.15	12.11	12.67	12.08	12.26	12.32
Fe ₂ O ₃ ^T	1.98	1.01	2.29	1.79	1.81	1.65	1.61	1.64
MnO	0.04	0.01	0.04	0.03	0.04	0.04	0.01	0.03
MgO	0.23	0.03	0.55	0.11	0.16	0.28	0.24	0.06
CaO	0.64	0.14	0.48	0.33	0.90	0.83	0.01	0.37
Na ₂ O	3.14	2.93	2.71	2.45	2.14	2.32	2.01	2.51
K ₂ O	4.68	4.67	5.05	4.12	4.52	3.85	4.89	4.52
P ₂ O ₅	0.06	0.02	0.07	0.02	0.04	0.04	0.02	0.03
LOI	0.30	0.40	0.90	0.70	1.30	1.80	0.60	0.70
TOTAL	100.20	99.88	99.09	98.67	98.75	99.31	98.56	98.46
CIPW Normative Mineralogy (0.5 Fe ratio)								
Q	38.26	43.19	37.26	46.76	44.12	46.92	46.81	44.23
C	1.49	2.13	2.57	3.14	2.79	2.75	3.77	2.76
Or	27.71	27.75	30.42	24.87	27.43	23.35	29.52	27.34
Ab	26.62	24.93	23.38	21.18	18.60	20.15	17.37	21.74
An	2.79	0.57	1.96	1.54	4.32	3.96	0.00	1.68
Di	0.00	0.00	0.00	0.00	0.00	0.00	0.00	0.00
Hy	0.91	0.30	1.73	0.76	0.93	1.15	0.96	0.57
Mt	1.44	0.80	1.69	1.33	1.35	1.23	1.19	1.22
Il	0.65	0.29	0.81	0.39	0.37	0.39	0.41	0.39
Ap	0.14	0.05	0.17	0.05	0.10	0.10	0.05	0.07
Trace elements (ppm)								
Ba	511	40	528	612	682	726	868	700
Rb	175	184	189	140	164	117	168	157
Sr	27	5	37	33	35	49	33	33
Y	63	103	76	51	57	52	54	50
Zr	271	180	314	208	198	206	220	206
Nb	21	24	26	17	16	17	18	18
Th	26	29	28	23	21	16	23	20
Pb	17	17	15	10	16	16	24	10
Ga	15	19	16	15	15	14	17	14
Zn	39	15	37	37	43	40	48	31
Cu	5	5	7	5	5	5	29	5
Ni	5	5	5	5	5	5	5	5
V	11	6	14	5	5	5	7	5
Cr	5	8	14	7	5	7	11	5

Table C.2.1. Continued.

Pluton	Gabbroic Plutons							
	Duck Lake Pluton							
	CW88-224	CW88-256	CW88-259	DL91-02	DL91-07	DL91-09	DL91-13	CW90-836C
Sample	224	256	259	02	07	09	13	836C
Major elements (wt. %)								
SiO ₂	43.10	42.64	47.00	45.68	41.01	38.10	34.91	43.51
TiO ₂	0.15	0.07	0.28	0.24	1.36	0.05	0.16	0.10
Al ₂ O ₃ T	18.91	22.49	21.17	17.72	18.08	13.57	5.36	24.86
Fe ₂ O ₃ T	6.32	7.50	4.62	7.08	16.39	12.84	19.21	5.17
MnO	0.10	0.11	0.09	0.12	0.15	0.21	0.19	0.08
MgO	11.37	10.86	6.31	11.00	7.55	21.75	28.35	8.83
CaO	14.86	11.63	17.97	13.10	10.81	6.69	1.53	11.70
Na ₂ O	1.29	1.28	1.63	0.73	1.81	0.30	0.00	0.98
K ₂ O	0.11	0.31	0.15	0.16	0.40	0.06	0.01	0.15
P ₂ O ₅	4.70	4.10	1.40	2.80	2.30	7.80	11.10	3.30
LOI	0.01	0.03	0.01	0.00	0.03	0.01	0.00	0.00
TOTAL	100.92	101.02	100.63	98.63	99.89	101.38	100.82	98.68
CIPW Normative Mineralogy (0.5 Fe ratio)								
Q	0.00	0.00	0.00	0.00	0.00	0.00	0.00	0.00
C	0.00	0.00	0.00	0.00	0.00	0.94	2.89	1.91
Or	0.68	1.90	0.90	0.99	2.44	0.38	0.07	0.93
Ab	5.36	11.22	8.69	6.47	15.83	2.73	0.00	8.72
An	47.42	56.66	50.51	46.71	41.36	35.64	8.55	61.02
Ne	3.26	0.00	2.84	0.00	0.00	0.00	0.00	0.00
Di	23.08	2.28	31.05	16.79	11.04	0.00	0.00	0.00
Hy	0.00	2.34	0.00	21.94	2.19	15.94	33.34	18.32
Ol	15.10	19.77	2.08	1.25	12.13	34.23	39.12	4.97
Mt	4.78	5.63	3.38	5.38	12.28	10.02	15.69	3.94
Il	0.30	0.14	0.54	0.48	2.67	0.10	0.34	0.20
Ap	0.02	0.07	0.02	0.00	0.07	0.03	0.00	0.00
Trace elements (ppm)								
Ba	18	51	26	42	72	23	13	55
Rb	5	7	5	5	9	5	5	5
Sr	338	330	342	259	304	179	41	438
Y	5	5	8	9	21	5	5	5
Zr	38	36	40	13	33	6	5	6
Nb	5	5	5	5	5	5	5	5
Th	10	10	10	10	10	10	10	10
Pb	10	10	10	10	10	10	10	10
Ga	16	15	17	12	19	9	7	11
Zn	56	58	31	49	80	78	66	30
Cu	5	13	121	19	209	6	6	5
Ni	233	218	45	76	59	592	838	144
V	75	18	140	136	437	37	111	47
Cr	559	140	49	198	36	750	2926	354

Table C.2.1. Continued.

Pluton Sample	Indiantown Pluton		Basaltic and Andesitic Dykes						
	CW89- 529C	CW90- 835B	CW90- 776	CW90- 779	CW90- 791	CW90- 821B	CW90- 822B	CW90- 834	NB91- 8038
Major elements (wt. %)									
SiO ₂	46.55	43.32	51.89	47.21	48.26	51.51	52.31	46.22	48.71
TiO ₂	0.23	0.15	0.86	0.68	1.50	1.63	1.78	3.16	1.24
Al ₂ O ₃	18.32	27.64	18.29	14.93	13.97	13.52	13.40	13.34	15.53
Fe ₂ O ₃ ^T	7.08	4.26	8.82	9.41	14.03	14.58	14.29	15.39	12.24
MnO	0.19	0.07	0.15	0.17	0.21	0.25	0.21	0.26	0.22
MgO	9.31	4.44	4.71	11.56	6.89	5.42	4.50	5.69	8.01
CaO	11.27	13.47	7.17	8.96	9.71	7.39	7.07	9.93	8.11
Na ₂ O	1.60	1.07	2.94	1.29	2.00	2.98	2.65	2.39	1.75
K ₂ O	1.94	0.45	1.55	1.61	0.92	0.62	1.27	0.94	1.92
P ₂ O ₅	3.40	3.40	0.26	0.15	0.20	0.21	0.23	0.51	0.15
LOI	0.01	0.00	2.40	3.60	2.10	1.50	1.90	1.60	2.90
TOTAL	99.90	98.27	99.04	99.57	99.79	99.61	99.61	99.43	100.78
CIPW Normative Mineralogy (0.5 Fe ratio)									
Q	0.00	0.00	6.70	0.00	5.49	9.96	12.41	4.78	3.07
C	0.00	0.95	0.00	0.00	0.00	0.00	0.00	0.00	0.00
Or	11.92	2.81	9.52	9.96	5.61	3.76	7.74	5.72	11.66
Ab	14.08	9.56	25.86	11.43	17.45	25.89	23.12	20.83	15.22
An	38.56	70.59	33.40	31.61	27.24	22.27	21.57	23.59	29.66
Ne	0.00	0.00	0.00	0.00	0.00	0.00	0.00	0.00	0.00
Di	15.39	0.00	1.44	10.94	16.74	11.15	10.43	18.69	8.47
Hy	0.46	10.31	14.11	24.68	13.57	12.44	10.03	7.49	20.02
Ol	13.77	2.20	0.00	2.52	0.00	0.00	0.00	0.00	0.00
Mt	5.34	3.26	6.65	7.14	10.49	10.85	10.68	11.49	9.12
Il	0.45	0.30	1.70	1.35	2.94	3.18	3.49	6.18	2.42
Ap	0.02	0.00	0.63	0.36	0.48	0.50	0.55	1.22	0.36
Trace elements (ppm)									
Ba	250	32	220	180	153	153	261	344	296
Rb	129	21	60	82	29	19	41	28	66
Sr	158	358	389	206	212	173	159	246	143
Y	12	5	16	18	38	39	47	46	31
Zr	17	7	83	80	112	117	181	235	85
Nb	5	5	5	5	5	5	9	17	5
Th	21	10	10	10	10	10	10	10	10
Pb	18	11	10	10	10	10	22	18	10
Ga	15	12	19	14	18	21	22	21	16
Zn	248	42	94	92	97	138	132	138	91
Cu	31	19	44	80	118	96	41	68	87
Ni	123	60	30	213	64	37	20	61	113
V	117	62	168	253	406	461	428	361	284
Cr	366	54	33	729	134	30	21	110	256

Table C.2.1. Continued.

Pluton Sample	Dykes			Orthogneiss					
	NB91- 8507B	NB91- 8554	NB91- 8619	CW88- 132A	CW88- 178	CW88- 181A	CW89- 537	CW89- 598B	NB89- 629A
Major elements (wt. %)									
SiO ₂	50.29	50.44	50.72	67.69	66.38	67.82	67.62	69.56	69.64
TiO ₂	1.49	0.88	0.98	0.51	0.65	0.44	0.55	0.40	0.43
Al ₂ O ₃	13.53	15.50	15.58	15.44	15.77	14.55	15.57	14.90	15.28
Fe ₂ O ₃ ^T	14.59	10.95	11.34	3.83	4.06	3.29	3.66	3.11	3.16
MnO	0.24	0.20	0.22	0.08	0.07	0.08	0.07	0.08	0.07
MgO	6.74	8.17	7.24	2.38	2.23	2.09	2.33	1.92	1.92
CaO	8.19	10.50	9.87	3.55	3.20	3.23	3.78	2.13	3.47
Na ₂ O	1.89	2.11	2.02	3.83	3.39	4.45	3.62	4.09	3.87
K ₂ O	0.88	0.53	0.87	1.60	2.17	1.83	1.44	2.20	1.58
P ₂ O ₅	0.23	0.11	0.12	0.10	0.17	0.10	0.13	0.09	0.09
LOI	2.40	1.60	1.60	1.20	1.90	1.40	1.20	1.60	0.80
TOTAL	100.47	100.99	100.56	100.21	99.99	99.28	99.97	100.08	100.31
CIPW Normative Mineralogy (0.5 Fe ratio).									
Q	10.30	4.61	6.30	28.35	28.94	25.64	29.94	30.34	30.91
C	0.00	0.00	0.00	1.21	2.49	0.00	1.52	2.17	1.12
Or	5.34	3.17	5.23	9.57	13.10	11.07	8.63	13.22	9.40
Ab	16.43	18.06	17.37	32.79	29.30	38.53	31.07	35.19	32.96
An	26.54	31.62	31.38	17.16	15.08	14.66	18.16	10.15	16.73
Ne	0.00	0.00	0.00	0.00	0.00	0.00	0.00	0.00	0.00
Di	10.87	16.10	13.95	0.00	0.00	0.85	0.00	0.00	0.00
Hy	16.20	16.46	15.26	6.90	6.42	5.73	6.63	5.65	5.54
Ol	0.00	0.00	0.00	0.00	0.00	0.00	0.00	0.00	0.00
Mt	10.87	8.03	8.36	2.81	3.01	2.44	2.69	2.29	2.31
Il	2.91	1.69	1.89	0.98	1.26	0.86	1.06	0.77	0.82
Ap	0.55	0.26	0.28	0.23	0.40	0.24	0.31	0.21	0.21
Trace elements (ppm)									
Ba	474	87	242	294	461	378	226	396	314
Rb	36	16	24	84	91	71	76	94	70
Sr	164	175	170	136	170	194	141	192	144
Y	37	22	21	37	24	17	27	27	21
Zr	122	50	54	180	188	177	181	174	172
Nb	5	5	5	12	5	14	10	13	13
Th	10	10	10	25	15	28	24	23	20
Pb	10	10	10	14	10	12	10	10	10
Ga	17	17	19	16	17	16	16	15	14
Zn	134	90	90	49	59	42	46	42	39
Cu	141	152	97	8	10	18	27	11	8
Ni	66	81	61	22	22	13	20	13	14
V	415	287	300	70	85	62	68	60	57
Cr	145	236	192	43	48	28	34	34	30

Table C.2.1. Continued.

Pluton	Orthogneiss		hornblende gneiss	
	KC79- 097	NB91- 8551	CW89- 531	NB92- 9080
Major elements (wt. %)				
SiO ₂	66.45	69.48	60.83	56.87
TiO ₂	0.60	0.44	0.97	1.04
Al ₂ O ₃	15.85	15.05	15.85	16.91
Fe ₂ O ₃ ^T	4.07	3.64	7.47	8.04
MnO	0.07	0.07	0.16	0.16
MgO	2.00	2.08	3.83	4.62
CaO	3.96	2.61	4.97	6.32
Na ₂ O	3.55	2.94	1.80	2.74
K ₂ O	1.76	1.73	2.11	1.05
P ₂ O ₅	0.14	0.09	0.16	0.17
LOI	2.10	1.90	1.30	1.20
TOTAL	100.55	100.03	99.45	99.12
CIPW Normative Mineralogy (0.5 Fe ratio)				
Q	28.12	37.68	26.15	16.51
C	1.26	3.89	2.00	0.19
Or	10.58	10.44	12.75	6.36
Ab	30.57	25.40	15.58	23.77
An	19.06	12.62	24.15	31.01
Ne	0.00	0.00	0.00	0.00
Di	0.00	0.00	0.00	0.00
Hy	5.91	6.22	11.58	13.75
Ol	0.00	0.00	0.00	0.00
Mt	3.00	2.69	5.54	5.98
Il	1.16	0.85	1.88	2.03
Ap	0.33	0.21	0.38	0.40
Trace elements (ppm)				
Ba	467	355	338	104
Rb	65	61	86	39
Sr	236	157	158	196
Y	19	13	41	36
Zr	139	172	184	233
Nb	8	11	11	10
Th	7	10	10	10
Pb	2	10	16	10
Ga	0	15	19	18
Zn	24	41	81	78
Cu	10	8	24	18
Ni	41	24	52	57
V	80	63	149	167
Cr	32	26	84	94

APPENDIX C.3

MICROPROBE DATA FROM PLUTONIC UNITS

Table C.3.1. Amphibole analyses from plutonic units in the Brookville Terrane.

Pluton Sample	Dioritic to Granodioritic Plutons													
	Ludgate Lake Granodiorite								NB92-9195b					
	NB91-8590				NB91-8622				C-1	R-1	C-2	R-2	C-3	R-3
	1	2	3	4	1	2	3	4						
SiO ₂	48.78	50.28	47.77	47.88	47.79	47.91	48.47	47.96	50.84	50.72	49.55	47.71	48.32	50.37
TiO ₂	0.86	0.57	0.96	1.04	1.02	1.04	1.01	1.02	0.54	0.70	0.70	0.92	1.00	0.88
Al ₂ O ₃	5.57	4.36	6.27	6.13	6.10	6.68	5.75	6.02	3.61	3.71	5.09	6.27	6.72	4.93
FeO	13.43	12.78	13.79	13.80	13.95	13.92	13.66	14.41	13.21	12.97	13.63	13.79	13.19	13.13
MnO	0.73	0.76	0.69	0.70	0.85	0.64	0.69	0.70	0.92	0.82	0.81	0.90	0.86	1.11
MgO	14.46	14.79	13.86	13.96	13.79	13.88	14.24	14.14	15.72	15.61	14.47	13.99	15.21	15.09
CaO	11.17	11.33	10.96	10.92	11.71	11.64	11.84	11.90	12.03	11.56	11.93	11.21	10.57	10.86
Na ₂ O	1.26	0.79	1.48	1.30	1.20	1.32	1.05	1.23	0.73	0.93	1.02	1.38	1.64	1.18
K ₂ O	0.52	0.26	0.37	0.34	0.48	0.43	0.48	0.43	0.23	0.26	0.35	0.29	0.26	0.18
Cr ₂ O ₃	0.00	0.00	0.00	0.00	0.00	0.00	0.00	0.00	0.00	0.00	0.00	0.00	0.00	0.00
TOTAL	96.78	95.92	96.15	96.07	96.89	97.46	97.19	97.81	97.83	97.28	97.55	96.46	97.77	97.73

Number of ions on the basis of 23 oxygen.

Si	7.21	7.43	7.12	7.14	7.10	7.06	7.15	7.07	7.41	7.42	7.27	7.10	7.06	7.33
Al ^{iv}	0.79	0.57	0.88	0.86	0.90	0.94	0.85	0.93	0.59	0.58	0.73	0.90	0.95	0.67
Al ^{vi}	0.18	0.19	0.23	0.22	0.17	0.22	0.15	0.12	0.03	0.06	0.15	0.20	0.21	0.17
Ti	0.10	0.06	0.11	0.12	0.11	0.12	0.11	0.11	0.06	0.08	0.08	0.10	0.11	0.10
Cr	0.00	0.00	0.00	0.00	0.00	0.00	0.00	0.00	0.00	0.00	0.00	0.00	0.00	0.00
Fe	1.66	1.58	1.72	1.72	1.73	1.72	1.69	1.78	1.61	1.59	1.67	1.72	1.61	1.60
Mn	0.09	0.10	0.09	0.09	0.11	0.08	0.09	0.09	0.11	0.10	0.10	0.11	0.11	0.14
Mg	3.19	3.26	3.08	3.10	3.05	3.05	3.13	3.11	3.41	3.40	3.16	3.10	3.31	3.27
Ca	1.77	1.80	1.75	1.74	1.86	1.84	1.87	1.88	1.88	1.81	1.88	1.79	1.65	1.69
Na	0.36	0.23	0.43	0.38	0.35	0.38	0.30	0.35	0.21	0.26	0.29	0.40	0.46	0.33
K	0.10	0.05	0.07	0.07	0.09	0.08	0.09	0.08	0.04	0.05	0.07	0.06	0.05	0.03
Mg/Mg+Fe	0.66	0.67	0.64	0.64	0.64	0.64	0.65	0.64	0.68	0.68	0.65	0.64	0.67	0.67

C = core; R = rim

Table C.3.1. Continued.

Pluton Sample	Dioritic to Granodioritic Plutons										French Village Pluton			
	Ludgate Lake Granodiorite NB92-9251				Rockwood Park Granodiorite CW89-509A						CW88-144			
	1	2	3	4	C-1	R-1	C-2	R-2	C-3	C-4	C-1	R-1	C-2	R-2
SiO ₂	50.21	50.04	48.95	49.36	46.84	43.95	43.99	42.94	44.76	46.16	46.12	42.60	45.35	43.54
TiO ₂	0.75	0.67	0.73	0.62	1.71	1.34	1.31	1.35	1.46	1.29	1.38	1.35	1.20	1.40
Al ₂ O ₃	3.97	4.40	5.63	5.37	7.33	8.67	8.91	9.18	8.00	7.39	7.28	9.61	7.73	8.67
FeO	13.27	13.48	13.27	13.57	15.25	17.22	16.82	17.20	15.82	15.70	13.74	17.13	15.45	16.14
MnO	0.89	0.71	0.86	0.74	0.61	0.65	0.57	0.55	0.63	0.62	0.60	0.58	0.61	0.57
MgO	15.32	15.20	14.62	15.09	12.36	10.49	11.03	10.36	11.53	11.88	13.26	10.07	11.97	10.44
CaO	11.68	11.69	11.62	11.26	11.84	12.02	12.14	11.91	12.02	12.01	11.98	12.03	11.96	11.77
Na ₂ O	0.85	1.09	1.04	1.37	1.23	1.20	1.09	1.23	1.11	1.03	1.18	1.24	1.04	1.13
K ₂ O	0.34	0.34	0.36	0.27	0.64	1.11	1.08	1.15	0.91	0.82	0.62	1.08	0.78	1.15
Cr ₂ O ₃	0.00	0.00	0.00	0.00	0.00	0.00	0.00	0.00	0.00	0.00	0.06	0.07	0.04	0.05
TOTAL	97.28	97.62	97.08	97.65	97.81	96.65	96.94	95.87	96.24	96.90	96.22	95.76	96.13	94.86

Number of ions on the basis of 23 oxygen.

Si	7.37	7.32	7.21	7.22	6.94	6.71	6.68	6.62	6.80	6.94	6.92	6.58	6.87	6.74
Al ^{iv}	0.64	0.68	0.80	0.78	1.06	1.29	1.32	1.38	1.20	1.07	1.09	1.42	1.13	1.26
Al ^{vi}	0.05	0.08	0.18	0.15	0.22	0.27	0.28	0.29	0.24	0.24	0.20	0.33	0.25	0.32
Ti	0.08	0.07	0.08	0.07	0.19	0.15	0.15	0.16	0.17	0.15	0.16	0.16	0.14	0.16
Cr	0.00	0.00	0.00	0.00	0.00	0.00	0.00	0.00	0.00	0.00	0.01	0.01	0.01	0.01
Fe	1.63	1.65	1.63	1.66	1.89	2.20	2.14	2.22	2.01	1.97	1.72	2.21	1.96	2.09
Mn	0.11	0.09	0.11	0.09	0.08	0.08	0.07	0.07	0.08	0.08	0.08	0.08	0.08	0.08
Mg	3.35	3.31	3.21	3.29	2.73	2.39	2.50	2.38	2.61	2.66	2.96	2.32	2.70	2.41
Ca	1.84	1.83	1.83	1.77	1.88	1.97	1.98	1.97	1.96	1.93	1.93	1.99	1.94	1.95
Na	0.24	0.31	0.30	0.39	0.35	0.36	0.32	0.37	0.33	0.30	0.34	0.37	0.31	0.34
K	0.06	0.06	0.07	0.05	0.12	0.22	0.21	0.23	0.18	0.16	0.12	0.21	0.15	0.23
Mg/Mg+Fe	0.67	0.67	0.66	0.67	0.59	0.52	0.54	0.52	0.57	0.57	0.63	0.51	0.58	0.54

Table C.3.1. Continued.

Pluton Sample	Dioritic to Granodioritic Plutons													
	French Village Pluton								CW88-246					
	CW88-153													
	C-1	R-1	C-2	R-2	C-3	R-3	C-4	R-4	C-1	R-1	C-2	R-2	C-3	R-3
SiO ₂	43.70	43.89	43.61	43.92	44.60	46.01	43.80	44.13	43.90	45.28	43.91	47.53	42.23	46.19
TiO ₂	1.26	1.28	0.87	0.94	1.16	0.95	1.38	0.95	2.04	1.82	1.30	1.46	3.08	1.10
Al ₂ O ₃	9.31	9.11	9.30	9.10	9.13	7.96	8.98	9.67	12.22	9.86	12.25	7.74	10.64	9.27
FeO	14.88	15.34	15.08	15.51	14.69	13.80	15.28	15.54	12.07	13.66	13.15	13.22	15.56	12.82
MnO	0.42	0.45	0.42	0.40	0.38	0.43	0.43	0.40	0.21	0.29	0.31	0.34	0.35	0.29
MgO	11.74	11.65	10.81	11.36	11.79	12.45	11.94	10.74	13.19	13.02	12.76	14.42	12.14	13.93
CaO	11.73	11.95	11.91	11.54	11.94	11.99	10.79	11.86	12.25	12.12	12.01	11.59	11.75	12.06
Na ₂ O	1.30	1.39	1.12	1.37	1.24	0.94	1.44	1.16	1.45	1.06	1.45	1.02	1.05	1.04
K ₂ O	0.73	0.70	0.72	0.71	0.66	0.49	0.56	0.71	0.36	0.60	0.40	0.37	0.57	0.43
Cr ₂ O ₃	0.05	0.05	0.02	0.07	0.06	0.03	0.04	0.07	0.00	0.02	0.06	0.02	0.03	0.05
TOTAL	95.12	95.81	93.86	94.92	95.65	95.05	94.64	95.23	97.69	97.73	97.60	97.71	97.40	97.18

Number of ions on the basis of 23 oxygen.

Si	6.68	6.68	6.76	6.74	6.76	6.96	6.72	6.74	6.42	6.67	6.46	6.94	6.34	6.79
Al ^{iv}	1.32	1.32	1.24	1.26	1.24	1.04	1.28	1.26	1.58	1.33	1.54	1.06	1.67	1.21
Al ^{vi}	0.36	0.32	0.46	0.39	0.39	0.38	0.35	0.49	0.53	0.38	0.59	0.28	0.22	0.40
Ti	0.15	0.15	0.10	0.11	0.13	0.11	0.16	0.11	0.23	0.20	0.14	0.16	0.35	0.12
Cr	0.01	0.01	0.00	0.01	0.01	0.00	0.01	0.01	0.00	0.00	0.01	0.00	0.00	0.01
Fe	1.90	1.95	1.96	1.99	1.86	1.75	1.96	1.99	1.48	1.68	1.62	1.62	1.95	1.58
Mn	0.05	0.06	0.06	0.05	0.05	0.06	0.06	0.05	0.03	0.04	0.04	0.04	0.04	0.04
Mg	2.68	2.64	2.50	2.60	2.66	2.81	2.73	2.45	2.88	2.86	2.80	3.14	2.71	3.05
Ca	1.92	1.95	1.98	1.90	1.94	1.94	1.77	1.94	1.92	1.91	1.89	1.81	1.89	1.90
Na	0.39	0.41	0.34	0.41	0.36	0.28	0.43	0.34	0.41	0.30	0.41	0.29	0.31	0.30
K	0.14	0.14	0.14	0.14	0.13	0.10	0.11	0.14	0.07	0.11	0.08	0.07	0.11	0.08
Mg/Mg+Fe	0.58	0.58	0.56	0.57	0.59	0.62	0.58	0.55	0.66	0.63	0.63	0.66	0.58	0.66

Table C.3.1. Continued.

Pluton Sample	Dioritic to Granodioritic Plutons												
	French Village Pluton CW88-246				Belmont Tonalite NB91-8513					NB91-8522			
	C-4	R-4	R-5	R-6	1	2	3	4	5	1	2	3	4
SiO ₂	43.10	46.92	47.65	46.76	47.40	46.92	46.31	48.20	46.41	48.35	47.98	47.82	48.31
TiO ₂	1.70	1.78	1.11	0.96	0.80	0.87	0.69	0.56	0.78	0.75	0.71	0.95	0.65
Al ₂ O ₃	12.74	8.38	8.42	8.41	6.73	6.89	7.62	6.37	7.61	6.28	6.68	6.66	6.03
FeO	13.00	12.12	13.43	13.03	14.73	14.62	15.10	13.37	15.24	13.61	13.87	14.37	13.95
MnO	0.26	0.24	0.27	0.27	0.56	0.64	0.36	0.52	0.54	0.43	0.50	0.69	0.25
MgO	12.79	13.18	13.62	13.83	13.12	13.01	12.53	13.89	12.54	13.94	13.86	13.51	13.81
CaO	12.13	12.76	12.02	12.13	11.30	11.51	11.44	11.72	11.31	11.42	11.50	10.83	11.47
Na ₂ O	1.62	0.84	0.94	0.91	0.95	0.94	1.08	0.93	1.09	1.03	0.99	1.14	0.90
K ₂ O	0.27	0.37	0.41	0.34	0.64	0.59	0.79	0.52	0.80	0.49	0.59	0.62	0.52
Cr ₂ O ₃	0.03	0.00	0.05	0.03	0.00	0.00	0.00	0.00	0.00	0.00	0.00	0.00	0.00
TOTAL	97.64	96.59	97.92	96.67	96.23	95.99	95.92	96.08	96.32	96.30	96.68	96.59	95.89

Number of ions on the basis of 32 oxygen.

Si	6.35	6.92	6.95	6.91	7.09	7.05	6.98	7.17	6.98	7.17	7.11	7.11	7.21
Al ^{IV}	1.65	1.08	1.05	1.09	0.91	0.95	1.02	0.83	1.03	0.83	0.89	0.89	0.80
Al ^{VI}	0.56	0.37	0.40	0.37	0.28	0.27	0.34	0.29	0.32	0.27	0.28	0.28	0.27
Ti	0.19	0.20	0.12	0.11	0.09	0.10	0.08	0.06	0.09	0.08	0.08	0.11	0.07
Cr	0.00	0.00	0.01	0.00	0.00	0.00	0.00	0.00	0.00	0.00	0.00	0.00	0.00
Fe	1.60	1.49	1.64	1.61	1.84	1.84	1.90	1.66	1.92	1.69	1.72	1.79	1.74
Mn	0.03	0.03	0.03	0.03	0.07	0.08	0.05	0.07	0.07	0.05	0.06	0.09	0.03
Mg	2.81	2.90	2.96	3.05	2.93	2.91	2.82	3.08	2.81	3.08	3.06	2.99	3.07
Ca	1.91	2.02	1.88	1.92	1.81	1.85	1.85	1.87	1.82	1.82	1.83	1.73	1.83
Na	0.46	0.24	0.27	0.26	0.28	0.27	0.32	0.27	0.32	0.30	0.29	0.33	0.26
K	0.05	0.07	0.08	0.06	0.12	0.11	0.15	0.10	0.15	0.09	0.11	0.12	0.10
Mg/Mg+Fe	0.64	0.66	0.64	0.65	0.61	0.61	0.60	0.65	0.60	0.65	0.64	0.63	0.64

Table C.3.1. Continued.

Pluton Sample	Dioritic to Granodioritic Plutons Perch Lake Granodiorite								Shadow Lake Granodiorite				NB91-8599-B	
	NB92-9027								NB91-8565					
	C-1	R-1	C-2	R-2	C-3	R-3	C-4	R-4	1	2	3	4	1	2
SiO ₂	44.94	46.33	45.32	45.33	46.22	46.31	45.18	45.49	47.87	45.78	47.21	46.93	46.55	46.34
TiO ₂	1.46	0.95	1.38	0.92	1.32	0.98	1.09	0.98	0.99	1.21	1.34	1.32	1.11	1.20
Al ₂ O ₃	7.38	7.27	7.53	7.64	7.16	6.73	7.85	7.48	6.02	7.64	6.98	6.56	6.82	6.71
FeO	17.04	16.86	17.03	17.21	16.86	16.75	16.94	16.92	13.68	14.96	14.21	14.33	16.51	16.67
MnO	0.49	0.52	0.35	0.53	0.59	0.55	0.51	0.44	0.60	0.71	0.71	0.75	0.60	0.55
MgO	11.49	11.93	11.79	11.73	12.10	12.32	11.28	11.59	13.92	12.71	13.29	13.51	12.02	11.96
CaO	12.01	12.07	11.78	11.74	11.67	11.87	11.69	11.83	11.47	11.08	11.30	11.20	12.08	11.82
Na ₂ O	1.37	1.11	1.33	1.15	1.26	1.21	1.36	1.44	0.88	1.15	1.06	1.30	1.32	1.12
K ₂ O	0.86	0.72	0.80	0.86	0.74	0.79	0.76	0.78	0.54	0.70	0.59	0.49	0.71	0.72
Cr ₂ O ₃	0.00	0.00	0.00	0.00	0.00	0.00	0.00	0.00	0.00	0.00	0.00	0.00	0.00	0.00
TOTAL	97.04	97.76	97.31	97.11	97.92	97.51	96.66	96.95	95.97	95.94	96.69	96.39	97.72	97.09

Number of ions on the basis of 23 oxygen.

Si	6.82	6.93	6.83	6.85	6.91	6.95	6.85	6.88	7.15	6.91	7.02	7.02	6.96	6.98
Al ^{iv}	1.19	1.07	1.17	1.15	1.09	1.05	1.15	1.12	0.85	1.09	0.98	0.98	1.04	1.02
Al ^{vi}	0.14	0.21	0.17	0.22	0.17	0.14	0.26	0.22	0.21	0.27	0.25	0.18	0.17	0.17
Ti	0.17	0.11	0.16	0.11	0.15	0.11	0.12	0.11	0.11	0.14	0.15	0.15	0.13	0.14
Cr	0.00	0.00	0.00	0.00	0.00	0.00	0.00	0.00	0.00	0.00	0.00	0.00	0.00	0.00
Fe	2.16	2.11	2.15	2.18	2.11	2.10	2.15	2.14	1.71	1.89	1.77	1.79	2.07	2.10
Mn	0.06	0.07	0.05	0.07	0.08	0.07	0.07	0.06	0.08	0.09	0.09	0.10	0.08	0.07
Mg	2.60	2.66	2.65	2.64	2.70	2.76	2.55	2.61	3.10	2.86	2.95	3.01	2.68	2.68
Ca	1.95	1.94	1.90	1.90	1.87	1.91	1.90	1.92	1.84	1.79	1.80	1.80	1.94	1.91
Na	0.40	0.32	0.39	0.34	0.37	0.35	0.40	0.42	0.26	0.34	0.31	0.38	0.38	0.33
K	0.17	0.14	0.15	0.17	0.14	0.15	0.15	0.15	0.10	0.14	0.11	0.09	0.14	0.14
Mg/Mg+Fe	0.55	0.56	0.55	0.55	0.56	0.57	0.54	0.55	0.65	0.60	0.63	0.63	0.57	0.56

Table C.3.1. Continued.

Pluton Sample	Dioritic to Granodioritic Plutons					Enclave				Talbot Road Granodiorite				
	Shadow Lake		Granodiorite			NB91-8597				NB92-9045				
	NB91-8599-B		NB92-9033			C-1	R-1	C-2	R-2	C-1	R-1	C-2	R-2	C-3
	3	4	1	2	3									
SiO ₂	46.52	45.94	46.37	46.41	47.05	47.05	46.23	46.79	45.87	45.90	46.15	45.84	45.37	45.84
TiO ₂	1.19	0.96	0.94	0.90	0.86	0.91	1.19	0.93	1.24	1.88	1.03	1.90	1.54	1.74
Al ₂ O ₃	7.08	7.14	6.25	6.71	5.66	6.90	7.57	6.79	7.59	7.42	7.35	7.42	7.41	7.34
FeO	16.70	16.66	16.24	16.84	16.24	15.36	15.43	14.71	15.42	14.66	16.49	15.78	16.03	16.33
MnO	0.40	0.53	1.14	1.13	1.09	0.00	0.47	0.36	0.57	0.41	0.59	0.52	0.70	0.56
MgO	12.03	11.80	12.24	11.80	12.42	12.89	12.26	12.84	12.33	13.19	12.46	12.46	12.05	12.47
CaO	11.97	12.04	11.57	11.63	11.43	11.57	11.45	11.49	11.48	11.77	11.82	11.58	11.72	11.37
Na ₂ O	1.30	1.21	1.52	1.27	1.16	1.04	1.07	1.02	1.07	1.26	1.19	1.44	1.29	1.51
K ₂ O	0.73	0.66	0.57	0.70	0.52	0.49	0.47	0.55	0.76	0.87	0.70	0.82	0.83	0.79
Cr ₂ O ₃	0.00	0.00	0.00	0.00	0.00	0.00	0.00	0.00	0.00	0.00	0.00	0.00	0.00	0.00
TOTAL	97.92	96.94	96.84	97.39	96.43	96.21	96.14	95.48	96.33	97.36	97.78	97.76	96.94	97.95

Number of ions on the basis of 23 oxygen.

Si	6.94	6.93	7.01	6.99	7.11	7.05	6.96	7.06	6.91	6.84	6.89	6.84	6.85	6.84
Al ^{iv}	1.06	1.07	0.99	1.01	0.89	0.95	1.04	0.94	1.09	1.16	1.11	1.16	1.16	1.16
Al ^{vi}	0.19	0.20	0.12	0.18	0.12	0.27	0.30	0.27	0.26	0.14	0.19	0.14	0.16	0.13
Ti	0.13	0.11	0.11	0.10	0.10	0.10	0.14	0.11	0.14	0.21	0.12	0.21	0.18	0.20
Cr	0.00	0.00	0.00	0.00	0.00	0.00	0.00	0.00	0.00	0.00	0.00	0.00	0.00	0.00
Fe	2.08	2.10	2.05	2.12	2.05	1.93	1.94	1.86	1.94	1.83	2.06	1.97	2.02	2.04
Mn	0.05	0.07	0.15	0.14	0.14	0.00	0.06	0.05	0.07	0.05	0.08	0.07	0.09	0.07
Mg	2.68	2.65	2.76	2.65	2.80	2.88	2.75	2.89	2.77	2.93	2.77	2.77	2.71	2.77
Ca	1.91	1.95	1.87	1.88	1.85	1.86	1.85	1.86	1.85	1.88	1.89	1.85	1.90	1.82
Na	0.38	0.35	0.45	0.37	0.34	0.30	0.31	0.30	0.31	0.36	0.35	0.42	0.38	0.44
K	0.14	0.13	0.11	0.13	0.10	0.09	0.09	0.11	0.15	0.17	0.13	0.16	0.16	0.15
Mg/Mg+Fe	0.56	0.56	0.57	0.56	0.58	0.60	0.59	0.61	0.59	0.62	0.57	0.59	0.57	0.58

Table C.3.1. Continued.

Pluton Sample	Dioritic to Granodioritic Plutons									Renforth Pluton				
	Talbot Road Granodiorite				NB92-9153					CW88-169				
	NB92-9045				C-1	R-1	C-2	R-2	R-3	C-1	R-1	C-2	R-2	C-3
SiO ₂	45.85	46.56	48.13	46.02	46.34	46.84	48.73	46.53	46.00	46.03	47.77	45.04	45.39	44.57
TiO ₂	1.56	1.69	0.94	1.44	1.43	0.97	0.84	0.84	1.18	1.56	0.93	1.83	1.69	1.20
Al ₂ O ₃	7.26	6.91	6.06	7.03	7.36	7.00	5.12	6.82	7.08	7.77	7.20	7.85	8.00	7.83
FeO	15.27	13.82	15.41	16.64	13.98	14.99	14.56	15.70	15.97	15.83	15.29	15.55	15.44	15.59
MnO	0.59	0.31	0.51	0.61	0.40	0.50	0.50	0.65	0.56	0.54	0.45	0.50	0.53	0.45
MgO	13.17	13.75	13.15	12.34	13.43	13.26	14.10	12.60	12.29	11.76	12.66	11.66	11.84	12.18
CaO	11.62	11.60	12.30	11.61	11.71	11.84	11.91	11.77	11.77	11.88	12.31	12.17	12.09	12.41
Na ₂ O	1.40	1.37	0.93	1.37	1.29	1.29	0.86	1.20	1.20	1.16	0.94	1.14	1.13	0.89
K ₂ O	0.79	0.69	0.60	0.70	0.69	0.69	0.42	0.64	0.63	0.92	0.76	0.98	0.93	0.78
Cr ₂ O ₃	0.00	0.00	0.00	0.00	0.00	0.00	0.00	0.00	0.00	0.00	0.00	0.00	0.00	0.00
TOTAL	97.51	96.70	98.03	97.76	96.63	97.38	97.04	96.75	96.68	97.45	98.31	96.72	97.04	95.90

Number of ions on the basis of 23 oxygen.

Si	6.84	6.94	7.11	6.89	6.92	6.97	7.22	6.99	6.93	6.88	7.03	6.80	6.82	6.79
Al ^{iv}	1.16	1.06	0.89	1.11	1.09	1.03	0.78	1.01	1.07	1.12	0.97	1.20	1.18	1.21
Al ^{vi}	0.12	0.15	0.16	0.13	0.21	0.20	0.11	0.20	0.19	0.25	0.28	0.20	0.24	0.19
Ti	0.18	0.19	0.10	0.16	0.16	0.11	0.09	0.10	0.13	0.18	0.10	0.21	0.19	0.14
Cr	0.00	0.00	0.00	0.00	0.00	0.00	0.00	0.00	0.00	0.00	0.00	0.00	0.00	0.00
Fe	1.91	1.72	1.90	2.08	1.75	1.87	1.80	1.97	2.01	1.98	1.88	1.96	1.94	1.99
Mn	0.08	0.04	0.06	0.08	0.05	0.06	0.06	0.08	0.07	0.07	0.06	0.06	0.07	0.06
Mg	2.93	3.05	2.89	2.75	2.99	2.94	3.11	2.82	2.76	2.62	2.78	2.62	2.65	2.77
Ca	1.86	1.85	1.95	1.86	1.87	1.89	1.89	1.90	1.90	1.90	1.94	1.97	1.95	2.03
Na	0.41	0.40	0.27	0.40	0.37	0.37	0.25	0.35	0.35	0.34	0.27	0.33	0.33	0.26
K	0.15	0.13	0.11	0.13	0.13	0.13	0.08	0.12	0.12	0.18	0.14	0.19	0.18	0.15
Mg/Mg+Fe	0.61	0.64	0.60	0.57	0.63	0.61	0.63	0.59	0.58	0.57	0.60	0.57	0.58	0.58

Table C.3.1. Continued.

Pluton Sample	Dioritic to Granodioritic Plutons						Narrows Tonalite								
	Renforth Pluton						CW89-616								
	R-3	CW88-189		CW88-192			C-1	R-1	C-2	R-2	C-3	R-3	C-4	R-4	
SiO ₂	56.15	51.49	51.29	50.50	51.06	49.37	50.26	47.96	49.07	46.40	48.23	46.41	49.57	48.64	
TiO ₂	1.57	0.50	0.51	0.58	0.48	0.75	0.85	1.34	0.93	1.53	1.45	1.80	0.65	1.20	
Al ₂ O ₃	7.77	3.56	4.05	4.43	3.96	4.40	6.43	7.51	6.81	8.07	7.77	8.53	5.79	7.51	
FeO	16.00	11.60	11.90	12.16	12.19	12.86	11.66	12.14	12.60	12.27	11.82	12.75	11.46	11.90	
MnO	0.41	0.97	0.97	0.84	0.82	0.72	0.44	0.38	0.39	0.31	0.28	0.30	0.31	0.33	
MgO	11.81	16.14	16.18	15.99	15.99	14.48	15.87	15.33	15.51	15.23	15.38	14.18	16.38	15.57	
CaO	12.10	11.96	11.88	11.74	11.60	11.86	11.71	11.49	11.12	11.59	11.63	12.01	11.40	11.46	
Na ₂ O	1.09	0.76	0.91	0.87	0.85	0.68	0.90	0.95	0.86	1.10	1.06	0.80	0.87	0.91	
K ₂ O	0.93	0.24	0.27	0.25	0.25	0.31	0.18	0.25	0.19	0.29	0.28	0.32	0.15	0.27	
Cr ₂ O ₃	0.00	0.00	0.00	0.00	0.02	0.02	0.06	0.06	0.04	0.00	0.03	0.08	0.33	0.07	
TOTAL	97.83	97.22	97.96	97.36	97.22	95.45	98.36	97.41	97.52	96.79	97.93	97.18	96.91	97.86	
Number of ions on the basis of 23 oxygen.															
Si	6.88	7.48	7.41	7.35	7.43	7.37	7.20	6.98	7.12	6.83	6.97	6.82	7.21	7.03	
Al ^{iv}	1.12	0.52	0.59	0.65	0.57	0.64	0.80	1.02	0.88	1.17	1.03	1.18	0.79	0.97	
Al ^{vi}	0.24	0.09	0.10	0.11	0.11	0.14	0.29	0.27	0.29	0.23	0.30	0.29	0.20	0.31	
Ti	0.18	0.06	0.06	0.06	0.05	0.08	0.09	0.15	0.10	0.17	0.16	0.20	0.07	0.13	
Cr	0.00	0.00	0.00	0.00	0.00	0.00	0.01	0.01	0.01	0.00	0.00	0.01	0.04	0.01	
Fe	1.99	1.41	1.44	1.48	1.48	1.60	1.40	1.48	1.53	1.51	1.43	1.57	1.39	1.44	
Mn	0.05	0.12	0.12	0.10	0.10	0.09	0.05	0.05	0.05	0.04	0.03	0.04	0.04	0.04	
Mg	2.62	3.50	3.48	3.47	3.47	3.22	3.39	3.33	3.36	3.34	3.31	3.10	3.55	3.35	
Ca	1.93	1.86	1.84	1.83	1.81	1.90	1.80	1.79	1.73	1.83	1.80	1.89	1.78	1.77	
Na	0.32	0.21	0.26	0.25	0.24	0.20	0.25	0.27	0.24	0.31	0.30	0.23	0.25	0.26	
K	0.18	0.04	0.05	0.05	0.05	0.06	0.03	0.05	0.04	0.05	0.05	0.06	0.03	0.05	
Mg/Mg+Fe	0.57	0.71	0.71	0.70	0.70	0.67	0.71	0.69	0.69	0.69	0.70	0.67	0.72	0.70	

Table C.3.1. Continued.

Pluton Sample	Narrows Tonalite		Monsogranitic to Granodioritic Plutons						Milkish Head Pluton				
	CW89-616		Fairville Granite				Chalet Lake Granite		NB92-9144				
	R-5	5-6	1	2	3	4	C-1	C-2	R-2	1	2	3	4
SiO ₂	48.20	46.86	42.17	41.33	42.73	42.94	40.63	40.44	40.28	49.51	48.25	48.22	46.82
TiO ₂	1.09	0.42	1.62	1.80	0.85	1.89	1.26	2.09	1.87	0.56	0.70	1.29	1.59
Al ₂ O ₃	7.05	8.94	8.77	8.97	8.20	9.03	9.69	9.25	9.40	4.57	5.94	6.56	6.74
FeO	11.96	14.40	25.55	25.02	26.14	22.91	25.16	24.87	24.66	13.40	14.31	11.96	13.60
MnO	0.35	0.43	0.69	0.62	0.75	0.42	0.84	0.86	0.87	0.80	0.67	0.45	0.52
MgO	15.50	12.83	5.39	5.41	5.32	6.92	4.56	4.37	4.28	14.83	14.34	15.36	14.11
CaO	11.36	12.32	10.03	9.55	9.68	9.90	10.51	10.18	10.41	11.65	11.52	11.37	11.38
Na ₂ O	0.96	0.78	1.61	1.72	1.59	1.69	1.50	1.99	2.05	1.15	1.01	1.23	1.50
K ₂ O	0.23	0.04	0.95	0.95	0.73	1.18	1.31	1.44	1.29	0.32	0.56	0.50	0.60
Cr ₂ O ₃	0.08	0.12	0.00	0.02	0.01	0.02	0.10	0.12	0.09	0.00	0.00	0.00	0.00
TOTAL	96.78	97.14	96.78	95.39	96.00	96.90	95.66	95.61	95.20	96.79	97.31	96.94	96.85

Number of ions on the basis of 23 oxygen.

Si	7.05	6.92	6.68	6.64	6.82	6.69	6.55	6.54	6.53	7.31	7.13	7.06	6.95
Al ^{iv}	0.95	1.08	1.32	1.37	1.18	1.31	1.45	1.47	1.47	0.69	0.87	0.94	1.05
Al ^{vi}	0.27	0.47	0.32	0.33	0.37	0.35	0.40	0.30	0.33	0.12	0.17	0.19	0.12
Ti	0.12	0.05	0.19	0.22	0.10	0.22	0.15	0.25	0.23	0.07	0.07	0.14	0.18
Cr	0.01	0.01	0.00	0.00	0.00	0.00	0.01	0.02	0.01	0.00	0.00	0.00	0.00
Fe	1.46	1.78	3.39	3.36	3.49	2.99	3.39	3.36	3.35	1.66	1.77	1.47	1.68
Mn	0.04	0.05	0.09	0.08	0.10	0.06	0.12	0.12	0.12	0.09	0.09	0.05	0.07
Mg	3.38	2.82	1.27	1.29	1.27	1.61	1.10	1.05	1.04	3.27	3.15	3.36	3.13
Ca	1.78	1.95	1.70	1.64	1.66	1.65	1.83	1.76	1.81	1.84	1.82	1.79	1.82
Na	0.27	0.22	0.50	0.54	0.49	0.51	0.47	0.62	0.65	0.32	0.30	0.35	0.44
K	0.04	0.01	0.19	0.20	0.15	0.24	0.27	0.30	0.27	0.07	0.12	0.09	0.12
Mg/Mg+Fe	0.70	0.61	0.27	0.28	0.27	0.35	0.24	0.24	0.24	0.66	0.64	0.70	0.65

Table C.3.1. Continued.

Pluton Sample	Monsogranitic to Granodioritic Plutons Hanson Stream Granodiorite													
	NB92-9039						NB92-9050							
	C-1	R-1	C-2	R-2	R-3	R-4	C-1	R-1	C-2	R-2	C-3	R-3	R-4	R-5
SiO ₂	47.39	46.99	47.89	47.32	46.69	46.71	47.64	47.67	50.39	50.72	51.18	50.63	47.49	48.21
TiO ₂	1.45	1.40	1.08	0.79	0.97	0.94	1.19	1.04	0.44	0.46	0.24	0.55	1.09	1.10
Al ₂ O ₃	6.72	6.79	6.31	6.27	6.72	6.71	6.68	6.56	4.60	4.78	3.98	4.14	6.78	6.12
FeO	13.71	15.29	14.01	15.07	15.42	16.35	13.94	14.08	13.25	13.47	13.39	13.20	13.87	13.24
MnO	0.62	0.93	0.56	0.64	0.71	0.63	0.73	0.85	0.67	0.91	0.69	0.74	0.71	0.62
MgO	14.17	12.75	14.31	13.19	12.63	12.57	14.23	14.02	15.21	14.96	15.40	15.29	14.41	14.93
CaO	11.39	11.11	11.47	11.98	11.87	11.78	12.02	12.06	12.12	12.28	12.38	12.33	11.58	11.61
Na ₂ O	1.24	1.23	1.24	1.00	1.04	0.10	1.34	1.17	0.95	0.88	0.89	0.84	1.45	1.43
K ₂ O	0.41	0.46	0.53	0.58	0.62	0.59	0.63	0.55	0.28	0.40	0.23	0.26	0.59	0.53
Cr ₂ O ₃	0.00	0.00	0.00	0.00	0.00	0.00	0.00	0.00	0.00	0.00	0.00	0.00	0.00	0.00
TOTAL	97.10	96.95	97.40	96.84	96.67	96.38	98.40	98.00	97.91	98.86	98.38	97.98	97.97	97.79

Number of ions on the basis of 23 oxygen.

Si	7.00	7.02	7.07	7.07	7.01	7.03	6.98	7.02	7.34	7.33	7.41	7.37	6.98	7.07
Al ^{iv}	1.00	0.99	0.94	0.93	0.99	0.97	1.02	0.99	0.66	0.67	0.59	0.63	1.02	0.93
Al ^{vi}	0.18	0.21	0.16	0.18	0.20	0.23	0.14	0.15	0.13	0.14	0.09	0.08	0.16	0.12
Ti	0.16	0.16	0.12	0.09	0.11	0.11	0.13	0.12	0.05	0.05	0.03	0.06	0.12	0.12
Cr	0.00	0.00	0.00	0.00	0.00	0.00	0.00	0.00	0.00	0.00	0.00	0.00	0.00	0.00
Fe	1.70	1.91	1.73	1.88	1.94	2.06	1.71	1.73	1.61	1.63	1.62	1.61	1.71	1.62
Mn	0.08	0.12	0.07	0.08	0.09	0.08	0.09	0.11	0.08	0.11	0.09	0.09	0.09	0.08
Mg	3.12	2.84	3.15	2.94	2.83	2.82	3.11	3.08	3.30	3.22	3.33	3.32	3.16	3.26
Ca	1.80	1.78	1.81	1.92	1.91	1.90	1.89	1.90	1.89	1.90	1.92	1.92	1.82	1.82
Na	0.36	0.36	0.36	0.29	0.30	0.03	0.38	0.33	0.27	0.25	0.25	0.24	0.41	0.41
K	0.08	0.09	0.10	0.11	0.12	0.11	0.12	0.10	0.05	0.07	0.04	0.05	0.11	0.10
Mg/Mg+Fe	0.65	0.60	0.65	0.61	0.59	0.58	0.65	0.64	0.67	0.66	0.67	0.67	0.65	0.67

Table C.3.1. Continued.

Pluton Sample	Monzogranitic to Granodioritic Plutons Hanson Stream Granodiorite NB92-9154							Syenogranitic to Monzogranitic Plutons Musquash Harbour Pluton (tonalite) NB92-9202A					
	C-1	R-1	C-2	R-2	R-3	R-4	R-5	1	2	3	4	5	6
	SiO ₂	47.13	49.02	47.38	48.65	48.35	48.16	49.65	47.31	46.32	46.02	47.98	46.52
TiO ₂	0.88	0.83	1.09	0.73	0.97	0.79	0.73	1.16	1.34	1.31	0.66	1.19	0.98
Al ₂ O ₃	6.29	5.15	6.76	5.06	5.97	5.83	5.08	6.56	7.22	6.93	5.84	7.15	8.01
FeO	14.65	13.46	14.51	14.13	13.96	14.43	13.50	16.03	16.96	16.51	15.58	16.29	15.80
MnO	0.74	0.84	0.75	0.78	0.77	0.57	0.75	0.47	0.37	0.27	0.53	0.39	0.33
MgO	13.26	14.15	13.09	13.80	13.86	13.88	14.74	12.94	11.96	12.15	12.93	12.95	13.20
CaO	11.90	12.03	12.22	12.03	11.79	11.95	12.15	11.44	11.35	11.59	11.76	11.56	10.44
Na ₂ O	1.12	0.99	1.14	1.04	1.26	1.02	1.02	0.96	1.10	1.12	0.94	1.30	1.04
K ₂ O	0.56	0.38	0.52	0.46	0.53	0.47	0.39	0.52	0.63	0.66	0.38	0.73	0.51
Cr ₂ O ₃	0.00	0.00	0.00	0.00	0.00	0.25	0.00	0.00	0.00	0.00	0.00	0.00	0.00
TOTAL	96.53	96.85	97.46	96.68	97.46	97.35	98.01	97.39	97.25	96.56	96.60	98.08	98.43

Number of ions on the basis of 23 oxygen

Si	7.06	7.25	7.02	7.24	7.13	7.13	7.25	7.04	6.95	6.95	7.18	6.91	7.02
Al ^{iv}	0.94	0.75	0.98	0.76	0.87	0.87	0.75	0.96	1.05	1.05	0.82	1.09	0.98
Al ^{vi}	0.17	0.15	0.21	0.13	0.17	0.14	0.12	0.19	0.22	0.18	0.21	0.16	0.40
Ti	0.10	0.09	0.12	0.08	0.11	0.09	0.08	0.13	0.15	0.15	0.07	0.13	0.11
Cr	0.00	0.00	0.00	0.00	0.00	0.03	0.00	0.00	0.00	0.00	0.00	0.00	0.00
Fe	1.84	1.67	1.80	1.76	1.72	1.79	1.65	2.00	2.13	2.09	1.95	2.02	1.93
Mn	0.09	0.11	0.09	0.10	0.10	0.07	0.09	0.06	0.05	0.04	0.07	0.05	0.04
Mg	2.96	3.12	2.89	3.06	3.05	3.06	3.21	2.87	2.67	2.73	2.88	2.87	2.87
Ca	1.91	1.91	1.94	1.92	1.86	1.90	1.90	1.82	1.82	1.88	1.89	1.84	1.63
Na	0.33	0.28	0.33	0.30	0.36	0.29	0.29	0.28	0.32	0.33	0.27	0.37	0.29
K	0.11	0.07	0.10	0.09	0.10	0.09	0.07	0.10	0.12	0.13	0.07	0.14	0.10
Mg/Mg+Fe	0.62	0.65	0.62	0.64	0.64	0.63	0.66	0.59	0.56	0.57	0.60	0.59	0.60

APPENDIX C.3. Continued.

Table C.3.2. Biotite analyses from plutonic units in the Brookville terrane.

Pluton	Dioritic to Granodioritic Plutons						Rockwood Park			French Village		Belmont		
	Ludgate Lake Granodiorite				Granodiorite			Pluton		Yonalite				
	NB91-8622		NB91-9195B		CW89-509A			CW88-	CW88-	NB91-8513				
Sample	1	2	3	4	1	2	3	1	2	3	144	153	1	2
SiO ₂	36.06	36.62	36.56	36.91	36.40	36.32	36.59	36.39	35.87	34.88	32.68	35.25	28.33	27.75
TiO ₂	3.80	4.01	4.03	4.10	3.79	3.55	3.58	2.68	3.29	2.80	1.79	3.13	0.00	0.00
Al ₂ O ₃	14.11	14.26	13.65	13.76	13.38	13.77	13.82	14.43	15.05	15.42	15.83	15.34	17.16	17.36
FeO	18.35	17.53	17.58	17.11	18.27	18.88	18.06	19.52	19.53	20.09	19.79	15.97	21.05	21.44
MnO	0.52	0.48	0.53	0.39	0.57	0.45	0.46	0.47	0.45	0.51	0.44	0.25	0.55	0.44
MgO	12.36	12.24	12.55	12.76	12.60	12.78	13.01	11.67	11.22	11.70	12.23	12.01	18.91	18.69
CaO	0.00	0.00	0.00	0.00	0.00	0.27	0.00	0.18	0.34	0.06	0.17	0.09	0.00	0.00
Na ₂ O	0.36	0.31	0.44	0.37	0.43	0.35	0.35	0.07	0.04	0.06	0.19	0.31	0.00	0.25
K ₂ O	8.98	9.28	9.38	9.45	9.18	8.66	8.98	8.37	8.15	7.60	7.40	9.68	0.00	0.00
Cr ₂ O ₃	0.00	0.00	0.00	0.00	0.00	0.00	0.00	0.00	0.00	0.00	0.07	0.06	0.00	0.00
TOTAL	94.54	94.73	94.72	94.85	94.62	95.03	94.85	93.78	93.94	93.12	90.59	92.09	86.00	85.93

Number of ions on the basis of 22 oxygen.

Si	5.55	5.59	5.60	5.63	5.60	5.56	5.59	5.64	5.54	5.45	5.27	5.52	4.68	4.60
Al ^{iv}	2.46	2.41	2.40	2.38	2.40	2.44	2.41	2.36	2.46	2.55	2.73	2.48	3.32	3.40
Al ^{vi}	0.10	0.16	0.07	0.10	0.03	0.05	0.08	0.27	0.29	0.29	0.28	0.36	0.02	0.00
Ti	0.44	0.46	0.46	0.47	0.44	0.41	0.41	0.31	0.38	0.33	0.22	0.37	0.00	0.00
Cr	0.00	0.00	0.00	0.00	0.00	0.00	0.00	0.00	0.00	0.00	0.01	0.01	0.00	0.00
Fe	2.36	2.24	2.25	2.18	2.35	2.42	2.31	2.53	2.52	2.62	2.67	2.09	2.91	2.98
Mn	0.07	0.06	0.07	0.05	0.07	0.06	0.06	0.06	0.06	0.07	0.06	0.03	0.08	0.06
Mg	2.83	2.79	2.87	2.90	2.89	2.92	2.96	2.69	2.58	2.72	2.94	2.80	4.65	4.62
Ca	0.00	0.00	0.00	0.00	0.00	0.04	0.00	0.03	0.06	0.01	0.03	0.02	0.00	0.00
Na	0.11	0.09	0.13	0.11	0.13	0.10	0.10	0.02	0.01	0.02	0.06	0.09	0.00	0.08
K	1.76	1.81	1.83	1.84	1.80	1.69	1.75	1.65	1.61	1.51	1.52	1.94	0.00	0.00
Mg/Mg+Fe	0.55	0.55	0.56	0.57	0.55	0.55	0.56	0.52	0.51	0.51	0.52	0.57	0.62	0.61

Table C.3.2. Continued.

Pluton	Dioritic to Granodioritic Plutons													
	Belmont Tonalite				Perch Lake Granodiorite				Shadow Lake Granodiorite			Enclave		
	NB91-8522				NB92-9027				NB92-9033			NB91-8597		
Sample	1	2	3	4	1	2	3	4	1	2	3	1	2	3
SiO ₂	34.46	35.30	36.14	34.83	35.44	36.44	36.03	36.45	36.15	36.44	37.07	36.30	36.17	35.60
TiO ₂	3.26	2.78	2.73	2.69	3.66	3.70	3.81	3.73	3.82	4.04	3.35	3.73	3.27	3.40
Al ₂ O ₃	14.74	14.45	14.50	14.93	14.05	13.75	14.45	13.86	13.96	13.95	13.40	14.19	14.21	14.50
FeO	17.80	17.69	17.75	17.44	19.64	18.91	19.28	19.15	19.56	18.97	18.17	18.19	17.72	19.33
MnO	0.45	0.23	0.26	0.36	0.30	0.00	0.36	0.25	0.57	0.44	0.56	0.23	0.26	0.28
MgO	14.08	13.25	13.04	14.58	11.74	11.84	11.08	11.61	11.09	11.13	12.34	11.86	11.86	11.09
CaO	0.17	0.39	0.00	0.13	0.00	0.00	0.00	0.00	0.00	0.00	0.00	0.00	0.00	0.00
Na ₂ O	0.19	0.29	0.24	0.34	0.23	0.22	0.27	0.42	0.26	0.29	0.27	0.31	0.30	0.23
K ₂ O	6.82	7.45	9.19	6.86	8.65	9.29	9.55	9.37	9.53	9.60	8.63	9.60	9.53	9.31
Cr ₂ O ₃	0.00	0.00	0.00	0.00	0.00	0.00	0.00	0.00	0.00	0.00	0.00	0.00	0.00	0.00
TOTAL	91.97	91.83	93.85	92.16	93.71	94.15	94.83	94.84	94.94	94.86	93.79	94.41	93.32	93.74

Number of ions on the basis of 22 oxygen.

Si	5.38	5.53	5.58	5.41	5.52	5.63	5.56	5.61	5.58	5.61	5.72	5.59	5.63	5.55
Al ^{iv}	2.62	2.47	2.43	2.59	2.48	2.37	2.44	2.39	2.42	2.39	2.29	2.41	2.38	2.45
Al ^{vi}	0.10	0.19	0.21	0.15	0.11	0.14	0.19	0.13	0.13	0.15	0.15	0.17	0.23	0.22
Ti	0.38	0.33	0.32	0.31	0.43	0.43	0.44	0.43	0.44	0.47	0.39	0.43	0.38	0.40
Cr	0.00	0.00	0.00	0.00	0.00	0.00	0.00	0.00	0.00	0.00	0.00	0.00	0.00	0.00
Fe	2.33	2.32	2.29	2.27	2.56	2.44	2.49	2.47	2.53	2.44	2.34	2.34	2.31	2.52
Mn	0.06	0.03	0.03	0.05	0.04	0.00	0.05	0.03	0.08	0.06	0.07	0.03	0.03	0.04
Mg	3.28	3.09	3.00	3.38	2.73	2.73	2.55	2.66	2.55	2.55	2.84	2.72	2.75	2.58
Ca	0.03	0.07	0.00	0.02	0.00	0.00	0.00	0.00	0.00	0.00	0.00	0.00	0.00	0.00
Na	0.06	0.09	0.07	0.10	0.07	0.07	0.08	0.13	0.08	0.09	0.08	0.09	0.09	0.07
K	1.36	1.49	1.81	1.36	1.72	1.83	1.88	1.84	1.88	1.89	1.70	1.89	1.89	1.85
Mg/Mg+Fe	0.59	0.57	0.57	0.60	0.52	0.53	0.51	0.52	0.50	0.51	0.55	0.54	0.54	0.51

Table C.3.2. Biotite analyses from plutonic units in the Brookville terrane.

Pluton	Dioritic to Granodioritic Plutons						Renforth Pluton CW88- 189	Narrows Tonalite			
	Talbot Road Granodiorite				NB92-9153			NB91-8513			
Sample	NB92-9045		3	4	1	2	3	189	1	2	3
	1	2									
SiO ₂	36.19	35.27	35.74	29.28	30.40	34.49	32.88	34.42	37.04	35.65	37.83
TiO ₂	4.04	2.98	3.83	0.78	3.25	3.56	3.22	3.10	3.17	2.71	2.57
Al ₂ O ₃	14.23	14.27	13.90	16.44	14.76	13.78	14.41	14.09	14.83	15.53	15.45
FeO	18.57	19.64	19.09	24.20	21.61	19.49	20.05	17.07	15.69	16.51	15.72
MnO	0.34	0.27	0.21	0.29	0.41	0.27	0.55	0.64	0.21	0.24	0.19
MgO	11.80	12.36	11.84	16.26	13.93	11.97	12.88	14.45	13.68	14.35	13.76
CaO	0.00	0.17	0.13	0.35	1.83	0.38	0.68	0.17	0.17	0.28	0.25
Na ₂ O	0.23	0.19	0.34	0.25	0.35	0.29	0.00	0.07	0.11	0.09	0.10
K ₂ O	9.56	7.91	8.78	0.50	2.95	7.54	5.59	8.15	8.73	7.25	8.05
Cr ₂ O ₃	0.00	0.00	0.00	0.17	0.00	0.00	0.00	0.07	0.00	0.00	0.00
TOTAL	94.96	93.06	93.86	88.52	89.49	91.77	90.26	92.23	93.63	92.61	93.92

Number of ions on the basis of 22 oxygen.

Si	5.55	5.51	5.55	4.78	4.95	5.48	5.29	5.40	5.64	5.48	5.69
Al ^{iv}	2.45	2.49	2.45	3.17	2.83	2.52	2.71	2.60	2.37	2.53	2.31
Al ^{vi}	0.13	0.14	0.09	0.00	0.00	0.06	0.02	0.00	0.29	0.29	0.44
Ti	0.47	0.35	0.45	0.10	0.40	0.43	0.39	0.37	0.36	0.31	0.29
Cr	0.00	0.00	0.00	0.02	0.00	0.00	0.00	0.01	0.00	0.00	0.00
Fe	2.38	2.57	2.48	3.31	2.94	2.59	2.70	2.24	2.00	2.12	1.98
Mn	0.04	0.04	0.03	0.04	0.06	0.04	0.08	0.09	0.03	0.03	0.02
Mg	2.70	2.88	2.74	3.96	3.38	2.83	3.09	3.38	3.10	3.28	3.09
Ca	0.00	0.03	0.02	0.06	0.32	0.07	0.12	0.03	0.03	0.05	0.04
Na	0.07	0.06	0.10	0.08	0.11	0.09	0.00	0.02	0.03	0.03	0.03
K	1.87	1.58	1.74	0.10	0.61	1.53	1.15	1.63	1.69	1.42	1.55
Mg/Mg+Fe	0.53	0.53	0.53	0.55	0.54	0.52	0.53	0.60	0.61	0.61	0.61

Table C.3.2. Biotite analyses from plutonic units in the Brookville terrane.

Pluton	Monzogranitic to Granodioritic Plutons									Syenogranite Plutons		
	Fairville Granite				Hammond River Granite			Hanson Stream Granodiorite				Musquash Harbour Pluton
	CW89-611				CW88-200			NB92-9154				NB92-9202A
Sample	1	2	3	4	1	2	3	1	2	3	4	
SiO ₂	34.87	34.99	31.30	33.45	33.39	35.19	30.54	35.89	33.95	36.46	36.56	26.71
TiO ₂	3.79	3.89	2.35	4.83	2.83	2.92	3.28	3.88	2.35	4.02	3.90	0.00
Al ₂ O ₃	13.52	13.57	14.20	13.01	17.87	17.77	18.13	13.72	15.37	13.51	13.47	18.57
FeO	28.26	28.62	30.32	27.39	19.05	18.99	21.55	18.39	19.30	18.28	17.97	23.60
MnO	0.41	0.33	0.39	0.28	0.77	0.81	0.94	0.57	0.76	0.43	0.53	0.65
MgO	5.40	5.28	6.41	5.39	9.01	9.10	9.87	12.56	13.41	12.57	12.61	17.14
CaO	0.01	0.04	0.25	2.36	0.06	0.00	2.59	0.00	0.31	0.00	0.00	0.00
Na ₂ O	0.06	0.09	0.06	0.05	0.12	0.11	0.02	0.32	0.35	0.33	0.22	0.31
K ₂ O	9.17	9.25	6.58	6.21	8.24	9.78	1.00	8.81	5.23	9.50	9.49	0.00
Cr ₂ O ₃	0.00	0.00	0.02	0.02	0.00	0.00	0.00	0.00	0.00	0.00	0.00	0.00
TOTAL	95.49	96.06	91.88	92.99	91.34	94.67	87.92	94.14	91.03	95.10	94.75	86.98
Number of ions on the basis of 22 oxygen												
Si	5.59	5.58	5.26	5.46	5.32	5.43	4.98	5.55	5.36	5.59	5.61	4.44
Al ^{iv}	2.41	2.42	2.75	2.50	2.68	2.57	3.02	2.46	2.64	2.42	2.39	3.56
Al ^{vi}	0.14	0.13	0.07	0.00	0.68	0.66	0.46	0.04	0.22	0.03	0.05	0.08
Ti	0.46	0.47	0.30	0.59	0.34	0.34	0.40	0.45	0.28	0.46	0.45	0.00
Cr	0.00	0.00	0.00	0.00	0.00	0.00	0.00	0.00	0.00	0.00	0.00	0.00
Fe	3.79	3.82	4.26	3.74	2.54	2.45	2.94	2.38	2.55	2.34	2.31	3.28
Mn	0.06	0.05	0.06	0.04	0.10	0.11	0.13	0.08	0.10	0.06	0.07	0.09
Mg	1.29	1.26	1.60	1.31	2.14	2.09	2.40	2.89	3.15	2.87	2.88	4.25
Ca	0.00	0.01	0.05	0.41	0.01	0.00	0.45	0.00	0.05	0.00	0.00	0.00
Na	0.02	0.03	0.02	0.02	0.04	0.03	0.01	0.10	0.11	0.10	0.07	0.10
K	1.88	1.88	1.41	1.29	1.66	1.92	0.21	1.74	1.05	1.86	1.86	0.00
Mg/Mg+Fe	0.25	0.25	0.27	0.26	0.46	0.46	0.45	0.55	0.55	0.55	0.56	0.56

APPENDIX C.3. Continued.

Table C.3.3. Plagioclase analyses from plutonic units in the Brookville terrane.

Pluton	Dioritic to Granodioritic Plutons Ludgate Lake Granodiorite													
	NB91-8590					NB91-8622					NB92-9195B			
	1r	1c	2c	2r	3	1c	1r	2	3	4	1c	1r	2	3
SiO ₂	62.79	62.53	59.96	61.09	57.67	57.45	59.24	61.71	62.05	61.33	63.73	63.82	64.71	64.74
TiO ₂	0.00	0.00	0.00	0.00	0.00	0.00	0.00	0.00	0.00	0.00	0.00	0.00	0.00	0.00
Al ₂ O ₃	22.75	23.06	24.07	24.03	26.02	26.30	25.47	24.09	23.66	23.66	22.61	22.52	21.86	21.72
FeO	0.31	0.00	0.33	0.00	0.00	0.20	0.20	0.00	0.21	0.00	0.00	0.25	0.00	0.00
MnO	0.00	0.00	0.00	0.00	0.00	0.00	0.00	0.20	0.00	0.00	0.00	0.00	0.00	0.00
MgO	0.00	0.00	0.00	0.00	0.00	0.00	0.00	0.00	0.00	0.00	0.00	0.00	0.00	0.00
CaO	2.44	4.61	6.05	5.40	7.91	8.36	7.51	5.66	5.39	5.56	4.09	3.92	3.30	3.35
Na ₂ O	7.11	8.13	7.31	7.89	6.79	6.70	7.37	8.31	8.02	8.17	9.02	8.92	9.09	9.49
K ₂ O	1.18	0.32	0.47	0.33	0.28	0.27	0.17	0.24	0.33	0.23	0.19	0.19	0.28	0.32
Cr ₂ O ₃	0.00	0.00	0.00	0.00	0.00	0.00	0.00	0.00	0.00	0.00	0.00	0.00	0.00	0.00
TOTAL	99.58	98.65	98.19	98.74	98.67	99.28	99.97	100.20	99.66	98.94	99.65	99.62	99.25	99.60
Number of ions on the basis of 32 oxygens														
Si	11.40	11.20	10.86	10.98	10.46	10.37	10.59	10.94	11.04	11.01	11.30	11.30	11.46	11.46
Al	4.87	4.86	5.14	5.09	5.57	5.60	5.38	5.16	4.96	4.99	4.70	4.70	4.58	4.54
Ti	0.00	0.00	0.00	0.00	0.00	0.00	0.00	0.00	0.00	0.00	0.00	0.00	0.00	0.00
Cr	0.00	0.00	0.00	0.00	0.00	0.00	0.00	0.00	0.00	0.00	0.00	0.00	0.00	0.00
Fe	0.05	0.00	0.05	0.00	0.00	0.03	0.03	0.00	0.03	0.00	0.00	0.03	0.00	0.00
Mn	0.00	0.00	0.00	0.00	0.00	0.00	0.00	0.03	0.00	0.00	0.00	0.00	0.00	0.00
Mg	0.00	0.00	0.00	0.00	0.00	0.00	0.00	0.00	0.00	0.00	0.00	0.00	0.00	0.00
Ca	0.47	0.88	1.17	1.02	1.54	1.63	1.44	1.09	1.02	1.06	0.77	0.74	0.64	0.64
Na	2.50	2.82	2.57	2.75	2.40	2.34	2.56	2.85	2.75	2.85	3.10	3.07	3.14	3.26
K	0.27	0.07	0.11	0.06	0.06	0.06	0.03	0.06	0.06	0.06	0.03	0.03	0.06	0.06
Mole proportions														
Or	0.08	0.02	0.03	0.02	0.02	0.02	0.01	0.01	0.02	0.01	0.01	0.01	0.02	0.02
Ab	0.77	0.75	0.67	0.71	0.60	0.58	0.63	0.72	0.72	0.72	0.79	0.80	0.82	0.82
An	0.15	0.23	0.31	0.27	0.39	0.40	0.36	0.27	0.27	0.27	0.20	0.19	0.16	0.16

c = core; r = rim; i = intermediate (between core and rim)

Table C.3.3. Continued.

Pluton	Dioritic to Granodioritic Plutons Ludgate Lake Granodiorite						Rockwood Park Granodiorite					French Village Pluton CW88-144		
	Sample	NB92-9251		3r	4	5	CW89-509A		2c	2r	3r	CW88-144		
	4	1r	2r				1c	1r				1c	1r	2c
SiO ₂	61.09	68.08	68.26	68.02	62.45	60.79	59.04	59.06	56.03	59.61	61.84	56.27	57.16	55.35
TiO ₂	0.00	0.00	0.00	0.00	0.00	0.00	0.03	0.01	0.00	0.00	0.00	0.03	0.00	0.00
Al ₂ O ₃	24.00	20.34	19.30	19.93	23.05	23.78	26.30	25.11	26.02	25.34	24.92	26.34	26.17	27.01
FeO	0.27	0.00	0.00	0.00	0.00	0.00	0.20	0.21	0.15	0.16	0.13	0.15	0.19	0.26
MnO	0.00	0.00	0.00	0.00	0.00	0.00	0.00	0.00	0.00	0.00	0.00	0.01	0.00	0.02
MgO	0.00	0.00	0.00	0.00	0.00	0.00	0.00	0.01	0.01	0.00	0.00	0.00	0.00	0.00
CaO	5.79	0.66	0.13	0.20	4.46	5.74	8.57	7.46	8.49	7.26	7.09	8.55	7.94	9.44
Na ₂ O	7.92	11.39	10.80	11.03	8.11	7.90	6.84	7.51	6.75	7.37	7.74	7.57	7.71	6.62
K ₂ O	0.29	0.00	0.00	0.00	0.56	0.35	0.22	0.19	0.17	0.35	0.15	0.15	0.16	0.20
Cr ₂ O ₃	0.00	0.00	0.00	0.00	0.00	0.00	0.00	0.00	0.00	0.00	0.00	0.02	0.00	0.01
TOTAL	99.35	100.47	98.49	99.19	98.63	98.55	101.20	99.56	97.62	100.08	101.88	99.08	99.33	98.91
Number of ions on the basis of 32 oxygens														
Si	10.91	11.84	12.06	11.94	11.20	10.94	10.46	10.61	10.31	10.64	10.81	10.24	10.34	10.10
Al	5.06	4.16	4.00	4.13	4.86	5.06	5.49	5.32	5.64	5.33	5.14	5.55	5.58	5.81
Ti	0.00	0.00	0.00	0.00	0.00	0.00	0.00	0.00	0.00	0.00	0.00	0.00	0.00	0.00
Cr	0.00	0.00	0.00	0.00	0.00	0.00	0.00	0.00	0.00	0.00	0.00	0.00	0.00	0.00
Fe	0.03	0.00	0.00	0.00	0.00	0.00	0.03	0.03	0.02	0.02	0.02	0.02	0.03	0.04
Mn	0.00	0.00	0.00	0.00	0.00	0.00	0.00	0.00	0.00	0.00	0.00	0.00	0.00	0.00
Mg	0.00	0.00	0.00	0.00	0.00	0.00	0.00	0.00	0.00	0.00	0.00	0.00	0.00	0.00
Ca	1.12	0.13	0.03	0.03	0.86	1.12	1.63	1.44	1.67	1.39	1.33	1.67	1.54	1.85
Na	2.75	3.84	3.71	3.74	2.82	2.75	2.35	2.62	2.41	2.55	2.62	2.67	2.71	2.34
K	0.06	0.00	0.00	0.00	0.13	0.06	0.05	0.04	0.04	0.08	0.03	0.04	0.04	0.05
Mole proportions														
Or	0.02	0.00	0.00	0.00	0.03	0.02	0.01	0.01	0.01	0.02	0.01	0.01	0.01	0.01
Ab	0.70	0.97	0.99	0.99	0.74	0.70	0.58	0.64	0.58	0.64	0.66	0.61	0.63	0.55
An	0.28	0.03	0.01	0.01	0.23	0.28	0.40	0.35	0.41	0.35	0.33	0.38	0.36	0.44

Table C.3.3. Continued.

Pluton	Dioritic to Granodioritic Plutons French Village Pluton													
	Sample CW88-144					Sample CW88-153				Sample CW88-246				
Sample	2r	3c	3r	4c	4r	1	2	3	4	1c	1r	2c	2r	3c
SiO ₂	55.67	56.07	56.83	56.39	56.72	53.79	58.75	52.96	56.53	54.27	57.82	54.65	55.74	54.19
TiO ₂	0.01	0.00	0.00	0.02	0.02	0.00	0.01	0.00	0.00	0.01	0.00	0.03	0.01	0.02
Al ₂ O ₃	27.12	26.68	26.55	26.84	26.15	27.39	25.22	28.40	25.88	28.09	26.66	27.95	27.59	28.36
FeO	0.22	0.23	0.18	0.19	0.19	0.27	0.15	0.18	0.15	0.12	0.07	0.00	0.00	0.10
MnO	0.02	0.01	0.00	0.04	0.00	0.00	0.00	0.03	0.00	0.00	0.00	0.00	0.00	0.00
MgO	0.00	0.00	0.00	0.00	0.00	0.00	0.00	0.00	0.00	0.01	0.01	0.01	0.00	0.00
CaO	9.22	8.92	8.46	9.11	8.42	10.97	7.18	10.86	8.22	10.91	9.16	10.52	10.19	11.05
Na ₂ O	8.09	7.09	6.88	6.50	7.25	6.75	8.08	5.73	8.45	5.41	6.45	5.86	5.86	5.57
K ₂ O	0.55	0.19	0.19	0.17	0.22	0.30	0.15	0.11	0.10	0.08	0.05	0.05	0.04	0.07
Cr ₂ O ₃	0.00	0.02	0.00	0.01	0.01	0.03	0.00	0.02	0.02	0.00	0.00	0.00	0.00	0.00
TOTAL	100.89	99.20	99.09	99.27	98.97	99.48	99.54	98.28	99.34	98.91	100.22	99.05	99.44	99.37
Number of ions on the basis of 32 oxygens														
Si	10.00	10.19	10.30	10.22	10.31	9.85	10.57	9.68	10.28	9.91	10.34	9.95	10.08	9.86
Al	5.67	5.72	5.67	5.73	5.60	5.91	5.35	6.17	5.55	6.05	5.62	6.00	5.88	6.08
Ti	0.00	0.00	0.00	0.00	0.00	0.00	0.00	0.00	0.00	0.00	0.00	0.00	0.00	0.00
Cr	0.00	0.00	0.00	0.00	0.00	0.00	0.00	0.00	0.00	0.00	0.00	0.00	0.00	0.00
Fe	0.03	0.04	0.03	0.03	0.03	0.04	0.02	0.03	0.02	0.02	0.01	0.00	0.00	0.02
Mn	0.00	0.00	0.00	0.00	0.00	0.00	0.00	0.00	0.00	0.00	0.00	0.00	0.00	0.00
Mg	0.00	0.00	0.00	0.00	0.00	0.00	0.00	0.00	0.00	0.00	0.00	0.00	0.00	0.00
Ca	1.78	1.74	1.64	1.77	1.64	2.15	1.38	2.15	1.60	2.13	1.76	2.05	1.98	2.15
Na	2.83	2.50	2.42	2.28	2.56	2.40	2.82	2.05	2.98	1.92	2.24	2.07	2.06	1.97
K	0.13	0.04	0.04	0.04	0.05	0.07	0.03	0.03	0.02	0.02	0.01	0.01	0.01	0.02
Mole proportions														
Or	0.03	0.01	0.01	0.01	0.01	0.02	0.01	0.01	0.01	0.01	0.00	0.00	0.00	0.00
Ab	0.60	0.58	0.59	0.56	0.60	0.52	0.67	0.49	0.65	0.47	0.56	0.50	0.51	0.48
An	0.38	0.41	0.40	0.43	0.39	0.47	0.33	0.51	0.35	0.53	0.44	0.50	0.49	0.52

Table C.3.3. Continued.

Pluton	Dioritic to Granodioritic Plutons Belmont Tonalite								Perch Lake Granodiorite				Shadow Lake Granodiorite	
	Sample	NB91-8513			NB91-8522				NB92-9027				NB91-8565	
		3r	1	2	3	1	2	3	4	1	2	3	4	1
SiO ₂	55.92	58.05	57.69	57.96	59.01	56.54	56.06	59.67	56.91	59.70	59.35	59.22	59.91	58.45
TiO ₂	0.01	0.00	0.00	0.00	0.00	0.00	0.00	0.00	0.00	0.00	0.00	0.00	0.00	0.00
Al ₂ O ₃	27.90	27.12	26.97	26.35	24.85	27.09	27.51	25.39	26.50	24.97	24.94	25.76	24.71	25.56
FeO	0.11	0.00	0.00	0.27	0.00	0.00	0.00	0.00	0.00	0.00	0.00	0.00	0.00	0.26
MnO	0.00	0.00	0.00	0.18	0.00	0.00	0.06	0.00	0.00	0.00	0.00	0.00	0.00	0.00
MgO	0.00	0.00	0.00	0.00	0.00	0.00	0.00	0.00	0.00	0.00	0.00	0.00	0.00	0.00
CaO	10.47	8.81	8.43	7.24	6.62	8.79	9.32	6.74	9.16	7.08	6.93	7.72	6.32	7.36
Na ₂ O	5.71	6.15	6.64	6.57	7.06	6.38	5.79	7.17	6.33	7.50	6.11	7.25	7.33	7.09
K ₂ O	0.06	0.15	0.12	0.62	0.14	0.12	0.14	0.23	0.09	0.16	2.27	0.18	0.19	0.23
Cr ₂ O ₃	0.00	0.00	0.00	0.00	0.00	0.00	0.25	0.00	0.00	0.00	0.00	0.00	0.00	0.00
TOTAL	100.17	100.28	99.84	99.17	97.68	98.91	99.07	99.20	98.90	99.41	99.60	100.13	98.45	98.95
Number of ions on the basis of 32 oxygens														
Si	10.05	10.34	10.34	10.46	10.72	10.24	10.14	10.69	10.30	10.69	10.69	10.56	10.82	10.56
Al	5.91	5.70	5.70	5.60	5.31	5.79	5.86	5.38	5.66	5.28	5.31	5.41	5.25	5.44
Ti	0.00	0.00	0.00	0.00	0.00	0.00	0.00	0.00	0.00	0.00	0.00	0.00	0.00	0.00
Cr	0.00	0.00	0.00	0.00	0.00	0.00	0.03	0.00	0.00	0.00	0.00	0.00	0.00	0.00
Fe	0.02	0.00	0.00	0.00	0.00	0.00	0.00	0.00	0.00	0.00	0.00	0.00	0.00	0.03
Mn	0.00	0.00	0.00	0.00	0.00	0.00	0.00	0.00	0.00	0.00	0.00	0.00	0.00	0.00
Mg	0.00	0.00	0.00	0.00	0.00	0.00	0.00	0.00	0.00	0.00	0.00	0.00	0.00	0.00
Ca	2.02	1.70	1.63	1.41	1.28	1.70	1.82	1.28	1.79	1.34	1.34	1.47	1.22	1.41
Na	1.99	2.11	2.30	2.30	2.50	2.24	2.05	2.50	2.21	2.59	2.14	2.50	2.56	2.50
K	0.01	0.03	0.03	0.13	0.03	0.03	0.03	0.06	0.00	0.03	0.51	0.03	0.03	0.06
Mole Proportions														
Or	0.00	0.01	0.01	0.04	0.01	0.01	0.01	0.01	0.00	0.00	0.13	0.01	0.01	0.01
Ab	0.50	0.55	0.58	0.60	0.65	0.56	0.53	0.65	0.56	0.66	0.54	0.62	0.67	0.63
An	0.50	0.44	0.41	0.37	0.34	0.43	0.47	0.34	0.44	0.34	0.34	0.37	0.32	0.36

Table C.3.3. Continued.

Pluton	Dioritic to Granodioritic Plutons Shadow Lake Granodiorite													
	Sample	NB91-8599B			NB92-9033				NB92-9258A					
	3	1	2	3	1	2	3	4	1c	1i	1r	2c	2i	2r
SiO ₂	59.30	60.37	59.93	58.21	61.51	61.06	60.99	60.95	61.37	59.79	66.69	61.17	59.92	66.79
TiO ₂	0.00	0.00	0.00	0.00	0.00	0.00	0.00	0.00	0.00	0.00	0.00	0.00	0.00	0.00
Al ₂ O ₃	25.51	24.63	24.68	26.16	23.73	23.76	23.76	23.81	24.03	24.89	20.66	23.94	24.57	20.72
FeO	0.29	0.00	0.00	0.20	0.23	0.00	0.00	0.26	0.31	0.21	0.00	0.00	0.00	0.00
MnO	0.00	0.00	0.00	0.00	0.00	0.00	0.00	0.00	0.00	0.00	0.00	0.00	0.00	0.00
MgO	0.00	0.00	0.00	0.00	0.00	0.00	0.00	0.00	0.00	0.00	0.00	0.00	0.00	0.00
CaO	7.18	6.53	6.71	8.38	5.59	5.73	5.78	5.72	5.87	6.87	1.44	5.35	6.70	1.41
Na ₂ O	7.28	7.88	7.63	6.74	7.77	7.72	7.80	7.83	7.99	7.59	10.01	7.92	7.46	10.37
K ₂ O	0.20	0.25	0.17	0.16	0.48	0.35	0.50	0.46	0.24	0.33	0.00	0.39	0.31	0.00
Cr ₂ O ₃	0.00	0.00	0.00	0.00	0.00	0.00	0.00	0.00	0.00	0.00	0.00	0.00	0.00	0.00
TOTAL	99.76	99.65	99.12	99.85	99.31	98.61	98.83	99.04	99.81	99.67	98.81	98.77	98.96	99.28
Number of ions on the basis of 32 oxygens.														
Si	10.62	10.78	10.75	10.43	11.01	10.98	10.98	10.94	10.94	10.72	11.78	10.98	10.78	11.74
Al	5.38	5.18	5.22	5.54	4.99	5.02	5.02	5.02	5.06	5.25	4.29	5.06	5.22	4.29
Ti	0.00	0.00	0.00	0.00	0.00	0.00	0.00	0.00	0.00	0.00	0.00	0.00	0.00	0.00
Cr	0.00	0.00	0.00	0.00	0.00	0.00	0.00	0.00	0.00	0.00	0.00	0.00	0.00	0.00
Fe	0.03	0.00	0.00	0.03	0.03	0.00	0.00	0.03	0.03	0.03	0.00	0.00	0.00	0.00
Mn	0.00	0.00	0.00	0.00	0.00	0.00	0.00	0.00	0.00	0.00	0.00	0.00	0.00	0.00
Mg	0.00	0.00	0.00	0.00	0.00	0.00	0.00	0.00	0.00	0.00	0.00	0.00	0.00	0.00
Ca	1.38	1.25	1.28	1.60	1.06	1.09	1.12	1.09	1.12	1.31	0.29	1.02	1.28	0.26
Na	2.53	2.72	2.66	2.34	2.69	2.69	2.72	2.72	2.75	2.62	3.42	2.75	2.59	3.55
K	0.03	0.06	0.03	0.03	0.10	0.06	0.13	0.10	0.06	0.06	0.00	0.10	0.06	0.00
Mole proportions														
Or	0.01	0.01	0.01	0.01	0.03	0.02	0.03	0.03	0.01	0.02	0.00	0.02	0.02	0.00
Ab	0.64	0.68	0.67	0.59	0.70	0.70	0.69	0.69	0.70	0.65	0.93	0.71	0.66	0.93
An	0.35	0.31	0.32	0.40	0.28	0.29	0.28	0.28	0.29	0.33	0.07	0.27	0.33	0.07

Table C.3.3. Continued.

Pluton Sample	Dioritic to Granodioritic Plutons Enclave					Talbot Road Granodiorite					Renforth Pluton CW88-169			
	3c	NB91-8597		3	4	NB92-9045			NB91-9153		3	4	1	2
SiO ₂	60.61	55.48	56.50	55.63	56.57	58.00	58.54	58.73	57.66	58.56	56.02	57.10	57.82	55.64
TiO ₂	0.00	0.00	0.00	0.00	0.00	0.00	0.00	0.00	0.00	0.00	0.00	0.00	0.03	0.02
Al ₂ O ₃	24.21	27.56	27.08	27.60	26.96	26.33	25.49	25.96	25.56	25.47	26.30	26.31	26.39	27.70
FeO	0.00	0.00	0.00	0.00	0.00	0.00	0.00	0.22	0.20	0.00	0.00	0.25	0.22	0.17
MnO	0.00	0.00	0.00	0.00	0.00	0.00	0.00	0.00	0.00	0.00	0.00	0.00	0.00	0.00
MgO	0.00	0.00	0.00	0.00	0.00	0.00	0.00	0.00	0.00	0.00	0.00	0.00	0.01	0.02
CaO	6.08	9.69	8.80	9.31	8.98	8.55	7.75	7.88	8.28	7.49	9.17	8.93	8.93	10.27
Na ₂ O	7.97	5.86	6.31	6.05	6.01	6.89	7.09	7.05	6.79	7.16	6.01	6.48	6.48	5.68
K ₂ O	0.17	0.19	0.14	0.00	0.22	0.92	0.24	0.10	0.18	0.13	0.22	0.12	0.38	0.21
Cr ₂ O ₃	0.00	0.00	0.00	0.00	0.00	0.00	0.00	0.00	0.00	0.00	0.00	0.00	0.00	0.00
TOTAL	99.04	98.77	98.83	98.59	98.75	100.69	99.11	99.93	98.68	98.82	97.73	99.17	100.25	99.71
Number of ions on the basis of 32 oxygens														
Si	10.88	10.08	10.20	10.11	10.27	10.40	10.56	10.50	10.46	10.56	10.27	10.34	10.36	10.06
Al	5.12	5.92	5.79	5.92	5.76	5.57	5.41	5.47	5.47	5.41	5.70	5.60	5.57	5.90
Ti	0.00	0.00	0.00	0.00	0.00	0.00	0.00	0.00	0.00	0.00	0.00	0.00	0.00	0.00
Cr	0.00	0.00	0.00	0.00	0.00	0.00	0.00	0.00	0.00	0.00	0.00	0.00	0.00	0.00
Fe	0.00	0.00	0.00	0.00	0.00	0.00	0.00	0.03	0.03	0.00	0.00	0.03	0.03	0.03
Mn	0.00	0.00	0.00	0.00	0.00	0.00	0.00	0.00	0.00	0.00	0.00	0.00	0.00	0.00
Mg	0.00	0.00	0.00	0.00	0.00	0.00	0.00	0.00	0.00	0.00	0.00	0.00	0.00	0.01
Ca	1.18	1.89	1.70	1.82	1.76	1.63	1.50	1.50	1.60	1.44	1.79	1.73	1.71	1.99
Na	2.78	2.08	2.21	2.14	2.11	2.40	2.46	2.43	2.40	2.50	2.14	2.27	2.25	1.99
K	0.03	0.03	0.03	0.00	0.06	0.03	0.06	0.03	0.03	0.03	0.06	0.03	0.09	0.05
Mole proportions														
Or	0.01	0.01	0.01	0.00	0.01	0.05	0.01	0.01	0.01	0.01	0.01	0.01	0.02	0.01
Ab	0.70	0.52	0.56	0.54	0.54	0.56	0.62	0.62	0.59	0.63	0.54	0.56	0.56	0.49
An	0.29	0.47	0.43	0.46	0.45	0.39	0.37	0.38	0.40	0.36	0.45	0.43	0.42	0.49

Table C.3.3. Continued.

Pluton	Dioritic to Granodioritic Plutons Renforth Pluton						Narrows Tonalite			Monzogranitic to Granodioritic Fairville Granite					
	Sample	CW88-189			CW88-192			CW89-616			CW88-272		CW89-611		
	3	1	2	3	1	2	1	2	3	1	2	1	2	3	
SiO ₂	55.99	58.78	64.67	59.03	61.71	59.59	58.48	61.55	55.94	60.47	59.26	59.44	63.91	59.39	
TiO ₂	0.03	0.00	0.00	0.01	0.00	0.00	0.03	0.00	0.01	0.00	0.00	0.03	0.00	0.00	
Al ₂ O ₃	27.97	24.97	21.43	25.08	23.80	25.21	25.54	24.32	27.58	24.78	26.29	25.88	23.60	25.78	
FeO	0.15	0.09	0.12	0.18	0.12	0.13	0.15	0.21	0.37	0.07	0.10	0.15	0.09	0.00	
MnO	0.00	0.00	0.02	0.00	0.00	0.00	0.00	0.00	0.00	0.00	0.00	0.03	0.00	0.00	
MgO	0.02	0.00	0.00	0.00	0.00	0.00	0.00	0.01	0.02	0.00	0.00	0.01	0.01	0.00	
CaO	10.66	6.18	2.68	7.08	5.48	6.88	8.30	6.29	9.95	6.38	6.81	8.10	5.18	6.82	
Na ₂ O	5.60	8.65	11.01	7.82	9.40	8.10	7.11	7.85	5.83	8.73	7.79	6.92	8.02	7.12	
K ₂ O	0.16	0.32	0.12	0.33	0.21	0.26	0.05	0.09	0.08	0.06	0.13	0.22	0.24	0.06	
Cr ₂ O ₃	0.00	0.00	0.00	0.02	0.00	0.00	0.00	0.00	0.00	0.00	0.00	0.00	0.00	0.00	
TOTAL	100.58	98.97	100.05	99.55	100.72	100.16	99.66	100.32	99.80	100.49	100.38	100.78	101.05	99.17	
Number of ions on the basis of 32 oxygens															
Si	10.04	10.63	11.46	10.62	10.93	10.64	10.51	10.90	10.09	10.74	10.53	10.55	11.17	10.64	
Al	5.91	5.32	4.47	5.32	4.97	5.31	5.41	5.08	5.87	5.19	5.51	5.42	4.86	5.45	
Ti	0.00	0.00	0.00	0.00	0.00	0.00	0.00	0.00	0.00	0.00	0.00	0.00	0.00	0.00	
Cr	0.00	0.00	0.00	0.00	0.00	0.00	0.00	0.00	0.00	0.00	0.00	0.00	0.00	0.00	
Fe	0.02	0.01	0.02	0.03	0.02	0.02	0.02	0.03	0.06	0.01	0.02	0.02	0.01	0.00	
Mn	0.00	0.00	0.00	0.00	0.00	0.00	0.00	0.00	0.00	0.00	0.00	0.00	0.00	0.00	
Mg	0.01	0.00	0.00	0.00	0.00	0.00	0.00	0.00	0.01	0.00	0.00	0.00	0.00	0.00	
Ca	2.05	1.20	0.51	1.36	1.04	1.32	1.60	1.19	1.92	1.21	1.30	1.54	0.97	1.31	
Na	1.95	3.03	3.78	2.73	3.23	2.80	2.48	2.70	2.04	3.01	2.69	2.38	2.72	2.47	
K	0.04	0.07	0.03	0.08	0.05	0.06	0.01	0.02	0.02	0.01	0.03	0.05	0.05	0.01	
Mole proportions															
Or	0.01	0.02	0.01	0.02	0.01	0.01	0.00	0.01	0.01	0.00	0.01	0.01	0.01	0.00	
Ab	0.48	0.71	0.88	0.65	0.75	0.67	0.61	0.69	0.51	0.71	0.67	0.60	0.73	0.65	
An	0.51	0.28	0.12	0.33	0.24	0.32	0.39	0.31	0.48	0.29	0.32	0.39	0.26	0.35	

Table C.3.3. Continued.

Pluton Sample	Monsogranitic to Granodioritic Plutons								Milkish Head Pluton						Hanson Stream Granodiorite	
	Chalet Lake Granite CW88-254		Hammond River Granite CW88-200				NB92-9144						NB92-9039			
	1	2	1	2	3	4	1c	1r	2c	2r	3r	4r	1	2		
SiO ₂	61.56	61.19	60.52	63.78	62.47	63.04	65.12	67.81	62.29	68.75	67.41	67.10	58.61	59.28		
TiO ₂	0.00	0.00	0.00	0.00	0.00	0.00	0.00	0.00	0.00	0.00	0.00	0.00	0.00	0.00		
Al ₂ O ₃	23.58	23.74	23.03	21.96	22.64	22.87	21.23	20.45	23.65	19.41	20.49	19.74	25.27	25.22		
FeO	0.18	0.27	0.08	0.10	0.08	0.11	0.00	0.00	0.00	0.00	0.00	0.00	0.31	0.30		
MnO	0.00	0.00	0.00	0.00	0.00	0.00	0.00	0.00	0.00	0.00	0.00	0.00	0.00	0.00		
MgO	0.00	0.00	0.00	0.00	0.00	0.00	0.00	0.00	0.00	0.00	0.00	0.00	0.00	0.00		
CaO	4.73	4.96	4.38	3.17	4.09	4.08	2.48	1.12	4.99	0.18	1.25	0.82	7.83	7.31		
Na ₂ O	9.81	9.46	10.58	10.80	10.06	10.13	9.19	10.02	8.25	10.78	9.63	9.16	6.88	7.28		
K ₂ O	0.12	0.11	0.34	0.32	0.25	0.18	0.32	0.00	0.47	0.00	0.21	0.13	0.28	0.21		
Cr ₂ O ₃	0.00	0.01	0.00	0.00	0.00	0.01	0.00	0.00	0.00	0.00	0.00	0.00	0.00	0.00		
TOTAL	99.98	99.74	98.93	100.13	99.59	100.42	98.34	99.40	99.65	99.12	98.99	96.95	99.18	99.60		
Number of ions on the basis of 32 oxygens																
Si	10.97	10.93	10.94	11.30	11.15	11.15	11.61	11.88	11.07	12.06	11.86	12.00	10.57	10.63		
Al	4.95	5.00	4.91	4.59	4.76	4.77	4.45	4.22	4.96	4.00	4.26	4.16	5.37	5.33		
Ti	0.00	0.00	0.00	0.00	0.00	0.00	0.00	0.00	0.00	0.00	0.00	0.00	0.00	0.00		
Cr	0.00	0.00	0.00	0.00	0.00	0.00	0.00	0.00	0.00	0.00	0.00	0.00	0.00	0.00		
Fe	0.03	0.04	0.01	0.02	0.01	0.02	0.00	0.00	0.00	0.00	0.00	0.00	0.05	0.05		
Mn	0.00	0.00	0.00	0.00	0.00	0.00	0.00	0.00	0.00	0.00	0.00	0.00	0.00	0.00		
Mg	0.00	0.00	0.00	0.00	0.00	0.00	0.00	0.00	0.00	0.00	0.00	0.00	0.00	0.00		
Ca	0.90	0.95	0.85	0.60	0.78	0.77	0.47	0.21	0.95	0.03	0.24	0.16	1.51	1.41		
Na	3.39	3.28	3.71	3.71	3.48	3.47	3.18	3.40	2.84	3.67	3.29	3.18	2.41	2.53		
K	0.03	0.03	0.08	0.07	0.06	0.04	0.07	0.00	0.11	0.00	0.05	0.03	0.06	0.05		
Mole proportions																
Or	0.01	0.01	0.02	0.02	0.01	0.01	0.02	0.00	0.03	0.00	0.01	0.01	0.02	0.01		
Ab	0.79	0.77	0.80	0.85	0.81	0.81	0.85	0.94	0.73	0.99	0.92	0.95	0.60	0.64		
An	0.21	0.22	0.18	0.14	0.18	0.18	0.13	0.06	0.24	0.01	0.07	0.05	0.38	0.35		

Table C.3.3. Continued.

Pluton	Monzogranitic to Granodioritic Plutons Hanson Stream Granodiorite								Syenogranitic Plutons Musquash Harbour Pluton				
	NB92-9039		NB92-9050				NB92-9154		NB92-9202A				
Sample	3	4	1c	1r	2c	2r	1c	2c	3	4	1c	1r	2c
SiO ₂	58.50	56.84	62.17	68.73	60.88	68.80	61.86	61.48	59.73	63.57	57.44	68.35	58.09
TiO ₂	0.00	0.00	0.00	0.00	0.00	0.00	0.00	0.00	0.00	0.00	0.00	0.00	0.00
Al ₂ O ₃	25.35	26.65	23.24	19.32	22.83	19.65	24.00	23.24	24.53	22.58	26.87	19.91	26.17
FeO	0.00	0.00	0.00	0.00	0.00	0.00	0.24	0.00	0.22	0.00	0.29	0.00	0.31
MnO	0.00	0.00	0.00	0.00	0.00	0.00	0.00	0.18	0.00	0.00	0.00	0.00	0.00
MgO	0.00	0.00	0.00	0.00	0.00	0.00	0.22	0.00	0.00	0.00	0.00	0.00	0.00
CaO	7.81	9.18	4.83	10.65	4.99	10.72	5.41	5.33	6.66	3.81	8.97	0.04	8.36
Na ₂ O	7.07	6.52	8.25	0.00	8.00	0.00	8.37	8.25	7.55	9.32	6.53	10.34	6.82
K ₂ O	0.26	0.18	0.28	0.00	0.13	0.00	0.26	0.26	0.46	0.00	0.19	0.00	0.20
Cr ₂ O ₃	0.00	0.00	0.00	0.00	0.00	0.00	0.00	0.00	0.00	0.00	0.00	0.00	0.00
TOTAL	98.99	99.37	98.77	98.70	96.83	99.17	100.36	98.74	99.15	99.28	99.98	99.95	99.96
Number of ions on the basis of 32 oxygens													
Si	10.56	10.27	11.13	12.02	11.11	11.98	10.95	11.06	10.75	11.29	10.30	12.00	10.43
Al	5.40	5.68	4.90	3.98	4.91	4.03	5.01	4.93	5.21	4.73	5.63	4.13	5.54
Ti	0.00	0.00	0.00	0.00	0.00	0.00	0.00	0.00	0.00	0.00	0.00	0.00	0.00
Cr	0.00	0.00	0.00	0.00	0.00	0.00	0.00	0.00	0.00	0.00	0.00	0.00	0.00
Fe	0.00	0.00	0.00	0.00	0.00	0.00	0.04	0.00	0.03	0.00	0.03	0.00	0.03
Mn	0.00	0.00	0.00	0.00	0.00	0.00	0.00	0.00	0.00	0.00	0.00	0.00	0.00
Mg	0.00	0.00	0.00	0.00	0.00	0.00	0.06	0.00	0.00	0.00	0.00	0.00	0.00
Ca	1.51	1.78	0.93	2.00	0.98	2.00	1.03	1.03	1.29	0.73	1.73	0.06	1.60
Na	2.48	2.29	2.86	0.00	2.83	0.00	2.87	2.88	2.64	3.21	2.27	3.52	2.37
K	0.06	0.04	0.06	0.00	0.03	0.00	0.06	0.06	0.11	0.00	0.03	0.00	0.03
Mole proportions													
Or	0.02	0.01	0.02	0.00	0.01	0.00	0.02	0.02	0.03	0.00	0.01	0.00	0.01
Ab	0.61	0.56	0.74	1.00	0.74	1.00	0.73	0.73	0.66	0.82	0.56	0.98	0.59
An	0.37	0.43	0.24	0.00	0.25	0.00	0.26	0.26	0.32	0.18	0.43	0.02	0.40

APPENDIX C.3. Continued.

Table C.3.4. K-feldspar analyses from plutonic units in the Brookville terrane.

Pluton	Dioritic to Granodioritic Plutons Ludgate Lake Granodiorite										Rockwood Park Granodiorite CW88-509A			
	NB91-8590		NB91-8622		NB92-9195B				NB92-9251			1	2	3
Sample	1	2	1	2	1	2	3	4	1	2	3	1	2	3
SiO ₂	64.05	64.40	64.82	64.87	64.31	64.31	64.81	64.69	64.57	64.21	63.22	65.20	66.57	65.91
TiO ₂	0.00	0.00	0.00	0.00	0.00	0.00	0.00	0.00	0.00	0.00	0.00	0.00	0.04	0.04
Al ₂ O ₃	17.94	18.27	18.37	18.51	18.09	18.27	18.00	18.14	18.19	18.13	18.426	18.67	18.36	18.36
FeO	0.00	0.00	0.00	0.00	0.00	0.00	0.00	0.19	0.00	0.00	0.00	0.08	0.06	0.11
MnO	0.00	0.00	0.00	0.00	0.00	0.00	0.00	0.00	0.00	0.00	0.00	0.00	0.01	0.02
MgO	0.00	0.00	0.00	0.00	0.00	0.00	0.00	0.00	0.00	0.13	0.00	0.01	0.01	0.01
CaO	0.00	0.00	0.00	0.00	0.00	0.00	0.00	0.00	0.00	0.00	0.00	0.02	0.00	0.03
Na ₂ O	0.30	0.27	0.71	0.46	0.32	0.48	0.51	0.69	0.29	0.45	0.32	0.64	0.57	0.51
K ₂ O	15.66	16.19	15.83	15.96	16.16	15.43	16.03	15.86	16.26	15.83	15.61	15.64	15.94	16.01
Cr ₂ O ₃	0.00	0.00	0.00	0.00	0.00	0.00	0.00	0.00	0.00	0.00	0.18	0.00	0.00	0.00
BaO	0.00	0.00	0.00	0.00	0.00	0.00	0.00	0.00	0.00	0.00	1.30	n.d.	n.d.	n.d.
TOTAL	97.95	99.13	99.73	99.81	98.88	98.68	99.34	99.37	99.31	98.76	99.05	100.26	101.56	100.99
Number of ions on the basis of 32 oxygens														
Si	12.06	12.00	11.94	12.00	12.03	12.00	12.03	12.03	12.00	12.00	11.90	11.98	12.07	12.04
Al	3.97	4.00	4.00	4.03	4.00	4.03	3.94	3.94	4.00	4.00	4.10	4.05	3.93	3.95
Ti	0.00	0.00	0.00	0.00	0.00	0.00	0.00	0.00	0.00	0.00	0.00	0.00	0.01	0.01
Cr	0.00	0.00	0.00	0.00	0.00	0.00	0.00	0.00	0.00	0.00	0.03	nd	nd	nd
Fe	0.00	0.00	0.00	0.00	0.00	0.03	0.00	0.00	0.00	0.00	0.00	0.01	0.01	0.02
Mn	0.00	0.00	0.00	0.00	0.00	0.00	0.00	0.00	0.00	0.00	0.00	0.00	0.00	0.00
Mg	0.00	0.00	0.00	0.00	0.00	0.00	0.00	0.00	0.00	0.03	0.00	0.00	0.00	0.00
Ca	0.00	0.00	0.00	0.00	0.00	0.00	0.00	0.00	0.00	0.00	0.00	0.00	0.00	0.01
Na	0.10	0.10	0.26	0.16	0.13	0.16	0.19	0.26	0.10	0.16	0.13	0.23	0.20	0.18
K	3.74	3.84	3.71	3.78	3.84	3.68	3.81	3.74	3.87	3.78	3.74	3.67	3.69	3.73
Ba	0.00	0.00	0.00	0.00	0.00	0.00	0.00	0.00	0.00	0.00	0.10	nd	nd	nd
Mole proportions														
Or	0.97	0.98	0.94	0.96	0.97	0.96	0.95	0.94	0.97	0.96	0.97	0.94	0.95	0.95
Ab	0.03	0.02	0.06	0.04	0.03	0.05	0.05	0.06	0.03	0.04	0.03	0.06	0.05	0.05
An	0.00	0.00	0.00	0.00	0.00	0.00	0.00	0.00	0.00	0.00	0.00	0.00	0.00	0.00

Table C.3.4. Continued.

Pluton	Dioritic to Granodioritic Plutons						Shadow Lake Granodiorite							
	Belmont Tonalite			Perch Lake Granodiorite			(perthite)				NB92-9033			
	NB91-8522			NB92-9027			NB91-8565			NB91-8599B		NB92-9033		
Sample	1	2	3	1	2	3	1	2	3	1	2	3	4	1
SiO ₂	64.53	64.54	64.30	64.53	64.18	64.66	67.73	68.47	66.83	64.60	64.66	64.59	64.84	63.94
TiO ₂	0.00	0.00	0.00	0.00	0.00	0.00	0.00	0.00	0.00	0.00	0.00	0.00	0.00	0.00
Al ₂ O ₃	18.38	18.32	18.45	18.27	18.30	18.44	19.52	19.61	20.72	18.42	18.64	18.56	18.43	18.25
FeO	0.00	0.00	0.00	0.00	0.00	0.00	0.00	0.00	0.00	0.00	0.00	0.00	0.00	0.00
MnO	0.00	0.00	0.00	0.00	0.00	0.00	0.00	0.00	0.00	0.00	0.00	0.00	0.00	0.00
MgO	0.00	0.00	0.00	0.00	0.13	0.00	0.00	0.00	0.00	0.00	0.00	0.00	0.00	0.00
CaO	0.00	0.00	0.00	0.00	0.00	0.00	0.43	0.32	1.50	0.00	0.00	0.00	0.00	0.00
Na ₂ O	1.02	0.67	0.59	1.00	0.30	0.44	10.18	10.88	9.59	0.56	0.37	0.61	0.23	1.00
K ₂ O	15.08	15.94	15.79	15.31	15.92	16.08	0.00	0.00	0.00	15.65	16.11	15.69	15.55	14.99
Cr ₂ O ₃	0.00	0.00	0.00	0.00	0.00	0.00	0.00	0.00	0.00	0.00	0.00	0.00	0.00	0.00
BaO	0.87	0.00	0.53	0.38	0.33	0.41	0.00	0.00	0.00	0.44	0.88	0.72	0.55	0.00
TOTAL	99.88	99.48	99.65	99.48	99.16	100.02	97.86	99.28	98.65	99.68	100.66	100.17	99.60	98.19
Number of ions on the basis of 32 oxygen														
Si	11.97	12.00	11.97	12.00	11.97	11.97	12.03	11.94	11.81	12.00	11.94	11.97	12.03	12.00
Al	4.03	4.00	4.03	4.00	4.03	4.03	4.10	4.03	4.32	4.03	4.06	4.06	4.03	4.03
Ti	0.00	0.00	0.00	0.00	0.00	0.00	0.00	0.00	0.00	0.00	0.00	0.00	0.00	0.00
Cr	0.00	0.00	0.00	0.00	0.00	0.00	0.00	0.00	0.00	0.00	0.00	0.00	0.00	0.00
Fe	0.00	0.00	0.00	0.00	0.00	0.00	0.00	0.00	0.00	0.00	0.00	0.00	0.00	0.00
Mn	0.00	0.00	0.00	0.00	0.00	0.00	0.00	0.00	0.00	0.00	0.00	0.00	0.00	0.00
Mg	0.00	0.00	0.00	0.00	0.03	0.00	0.00	0.00	0.00	0.00	0.00	0.00	0.00	0.00
Ca	0.00	0.00	0.00	0.00	0.00	0.00	0.10	0.06	0.29	0.00	0.00	0.00	0.00	0.00
Na	0.35	0.26	0.22	0.35	0.10	0.16	3.49	3.68	3.30	0.19	0.13	0.22	0.10	0.35
K	3.58	3.78	3.74	3.62	3.78	3.81	0.00	0.00	0.00	3.71	3.78	3.71	3.68	3.58
Ba	0.06	0.00	0.03	0.03	0.03	0.03	0.00	0.00	0.00	0.03	0.06	0.06	0.03	0.00
Mole Proportions														
Or	0.91	0.94	0.95	0.91	0.97	0.96	0.00	0.00	0.00	0.95	0.97	0.94	0.98	0.91
Ab	0.09	0.06	0.05	0.09	0.03	0.04	0.98	0.98	0.92	0.05	0.03	0.06	0.02	0.09
An	0.00	0.00	0.00	0.00	0.00	0.00	0.02	0.02	0.08	0.00	0.00	0.00	0.00	0.00

Table C.3.4. Continued.

Pluton	Dioritic to Granodioritic Plutons Shadow Lake Granodiorite						Enclave		Talbot Road Tonalite					
	NB92-9033		4	5	NB92-9258			NB91-8E97		NB92-9045			NB92-9153	
Sample	2	3			1	2	3	1	2	1	2	3	1	2
SiO ₂	64.65	64.00	63.89	64.66	66.04	64.86	66.46	64.75	64.14	64.66	65.04	64.45	64.36	64.80
TiO ₂	0.00	0.00	0.00	0.00	0.00	0.00	0.00	0.00	0.00	0.00	0.00	0.00	0.00	0.00
Al ₂ O ₃	17.93	18.21	18.24	18.43	18.61	18.41	18.92	18.27	18.37	18.27	18.47	18.13	18.18	18.41
FeO	0.00	0.00	0.00	0.00	0.00	0.00	0.00	0.00	0.00	0.00	0.00	0.00	0.00	0.00
MnO	0.00	0.00	0.00	0.00	0.00	0.00	0.00	0.00	0.00	0.00	0.00	0.00	0.00	0.00
MgO	0.00	0.00	0.00	0.00	0.00	0.00	0.00	0.00	0.00	0.00	0.00	0.00	0.00	0.00
CaO	0.00	0.00	0.00	0.00	0.00	0.00	0.00	0.00	0.00	0.00	0.00	0.00	0.00	0.00
Na ₂ O	1.68	0.56	0.46	1.85	0.51	0.22	4.43	0.63	0.66	1.03	0.54	0.79	0.84	0.56
K ₂ O	13.69	15.72	15.93	13.93	14.33	16.34	11.07	15.90	15.68	15.46	16.05	15.76	15.64	15.70
Cr ₂ O ₃	0.00	0.00	0.00	0.00	0.00	0.00	0.00	0.00	0.00	0.00	0.00	0.00	0.00	0.00
BaO	0.00	0.00	0.34	0.30	0.00	0.00	0.00	0.55	0.61	0.00	0.00	0.00	0.00	0.00
TOTAL	97.95	98.49	98.85	99.17	99.47	99.82	100.88	100.10	99.45	99.42	100.10	99.12	99.02	99.47

Number of ions on the basis of 32 oxygen.

Si	12.06	12.00	11.97	11.97	12.10	12.00	11.97	12.00	11.97	12.00	12.00	12.00	12.00	12.00
Al	3.94	4.03	4.03	4.03	4.03	4.00	4.00	4.00	4.03	4.00	4.00	3.97	4.00	4.03
Ti	0.00	0.00	0.00	0.00	0.00	0.00	0.00	0.00	0.00	0.00	0.00	0.00	0.00	0.00
Cr	0.00	0.00	0.00	0.00	0.00	0.00	0.00	0.00	0.00	0.00	0.00	0.00	0.00	0.00
Fe	0.00	0.00	0.00	0.00	0.00	0.00	0.00	0.00	0.00	0.00	0.00	0.00	0.00	0.00
Mn	0.00	0.00	0.00	0.00	0.00	0.00	0.00	0.00	0.00	0.00	0.00	0.00	0.00	0.00
Mg	0.00	0.00	0.00	0.00	0.00	0.00	0.00	0.00	0.00	0.00	0.00	0.00	0.00	0.00
Ca	0.00	0.00	0.00	0.00	0.00	0.00	0.00	0.00	0.00	0.00	0.00	0.00	0.00	0.00
Na	0.61	0.19	0.16	0.67	0.19	0.06	1.54	0.22	0.22	0.38	0.19	0.29	0.32	0.19
K	3.26	3.74	3.81	3.30	3.36	3.87	2.53	3.74	3.74	3.65	3.78	3.74	3.71	3.71
Ba	0.00	0.00	0.03	0.03	0.00	0.00	0.00	0.03	0.03	0.00	0.00	0.00	0.00	0.00

Mole proportions

Or	0.84	0.95	0.96	0.83	0.95	0.98	0.62	0.94	0.94	0.91	0.95	0.93	0.92	0.95
Ab	0.16	0.05	0.04	0.17	0.05	0.02	0.38	0.06	0.06	0.09	0.05	0.07	0.08	0.05
An	0.00	0.00	0.00	0.00	0.00	0.00	0.00	0.00	0.00	0.00	0.00	0.00	0.00	0.00

Table C.3.4. Continued.

Pluton Sample	Monzogranite to Granodioritic Plutons												
	NB92- 9153	Renforth Pluton CW88- 189	Fairville Granite				Chalet Lake Granite			Hammond River Granite			
			CW88-272		CW89-611		CW88-254			CW88-200			
			1	2	1	2	1	2	3	1	2	3	4
SiO ₂	64.69	64.15	64.02	63.94	67.09	65.70	63.22	63.25	63.97	63.59	64.21	62.95	64.21
TiO ₂	0.00	0.03	0.00	0.00	0.02	0.00	0.05	0.05	0.02	0.01	0.00	0.00	0.00
Al ₂ O ₃	17.93	18.90	18.22	18.25	18.34	18.74	18.43	18.17	18.59	18.73	18.58	18.40	19.70
FeO	0.00	0.18	0.09	0.00	0.04	0.00	0.14	0.10	0.16	0.13	0.12	0.09	0.09
MnO	0.00	0.02	0.00	0.00	0.00	0.00	0.04	0.00	0.04	0.05	0.02	0.00	0.00
MgO	0.00	0.00	0.00	0.00	0.01	0.00	0.00	0.00	0.00	0.00	0.00	0.00	0.00
CaO	0.00	0.20	0.03	0.04	0.01	0.00	0.03	0.03	0.07	0.02	0.01	0.00	0.05
Na ₂ O	0.36	1.59	0.67	0.52	0.28	0.41	0.51	0.48	0.71	0.27	1.06	0.50	1.92
K ₂ O	16.07	14.83	16.55	16.74	16.57	16.29	16.59	16.73	16.57	15.25	15.31	16.59	14.25
Cr ₂ O ₃	0.00	0.03	0.00	0.00	0.00	0.00	0.04	0.03	0.00	0.02	0.04	0.02	0.00
BaO	0.00	n.d.	n.d.	n.d.	n.d.	n.d.	n.d.	n.d.	n.d.	n.d.	n.d.	n.d.	n.d.
TOTAL	99.05	99.93	99.58	99.49	102.36	101.14	99.05	98.84	100.13	98.07	99.35	98.55	100.22

Number of ions on the basis of 32 oxygen.

Si	12.00	11.86	11.94	11.94	12.09	11.99	11.88	11.91	11.88	11.94	11.93	11.88	11.79
Al	3.94	4.12	4.01	4.02	3.90	4.03	4.08	4.04	4.07	4.15	4.07	4.09	4.26
Ti	0.00	0.00	0.00	0.00	0.00	0.00	0.00	0.00	0.00	0.00	0.00	0.00	0.00
Cr	0.00	0.00	0.00	0.00	0.00	0.00	0.00	0.00	0.00	0.00	0.00	0.00	0.00
Fe	0.00	0.03	0.01	0.00	0.01	0.00	0.02	0.02	0.03	0.02	0.02	0.01	0.01
Mn	0.00	0.00	0.00	0.00	0.00	0.00	0.00	0.00	0.00	0.00	0.00	0.00	0.00
Mg	0.00	0.00	0.00	0.00	0.00	0.00	0.00	0.00	0.00	0.00	0.00	0.00	0.00
Ca	0.00	0.04	0.01	0.01	0.00	0.00	0.01	0.01	0.01	0.00	0.00	0.00	0.01
Na	0.13	0.57	0.24	0.19	0.10	0.15	0.19	0.18	0.26	0.10	0.38	0.18	0.68
K	3.81	3.50	3.94	3.99	3.81	3.79	3.98	4.02	3.93	3.65	3.63	3.99	3.34
Ba	0.00	n.d.	n.d.	n.d.	n.d.	n.d.	n.d.	n.d.	n.d.	n.d.	n.d.	n.d.	n.d.

Mole proportions

Or	0.97	0.85	0.94	0.95	0.97	0.96	0.95	0.96	0.94	0.89	0.90	0.96	0.83
Ab	0.03	0.14	0.06	0.05	0.03	0.04	0.05	0.04	0.06	0.11	0.10	0.04	0.17
An	0.00	0.01	0.00	0.00	0.00	0.00	0.00	0.00	0.00	0.00	0.00	0.00	0.00

Table C.3.4. Continued.

Pluton	Monzogranitic to Granodioritic Plutons													
	Milkish Head Pluton			Hanson Stream Granodiorite										
	Sample	NB92-9144			NB92-9039				NB92-9050				NB92-9154	
	1	2	3	1	2	3	4	1	2	3	4	1	2	3
SiO ₂	64.80	64.29	64.49	64.08	63.78	65.11	64.82	64.95	64.18	64.61	64.43	64.71	64.52	64.29
TiO ₂	0.00	0.00	0.00	0.00	0.00	0.00	0.00	0.00	0.00	0.00	0.00	0.00	0.00	0.00
Al ₂ O ₃	18.28	18.19	18.31	18.01	18.11	18.32	18.44	18.31	18.18	18.20	18.29	18.19	18.22	18.34
FeO	0.00	0.00	0.00	0.00	0.00	0.00	0.00	0.00	0.00	0.00	0.00	0.00	0.00	0.00
MnO	0.00	0.00	0.00	0.00	0.00	0.00	0.00	0.00	0.00	0.00	0.00	0.00	0.00	0.00
MgO	0.00	0.00	0.00	0.00	0.00	0.14	0.14	0.00	0.00	0.00	0.20	0.00	0.00	0.00
CaO	0.00	0.00	0.00	0.00	0.00	0.00	0.00	0.00	0.00	0.00	0.17	0.00	0.00	0.00
Na ₂ O	2.27	0.41	0.33	0.48	0.64	0.80	0.58	0.42	0.24	0.22	0.25	0.51	0.75	0.47
K ₂ O	14.26	15.97	16.08	15.87	15.05	15.51	15.96	15.87	15.99	16.34	16.16	16.04	15.20	15.95
Cr ₂ O ₃	0.00	0.00	0.00	0.00	0.00	0.00	0.00	0.00	0.00	0.00	0.00	0.00	0.00	0.00
BaO	0.00	0.00	0.00	0.00	0.00	0.00	0.00	0.00	0.00	0.00	0.00	0.00	0.00	0.00
TOTAL	99.61	98.86	99.21	98.44	97.58	99.88	99.94	99.55	98.59	99.37	99.50	99.45	98.69	99.05
Number of ions on the basis of 32 oxygen.														
Si	11.97	12.01	12.00	12.02	12.02	12.01	11.98	12.03	12.01	12.02	11.97	12.02	12.03	11.99
Al	3.97	4.00	4.03	3.98	4.02	3.98	4.02	4.00	4.01	3.99	4.01	3.98	4.00	4.03
Ti	0.00	0.00	0.00	0.00	0.00	0.00	0.00	0.00	0.00	0.00	0.00	0.00	0.00	0.00
Cr	0.00	0.00	0.00	0.00	0.00	0.00	0.00	0.00	0.00	0.00	0.00	0.00	0.00	0.00
Fe	0.00	0.00	0.00	0.00	0.00	0.00	0.00	0.00	0.00	0.00	0.00	0.00	0.00	0.00
Mn	0.00	0.00	0.00	0.00	0.00	0.00	0.00	0.00	0.00	0.00	0.00	0.00	0.00	0.00
Mg	0.00	0.00	0.00	0.00	0.00	0.04	0.04	0.00	0.00	0.00	0.06	0.00	0.00	0.00
Ca	0.00	0.00	0.00	0.00	0.00	0.00	0.00	0.00	0.00	0.00	0.03	0.00	0.00	0.00
Na	0.81	0.15	0.12	0.18	0.23	0.29	0.21	0.15	0.09	0.08	0.09	0.18	0.27	0.17
K	3.36	3.81	3.82	3.80	3.62	3.65	3.76	3.75	3.82	3.88	3.83	3.80	3.61	3.79
Ba	0.00	0.00	0.00	0.00	0.00	0.00	0.00	0.00	0.00	0.00	0.00	0.00	0.00	0.00
Mole proportions														
Or	0.81	0.96	0.97	0.96	0.94	0.93	0.95	0.96	0.98	0.98	0.97	0.95	0.93	0.96
Ab	0.20	0.04	0.03	0.04	0.06	0.07	0.05	0.04	0.02	0.02	0.02	0.05	0.07	0.04
An	0.00	0.00	0.00	0.00	0.00	0.00	0.00	0.00	0.00	0.00	0.01	0.00	0.00	0.00

APPENDIX C.3. Continued.

Table C.3.5. Opaque mineral analyses from plutonic units in the Brookville terrane.

Pluton	Dioritic to Granodioritic Plutons Ludgate Lake Granodiorite						French Village Pluton CW88-153		Belmont Tonalite				
	NB91- 8590	NB91-8622 1 2		NB92-9195B 1 2		NB92- 9251	1	2	NB91-8513 1 2		NB91-8522 1 2		3
SiO ₂	0.20	0.15	0.23	0.18	0.21	0.19	0.10	0.00	0.00	0.00	0.15	0.00	1.52
TiO ₂	0.23	0.00	0.00	0.00	0.00	0.00	0.19	0.00	0.00	0.00	0.00	0.00	1.66
Al ₂ O ₃	0.00	0.00	0.00	0.00	0.00	0.00	30.25	31.87	0.00	0.00	0.00	0.00	0.95
FeO	90.71	90.66	91.08	91.75	91.88	91.93	68.86	67.51	91.23	90.57	86.97	87.29	84.07
MnO	0.00	0.00	0.00	0.00	0.00	0.00	0.24	0.00	0.00	0.00	0.00	0.00	0.00
MgO	0.00	0.00	0.00	0.00	0.00	0.00	0.28	0.25	0.00	0.00	0.00	0.00	1.11
CaO	0.00	0.00	0.00	0.00	0.00	0.00	0.20	0.30	0.00	0.00	0.00	0.11	0.10
Na ₂ O	0.41	0.27	0.36	0.43	0.26	0.37	0.33	0.02	0.31	0.35	0.00	0.41	0.37
K ₂ O	0.00	0.00	0.00	0.00	0.00	0.00	0.00	0.01	0.00	0.00	0.00	0.00	0.00
Cr ₂ O ₃	0.00	0.00	0.00	0.00	0.00	0.00	0.16	0.12	0.47	0.74	0.00	0.83	0.00
TOTAL	91.55	91.08	91.67	92.36	92.36	92.49	100.61	100.08	92.01	91.76	87.13	88.63	89.78

Number of ions on the basis of 6 oxygen.

Magnetite	0.99	1.00	1.00	1.00	1.00	1.00	0.42	0.40	1.00	1.00	1.00	1.00	0.88
Mg-Ferrite	0.00	0.00	0.00	0.00	0.00	0.00	0.00	0.00	0.00	0.00	0.00	0.00	0.04
Jacobsite	0.00	0.00	0.00	0.00	0.00	0.00	0.01	0.00	0.00	0.00	0.00	0.00	0.00
Chromite	0.00	0.00	0.00	0.00	0.00	0.00	0.00	0.00	0.00	0.00	0.00	0.00	0.00
Spinel	0.00	0.00	0.00	0.00	0.00	0.00	0.01	0.01	0.00	0.00	0.00	0.00	0.02
Hercynite	0.00	0.00	0.00	0.00	0.00	0.00	0.56	0.59	0.00	0.00	0.00	0.00	0.00
Ulvospinel	0.01	0.00	0.00	0.00	0.00	0.00	0.01	0.00	0.00	0.00	0.00	0.00	0.05

c = core; r = rim

Table C.3.5. Continued.

Pluton Sample	Dioritic to Granodioritic Plutons										Enclave NB91- 8597	Talbot Road Granodiorite		
	Perch Lake Granodiorite		Shadow Lake Granodiorite						NB92-9045			NB92- 9153		
	NB92-9027 1	2	NB91-8565 1	2	NB91-8599B 1	2	NB92-9033 1	2	NB92-9258 1	2			1c	1r
SiO ₂	0.22	0.23	0.25	0.21	0.00	0.23	0.17	0.27	0.23	0.18	0.21	0.00	0.25	0.00
TiO ₂	0.39	0.00	0.23	0.36	0.00	0.23	0.00	0.00	0.00	0.00	0.00	0.00	0.21	0.00
Al ₂ O ₃	0.00	0.00	0.00	0.22	0.00	0.00	0.17	0.00	0.00	0.00	0.00	0.00	0.00	0.00
FeO	91.19	91.14	89.54	87.26	92.00	92.15	91.32	92.04	90.47	91.42	91.15	90.34	90.54	90.78
MnO	0.00	0.00	0.00	0.00	0.00	0.00	0.00	0.00	0.00	0.00	0.00	0.00	0.00	0.00
MgO	0.00	0.00	0.00	0.00	0.00	0.00	0.00	0.00	0.00	0.00	0.00	0.00	0.00	0.00
CaO	0.17	0.00	0.00	0.00	0.00	0.00	0.00	0.00	0.11	0.11	0.00	0.00	0.00	0.00
Na ₂ O	0.50	0.36	0.39	0.35	0.41	0.39	0.34	0.40	0.51	0.50	0.00	0.35	0.41	0.39
K ₂ O	0.00	0.00	0.00	0.00	0.00	0.00	0.00	0.00	0.00	0.00	0.00	0.00	0.00	0.00
Cr ₂ O ₃	0.00	0.22	0.00	0.00	0.00	0.27	0.00	0.00	0.00	0.00	0.00	0.00	0.00	0.16
TOTAL	92.48	91.94	90.41	88.40	92.41	93.26	92.00	92.71	91.32	92.21	91.35	90.69	91.40	91.33

Number of ions on the basis of 6 oxygen.

Magnetite	0.99	1.00	0.99	0.98	1.00	1.00	1.00	1.00	1.00	1.00	1.00	1.00	0.99	1.00
Mg-Ferrite	0.00	0.00	0.00	0.00	0.00	0.00	0.00	0.00	0.00	0.00	0.00	0.00	0.00	0.00
Jacobsite	0.00	0.00	0.00	0.00	0.00	0.00	0.00	0.00	0.00	0.00	0.00	0.00	0.00	0.00
Chromite	0.00	0.00	0.00	0.00	0.00	0.00	0.00	0.00	0.00	0.00	0.00	0.00	0.00	0.00
Spinel	0.00	0.00	0.00	0.00	0.00	0.00	0.00	0.00	0.00	0.00	0.00	0.00	0.00	0.00
Hercynite	0.00	0.00	0.00	0.01	0.00	0.00	0.00	0.00	0.00	0.00	0.00	0.00	0.00	0.00
Ulvospinel	0.01	0.00	0.01	0.01	0.00	0.00	0.00	0.00	0.00	0.00	0.00	0.00	0.01	0.00

Table C.3.5. Continued.

Pluton	Narrows Tonalite Sample CW89- 616	Monzogranitic to Granodioritic Plutons						Hanson Stream Granodiorite						
		Fairville Granite		Hammond R. Granite		Milkish H. Pluton		NB92-9039		NB92-9050		NB92-9154		
		CW88-272	CW89-	CW88-200	NB92-9144	NB92-9039	NB92-9050	NB92-9154						
		1	2	1	2	1	2	1	2	1	2	1	2	
SiO ₂	0.00	0.00	0.00	0.25	0.00	0.00	0.15	0.00	0.20	0.15	0.16	0.00	0.19	0.18
TiO ₂	0.16	0.16	0.16	0.00	0.40	0.18	0.28	0.26	0.00	0.00	0.00	0.21	0.00	0.25
Al ₂ O ₃	0.00	0.17	0.09	0.00	0.14	0.09	0.18	0.09	0.00	0.00	0.00	0.00	0.00	0.00
FeO	92.16	89.95	92.35	92.08	85.51	92.36	91.25	92.30	91.14	93.09	91.41	91.77	91.85	91.51
MnO	0.13	0.31	0.10	0.00	0.33	0.31	0.00	0.08	0.00	0.00	0.00	0.00	0.00	0.00
MgO	0.02	0.00	0.00	0.00	0.00	0.03	0.00	0.00	0.00	0.00	0.00	0.00	0.00	0.00
CaO	0.09	0.07	0.00	0.00	0.08	0.08	0.00	0.00	0.00	0.00	0.00	0.00	0.00	0.00
Na ₂ O	0.01	0.00	0.00	0.21	0.00	0.17	0.42	0.03	0.44	0.57	0.32	0.50	0.44	0.49
K ₂ O	0.04	0.05	0.00	0.00	0.05	0.10	0.00	0.00	0.00	0.00	0.00	0.00	0.00	0.00
Cr ₂ O ₃	0.00	0.19	0.14	0.01	0.16	0.18	0.38	0.42	0.18	0.00	0.00	0.00	0.00	0.00
TOTAL	92.61	90.90	92.84	92.55	86.65	93.50	92.66	93.18	91.96	93.80	91.88	92.48	92.49	92.43
Number of ions on the basis of 4 oxygen.														
Magnetite	0.99	0.98	1.00	1.00	0.97	0.98	0.98	0.98	1.00	1.00	1.00	0.99	1.00	0.99
Mg-Ferrite	0.00	0.00	0.00	0.00	0.00	0.00	0.00	0.00	0.00	0.00	0.00	0.00	0.00	0.00
Jacobsite	0.00	0.01	0.00	0.00	0.01	0.01	0.00	0.00	0.00	0.00	0.00	0.00	0.00	0.00
Chromite	0.00	0.00	0.00	0.00	0.00	0.00	0.01	0.01	0.00	0.00	0.00	0.00	0.00	0.00
Spinel	0.00	0.00	0.00	0.00	0.00	0.00	0.00	0.00	0.00	0.00	0.00	0.00	0.00	0.00
Hercynite	0.00	0.00	0.00	0.00	0.00	0.00	0.00	0.00	0.00	0.00	0.00	0.00	0.00	0.00
Ulvospinel	0.01	0.01	0.01	0.00	0.01	0.01	0.01	0.01	0.00	0.00	0.00	0.01	0.00	0.01

APPENDIX D

MICROPROBE DATA FROM METAMORPHIC UNITS

Table D.1. Biotite analyses.

Rock Sample	Brookville Gneiss migmatite CW88-181B				paragneiss CW88-181C			migmatite CW88-218		paragneiss CW88-220			migmatite CW88-240	
	1	2	3	4	1	2	3	1	2	1	2	3	1	2
	SiO ₂	34.86	34.88	35.21	34.48	34.76	34.57	34.67	36.03	36.14	34.36	34.76	35.32	35.38
TiO ₂	2.67	2.77	2.79	2.77	3.15	2.92	3.27	1.07	2.81	3.63	3.90	3.06	2.54	3.32
Al ₂ O ₃	18.87	19.06	18.80	18.57	17.80	17.63	17.55	19.54	19.24	18.49	18.12	18.97	19.13	18.28
FeO	18.94	19.18	19.08	18.10	20.34	20.14	20.21	16.08	16.28	18.94	19.61	18.33	17.80	19.26
MnO	0.20	0.19	0.17	0.15	0.34	0.27	0.23	0.34	0.48	0.26	0.20	0.24	0.36	0.28
MgO	9.64	9.41	9.50	10.00	8.97	9.55	9.30	12.79	11.00	9.61	9.07	9.88	10.50	9.22
CaO	0.00	0.00	0.00	0.01	0.00	0.00	0.00	0.00	0.00	0.00	0.00	0.00	0.00	0.00
Na ₂ O	0.13	0.15	0.11	0.14	0.08	0.09	0.08	0.16	0.16	0.12	0.07	0.18	0.18	0.08
K ₂ O	9.61	9.83	9.69	9.60	9.75	9.93	9.87	9.35	9.57	9.43	9.81	9.77	9.51	9.96
Cr ₂ O ₃	0.00	0.03	0.04	0.04	0.06	0.03	0.00	0.00	0.00	0.02	0.04	0.04	0.01	0.03
TOTAL	94.92	95.50	95.39	93.86	95.25	95.13	95.18	95.36	95.68	94.86	95.58	95.79	95.41	95.64

Number of ions on the basis of 22 oxygen.

Si	5.34	5.32	5.36	5.33	5.36	5.34	5.35	5.39	5.40	5.27	5.32	5.34	5.35	5.37
Al ^{iv}	2.66	2.68	2.64	2.68	2.64	2.66	2.65	2.61	2.60	2.73	2.69	2.66	2.65	2.63
Al ^{vi}	0.74	0.74	0.74	0.71	0.59	0.55	0.54	0.83	0.79	0.62	0.58	0.72	0.76	0.65
Ti	0.31	0.32	0.32	0.32	0.37	0.34	0.38	0.12	0.32	0.42	0.45	0.35	0.29	0.38
Cr	0.00	0.00	0.01	0.01	0.01	0.00	0.00	0.00	0.00	0.00	0.01	0.01	0.00	0.00
Fe	2.42	2.45	2.43	2.34	2.62	2.60	2.61	2.01	2.04	2.43	2.51	2.32	2.25	2.46
Mn	0.03	0.03	0.02	0.02	0.04	0.04	0.03	0.04	0.06	0.03	0.03	0.03	0.05	0.04
Mg	2.20	2.14	2.16	2.30	2.06	2.20	2.14	2.85	2.45	2.20	2.07	2.23	2.37	2.10
Ca	0.00	0.00	0.00	0.00	0.00	0.00	0.00	0.00	0.00	0.00	0.00	0.00	0.00	0.00
Na	0.04	0.04	0.03	0.04	0.02	0.03	0.02	0.05	0.05	0.04	0.02	0.05	0.05	0.02
K	1.88	1.91	1.88	1.89	1.92	1.96	1.94	1.78	1.83	1.85	1.91	1.89	1.83	1.94
Mg/Mg+Fe	0.48	0.47	0.47	0.50	0.44	0.46	0.45	0.59	0.55	0.48	0.45	0.49	0.51	0.46

Table D.1. Continued.

Rock Sample	Brookville Gneiss											ortho- gneiss CW88 -132A 1		
	migma- tite CW88 -240		paragneiss CW89-534A			CW89-569			CW89-644					
	3	1	2	3	1	2	3	4	1	2	3		4	5
SiO ₂	33.87	34.05	34.09	33.79	34.25	33.73	34.68	34.87	36.36	34.90	32.24	33.35	33.77	34.97
TiO ₂	3.21	3.28	2.78	3.29	3.69	3.03	3.29	3.46	1.64	2.66	1.62	1.45	2.09	3.38
Al ₂ O ₃	17.96	17.24	17.37	17.63	18.52	18.51	18.61	18.20	19.61	18.68	18.42	18.83	18.20	14.80
FeO	19.51	19.62	20.39	19.68	19.20	20.29	19.21	19.81	16.13	20.31	21.39	21.43	20.59	17.74
MnO	0.31	0.32	0.25	0.29	0.22	0.19	0.22	0.23	0.34	0.24	0.28	0.26	0.28	0.51
MgO	9.26	9.69	10.27	9.69	8.48	8.98	8.96	8.88	12.17	8.92	10.29	9.66	9.38	11.70
CaO	0.00	0.00	0.00	0.00	0.09	0.04	0.00	0.00	0.04	0.00	0.00	0.00	0.00	0.04
Na ₂ O	0.07	0.08	0.12	0.13	0.14	0.13	0.12	0.12	0.12	0.12	0.02	0.05	0.06	0.08
K ₂ O	9.93	9.69	8.87	9.73	9.35	9.01	9.78	9.90	9.63	9.67	8.31	8.97	9.62	9.06
Cr ₂ O ₃	0.00	0.03	0.05	0.00	0.03	0.01	0.05	0.00	0.00	0.02	0.00	0.00	0.02	0.00
TOTAL	94.12	94.00	94.19	94.23	93.97	93.92	94.92	95.47	96.04	95.52	92.57	94.00	94.01	92.28
Number of ions on the basis of 22 oxygen.														
Si	5.28	5.32	5.30	5.27	5.31	5.26	5.33	5.34	5.40	5.35	5.13	5.22	5.29	5.50
Al ^{iv}	2.72	2.69	2.70	2.74	2.69	2.74	2.67	2.66	2.60	2.65	2.87	2.78	2.71	2.50
Al ^{vi}	0.58	0.49	0.49	0.50	0.69	0.66	0.70	0.63	0.84	0.72	0.59	0.70	0.65	0.25
Ti	0.38	0.39	0.33	0.39	0.43	0.36	0.38	0.40	0.18	0.31	0.19	0.17	0.25	0.40
Cr	0.00	0.00	0.01	0.00	0.00	0.00	0.01	0.00	0.00	0.00	0.00	0.00	0.00	0.00
Fe	2.54	2.56	2.65	2.57	2.49	2.64	2.47	2.54	2.00	2.60	2.85	2.81	2.70	2.34
Mn	0.04	0.04	0.03	0.04	0.03	0.03	0.03	0.03	0.04	0.03	0.04	0.03	0.04	0.07
Mg	2.15	2.25	2.38	2.25	1.96	2.09	2.05	2.03	2.70	2.04	2.44	2.25	2.19	2.74
Ca	0.00	0.00	0.00	0.00	0.02	0.01	0.00	0.00	0.01	0.00	0.00	0.00	0.00	0.01
Na	0.02	0.02	0.04	0.04	0.04	0.04	0.04	0.04	0.04	0.04	0.01	0.02	0.02	0.02
K	1.98	1.93	1.76	1.93	1.85	1.79	1.92	1.94	1.83	1.89	1.69	1.79	1.92	1.82
Mg/Mg+Fe	0.46	0.47	0.47	0.47	0.44	0.44	0.45	0.44	0.57	0.44	0.46	0.45	0.45	0.54

Table D.1. Continued.

Rock Sample	Brookville Gneiss orthogneiss														
	CW88-132A					CW88-178				CW880181A			CW89-629A		
	2	3	4	5	6	1	2	3	4	1	2	3	1	2	
SiO ₂	35.98	36.75	37.07	27.25	31.60	33.75	32.85	29.08	33.18	36.52	37.19	36.86	36.54	35.63	
TiO ₂	3.28	3.24	2.90	0.15	1.28	2.65	2.51	1.35	0.77	2.87	2.86	2.94	2.66	2.70	
Al ₂ O ₃	14.52	14.25	14.62	18.94	16.88	16.61	17.25	17.78	18.54	15.86	15.59	15.84	15.92	15.72	
FeO	18.03	17.98	17.67	20.96	20.30	20.42	21.45	22.88	20.98	19.11	18.56	18.60	18.81	18.99	
MnO	0.53	0.49	0.52	0.74	0.63	0.32	0.33	0.40	0.31	0.48	0.50	0.46	0.48	0.51	
MgO	11.60	11.98	12.50	18.69	16.14	10.73	11.24	14.23	11.40	10.91	11.07	10.84	10.92	10.88	
CaO	0.05	0.04	0.00	0.04	0.06	0.09	0.14	0.51	0.14	0.00	0.00	0.00	0.00	0.02	
Na ₂ O	0.11	0.10	0.12	0.01	0.03	0.05	0.02	0.01	0.01	0.05	0.05	0.05	0.10	0.08	
K ₂ O	9.30	9.19	9.59	0.04	1.83	7.40	6.01	0.83	3.70	9.62	9.55	9.41	9.57	9.83	
Cr ₂ O ₃	0.00	0.00	0.00	0.00	0.00	0.00	0.00	0.00	0.00	0.00	0.00	0.00	0.00	0.00	
TOTAL	93.40	94.02	94.99	86.82	88.75	92.02	91.80	87.07	89.03	95.42	95.37	95.00	95.00	94.36	

Number of ions on the basis of 22 oxygen.

Si	5.60	5.66	5.65	4.46	5.05	5.34	5.20	4.80	5.30	5.57	5.65	5.62	5.59	5.52
Al ^{iv}	2.41	2.34	2.35	3.54	2.96	2.66	2.80	3.20	2.70	2.43	2.35	2.38	2.41	2.48
Al ^{vi}	0.26	0.25	0.27	0.12	0.22	0.44	0.42	0.25	0.80	0.42	0.44	0.47	0.46	0.39
Ti	0.38	0.38	0.33	0.02	0.15	0.32	0.30	0.17	0.09	0.33	0.33	0.34	0.31	0.32
Cr	0.00	0.00	0.00	0.00	0.00	0.00	0.00	0.00	0.00	0.00	0.00	0.00	0.00	0.00
Fe	2.35	2.32	2.25	2.87	2.71	2.70	2.84	3.16	2.81	2.44	2.36	2.37	2.41	2.46
Mn	0.07	0.06	0.07	0.10	0.09	0.04	0.04	0.06	0.04	0.06	0.06	0.06	0.06	0.07
Mg	2.69	2.75	2.84	4.56	3.84	2.53	2.65	3.50	2.72	2.48	2.51	2.46	2.49	2.51
Ca	0.01	0.01	0.00	0.01	0.01	0.02	0.02	0.09	0.02	0.00	0.00	0.00	0.00	0.00
Na	0.03	0.03	0.04	0.00	0.01	0.02	0.01	0.90	0.00	0.02	0.02	0.02	0.03	0.02
K	1.85	1.81	1.86	0.01	0.37	1.49	1.21	0.18	0.76	1.87	1.85	1.83	1.87	1.94
Mg/Mg+Fe	0.53	0.54	0.56	0.61	0.59	0.48	0.48	0.53	0.49	0.50	0.52	0.51	0.51	0.51

Table D.1. Continued.

Rock Sample	Brookville Gneiss							quartzo-feldspathic blastomylonite						
	orthogneiss		paragneissic		boudin			NB92-9079B						
	CW89-629A		CW89-662A					1-G1	2-G2	3-G3	4-G4r	5-G4c	6-G5c	7-G5r
	3	4	1	2	3	4	5							
SiO ₂	35.04	31.11	34.70	35.26	34.54	35.08	35.21	33.63	34.31	35.50	34.44	34.12	34.77	35.34
TiO ₂	2.72	1.48	2.47	2.15	3.13	2.23	0.72	1.42	1.23	1.27	1.63	1.46	2.41	1.45
Al ₂ O ₃	15.80	17.48	20.02	20.09	19.67	20.07	20.74	19.50	19.87	20.55	20.05	20.08	18.86	19.83
FeO	19.31	22.16	19.80	19.33	20.36	19.27	18.46	21.60	22.42	22.33	21.97	22.16	21.90	20.04
MnO	0.50	0.65	0.15	0.15	0.15	0.16	0.15	0.00	0.00	0.00	0.00	0.00	0.00	0.00
MgO	11.24	13.69	8.54	8.97	7.99	8.88	10.33	7.73	8.02	8.49	7.71	7.47	8.03	9.70
CaO	0.01	0.44	0.00	0.00	0.00	0.00	0.00	0.13	0.00	0.00	0.00	0.00	0.00	0.00
Na ₂ O	0.04	0.03	0.16	0.11	0.15	0.13	0.16	0.47	0.48	0.46	0.46	0.49	0.42	0.50
K ₂ O	9.27	3.16	9.62	9.40	9.41	9.71	9.57	8.59	8.51	8.52	8.69	8.93	9.05	8.66
Cr ₂ O ₃	0.00	0.00	0.00	0.03	0.10	0.00	0.00	0.00	0.56	0.39	0.00	0.21	0.00	0.00
TOTAL	93.93	90.20	95.46	95.49	95.50	95.53	95.34	93.05	95.40	97.51	94.95	94.92	95.43	95.53

Number of ions on the basis of 22 oxygen.

Si	5.45	4.98	5.29	5.35	5.28	5.33	5.33	5.30	5.28	5.32	5.31	5.29	5.35	5.36
Al ^{iv}	2.55	3.02	2.71	2.65	2.72	2.67	2.67	2.70	2.72	2.68	2.69	2.72	2.65	2.64
Al ^{vi}	0.35	0.28	0.89	0.94	0.83	0.92	1.03	0.93	0.89	0.94	0.96	0.95	0.77	0.90
Ti	0.32	0.18	0.28	0.25	0.36	0.26	0.08	0.17	0.14	0.14	0.19	0.17	0.28	0.17
Cr	0.00	0.00	0.00	0.00	0.01	0.00	0.00	0.00	0.07	0.05	0.00	0.03	0.00	0.00
Fe	2.51	2.97	2.53	2.45	2.60	2.45	2.34	2.85	2.89	2.80	2.83	2.87	2.82	2.54
Mn	0.07	0.09	0.02	0.02	0.02	0.02	0.02	0.00	0.00	0.00	0.00	0.00	0.00	0.00
Mg	2.61	3.27	1.94	2.03	1.82	2.01	2.33	1.82	1.84	1.90	1.77	1.73	1.84	2.19
Ca	0.00	0.08	0.00	0.00	0.00	0.00	0.00	0.02	0.00	0.00	0.00	0.00	0.00	0.00
Na	0.01	0.01	0.05	0.03	0.04	0.04	0.05	0.14	0.14	0.13	0.14	0.15	0.12	0.15
K	1.84	0.65	1.87	1.87	1.84	1.88	1.85	1.73	1.67	1.63	1.71	1.77	1.78	1.68
Mg/Mg+Fe	0.51	0.52	0.44	0.45	0.41	0.45	0.50	0.39	0.39	0.40	0.39	0.38	0.40	0.46

G# indicates associated garnet (Table D.6);
 c = inclusion in core; r = inclusion in rim

Table D.1. Continued.

Rock Sample	Brookville Gneiss marble in paragneiss						Ashburn Formation marble							
	CW89-592C			CW89-629C			CW88-204							
	1	2	3	1	2	3	4	5	6	1	2	3	4	5
SiO ₂	40.85	41.60	40.90	39.49	39.93	39.40	39.46	39.56	39.82	37.69	38.31	37.80	37.30	38.14
TiO ₂	0.48	0.24	0.32	0.71	0.37	0.51	0.43	0.49	0.45	0.96	0.31	0.56	0.53	0.68
Al ₂ O ₃	13.89	12.29	13.56	16.92	16.80	17.45	18.05	17.89	17.33	16.87	12.80	14.99	15.45	16.13
FeO	1.24	1.14	1.46	1.87	1.84	1.92	1.96	2.01	1.96	3.34	2.71	3.86	3.73	3.91
MnO	0.00	0.00	0.00	0.00	0.00	0.00	0.00	0.00	0.00	0.00	0.00	0.00	0.00	0.00
MgO	26.90	28.21	27.46	25.79	26.11	26.03	25.98	25.99	26.02	26.20	31.07	28.77	28.60	26.92
CaO	0.00	0.00	0.13	0.25	0.00	0.22	0.00	0.00	0.19	0.11	0.00	0.09	0.00	0.00
Na ₂ O	0.07	0.02	0.05	0.41	0.32	0.35	0.35	0.32	0.33	1.20	0.33	0.33	0.53	0.83
K ₂ O	10.21	9.65	9.38	9.96	10.00	9.99	10.23	10.12	10.24	7.59	5.46	6.51	6.60	8.08
Cr ₂ O ₃	0.00	0.00	0.04	0.00	0.00	0.00	0.00	0.00	0.00	0.00	0.00	0.00	0.00	0.00
TOTAL	93.64	93.15	93.30	95.39	95.37	95.87	96.46	96.38	96.32	93.96	90.98	92.90	92.73	94.69
Number of ions on the basis of 22 oxygen.														
Si	5.81	5.93	5.82	5.53	5.59	5.50	5.47	5.49	5.53	5.36	5.54	5.41	5.36	5.41
Al ^{iv}	2.19	2.06	2.18	2.47	2.41	2.51	2.53	2.52	2.47	2.64	2.18	2.53	2.62	2.59
Al ^{vi}	0.14	0.00	0.09	0.33	0.36	0.36	0.42	0.41	0.37	0.19	0.00	0.00	0.00	0.10
Ti	0.05	0.03	0.03	0.08	0.04	0.05	0.05	0.05	0.05	0.10	0.03	0.06	0.06	0.07
Cr	0.00	0.00	0.00	0.00	0.00	0.00	0.00	0.00	0.00	0.00	0.00	0.00	0.00	0.00
Fe	0.15	0.14	0.17	0.22	0.22	0.22	0.23	0.23	0.23	0.40	0.33	0.46	0.45	0.46
Mn	0.00	0.00	0.00	0.00	0.00	0.00	0.00	0.00	0.00	0.00	0.00	0.00	0.00	0.00
Mg	5.70	5.99	5.82	5.39	5.44	5.41	5.37	5.37	5.39	5.56	6.70	6.14	6.12	5.69
Ca	0.00	0.00	0.02	0.04	0.00	0.03	0.00	0.00	0.03	0.02	0.00	0.01	0.00	0.00
Na	0.02	0.01	0.01	0.11	0.09	0.10	0.10	0.09	0.09	0.33	0.09	0.09	0.15	0.23
K	1.85	1.75	1.70	1.78	1.79	1.78	1.81	1.79	1.81	1.38	1.01	1.19	1.21	1.46
Mg/Mg+Fe	0.98	0.98	0.97	0.96	0.96	0.96	0.96	0.96	0.96	0.93	0.95	0.93	0.93	0.93

Table D.1. Continued.

Rock Sample	Ashburn Formation							Hammondvale metamorphic unit mica schist							
	marble CW88-204		CW90-764					CW90-812			NB87-4090				
	6	7	8	9	10	11	12	1	2	3	4	5	1	2	
SiO ₂	38.51	39.83	41.96	39.15	40.08	39.25	39.32	40.65	40.87	39.25	40.80	41.34	35.75	36.02	
TiO ₂	0.74	0.59	0.71	0.63	0.91	0.97	0.67	0.53	0.75	0.60	0.63	0.81	1.81	1.73	
Al ₂ O ₃	16.97	15.31	13.99	14.57	14.37	15.68	14.97	16.08	15.88	17.34	16.10	15.83	18.54	17.74	
FeO	3.44	3.13	1.47	2.33	1.31	1.41	2.44	0.90	1.01	0.94	0.78	0.92	18.09	18.10	
MnO	0.00	0.00	0.00	0.18	0.00	0.00	0.00	0.00	0.00	0.00	0.00	0.00	0.16	0.15	
MgO	25.56	26.53	27.47	27.77	27.25	26.33	27.52	27.06	26.12	26.88	26.12	26.47	11.05	11.50	
CaO	0.00	0.00	2.79	0.00	0.00	0.00	0.12	0.00	0.00	0.12	0.00	0.11	0.00	0.02	
Na ₂ O	1.07	1.05	0.28	0.00	0.16	0.29	0.16	0.26	0.22	0.29	0.00	0.25	0.29	0.24	
K ₂ O	8.57	8.67	6.44	8.37	9.73	9.74	7.56	9.38	9.63	8.58	9.70	9.87	10.10	9.19	
Cr ₂ O ₃	0.00	0.00	0.00	0.00	0.00	0.00	0.00	0.00	0.00	0.00	0.00	0.00	0.05	0.00	
TOTAL	94.85	95.11	95.11	92.99	93.80	93.68	92.77	94.85	94.48	94.00	94.13	95.61	95.84	94.69	
Number of ions on the basis of 22 oxygen.															
Si	5.45	5.61	5.80	5.60	5.69	5.59	5.61	5.67	5.72	5.51	5.73	5.73	5.40	5.48	
Al ^{iv}	2.56	2.40	2.20	2.40	2.31	2.42	2.39	2.33	2.28	2.49	2.28	2.27	2.60	2.52	
Al ^{vi}	0.27	0.15	0.07	0.06	0.09	0.22	0.12	0.31	0.35	0.38	0.39	0.31	0.71	0.67	
Ti	0.08	0.06	0.07	0.07	0.10	0.10	0.07	0.06	0.08	0.06	0.07	0.08	0.21	0.20	
Cr	0.00	0.00	0.00	0.00	0.00	0.00	0.00	0.00	0.00	0.00	0.00	0.00	0.01	0.00	
Fe	0.41	0.37	0.17	0.28	0.16	0.17	0.29	0.10	0.12	0.11	0.09	0.11	2.29	2.30	
Mn	0.00	0.00	0.00	0.02	0.00	0.00	0.00	0.00	0.00	0.00	0.00	0.00	0.02	0.02	
Mg	5.39	5.56	5.66	5.92	5.77	5.58	5.85	5.62	5.45	5.62	5.46	5.47	2.49	2.61	
Ca	0.00	0.00	0.41	0.00	0.00	0.00	0.02	0.00	0.00	0.02	0.00	0.02	0.00	0.00	
Na	0.29	0.29	0.08	0.00	0.04	0.08	0.05	0.07	0.06	0.08	0.00	0.07	0.85	0.07	
K	1.55	1.56	1.13	1.53	1.76	1.77	1.38	1.67	1.72	1.54	1.74	1.74	1.95	1.79	
Mg/Mg+Fe	0.93	0.94	0.97	0.96	0.97	0.97	0.95	0.98	0.98	0.98	0.98	0.98	0.52	0.53	

APPENDIX D. Continued.

Table D.2. Plagioclase analyses.

Rock Sample	Brookville Gneiss migmatite				paragneiss			migma tite CW88 -218	paragneiss			migmatite		
	CW88-181B				CW88-181C				CW88-220			CW88-240		
	1	2	3	4	1	2	3	1	1	2	3	1	2	3
SiO ₂	57.01	57.89	56.72	56.21	58.28	60.91	60.97	58.72	57.05	59.72	59.42	59.69	57.21	58.15
TiO ₂	0.00	0.00	0.00	0.00	0.00	0.00	0.00	0.00	0.00	0.00	0.00	0.00	0.00	0.00
Al ₂ O ₃	27.40	27.17	27.40	27.95	25.47	24.64	25.12	26.01	26.96	26.53	25.91	25.95	26.04	26.27
FeO	0.00	0.00	0.00	0.00	0.00	0.00	0.00	0.00	0.00	0.00	0.00	0.00	0.00	0.00
MnO	0.00	0.00	0.00	0.00	0.00	0.00	0.00	0.00	0.00	0.00	0.00	0.00	0.00	0.00
MgO	0.00	0.00	0.00	0.00	0.00	0.00	0.00	0.00	0.00	0.00	0.00	0.00	0.00	0.00
CaO	8.80	8.46	9.12	9.77	6.44	5.54	6.07	7.13	7.90	7.38	7.35	7.30	7.22	7.28
Na ₂ O	6.55	6.51	6.70	6.25	7.80	8.44	7.42	7.47	6.99	7.16	7.29	7.03	7.23	7.44
K ₂ O	0.00	0.08	0.00	0.00	0.00	0.00	0.07	0.00	0.02	0.04	0.26	0.03	0.03	0.04
Cr ₂ O ₃	0.00	0.00	0.00	0.00	0.00	0.00	0.00	0.00	0.00	0.00	0.00	0.00	0.00	0.00
TOTAL	99.76	100.11	99.94	100.18	97.99	99.53	99.65	99.33	98.92	100.83	100.23	100.01	97.73	99.18
Number of ions on the basis of 32 oxygen.														
Si	10.23	10.33	10.19	10.08	10.59	10.86	10.83	10.54	10.31	10.54	10.58	0.00	10.45	10.47
Al ^{iv}	5.80	5.72	5.80	5.91	5.46	5.18	5.26	5.50	5.75	5.52	5.44	5.44	5.61	5.57
Al ^{vi}	0.00	0.00	0.00	0.00	0.00	0.00	0.00	0.00	0.00	0.00	0.00	0.00	0.00	0.00
Ti	0.00	0.00	0.00	0.00	0.00	0.00	0.00	0.00	0.00	0.00	0.00	0.00	0.00	0.00
Cr	0.00	0.00	0.00	0.00	0.00	0.00	0.00	0.00	0.00	0.00	0.00	0.00	0.00	0.00
Fe	0.00	0.00	0.00	0.00	0.00	0.00	0.00	0.00	0.00	0.00	0.00	0.00	0.00	0.00
Mn	0.00	0.00	0.00	0.00	0.00	0.00	0.00	0.00	0.00	0.00	0.00	0.00	0.00	0.00
Mg	0.00	0.00	0.00	0.00	0.00	0.00	0.00	0.00	0.00	0.00	0.00	0.00	0.00	0.00
Ca	1.69	1.62	1.76	1.88	1.25	1.06	1.16	1.37	1.53	1.40	1.40	1.39	1.41	1.40
Na	2.28	2.25	2.33	2.17	2.75	2.92	2.56	2.60	2.45	2.45	2.52	2.42	2.56	2.60
K	0.00	0.02	0.00	0.00	0.00	0.00	0.02	0.00	0.01	0.01	0.06	0.01	0.01	0.01
Mole proportions														
Or	0.00	0.01	0.00	0.00	0.00	0.00	0.00	0.00	0.00	0.00	0.02	0.00	0.00	0.00
Ab	0.57	0.58	0.57	0.54	0.69	0.73	0.69	0.66	0.62	0.64	0.63	0.63	0.64	0.65
An	0.43	0.42	0.43	0.46	0.31	0.27	0.31	0.35	0.38	0.36	0.35	0.36	0.36	0.35

APPENDIX D. Continued.

Table D.2. Plagioclase analyses.

Rock	Brookville Gneiss													
	migma-	paragneiss						orthogneiss						
	tite CW88	CW89-534A			CW89-569			CW89-664			CW88-132A			
Sample	-240	1	2	3	1	2	3	1	2	3	1	2	3	4
SiO ₂	58.91	58.82	59.85	58.13	58.18	58.55	57.87	60.35	60.66	59.48	60.54	58.81	60.17	60.76
TiO ₂	0.00	0.00	0.00	0.00	0.00	0.00	0.00	0.00	0.00	0.00	0.01	0.02	0.00	0.00
Al ₂ O ₃	25.85	25.88	25.61	26.03	26.76	26.47	26.54	24.88	25.57	25.41	24.80	25.21	24.89	25.17
FeO	0.02	0.00	0.01	0.00	0.06	0.00	0.00	0.00	0.04	0.00	0.14	0.17	0.16	0.10
MnO	0.00	0.00	0.00	0.00	0.00	0.00	0.00	0.00	0.00	0.00	0.00	0.00	0.00	0.00
MgO	0.00	0.00	0.00	0.00	0.00	0.00	0.00	0.00	0.00	0.00	0.01	0.02	0.00	0.00
CaO	7.45	6.64	6.18	6.83	7.39	7.40	7.53	6.75	6.88	6.89	7.03	7.28	7.18	6.59
Na ₂ O	7.41	7.38	7.61	7.06	6.85	6.95	7.04	8.08	8.09	7.91	7.22	6.91	7.35	7.39
K ₂ O	0.06	0.14	0.13	0.06	0.00	0.06	0.10	0.00	0.00	0.00	0.26	0.25	0.21	0.56
Cr ₂ O ₃	0.00	0.00	0.00	0.00	0.00	0.00	0.00	0.00	0.00	0.00	0.00	0.00	0.00	0.00
TOTAL	99.70	98.86	99.39	98.11	99.24	99.43	99.08	100.06	101.24	99.69	100.01	98.67	99.96	100.57
Number of ions on the basis of 32 oxygen.														
Si	10.55	10.59	10.69	10.54	10.44	10.49	10.43	10.74	10.68	10.64	10.78	10.63	10.73	10.76
Al ^{iv}	5.46	5.49	5.40	5.56	5.66	5.59	5.64	5.22	5.31	5.36	5.21	5.37	5.23	5.26
Al ^{vi}	0.00	0.00	0.00	0.00	0.00	0.00	0.00	0.00	0.00	0.00	0.00	0.00	0.00	0.00
Ti	0.00	0.00	0.00	0.00	0.00	0.00	0.00	0.00	0.00	0.00	0.00	0.00	0.00	0.00
Cr	0.00	0.00	0.00	0.00	0.00	0.00	0.00	0.00	0.00	0.00	0.00	0.00	0.00	0.00
Fe	0.00	0.00	0.00	0.00	0.01	0.00	0.00	0.00	0.01	0.00	0.02	0.03	0.02	0.02
Mn	0.00	0.00	0.00	0.00	0.00	0.00	0.00	0.00	0.00	0.00	0.00	0.00	0.00	0.00
Mg	0.00	0.00	0.00	0.00	0.00	0.00	0.00	0.00	0.00	0.00	0.00	0.01	0.00	0.00
Ca	1.43	1.28	1.18	1.33	1.42	1.42	1.45	1.29	1.30	1.32	1.34	1.41	1.37	1.25
Na	2.57	2.58	2.64	2.48	2.38	2.41	2.46	2.79	2.76	2.74	2.49	2.42	2.54	2.54
K	0.01	0.03	0.03	0.01	0.00	0.01	0.02	0.00	0.00	0.00	0.06	0.06	0.05	0.13
Mole proportions														
Or	0.00	0.01	0.01	0.00	0.00	0.00	0.01	0.00	0.00	0.00	0.02	0.02	0.01	0.03
Ab	0.64	0.66	0.69	0.65	0.63	0.63	0.63	0.68	0.68	0.68	0.64	0.62	0.64	0.65
An	0.36	0.33	0.31	0.35	0.37	0.37	0.37	0.32	0.32	0.33	0.35	0.36	0.35	0.32

APPENDIX D. Continued.

Table D.2. Plagioclase analyses.

Rock Sample	Brookville Gneiss orthogneiss												
	CW88-178				CW88-181A					CW89-629A			
	1	2	3	4	1	2	3	4	5	1	2	3	4
SiO ₂	59.17	58.68	60.24	59.72	61.17	60.32	61.69	61.97	61.96	61.66	61.62	59.97	60.11
TiO ₂	0.00	0.03	0.00	0.01	0.01	0.00	0.00	0.02	0.02	0.01	0.01	0.02	0.01
Al ₂ O ₃	26.05	26.09	24.93	25.73	24.50	25.08	24.50	24.64	24.36	25.01	24.71	25.34	25.00
FeO	0.04	0.05	0.06	0.00	0.09	0.12	0.12	0.08	0.08	0.14	0.19	0.11	0.10
MnO	0.00	0.00	0.01	0.00	0.00	0.00	0.00	0.00	0.01	0.00	0.00	0.00	0.00
MgO	0.01	0.01	0.00	0.00	0.00	0.01	0.01	0.00	0.01	0.00	0.01	0.00	0.00
CaO	8.10	8.06	7.45	7.76	6.45	6.78	6.42	6.39	6.37	6.81	6.87	7.08	6.87
Na ₂ O	7.15	7.13	7.37	7.48	7.87	7.41	7.86	7.78	7.80	7.62	7.58	7.72	7.67
K ₂ O	0.18	0.12	0.19	0.11	0.19	0.24	0.22	0.23	0.18	0.30	0.27	0.03	0.22
Cr ₂ O ₃	0.00	0.00	0.00	0.00	0.00	0.00	0.00	0.00	0.00	0.00	0.00	0.00	0.00
TOTAL	100.70	100.17	100.25	100.81	100.28	99.96	100.82	101.11	100.79	101.55	101.26	100.27	99.98

Number of ion on the basis of 32 oxygen.

Si	10.51	10.48	10.72	10.58	10.85	10.74	10.88	10.89	10.92	10.81	10.83	10.67	10.72
Al ^{iv}	5.45	5.49	5.23	5.38	5.12	5.27	5.09	5.10	5.06	5.17	5.12	5.31	5.26
Al ^{vi}	0.00	0.00	0.00	0.00	0.00	0.00	0.00	0.00	0.00	0.00	0.00	0.00	0.00
Ti	0.00	0.00	0.00	0.00	0.00	0.00	0.00	0.00	0.00	0.00	0.00	0.00	0.00
Cr	0.00	0.00	0.00	0.00	0.00	0.00	0.00	0.00	0.00	0.00	0.00	0.00	0.00
Fe	0.01	0.01	0.01	0.00	0.01	0.02	0.02	0.01	0.01	0.02	0.03	0.02	0.02
Mn	0.00	0.00	0.00	0.00	0.00	0.00	0.00	0.00	0.00	0.00	0.00	0.00	0.00
Mg	0.00	0.00	0.00	0.00	0.00	0.00	0.00	0.00	0.00	0.00	0.00	0.00	0.00
Ca	1.54	1.54	1.42	1.47	1.23	1.29	1.21	1.20	1.20	1.28	1.29	1.35	1.31
Na	2.46	2.47	2.54	2.57	2.71	2.56	2.69	2.65	2.67	2.59	2.58	2.66	2.65
K	0.04	0.03	0.04	0.03	0.04	0.06	0.05	0.05	0.04	0.07	0.06	0.01	0.05

Mole proportions

Or	0.01	0.01	0.01	0.01	0.01	0.01	0.01	0.01	0.01	0.02	0.02	0.00	0.01
Ab	0.61	0.61	0.64	0.63	0.68	0.66	0.68	0.68	0.68	0.66	0.66	0.66	0.66
An	0.38	0.38	0.36	0.36	0.31	0.33	0.31	0.31	0.31	0.33	0.33	0.34	0.33

APPENDIX D. Continued.

Table D.2. Plagioclase analyses.

Rock Sample	Brookville Gneiss						marble				Ashburn Formation mica schist			
	paragneissic boudin			blastomylonite			CW89-596B		CW89-629C		CW90-767			
	1	2	3	1	2	3	1	2	1	2	1	2	3	4
SiO ₂	62.51	65.78	65.51	62.42	60.84	63.86	43.20	42.99	43.01	43.26	64.41	68.54	65.83	66.42
TiO ₂	0.00	0.00	0.00	0.00	0.00	0.00	0.00	0.00	0.00	0.00	0.00	0.00	0.00	0.00
Al ₂ O ₃	23.87	22.20	22.12	24.62	26.15	23.10	37.00	37.31	37.23	37.40	22.32	19.78	23.07	21.02
FeO	0.00	0.00	0.00	0.20	0.57	0.37	0.00	0.00	0.00	0.00	0.00	0.00	0.00	0.00
MnO	0.00	0.00	0.00	0.00	0.00	0.00	0.00	0.00	0.00	0.00	0.00	0.00	0.00	0.00
MgO	0.00	0.00	0.00	0.15	0.18	0.19	0.00	0.00	0.00	0.00	0.00	0.00	0.00	0.00
CaO	4.85	3.09	2.98	3.73	3.51	1.84	20.75	20.62	20.85	20.52	3.34	0.11	3.40	2.22
Na ₂ O	8.75	8.91	9.56	7.56	6.27	6.21	0.00	0.00	0.14	0.00	9.42	11.40	8.51	10.19
K ₂ O	0.00	0.05	0.00	1.15	1.52	2.49	0.00	0.00	0.00	0.00	0.11	0.00	0.05	0.00
Cr ₂ O ₃	0.00	0.00	0.00	0.12	0.00	0.00	0.00	0.00	0.00	0.00	0.00	0.00	0.00	0.00
TOTAL	99.97	100.03	100.17	99.94	99.04	98.05	100.95	100.92	101.23	101.18	99.60	99.83	100.80	99.85

Number of ions on the basis of 32 oxygen.

Si	11.06	11.52	11.48	11.05	10.85	11.43	7.94	7.90	7.90	7.93	11.38	11.97	11.43	11.66
Al ^{iv}	4.98	4.58	4.57	5.14	5.50	4.88	8.02	8.09	8.06	8.08	4.65	4.07	4.71	4.35
Al ^{vi}	0.00	0.00	0.00	0.00	0.00	0.00	0.00	0.00	0.00	0.00	0.00	0.00	0.00	0.00
Ti	0.00	0.00	0.00	0.00	0.00	0.00	0.00	0.00	0.00	0.00	0.00	0.00	0.00	0.00
Cr	0.00	0.00	0.00	0.00	0.00	0.00	0.00	0.00	0.00	0.00	0.00	0.00	0.00	0.00
Fe	0.00	0.00	0.00	0.03	0.09	0.06	0.00	0.00	0.00	0.00	0.00	0.00	0.00	0.00
Mn	0.00	0.00	0.00	0.00	0.00	0.00	0.00	0.00	0.00	0.00	0.00	0.00	0.00	0.00
Mg	0.00	0.00	0.00	0.04	0.05	0.05	0.00	0.00	0.00	0.00	0.00	0.00	0.00	0.00
Ca	0.92	0.58	0.56	0.71	0.67	0.35	4.09	4.06	4.10	4.03	0.63	0.02	0.63	0.42
Na	3.00	3.02	3.25	2.60	2.17	2.16	0.00	0.00	0.05	0.00	3.23	3.86	2.87	3.47
K	0.00	0.01	0.00	0.26	0.35	0.57	0.00	0.00	0.00	0.00	0.03	0.00	0.01	0.00

Mole proportions

Or	0.00	0.00	0.00	0.07	0.11	0.19	0.00	0.00	0.00	0.00	0.01	0.00	0.00	0.00
Ab	0.77	0.84	0.85	0.73	0.68	0.70	0.00	0.00	0.01	0.00	0.83	1.00	0.82	0.89
An	0.23	0.16	0.15	0.20	0.21	0.12	1.00	1.00	0.99	1.00	0.16	0.00	0.18	0.11

APPENDIX D. Continued.

Table D.2. Plagioclase analyses.

Rock Sample	Ashburn Formation mica schist		Hammondvale metamorphic unit mica schist							
	CW90-767		NB87-4090		NB87-4107		CW88-115A		3	4
	5	6	1	2	1	2	1	2		
SiO ₂	66.02	62.56	67.53	61.49	60.91	68.87	68.81	69.29	68.90	68.80
TiO ₂	0.00	0.00	0.00	0.00	0.00	0.00	0.00	0.00	0.00	0.00
Al ₂ O ₃	21.56	24.69	20.06	24.80	24.71	19.83	19.79	19.77	19.47	19.72
FeO	0.00	0.00	0.02	0.03	0.00	0.02	0.00	0.00	0.00	0.00
MnO	0.00	0.00	0.00	0.00	0.00	0.00	0.00	0.00	0.00	0.00
MgO	0.00	0.00	0.00	0.00	0.00	0.00	0.00	0.00	0.00	0.00
CaO	1.67	4.88	0.40	6.00	6.32	0.09	0.25	0.12	0.13	0.11
Na ₂ O	9.75	8.09	12.02	8.69	8.33	12.76	11.32	10.31	10.00	11.10
K ₂ O	0.09	0.10	0.22	0.09	0.19	0.00	0.00	0.14	0.10	0.00
Cr ₂ O ₃	0.00	0.00	0.00	0.00	0.00	0.00	0.00	0.00	0.00	0.00
TOTAL	99.09	100.32	100.25	101.10	100.45	101.57	100.17	99.63	98.60	99.73

Number of ions on the basis of 32 oxygen.

Si	11.64	11.01	11.82	10.82	10.80	11.89	11.98	12.07	12.11	12.01
Al ^{iv}	4.48	5.12	4.14	5.15	5.17	4.04	4.06	4.06	4.03	4.06
Al ^{vi}	0.00	0.00	0.00	0.00	0.00	0.00	0.00	0.00	0.00	0.00
Ti	0.00	0.00	0.00	0.00	0.00	0.00	0.00	0.00	0.00	0.00
Cr	0.00	0.00	0.00	0.00	0.00	0.00	0.00	0.00	0.00	0.00
Fe	0.00	0.00	0.00	0.00	0.00	0.00	0.00	0.00	0.00	0.00
Mn	0.00	0.00	0.00	0.00	0.00	0.00	0.00	0.00	0.00	0.00
Mg	0.00	0.00	0.00	0.00	0.00	0.00	0.00	0.00	0.00	0.00
Ca	0.32	0.92	0.08	1.13	1.20	0.02	0.05	0.02	0.02	0.02
Na	3.33	2.76	4.08	2.97	2.86	4.27	3.82	3.48	3.41	3.76
K	0.02	0.02	0.05	0.02	0.04	0.00	0.00	0.03	0.02	0.00

Mole proportions

Or	0.01	0.01	0.01	0.01	0.01	0.00	0.00	0.01	0.01	0.00
Ab	0.91	0.75	0.97	0.72	0.70	1.00	0.99	0.99	0.99	1.00
An	0.09	0.25	0.02	0.28	0.29	0.00	0.01	0.01	0.01	0.01

APPENDIX D. Continued.

Table D.3. Potassium feldspar analyses.

Rock Sample	Brookville Gneiss migmatite CW88-181C			paragneiss CW89-569		orthogneiss CW88-132A				CW88-178		
	1	2	3	1	2	1	2	3	4	1	2	3
SiO ₂	64.19	62.74	63.61	64.90	65.11	65.11	66.27	65.95	65.70	68.13	68.27	67.06
TiO ₂	0.01	0.00	0.00	0.01	0.00	0.04	0.03	0.02	0.04	0.03	0.00	0.04
Al ₂ O ₃	18.29	18.89	18.92	18.94	18.89	18.43	18.41	18.55	18.26	18.14	18.08	18.33
FeO	0.01	0.00	0.00	0.00	0.00	0.09	0.05	0.06	0.06	0.08	0.04	0.00
MnO	0.01	0.00	0.00	0.00	0.00	0.01	0.00	0.00	0.03	0.01	0.01	0.00
MgO	0.00	0.00	0.00	0.00	0.00	0.00	0.01	0.01	0.01	0.01	0.01	0.01
CaO	0.00	0.00	0.00	0.03	0.00	0.02	0.04	0.05	0.00	0.00	0.00	0.00
Na ₂ O	1.08	0.50	0.78	1.07	0.88	0.98	0.71	0.98	0.87	0.16	0.19	0.25
K ₂ O	14.44	15.80	15.47	14.80	15.69	15.18	15.61	15.39	15.42	16.63	16.24	16.41
Cr ₂ O ₃	0.00	0.00	0.00	0.00	0.00	0.00	0.00	0.00	0.00	0.00	0.00	0.00
TOTAL	98.03	97.93	98.78	99.75	100.57	99.86	101.13	101.01	100.39	103.19	102.84	102.10
Number of ions on the basis of 32 oxygen.												
Si	12.01	11.85	11.88	11.95	11.94	12.01	12.06	12.02	12.05	12.17	12.20	12.11
Al ^{iv}	4.04	4.21	4.17	4.11	4.08	4.01	3.95	3.99	3.95	3.82	3.81	3.90
Al ^{vi}	0.00	0.00	0.00	0.00	0.00	0.00	0.00	0.00	0.00	0.00	0.00	0.00
Ti	0.00	0.00	0.00	0.00	0.00	0.00	0.00	0.00	0.00	0.00	0.00	0.00
Cr	0.00	0.00	0.00	0.00	0.00	0.00	0.00	0.00	0.00	0.00	0.00	0.00
Fe	0.00	0.00	0.00	0.00	0.00	0.01	0.01	0.01	0.01	0.01	0.01	0.00
Mn	0.00	0.00	0.00	0.00	0.00	0.00	0.00	0.00	0.00	0.00	0.00	0.00
Mg	0.00	0.00	0.00	0.00	0.00	0.00	0.00	0.00	0.00	0.00	0.00	0.00
Ca	0.00	0.00	0.00	0.01	0.00	0.00	0.01	0.01	0.00	0.00	0.00	0.00
Na	0.39	0.18	0.28	0.38	0.31	0.35	0.25	0.35	0.31	0.06	0.07	0.09
K	3.45	3.81	3.69	3.48	3.67	3.57	3.62	3.58	3.61	3.79	3.70	3.78
Mole proportion												
Or	0.90	0.95	0.93	0.90	0.92	0.91	0.93	0.91	0.92	0.99	0.98	0.98
Ab	0.10	0.05	0.07	0.10	0.08	0.09	0.07	0.09	0.08	0.01	0.02	0.02
An	0.00	0.00	0.00	0.00	0.00	0.00	0.00	0.00	0.00	0.00	0.00	0.00

APPENDIX D. Continued.

Table D.3. Potassium feldspar analyses.

Rock Sample	Brookville Gneiss orthogneiss CW88-181A			CW89-629A			paragneissic boudin CW89-662A			marble CW89-596B		CW89-629C
	1	2	3	1	2	3	1	2	3	1	2	1
	SiO ₂	66.35	66.06	66.51	65.26	64.98	65.54	67.42	66.19	67.46	64.21	66.26
TiO ₂	0.04	0.03	0.05	0.02	0.03	0.00	0.00	0.00	0.00	0.00	0.00	0.00
Al ₂ O ₃	18.44	18.39	18.47	18.31	18.58	18.50	18.90	18.88	18.77	17.48	17.25	17.31
FeO	0.09	0.00	0.09	0.02	0.06	0.03	0.00	0.00	0.00	0.00	0.00	0.00
MnO	0.01	0.00	0.00	0.00	0.00	0.00	0.00	0.00	0.00	0.00	0.00	0.00
MgO	0.00	0.00	0.01	0.00	0.01	0.00	0.00	0.00	0.00	0.00	0.00	0.00
CaO	0.00	0.00	0.00	0.00	0.00	0.00	0.00	0.00	0.00	0.05	0.06	0.04
Na ₂ O	0.73	0.74	0.80	0.78	0.72	0.76	1.58	0.93	1.65	0.42	0.43	0.41
K ₂ O	15.77	15.75	15.53	15.50	15.66	15.97	14.36	15.65	14.28	16.10	16.41	16.30
Cr ₂ O ₃	0.00	0.00	0.00	0.00	0.00	0.00	0.00	0.00	0.00	0.01	0.00	0.00
TOTAL	101.43	100.97	101.46	99.89	100.04	100.80	102.26	101.65	102.16	98.27	100.41	99.36

Number of ions on the basis of 32 oxygen.

Si	12.05	12.05	12.06	12.03	11.98	12.00	12.06	11.99	12.07	12.08	12.19	12.15
Al ^{iv}	3.95	3.96	3.95	3.98	4.04	3.99	3.98	4.03	3.96	3.88	3.74	3.80
Al ^{vi}	0.00	0.00	0.00	0.00	0.00	0.00	0.00	0.00	0.00	0.00	0.00	0.00
Ti	0.00	0.00	0.00	0.00	0.00	0.00	0.00	0.00	0.00	0.00	0.00	0.00
Cr	0.00	0.00	0.00	0.00	0.00	0.00	0.00	0.00	0.00	0.00	0.00	0.00
Fe	0.01	0.00	0.01	0.00	0.01	0.01	0.00	0.00	0.00	0.00	0.00	0.00
Mn	0.00	0.00	0.00	0.00	0.00	0.00	0.00	0.00	0.00	0.00	0.00	0.00
Mg	0.00	0.00	0.00	0.00	0.00	0.00	0.00	0.00	0.00	0.00	0.00	0.00
Ca	0.00	0.00	0.00	0.00	0.00	0.00	0.00	0.00	0.00	0.01	0.01	0.01
Na	0.26	0.26	0.28	0.28	0.26	0.27	0.55	0.33	0.57	0.15	0.15	0.15
K	3.66	3.67	3.59	3.65	3.68	3.73	3.28	3.62	3.26	3.87	3.85	3.87

Mole proportions

Or	0.93	0.93	0.93	0.93	0.94	0.93	0.86	0.92	0.85	0.96	0.96	0.96
Ab	0.07	0.07	0.07	0.07	0.07	0.07	0.14	0.08	0.15	0.04	0.04	0.04
An	0.00	0.00	0.00	0.00	0.00	0.00	0.00	0.00	0.00	0.00	0.00	0.00

APPENDIX D. Continued.

Table D.4. Amphibole analyses.

Brookville Gneiss												
Rock	marble											
Sample	CW89-596B											
	1	2	3	4	5	6	7	8	9	10	11	12
SiO ₂	52.44	56.24	58.22	56.79	53.52	59.05	55.00	55.64	58.06	55.62	56.62	56.08
TiO ₂	0.12	0.08	0.00	0.04	0.21	0.00	0.08	0.07	0.00	0.04	0.05	0.00
Al ₂ O ₃	5.93	2.81	1.67	2.03	5.23	0.69	3.44	3.46	1.13	3.43	1.85	3.13
FeO	9.53	7.61	6.92	8.12	8.82	6.38	8.30	7.97	8.63	8.16	9.85	8.01
MnO	0.03	0.00	0.00	0.00	0.01	0.01	0.00	0.01	0.04	0.02	0.00	0.00
MgO	16.48	18.73	19.55	18.87	17.17	20.34	18.22	18.19	18.46	17.98	17.54	18.32
CaO	12.26	12.53	12.64	12.62	12.34	12.75	12.51	12.50	12.71	12.66	12.50	12.53
Na ₂ O	0.74	0.33	0.17	0.25	0.68	0.08	0.43	0.42	0.09	0.39	0.25	0.37
K ₂ O	0.47	0.08	0.00	0.07	0.29	0.00	0.15	0.15	0.00	0.13	0.02	0.07
Cr ₂ O ₃	0.02	0.01	0.00	0.02	0.02	0.00	0.03	0.03	0.00	0.06	0.03	0.00
TOTAL	98.02	98.42	99.17	98.81	98.29	99.30	98.16	98.44	99.12	98.49	98.71	98.51
Number of ions on the basis of 23 oxygen.												
Si	7.43	7.81	7.97	7.87	7.52	8.05	7.70	7.75	8.02	7.75	7.91	7.79
Al ^{iv}	0.57	0.19	0.03	0.13	0.48	0.00	0.30	0.25	0.00	0.25	0.09	0.21
Al ^{vi}	0.42	0.27	0.24	0.20	0.39	0.16	0.27	0.31	0.20	0.31	0.21	0.31
Ti	0.01	0.01	0.00	0.00	0.02	0.00	0.01	0.01	0.00	0.00	0.01	0.00
Cr	0.00	0.00	0.00	0.00	0.00	0.00	0.00	0.00	0.00	0.01	0.00	0.00
Fe	1.13	0.88	0.79	0.94	1.04	0.73	0.97	0.93	1.00	0.95	1.15	0.93
Mn	0.00	0.00	0.00	0.00	0.00	0.00	0.00	0.00	0.01	0.00	0.00	0.00
Mg	3.48	3.88	3.99	3.90	3.60	4.13	3.80	3.77	3.80	3.73	3.65	3.79
Ca	1.86	1.86	1.85	1.87	1.86	1.86	1.88	1.87	1.88	1.89	1.87	1.87
Na	0.20	0.09	0.05	0.07	0.19	0.02	0.12	0.11	0.02	0.11	0.07	0.10
K	0.09	0.01	0.00	0.01	0.05	0.00	0.03	0.03	0.00	0.02	0.00	0.01
Mg/Mg+Fe	0.76	0.81	0.83	0.81	0.78	0.85	0.80	0.80	0.79	0.80	0.76	0.80

APPENDIX D. Continued.

Table D.4. Amphibole analyses.

Rock Sample	Brookville Gneiss marble								Ashburn Formation marble				
	CW89-598C			CW89-629C					CW88-204				
	1	2	3	1	2	3	4	1	2	3	4	5	
SiO ₂	59.86	59.54	57.94	55.48	56.19	51.88	57.16	53.91	57.90	54.25	56.62	58.26	
TiO ₂	0.00	0.09	0.11	0.00	0.00	0.23	0.00	0.00	0.00	0.00	0.00	0.00	
Al ₂ O ₃	0.35	0.73	1.77	4.13	3.49	5.96	2.53	3.52	0.66	3.19	1.05	0.51	
FeO	0.63	0.63	0.71	1.01	1.41	1.38	1.18	2.23	1.89	2.07	1.67	1.60	
MnO	0.00	0.00	0.00	0.00	0.00	0.00	0.00	0.00	0.00	0.00	0.00	0.00	
MgO	24.41	24.14	23.53	23.65	23.85	21.92	24.58	23.54	24.46	24.29	24.79	24.71	
CaO	12.63	13.07	12.82	14.27	13.68	15.33	13.95	13.67	13.58	13.10	13.50	13.62	
Na ₂ O	0.14	0.28	0.51	0.60	0.48	0.78	0.44	1.72	0.59	2.00	1.14	0.51	
K ₂ O	0.00	0.00	0.00	0.10	0.19	0.21	0.08	0.08	0.00	0.10	0.06	0.00	
Cr ₂ O ₃	0.00	0.01	0.04	0.00	0.00	0.17	0.00	0.00	0.00	0.00	0.00	0.00	
TOTAL	98.02	98.49	97.43	99.24	99.29	97.87	99.91	98.66	99.06	98.99	98.84	99.21	
Number of ions on the basis of 23 oxygen.													
Si	8.06	7.99	7.88	7.49	7.58	7.15	7.65	7.41	7.83	7.42	7.70	7.85	
Al ^{iv}	0.00	0.01	0.12	0.51	0.42	0.81	0.35	0.57	0.10	0.51	0.17	0.08	
Al ^{vi}	0.11	0.11	0.16	0.15	0.13	0.16	0.05	0.00	0.00	0.00	0.00	0.00	
Ti	0.00	0.01	0.01	0.00	0.00	0.02	0.00	0.00	0.00	0.00	0.00	0.00	
Cr	0.00	0.00	0.00	0.00	0.00	0.00	0.00	0.00	0.00	0.00	0.00	0.00	
Fe	0.07	0.07	0.08	0.11	0.16	0.16	0.13	0.26	0.21	0.24	0.19	0.18	
Mn	0.00	0.00	0.00	0.00	0.00	0.00	0.00	0.00	0.00	0.00	0.00	0.00	
Mg	4.90	4.83	4.77	4.76	4.79	4.53	4.90	4.82	4.93	4.95	5.03	4.96	
Ca	1.82	1.88	1.87	2.07	1.98	2.28	2.00	2.01	1.97	1.92	1.97	1.97	
Na	0.04	0.07	0.13	0.16	0.13	0.21	0.11	0.46	0.16	0.53	0.30	0.13	
K	0.00	0.00	0.00	0.02	0.03	0.04	0.01	0.01	0.00	0.02	0.01	0.00	
Mg/Mg+Fe	0.99	0.99	0.98	0.98	0.97	0.97	0.97	0.95	0.96	0.95	0.96	0.97	

APPENDIX D. Continued.

Table D.4. Amphibole analyses.

Rock Sample	Ashburn Formation									
	marble CW90-764						CW90-812			
	1	2	3	4	5	6	1	2	3	4
SiO ₂	53.78	55.40	57.31	54.14	53.16	54.76	57.25	54.40	55.99	57.36
TiO ₂	0.26	0.20	0.18	0.26	0.56	0.18	0.25	0.15	0.19	0.17
Al ₂ O ₃	3.75	2.40	0.83	3.52	4.25	1.17	1.81	1.60	3.75	1.44
FeO	1.08	0.95	0.85	1.03	1.11	0.46	0.44	0.82	0.31	0.64
MnO	0.00	0.00	0.00	0.00	0.00	0.00	0.00	0.00	0.00	0.00
MgO	23.71	24.33	24.94	24.25	23.95	23.12	24.80	23.88	24.19	24.29
CaO	13.58	13.84	13.75	13.82	13.84	17.04	14.28	10.43	14.09	14.06
Na ₂ O	1.14	0.93	0.50	1.25	1.66	0.13	0.14	0.15	0.46	0.22
K ₂ O	0.11	0.07	0.00	0.14	0.15	0.00	0.00	0.00	0.12	0.15
Cr ₂ O ₃	0.00	0.00	0.15	0.00	0.00	0.00	0.00	0.00	0.00	0.00
TOTAL	97.41	98.12	98.51	98.41	98.69	96.85	98.98	91.44	99.10	98.30

Number of ions on the basis of 23 oxygen.

Si	7.43	7.59	7.77	7.41	7.29	7.63	7.71	7.85	7.54	7.78
Al ^{IV}	0.57	0.39	0.13	0.57	0.69	0.19	0.29	0.15	0.46	0.22
Al ^{VI}	0.04	0.00	0.00	0.00	0.00	0.00	0.00	0.12	0.13	0.01
Ti	0.03	0.02	0.02	0.03	0.06	0.02	0.03	0.02	0.02	0.02
Cr	0.00	0.00	0.02	0.00	0.00	0.00	0.00	0.00	0.00	0.00
Fe	0.12	0.11	0.10	0.12	0.13	0.05	0.05	0.10	0.03	0.07
Mn	0.00	0.00	0.00	0.00	0.00	0.00	0.00	0.00	0.00	0.00
Mg	4.88	4.96	5.04	4.95	4.89	4.80	4.98	5.13	4.85	4.91
Ca	2.01	2.03	2.00	2.03	2.03	2.54	2.06	1.61	2.03	2.04
Na	0.30	0.25	0.13	0.33	0.44	0.04	0.04	0.04	0.12	0.06
K	0.02	0.01	0.00	0.02	0.03	0.00	0.00	0.00	0.02	0.03
Mg/Mg+Fe	0.98	0.98	0.98	0.98	0.98	0.99	0.99	0.98	0.99	0.99

APPENDIX D. Continued.

Table D.5. Clinopyroxene analyses.

Rock	Brookville Gneiss marble					Ashburn Formation marble				
	CW89-596B		CW89-598C	CW89-629C		CW88-204		3	4	5
	1	2	1	1	2	1	2			
SiO ₂	51.04	49.08	54.01	53.64	54.81	54.78	54.94	54.35	55.26	55.37
TiO ₂	1.03	1.55	0.00	0.22	0.00	0.00	0.23	0.00	0.00	0.00
Al ₂ O ₃	5.05	5.46	1.27	1.60	0.99	0.29	0.94	1.11	0.46	0.00
FeO	0.90	1.06	1.20	1.04	1.20	1.56	1.62	1.86	1.43	1.36
MnO	0.16	0.00	0.00	0.00	0.00	0.00	0.00	0.00	0.00	0.13
MgO	16.80	16.12	18.50	18.99	18.20	18.43	18.04	18.16	18.46	18.72
CaO	26.37	27.36	25.58	25.01	26.58	26.23	26.29	25.83	26.35	26.08
Na ₂ O	0.00	0.00	0.00	0.00	0.00	0.20	0.30	0.28	0.31	0.28
K ₂ O	0.00	0.00	0.00	0.00	0.00	0.00	0.00	0.00	0.00	0.00
Cr ₂ O ₃	0.00	0.00	0.00	0.15	0.17	0.00	0.00	0.00	0.00	0.00
TOTAL	101.35	100.63	100.56	100.64	101.94	101.48	102.35	101.59	102.26	101.94

Number of ions on the basis of 6 oxygen.

Si	1.84	1.79	1.95	1.93	1.96	1.97	1.96	1.95	1.97	1.98
Al ^{iv}	0.16	0.21	0.05	0.07	0.04	0.01	0.04	0.05	0.02	0.00
Al ^{vi}	0.05	0.03	0.00	0.00	0.00	0.00	0.00	0.00	0.00	0.00
Ti	0.03	0.04	0.00	0.01	0.00	0.00	0.01	0.00	0.00	0.00
Cr	0.00	0.00	0.00	0.00	0.01	0.00	0.00	0.00	0.00	0.00
Fe	0.03	0.03	0.04	0.03	0.04	0.05	0.05	0.06	0.04	0.04
Mn	0.01	0.00	0.00	0.00	0.00	0.00	0.00	0.00	0.00	0.00
Mg	0.90	0.88	1.00	1.02	0.97	0.99	0.96	0.97	0.98	1.00
Ca	1.02	1.07	0.99	0.97	1.02	1.01	1.00	0.99	1.01	1.00
Na	0.00	0.00	0.00	0.00	0.00	0.01	0.02	0.02	0.02	0.02
K	0.00	0.00	0.00	0.00	0.00	0.00	0.00	0.00	0.00	0.00

Mole proportions

Wo	0.49	0.51	0.48	0.47	0.50	0.50	0.50	0.49	0.50	0.49
En	0.49	0.47	0.50	0.52	0.49	0.49	0.49	0.49	0.49	0.49
Fs	0.02	0.02	0.02	0.02	0.02	0.02	0.01	0.02	0.01	0.01

APPENDIX D. Continued.

Table D.6. Garnet analyses.

Rock Sample	Brookville Gneiss blastomylonite NB92-9079B							Hammondvale metamorphic unit mica schist NB87-4090 CW88-115A			
	1c	2c	3c	4c	4r	5c	5r	1c	1r	1	2
	SiO ₂	36.94	36.99	37.00	36.87	36.88	36.90	36.68	36.58	37.12	37.25
TiO ₂	0.00	0.00	0.00	0.00	0.00	0.00	0.00	0.07	0.14	0.00	0.00
Al ₂ O ₃	20.92	20.97	21.14	21.28	21.37	20.98	20.64	21.52	21.45	20.76	20.70
FeO	37.44	37.33	38.11	37.93	38.06	37.33	38.04	26.32	26.40	25.96	26.02
MnO	0.00	0.21	0.17	0.19	0.38	0.00	0.16	4.94	3.05	8.11	8.07
MgO	2.93	3.04	3.17	2.71	2.17	3.26	2.48	0.94	0.90	1.74	1.79
CaO	1.47	1.18	0.97	1.40	1.44	1.13	1.35	9.12	11.27	5.80	5.85
Na ₂ O	0.24	0.24	0.23	0.31	0.00	0.24	0.22	0.00	0.06	0.24	0.21
K ₂ O	0.00	0.00	0.00	0.00	0.00	0.00	0.00	0.00	0.00	0.00	0.00
Cr ₂ O ₃	0.00	0.00	0.00	0.00	0.00	0.00	0.00	0.06	0.03	0.00	0.00
TOTAL	99.94	99.95	100.79	100.67	100.29	99.85	99.59	99.55	100.42	99.86	99.95

Number of ions on the basis of 24 oxygen.

Si	5.95	5.96	5.91	5.90	5.96	5.94	5.96	5.89	5.90	5.99	5.99
Al ^{iv}	0.05	0.04	0.09	0.10	0.04	0.06	0.04	0.11	0.10	0.01	0.01
Al ^{vi}	3.92	3.94	3.89	3.92	4.03	3.92	3.91	3.97	3.91	3.92	3.91
Ti	0.00	0.00	0.00	0.00	0.00	0.00	0.00	0.01	0.02	0.00	0.00
Cr	0.00	0.00	0.00	0.00	0.00	0.00	0.00	0.01	0.00	0.00	0.00
Fe ³	0.20	0.18	0.27	0.28	0.01	0.21	0.20	0.12	0.17	0.17	0.16
Fe ²	4.84	4.85	4.83	4.80	5.14	4.81	4.96	3.43	3.34	3.32	3.33
Mn	0.00	0.03	0.02	0.03	0.05	0.00	0.02	0.67	0.41	1.10	1.10
Mg	0.70	0.73	0.75	0.65	0.52	0.78	0.60	0.23	0.21	0.42	0.42
Ca	0.25	0.20	0.17	0.24	0.25	0.19	0.23	1.57	1.92	1.00	1.01
Na	0.07	0.07	0.07	0.10	0.00	0.07	0.07	0.00	0.02	0.07	0.07

Mole proportions

Alm	0.84	0.84	0.84	0.84	0.86	0.83	0.85	0.59	0.58	0.57	0.57
Sp	0.00	0.00	0.00	0.00	0.01	0.00	0.00	0.11	0.07	0.19	0.19
Py	0.12	0.12	0.13	0.11	0.09	0.13	0.10	0.04	0.04	0.07	0.07
Gr	0.01	0.01	0.00	0.01	0.04	0.00	0.01	0.26	0.32	0.13	0.13
And	0.03	0.03	0.03	0.03	0.00	0.03	0.03	0.00	0.00	0.04	0.04

c = core; r = rim

APPENDIX D. Continued.

Table D.7. Muscovite analyses.

Rock Sample	Brookville Gneiss						Ashburn Formation							
	paragneiss CW88-181C			migmatite CW88-218		paragneiss CW89-644			paragneissic boudin CW89-662A			mica schist CW90-767		
	1	2	3	1	2	1	2	3	1	2	3	1	2	3
SiO ₂	47.18	46.24	47.54	48.69	47.61	47.98	47.47	48.18	47.92	47.02	47.26	47.28	49.23	46.63
TiO ₂	1.01	0.94	1.25	0.25	0.25	0.00	0.88	0.57	0.14	0.03	0.03	0.84	0.49	1.11
Al ₂ O ₃	33.56	33.61	33.57	34.15	34.33	35.07	34.17	34.92	36.47	36.01	36.32	35.46	32.97	35.31
FeO	3.36	3.46	3.22	3.16	3.35	2.43	2.43	2.59	0.99	0.93	1.02	1.22	1.83	1.14
MnO	0.00	0.00	0.00	0.00	0.00	0.00	0.00	0.00	0.00	0.00	0.00	0.00	0.00	0.00
MgO	0.63	0.62	0.58	0.79	0.79	0.65	0.64	0.53	0.69	0.66	0.62	0.54	1.38	0.57
CaO	0.00	0.00	0.00	0.00	0.00	0.00	0.00	0.00	0.00	0.00	0.00	0.00	0.00	0.00
Na ₂ O	0.26	0.32	0.25	0.40	0.43	0.55	0.48	0.49	0.42	0.35	0.38	1.13	0.50	0.95
K ₂ O	10.51	10.55	9.91	9.81	10.29	10.01	9.96	9.95	10.30	10.11	9.96	10.17	10.53	10.03
Cr ₂ O ₃	0.00	0.06	0.00	0.00	0.00	0.00	0.00	0.00	0.00	0.00	0.00	0.04	0.00	0.05
TOTAL	96.51	95.80	96.32	97.25	97.05	96.69	96.03	97.23	96.93	95.11	95.59	96.68	96.93	95.79
Number of ions on the basis of 22 oxygen.														
Si	6.26	6.19	6.28	6.35	6.26	6.29	6.27	6.28	6.22	6.22	6.22	6.19	6.44	6.16
Al ^{IV}	1.75	1.81	1.72	1.65	1.74	1.71	1.73	1.72	1.78	1.78	1.79	1.81	1.56	1.84
Al ^{VI}	3.50	3.50	3.52	3.61	3.59	3.70	3.60	3.65	3.81	3.84	3.85	3.67	3.52	3.66
Ti	0.10	0.10	0.12	0.03	0.03	0.00	0.09	0.06	0.01	0.00	0.00	0.08	0.05	0.11
Cr	0.00	0.01	0.00	0.00	0.00	0.00	0.00	0.00	0.00	0.00	0.00	0.00	0.00	0.01
Fe	0.37	0.39	0.36	0.35	0.37	0.27	0.27	0.28	0.11	0.10	0.11	0.13	0.20	0.13
Mn	0.00	0.00	0.00	0.00	0.00	0.00	0.00	0.00	0.00	0.00	0.00	0.00	0.00	0.00
Mg	0.12	0.12	0.11	0.15	0.16	0.13	0.13	0.10	0.13	0.13	0.12	0.11	0.27	0.11
Ca	0.00	0.00	0.00	0.00	0.00	0.00	0.00	0.00	0.00	0.00	0.00	0.00	0.00	0.00
Na	0.07	0.08	0.06	0.10	0.11	0.14	0.12	0.12	0.11	0.09	0.10	0.29	0.13	0.24
K	1.78	1.80	1.67	1.63	1.73	1.67	1.68	1.66	1.71	1.71	1.67	1.70	1.76	1.69
Mole proportions														
Musc	0.96	0.96	0.96	0.94	0.94	0.92	0.93	0.93	0.94	0.95	0.95	0.86	0.93	0.87
Para	0.04	0.04	0.04	0.06	0.06	0.08	0.07	0.07	0.06	0.05	0.05	0.14	0.07	0.13
Marg	0.00	0.00	0.00	0.00	0.00	0.00	0.00	0.00	0.00	0.00	0.00	0.00	0.00	0.00

APPENDIX D. Continued.

Table D.7. Muscovite analyses.

Rock Sample	Ashburn Formation mica schist CW90-767					Famondvale metamorphic unit mica schist NB87-4086					NB87-4090			
	4	5	6	7	8	1	2	3	4	5	1	2	3	4
SiO ₂	46.73	47.25	46.95	46.86	46.11	51.33	51.39	51.93	50.03	51.87	47.97	48.84	48.92	49.29
TiO ₂	1.16	1.18	1.02	0.93	1.35	0.19	0.45	0.07	0.43	0.09	0.55	0.37	0.44	0.51
Al ₂ O ₃	35.36	35.25	34.81	34.07	35.23	30.45	32.83	29.15	31.83	28.07	31.27	31.28	31.81	31.01
FeO	1.25	1.24	1.46	1.49	1.22	1.98	1.76	1.86	1.61	1.97	3.55	3.41	3.32	3.65
MnO	0.00	0.00	0.00	0.00	0.00	0.00	0.00	0.00	0.00	0.00	0.00	0.00	0.00	0.00
MgO	0.47	0.54	0.58	0.71	0.46	3.02	2.45	3.15	2.24	3.16	1.75	1.80	1.58	1.81
CaO	0.00	0.00	0.00	0.00	0.00	0.00	0.00	0.00	0.00	0.00	0.00	0.00	0.00	0.00
Na ₂ O	1.15	1.05	0.98	0.92	0.81	0.30	0.69	0.44	0.74	0.36	0.79	0.60	0.54	0.72
K ₂ O	9.88	9.82	9.82	9.60	9.36	9.19	8.51	9.51	9.94	10.19	9.99	10.17	10.76	10.42
Cr ₂ O ₃	0.05	0.00	0.05	0.00	0.00	0.00	0.00	0.00	0.03	0.05	0.01	0.00	0.03	0.00
TOTAL	96.05	96.33	95.67	94.58	94.54	96.46	98.08	96.11	96.85	95.76	95.88	96.47	97.40	97.41

Number of ions on the basis of 22 oxygen.

Si	6.16	6.20	6.21	6.26	6.15	6.68	6.55	6.79	6.52	6.84	6.40	6.47	6.43	6.48
Al ^{iv}	1.84	1.80	1.79	1.74	1.85	1.32	1.46	1.21	1.48	1.16	1.60	1.53	1.57	1.52
Al ^{vi}	3.65	3.65	3.64	3.63	3.69	3.35	3.48	3.28	3.41	3.21	3.33	3.35	3.36	3.29
Ti	0.12	0.12	0.10	0.09	0.14	0.02	0.04	0.01	0.04	0.01	0.06	0.04	0.04	0.05
Cr	0.01	0.00	0.01	0.00	0.00	0.00	0.00	0.00	0.00	0.01	0.00	0.00	0.00	0.00
Fe	0.14	0.14	0.16	0.17	0.14	0.22	0.19	0.20	0.18	0.22	0.40	0.38	0.37	0.40
Mn	0.00	0.00	0.00	0.00	0.00	0.00	0.00	0.00	0.00	0.00	0.00	0.00	0.00	0.00
Mg	0.09	0.11	0.11	0.14	0.09	0.59	0.47	0.61	0.44	0.62	0.35	0.36	0.31	0.36
Ca	0.00	0.00	0.00	0.00	0.00	0.00	0.00	0.00	0.00	0.00	0.00	0.00	0.00	0.00
Na	0.29	0.27	0.25	0.24	0.21	0.08	0.17	0.11	0.19	0.09	0.20	0.15	0.14	0.18
K	1.66	1.64	1.66	1.64	1.59	1.53	1.38	1.59	1.65	1.72	1.70	1.72	1.81	1.75

Mole proportion

Or	0.85	0.86	0.87	0.87	0.88	0.95	0.89	0.93	0.90	0.95	0.89	0.92	0.93	0.90
Ab	0.15	0.14	0.13	0.13	0.12	0.05	0.11	0.07	0.10	0.05	0.11	0.08	0.07	0.10
An	0.00	0.00	0.00	0.00	0.00	0.00	0.00	0.00	0.00	0.00	0.00	0.00	0.00	0.00

APPENDIX D. Continued.

Table D.7. Muscovite analyses.

Rock Sample	Hammondvale metamorphic unit										marble				
	mica schist										CW88-101				
	NB87-4090				NB87-4107										
	5	6	7	8	1	2	3	4	5	1	2	3	4	5	
SiO ₂	49.00	49.18	46.81	49.05	50.90	49.84	50.39	51.40	50.87	48.49	49.63	49.68	49.47	48.92	
TiO ₂	0.49	0.48	0.53	0.45	0.38	0.30	0.41	0.45	0.28	0.54	0.24		0.39	0.23	
Al ₂ O ₃	32.80	33.34	33.70	31.77	28.03	28.32	30.33	29.55	28.18	31.87	30.91	30.66	31.47	31.81	
FeO	3.70	3.56	3.19	3.20	3.97	3.72	4.03	3.77	3.93	1.11	1.09	0.99	1.15	1.03	
MnO	0.00	0.00	0.00	0.00	0.01	0.00	0.00	0.00	0.00	0.00	0.00	0.00	0.00	0.00	
MgO	1.73	1.69	0.92	1.49	2.63	2.46	2.46	2.57	2.53	2.59	3.13	3.27	3.09	2.75	
CaO	0.00	0.00	0.00	0.00	0.00	0.00	0.00	0.00	0.01	0.00	0.00	0.00	0.00	0.00	
Na ₂ O	0.50	1.08	0.66	0.51	0.13	0.23	0.16	0.22	0.29	0.59	0.20	0.22	0.64	0.25	
K ₂ O	9.26	8.50	10.16	10.42	11.19	11.10	9.20	9.77	9.37	8.87	9.19	9.47	8.39	9.43	
Cr ₂ O ₃	0.00	0.00	0.00	0.04	0.00	0.01	0.00	0.00	0.00	0.00	0.00	0.00	0.00	0.00	
TOTAL	97.48	97.83	95.97	96.93	97.24	95.98	96.98	97.73	95.46	94.05	94.38	94.28	94.59	94.42	
Number of ions on the basis of 22 oxygen.															
Si	6.39	6.36	6.24	6.46	6.73	6.67	6.60	6.69	6.77	6.46	6.58	6.60	6.53	6.50	
Al ^{iv}	1.61	1.64	1.77	1.54	1.27	1.33	1.41	1.32	1.23	1.54	1.42	1.40	1.47	1.50	
Al ^{vi}	3.43	3.45	3.53	3.39	3.10	3.14	3.28	3.22	3.19	3.46	3.41	3.41	3.43	3.48	
Ti	0.05	0.05	0.05	0.05	0.04	0.03	0.04	0.04	0.03	0.05	0.02	0.00	0.04	0.02	
Cr	0.00	0.00	0.00	0.00	0.00	0.00	0.00	0.00	0.00	0.00	0.00	0.00	0.00	0.00	
Fe	0.40	0.39	0.36	0.35	0.44	0.42	0.44	0.41	0.44	0.12	0.12	0.11	0.13	0.12	
Mn	0.00	0.00	0.00	0.00	0.00	0.00	0.00	0.00	0.00	0.00	0.00	0.00	0.00	0.00	
Mg	0.34	0.33	0.18	0.29	0.52	0.49	0.48	0.50	0.50	0.51	0.62	0.65	0.61	0.55	
Ca	0.00	0.00	0.00	0.00	0.00	0.00	0.00	0.00	0.00	0.00	0.00	0.00	0.00	0.00	
Na	0.13	0.27	0.17	0.13	0.03	0.06	0.04	0.06	0.08	0.15	0.05	0.06	0.16	0.06	
K	1.54	1.40	1.73	1.75	1.89	1.90	1.54	1.62	1.59	1.51	1.55	1.61	1.41	1.60	
Mole proportion															
Or	0.92	0.84	0.91	0.93	0.98	0.97	0.97	0.97	0.95	0.91	0.97	0.97	0.90	0.96	
Ab	0.08	0.16	0.09	0.07	0.02	0.03	0.03	0.03	0.05	0.09	0.03	0.03	0.10	0.04	
An	0.00	0.00	0.00	0.00	0.00	0.00	0.00	0.00	0.00	0.00	0.00	0.00	0.00	0.00	

APPENDIX D. Continued.

Table D.7. Muscovite analyses.

Rock Sample	Hammondvale metamorphic unit							
	marble CW88-101				mica schist CW88-115A			
	6	7	8	9	1	2	3	4
SiO ₂	49.60	50.00	48.50	50.18	47.89	49.27	47.98	46.61
TiO ₂	0.23	0.27	0.49	0.20	0.79	0.73	0.85	0.37
Al ₂ O ₃	30.63	31.84	32.44	30.67	28.89	28.95	29.38	30.20
FeO	1.05	0.69	0.98	1.11	5.11	4.31	4.84	5.33
MnO	0.00	0.00	0.00	0.00	0.00	0.00	0.00	0.00
MgO	3.24	2.27	2.38	3.21	1.95	2.07	2.11	1.78
CaO	0.00	0.00	0.00	0.00	0.00	0.00	0.00	0.44
Na ₂ O	0.50	0.11	0.60	0.32	0.33	0.21	0.45	0.53
K ₂ O	8.77	8.93	9.03	8.89	8.51	8.43	8.92	8.53
Cr ₂ O ₃	0.00	0.00	0.00	0.00	0.00	0.00	0.00	0.00
TOTAL	94.01	94.11	94.41	94.57	93.47	93.97	94.53	93.79
Number of ions on the basis of 22 oxygen								
Si	6.59	6.61	6.44	6.63	6.55	6.65	6.50	6.38
Al ^{iv}	1.41	1.39	1.57	1.37	1.46	1.35	1.51	1.62
Al ^{vi}	3.39	3.57	3.51	3.40	3.20	3.25	3.18	3.25
Ti	0.02	0.03	0.05	0.02	0.08	0.07	0.09	0.04
Cr	0.00	0.00	0.00	0.00	0.00	0.00	0.00	0.00
Fe	0.12	0.08	0.11	0.12	0.58	0.49	0.55	0.61
Mn	0.00	0.00	0.00	0.00	0.00	0.00	0.00	0.00
Mg	0.64	0.45	0.47	0.63	0.40	0.42	0.43	0.36
Ca	0.00	0.00	0.00	0.00	0.00	0.00	0.00	0.07
Na	0.13	0.03	0.15	0.08	0.09	0.06	0.12	0.14
K	1.49	1.51	1.53	1.50	1.48	1.45	1.54	1.49
Mole proportion								
Or	0.92	0.98	0.91	0.95	0.94	0.96	0.93	0.88
Ab	0.08	0.02	0.09	0.05	0.06	0.04	0.07	0.08
An	0.00	0.00	0.00	0.00	0.00	0.00	0.00	0.04

APPENDIX D. Continued.

Table D.8. Cordierite and epidote analyses.

Rock Sample	Brookville Gneiss												
	Cordierite migmatite CW88-181B			leucosome CW88-218		melanosome		paragneiss CW88-220			migmatite CW88-240		
	1	2	3	1	2	1	2	1	2	3	1	2	3
SiO ₂	50.32	50.66	49.59	47.28	47.86	47.40	47.47	47.47	47.88	48.01	47.01	44.40	48.17
TiO ₂	0.03	0.02	0.02	0.00	0.00	0.00	0.00	0.00	0.00	0.00	0.00	0.00	0.00
Al ₂ O ₃	27.66	27.84	27.47	33.09	33.33	33.19	33.24	30.38	30.50	30.53	28.58	28.16	28.43
FeO	5.02	4.44	5.34	6.94	6.71	7.20	7.25	5.67	5.46	5.25	5.85	6.77	5.60
MnO	0.08	0.00	0.08	0.67	0.71	0.71	0.67	0.03	0.04	0.03	0.04	0.09	0.05
MgO	3.83	3.52	3.86	8.74	8.99	8.81	8.75	2.89	2.78	2.54	4.11	5.57	4.10
CaO	0.20	0.26	0.26	0.00	0.00	0.00	0.00	0.39	0.38	0.36	0.54	0.57	0.54
Na ₂ O	0.05	0.10	0.07	0.21	0.19	0.20	0.23	0.06	0.11	0.08	0.07	0.04	0.05
K ₂ O	7.86	8.08	7.87	0.00	0.00	0.00	0.00	7.10	7.50	7.69	6.09	5.45	6.74
Cr ₂ O ₃	0.00	0.00	0.00	0.00	0.00	0.00	0.00	0.00	0.00	0.00	0.00	0.00	0.00
TOTAL	95.05	94.92	94.56	96.93	97.79	97.51	97.61	93.99	94.65	94.49	92.29	91.05	93.68

Number of ions on the basis of 18 oxygen.

Si	5.49	5.52	5.46	4.93	4.94	4.92	4.92	5.25	5.26	5.28	5.28	5.10	5.34
Al ^{iv}	0.51	0.48	0.54	1.07	1.06	1.08	1.08	0.75	0.74	0.72	0.72	0.90	0.66
Al ^{vi}	3.06	3.10	3.03	3.00	2.99	2.98	2.98	3.21	3.22	3.24	3.07	2.91	3.06
Ti	0.00	0.00	0.00	0.00	0.00	0.00	0.00	0.00	0.00	0.00	0.00	0.00	0.00
Cr	0.00	0.00	0.00	0.00	0.00	0.00	0.00	0.00	0.00	0.00	0.00	0.00	0.00
Fe	0.46	0.41	0.49	0.61	0.58	0.63	0.63	0.52	0.50	0.48	0.55	0.65	0.52
Mn	0.01	0.00	0.01	0.06	0.06	0.06	0.06	0.00	0.00	0.00	0.00	0.01	0.01
Mg	0.62	0.57	0.63	1.36	1.38	1.36	1.35	0.48	0.46	0.42	0.69	0.95	0.68
Ca	0.02	0.03	0.03	0.00	0.00	0.00	0.00	0.05	0.05	0.04	0.07	0.07	0.06
Na	0.01	0.02	0.02	0.04	0.04	0.04	0.05	0.01	0.02	0.02	0.02	0.01	0.01
K	1.10	1.12	1.11	0.00	0.00	0.00	0.00	1.00	1.05	1.08	0.87	0.80	0.95

APPENDIX D. Continued.

Table D.8. Cordierite and epidote analyses.

Rock	Brookville Gneiss Cordierite paragneissic boudin				Hammondvale metamorphic unit Epidote mica schist inclusion in albite			matrix
	Sample CW89-662A				Sample CW88-115A			
	1	2	3	4	1	2	3	
SiO ₂	45.09	45.72	41.19	41.38	37.83	37.69	37.72	
TiO ₂	0.00	0.00	0.00	0.00	0.00	0.00	0.00	
Al ₂ O ₃	36.77	35.27	35.04	34.96	24.38	24.12	24.30	
FeO	3.67	3.70	5.94	5.79	10.86	10.66	10.69	
MnO	0.00	0.00	0.03	0.02	0.36	0.55	0.41	
MgO	2.18	1.75	4.28	4.20	0.00	0.00	0.00	
CaO	0.21	0.41	0.27	0.28	22.95	22.15	22.57	
Na ₂ O	0.02	0.04	0.01	0.02	0.17	0.15	0.15	
K ₂ O	1.59	2.79	0.64	0.69	0.00	0.00	0.00	
Cr ₂ O ₃	0.00	0.04	0.01	0.00	0.00	0.00	0.00	
TOTAL	89.53	89.72	87.41	87.34	96.53	95.31	95.84	
	Number of ions in the basis of 18 oxygen.				Number of ions on the basis of 12.5 oxygen.			
Si	4.99	5.09	4.74	4.76	3.03	3.05	3.04	
Al ^{IV}	1.01	0.91	1.26	1.24	0.00	0.00	0.00	
Al ^{VI}	3.78	3.71	3.49	3.50	2.30	2.30	2.31	
Ti	0.00	0.00	0.00	0.00	0.00	0.00	0.00	
Cr	0.00	0.00	0.00	0.00	0.00	0.00	0.00	
Fe	0.34	0.34	0.57	0.56	0.65	0.65	0.65	
Mn	0.00	0.00	0.00	0.00	0.02	0.04	0.03	
Mg	0.36	0.29	0.73	0.72	0.00	0.00	0.00	
Ca	0.03	0.05	0.03	0.04	1.97	1.92	1.95	
Na	0.00	0.01	0.00	0.00	0.03	0.05	0.02	
K	0.22	0.40	0.09	0.10	0.00	0.00	0.00	

APPENDIX D. Continued.

Table D.9. Calcite analyses.

Rock Sample	Brookville Gneiss marble													
	CW89-596B				CW89-598C				CW89-629C					
	1	2	3	4	1	2	3	4	5	6	7	1	2	3
SiO ₂	0.00	0.00	0.00	0.00	0.00	0.00	0.00	0.00	0.00	0.00	0.00	0.00	0.00	0.10
TiO ₂	0.00	0.00	0.00	0.00	0.00	0.00	0.00	0.00	0.00	0.00	0.00	0.00	0.00	0.00
Al ₂ O ₃	0.00	0.00	0.00	0.00	0.00	0.00	0.00	0.00	0.00	0.00	0.00	0.00	0.00	0.00
FeO	0.14	0.17	0.16	0.19	0.08	0.06	0.06	0.08	0.03	0.05	0.09	0.00	0.16	0.00
MnO	0.02	0.04	0.04	0.04	0.00	0.00	0.00	0.00	0.00	0.00	0.00	0.00	0.00	0.00
MgO	0.20	0.12	0.10	0.11	1.28	1.08	0.89	0.80	0.95	0.67	1.22	0.73	0.73	0.12
CaO	57.13	55.15	58.57	55.97	57.26	57.64	57.40	58.46	54.46	49.12	53.86	57.49	54.97	58.20
Na ₂ O	0.00	0.00	0.00	0.00	0.00	0.00	0.00	0.00	0.00	0.00	0.00	0.00	0.00	0.11
K ₂ O	0.00	0.00	0.00	0.00	0.00	0.00	0.00	0.00	0.00	0.00	0.00	0.00	0.00	0.00
TOTAL	57.48	55.48	58.87	56.31	58.62	58.78	58.35	59.34	55.44	49.84	55.17	58.22	55.86	58.52

Number of ions on the basis of 6 oxygen.

Si	0.00	0.00	0.00	0.00	0.00	0.00	0.00	0.00	0.00	0.00	0.00	0.00	0.00	0.01
Al	0.00	0.00	0.00	0.00	0.00	0.00	0.00	0.00	0.00	0.00	0.00	0.00	0.00	0.00
Ti	0.00	0.00	0.00	0.00	0.00	0.00	0.00	0.00	0.00	0.00	0.00	0.00	0.00	0.00
Fe	0.01	0.02	0.01	0.02	0.01	0.01	0.01	0.01	0.00	0.01	0.01	0.00	0.01	0.00
Mn	0.00	0.00	0.00	0.00	0.00	0.00	0.00	0.00	0.00	0.00	0.00	0.00	0.00	0.00
Mg	0.03	0.02	0.02	0.02	0.18	0.15	0.13	0.11	0.14	0.11	0.18	0.10	0.11	0.02
Ca	5.96	5.96	5.97	5.96	5.81	5.84	5.87	5.88	5.85	5.88	5.81	5.90	5.88	5.93
Na	0.00	0.00	0.00	0.00	0.00	0.00	0.00	0.00	0.00	0.00	0.00	0.00	0.00	0.02
K	0.00	0.00	0.00	0.00	0.00	0.00	0.00	0.00	0.00	0.00	0.00	0.00	0.00	0.00

APPENDIX D. Contin 22.

Table D.9. Calcite analyses.

Rock Sample	Brookville Gneiss marble CW88-629C		Ashburn Formation marble CW88-204							CW90-764			
	4	5	1	2	3	4	5	6	7	1	2	3	4
	SiO ₂	0.10	0.00	0.25	0.28	0.97	0.16	0.10	0.14	0.08	0.08	0.00	0.17
TiO ₂	0.00	0.00	0.00	0.00	0.00	0.00	0.00	0.00	0.00	0.00	0.00	0.00	0.00
Al ₂ O ₃	0.00	0.08	0.00	0.00	0.00	0.00	0.00	0.00	0.00	0.00	0.00	0.00	0.00
FeO	0.00	0.16	0.00	0.00	0.00	0.00	0.29	0.38	0.00	0.17	0.00	0.16	0.19
MnO	0.00	0.00	0.00	0.00	0.00	0.00	0.00	0.00	0.00	0.00	0.00	0.00	0.00
MgO	0.70	0.60	0.13	0.15	0.51	0.00	1.25	1.47	0.00	0.31	0.93	1.36	0.28
CaO	58.74	57.28	57.52	51.84	57.66	58.32	56.59	55.66	55.96	58.70	57.46	57.38	58.05
Na ₂ O	0.00	0.00	0.00	0.14	0.00	0.00	0.00	0.00	0.00	0.00	0.00	0.00	0.00
K ₂ O	0.06	0.00	0.00	0.00	0.00	0.00	0.00	0.00	0.00	0.00	0.06	0.00	0.00
TOTAL	59.60	58.11	57.89	52.41	59.14	58.49	58.23	57.65	56.04	59.25	58.46	59.07	59.03

Number of ions on the basis of 6 oxygen.

Si	0.01	0.00	0.02	0.03	0.09	0.02	0.01	0.01	0.01	0.01	0.00	0.02	0.05
Al	0.00	0.01	0.00	0.00	0.00	0.00	0.00	0.00	0.00	0.00	0.00	0.00	0.00
Ti	0.00	0.00	0.00	0.00	0.00	0.00	0.00	0.00	0.00	0.00	0.00	0.00	0.00
Fe	0.00	0.01	0.00	0.00	0.00	0.00	0.02	0.03	0.00	0.01	0.00	0.01	0.02
Mn	0.00	0.00	0.00	0.00	0.00	0.00	0.00	0.00	0.00	0.00	0.00	0.00	0.00
Mg	0.10	0.08	0.02	0.02	0.07	0.00	0.18	0.21	0.00	0.04	0.13	0.19	0.04
Ca	5.88	5.89	5.93	5.90	5.74	5.97	5.78	5.73	5.98	5.93	5.86	5.77	5.35
Na	0.00	0.00	0.00	0.02	0.00	0.00	0.00	0.00	0.00	0.00	0.00	0.00	0.00
K	0.01	0.00	0.00	0.00	0.00	0.00	0.00	0.00	0.00	0.00	0.01	0.00	0.00

APPENDIX D. Continued.

Table D.9. Calcite analyses.

Rock Sample	Ashburn Formation marble CW90-812				Hammondvale metamorphic unit marble CW88-101		
	1	2	3	4	1	2	3
	SiO ₂	0.16	0.15	0.00	0.09	0.00	0.00
TiO ₂	0.00	0.00	0.00	0.00	0.00	0.00	0.00
Al ₂ O ₃	0.00	0.11	0.00	0.00	0.00	0.00	0.00
FeO	0.00	0.00	0.00	0.00	0.00	0.00	0.17
MnO	0.00	0.00	0.00	0.00	0.00	0.25	0.00
MgO	1.10	2.01	1.26	0.37	0.16	0.00	0.21
CaO	55.48	57.05	56.77	56.93	57.91	58.60	57.80
Na ₂ O	0.00	0.00	0.00	0.00	0.00	0.00	0.00
K ₂ O	0.00	0.00	0.00	0.00	0.00	0.00	0.00
TOTAL	56.74	59.31	58.03	57.39	58.08	58.86	58.29

Number of ions on the basis of 6 oxygen.

Si	0.02	0.01	0.00	0.01	0.00	0.00	0.01
Al	0.00	0.01	0.00	0.00	0.00	0.00	0.00
Ti	0.00	0.00	0.00	0.00	0.00	0.00	0.00
Fe	0.00	0.00	0.00	0.00	0.00	0.00	0.01
Mn	0.00	0.00	0.00	0.00	0.00	0.02	0.00
Mg	0.16	0.28	0.18	0.05	0.02	0.00	0.03
Ca	5.79	5.66	5.82	5.91	5.98	5.98	5.93
Na	0.00	0.00	0.00	0.00	0.00	0.00	0.00
K	0.00	0.00	0.00	0.00	0.00	0.00	0.00

APPENDIX D. Continued.

Table D.10. Dolomite analyses.

Rock Sample	Brookville Gneiss marble CW89-598C								Ashburn Formation marble CW89-663					CW90 -764
	1	2	3	4	5	6	7	8	1	2	3	4	5	1
SiO ₂	0.00	0.00	0.00	0.00	0.00	0.00	0.00	0.00	0.00	0.00	0.00	0.00	0.00	0.00
TiO ₂	0.00	0.00	0.00	0.00	0.00	0.00	0.00	0.00	0.00	0.00	0.00	0.00	0.00	0.00
Al ₂ O ₃	0.00	0.00	0.00	0.00	0.00	0.00	0.00	0.00	0.00	0.00	0.00	0.00	0.00	0.00
FeO	0.32	0.45	0.56	0.55	0.47	0.46	0.54	0.48	0.00	0.01	0.03	0.00	0.00	0.72
MnO	0.00	0.00	0.00	0.00	0.00	0.00	0.00	0.00	0.00	0.00	0.00	0.00	0.00	0.00
MgO	10.72	20.83	19.93	21.24	20.91	21.32	20.92	21.04	23.33	21.53	21.94	21.49	21.86	21.55
CaO	44.33	29.95	30.99	29.84	30.11	28.97	29.49	29.56	31.83	29.55	29.36	29.58	29.66	31.29
Na ₂ O	0.00	0.00	0.00	0.00	0.00	0.00	0.00	0.00	0.00	0.00	0.00	0.00	0.00	0.00
K ₂ O	0.00	0.00	0.00	0.00	0.00	0.00	0.00	0.00	0.00	0.00	0.00	0.00	0.00	0.00
TOTAL	55.37	51.23	51.48	51.63	51.49	50.75	50.95	51.08	55.16	51.09	51.33	51.07	51.52	53.56

Number of ions on the basis of 6 oxygen.

Si	0.00	0.00	0.00	0.00	0.00	0.00	0.00	0.00	0.00	0.00	0.00	0.00	0.00	0.00
Al	0.00	0.00	0.00	0.00	0.00	0.00	0.00	0.00	0.00	0.00	0.00	0.00	0.00	0.00
Ti	0.00	0.00	0.00	0.00	0.00	0.00	0.00	0.00	0.00	0.00	0.00	0.00	0.00	0.00
Fe	0.03	0.04	0.04	0.04	0.04	0.04	0.04	0.04	0.00	0.00	0.00	0.00	0.00	0.05
Mn	0.00	0.00	0.00	0.00	0.00	0.00	0.00	0.00	0.00	0.00	0.00	0.00	0.00	0.00
Mg	1.50	2.93	2.81	2.96	2.93	3.02	2.96	2.97	3.03	3.02	3.06	3.02	3.04	2.91
Ca	4.47	3.03	3.14	2.99	3.03	2.95	3.00	3.00	2.97	2.98	2.94	2.98	2.96	3.04
Na	0.00	0.00	0.00	0.00	0.00	0.00	0.00	0.00	0.00	0.00	0.00	0.00	0.00	0.00
K	0.00	0.00	0.00	0.00	0.00	0.00	0.00	0.00	0.00	0.00	0.00	0.00	0.00	0.00

APPENDIX D. Continued.

Table D.10. Dolomite analyses.

Rock Sample	Ashburn Formation marble CW90-812			
	1	2	3	4
SiO ₂	0.00	0.12	0.00	0.12
TiO ₂	0.00	0.00	0.00	0.00
Al ₂ O ₃	0.00	0.00	0.00	0.00
FeO	0.39	0.39	0.18	0.43
MnO	0.00	0.00	0.00	0.00
MgO	22.16	22.15	21.90	21.97
CaO	31.54	31.58	32.19	31.54
Na ₂ O	0.00	0.00	0.00	0.12
K ₂ O	0.00	0.00	0.00	0.00
TOTAL	54.10	54.25	54.27	54.17

Number of ions on the basis of 6 oxygen.

Si	0.00	0.01	0.00	0.01
Al	0.00	0.00	0.00	0.00
Ti	0.00	0.00	0.00	0.00
Fe	0.03	0.03	0.01	0.03
Mn	0.00	0.00	0.00	0.00
Mg	2.95	2.94	2.91	2.92
Ca	3.02	3.01	3.08	3.01
Na	0.00	0.00	0.00	0.02
K	0.00	0.00	0.00	0.00

APPENDIX E

E.1. U-Pb ANALYTICAL TECHNIQUES

U-Pb data presented in this study were acquired at the geochronology laboratory in the Earth Sciences Department at Memorial University of Newfoundland under the supervision of Dr. G. R. Dunning.

Minerals dated were zircon and titanite. These minerals were separated from samples weighing approximately 25 to 30 kg by standard crushing, grinding, Wilfley table, heavy liquid, and magnetic techniques (Hutchison, 1974). Mineral separates were then sieved into a number of size fractions. Zircon and titanite were selected from the -100/+200 mesh size for analysis and hand picking in ethyl alcohol under a microscope.

The criteria used for selection of zircon included optimum clarity, uniform morphology, lack of cracks and inclusions, and the absence of obvious "cored" grains. Zircon grains from the Ludgate Lake Granodiorite (NB92-9010) were mounted and polished, then analyzed using the backscatter and catholuminescence images on the electron microprobe. This was done to document morphological characteristics which are used in the interpretation of the U-Pb results.

The criteria for selection of titanite are similar to those for zircon; however, grains that were very dark in colour were picked because of their high U content. This reduces the uncertainties associated with the common Pb correction.

All zircon and titanite fractions were air abraded following the technique of Krogh (1982), using pyrite as an abrasion medium, and re-picked to further purify the concentrates. All fractions were then washed with 3N HNO₃, water, and acetone, spiked with a mixed ²⁰⁵Pb/²³⁵U tracer and dissolved with HF and HNO₃ in Teflon capsules (zircon) at 220°C for 5 days or in Savillex screw-top capsules (titanite) at 90°C for 3 to 5 days. U and Pb were collected using ion-exchange chemistry,

modified after Krogh (1973) and Parrish et al. (1987), loaded on a Re filament, and analyzed on a Finnigan MAT 262 mass spectrometer.

Measured isotopic ratios were corrected for fractionation in the mass spectrometer, and corrected for Pb and U blank (5-15 pg), and further corrected for common Pb using the isotopic composition predicted by the model of Stacey and Kramers (1975). Linear regression and calculation of intercepts and errors (95% confidence level) were carried out using the method of Davis (1982).

Table E.1. U/Pb data

Mineral fraction	Weight (mg)	U (ppm)	Pb (ppm)	Pb (pg)	$\frac{^{206}\text{Pb}}{^{204}\text{Pb}}$	Corrected Atomic Ratios ¹			Age (Ma)			
						$\frac{^{206}\text{Pb}}{^{238}\text{U}}$	$\frac{^{207}\text{Pb}}{^{235}\text{U}}$	$\frac{^{207}\text{Pb}}{^{206}\text{Pb}}$	$\frac{^{206}\text{Pb}}{^{238}\text{U}}$	$\frac{^{207}\text{Pb}}{^{235}\text{U}}$	$\frac{^{207}\text{Pb}}{^{206}\text{Pb}}$	
<u>FRENCH VILLAGE QUARTZ DIORITE</u>												
Z1 N+149abr	0.064	161	16.6	12	4591	0.08687±0.09	0.6971±0.10	0.05820±0.04				537
Z2 W+149abr	0.026	104	10.3	4	3476	0.08701±0.11	0.6981±0.12	0.05819±0.07				537
Z3 N+149abr	0.107	208	21.6	23	5206	0.08681±0.08	0.6974±0.10	0.05827±0.04				540
<u>FAIRVILLE GRANITE</u>												
Z1 long euh abr	0.153	182	17.2	86	1829	0.08949±0.32	0.7291±0.30	0.05909±0.10	552	556		570
Z2 long euh abr	0.221	143	13.5	49	3448	0.08896±0.30	0.7214±0.26	0.05882±0.08	549	552		560
Z3 gem prism abr	0.173	196	18.8	60	3254	0.09114±0.38	0.7637±0.34	0.06078±0.12	562	576		631
<u>LUDGATE LAKE GRANODIORITE</u>												
Z1 long euh abr	0.136	161	15.3	111	1098	0.08731±0.46	0.7041±0.40	0.05849±0.14	540	541		548
Z2 stubby abr	0.421	159	14.9	103	3577	0.08732±0.32	0.7043±0.28	0.05850±0.08	540	541		548
Z3 clr gem abr	0.246	168	15.9	66	3436	0.08711±0.30	0.7013±0.26	0.05839±0.08	538	540		544
T1 brown abr	0.345	385	40.2	526	1376	0.08585±0.30	0.6913±0.28	0.05840±0.08	531	534		545
T2 brown abr	0.176	307	33.2	365	823	0.08686±0.42	0.7011±0.40	0.05855±0.14	537	539		550

¹ Ratios corrected for blank Pb and U and common Pb; errors are 1 sigma for French Village quartz diorite and 2 sigma for all others.

ABBREVIATIONS: N=non-magnetic at <1°, 1.7 amps on Franz magnetic separated; W=non-magnetic at <2°, 1.7 amps; 149 refers to size in microns; euh=euhedral; clr=clear; abr=abraded.

APPENDIX E: Continued.**E.2. $^{40}\text{Ar}/^{39}\text{Ar}$ ANALYTICAL TECHNIQUES, ERROR ANALYSIS, INTERPRETATION OF AGE SPECTRA, AND DATA**

$^{40}\text{Ar}/^{39}\text{Ar}$ data were obtained at the argon laboratory in the Earth Sciences Department at Dalhousie University, Halifax, Nova Scotia under the supervision of Dr. P.H. Reynolds.

Samples selected for this study were based on the following criteria:

1) Samples were fresh and unaltered to avoid grains which may have lost or gained K (e.g. chloritized biotite and hornblende). Grains that are deformed were also avoided (e.g. fractured hornblende and kinked mica).

2) Grains with intergrown phases were avoided. A small amount of high K-phase (biotite) may produce enough radiogenic Ar to obscure that produced by the phase (hornblende) intended for dating.

3) In metamorphic rocks it is important to recognize different generations of mineral phases so they can be separated or used in the interpretation of the resulting spectrum.

Hornblende, phlogopite, biotite, and muscovite were obtained by crushing 5 kg of sample, sieved to various size fractions and hand-picked. Concentrates from finer-grained samples were obtained by standard magnetic and heavy-liquid techniques. All concentrates were then ultrasonically washed in distilled water and hand-picked under a binocular microscope to increase purity. Small sample volumes of 10 mg were obtained and analyzed by the VG3600 Mass Spectrometer.

The standard techniques used in $^{40}\text{Ar}/^{39}\text{Ar}$ dating are well known. A detailed discussion of modern technical aspects are outlined in McDougall and Harrison (1988) and analytical procedures for the argon laboratory at Dalhousie University are summarized by Haggart (1991).

The standard flux monitor used in this study was MMhb-1

(hornblende) with a calculated K-Ar age of 519.4 ± 3.2 (Alexander et al., 1978). These were placed at regular intervals in the irradiation canister, allowing the determination of the irradiation parameter, J . J -values were measured for each standard and plotted against position in the canister. A best-fit line using the York (1969) method was employed and J -values each sample were determined by interpolation along the line. Error in J is the major source of error in the final age assigned to the sample. The errors on the J -values are quoted at 1 sigma and are noted on their data summary sheets in Appendix 4.3.

Errors on individual steps (quoted at 1 sigma in Appendix 4.3) are based on uncertainties in the correction for atmospheric argon and measurement of ^{40}Ar and ^{39}Ar peaks. In addition, step errors are dependent on corrections in mass discriminations and interfering isotopes. The final age calculation incorporates errors in the J value and "mass spectrometer" measurements and is quoted at 2 sigma. The final age does not incorporate errors associated with the hornblende standard which are less than 1%.

The $^{40}\text{Ar}/^{39}\text{Ar}$ step heating approach provides considerable information on the distribution of Ar in a sample. The original theory of Ar diffusion (Turner, 1968) predicted that thermally undisturbed samples will yield perfectly flat age spectra (plateau) that correspond to the time of closure to argon diffusion. Samples that are thermal disturbed are predicted to exhibit age gradients depending on the intensity of the event.

In reality there is considerable deviation from the theoretical model of Turner (1968) probably due to violations in the assumptions of the model. This led to the establishment of various criteria for spectrum interpretation. The most common assumption is that the data exhibit a plateau before a geologically meaningful age can be assigned. This resulted in various definitions of a "plateau" (cf. Dalrymple and Lanphere, 1974; Fleck et al., 1977; Lanphere and Dalrymple, 1978; Berger and York, 1981; Snee et al., 1988; Dallmeyer and Nance, 1990). However,

the presence or absence of a plateau is not considered a valid criterion for acceptance or rejection of an analysis (cf. Lee, 1993).

Many of the samples dated in this study display age spectra that have irregular shapes; however, all samples have been tested for the presence of a "plateau" in their spectra using the criteria established by Fleck et al. (1977). Plateau ages quoted by Dallmeyer and Nance (1989, 1990, 1992), Dallmeyer et al. (1990) and Nance and Dallmeyer (in press) are calculated similar to the criteria of Fleck et al. (1977). However, an additional intralaboratory uncertainty of $\pm 1\%$ is introduced in their calculations that results in a less stringent definition of the "plateau" age.

Relatively flat spectra that do not statistically define a plateau yet yield reasonable ages are interpreted to define a "near-plateau" age (Schermer et al., 1990). Many of the mica analyses display age gradients or stepped spectra and geologically meaningful ages can be acquired from the high temperature steps (most argon retentive) that are interpreted to reflect a minimum age for the sample.

APPENDIX E: Continued.

ANALYTICAL DATA

CW89-169 HB CAN L SUMMARY

oC	mV 39	% 39	AGE (Ma)	% ATM 37/39	36/40	39/40	% IIC
750	12.5	2.1	507.2 +/- 20.5	72.2 13.15	.002443	.001912	1.54
850	15.5	2.6	418.4 +/- 10.4	57.3 4.88	.00194	.003652	.63
900	10.9	1.8	402.6 +/- 4.4	15 4.48	.00051	.007588	.59
950	23.2	3.9	440.1 +/- 2.9	8.2 6.12	.00028	.007416	.77
975	19.1	3.2	475.1 +/- 3.4	8.1 7.68	.000276	.006809	.93
1000	25.3	4.2	516.4 +/- 2.8	4.8 7.39	.000164	.006412	.85
1025	78.3	13.2	523.8 +/- 2.3	2.1 6.5	.000074	.006487	.75
1050	154.3	26	516.9 +/- 2.2	1.4 6.01	.00005	.006633	.69
1075	84.1	14.1	511.9 +/- 2.3	1.6 5.62	.000057	.006693	.65
1100	26	4.4	480.3 +/- 3.5	4.2 5.3	.000145	.00701	.63
1125	18.1	3	426.7 +/- 8.8	14 5.93	.000474	.0072	.76
1200	95.6	16.1	513.1 +/- 2.9	3.2 7.8	.000108	.006574	.9
1300	23.8	4	507.9 +/- 3.3	6.2 6.25	.00021	.006443	.73
1350	5.3	.9	484.6 +/- 11.4	21.8 6.39	.000738	.005669	.76

TOTAL GAS AGE = 502.4 Ma

J = .002235

ERROR ESTIMATES AT ONE SIGMA LEVEL

37/39,36/40 AND 39/40 Ar RATIOS ARE CORRECTED FOR INTERFERING ISOTOPES

% IIC - INTERFERING ISOTOPES CORRECTION

CW88-246 HB SUMMARY

oC	mV 39	% 39	AGE (Ma)	% ATM 37/39	36/40	39/40	% IIC
750	12.8	2.8	381.4 +/- 12.5	62.7 3.27	.002122	.003537	.44
850	19.7	4.3	468.3 +/- 5.8	30.3 2.63	.001028	.005247	.32
900	11.6	5	426.8 +/- 3.7	13.5 1.29	.000458	.007236	.16
950	15.5	3.4	459.5 +/- 3.6	9.9 1.74	.000336	.006937	.21
975	10.9	2.4	520.8 +/- 5.9	13.5 3.79	.000458	.005771	.43
1000	13.8	3	533.1 +/- 4.8	10.4 7.48	.000353	.005819	.85
1025	18.6	4.1	528.8 +/- 3.4	5.9 8.62	.0002	.006171	.99
1050	49.6	10.9	533.5 +/- 2.5	3.7 9.13	.000125	.006251	1.04
1075	65.2	14.4	536.3 +/- 2.4	1.7 9.52	.00006	.006339	1.08
1100	46.5	10.2	540 +/- 2.4	2.4 11.04	.000083	.006245	1.25
1140	23	5	541.7 +/- 3.3	5 9.81	.000169	.00606	1.11
1200	126.5	27.9	543.7 +/- 2.3	2.6 9.38	.00009	.006183	1.06
1300	26.5	5.8	545.1 +/- 3.4	14.8 9.59	.000503	.00539	1.08
1375	11	2.4	569.2 +/- 10.5	45.5 9.6	.001542	.003277	1.06

TOTAL GAS AGE = 526.8 Ma

J = .002235

ERROR ESTIMATES AT ONE SIGMA LEVEL

37/39,36/40 AND 39/40 Ar RATIOS ARE CORRECTED FOR INTERFERING ISOTOPES

% IIC - INTERFERING ISOTOPES CORRECTION

CW88-509A HB SUMMARY

oC	mV 39	% 39	AGE (Ma)	% ATM 37/39	36/40	39/40	% IIC	
750	13.9	1.6	425.7 +/- 3.9	22.3	1	.000755	.00652	.12
850	22.4	2.7	363.8 +/- 2.5	13.7	.91	.000467	.008621	.12
900	15.7	1.9	401.2 +/- 3.9	16.6	3.75	.000564	.007473	.49
950	19.4	2.3	442.5 +/- 4.1	11.6	6.41	.000394	.007101	.8
975	13.6	1.6	542.4 +/- 4.9	11.4	10.13	.000388	.005638	1.14
1000	34.4	4.1	554.3 +/- 2.8	5.4	7.11	.000183	.005874	.79
1025	107.8	13.1	549.1 +/- 2.4	2.2	6.28	.000074	.006141	.7
1050	273.8	33.3	538.5 +/- 2.2	1.1	6.4	.000039	.006349	.72
1075	134.3	16.3	533 +/- 2.3	1	6.77	.000037	.006429	.77
1100	24	2.9	503.4 +/- 2.7	4.8	7.21	.000163	.006607	.84
1125	16.2	1.9	515.1 +/- 3.3	7.4	9.5	.000252	.006256	1.1
1150	24.2	2.9	519.2 +/- 4.2	9.2	10.33	.000313	.00608	1.19
1200	82.6	10	540.2 +/- 2.6	4.4	8.22	.000151	.006113	.93
1250	15.5	1.8	526.8 +/- 5.3	19.7	9.08	.000668	.005287	1.04
1300	14	1.7	541.8 +/- 6.3	22.5	8.8	.000763	.004939	.99
1350	7.1	.8	545.5 +/- 10.2	39	8.88	.001321	.003856	1
1400	2.3	.2	544.6 +/- 54.8	58.5	7.58	.001981	.002628	.85

TOTAL GAS AGE = 526.6 Ma

J = .002235

ERROR ESTIMATES AT ONE SIGMA LEVEL

37/39, 36/40 AND 39/40 Ar RATIOS ARE CORRECTED FOR INTERFERING ISOTOPES

% IIC - INTERFERING ISOTOPES CORRECTION

CW89-611 SUMMARY

oC	mV 39	% 39	AGE (Ma)	% ATM 37/39	36/40	39/40	% IIC	
650	6.2	.8	47.3 +/- 28.7	98.5	5.68	.003336	.001248	4.15
750	11.7	1.6	351.1 +/- 8.4	75.6	2.31	.002559	.002654	.34
850	17.8	2.4	405.9 +/- 5.5	62.5	4.32	.002115	.003475	.58
950	162	22.4	552.6 +/- 1.2	4	4.58	.000137	.006261	.52
975	148	20.5	534.8 +/- 1.1	2.2	3.89	.000076	.006625	.45
1000	119.8	16.6	537.9 +/- 1.1	2.2	3.7	.000077	.006579	.43
1025	16.1	2.2	514.7 +/- 2.3	6.6	4.06	.000224	.006615	.48
1050	40.4	5.6	493.5 +/- 1.2	4.7	4.83	.000159	.007084	.58
1100	194.4	26.9	533.7 +/- 1.1	2.7	4.24	.000092	.00661	.49
1225	4	.5	525.9 +/- 9.2	65.3	6.3	.002212	.002392	.74

TOTAL GAS AGE = 526.6 Ma

J = .00234

ERROR ESTIMATES AT ONE SIGMA LEVEL

37/39, 36/40 AND 39/40 Ar RATIOS ARE CORRECTED FOR INTERFERING ISOTOPES

% IIC - INTERFERING ISOTOPES CORRECTION

NB91-2597 Hb SUMMARY

OC	mV 39	% 39	AGE (Ma)	% ATM 37/39	36/40	39/40	% IIC
750	8.5	2.4	418.2 +/- 11.3	29.4	2.52	.000998	.006241 .33
950	10.1	2.9	504.1 +/- 7.9	21	4.34	.000714	.005651 .51
975	3.7	1	482.9 +/- 17.7	31.3	5.14	.001061	.005164 .62
1000	10.8	3.1	521.9 +/- 7.4	8.2	6.72	.000279	.006316 .78
1025	109.2	31.6	527.7 +/- 2.3	1.3	7.82	.000044	.006706 .91
1045	26.8	7.7	524.8 +/- 3.8	5.1	7.21	.000173	.006489 .84
1065	15.8	4.5	525.6 +/- 5.1	7.3	7.07	.000249	.006324 .82
1100	12.9	3.7	540.7 +/- 6.6	10.2	7.54	.000347	.005929 .86
1150	32.9	9.5	527 +/- 2.6	3.7	8.11	.000126	.006551 .94
1200	40.3	11.6	533.2 +/- 2.5	3.9	7.54	.000134	.006448 .87
1250	45.6	13.2	520.3 +/- 2.6	4.5	8	.000153	.006594 .94
1300	19.2	5.5	529.2 +/- 3.4	12.2	7.83	.000414	.005944 .91
1350	8.4	2.4	498.5 +/- 12.1	41.7	8.01	.001412	.004226 .96

TOTAL GAS AGE = 522.9001 Ma

J = .00231

ERROR ESTIMATES AT ONE SIGMA LEVEL

37/39,36/40 AND 39/40 Ar RATIOS ARE CORRECTED FOR INTERFERING ISOTOPES

% IIC - INTERFERING ISOTOPES CORRECTION

NB91-8599 HORNBLLENDE SUMMARY

oC	mV 39	% 39	AGE (Ma)	% ATM 37/39	36/40	39/40	% IIC	
750	3.5	1.2	8272.9 +/- 1017.6	.3	7.62	.000011	.000023	.49
950	21	7.6	597.4 +/- 6.9	34.4	10.36	.001164	.003861	1.13
975	7.9	2.8	586.2 +/- 14	25.5	8.81	.000863	.004483	.97
1000	23.1	8.3	537.9 +/- 3.1	7.8	7.58	.000266	.005875	.85
1025	70.8	25.7	543.8 +/- 2.5	3.9	7.09	.000132	.006311	.81
1050	54.7	19.8	541.9 +/- 2.7	3.2	6.94	.000111	.00638	.79
1070	33.4	12.1	543.3 +/- 2.9	5.1	6.85	.000172	.006241	.78
1090	15	5.4	542.1 +/- 5	16.4	7.17	.000555	.005511	.82
1115	13.1	4.7	556.1 +/- 4.7	12	7.34	.000407	.005631	.83
1150	13.3	4.8	552 +/- 8.2	17.2	7.78	.000585	.00534	.88
1200	19.2	6.9	568.5 +/- 5.5	17.9	7.24	.000607	.00512	.81

TOTAL GAS AGE = 1727 Ma

J = .002312

ERROR ESTIMATES AT ONE SIGMA LEVEL

37/39,36/40 AND 39/40 Ar RATIOS ARE CORRECTED FOR INTERFERING ISOTOPES

% IIC - INTERFERING ISOTOPES CORRECTION

CW88-509 BIOTITE SUMMARY

oC	mV 39	% 39	AGE (Ma)	% ATM 37/39	36/40	39/40	% IIC	
600	30	3.1	399.5 +/- 2.1	11.3	1.41	.000385	.00836	.19
650	99	10.5	408.6 +/- 1.8	3.9	1.16	.000133	.008839	.15
700	156	16.5	508.5 +/- 2.1	1	.58	.000036	.007108	.07
750	187	19.8	510.4 +/- 2.1	.8	.36	.000029	.007091	.04
800	33	3.5	511.3 +/- 2.3	2.6	1.31	.00009	.006949	.15
850	73	7.7	514.6 +/- 2.1	1.4	.66	.00005	.006981	.07
900	111	11.8	509.9 +/- 2.1	.8	.68	.000028	.007101	.08
950	81	8.6	509.5 +/- 2.1	.6	.4	.00002	.007125	.04
1000	97	10.3	506.3 +/- 3.1	.8	.55	.000027	.007162	.06
1050	73	7.7	504.5 +/- 2.1	1.6	2.4	.000057	.007126	.28

TOTAL GAS AGE = 495.5 Ma

J = .00234

ERROR ESTIMATES AT ONE SIGMA LEVEL

37/39, 36/40 AND 39/40 Ar RATIOS ARE CORRECTED FOR INTERFERING ISOTOPES

% IIC - INTERFERING ISOTOPES CORRECTION

CW88-204 PHLOGOPITE SUMMARY

oC	mV 39	% 39	AGE (Ma)	% ATM 37/39	36/40	39/40	% IIC
650	23.7	2.9	44.8 +/- 3	77.7 .13	.00263	.019691	.1
720	16.4	2	78.3 +/- 4.8	75.5 .25	.002555	.012268	.11
800	14.9	1.8	496.8 +/- 10.9	48.3 .07	.001637	.00362	0
840	26.6	3.3	503.4 +/- 3.2	15 .02	.00051	.005867	0
870	39.6	4.9	549.2 +/- 3.1	9 .01	.000307	.005683	0
900	73	9.1	559.9 +/- 2.7	5.2 .01	.000176	.005793	0
930	83.8	10.4	557.5 +/- 2.5	1.9 0	.000065	.0060 [~] 4	0
960	104	13	559 +/- 2.3	1.6 0	.000056	.006022	0
990	98.2	12.3	572.3 +/- 2.4	1.5 0	.000053	.005863	0
1020	94.4	11.8	566.4 +/- 2.4	2 .01	.00007	.005905	0
1070	88.2	11	546 +/- 2.3	1.4 .01	.000049	.006201	0
1120	94.4	11.8	537.5 +/- 2.4	2.3 .01	.00008	.006255	0
1200	34	4.2	540.4 +/- 3.4	12.2 .03	.000414	.005588	0
1300	5.8	.7	1674.2 +/- 170.2	18.8 .08	.000636	.00118	0
1400	1.2	.1	2354.2 +/- 278.6	40.5 .64	.001373	.000491	.04

TOTAL GAS AGE = 547.2 Ma

J = .002225

ERROR ESTIMATES AT ONE SIGMA LEVEL

37/39, 36/40 AND 39/40 Ar RATIOS ARE CORRECTED FOR INTERFERING ISOTOPES

% IIC - INTERFERING ISOTOPES CORRECTION

CW89-598C PHLOGOPITE SUMMARY

OC	mV 39	% 39	AGE (Ma)	% ATM 37/39	36/40	39/40	% IIC
650	24.8	3.3	52.2 +/- 1.4	52.7 .01	.001736	.035776	.01
720	19.6	2.6	123.4 +/- 2.6	37.6 .04	.001272	.019594	.01
800	16.5	2.2	584.1 +/- 7.3	8.9 .04	.000301	.005299	0
840	11.9	1.5	600.4 +/- 7.4	9.3 .02	.000317	.005104	0
870	7.3	.9	569.4 +/- 14.3	13.6 .03	.000462	.005174	0
900	17.7	2.3	533.9 +/- 4.5	7.1 .01	.000241	.005998	0
930	76	10.1	522.1 +/- 2.4	.6 0	.000022	.006583	0
960	136.1	18.1	511 +/- 2.3	.9 0	.000003	.006731	0
990	99.4	13.2	525.8 +/- 2.2	1.1 0	.000004	.006495	0
1020	85.3	11.3	536.2 +/- 2.4	1.6 0	.000055	.006322	0
1050	79.6	10.5	540.2 +/- 2.5	2.5 .01	.000086	.006208	0
1100	70.7	9.4	542.8 +/- 2.5	3.5 .02	.00012	.00611	0
1150	68.3	9	541.2 +/- 2.6	4.2 .01	.000143	.006089	0
1200	29.1	3.8	543.3 +/- 4	12 .02	.000406	.005569	0
1250	6.5	.8	770.4 +/- 30.6	12.4 .12	.00042	.003656	.01
1300	1.2	.1	1188 +/- 243	62.6 .84	.002121	.00089	.07
1400	.7	.1	-11.6 +/- 972.1	100.1	2.13	.003389	.0006 5.49

TOTAL GAS AGE = 512.2 Ma

J = .002225

ERROR ESTIMATES AT ONE SIGMA LEVEL

37/39, 36/40 AND 39/40 Ar RATIOS ARE CORRECTED FOR INTERFERING ISOTOPES

% IIC - INTERFERING ISOTOPES CORRECTION

CW89-629 PHLOGOPITE SUMMARY

oC	mV 39	% 39	AGE (Ma)	% ATM 37/39	36/40	39/40	% IIC
650	30.2	1.4	70.1 +/- 1.2	39.7 .03	.001346	.033752	.01
700	10.9	.5	322 +/- 4.1	20.6 .05	.000699	009028	0
765	17.8	.8	629 +/- 5.9	7 .03	.000237	.004958	0
800	22.2	1	603 +/- 4.2	.2 .03	.000006	.005593	0
830	14.5	7	541 +/- 7.3	8.8 .06	.000299	.065797	0
860	13.9	.6	519.2 +/- 7.1	12 .05	.000407	.005866	0
890	23.1	1.1	537.9 +/- 4.8	8.7 .05	.000294	.005846	0
930	57.9	2.8	534.9 +/- 2.6	4.3 .01	.000146	.006164	0
960	67.5	3.2	541.5 +/- 2.4	2.3 .01	.000078	.006205	0
990	91.2	4.4	547.4 +/- 2.6	1.6 .01	.000057	.006168	0
1020	147.5	7.1	547.3 +/- 2.4	1.1 0	.000038	.006203	0
1070	291.3	14.1	537.5 +/- 2.2	.7 0	.000023	.006353	0
1120	435.4	21.1	533.2 +/- 2.2	.7 0	.000026	.006417	0
1200	584.7	28.3	532.5 +/- 2.2	1 0	.000035	.00641	0
1300	235	11.4	531.5 +/- 2.3	4.1 .01	.000141	.00622	0
1400	16.3	.7	539.5 +/- 13.1	52 .1	.00176	.003061	.01

TOTAL GAS AGE = 530 Ma

J = .002225

ERROR ESTIMATES AT ONE SIGMA LEVEL

37/39, 36/40 AND 39/40 Ar RATIOS ARE CORRECTED FOR INTERFERING ISOTOPES

% IIC - INTERFERING ISOTOPES CORRECTION

CW90-764 PHLOGOPITE SUMMARY

OC	mV 39	% 39	AGE (Ma)	% ATM 37/39	36/40	39/40	% IIC
650	11.3	.8	55.7 +/- 4	71.4 .14	.002417	.020249	.08
700	17.2	1.3	46.1 +/- 2	61.2 .13	.002073	.033266	.09
750	9.3	.7	225.8 +/- 7	45.7 .11	.001549	.009054	.02
800	13.2	1	543.6 +/- 6.3	23.5 .04	.000796	.004842	0
830	35.9	2.7	532.4 +/- 3.7	6.9 0	.000234	.006039	0
860	50.5	3.8	497.3 +/- 2.9	4.3 0	.000147	.006711	0
890	73.4	5.6	510 +/- 2.6	2.9 0	.000099	.006617	0
920	103	7.9	518.1 +/- 2.5	2 0	.000068	.00656	0
950	135	10.4	519.8 +/- 2.3	1.6 0	.000054	.006562	0
980	160.8	12.4	527.2 +/- 2.3	1.2 -.01	.000043	.006477	0
1010	209.2	16.1	528.1 +/- 2.2	1 0	.000035	.006479	0
1040	185.8	14.3	529.9 +/- 2.3	1.1 0	.000037	.006449	0
1070	113.8	8.7	534.6 +/- 2.4	1.5 0	.000053	.006355	0
1120	102.2	7.8	532.1 +/- 2.4	2.7 .01	.000093	.006313	0
1200	69.2	5.3	533.6 +/- 2.9	10.7 .06	.000363	.005776	0
1300	5.2	.4	530.6 +/- 70.3	66.3 .55	.002244	.002192	.06
1400	1.6	.1	1031.5 +/- 289.1	74.9 1.73	.002535	.000723	.15

TOTAL GAS AGE = 515.3 Ma

J = .002228

ERROR ESTIMATES AT ONE SIGMA LEVEL

37/39, 36/40 AND 39/40 Ar RATIOS ARE CORRECTED FOR INTERFERING ISOTOPES

% IIC - INTERFERING ISOTOPES CORRECTION

CW90-812 PHLOGOPITE SUMMARY

OC	mV 39	% 39	AGE (Ma)	% ATM 37/39	36/40	39/40	% IIC
650	16.5	1.2	96.5 +/- 3.1	51.5 .03	.001745	.01961	.01
700	10.6	.8	245.7 +/- 6	38.2 .07	.001294	.009418	.01
760	14.4	1.1	478 +/- 5.3	16.7 .02	.000567	.006107	0
800	15.7	1.2	543.7 +/- 4.6	10.5 .03	.000358	.005659	0
830	12.9	1	510.3 +/- 8.5	11.3 .01	.000385	.006034	0
860	17.9	1.4	512.5 +/- 6.2	9.6 0	.000326	.006121	0
890	44.5	3.4	513.1 +/- 3.4	3.6 0	.000123	.00652	0
920	88.3	6.9	517.7 +/- 2.5	1.5 0	.000051	.006596	0
950	96.9	7.6	520.4 +/- 2.3	1.1 0	.000037	.006583	0
980	102.8	8	525 +/- 2.3	.9 0	.000031	.006529	0
1010	144.4	11.3	524.9 +/- 2.2	.6 0	.000022	.006548	0
1040	199.5	15.6	518.8 +/- 2.2	.5 0	.000016	.006648	0
1070	212.5	16.6	514.5 +/- 2.2	.7 0	.000024	.006697	0
1120	165.3	12.9	511.9 +/- 2.2	1.3 0	.000044	.006696	0
1200	114	8.9	514.3 +/- 2.4	3.3 0	.000111	.006525	0
1300	14.6	1.1	529.1 +/- 10.5	26.6 .07	.0009	.004794	0
1400	1.9	.1	521.8 +/- 104.7	78.4 .21	.002655	.001429	.02

TOTAL GAS AGE = 510.6 Ma

J = .002227

ERROR ESTIMATES AT ONE SIGMA LEVEL

37/39, 36/40 AND 39/40 Ar RATIOS ARE CORRECTED FOR INTERFERING ISOTOPES

% IIC - INTERFERING ISOTOPES CORRECTION

CW88-101 MUSCOVITE SUMMARY

oC	mV 39	% 39	AGE (Ma)	% ATM 37/39	36/40	39/40	% IIC
650	71.9	4.8	483 +/- 2.3	2.5 .01	.000086	.007339	0
700	42.3	2.8	559.5 +/- 2.9	1.9 0	.000064	.006236	0
750	81.7	5.4	573.8 +/- 2.6	1.7 0	.000058	.006067	0
800	117.6	7.8	593.2 +/- 2.5	.7 -.01	.000025	.005895	0
825	153.8	10.2	603.9 +/- 2.6	.6 0	.000021	.00578	0
850	108.3	7.2	605.6 +/- 2.5	.7 0	.000026	.005751	0
875	118.9	7.9	601.7 +/- 2.6	.6 -.01	.000023	.0058	0
900	113	7.5	602.8 +/- 2.6	.4 0	.000015	.005802	0
930	105.9	7	605.2 +/- 2.6	.6 0	.000021	.005763	0
960	156.1	10.4	607.4 +/- 2.5	.3 0	.000012	.005755	0
990	134.1	8.9	611 +/- 2.7	.4 -.01	.000014	.005711	0
1020	118	7.8	615.2 +/- 2.6	.7 0	.000026	.005644	0
1070	129.1	8.6	614 +/- 2.7	.4 0	.000015	.005677	0
1120	22.5	1.5	609.1 +/- 5.2	3.5 .01	.000119	.005554	0
1200	14.2	.9	620.5 +/- 6.4	10.8 .01	.000365	.005023	0
1400	9.8	.6	628.1 +/- 20.2	61.4 1.37	.002079	.00214	.14

TOTAL GAS AGE = 597.7 Ma

J = .002313

ERROR ESTIMATES AT ONE SIGMA LEVEL

37/39, 36/40 AND 39/40 Ar RATIOS ARE CORRECTED FOR INTERFERING ISOTOPES

% IIC - INTERFERING ISOTOPES CORRECTION

CW88-115A PHLOGOPITE SUMMARY

oC	mV	39	% 39	AGE (Ma)	% ATM	37/39	36/40	39/40	% IIC
650	24.8	1.7	477.2 +/- 4.7	7.4	.09	.000252	.006798	.01	
700	16.3	1.1	541.4 +/- 5.6	6.3	.04	.000216	.005949	0	
750	37.6	2.5	536.8 +/- 2.9	3.4	.02	.000118	.006194	0	
800	52.1	3.5	546.3 +/- 2.8	2.1	.04	.000071	.006156	0	
830	76.6	5.2	570.5 +/- 2.5	1.3	.03	.000044	.005901	0	
860	167.7	11.5	586.9 +/- 2.5	.6	.01	.00002	.00575	0	
890	194.9	13.4	590.7 +/- 2.5	.5	.01	.000017	.005712	0	
920	191.1	13.1	596.1 +/- 2.5	.4	.01	.000016	.005652	0	
950	175.4	12	601.8 +/- 2.5	.5	.01	.000019	.005586	0	
980	143.1	9.8	600 +/- 2.6	.6	.01	.000021	.0056	0	
1010	130.5	8.9	603.6 +/- 2.6	.7	.01	.000024	.005557	0	
1040	102.5	7	604.2 +/- 2.6	.8	.01	.000029	.005543	0	
1070	65.8	4.5	602.8 +/- 3.1	1.8	.02	.000061	.005504	0	
1120	34.2	2.3	607.7 +/- 4.6	2.6	.05	.00009	.005405	0	
1200	19.9	1.3	598.8 +/- 4.8	5.4	.11	.000184	.005343	.01	
1400	17.7	1.2	600 +/- 7.1	20.3	.09	.000688	.00449	.01	

TOTAL GAS AGE = 590.1 Ma

J = .002225

ERROR ESTIMATES AT ONE SIGMA LEVEL

37/39, 36/40 AND 39/40 Ar RATIOS ARE CORRECTED FOR INTERFERING ISOTOPES

% IIC - INTERFERING ISOTOPES CORRECTION

CW89-767 SUMMARY

oC	mV 39	% 39	AGE (Ma)	% ATM 37/39	36/40	39/40	% IIC
650	16.9	2.8	410.3 +/- 3.7	5.8	.12	.000198	.008531 .01
700	16.3	2.7	478.3 +/- 5.9	5.3	.04	.000181	.007214 0
750	23.2	3.8	496.1 +/- 4.1	2.1	.04	.000072	.007155 0
775	21.7	3.6	501.3 +/- 3.7	2	.02	.00007	.007073 0
810	37.6	6.2	504.2 +/- 3	.9	.01	.000032	.007108 0
840	86.3	14.4	498.9 +/- 2.2	.5	0	.000018	.007224 0
870	108.9	18.1	505.7 +/- 2.2	2.3	0	.000044	.007059 0
900	56.8	9.4	508.9 +/- 2.4	1.7	.01	.000057	.00698 0
930	43.3	7.2	505.8 +/- 3	3.8	.01	.00013	.006875 0
960	41.3	6.9	503.9 +/- 2.9	6.2	.04	.000213	.006729 0
990	26.6	4.4	510.6 +/- 3.1	6	.05	.000205	.006644 0
1020	28.3	4.7	508.7 +/- 3	5.6	.08	.000192	.0067 .01
1070	40.6	6.7	508.7 +/- 3.5	3.5	.13	.000118	.006855 .01
1130	38.6	6.4	509.7 +/- 2.5	4	.12	.000137	.006801 .01
1200	8.6	1.4	548.1 +/- 14.9	20.6	.34	.000699	.00517 .03
1300	2.8	.4	661 +/- 68.7	48.8	.93	.001653	.002674 .09

TOTAL GAS AGE = 503.1 Ma

J = .002315

ERROR ESTIMATES AT ONE SIGMA LEVEL

37/39, 36/40 AND 39/40 Ar RATIOS ARE CORRECTED FOR INTERFERING ISOTOPES

% IIC - INTERFERING ISOTOPES CORRECTION

NB87-4090 MUSCOVITE SUMMARY

oC	mV 39	% 39	AGE (Ma)	% ATM 37/39	36/40	39/40	% IIC
650	34.4	2.4	519.4 +/- 3.7	2.9 .01	.000098	.006477	0
700	35.1	2.4	574.9 +/- 2.9	2.6 .01	.000089	.005775	0
750	45.8	3.2	583.3 +/- 3.2	2.2 0	.000077	.005698	0
800	54.8	3.8	597.4 +/- 3.4	1.5 0	.00005	.005586	0
835	198.2	13.9	605.9 +/- 2.5	.6 -.01	.000021	.005542	0
860	223.8	15.7	609.4 +/- 2.5	.3 0	.000012	.005519	0
890	243.3	17	610.3 +/- 2.5	.3 -.01	.000011	.005512	0
920	146.9	10.3	609.4 +/- 2.6	.4 0	.000015	.005514	0
950	143.1	10	611.2 +/- 2.6	.4 0	.000014	.005496	0
980	143.8	10	616.3 +/- 2.6	.4 0	.000016	.005441	0
1010	81.8	5.7	617.7 +/- 3.1	.8 -.01	.000027	.005408	0
1040	32.5	2.2	616.8 +/- 3.5	2.2 .01	.000074	.005341	0
1070	14.9	1	616.9 +/- 6.7	5.2 .01	.000178	.005172	0
1120	10.5	.7	619.1 +/- 7	12.1 0	.000411	.004777	0
1200	8.2	.5	838.7 +/- 33.6	23 .05	.000778	.002896	0
1300	5.4	.3	850.3 +/- 33.6	50.8 .11	.001722	.001815	.01
1400	1.2	0	2896.7 +/- 160.4	49 1.2	.001661	.000284	.08

TOTAL GAS AGE = 612.9 Ma

J = .002227

ERROR ESTIMATES AT ONE SIGMA LEVEL

37/39,36/40 AND 39/40 Ar RATIOS ARE CORRECTED FOR INTERFERING ISOTOPES

% IIC - INTERFERING ISOTOPES CORRECTION

APPENDIX E. Continued.

E.3. CONVERSION OF ($^{37}\text{Ar}/^{39}\text{Ar}$) TO (Ca/K)

During irradiation of a sample, ^{37}Ar and ^{39}Ar are produced in amounts proportional to Ca and K, respectively. However, neutron flux spectra can differ for various reactors and a conversion factor is needed. This is achieved using the relationship $K = (\text{Ca}/\text{K}) / (^{37}\text{Ar}/^{39}\text{Ar})$. The reactor used in this study is the McMaster University nuclear reactor in Hamilton, Ontario.

On the basis of whole-rock bulk geochemical analyses, Stukas (1977) reported an average value of 2.3 ± 0.2 . Later work by Onstott and Peacock (1987) reported a coefficient of 1.82 ± 0.17 . Recent work using internal standards from the Ar laboratory at Dalhousie University suggest that a factor of 1.93 should be quoted (P.H. Reynolds, personal communication, 1994). This value is used in this study.

Knowing the irradiation parameter typical of the nuclear reactor used, the Ca/K ratios for each temperature increment can be calculated from the $^{37}\text{Ar}/^{39}\text{Ar}$ ratios. This can then be compared to the Ca/K of the phase in question as determined by electron microprobe analyses as an independent check on the data. In this study the $^{37}\text{Ar}/^{39}\text{Ar}$ ratios were used on the age spectrum plots, therefore the microprobe data was converted by the 1.93 factor and plotted on these diagrams.

APPENDIX E: Continued.

E.4.1. LOCATION AND DETAILED DESCRIPTION OF U-Pb SAMPLES*Sample NB92-9012 - Fairville Granite (Wardle, 1978)*

Location: long W = 66°06'19" lat N = 45°15'40"

Description: Coarse-grained, unfoliated, hypidiomorphic, inequigranular biotite monzogranite. Sample comprises plagioclase (37%), quartz (29%), K-feldspar (24%), biotite (7%), and hornblende (2%). Accessory minerals include apatite, zircon, and opaque minerals (1%). No titanite. Plagioclase (<5 mm) forms subhedral, zoned grains of oligoclase to andesine (An₂₅₋₃₅) partially altered to sericite. K-feldspar (<10 mm) is euhedral to subhedral and commonly comprises microperthite microcline. Quartz (<5 mm) exhibits undulose extinction and is interstitial. Myrmekite is common along plagioclase-K-feldspar contacts. Pleochroic (green to brown) biotite (2 mm) is interstitial, extensively chloritized with inclusions of small epidote and apatite grains and lens-shaped unstrained muscovite. Euhedral hornblende (<5 mm) forms entirely chloritized discrete grains with numerous inclusions of opaque minerals.

Age: Lower intercept U-Pb zircon age of 548 ± 2 Ma; upper intercept U-Pb zircon age of 1997 ± 260/-215 Ma.

Sample NB92-9010 - Ludgate Lake Granodiorite (White and Barr, 1991)

Location: long W = 66°13'56" lat N = 45°12'02"

Description: Medium-grained, unfoliated, hypidiomorphic, inequigranular biotite granodiorite. Sample comprises plagioclase (53%), quartz (27%), K-feldspar (9%), biotite (7%), and hornblende (3%). Accessory minerals include apatite, zircon, titanite, and opaque minerals (1%). Plagioclase (<5 mm) forms subhedral, zoned grains of oligoclase to andesine (An₂₅₋₃₅) partially to entirely altered to sericite and saussurite. Commonly rimmed by thin, unaltered albite.

Quartz (<4 mm) is rounded with embayed and serrated grain margins and exhibits undulose extinction. K-feldspar (3 mm) is microperthite and is interstitial. Pleochroic (green to brown) biotite (<2 mm) is extensively chloritized with inclusions of epidote and quartz grains, opaque minerals, and lens-shaped unstrained muscovite. Pleochroic (light to dark green), commonly twinned hornblende are partially altered to chlorite and form laths (<4 mm) and fine-grained aggregates associated with biotite, apatite and opaque minerals. Titanite is commonly twinned and is either interstitial or forms small laths (<2 mm).

Age: Upper intercept U-Pb zircon and titanite age of 546 ± 2 Ma.

Sample CW89-509A - Rockwood Park Granodiorite (White et al. 1990)

Location: long W = 66°04'53" lat N = 45°17'00"

Description: Medium- to coarse-grained, foliated, hypidiomorphic, inequigranular hornblende-biotite granodiorite. Sample comprises plagioclase (44), quartz (31%), K-feldspar (9%), biotite (9%), and hornblende (7%). Accessory minerals include apatite, zircon, titanite, and opaque minerals (1%). Plagioclase forms large (5 mm), weakly aligned euhedral to subhedral zoned grains of andesine (An₃₅) partially altered to sericite and saussurite. Quartz (<5 mm) and microcline are interstitial to plagioclase. Pleochroic (light to dark brown) biotite (<4 mm) is commonly inclusion-free and locally chloritized along cleavage planes. Light to dark green hornblende form euhedral, twinned laths (5 mm) that are aligned parallel to foliation and contain inclusions of opaque minerals, quartz, and rare altered plagioclase. Hornblende cleavage planes are locally partially replaced by chlorite. Euhedral titanite (2 mm) are located at grain boundaries between hornblende and other minerals.

Age: Concordant U-Pb zircon and titanite age of 538 ± 1 Ma.

Sample CW88-246 - French Village Quartz Diorite (White et al. 1990)

Location: long W = 65°57'47" lat N = 45°22'34"

Description: Medium- to coarse-grained, unfoliated, subporphyritic quartz diorite. Sample comprises plagioclase (47%), quartz (8%), hornblende (39%), and biotite (4%). Accessory minerals include apatite, zircon, and opaque minerals (2%). Plagioclase forms subhedral stubby laths (2.0-2.5 mm) of weakly zoned andesine to labradorite (An₅₀) variably altered to sericite and saussurite. These grains are set in a fine-grained (<1 mm) matrix of interlocking, unaltered, subhedral plagioclase. Quartz forms minor rounded grains (<0.5 mm) that exhibit undulose extinction. Large (1 cm) euhedral hornblende are pleochroic (green to light yellow-green), twinned and optically zoned. Cores contain very small (<0.1) inclusions of opaque minerals, biotite, apatite, and epidote. The rims are mottled, relatively inclusion-free with the exception of rare altered plagioclase grains and biotite. Smaller (<2 mm) grains are untwinned and inclusion-free. Pleochroic (light green to brown) biotite is chloritized along grain margins and cleavage planes with inclusions of small epidote and lens-shaped unstrained muscovite.

Age: Concordant U-Pb zircon age of 537 ± 2 Ma.

Sample CW88-181A - Orthogneiss = (MLNB-726 of Bevier et al. 1990)

Location: long W = 66°01'59" lat N = 45°18'52"

Description: Strongly foliated, relatively homogeneous tonalitic orthogneiss consisting of plagioclase (An₃₀₋₃₅) (41%), quartz (39%), K-feldspar (4%), and biotite (15%). Accessory minerals include apatite, zircon, titanite, and opaque minerals (2%). Gneissic layering is defined by alternation biotite-rich and quartzofeldspathic layers. Weak mineral lineation defined by elongate quartz and feldspar and quartz aggregates. Plagioclase (<2 mm) (partially sericitized and saussuritized), quartz (1 mm), and microcline (<3 mm) form, xenoblastic and poikiloblastic grains of with numerous inclusions of rounded quartz

and biotite in the plagioclase. Pleochroic (light to dark brown), subidioblastic biotite (<1 mm) is locally replaced by chlorite and epidote. Titanite occur as inclusions in the biotite.

Age: Upper intercept U-Pb zircon age of 605 ± 3 Ma. Pb/Pb titanite age of 564 ± 6 Ma.

Sample CW88-181B - Migmatitic Paragneiss = (MLNB-727 of Bevier et al. 1990)

Location: long W = $66^{\circ}02'03''$ lat N = $45^{\circ}18'54''$

Description: Fine- to medium-grained migmatitic paragneiss with a moderately well developed banding defined by thin (2-5 mm) alternating biotite-rich and quartzofeldspathic layers consisting of plagioclase (An₃₀) (35%), quartz (35%), biotite (25%), and K-feldspar and cordierite (<5%). Accessory minerals include apatite, titanite, zircon, and opaque minerals. Concordant leucosome bands (up to 10 mm wide) consist of quartz (50%), plagioclase (40%), and minor K-feldspar (10%). Thin (< 5 mm) biotite-rich melanosome layers border leucosomes. Plagioclase (altered to sericite), quartz, cordierite, and K-feldspar are xenoblastic and locally poikilitic with inclusions of biotite and quartz. Subidioblastic biotite is replaced by chlorite and epidote. Myrmekite is common. Muscovite replaces K-feldspar, plagioclase cores, and cordierite.

Age: Youngest detrital zircon age of 641 ± 3.2 Ma.

Sample CW88-181C - Paragneiss = (MLNB-728 of Bevier et al. 1990)

Location: long W = $66^{\circ}02'07''$ lat N = $45^{\circ}18'54''$

Description: Fine- to medium-grained paragneiss with a well developed gneissic banding defined by thin (2-5 mm) alternating biotite-rich and quartzofeldspathic layers. Gneiss consists of plagioclase (An₃₅) (35%), quartz (35%), biotite (20%), and K-feldspar and cordierite (<10%). Accessory minerals include apatite, titanite, zircon, and opaque minerals. Texturally similar to sample CW88-181B without the

leucosome and melanosome layers.

Age: Youngest detrital zircon age of 943 ± 3 Ma.

E.4.2. LOCATION AND DETAILED DESCRIPTION OF $^{40}\text{Ar}/^{39}\text{Ar}$ SAMPLES

A4.2.1. Plutonic Units

Sample CW88-169 - Renforth Pluton (Currie et al., 1981)

Location: long W = $65^{\circ}58'21''$ lat N = $45^{\circ}23'21''$

Description: Medium-grained, unfoliated, hypidiomorphic, inequigranular hornblende tonalite. Sample comprises plagioclase (57%), quartz (23%), hornblende (13%), biotite (4%), and K-feldspar (2%). Accessory minerals include apatite, titanite, zircon, and opaque minerals (1%). Plagioclase (<4 mm) forms subhedral, moderately zoned grains of andesine (An₄₅) partially altered to sericite. K-feldspar (<2 mm) is anhedral, interstitial, and microcline. Quartz (2 mm) is subhedral to anhedral. Hornblende (<3 mm) is typically anhedral, green to green-brown, with inclusions opaque minerals and biotite and plagioclase near the rims. However, larger euhedral hornblende (5 mm) form entirely chloritized grains with numerous inclusions of opaque minerals. Myrmekite is common along plagioclase-K-feldspar contacts. Brown biotite (<2 mm) is subhedral and chloritized with inclusions of small epidote and apatite grains and lens-shaped unstrained muscovite.

Age: $^{40}\text{Ar}/^{39}\text{Ar}$ hornblende age of 511 ± 5 Ma

Sample CW88-246 - French Village Quartz Diorite

Location: long W = $65^{\circ}57'47''$ lat N = $45^{\circ}22'34''$

Description: Same as U-Pb sample CW88-246

Age: $^{40}\text{Ar}/^{39}\text{Ar}$ hornblende age of 540 ± 5 Ma.

Sample CW89-509A - Rockwood Park Granodiorite

Location: long W = 66°04'53" lat N = 45°17'00"

Description: Same as U-Pb sample CW89-509A

Age: $^{40}\text{Ar}/^{39}\text{Ar}$ hornblende age of 538 ± 5 Ma.

$^{40}\text{Ar}/^{39}\text{Ar}$ biotite plateau age of 511 ± 3 Ma.

Sample CW89-611 - Fairville Granite

Location: long W = 66°06'02" lat N = 45°15'55"

Description: Coarse-grained, unfoliated, hypidiomorphic, inequigranular hornblende monzogranite. Sample comprises plagioclase (38%), quartz (25%), K-feldspar (23%), hornblende (9%), and biotite (4%). Accessory minerals include apatite, zircon, titanite, and opaque minerals (1%). Plagioclase (5 mm) forms subhedral, zoned grains of andesine (An_{35}) with rare albite rims partially altered to sericite. K-feldspar (<10 mm) is euhedral to subhedral and commonly comprises perthitic microcline. Quartz (<5 mm) exhibits undulose extinction and is interstitial. Myrmekite is common along plagioclase-K-feldspar contacts. Green to brown biotite is interstitial, partially chloritized. Euhedral green hornblende (<5 mm) forms partially chloritized discrete grains with numerous inclusions of opaque minerals.

Age: $^{40}\text{Ar}/^{39}\text{Ar}$ hornblende age of 536 ± 3 Ma.

Sample NB91-8597 - Shadow Lake Granodiorite "enclave"

Location: long W = 66°20'39" lat N = 45°11'22"

Description: Medium-grained, unfoliated, allotriomorphic, inequigranular quartz diorite. Sample comprises plagioclase (52%), quartz (13%), hornblende (24%), and biotite (11%). Accessory minerals include apatite, titanite, zircon, and opaque minerals (<1%). Plagioclase forms typically unaltered subhedral to anhedral laths (2.0-2.5 mm) of patchy zoned labradorite (An_{50}). Quartz forms minor interstitial grains (<0.5 mm) that exhibit undulose extinction.

Anhedral hornblende (0.5 mm) are pleochroic (green to light blue), twinned, relatively inclusion-free with mottled zoning. Pleochroic brown biotite is chloritized along grain margins and cleavage planes.

Age: $^{40}\text{Ar}/^{39}\text{Ar}$ hornblende age of 527 ± 5 Ma.

Sample NB91-8599B - Shadow Lake Granodiorite

Location: long W = $66^{\circ}22'45''$ lat N = $45^{\circ}10'49''$

Description: Medium-grained, hypidiomorphic, inequigranular hornblende granodiorite. Sample comprises plagioclase (52%), quartz (12%), K-feldspar (4%), biotite (11%), and hornblende (19%). Accessory minerals include apatite, zircon, titanite, and opaque minerals (<1%). Plagioclase forms small (3 mm), euhedral to subhedral zoned grains of andesine (An_{35}) partially altered to sericite and saussurite. Quartz (<5 mm) and microcline are interstitial to plagioclase. Pleochroic green biotite (<4 mm) is commonly inclusion-free and locally chloritized along cleavage planes. Light to dark green hornblende form euhedral, twinned laths (5 mm) that contain inclusions of opaque minerals, quartz, and rare altered plagioclase. Hornblende cleavage planes are locally partially replaced by chlorite.

Age: $^{40}\text{Ar}/^{39}\text{Ar}$ hornblende age of 543 ± 5 Ma.

A4.2.2. Green Head Group

Sample CW88-204 - Marble

Location: long W = $65^{\circ}53'09''$ lat N = $45^{\circ}26'22''$

Description: Medium-grained, layered, marble. Sample comprises calcite (95%), phlogopite (3%), tremolite (<1%), and diopside (<1%). Rounded quartz, plagioclase, and microcline are rare. Accessory mineral include titanite, apatite, tourmaline, and opaque minerals (<1%). Calcite (<4 mm) is slightly elongate parallel to layering and typically has serrated boundaries. Phlogopite (<1 mm) is unaltered, inclusion-free, idioblastic, and elongate parallel to layering. Tremolite and

diopside (<0.5 mm) are subidioblastic to xenoblastic and scattered throughout the thin section. Tremolite locally replaces the diopside rims. Titanite, apatite, and tourmaline are idioblastic and typically strongly zoned.

Age: $^{40}\text{Ar}/^{39}\text{Ar}$ phlogopite age of 538 ± 6 Ma.

Sample CW90-764 - Marble

Location: long W = $65^{\circ}52'16''$ lat N = $45^{\circ}27'54''$

Description: Coarse-grained, weakly layered, granoblastic marble. Sample comprises calcite (95%), phlogopite (2%), tremolite (<1%), diopside (<1%), and forsterite (<1%). Rounded quartz, plagioclase, and microcline are rare. Accessory mineral include titanite, apatite, and opaque minerals (<1%). Calcite (5 mm) is typically granoblastic with locally developed serrated boundaries. Phlogopite (<1 mm) is relatively unaltered, idioblastic, inclusion-free, and parallel to layering. Locally it is partially chloritized near tremolite. Tremolite and diopside (<0.5 mm) are subidioblastic to xenoblastic, locally pseudomorphed by chlorite and associated epidote. Rounded forsterite is entirely replaced by serpentine and/or chlorite. Titanite and apatite are idioblastic.

Age: $^{40}\text{Ar}/^{39}\text{Ar}$ phlogopite age of 530 ± 5 Ma.

Sample CW90-767 - Mica schist

Location: long W = $65^{\circ}52'34''$ lat N = $45^{\circ}27'48''$

Description: Medium-grained, strongly foliated mica schist. Sample comprises muscovite (30%), quartz (<35%), feldspar (<35%), and cordierite (<1%). Accessory minerals include opaque minerals and apatite. Foliation is locally strongly crenulated. Muscovite (<4 mm) is unaltered, idioblastic, and inclusion-free. Quartz and feldspar (<0.5 mm) form granoblastic layers and pods parallel to foliation. Cordierite (<0.5 mm) is xenoblastic and skeletal and entirely replaced by sericite and rare coarse muscovite. It is interpreted to be the

result of contact metamorphism.

Age: $^{40}\text{Ar}/^{39}\text{Ar}$ muscovite age of 507 ± 5 Ma.

Sample CW90-812 - Marble

Location: long W = $66^{\circ}01'07''$ lat N = $45^{\circ}20'47''$

Description: Medium-to fine-grained, strongly layered, marble.

Sample comprises calcite (95%), phlogopite (4%), and tremolite (<1%). Accessory mineral include titanite, apatite, and opaque minerals (<1%). Calcite (2 mm) is typically granoblastic in the medium-grained layers but is slightly elongate with serrated boundaries in the coarse-grained layers (<4 mm). Phlogopite (<1 mm) is relatively unaltered, idioblastic to subidioblastic, inclusion-free, and elongate parallel to layering. Tremolite (<2 mm) is subidioblastic to xenoblastic and is locally replaced by chlorite. Titanite and apatite are idioblastic. Opaque minerals are cubic.

Age: $^{40}\text{Ar}/^{39}\text{Ar}$ phlogopite age of 515 ± 5 Ma.

A4.2.3 Brookville Gneiss

Sample CW89-598C - Marble

Location: long W = $66^{\circ}01'59''$ lat N = $45^{\circ}18'52''$

Description: Coarse-grained granoblastic marble. Sample comprises calcite and dolomite (95%), phlogopite (1%), tremolite (1%), forsterite (1%), and diopside (1%). Accessory minerals include titanite, apatite, tourmaline, and opaque minerals (1%). Calcite and dolomite (5 mm) are granoblastic with moderately developed serrated boundaries. Phlogopite (<2 mm) is randomly oriented, idioblastic, inclusion-free, and typically unaltered. Tremolite (2 mm) and diopside (<1 mm) are subidioblastic to xenoblastic and commonly replaced by chlorite and associated epidote. Forsterite (<0.5 mm) is partially pseudomorphed by serpentine.

Age: $^{40}\text{Ar}/^{39}\text{Ar}$ phlogopite age of 541 ± 5 Ma.

Sample CW89-629C - Marble

Location: long W = 66°01'38" lat N = 45°19'25"

Description: Same as for sample CW89-598C, although diopside and forsterite is rare and completely replaced by serpentine and/or chlorite. Rounded anorthite (<0.5 mm) common.

Age: $^{40}\text{Ar}/^{39}\text{Ar}$ phlogopite age of 534 ± 5 Ma.

A4.2.4. Hammondvale Metamorphic Unit**Sample NB87-4090 - Mica schist**

Location: long W = 65°28'32" lat N = 45°34'45"

Description: Coarse-grained, well foliated mica schist. Sample comprises muscovite (40%), albite (40%), quartz (<15%), garnet (<5%), orthoclase (<1%), and biotite (<1%). Accessory minerals include opaque minerals, tourmaline, apatite, titanite, epidote, and zircon. Albite and garnet form large (<10 mm) subidioblastic porphyroblasts with straight to curved inclusion trails defined by elongate quartz, tourmaline, epidote, opaque minerals, muscovite, chlorite, and biotite. Coarse muscovite (<10 mm) defines the main external schistosity and is commonly draped around porphyroblasts. It is relatively inclusion-free and unaltered. Orthoclase forms small patches on albite, especially near pressure shadows. It also occurs as small (<5 mm) porphyroblasts in the matrix with inclusions of elongate quartz. Biotite (<2 mm) is associated with the matrix muscovite and inclusions in albite. It is typically partially altered to chlorite.

Age: $^{40}\text{Ar}/^{39}\text{Ar}$ muscovite age of 617 ± 6 Ma.

Sample CW88-101 - Marble

Location: long W = 65°29'03" lat N = 45°35'20"

Description: Medium-grained muscovite-bearing marble. Sample comprises muscovite (50%) and calcite (50%), with accessory apatite, titanite, tourmaline, and opaque minerals (<1%). Muscovite (5 mm)

defines the foliation and is locally crenulated. It is typically idioblastic, unaltered, inclusion-free, and locally intensely crenulated. Calcite (<5 mm) is locally granoblastic with serrated boundaries. With the exception of the opaque minerals all accessory minerals are idioblastic. Apatite and tourmaline are typically well zoned.

Age: $^{40}\text{Ar}/^{39}\text{Ar}$ muscovite age of 613 ± 6 Ma.

Sample CW88-115A - Mica schist

Location: long W = $65^{\circ}29'17''$ lat N = $45^{\circ}33'53''$

Description: Same as for sample NB87-4090, although this sample is more deformed with well developed asymmetric albite porphyroblasts and quartz ribbons.

Age: $^{40}\text{Ar}/^{39}\text{Ar}$ muscovite age of 603 ± 6 Ma.

REFERENCES

- Abdel-Rahman, A.M. 1994. Nature of biotites from alkaline, calc-alkaline, and peraluminous magmas. *Journal of Petrology*, 35: 525-541.
- Alcock, F.J. 1938. Geology of the Saint John Region, New Brunswick. Geological Survey of Canada, Memoir 216, 65 p.
- Alcock, F.J. 1941. The geology of Long Reach, Kings County, New Brunswick. The Royal Society of Canada, Proceedings and Transactions, Third Series, 35: 17-21.
- Alcock, F.J. 1948. Problems of New Brunswick Geology - Presidential Address. The Royal Society of Canada, Proceedings and Transactions, Third Series, 42: 1-15.
- Alcock, F.J. 1959. Geology of the Musquash area; Charlotte, King's and Saint John counties, New Brunswick. Geological Survey of Canada, Map 1084A. Scale 1 inch = 1 mile.
- Alcock, F.J. and Perry, S.C. 1960. St. George. Geological Survey of Canada, Map 1094A. Scale 1 inch = 1 mile.
- Ami, H.M. 1900. On the geology of the principle cities in Eastern Canada. The Royal Society of Canada, Proceedings and Transactions, Second Series, 6: 125-171.
- Anderson, J.L. 1980. Mineral equilibria and crystallization conditions in the late Precambrian Wolf River rapakivi massif, Winsconsin. *American Journal of Science*, 280; 298-332.
- Anderson, J.L. and Smith, D.R. 1995. The effects of temperature and f_{O_2} on the Al-in-hornblende barometer. *American Mineralogist*, 80: 549-559.
- Anovitz, L.M. and Essene, E.J. 1987. Phase equilibria in the system $CaCO_3$ - $MgCO_3$ - $FeCO_3$. *Journal of Petrology*, 28: 389-414.
- Arculus, R.J. 1987. The significance of source versus process in the tectonic controls of magma genesis. In *Tectonic controls on magma chemistry*. Edited by S.D. Weaver and R.W. Johnson. Elsevier, Amsterdam, pp. 1-12.
- Armitage, A.E. 1989. Geology and petrology of the crystalline rocks of the Whycomagh area, Cape Breton Island, Nova Scotia. Unpublished B.Sc. thesis, Acadia University, Wolfville, Nova Scotia, 120 p.
- Ayuso, R.A., Barr, S.M., and Longstaffe, F.J. in press. Pb and O isotopic constraints on the source of granite rocks from Cape Breton Island, Nova Scotia. *American Journal of Science*.
- Bailey, L.W. 1865. Geology of New Brunswick. *The Canadian Naturalist and Geologist*, 2: 232-239, 314-318.
- Bailey, L.W. 1872. Report of Progress of Geological Investigations in New Brunswick. Geological Survey of Canada, Report of Progress for 1871-72, pp. 142-145.
- Bailey, L.W. 1879. Report on the Pre-Silurian (Huronian) and Cambrian, or Primordial Silurian Rocks. Geological Survey of Canada, Report of Progress for 1877-78, Part DD, pp. 1-34.
- Bailey, L.W. 1881. On the progress of geological investigation in New Brunswick, 1870-1880. *The American Association for the Advancement of Science*, 29: 415-421.
- Bailey, L.W. 1890a. On some relations between the geology of Eastern Maine and New Brunswick. *Royal Society of Canada, Proceedings and Transactions*, 7: 57-68.
- Bailey, L.W. 1890b. Presidential Address: On the progress of geological investigations in New Brunswick. *Royal Society of Canada, Proceedings and Transactions*, 7: 3-17.
- Bailey, L.W. 1899. The Mineral Resources of the Province of New Brunswick. Geological Survey of Canada Annual Report for 1897 (New Series), Report M, pp. 1-128.
- Bailey, L.W. 1904. The volcanic rocks of New Brunswick. *Royal Society of Canada, Proceedings and Transactions, Second Series*, 10: 123-138.

- Bailey, L.W. and Matthew, G.F. 1872. Preliminary report on the geology of southern New Brunswick. Geological Survey of Canada, Report of Progress for 1870-71, pp. 13-240.
- Bailey, L.W. and Matthew, G.F. 1919. Some problems of New Brunswick geology. The Royal Society of Canada, Proceedings and Transactions, Third Series, 12: 105-130.
- Bailey, L.W., Matthew, G.F., and Ellis, R.W. 1880. Report on the geology of southern New Brunswick, embracing the counties of Charlotte, Sunbury, Queens, Kings, Saint John and Albert. Geological Survey of Canada, Report of Progress for 1878-79, Part D, pp. 1-26.
- Bailey, L.W., Matthew, G.F., and Hartt, C.F. 1865. Observations on the geology of southern New Brunswick. Fredericton, New Brunswick.
- Bailey, R.H., Skehan, J.W., Dreier, R.B., and Webster, M.J. 1989. Olistostromes of the Avalonian terrane of southeastern New England. Geological Society of America Special Paper 228, pp. 93-112.
- Barbarin, B. and Didier, J. 1992. Genesis and evolution of mafic microgranular enclaves through various types of interaction between coexisting felsic and mafic magmas. Transactions of the Royal Society of Edinburgh: Earth Sciences, 83: 145-153.
- Barbey, P. 1991. Restite in migmatites and autochthonous granites: their main features and their genesis. In Enclaves and Granite Petrology. Edited by J. Didier and B. Barbarian. Developments in Petrography 13. Elsevier, Amsterdam, pp. 479-492.
- Barr, S.M. 1990. Granitoid rocks and terrane characterization: an example from the northern Appalachian Orogen. Geological Journal, 25: 295-304.
- Barr, S.M. and Hegner, E. 1992. Nd isotopic compositions of felsic igneous rocks in Cape Breton Island, Nova Scotia. Canadian Journal of Earth Sciences, 29: 650-657.
- Barr, S.M. and Kerr, A. in press. Late Precambrian plutons in the Avalon terrane of New Brunswick, Nova Scotia, and Newfoundland. In Magmatism in the Appalachian Orogen. Edited by A.K. Sinha, J. Whalen, and J. Hogan. Geological Society of America Memoir.
- Barr, S.M. and Raeside, R.P. 1986. Pre-Carboniferous tectonostratigraphic subdivisions of Cape Breton Island. Maritime Sediments and Atlantic Geology, 22: 252-263.
- Barr, S.M. and Raeside, R.P. 1989. Tectonostratigraphic terranes in Cape Breton Island, Nova Scotia: implications for the configuration of the northern Appalachian orogen. Geology, 17: 822-825.
- Barr, S.M. and White, C.E. 1988. Petrochemistry of contrasting Late Precambrian volcanic and plutonic associations, Caledonian Highlands, southern New Brunswick. Maritime Sediments and Atlantic Geology, 24: 353-372.
- Barr, S.M. and White, C.E. 1989. Re-interpretation of Precambrian stratigraphy in southern New Brunswick. In Project Summaries for 1989, Fourteenth Annual Review of Activities. Edited by S.A. Abbott. New Brunswick Department of Natural Resources and Energy, Minerals and Energy Division, Information Circular 89-2, pp. 182-189.
- Barr, S.M. and White, C.E. 1991a. Revised stratigraphy of the Avalon Terrane of southern New Brunswick. In Geology of the Coastal Lithotectonic Block and Neighboring Terranes, Eastern Maine and Southern New Brunswick. Edited by A. Ludman. Eighty-third New England Intercollegiate Geological Conference, pp. 1-12.
- Barr, S.M. and White, C.E. 1991b. Late Precambrian-Early Cambrian geology, Saint John-St. Martins area, southern New Brunswick. Geological Survey of Canada, Open File 2353. Scale 1:50,000.
- Barr, S.M. and White, C.E. 1994. Contrasts in Late Precambrian-Paleozoic magmatism between Avalon Terrane *sensu stricto* and other Gondwanan terranes in New Brunswick and Cape Breton Island. Northeastern Geological Society of America 29th Annual Meeting, Abstracts with Programs, 29: 5.

- Barr, S.M. and White, C.E. 1996. Tectonic setting of Avalonian volcanic and plutonic rocks in the Caledonian Highlands, southern New Brunswick. *Canadian Journal of Earth Science*, 33:
- Barr, S.M. and White, C.E. In press. Contrasts in late Precambrian-early Paleozoic tectonothermal history between Avalon Composite Terrane *sensu stricto* and other peri-Gondwanan terranes in southern New Brunswick and Cape Breton Island, Canada. In *Avalonian and related peri-Gondwanan terranes of the Circum-North Atlantic*. Edited by R.D. Nance and M.D. Thompson. Geological Society of America Special Paper.
- Barr, S.M., White, C.E., and Bevier, M.L. 1990a. Contrasting petrochemistry and age of plutonic rocks in the Saint John area and Caledonian Highlands Kings and Saint John counties, southern New Brunswick. In *Project Summaries for 1990, Fifteenth Annual Review of Activities*. Edited by S.A. Abbott. New Brunswick Department of Natural Resources and Energy, Minerals and Energy Division, Information Circular 90-2, pp. 178-186.
- Barr, S.M., Dunning, G.R., Raeside, R.P., and Jamieson, R.A. 1990b. Contrasting U-Pb ages from plutons in the Bras d'Or and Mira terranes of Cape Breton Island, Nova Scotia. *Canadian Journal of Earth Sciences*, 27: 1200-1208.
- Barr, S.M., Bevier, M.L., White, C.E., and Doig, R. 1994. Magmatic evolution of the Caledonia (Avalon) terrane of southern New Brunswick based on U-Pb (zircon) geochronology. In *Current Research*, compiled and edited by S.A. Abbott, New Brunswick Department of Natural Resources, Information Circular 93-1, pp. 4-11.
- Barr, S.M., Bevier, M.L., White, C.E., and Doig, R. 1994. Magmatic history of the Avalon terrane of southern New Brunswick, Canada, based on U-Pb (zircon) geochronology. *Journal of Geology*, 102: 399-409.
- Barr, S.M., White, C.E., McLeod, M.J., and Johnson, S.C. 1995. Characterization of terranes in southern New Brunswick and correlative terranes in Nova Scotia and Newfoundland. Abstract in *Geological Society of America, Northeastern Section, Abstracts with Programs*, 27: 28.
- Beach, A. 1980. Retrogressive metamorphic processes in shear zones with special reference to the Lewisian Complex. *Journal of Structural Geology*, 2: 257-265.
- Belt, E.S. 1968. Post-Acadian rifts and related fabrics, eastern Canada. In *Studies in Appalachian Geology-Northern and Maritime*. Edited by E-an Zen. New York Interscience, pp. 95-113.
- Belyea, H.R. 1939. The geology of the Musquash area, New Brunswick. Unpublished Ph.D. Thesis, Northwestern University, Evanston, Illinois, 189 p.
- Belyea, H.R. 1944. Plutonic rocks of the Musquash area, New Brunswick. *Acadian Naturalist*, 1: 87-102.
- Belyea, H.R. 1945. Plutonic rocks of the Musquash area, New Brunswick - II. *Acadian Naturalist*, 2: 18-27.
- Berger, G.W. 1975. $^{40}\text{Ar}/^{39}\text{Ar}$ step heating of thermally overprinted biotite, hornblende, and potassium feldspar from Eldora, Colorado. *Earth and Planetary Science Letters*, 26: 387-408.
- Berman, R.G. 1988. Internally-consistent thermodynamic data for minerals in the system $\text{Na}_2\text{O}-\text{K}_2\text{O}-\text{CaO}-\text{MgO}-\text{FeO}-\text{Fe}_2\text{O}_3-\text{Al}_2\text{O}_3-\text{SiO}_2-\text{TiO}_2-\text{H}_2\text{O}-\text{CO}_2$. *Journal of Petrology*, 29: 445-522.
- Berman, R.G. 1990. Mixing properties of Ca-Mg-Fe-Mn garnets. *American Mineralogist*, 78: 328-244.
- Berman, R.G. 1991. Thermobarometry using multi-equilibrium calculations: a new technique, with petrological applications. *Canadian Mineralogist*, 29: 833-855.
- Bevier, M.L. and Barr, S.M. 1990. U-Pb age constraints on the stratigraphy and tectonic history of the Avalon terrane, New Brunswick, Canada. *Journal of Geology*, 98: 53-63.

- Bevier, M.L., White, C.E., and Barr, S.M. 1990. Late Precambrian U-Pb ages for the Brookville Gneiss, southern New Brunswick. *Journal of Geology*, 98: 955-965.
- Bevier, M.L., White, C.E., and Barr, S.M. 1991. A new U-Pb date for the French Village quartz diorite, Saint John County, southern New Brunswick. In *Project Summaries for 1991, Sixteenth Annual Review of Activities*. Edited by S.A. Abbott. New Brunswick Department of Natural Resources and Energy, Minerals and Energy Division, Information Circular 91-2, pp. 195-198.
- Bevier, M.L., Barr, S.M., White, C.E., and Macdonald, A.S. 1993. U-Pb geochronological constraints on the volcanic evolution of the Mira (Avalon) terrane, southeastern Cape Breton Island. *Canadian Journal of Earth Sciences*, 30: 1-10.
- Blundy, J.D. and Holland, T.J.B. 1990. Calcic amphibole equilibria and a new amphibole-plagioclase geothermometer. *Contributions to Mineralogy and Petrology*, 104: 208-224.
- Bouma, A.H. 1962. *Sedimentology of Some Flysch Deposits*. Elsevier, Amsterdam, 168 p.
- Boyle, D.R. and Stirling, J.A.R. 1994. Geochemistry, mineralogy, and possible origin of the Coverdale Ti-P-ferrogabbro complex, New Brunswick. In *Nineteenth Annual Review of Activities*. Edited by S.A.A. Merlini. New Brunswick Department of Natural Resources and Energy, Minerals and Energy Division, Miscellaneous Report 14, pp. 4.
- Bradley, D.C. 1982. Subsidence in late Paleozoic basins in the Northern Appalachians. *Tectonics*, 1: 107-123.
- Brown, R.L. 1972. Appalachian structural style in southern New Brunswick. *Canadian Journal of Earth Sciences*, 9: 43-53.
- Brown, R.L. and Helmstaedt, H. 1970. Deformation history in part of the Lubec-Belleisle zone of southern New Brunswick. *Canadian Journal of Earth Sciences*, 7: 748-767.
- Butt, K.A. 1976. Genesis of granitic stocks in southwestern New Brunswick. Unpublished Ph.D. Thesis, University of New Brunswick, Fredericton, New Brunswick, 235 p.
- Campbell, J.E. 1990. Geology of the eastern Creignish Hills. Unpublished M.Sc. thesis, Acadia University, Wolfville, Nova Scotia, 164 p.
- Cas, R.A.F. and Wright, J.V. 1987. *Volcanic successions: modern and ancient*. Allen and Unwin, London, 528 p.
- Casseday, R.P., R.D. Nance, Doig, R., Dallmeyer, R.D., and Murphy, J.B. 1991. Earliest Silurian age for the bimodal Kingston dike complex: Evidence for sinistral accretion of the Avalon Composite Terrane in southern New Brunswick, Canada. *Northeastern and Southeastern Geological Society of America 26th Annual Meeting, Abstracts with Programs*, 23: 15.
- Caudill, M.R. 1989. Sedimentology of the Carboniferous Balls Lake and Lancaster formations, Saint John Harbour, southern New Brunswick. Unpublished M.Sc. Thesis, Ohio University, Athens, Ohio, 236 p.
- Caudill, M.R. and Nance, R.D. 1986. Variscan tectono-stratigraphy of the Mispec Group, southern New Brunswick: stratigraphy and depositional setting. In *Current Research, Part A, Geological Survey of Canada, Paper 86-1A*, pp. 343-350.
- Cawthorn, R.G., Strong, D.F., and Brown, P.A. 1976. Origin of corundum-normative intrusive and extrusive magmas. *Nature*, 259: 102-104.
- Chappell, B.W. and White, A.J.R. 1974. Two contrasting granite types. *Pacific Geology*, 8: 173-174.
- Chappell, B.W. and White, A.J.R. 1991. Restite enclaves and the restite model. In *Enclaves and Granite Petrology*. Edited by J. Didier and B. Barbarian. *Developments in Petrography* 13. Elsevier, Amsterdam, pp. 375-381.
- Cook, S.J. and Bowman, J.R. 1994. Contact metamorphism surrounding the Alta stock: thermal constraints and evidence of advective heat transport from calcite and dolomite geothermometry. *American Mineralogist*, 79: 513-525.

- Cormier, R.F. 1969. Radiometric dating of the Coldbrook Group of southern New Brunswick, Canada. *Canadian Journal of Earth Sciences*, 6: 393-398.
- Cullers, R.L., Griffin, T., Bickford, M.E., and Anderson, J.L. 1992. Origin and chemical evolution of the 1360 Ma San Isabel batholith, Wet Mountains, Colorado: a mid-crustal granite of anorogenic affinities. *Geological Society of America Bulletin*, 104: 316-328.
- Cumming, C.L. 1916. The igneous rocks of Saint John, New Brunswick. Unpublished Ph.D. Thesis, Princeton University, Princeton, New Jersey, 344 p.
- Currie, K.L. 1983. Repeated basement reactivation in the northeastern Appalachians. *Geological Journal*, 18: 223-239.
- Currie, K.L. 1984. A reconsideration of some geological relations near Saint John, New Brunswick. In *Current Research, Part A, Geological Survey of Canada, Paper 84-1A*, pp. 193-201.
- Currie, K.L. 1985. Geology of the Saint John region, New Brunswick. Geological Survey of Canada, Open File 1027. Scale 1:50,000.
- Currie, K.L. 1986a. The stratigraphy and structure of the Avalonian terrane around Saint John, New Brunswick. *Maritime Sediments and Atlantic Geology*, 22: 278-295.
- Currie, K.L. 1986b. The boundaries of the Avalon tectono-stratigraphic zones, Musquash Harbour-Loch Alva region, southern New Brunswick. In *Current Research, Part A, Geological Survey of Canada, Paper 86-1A*, pp. 333-341.
- Currie, K.L. 1987a. Late Precambrian igneous activity and its tectonic implications, Musquash-Loch Alva region, southern New Brunswick. In *Current Research, Part A, Geological Survey of Canada, Paper 87-1A*, pp. 663-671.
- Currie, K.L. 1987b. Geological map of the Musquash-Loch Alva region, southern New Brunswick. Geological Survey of Canada, Open File 1441. Scale 1:50,000.
- Currie, K.L. 1987c. The Avalon terrane around Saint John, New Brunswick and its deformed Carboniferous cover. *Geological Society of America, Centennial Field Guide, Northeastern Section*, pp. 403-408.
- Currie, K.L. 1988a. The western end of the Avalon zone in southern New Brunswick. *Maritime Sediments and Atlantic Geology*, 24: 339-352.
- Currie, K.L. 1988b. Saint George map area: the end of the Avalon zone in southern New Brunswick. In *Current Research, Part B, Geological Survey of Canada, Paper 88-1B*, pp. 9-16.
- Currie, K.L. 1989a. Geological map of the Saint John-Saint George region, southern New Brunswick. Geological Survey of Canada, Open File 1974. Scale 1:50,000.
- Currie, K.L. 1989b. Revised Late Precambrian stratigraphy near Saint John, New Brunswick. In *Current Research, Part B, Geological Survey of Canada, Paper 89-1B*, pp. 39-45.
- Currie, K.L. 1991. A note on the stratigraphy of the Martinon Formation, Saint John, New Brunswick. In *Current Research, Part D, Geological Survey of Canada, Paper 91-1D*, pp. 9-13.
- Currie, K.L. 1992. The "Lorneville Beds": a latest Precambrian sequence near Saint John, New Brunswick. In *Current Research, Part D, Geological Survey of Canada, Paper 92-1D*, pp. 35-43.
- Currie, K.L. and Hunt, P.A. 1991. Late Precambrian activity near Saint John, New Brunswick. In *Radiogenic Age and Isotopic Studies: Report 4, Geological Survey of Canada, Paper 90-2*, pp. 11-17.
- Currie, K.L. and Nance, R.D. 1983. A reconsideration of the Carboniferous rocks of Saint John, New Brunswick. In *Current Research, Part A, Geological Survey of Canada, Paper 83-1A*, pp. 29-36.
- Currie, K.L., Nance, R.D., Pajari, G.E., and Pickerill, R.K. 1981. Some aspects of the pre-Carboniferous geology of Saint John, New Brunswick. In *Current Research, Part A, Geological Survey of Canada, Paper 81-1A*, pp. 23-30.

- Dahl, P.S. 1994. Closing in or argon closure temperatures?: an extended "ionic porosity" model for thermochronometric minerals, with application to amphiboles. In Abstracts of the Eighth International Conference on Geochronology, Cosmochronology, and Isotope Geology. Edited by M.A. Lanphere, G.B. Dalrymple, and B.D. Turrin. U.S. Geological Survey Circular 1107, pp. 72.
- Dallmeyer, R.D. and Keppie, J.D. 1993. $^{40}\text{Ar}/^{39}\text{Ar}$ mineral ages from the southern Cape Breton Highlands and Creignish Hills, Cape Breton Island, Canada: evidence for a polyphase tectonothermal evolution. *Journal of Geology*, 101: 467-482.
- Dallmeyer, R.D. and Nance, R.D. 1989. $^{40}\text{Ar}/^{39}\text{Ar}$ mineral age record of polyphase tectonothermal activity in the Avalon Terrane of southern New Brunswick. In Geological Association of Canada and Mineralogical Association of Canada Program with Abstracts, 14: A126.
- Dallmeyer, R.D. and Nance, R.D. 1990. $^{40}\text{Ar}/^{39}\text{Ar}$ ages of detrital muscovite within early Paleozoic overstep sequences, Avalon composite terrane, southern New Brunswick: implications for extent of late Paleozoic tectonothermal overprint. *Canadian Journal of Earth Sciences*, 27: 1209-1214.
- Dallmeyer, R.D. and Nance, R.D. 1992. Tectonic implications of $^{40}\text{Ar}/^{39}\text{Ar}$ mineral ages from Late Precambrian-Cambrian plutons, Avalon Composite Terrane, southern New Brunswick, Canada. *Canadian Journal of Earth Sciences*, 29: 2445-2462.
- Dallmeyer, R.D., Doig, R., Nance, R.D., and Murphy, J.B. 1990. $^{40}\text{Ar}/^{39}\text{Ar}$ and U-Pb mineral ages from the Brookville Gneiss and Green Head Group: implications for terrane analysis and evolution of Avalonian "basement" in southern New Brunswick. *Atlantic Geology*, 26: 247-257.
- Dalrymple, G.B. and Lanphere, M.A. 1974. $^{40}\text{Ar}/^{39}\text{Ar}$ age spectra of some undisturbed terrestrial samples. *Geochemica et Cosmochimica Acta*, 38: 715-738.
- Davis, D.W. 1993. Report on U-Pb geochronology of metasediments in Nova Scotia (March, 1993). Unpublished report, Royal Ontario Museum, Toronto, Ontario, 8 p.
- Davis, D.W. 1994. Report on U-Pb geochronology of Avalonian rocks in Nova Scotia (March, 1994). Unpublished report, Royal Ontario Museum, Toronto, Ontario, 13 p.
- Dawson, J.W. 1855. *Acadian Geology: an Account of the Geological Structure and Mineral Resources of Nova Scotia and portions of the Neighbouring Provinces of British America*. Edinburgh, Scotland, 388 p.
- Dawson, J.W. 1861. On the Pre-Carboniferous flora of New Brunswick, Maine and Eastern Canada. *The Canadian Naturalist and Geologist and Proceedings of the Natural History Society of Montreal*, 6: 161-180.
- Dawson, J.W. 1862. On the flora of the Devonian Period in northeastern America. *Quarterly Journal of the Geological Society of London*, 18: 296-330.
- Dawson, J.W. 1868. *Acadian Geology; the Geological Structure, Organic Remains and Mineral Resources of Nova Scotia, New Brunswick and Prince Edward Island*, MacMillian and Co., London, 694 p.
- Dawson, J.W. 1878. Supplement to the second edition of *Acadian Geology*. In *The Geology of Nova Scotia, New Brunswick and Prince Edward Island, or Acadian Geology*, 4th Edition 1891, London, pp. 1-102.
- Dawson, J.W. 1891. Supplementary note to the 4th Edition. In *The Geology of Nova Scotia, New Brunswick and Prince Edward Island, or Acadian Geology*, 4th Edition 1891, London, pp.1-37.
- Deer, W.A., Howie, R.A., and Zussman, J. 1992. *An introduction to the rock-forming minerals*. Longman Scientific and Technical. Essex, England, 696 p.

- Deveau, K.A. 1989. Petrography of the Golden Grove Intrusive Suite in the area northeast of Saint John, New Brunswick. Unpublished B.Sc. thesis, Acadia University, Wolfville, Nova Scotia, 145 p.
- Dickson, W.L. 1983. Geology, geochemistry, and petrology of the Precambrian and Carboniferous igneous rocks between Saint John and Beaver Harbour, southern New Brunswick. Unpublished Ph.D. thesis, University of New Brunswick, Fredericton, New Brunswick, 409 p.
- Dodson, M.H. 1973. Closure temperature in cooling geochronological and petrological systems. *Contributions to Mineralogy and Petrology*, 40: 259-274.
- Doig, R., Nance, R.D., Murphy, J.B., and Casseday, R.P. 1990. Evidence for Silurian sinistral accretion of Avalon composite terrane in Canada. *Journal of the Geological Society, London*, 147: 927-930.
- Dunning, G.R. and O'Brien, S.J. 1989. Late Proterozoic-early Paleozoic crust in the Hermitage flexure, Newfoundland Appalachians: U-Pb ages and tectonic significance. *Geology*, 17: 548-551.
- Dostal, J. and McCutcheon, S.R. 1990. Geochemistry of Late Proterozoic basaltic rocks from southeastern New Brunswick, Canada. *Precambrian Research*, 47: 83-98.
- Dunning, G.R., Barr, S.M., Raeside, R.P., and Jamieson, R.A. 1990. U-Pb zircon, titanite, and monazite ages in the Bras d'Or and Aspy terranes of Cape Breton Island, Nova Scotia: implications for igneous and metamorphic history. *Geological Society of America Bulletin*, 102: 322-350.
- Eby, G.N. and Currie, K.L. 1993. Petrology and geochemistry of the Kingston Complex - a bimodal sheeted dyke suite in southern New Brunswick. *Atlantic Geology*, 29: 121-135.
- Ellis, D.J. and Obata, M. 1992. Migmatite and melt segregation at Cooma, New South Wales. *Transactions of the Royal Society of Edinburgh: Earth Sciences*, 83: 95-106.
- Ells, R.W. 1879. Report on the Pre-Silurian rocks of Albert, Eastern Kings and Saint John counties, southern New Brunswick. *Geological Survey of Canada, Report of Progress for 1877-78, Part D*, pp. 1-13.
- Ells, R.W. 1886. Report on the geological formations of eastern Albert and Westmoreland Counties in the northeast and of portions of Cumberland and Colchester Counties in Nova Scotia. *Geological and Natural History Survey of Canada, Annual Report for 1885, Part E*, pp. 1-71.
- Ells, R.W. 1905. Some interesting problems in New Brunswick geology. *Royal Society of Canada, Proceedings and Transactions, Second Series*, 11: 21-35.
- Ells, R.W. 1906. Southern New Brunswick. *Geological Survey of Canada, Summary Report for the Calendar Year 1906*, pp. 131-139.
- Ells, R.W. 1907. The geology and mineral resources of New Brunswick. *Geological Survey of Canada, Department of Mines, Separate Report 983*, 135 p.
- Ells, R.W. 1908. Surveys in southern New Brunswick. *Department of Mines, Geological Survey Branch, Summary Report for the Calendar Year 1907*, pp. 74-76.
- Fairbairn, H.W., Bottino, M.L., Pinson, W.H., Jr., and Hurley, P.M. 1966. Whole-rock age and initial $^{87}\text{Sr}/^{86}\text{Sr}$ of volcanics underlying fossiliferous Lower Cambrian in the Atlantic Provinces of Canada. *Canadian Journal of Earth Sciences*, 3: 509-521.
- Farrow, C.E.G. and Barr, S.M. 1992. Petrography of high alumina hornblende and magmatic epidote bearing plutons, southeastern Cape Breton Island, Nova Scotia. *Canadian Mineralogist*, 30: 377-392.
- Faure, G. 1986. Principles of isotope geology, 2nd edition. Wiley, New York, New York, 464 p.
- Ferry, J.M. 1983. Mineral reactions and element migration during metamorphism of calcareous sediments from the Vassalboro Formation, south-central Maine. *American Mineralogist*, 68: 334-354.

- Ferry, J.M. and Spear, F.S. 1982. Experimental calibration of the partitioning of Fe and Mg between biotite and garnet. *Contributions to Mineralogy and Petrology*, 66: 113-117.
- Fleck, R.J., Sutter, J.F., and Elliot, D.H. 1977. Interpretation of discordant $^{40}\text{Ar}/^{39}\text{Ar}$ age-spectra of Mesozoic tholeiites from Antarctica. *Geochemica et Cosmochimica Acta*, 41: 15-32.
- Fryer, B.J., Kerr, A., Jenner, G.A., and Longstaffe, F.J. 1992. Probing the crust with plutons: regional isotopic geochemistry of granitoid intrusions across insular Newfoundland. Newfoundland Geological Surveys Branch Report 92-1, pp. 119-140.
- Fyffe, L.R. and Fricker, A. 1987. Tectonostratigraphic terrane analysis of New Brunswick. *Maritime Sediments and Atlantic Geology*, 23: 113-122.
- Fuhrman, M.L. and Lindsley, D.H. 1988. Ternary-feldspar modelling and thermometry. *American Mineralogist*, 73: 201-215.
- Gesner, A. 1839. First Report on the Geological Survey of the Province of New Brunswick. Saint John, New Brunswick, 87 p.
- Gesner, A. 1840. Second Report on the Geological Survey of the Province of New Brunswick. Saint John, New Brunswick, 76 p.
- Gesner, A. 1841. Third Report on the Geological Survey of the Province of New Brunswick. Saint John, New Brunswick, 88 p.
- Gesner, A. 1842. Third Report on the Geological Survey of the Province of New Brunswick. Saint John, New Brunswick, 101 p.
- Gesner, A. 1843. Report on the Geological Survey of the Province of New Brunswick, with a Topographical Account of the Public Lands and the Districts Explored in 1842. Saint John, New Brunswick, 88 p.
- Gesner, A. 1847. New Brunswick, with Notes for Emigrants. London, 388 p.
- Getty, S.R. and Gromet, L.P. 1992. Geochronological constraints on ductile deformation, crustal extension, and doming about a basement cover boundary, New England Appalachians. *American Journal of Science*, 292: 421-444.
- Ghent, E.D., Robbins, D.B., and Stout, M.L. 1979. Geothermometry, geobarometry, and fluid compositions of metamorphosed calc-silicates and pelites, Mica Creek, British Columbia. *American Mineralogist*, 64: 874-885.
- Ghent, E.D., Stout, M.Z., and Parrish, R.R. 1988. Determination of metamorphic pressure-temperature-time (P-T-t) paths. In Short course on heat, metamorphism, and tectonics. Edited by E.G. Nisbet and C.M.R. Fowler. Mineralogical Association of Canada Short Course Handbook, 14: 155-188.
- Gibbons, W. 1990. Transcurrent ductile shear zones and the dispersal of the Avalon superterrane. In *The Cadomian Orogeny*. Edited by R.S. D'Lemos, Strachan, R.S., and Topley, C.G. Geological Society Special Publication 51, pp. 407-423.
- Giles, P.S. and Ruitenberg, A.A. 1977. Stratigraphy, paleo-geography, and tectonic setting of the Coldbrook Group in the Caledonia Highlands of southern New Brunswick. *Canadian Journal of Earth Sciences*, 14: 1263-1275.
- Gill, J.B. 1981. *Orogenic andesites and plate tectonics*. Springer-Verlag, New York, 390 p.
- Golberg, J.M. and Leyreloup, A.F. 1990. High temperature-low pressure Cretaceous metamorphism related to crustal thinning (Eastern North Pyrenean Zone, France). *Contributions to Mineralogy and Petrology*, 104: 194-207.
- Grammatikopoulos, A.L. 1992. Petrogenesis, age and economic potential of gabbroic plutons in the Avalon Terrane in southern New Brunswick and southeastern Cape Breton Island. Unpublished M.Sc. Thesis, Acadia University, Wolfville, Nova Scotia, 378 p.
- Grant, E.B. 1972. The structure and development of part of the Kingston Uplift, Kings County, New Brunswick. Unpublished M.Sc. Thesis, Carleton University, Ottawa, Ontario, 88 p.

- Grant, R.H. 1972. Geology of map area N-29, Loch Alva-part of Musquash Reserve and Reservoir. New Brunswick Department of Natural Resources, Mineral Resources Branch. Scale 1 inch to 1320 feet.
- Greenough, J.D., McCutcheon, S.R., and Papezik, V.S. 1985. Petrology and geochemistry of Cambrian volcanic rocks from the Avalon Zone in New Brunswick. *Canadian Journal of Earth Sciences*, 22: 881-892.
- Gromet, L.P. 1991. Direct dating of deformational fabrics. In short course handbook on applications of radiogenic isotope systems to problems in geology. Edited by L. Heaman and J.N. Ludden. Mineralogical Association of Canada, 19: 167-189.
- Guidotti, C.V. 1984. Micas in metamorphic rocks. In *Micas*. Edited by S.W. Bailey. Mineralogical Society of America Reviews in Mineralogy, 13: 357-493.
- Gupta, V.K. 1975. Aeromagnetic and gravity interpretation of the Caledonia area, southern New Brunswick. Unpublished Ph.D. Thesis, University of New Brunswick, Fredericton, New Brunswick, 201 p.
- Gussow, W.C. 1953. Carboniferous stratigraphy and structural geology of New Brunswick, Canada. *Bulletin of the American Association of Petroleum Geologists*, 37: 1713-1816.
- Halliday, A.N., Stephens, W.E., and Harmon, R.S. 1971. Isotopic and chemical constraints on the development of peraluminous Caledonian and Acadian granites. *Canadian Mineralogist*, 19: 205-216.
- Hamilton, J.B. 1965. Limestone in New Brunswick. New Brunswick Mines Branch, Mineral Resources, Report no. 2, 147 p.
- Hamilton, J.B. 1968. Carbonate deposits in the Nauwigewauk, Elliott Road and Torryburn areas, Kings County. New Brunswick Department of Natural Resources, Mineral Resources Branch, Report of Investigation 8, 18 p.
- Hammarstrom, J.M. and Zen, E-an. 1986. Aluminum in hornblende: an empirical igneous geobarometer. *American Mineralogist*, 71: 1297-1313.
- Hanes, J.A. 1991. K-Ar and $^{40}\text{Ar}/^{39}\text{Ar}$ geochronology: methods and applications. In short course handbook on applications of radiogenic isotope systems to problems in geology. Edited by L. Heaman and J.N. Ludden. Mineralogical Association of Canada, 19: 27-57.
- Hanson, G.N. 1980. Rare Earth Elements in petrogenetic studies of igneous systems. *Annual Reviews of Earth and Planetary Sciences*, 8: 371-406.
- Harrison, T.M. 1981. Diffusion of ^{40}Ar in hornblende. *Contributions to Mineralogy and Petrology*, 78: 324-331.
- Harrison, T.M. and Fitz Gerald, J.D. 1986. Exsolution in hornblende and its consequences for $^{40}\text{Ar}/^{39}\text{Ar}$ age spectra and closure temperature. *Geochemica et Cosmochimica Acta*, 50: 247-253.
- Harrison, T.M. and McDougall, I. 1980. Investigations of an intrusive contact, northwest Nelson, New Zealand-II. Diffusion of radiogenic and excess ^{40}Ar in hornblende revealed by $^{40}\text{Ar}/^{39}\text{Ar}$ age spectrum analysis. *Geochemica et Cosmochimica Acta*, 44: 2005-2020.
- Harrison, T.M. and McDougall, I. 1981. Excess ^{40}Ar in metamorphic rocks from Broken Hill, New South Wales: implications for $^{40}\text{Ar}/^{39}\text{Ar}$ age spectra and the thermal history of the region. *Earth and Planetary Science Letters*, 55: 123-149.
- Harrison, T.M., Duncan, I., and McDougall, I. 1985. Diffusion of ^{40}Ar in biotite: temperature, pressure, and compositional effects. *Geochemica et Cosmochimica Acta*, 49: 2461-2468.
- Hartt, C.F. 1865. Preliminary notice of a fauna of the Primordial Period in the vicinity of Saint John, New Brunswick. *The Canadian Naturalist and Geologist*, 2: 318-320.
- Haselton, H.T.Jr., Hovis, G.L., Hemingway, B.S., and Robie, R.A. 1983. Calorimetric investigation of the excess entropy of mixing in analbite-sanidine solid solutions: lack of evidence for Na, K short-range order and implications for two-feldspar thermometry. *American Mineralogist*, 68: 398-413.

- Hayes, A.O. 1914. Geology of the Saint John map-area, New Brunswick. Geological Survey of Canada, Department of Mines Summary Report for 1913, pp. 228-243.
- Hayes, A.O. and Howell, B.F. 1937. Geology of Saint John, New Brunswick. Geological Society of America, Special Paper 5, 146 p.
- Heaman, L. and Parrish, R. 1991. U-Pb geochronology of accessory minerals. In short course handbook on applications of radiogenic isotope systems to problems in geology. Edited by L. Heaman and J.N. Ludden. Mineralogical Association of Canada, 19: 59-102.
- Heizler, M.T. and Harrison, T.M. 1988. Multiple trapped argon isotope components revealed by $^{40}\text{Ar}/^{39}\text{Ar}$ isochron analysis. *Geochemica et Cosmochimica Acta*, 52: 1295-1303.
- Helmstaedt, H. 1968. Structural analysis of the Beaver Harbour area, Charlotte County, New Brunswick. Unpublished Ph.D. Thesis, University of New Brunswick, Fredericton, New Brunswick, 196 p.
- Hibbard, M.J. 1991. Textural anatomy of twelve magma-mixed granitoid systems. In *Enclaves and Granite Petrology*. Edited by J. Didier and B. Barbarian. Developments in Petrography 13. Elsevier, Amsterdam, pp. 431-444.
- Hodges, K.V. and Spear, F.S. 1982. Geothermometry, geobarometry, and the Al_2O_3 triple point at Mt. Moosilauke, New Hampshire. *American Mineralogist*, 67: 1118-1134.
- Hoffer, E. 1976. The reaction sillimanite+biotite+quartz=cordierite+K-feldspar+ H_2O and partial melting in the system $\text{K}_2\text{O}-\text{FeO}-\text{MgO}-\text{Al}_2\text{O}_3-\text{SiO}_2-\text{H}_2\text{O}$. *Contributions to Mineralogy and Petrology*, 55: 127-130.
- Hofmann, H.J. 1974. The stromatolite *Archaeozoon acadense* from the Proterozoic Green Head Group of Saint John, New Brunswick. *Canadian Journal of Earth Sciences*, 11: 1098-1115.
- Holdway, M.J. 1971. Stability of andalusite and the aluminum silicate phase diagram. *American Journal of Science*, 271: 97-131.
- Holdway, M.J. and Lee, S.M. 1977. Fe-Mg cordierite stability in high-grade pelitic rocks based on experimental, theoretical, and natural observations. *Contributions to Mineralogy and Petrology*, 63: 175-198.
- Hollister, L.S., Grisson, G.C., Peters, E.K., Stowell, H.H., and Sisson, V.B. 1987. Confirmation of the empirical calibration of Al in hornblende with pressure of solidification of calc-alkaline plutons. *Geology*, 17: 837-841.
- Holness, M.B. 1992. Metamorphism and fluid infiltration of the calc-silicate aureole of the Beinn an Dubhaich Granite, Skye. *Journal of Petrology*, 33: 1261-1293.
- Hsu, K.J. 1974. Melanges and their distinction from olistostromes. In *Modern and ancient geosynclinal sedimentation*. Edited by R.H. Dott and R.J. Shaver. Paleontologists and Mineralogists Special Publication 19, pp. 321-333.
- Hutchinson, R.D. 1952. The stratigraphy and trilobite faunas of the Cambrian sedimentary rocks of Cape Breton Island, Nova Scotia. Geological Survey of Canada, Memoir 262, 124 p.
- International Subcommission on Stratigraphic Classification. 1987. Stratigraphic classification and nomenclature of igneous and metamorphic rock bodies. *Geology*, 99: 440-442.
- Irvine, T.N. and Baragar, W.R.A. 1971. A guide to the chemical classification of the common volcanic rocks. *Canadian Journal of Earth Sciences*, 8: 523-548.
- Jamieson, R.A. 1984. Low pressure cordierite-bearing migmatites from Kellys Mountain, Nova Scotia. *Contributions to Mineralogy and Petrology*, 36: 309-320.
- Jamieson, R.A. 1990. Metamorphism of an Early Paleozoic continental margin, western Baie Verte Peninsula, Newfoundland. *Journal of Metamorphic Geology*, 8: 269-288.
- Jamieson, R.A. and O'Beirne-Ryan, A.M. 1991. Decomposition-induced growth of albite porphyroblasts, Fleur de Lys Supergroup, western Newfoundland. *Journal of Metamorphic Geology*, 9: 433-439.

- Johannes, W. 1984. Beginning of melting in the granite system Qz-Or-Ab-An-H₂O. *Contributions to Mineralogy and Petrology*, 86: 264-273.
- Johannes, W. 1988. What controls partial melting in migmatites? *Journal of Metamorphic Geology*, 6: 451-465.
- Johnson, S.C. and McLeod, M.J. 1994. Tectonic significance of the New River belt: a unique segment along the western margin of the Avalon composite terrane, southern New Brunswick. *Geological Society of America 1994 Abstracts with Programs*, 26: 26.
- Kaneoka, I. and Aoki, K.-I. 1978. ⁴⁰Ar/³⁹Ar analyses of phlogopite nodules and phlogopite-bearing peridotites in South African kimberlites. *Earth and Planetary Science Letters*, 40: 119-129.
- Keen, C.E., Kay, W.A., Keppie, D., Marillier, F., Pe-Piper, G., and Waldron, J.W.F. 1991. Deep seismic reflection data from the Bay of Fundy and Gulf of Maine: tectonic implications for the northern Appalachians. *Canadian Journal of Earth Sciences*, 28: 1096-1111.
- Kneller, B.C. and Leslie, A.G. 1984. Amphibolite facies metamorphism in shear zones in the Buchan area of N.E. Scotland. *Journal of Metamorphic Geology*, 2: 83-94.
- Keppie, J.D. 1982. Geology and tectonics of Nova Scotia. In *Guidebook for Avalon and Meguma zones*. Edited by A.F. King. Memorial University of Newfoundland, Report 5, pp. 125-139.
- Keppie, J.D. 1985. The Appalachian collage. In *The Caledonide Orogen-Scandinavia and Related Areas*. Edited by D.G. Gee and B.A. Sturt. J. Wiley and Sons, New York, pp. 1217-1226.
- Keppie, J.D. 1989. Northern Appalachian terranes and their accretionary history. In *Terranes in the Circum-Atlantic Paleozoic Orogens*. Edited by R.D. Dallmeyer. Geological Society of America, Special Paper 20, pp. 159-192.
- Keppie, J.D. and Dallmeyer, R.D. 1989. ⁴⁰Ar/³⁹Ar mineral ages from Kellys Mountain, Cape Breton Island, Nova Scotia: implications for the tectonothermal evolution of the Avalon terrane. *Canadian Journal of Earth Sciences*, 26: 1509-1516.
- Keppie, J.D. and Dostal, J. 1991. Late Proterozoic Tectonic Model for the Avalon Terrane in Maritime Canada. *Tectonics*, 10: 842-850.
- Keppie, J.D. and Krogh, T.E. 1990. Detrital zircon ages from Late Precambrian conglomerate, Avalon Composite Terrane, Nova Scotia. *Geological Society of America 1990 Abstracts with Programs*, 22: 27-28.
- Keppie, J.D., Nance, R.D., Murphy, J.B., and Dostal, J. 1991. Northern Appalachians: Avalon and Meguma terranes. In *The West African Orogens and Circum-Atlantic Correlatives*. Edited by R.D. Dallmeyer and J.P. Lecorche. Springer, Heidelberg, Germany, pp. 315-333.
- Kozoil, A.M. and Newton, R.C. 1988. Redetermination of the anorthite breakdown reaction and improvement of the plagioclase-garnet-Al₂SiO₅-quartz geobarometer. *American Mineralogist*, 103: 423-433.
- Lalonde, A.E. and Bernard, P. 1993. Composition and colour of biotite from granites: two useful properties in the characterization of plutonic suites from the Hepburn internal zone of Wopmay Orogen, Northwest Territories. *Canadian Mineralogist*, 31: 203-217.
- Lameyre, J. and Bowen, P. 1982. Plutonic rock types series: discrimination of various granitoid series and related rocks. *Journal of Volcanology and Geothermal Research*, 14: 169-186.
- Landing, E. 1991a. Upper Precambrian through Lower Cambrian of Cape Breton Island: faunas, paleoenvironments, and stratigraphic revision. *Journal of Paleontology*, 65: 507-595.
- Landing, E. 1991b. A unified uppermost Precambrian through Lower Cambrian stratigraphy for Avalonian North America. *Geological Society of America 1991 Abstracts with Programs*, 23: 56.
- Landing, E. 1994. Avalon - an insular continent by the latest Precambrian. *Geological Society of America 1994 Abstracts with Programs*, 26: 31.
- Lapworth, C. 1879. On the tripartite classifications of the Lower Paleozoic rocks. *Geological Magazine*, 6: 1-15.

- Leake, B.E. 1978. Nomenclature of amphiboles. *The Canadian Mineralogist*, 16: 501-520.
- Leake, B.E. and Ahmed Said, Y. 1994. Hornblende barometry of the Galway batholith, Ireland: an empirical test. *Mineralogy and Petrology*, 51: 243-250.
- Leavitt, E.M. 1963. The geology of the Precambrian Green Head Group in the Saint John New Brunswick area. Unpublished M.Sc Thesis, University of New Brunswick, Fredericton, New Brunswick, 146 p.
- Leavitt, E.M. and Hamilton, J.B. 1962. Geology of Saint John area. West and East half. New Brunswick Department of Natural Resources Branch. Maps 62-4A and 62-4B. Scale 1 inch = 1320 feet.
- Leech, G.B., Lowdon, J.A., Sockwell, C.H., and Wanless, R.K. 1963. Age Determinations and Geological Studies, Report 4. Geological Survey of Canada, Department of Energy, Mines and Resources, Paper 63-17, pp. 102-103.
- Leger, A. and Williams, P.F. 1986. Transcurrent faulting history of southern New Brunswick. In *Current Research, Part B, Geological Survey of Canada, Paper 86-1B*, pp. 111-120.
- Leterrier, J., Maury, R.C., Thonon, P., Girard, D., and Marchal, M. 1982. Clinopyroxene composition as a method of identification of the magmatic affinities of paleo-volcanic series. *Earth and Planetary Science Letters*, 59: 139-154.
- Lo, C.-H. and Onstott, T.C. 1989. ^{39}Ar recoil artifacts in chloritized biotite. *Geochimica et Cosmochimica Acta*, 53: 2697-2711.
- Logan, W.E. 1858a. On the division of the Azoic rocks of Canada into Huronian and Laurentian. *The American Association for the Advancement of Science*, 11: 44-47.
- Logan, W.E. 1858b. On the probable subdivision of the Laurentian Series of rocks of Canada. *The American Association for the Advancement of Science*, 11: 47-51.
- Lux, D.R., DeYoreo, J.J., Guidotti, C.V., and Decker, E.R. 1986. Role of plutonism in low-pressure metamorphic belt formation. *Nature*, 323: 794-797.
- Maaloe, S. 1992. Melting and diffusion processes in closed-system migmatization. *Journal of Metamorphic Geology*, 10: 503-516.
- MacKenzie, G.S. 1951. Preliminary geology map of Westfield. Geological Survey of Canada Map 51-15. Scale 1:40,000.
- MacKenzie, G.S. 1964. Geology of Saint John New Brunswick. Geological Survey of Canada Map 1113A (with marginal notes). Scale 1 inch to 1 mile.
- Mather, J.D. 1970. The biotite isograd and the lower greenschist facies in the Dalradian rocks of Scotland. *Journal of Petrology*, 11: 253-275.
- Matthew, G.F. 1863. Observations on the geology of Saint John County, New Brunswick. *The Canadian Naturalist and Geologist*, 8: 241-259.
- Matthew, G.F. 1865. On the Azoic and Paleozoic rocks of southern New Brunswick. *The Quarterly Journal of the Geological Society of London, Proceedings of the Geological Society*, pp. 422-434.
- Matthew, G.F. 1868. On the Azoic and Paleozoic rocks of southern New Brunswick. *The Canadian Naturalist and Geologist, New Series* 3: 387-391.
- Matthew, G.F. 1878. Report on the slate formations of the northern part of Charlotte County, New Brunswick, with a summary of geological observations in the southeastern part of the same county. Geological Survey of Canada, Report of Progress for 1876-77, pp. 322-350.
- Matthew, G.F. 1890a. Eozoon and other organisms in Laurentian rocks at Saint John. *Natural History of New Brunswick Bulletin* 9: 36-41.
- Matthew, G.F. 1890b. On the occurrence of sponges in Laurentian rocks at Saint John, New Brunswick. *Natural History of New Brunswick Bulletin* 9: 42-45.
- Matthew, G.F. 1896. Report on the Summer Camp at Lepreau Basin. *Natural History of New Brunswick Bulletin, Appendix* 1, 3: 88-93.

- Matthew, G.F. 1897. Abraham Gesner. A review of his scientific work. *Natural History of New Brunswick Bulletin* 3: 3-48.
- Matthew, G.F. 1899. A Paleozoic terrane beneath the Cambrian. *New York Academy of Science, Annual*, 12: 137-142.
- Matthew, G.F. 1903. Report on the Cambrian rocks at Cape Breton. *Geological Survey of Canada, Report* 797, 246 p.
- Matthew, G.F. 1908a. Geological Cycles in the Maritime Provinces of Canada. *Royal Society of Canada, Proceedings and Transactions, Third Series*, 2: 121-143.
- Matthew, G.F. 1908b. The physical evolution of Acadia, Part 1, The Insular Stage, or Precambrian to Devonian development. *Natural History Society of New Brunswick, Bulletin*, 6: 3-16.
- Matthew, G.F. 1911. Rocks and minerals of Rockwood Park. *Natural History Society of New Brunswick, Bulletin*, 6: 339-341.
- Matthew, G.F. 1921. On the Mispec Group (Devonian). *The Royal Society of Canada, Proceedings and Transactions, Third Series*, 15: 105-109.
- Matthew, G.F. and Bailey, L.W. 1869a. The metamorphic rocks of New Brunswick and Maine. *The Canadian Naturalist, New Series*, 4: 326-328.
- Matthew, G.F. and Bailey, L.W. 1869b. Remarks on the age and relations of the metamorphic rocks of New Brunswick and Maine. *American Naturalist*, 3: 442-444.
- Matthew, G.F. and Bailey, L.W. 1870. Remarks on the age and relations of the metamorphic rocks of New Brunswick and Maine. *The American Association for the Advancement of Science, Proceedings*, 18: 179-195.
- Matthew, W.D. 1894a. The crystalline rocks near Saint John, New Brunswick, Canada. *Natural History Society of New Brunswick Bulletin*, 3: 16-33.
- Matthew, W.D. 1894b. The intrusive rocks near Saint John New Brunswick. *New York Academy of Sciences Transactions*, 13: 185-203.
- Matthew, W.D. 1895. The effusive and dyke rocks near Saint John New Brunswick. *New York Academy of Sciences Transactions*, 14: 187-218.
- Matthew, W.D. 1896. The volcanic rocks of the Maritime Provinces of Canada. *Natural History Society of New Brunswick*, 3: 76-83.
- McCutcheon, S.R. 1978. Geology of the Apohaqui-Markhamville area, Map area R-25 (21H/11W, 21H/12E). *New Brunswick Department of Natural Resources, Minerals Resources Branch, Map Report* 78-5, 41 p.
- McCutcheon, S.R. 1981. Stratigraphy and paleogeography of the Windsor Group, southern New Brunswick. Unpublished M.Sc. Thesis, Acadia University, Wolfville, Nova Scotia, 206 p.
- McCutcheon, S.R. 1984. Geology of the gold-bearing rocks in the Lorneville-Lepreau area. *In Ninth Annual Review of Activities, New Brunswick Department of Natural Resources, Minerals Resources Division, Information Circular* 4-2, pp. 2-6.
- McCutcheon, S.R. 1985. Geology of the gold-bearing rocks in the Lorneville-Lepreau area. Part of NTS map 21G/1, *New Brunswick Department of Natural Resources, Minerals Resources Branch, Map Plate* 85-28. Scale 1:50,000.
- McCutcheon, S.R. and Robinson, P.T. 1987. Geological constraints on the genesis of the Maritimes Basin, Atlantic Canada. *In Sedimentary Basins and Basin-Forming Mechanisms. Edited by C. Beaumont and A.J. Tankard. Canadian Society of Petroleum Geologists, Memoir* 12, pp. 287-297.
- McCutcheon, S.R. and Ruitenberg, A.A. 1987. Geology of Mineral Deposits, Annidale-Nerepis area. *New Brunswick Department of Natural Resources, Minerals Resources Division, Memoir* 2, 141 p.
- McCutcheon, S.R., McLeod, M.J., and Ruitenberg, A.A. 1982. Southern New Brunswick-Field Trip Introduction. *In Guidebook for Avalon and Meguma zones. Edited by A.F. King. Memorial University of Newfoundland, Report* 9, pp. 277-284.

- McDougall, I. and Harrison, T.M. 1988. Geochronology and thermochronology by the $^{40}\text{Ar}/^{39}\text{Ar}$ method. Oxford University Press. New York, New York, 212 p.
- McLellan, E.L. 1983. Problems of structural analysis in migmatite terranes. In *Migmatites, Melting and Metamorphism*. Edited by M.P. Atherton and Gribble, C.D. Proceedings of the Geochemical Group of the Mineralogical Society, p. 299-302.
- McLeod, M.J., Ruitenberg, A.A., and Krogh, T.E. 1992. Geology and U-Pb geochronology of the Annidale Group, southern New Brunswick: Lower Ordovician volcanic and sedimentary rocks formed near the southeastern margin of Iapetus Ocean. *Atlantic Geology*, 28: 181-192.
- McLeod, M.J., Johnson, S.C., and Ruitenberg, A.A. 1994. Geological map of southern New Brunswick. New Brunswick Department of Natural Resources and Energy, Mineral Resources, Maps NR-5 and NR-6.
- McMullin, D.W.A. 1991. Thermobarometry of pelitic rocks using equilibria between quartz-garnet-aluminosilicate-muscovite-biotite, with application to rocks of the Quesnel Lake area, British Columbia. Unpublished Ph.D. thesis, University of British Columbia, Vancouver, British Columbia, 291 p.
- McMullin, D.W.A., Berman, R.G., and Greenwood, H.J. 1991. Calibration of the SGAM thermobarometer for pelitic rocks using data from phase-equilibrium and natural assemblages. *Canadian Mineralogist*, 29: 889-908.
- Meschede, M. 1986. A method of discriminating between different types of mid-ocean ridge basalts and continental tholeiites with the Nb-Zr-Y diagram. *Chemical Geology*, 56: 207-218.
- Murphy, J.B. and Nance, R.D. 1989. Model for the evolution of the Avalonian-Cadomian belt. *Geology*, 17: 735-738.
- Murphy, J.B. and Nance, R.D. 1991. Supercontinent model for the contrasting character of Late Proterozoic orogenic belts. *Geology*, 19: 469-472.
- Murphy, J.B., Keppie, J.D., Nance, R.D., and Dostal, J. 1990. The Avalon composite terrane of Nova Scotia. In *Avalonian and Cadomian Geology of the North Atlantic*. Edited by R.A. Strachan and G.K. Taylor, pp. 195-213.
- Murphy, J.B., Barr, S.M., Currie, K.L., Keppie, J.D., Nance, R.D., and White, C.E. 1992. The Avalon Terrane in Maritime Canada. Geological Association of Canada, Mineralogical Association of Canada, Joint Annual Meeting, Wolfville, Nova Scotia. Field Trip C-12, Guidebook, 164 p.
- Murry, D.P. 1988. Post-Acadian metamorphism in the Appalachians. In *The Caledonian-Appalachian Orogen*. Edited by A.L. Harris and D.J. Fettes. Geological Society Special Publication No. 38, pp. 597-609.
- Nadon, G.C. and Middleton, G.V. 1985. The stratigraphy and sedimentology of the Fundy Group (Triassic) of the St. Martin's area, New Brunswick. *Canadian Journal of Earth Sciences*, 22: 1183-1203.
- Nance, R.D. 1982. Structural recognition of the Green Head Group, Saint John, New Brunswick. In *Current Research, Part A, Geological Survey of Canada, Paper 82-1A*, pp. 37-43.
- Nance, R.D. 1985. Alleghenian deformation in the Mispic Group, Saint John Harbour. In *Current Research, Part A, Geological Survey of Canada, Paper 85-1A*, pp. 7-13.
- Nance, R.D. 1986a. Late Carboniferous tectonostratigraphy in the Avalon Terrane of southern New Brunswick. *Maritime Sediments and Atlantic Geology*, 22: 308-326.
- Nance, R.D. 1986b. Precambrian evolution of the Avalon terrane in the northern Appalachians: A review. *Maritime Sediments and Atlantic Geology*, 22: 214-238.
- Nance, R.D. 1987a. Model for the Precambrian evolution of the Avalon terrane in southern New Brunswick, Canada. *Geology*, 15: 753-756.

- Nance, R.D. 1987b. Dextral transpression and Late Carboniferous sedimentation in the Fundy Coastal Zone of southern New Brunswick. *In Sedimentary Basins and Basin-Forming Mechanisms. Edited by C. Beaumont and A.J. Tankard. Canadian Society of Petroleum Geologists, Memoir 12, pp. 363-377.*
- Nance, R.D. 1988. Tectonic evolution of the Avalon Terrane in southern New Brunswick, Canada. *Trabajos de Geologia, 17: 167-188.*
- Nance, R.D. 1990. Late Precambrian - Early Paleozoic evolution of part of the Avalon terrane in southern New Brunswick, Canada. *In The Cadomian Orogeny. Edited by R.S. D'Lemos, R.A. Strachan, and C.G. Topley. Geological Society Special Publication No. 51, pp. 363-382.*
- Nance, R.D. and Dallmeyer, R.D. 1993. $^{40}\text{Ar}/^{39}\text{Ar}$ amphibole ages from the Kingston Complex, New Brunswick: evidence for Silurian-Devonian tectonothermal activity and implications for the accretion of the Avalon Composite Terrane. *The Journal of Geology, 101: 375-388.*
- Nance, R.D. and Dallmeyer, R.D. 1994. Structural and $^{40}\text{Ar}/^{39}\text{Ar}$ mineral age constraints for the tectonothermal evolution of the Green Head Group and Brookville Gneiss, southern New Brunswick, Canada; implications for the configuration of the Avalon composite terrane. *Geological Journal, 29: 293-322.*
- Nance, R.D. and Murphy, J.B. 1994. Contrasting basement isotopic signatures and the palinspastic restoration of peripheral orogens: example from the Neoproterozoic Avalonian-Cadomian belt. *Geology, 22: 617-620.*
- Nance, R.D. and Warner, J.B. 1986. Variscan tectonostratigraphy of the Mispic Group, southern New Brunswick: structural geometry and deformational history. *In Current Research, Part A, Geological Survey of Canada, Paper 86-1A, pp. 351-358.*
- Nance, R.D., Currie, K.L., and Murphy, J.B. 1990. The Avalon Zone of New Brunswick. *In Avalonian and Cadomian Geology of the North Atlantic. Edited by R.A. Strachan and G.K. Taylor, pp. 214-236.*
- Nance, R.D., Murphy, J.B., Strachan, R.A., D'Lemos, R.S., and Taylor, G.K. 1991. Late Proterozoic tectonostratigraphic evolution of the Avalonian and Cadomian terranes. *Precambrian Research, 53: 41-78.*
- Neale, E.R.W., Beland, J., Potter, R.R. and Poole, W.H. 1961. A preliminary tectonic map of the Canadian Appalachian region based on folding. *Canadian Institute of Mining and Metallurgy, 54: 687-694.*
- Neuman, R.B. 1984. Geology and paleobiology of islands in the Ordovician Iapetus ocean: Review and implications. *Geological Society of America Bulletin, 95: 1188-1201.*
- Newton, R.C. and Haselton, H.T. 1981. Thermodynamics of the garnet-plagioclase- Al_2SiO_5 -quartz geobarometer. *In Thermodynamics of Minerals and Melts. Edited by R.C. Newton, A. Navrotsky, and B.J. Wood. Advances in Physical Geochemistry 1. New York: Springer-Verlag, pp. 131-147.*
- Nicholls, I.A. and Harris, K.L. 1980. Experimental rare earth element partition coefficients for garnet, clinopyroxene and amphibole coexisting with andesitic and basaltic liquids. *Geochimica et Cosmochimica Acta, 34: 331-340.*
- Obradovich, J.D. and Cobban, W.A. 1975. A time-scale for the late Cretaceous of the western interior of North America. *Geological Association of Canada, Special Paper 13, pp. 31-54.*
- O'Brien, B.H. 1976. The geology of parts of the Coldbrook Group, southern New Brunswick. Unpublished M.Sc. Thesis, University of New Brunswick, Fredericton, New Brunswick, 214 p.
- O'Brien, B.H., O'Brien, S.J., and Dunning, G.R. 1991. Silurian cover, Late Precambrian-Early Ordovician basement, and the chronology of Silurian orogenesis in the Hermitage Flexure (Newfoundland Appalachians). *American Journal of Science, 291: 760-799.*

- O'Brien, B.H., O'Brien, S.J., Dunning, G.R., and Tucker, R.D. 1993. Episodic reactivation of a Late Precambrian mylonite zone on the Gondwanan margin of the Appalachians, southern Newfoundland. *Tectonic*, 12: 1043-1055.
- O'Brien, B.H., Wardle, R.J., and King, A.F. 1983. The Avalon Zone: A Pan-African terrane in the Appalachian Orogen of Canada. *Geological Journal*, 18: 195-222.
- Olszewski, W.J., Jr. and Gaudette, H.E. 1982. Age of the Brookville gneiss and associated rocks, southeastern New Brunswick. *Canadian Journal of Earth Sciences*, 19: 2158-2166.
- Olszewski, W.J., Jr., Gaudette, H.E., and Poole, W.H. 1980. Rb-Sr whole rock and U-Pb zircon ages from the Green Head Group, New Brunswick. *Northeast Geological Society of America 15th Annual Meeting, Abstract with Programs*, 12: 76.
- Onstott, T.C. and Peacock, M.W. 1987. Argon retentivity of hornblendes: a field experiment in a slowly cooled metamorphic terrane. *Geochimica et Cosmochimica Acta*, 51: 2891-2903.
- Park, A.F., Williams, P.F., Ralser, S., and Leger, A. 1994. Geometry and kinematics of a major crustal shear zone segment in the Appalachians of southern New Brunswick. *Canadian Journal of Earth Sciences*, 31: 1523-1535.
- Parker, J.S.D. 1984. Geological relationships of basement to cover, Musquash Harbour to Black River, Saint John area, southern New Brunswick. Unpublished M.Sc. Thesis, University of New Brunswick, Fredericton, New Brunswick, 326 p.
- Parrish, R.R., Roddick, J.C., Loveridge, D., and Sullivan, R.W. 1987. Uranium-lead analytical techniques at the Geochronology laboratory, Geological Survey of Canada. In *Radiogenic age and isotopic studies, Report 1. Geological Survey of Canada, Paper 87-2*, pp. 3-7.
- Patel, I.M. 1973. Saint John area. In *Geology of New Brunswick. Edited by N. Rast. 1973 New England Intercollegiate Geological Conference*, pp. 115-118.
- Paterson, S.R., Vernon, R.H., and Tobisch, O.T. 1989. A review of criteria for the identification of magmatic and tectonic foliations in granitoids. *Journal of Structural Geology*, 11: 349-363.
- Patino Douce, A.E. and Johnson, A.D. 1991. Phase equilibria and melt productivity in the pelitic system: implications for the origin of peraluminous granitoids and aluminous granulites. *Contributions to Mineralogy and Petrology*, 107: 202-218.
- Pattison, D. and Harte, B. 1985. A petrogenetic grid for pelites in the Ballachulish and other Scottish thermal aureoles. *Journal of the Geological Society of London*, 142: 7-28.
- Pearce, J.A. and Cann, J.R. 1973. Tectonic setting of basic volcanic rocks determined using trace element analyses. *Earth and Planetary Science Letters*, 19: 290-300.
- Pearce, J.A., Harris, N.B.W., and Tindle, A.G. 1984. Trace element discrimination diagrams for the tectonic interpretation of granite rocks. *Journal of Petrology*, 69: 33-47.
- Peters, M.T. and Wickham, S.M. 1994. Petrology of upper amphibolite facies marbles from the East Humboldt Range, Nevada, USA; evidence for high-temperature, retrograde, hydrous volatile fluxes at mid-crustal levels. *Journal of Petrology*, 35: 205-238.
- Pickerill, R.K., Carter, D., and St. Peter, C. 1985. The Albert Formation - oil shale, lakes, fans, and deltas. *Geological Association of Canada Annual Meeting, Fredericton, New Brunswick, Excursion Guide 6*.
- Pimentel, M.M., and Fuck, R.A. 1992. Neoproterozoic crustal accretion in central Brazil. *Geology*, 20: 375-379.
- Pitcher, W.S. 1994. The nature and origin of granite. *Blackie Academic and Professional, London*, 321 p.

- Plint, A.G. and van de Poll, H.W. 1982. Alluvial fan and piedmont sedimentation in the Tynemouth Creek Formation (Lower Pennsylvanian) of southern New Brunswick. *Maritime Sediments and Atlantic Geology*, 18: 104-128.
- Plint, A.G. and van de Poll, H.W. 1984. Structural and sedimentary history of the Quaco Head area, southern New Brunswick. *Canadian Journal of Earth Sciences*, 21: 753-761.
- Plint, H.E. and Ross, G.M. 1993. $^{40}\text{Ar}/^{39}\text{Ar}$ geochronology of selected crystalline basement samples from the Alberta Basin: the timing of Proterozoic assembly of the subsurface of western Canada. In *Radiogenic age and isotopic studies: Report 7. Geological Survey of Canada Paper 93-2*, pp. 71-82.
- Poole, W.H. 1967. Tectonic Evolution of Appalachian Region of Canada. In *Collected Papers on the geology of the Atlantic Region. Edited by E.R.W. Neale and H. Williams. The Geological Association of Canada, Special Paper No. 4*, pp. 9-51.
- Poole, W.H. 1976. Plate tectonic evolution of the Canadian Appalachian Region. *Geological Survey of Canada, Paper 76-1B*, pp. 113-126.
- Poole, W.H. 1980. Rb-Sr age of some granitic rocks between Ludgate Lake and Negro Harbour, southwestern New Brunswick. In *Current Research, Part C, Rb-Sr and U-Pb Isotopic Age Studies, Geological Survey of Canada, Paper 80-1C*, pp. 170-173.
- Poole, W.H. and Rodgers, J. 1972. Appalachian geotectonic elements of the Atlantic Provinces and southern Quebec. In *Twenty-fourth International Geological Congress Guidebook. Edited by D.J. Glass. Excursion A63 and C63*, 200 p.
- Poole, W.H., Kelley, D.G., and Neale, E.R.W. 1964. Age and correlation problems in the Appalachian Region of Canada. In *Geochronology in Canada. Edited by F.F. Osborne. The Royal Society of Canada Special Publication, No. 8*, pp. 61-84.
- Poole, W.H., Sanford, B.V., Williams, H., and Kelly, D.G. 1970. Geology of southeastern Canada. In *Geology and Economic Minerals of Canada. Edited by R.J.W. Douglas. Geological Survey of Canada, Department of Energy, Mines and Resources, Economic Geology Report No. 1*, pp. 228-304.
- Postma, G. 1986. Classification for sediment gravity-flow deposits based on flow conditions during sedimentation. *Geology*, 14: 291-294.
- Potter, R.R., Bingley, J.M., and Smith, J.C. 1972. Appalachian stratigraphy and structure of the Maritime Provinces. In *Twenty-fourth International Geological Congress Guidebook. Edited by D.J. Glass. Excursion A57-C57*, 48 p.
- Powell, R., Condcliffe, D.M., and Condcliffe, E. 1984. Calcite-dolomite geothermometry in the system $\text{CaCO}_3\text{-MgCO}_3\text{-FeCO}_3$: an experimental study. *Journal of Metamorphic Geology*, 2: 33-41.
- Raeside, R.P. and Barr, S.M. 1990. Geology and tectonic development of the Bras d'Or suspect terrane, Cape Breton Island. *Canadian Journal of Earth Sciences*, 27: 1371-1381.
- Rast, N. 1979. Precambrian meta-diabase of southern New Brunswick - the opening of the Iapetus Ocean? *Tectonophysics*, 59: 127-137.
- Rast, N. 1989. The evolution of the Appalachian Chain. In *The Geology of North America-An Overview. Edited by A.W. Bailey and A.R. Palmer. Geological Society of America, The Geology of North America, A: 323-348*.
- Rast, N. and Currie, K.L. 1976. On the position of the Variscan Front in southern New Brunswick and its relation to Precambrian basement. *Canadian Journal of Earth Sciences*, 13: 194-196.
- Rast, N. and Dickson, W.L. 1982. The Pocologan mylonite zone. In *Major Structural Zones and Faults of the Northern Appalachians. Edited by P. St-Julien and J. Beland. Geological Society of Canada, Special Paper 24*, pp. 249-261.
- Rast, N. and Grant, R.H. 1973a. Transatlantic correlation of the Variscan - Appalachian Orogeny. *American Journal of Science*, 273: 572-579.

- Rast, N. and Grant, R.H. 1973b. The Variscan Front in southern New Brunswick. In *Geology of New Brunswick*. Edited by N. Rast. 1973 New England Intercollegiate Geological Conference, pp. 4-11.
- Rast, N. and Skehan, S.J., J.W. 1983. The evolution of the Avalonian Plate. *Tectonophysics*, 100: 257-286.
- Rast, N. and Skehan, S.J., J.W. 1991. Tectonic relationships of Carboniferous and Precambrian rocks in southwestern New Brunswick. 1991. In *Geology of the Coastal Lithotectonic Block and Neighboring Terranes, Eastern Maine and Southern New Brunswick*. Edited by A. Ludman. Eighty-third New England Intercollegiate Geological Conference, pp. 209-221.
- Rast, N. and Stringer, P. 1974. Recent advances and the interpretation of the geological structure of New Brunswick. *Geoscience Canada*, 1: 15-25.
- Rast, N., Kennedy, M.J., and Blackwood, R.F. 1976a. Comparison of some tectonostratigraphic zones in the Appalachians of Newfoundland and New Brunswick. *Canadian Journal of Earth Sciences*, 13: 868-875.
- Rast, N., O'Brien, B.H., and Wardle, R.J. 1976b. Relationships between Precambrian and lower Paleozoic rocks of the "Avalon Platform" in New Brunswick, the northeast Appalachians, and the British Isles. *Tectonophysics*, 30: 315-338.
- Rast, N., Dickson, W.L., and Grant, R.H. 1978a. Precambrian basement in southwestern New Brunswick. In *Guidebook for field trips in southeastern Maine and southwestern New Brunswick*. Edited by A. Ludman. Seventieth New England Intercollegiate Geological Conference, pp. 108-119.
- Rast, N., Grant, R.H., Parker, J.S.D., and Teng, H.C. 1978b. The Carboniferous deformed rocks west of Saint John, New Brunswick. In *Guidebook for field trips in southeastern Maine and southwestern New Brunswick*. Edited by A. Ludman. Seventieth New England Intercollegiate Geological Conference, pp. 162-173.
- Rex, D.C., Guise, P.G., and Wartho, J.-A. 1993. Disturbed $^{40}\text{Ar}/^{39}\text{Ar}$ spectra from hornblendes: thermal loss or contamination. *Chemical Geology, Isotope Geoscience Section*, 103: 271-281.
- Reynolds, P.H., Jamieson, R.A., Barr, S.M., and Raeside, R.P. 1989. An $^{40}\text{Ar}/^{39}\text{Ar}$ study of the Cape Breton Islands, Nova Scotia: thermal histories and tectonic implication. *Canadian Journal of Earth Sciences*, 26: 2081-2091.
- Richards, N.A. 1971. Structure in the Precambrian and Paleozoic rocks at Saint John, New Brunswick. Unpublished M.Sc Thesis, University of New Brunswick, Fredericton, New Brunswick, 73 p.
- Roberts, W. and Williams, P.F. 1993. Evidence for early Mesozoic extensional faulting in Carboniferous rocks, southern New Brunswick, Canada. *Canadian Journal of Earth Sciences*, 30: 1324-1331.
- Robb, J. 1841. Remarks upon certain geological features of the River Saint John in New Brunswick, with an account of the falls upwards from the sea, which occur near its embouchure in the Bay of Fundy. *British Association for the Advancement of Science, Report of the Tenth Meeting*, pp. 115-118.
- Robb, J. 1950a. The agricultural capabilities of the province as indicated by its geological structure (with map and marginal notes by Dr. James Robb). In J.F.W. Johnston: *Report on the Agricultural Capabilities of the Province of New Brunswick*, Fredericton, New Brunswick, pp. 5-9.
- Robb, J. 1950b. Existence of coal in New Brunswick. In J.F.W. Johnston: *Report on the Agricultural Capabilities of the Province of New Brunswick*, Fredericton, New Brunswick, pp. 16-18.
- Roddick, J.C., Quigg, F.B., and Hunt, P.A. 1992. Miscellaneous $^{40}\text{Ar}/^{39}\text{Ar}$ ages and analytical procedures. In *Radiogenic age and isotopic studies: Report 6*. Geological Survey of Canada Paper 92-2, pp. 171-177.

- Rodgers, J. 1967. Chronology of tectonic movements in the Appalachian Region of eastern North America. *American Journal of Science*, 265: 408-427.
- Rodgers, J. 1970. The tectonics of the Appalachians. Wiley-Interscience, New York, 271 p.
- Rodgers, J. 1972. Latest Precambrian (post-Grenville) rocks of the Appalachian Region. *American Journal of Science*, 272: 507-520.
- Rothstein, D.A. and Hoisch, T.D. 1994. Multiple intrusions and low-pressure metamorphism in the central Old Woman Mountains, southeastern California: constraints from thermal modelling. *Journal of Metamorphic Geology*, 12: 723-734.
- Ruitenbergh, A.A. 1969. Mineral deposits in granitic intrusions and related metamorphic aureoles in parts of the Welsford, Loch Alva, Musquash, and Pennfield areas. New Brunswick Department of Natural Resources, Mineral Resources Division, Report of Investigation No. 9, 24 p.
- Ruitenbergh, A.A. and McCutcheon, S.R. 1980. Volcanism and mineralization in southwestern New Brunswick. Geological Association of Canada/Mineralogical Association of Canada, Field Trip Guidebook 17, Halifax, Nova Scotia, 36 p.
- Ruitenbergh, A.A., Venugopal, D.V., and Giles, P.S. 1973a. "Fundy Cataclastic Zone," New Brunswick: evidence for post-Acadian penetrative deformation. *Geological Society of America Bulletin*, 84: 3029-3044.
- Ruitenbergh, A.A., Giles, P.S., Venugopal, D.V., and McCutcheon, S.R. 1973b. A brief summary of the Late Precambrian rocks in the Caledonia Highlands of southeastern New Brunswick. *Maritime Sediments*, 9: 83-87.
- Ruitenbergh, A.A., Giles, P.S., and Venugopal, D.V. 1973c. Stratigraphy and structure of Late Precambrian rocks in the Caledonia Highlands, New Brunswick. Abstract in *Maritime Sediments*, 9: 66-67.
- Ruitenbergh, A.A., Giles, P.S., Venugopal, D.V., Buttimer, S.M., McCutcheon, S.R., and Chandra, J. 1975. Geological maps to accompany: Geology and mineral deposits, Caledonia area. New Brunswick Department of Natural Resources, Mineral Resources Division.
- Ruitenbergh, A.A., Fyffe, L.R., McCutcheon, S.R., St. Peter, C.J., Irrinki, R.R., and Venugopal, D.V. 1977. Evolution of pre-Carboniferous Tectonostratigraphic zones in the New Brunswick Appalachians. *Geoscience Canada*, 4: 171-181.
- Ruitenbergh, A.A., Giles, P.S., Venugopal, D.V., Buttimer, S.M., McCutcheon, S.R., and Chandra, J. 1979. Geology and Mineral Deposits, Caledonia area. New Brunswick Department of Natural Resources, Mineral Resources Branch, Memoir 1, 213 p.
- Ruther, M.J., Van der Laan, S.R., and Willie, P.J. 1989. Experimental igneous barometer: aluminum in hornblende at 10 Kbar pressure. *Geology*, 17: 897-900.
- St. Peter, C. 1993. Maritimes Basin evolution: key geologic and seismic evidence from the Moncton Subbasin of New Brunswick. *Atlantic Geology*, 29: 233-270.
- St. Peter, C. and Fyffe, L.R. 1990. Structural trends and basement rock subdivisions in the western Gulf of St. Lawrence: Discussion. *Atlantic Geology*, 26: 277-279.
- Samson, S.D. in press. Is the Carolina terrane part of Avalon. In *New Perspectives in the Appalachian-Caledonia Orogen*. Edited by J.P. Hibbard, C.R. van Staal, and P.A. Cawood. Geological Association of Canada, Special Paper 41.
- Sangster, A.L., Hunt, P.A., and Mortensen, J.K. 1990. U-Pb geochronology of the Lime Hill gneissic complex, Cape Breton Island, Nova Scotia. *Atlantic Geology*, 26: 229-236.

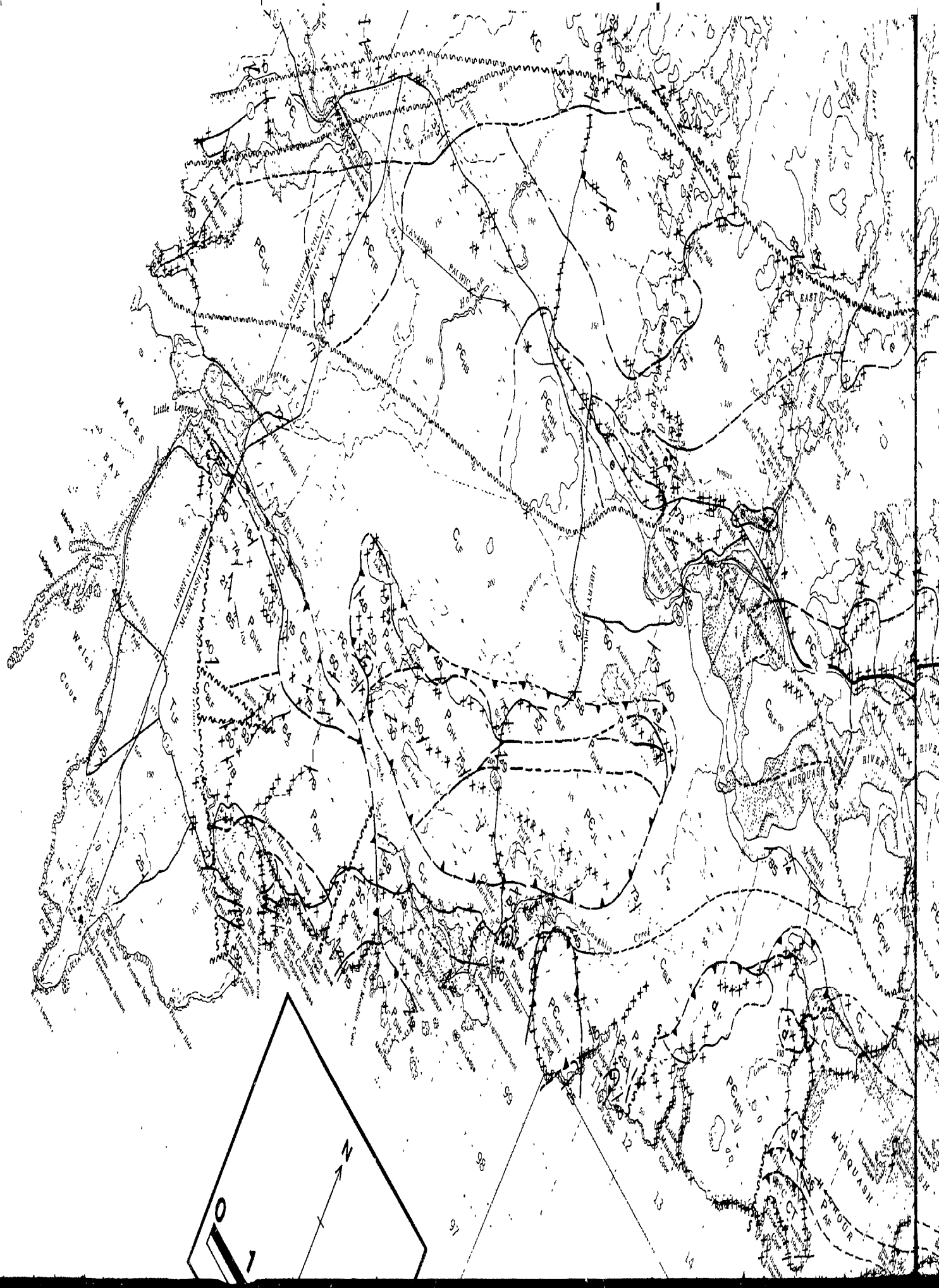
- Sarjeant, W.A.S. and Stringer, P. 1978. Triassic reptile tracks in the Lepreau Formation, southern New Brunswick, Canada. *Canadian Journal of Earth Sciences*, 15: 594-602.
- Scaillet, S., Feraud, G., Ballevre, M., and Amouric, M. 1992. Mg/Fe and [(Mg,Fe)Si-Al₂] compositional control on argon behaviour in high-pressure white micas: a ⁴⁰Ar/³⁹Ar continuous laser-probe study from the Dora-Maira nappe of the internal western Alps, Italy. *Geochimica et Cosmochimica Acta*, 56: 2851-2872.
- Schenk, P.E. 1971. Southeastern Atlantic Canada, northwest Africa, and Continental Drift. *Canadian Journal of Earth Sciences*, 8: 1218-1251.
- Schenk, P.E. 1978. Synthesis of the Canadian Appalachians. In *Caledonian-Appalachian Orogen of the North Atlantic Region*; Geological Survey of Canada Paper 78-13, pp. 111-136.
- Shand, S.J. 1947. Eruptive rocks. Their genesis, composition, classification, and their relation to ore-deposits, 3rd edition. J. Wiley and Sons, New York, 488 p.
- Shelly, D. 1993. Igneous and metamorphic rocks under the microscope: classification, textures, microstructures, and mineral preferred orientations. Chapman and Hall, London, 445 p.
- Shervais, J.W. 1977. Ti-V plots and the petrogenesis of modern and ophiolitic lavas. *Earth and Planetary Science Letters*, 59: 101-118.
- Simpson, C. and Schmidt, S.M. 1983. An evaluation of the criteria to deduce the sense of movement in sheared rocks. *Geological Society of America Bulletin*, 94: 1281-1288.
- Skehan, S.J., J.W. 1988. Evolution of the Iapetus Ocean and its borders in the pre-Arenig times: a synthesis. In *The Caledonian - Appalachian Orogen*. Edited by A.L. Harris and D.J. Fettes. Geological Society Special Publication No. 28, pp. 185-229.
- Skehan, S.J., J.W. and Rast, N. 1983. Relationships between Precambrian and Lower Paleozoic rocks of southeastern New England and other North Atlantic Avalonian terranes. In *Regional trends in the geology of the Appalachian - Caledonian - Hercynian - Mauritanide Orogen*. Edited by P.E. Schenk, pp. 131-162.
- Skehan, S.J., J.W., Murray, D.P., Palmer, A.R., and Smith, A.T. 1978. Significance of fossiliferous Middle Cambrian rocks of Rhode Island to the history of Avalonian microcontinent. *Geology*, 6: 694-698.
- Smith, J.C. 1966. Geology of southwestern New Brunswick. In *Geology of parts of Atlantic Provinces Guidebook*. Edited by W.H. Poole. The Geological Association of Canada and the Mineralogical Association of Canada, pp. 1-18.
- Snee, L.W. 1982. Determination of thermal histories in complex plutonic terranes by use of details of ⁴⁰Ar/³⁹Ar age-spectrum diagrams. Abstract in EOS, Transactions of the American Geophysical Union, 63: 453.
- Snee, L.W., Sutter, J.F., and Kelly, W.C. 1988. Thermochronology of economic mineral deposits: dating the stages of mineralization at Panasqueira, Portugal, by high-precision ⁴⁰Ar/³⁹Ar age spectrum techniques on muscovite. *Economic Geology*, 83: 335-354.
- Spear, F.S. 1991. On the interpretation of peak metamorphic temperatures in light of garnet diffusion during cooling. *Journal of Metamorphic Geology*, 9: 379-388.
- Spear, F.S. and Cheney, J.T. 1989. A petrogenetic grid for pelitic schists in the system SiO₂-Al₂O₃-FeO-MgO-K₂O-H₂O. *Contributions to Mineralogy and Petrology*, 101: 149-164.
- Steiger, R.H. and Jager, E. 1977. Subcommittee on geochronology: convention on the use of decay constants in geo- and cosmochronology. *Earth and Planetary Science Letters*, 36: 359-362.

- Stevens, R.D., DeLabio, R.N., and Lachance, G.R. 1982. Age Determinations and Geological Studies, K-Ar Isotopic Ages, Report 15. Geological Survey of Canada, Department of Energy, Mines and Resources, Paper 81-2, pp. 45.
- Stopes, H.C. 1914. The "Fern Ledges" Carboniferous Flora of Saint John, New Brunswick. Geological Survey of Canada, Memoir 41, 142 p.
- Stormer, J.C.Jr. 1975. A practical two-feldspar geothermometer. *American Mineralogist*, 60: 667-674.
- Streckeisen, A.L. 1976. To each plutonic rock its proper name. *Earth Science Reviews*, 12: 1-33.
- Streckeisen, A.L. 1979. Classification and nomenclature of volcanic rocks, lamprophyres, carbonitites, and melilitic rocks: recommendations and suggestions of the IUGS subcommission on the systematics of igneous rocks. *Geology*, 7: 331-335.
- Stringer, P. 1978. Folding and cleavage in Triassic rocks of southwestern New Brunswick. In *Guidebook for field trips in southeastern Maine and southwestern New Brunswick*. Edited by A. Ludman. Seventieth New England Intercollegiate Geological Conference, pp. 57-77.
- Stringer, P. and Burke, K.B.S. 1985. Structure in southwestern New Brunswick. The Geological Association of Canada and the Mineralogical Association of Canada Field Excursion 9, Fredericton, New Brunswick, 34 p.
- Stringer, P. and Wardle, R.J. 1973. Post-Carboniferous and post-Triassic structures in southern New Brunswick. In *Geology of New Brunswick*. Edited by N. Rast. New England Intercollegiate Geological Conference, Field Guide to Excursions, pp. 88-95.
- Strong, D.F., Dickson, W.L., and Pickerill, R.K. 1979. Chemistry and prehnite-pumpellyite facies metamorphism of calc-alkaline Carboniferous volcanic rocks of southeastern New Brunswick. *Canadian Journal of Earth Sciences*, 16: 1071-1085.
- Stukas, V. 1978. Plagioclase release patterns: a high resolution $^{40}\text{Ar}/^{39}\text{Ar}$ study. Unpublished Ph.D. thesis, Dalhousie University, Halifax, Nova Scotia, 162 p.
- Subhas, T. 1970. Structural analysis of the Musquash area, Saint John County, New Brunswick. Unpublished M.Sc. Thesis, University of New Brunswick, Fredericton, New Brunswick, 97 p.
- Tanoli, S.K. and Pickerill, R.K. 1988. Lithostratigraphy of the Cambrian-Lower Ordovician Saint John Group, southern New Brunswick. *Canadian Journal of Earth Sciences*, 25: 669-690.
- Tanoli, S.K. and Pickerill, R.K. 1990. Lithofacies and basinal development of the type 'Echeminian Series' (Lower Cambrian Ratcliffe Brook Formation), Saint John area, southern New Brunswick. *Atlantic Geology*, 26: 57-78.
- Thompson, A.B. 1976. Mineral reactions in pelitic rocks: Parts I and II. *American Journal of Science*, 276: 401-454.
- Thompson, J.B. Jr. 1979. The tschermak substitution and reactions in pelitic schists. In *Problems in Physicochemical Petrology*. Edited by V.A. Zharikov, V.I. Fonarev, and S.P. Korikouskii. Academy of Sciences. Moscow, pp. 146-159.
- Thornton, C.P. and Tuttle, O.F. 1960. Chemistry of igneous rocks. I. differentiation index. *American Journal of Science*, 258: 664-684.
- Tindle, A.G. and Pearce, J.A. 1981. Petrogenetic modelling of in situ fractional crystallization in the zoned Loch Doon Pluton, Scotland. *Contributions to Mineralogy and Petrology*, 78: 196-207.
- Tracy, R.J. 1982. Compositional zoning and inclusions in metamorphic minerals. In *Characterization of Metamorphism through Mineral Equilibria*. Edited by J.M. Ferry. Mineralogical Society of America Reviews in Mineralogy, 10: 355-397.
- Tucker, R.D., Raheim, A., Krogh, T.E., and Corfu, F. 1987. Uranium-lead zircon and titanite ages from the northern portion of the Western Gneiss Region, south-central Norway. *Earth and Planetary Science Letters*, 81: 203-211.

- Turner, F.J. 1980. *Metamorphic petrology: mineralogical, field, and tectonic aspects*, second edition. McGraw-Hill International Series in the Earth and Planetary Sciences, New York, New York, 524 p.
- Turner, G. 1968. The distribution of potassium and argon in chondrites. *In Origin and distribution of the elements. Edited by L.H. Ahrens*, pp. 387-398.
- Turner, G., Miller, J.A., and Grasby, R.L. 1966. The thermal history of the Bruderheim meteorite. *Earth and Planetary Science Letters*, 1: 155-157.
- van de Poll, H.W. 1970. *Stratigraphical and sedimentological aspects of Pennsylvanian strata in southern New Brunswick*. Unpublished Ph.D. Thesis, University of Wales, 140 p.
- Van Hise, C.R. 1892. Archean and Algonkian. *United States Geological Survey Bulletin No. 86*, 549 p.
- Wanless, R.K., Stevens, R.D., Lachance, G.R., and Rimsaite, J.Y.H. 1966. Age Determinations and Geological Studies, K-Ar Isotopic Ages, Report 6. Geological Survey of Canada, Department of Energy, Mines and Resources, Paper 65-17, pp. 93.
- Wanless, R.K., Stevens, R.D., Lachance, G.R., and Delabio, R.N. 1972. Age Determinations and Geological Studies, K-Ar Isotopic Ages, Report 9. Geological Survey of Canada, Department of Energy, Mines and Resources, Paper 69-2A, pp. 69.
- Wanless, R.K., Stevens, R.D., Lachance, G.R., and Delabio, R.N. 1972. Age Determinations and Geological Studies, K-Ar Isotopic Age, Report 10. Geological Survey of Canada, Department of Energy, Mines and Resources, Paper 71-2, pp. 68-69.
- Wanless, R.K., Stevens, R.D., Lachance, G.R., and Delabio, R.N. 1973. Age Determinations and Geological Studies, K-Ar Isotopic Ages, Report 11. Geological Survey of Canada, Department of Energy, Mines and Resources, Paper 73-2, pp. 83-85.
- Wardle, R.J. 1978. *The stratigraphy and tectonics of the Green Head Group: Its relation to Hadrynian and paleozoic rocks, southern New Brunswick*. Unpublished Ph.D. Thesis, University of New Brunswick, Fredericton, New Brunswick, 295 p.
- Wardle, R.J. and O'Brien, B.H. 1973. Structure and magmatic sequence in the Coldbrook and Green Head groups, southern New Brunswick. *Abstract in Maritime Sediments*, 9: 67.
- Watters, S.E. 1993. *Structure and alteration related to Hercynian gold deposition, Cape Spencer, New Brunswick, Canada*. Unpublished Ph.D. Thesis, University of Western Ontario, London, Ontario, 351 p.
- Webb, G.W. 1963. Occurrence and exploration significance of strike-slip faults in southern New Brunswick, Canada. *Bulletin of the American Association of Petroleum Geologists*, 47: 1904-1927.
- Weeks, L.J. 1957. The Appalachian Region. *In Geology and Economic Minerals of Canada*, 4th Edition. Edited by C.H. Stockwell. Geological Survey of Canada, Economic Geology Series No. 1, pp. 123-205.
- Whalen, J.B., Currie, K.L., and Chappell, B.W. 1987. A-type granites: geochemical characteristics, discrimination and petrogenesis. *Contributions to Mineralogy and Petrology*, 95: 407-419.
- Whalen, J.B., Jenner, G.A., Currie, K.L., Barr, S.M., Longstaffe, F.J., and Hegner, E. 1994. Geochemical and isotopic characteristics of granitoids of the Avalon Zone, southern New Brunswick: possible evidence of repeated delamination events. *Journal of Geology*, 102: 269-282.
- White, C.E. 1994. *Geology of the Brookville terrane, southern New Brunswick, Canada: Implications for extent of the Avalon Terrane*. Northeastern Geological Society of America 29th Annual Meeting, Abstracts with Programs, 29: 80.

- White, C.E. and Barr, S.M. 1991. Contrasting plutonic units in the Brookville and Caledonia Terranes in the Saint John area of southern New Brunswick. In *Geology of the Coastal Lithotectonic Block and Neighboring Terranes, Eastern Maine and Southern New Brunswick*. Edited by A. Ludman. Eighty-third New England Intercollegiate Geological Conference, pp. 374-388.
- White, C.E. and Barr, S.M. in press. Geology of the Brookville terrane, southern New Brunswick, Canada. In *Avalonian and related periGondwanan terranes of the Circum-North Atlantic*. Edited by R.D. Nance and M.D. Thompson. Geological Society of America Special Paper.
- White, C.E. and Deveau, K.A. 1989. Petrology of the Brookville Gneiss and Golden Grove Intrusive Suite, southern New Brunswick. Abstract in *Atlantic Geology*, 25: 171.
- White, C.E., Barr, S.M., and Bevier, M.L. 1990a. Late Precambrian ages for the Brookville Gneiss, southern New Brunswick: implications for stratigraphy of the Avalon Terrane. Abstract in *Atlantic Geology*, 26: 189.
- White, C.E., Barr, S.M., Bevier, M.L., and Deveau, K.A. 1990b. Field relations, composition, and age of plutonic units in the Saint John area of southern New Brunswick. *Atlantic Geology*, 26: 259-270.
- White, C.E., Bevier, M.L., and Barr, S.M. 1990c. New U-Pb ages for the Brookville Gneiss and revised Avalonian stratigraphy in the Canadian Appalachian orogen. Northeast Geological Society of America 25th Annual Meeting, Abstract with Programs, 22: 78.
- White, C.E., Culshaw, N.G., and Barr, S.M. 1991. Significance of calcite mylonites along the Brookville-Caledonia terrane boundary, New Brunswick, Canada. Northeastern and Southeastern Geological Society of America 26th Annual Meeting, Abstracts with Programs, 23: 148.
- White, C.E., Barr, S.M., Bevier, M.L., Kamo, S. 1994. A revised interpretation of Cambrian and Ordovician rocks in the Bourinot belt of central Cape Breton Island, Nova Scotia. *Atlantic Geology*, 30: 123-142.
- White, R.W. and Clarke, G.L. 1994. Garnet-forming reactions and recrystallization in high-grade mylonite zones, MacRobertson Land, east Antarctic. *Journal of Metamorphic Geology*, 12: 853-865.
- Wickham, S.M. and Oxburgh, E.R. 1987. Low-pressure regional metamorphism in the Pyrenees and its implications for the thermal evolution of rifted continental crust. *Philosophical Transactions of the Royal Society of London*, A321: 219-242.
- Williams, P.F. and Hy, C. 1990. Origin and deformational and metamorphic history of gold-bearing quartz veins on the Eastern Shore of Nova Scotia. In *Mineral deposit studies in Nova Scotia 1*. Edited by A.L. Sangster. Geological Survey of Canada, Paper 90-8, pp. 169-194.
- Williams, G.L., Fyffe, L.R., Wardle, R.L., Colman-Sadd, S.P., and Boehner, R.C. 1985. *Lexicon of Canadian Stratigraphy, Volume VI, Atlantic Region*. Canadian Society of Petroleum Geologists, Calgary, 572 p.
- Williams, H. 1964. The Appalachians in northeastern Newfoundland - a two-sided symmetrical system. *American Journal of Science*, 262: 1137-1158.
- Williams, H. 1978. Tectonic lithofacies map of the Appalachians. Memorial University Map No. 1, Department of Geology, Memorial University of Newfoundland, Canada.
- Williams, H. 1979. The Appalachian Orogen in Canada. *Canadian Journal of Earth Sciences*, 16: 792-807.
- Williams, H. and Hatcher, R.D., Jr. 1983. Appalachian suspect terranes. In *Contributions to the tectonics and geophysics of Mountain Chains*. Edited by R.D. Hatcher, Jr., H. Williams and I. Zietz. Geological Society of America, Memoir 158, pp. 33-53.

- Williams, H., Kennedy, M.J., and Neale, E.R.W. 1972. The Appalachian structural province. In *Variations in Tectonic Styles in Canada*. Edited by R.A. Price and R.J.W. Douglas. The Geological Association of Canada, Special Paper No. 11, pp. 182-261.
- Winchester, J.A. and Floyd, P.A. 1977. Geochemical discrimination of different magma series and their differentiation products using immobile elements. *Chemical Geology*, 20: 321-355.
- Wright, W.J. and Clements, C.S. 1943. Coal deposits of Lepreau-Musquash district, New Brunswick. *Acadian Naturalist*, 1: 5-27.
- Xu, G., Powell, R., Wilson, C.J.L., and Will, T.M. 1994. Contact metamorphism around the Stawell granite, Victoria, Australia. *Journal of Metamorphic Geology*, 12: 609-624.
- Yardley, B.W.D. 1989. An introduction to metamorphic petrology. Longman Earth Science Series, New York, New York, 248 p.
- Young, G.A. 1913. Saint John and Vicinity. In *Geological Survey of Canada Guide Book No. 1 - Excursions in Eastern Quebec and the Maritime Provinces, Part 2*, pp. 369-395.
- Yu, Y. and Morse, S.A. 1992. Age and cooling history of the Kiglapait Intrusion from an $^{40}\text{Ar}/^{39}\text{Ar}$ study. *Geochimica et Cosmochimica Acta*, 56: 2471-2485.
- Zain Eldeen, U. 1991. The geology of the Dipper Harbour area, southern New Brunswick, Canada. Unpublished M.Sc. Thesis, Ohio University, Athens, Ohio, 151 p.
- Zain Eldeen, U., Yan, N., Manuel, L.M., Nance, R.D., Doig, R., and Dallmeyer, R.D. 1991. Late Carboniferous sedimentation and tectonics in the Chance Harbour-Dipper Harbour area, southern New Brunswick, Canada. *Northeast Geological Society of America, Abstracts with Programs*, 23: 153.
- Zen, E-an. 1983. Exotic terranes in the New England Appalachians-limits, candidates, and ages: a speculative essay. In *Contributions to the tectonics and geophysics of Mountain Chains*. Edited by R.D. Hatcher, Jr., H. Williams, and I. Zietz. Geological Society of America, Memoir 158, pp. 55-81.





NEW RIVER BEACH FAULT

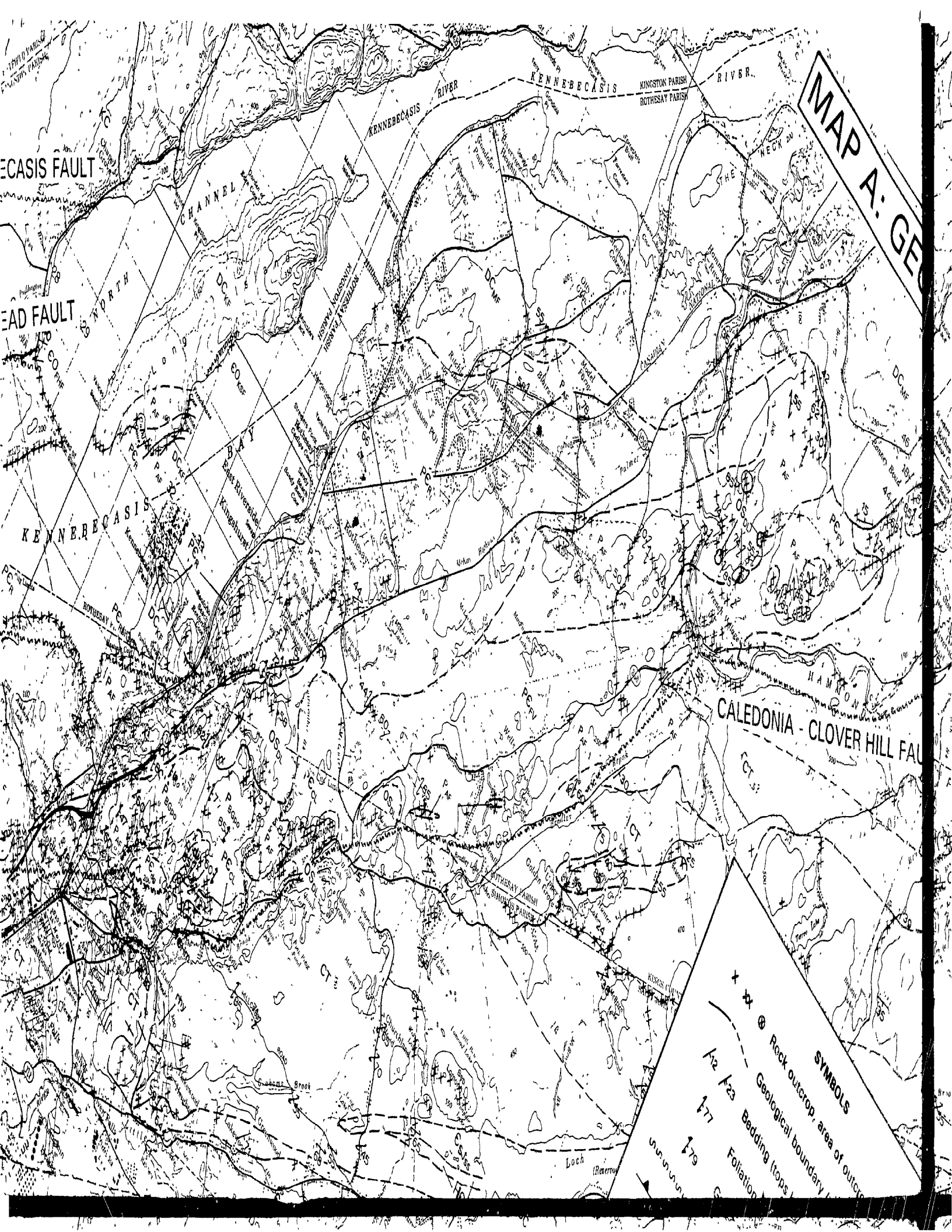
KENNEBECASIS

MILKISH HEAD FAULT

GRAND BAY

CALEDONIA - CLOVER HILL FAULT

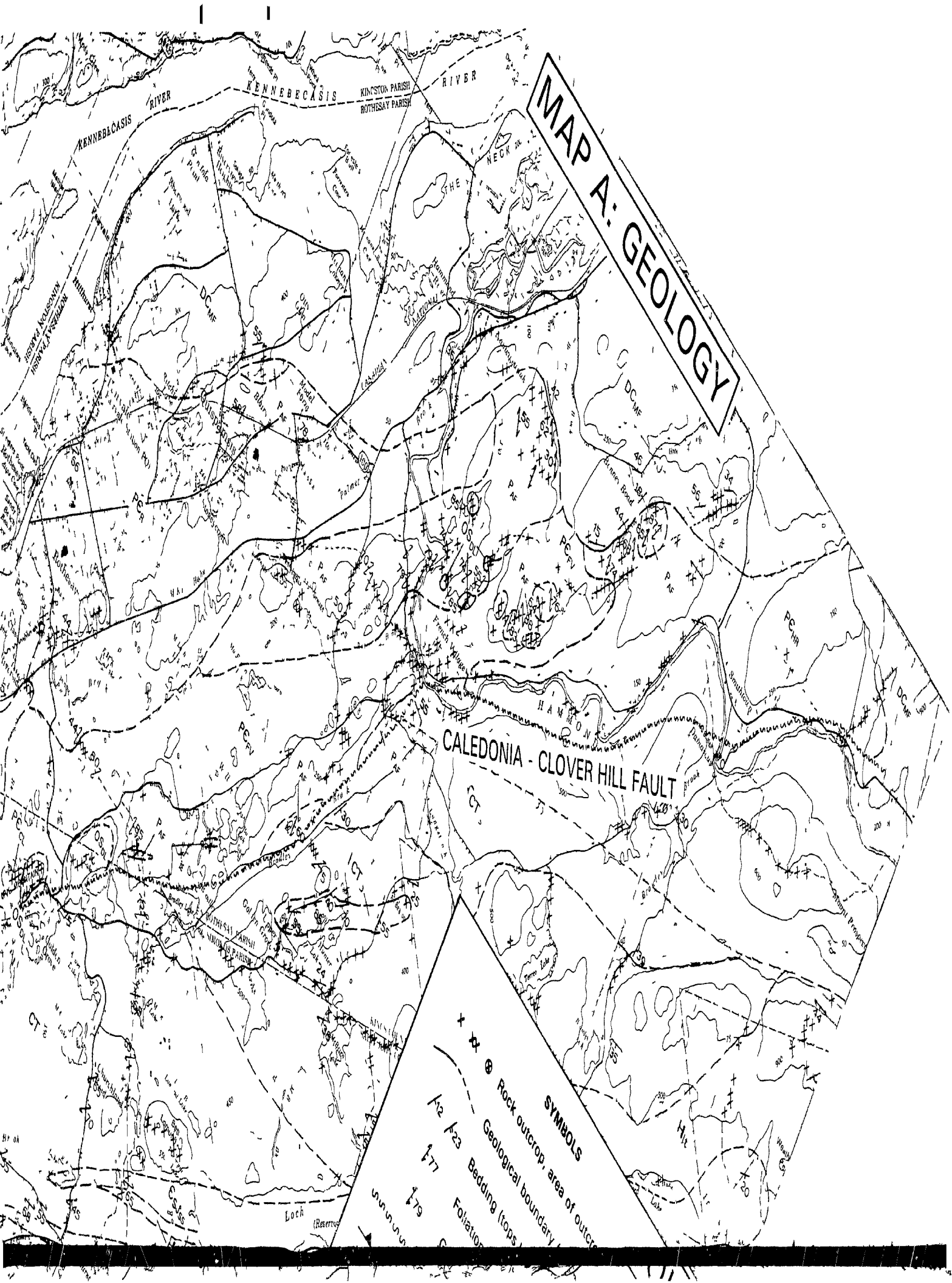
MAP A: GE

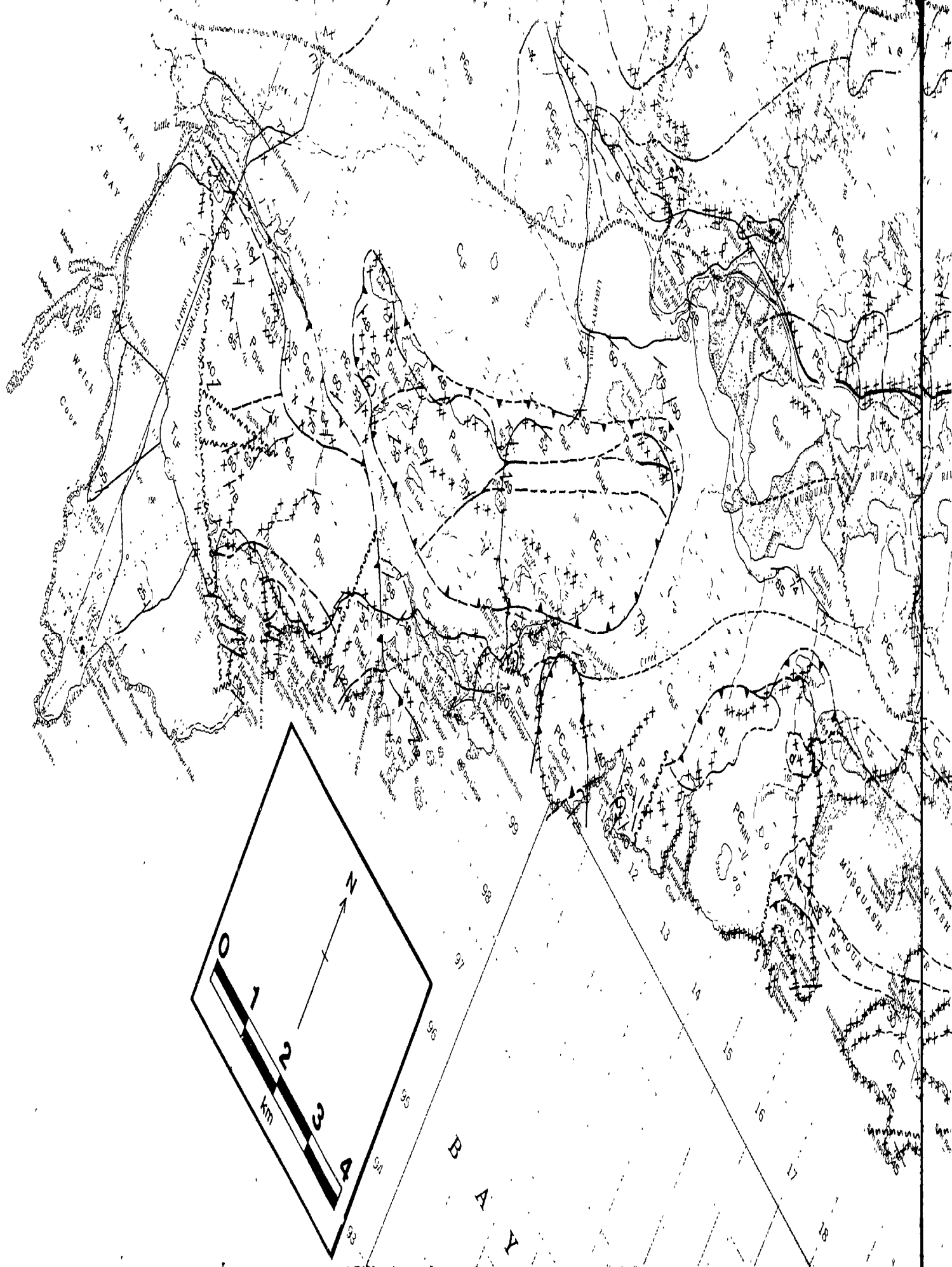


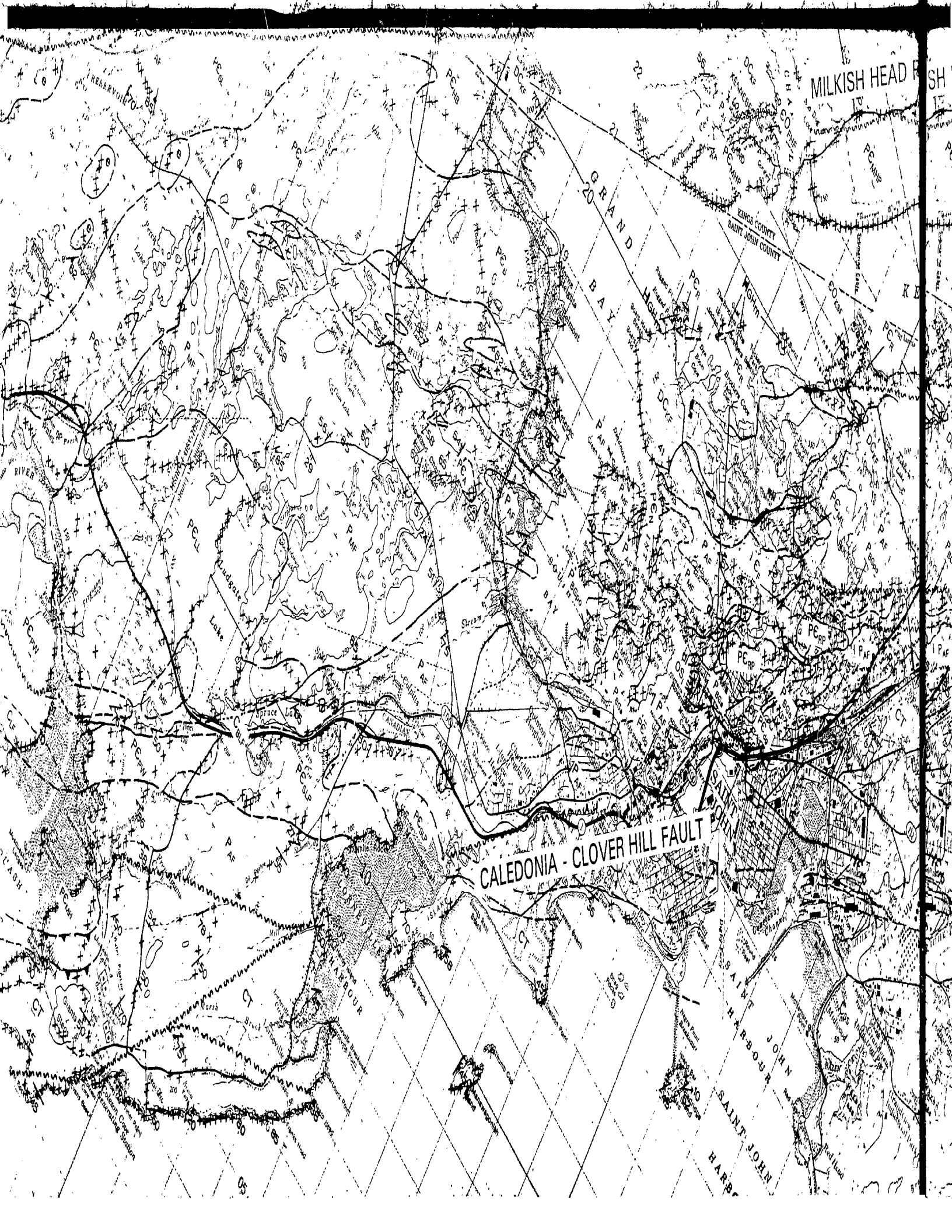
SYMBOLS

- + x ⊗ Rock outcrop, area of outcrop
- 1/2 1/3 Bedding (tops)
- 177 178 Foliation

MAP A: GEOLOGY







MILKISH HEAD

GRAND BAY

KINGS COUNTY
SAINT JOHN COUNTY

CALEDONIA - CLOVER HILL FAULT

SAINT JOHN
HARBOR

HEAD FAULT

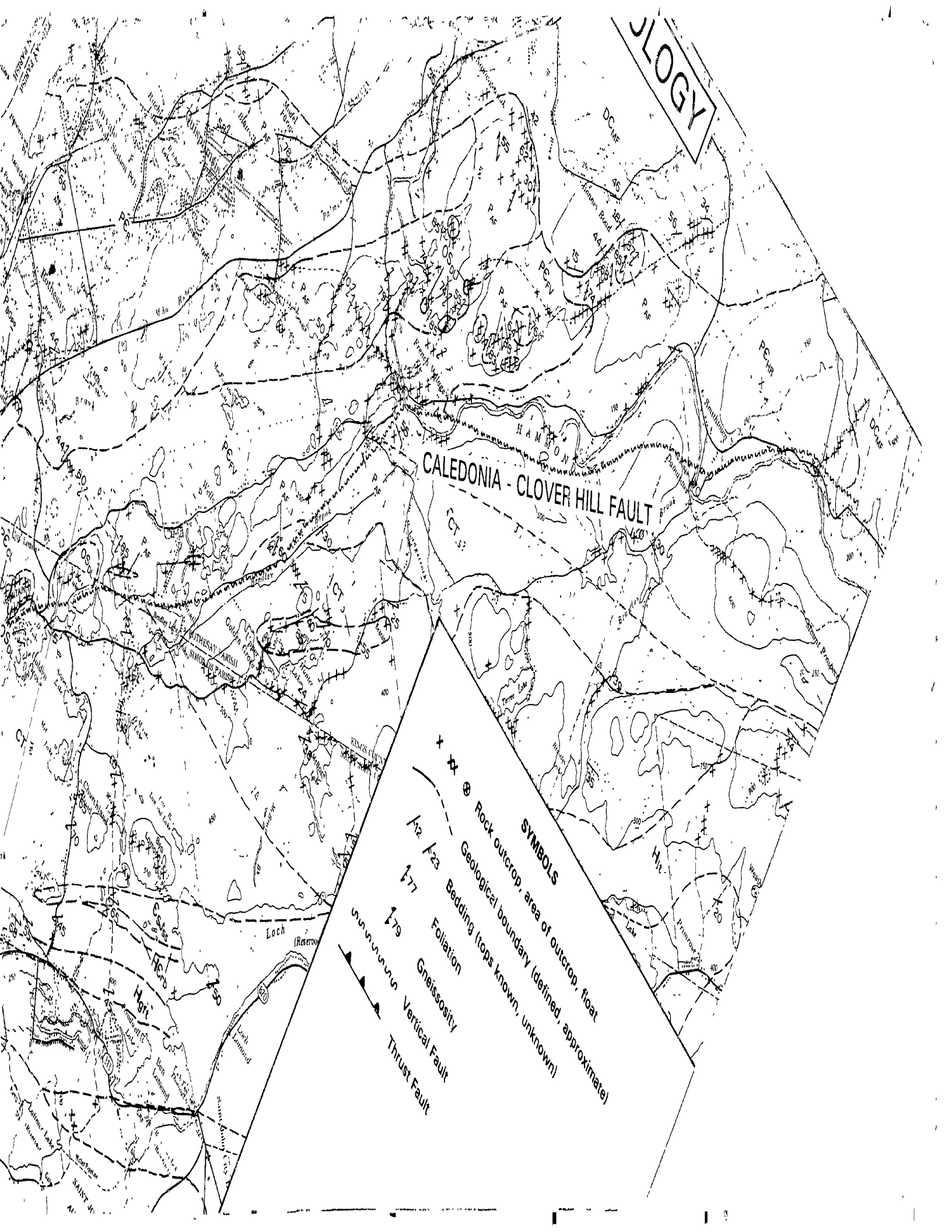
KENNERECASIS

BAY

CALEDONIA - CLOVER HILL



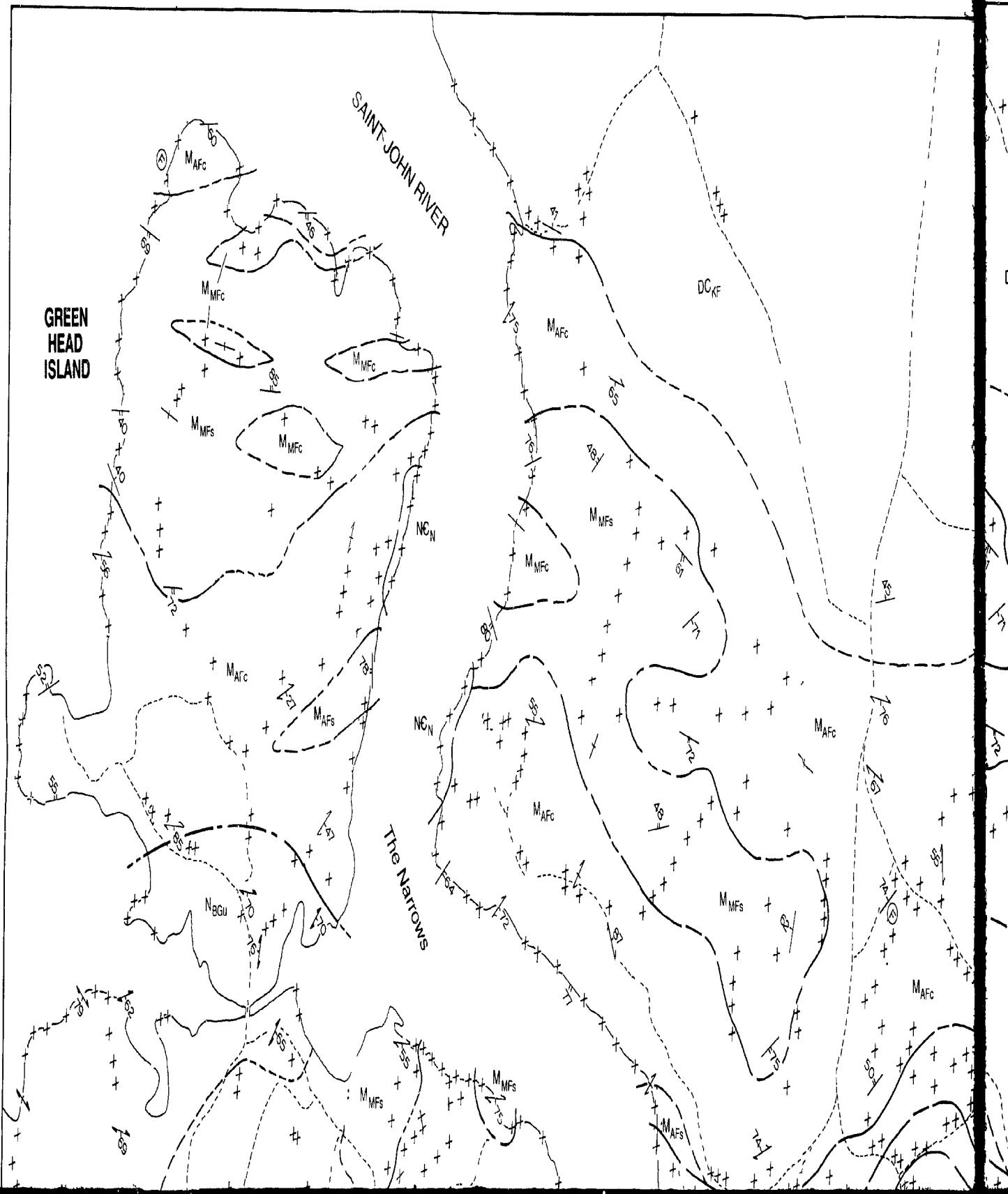
GEOLOGY

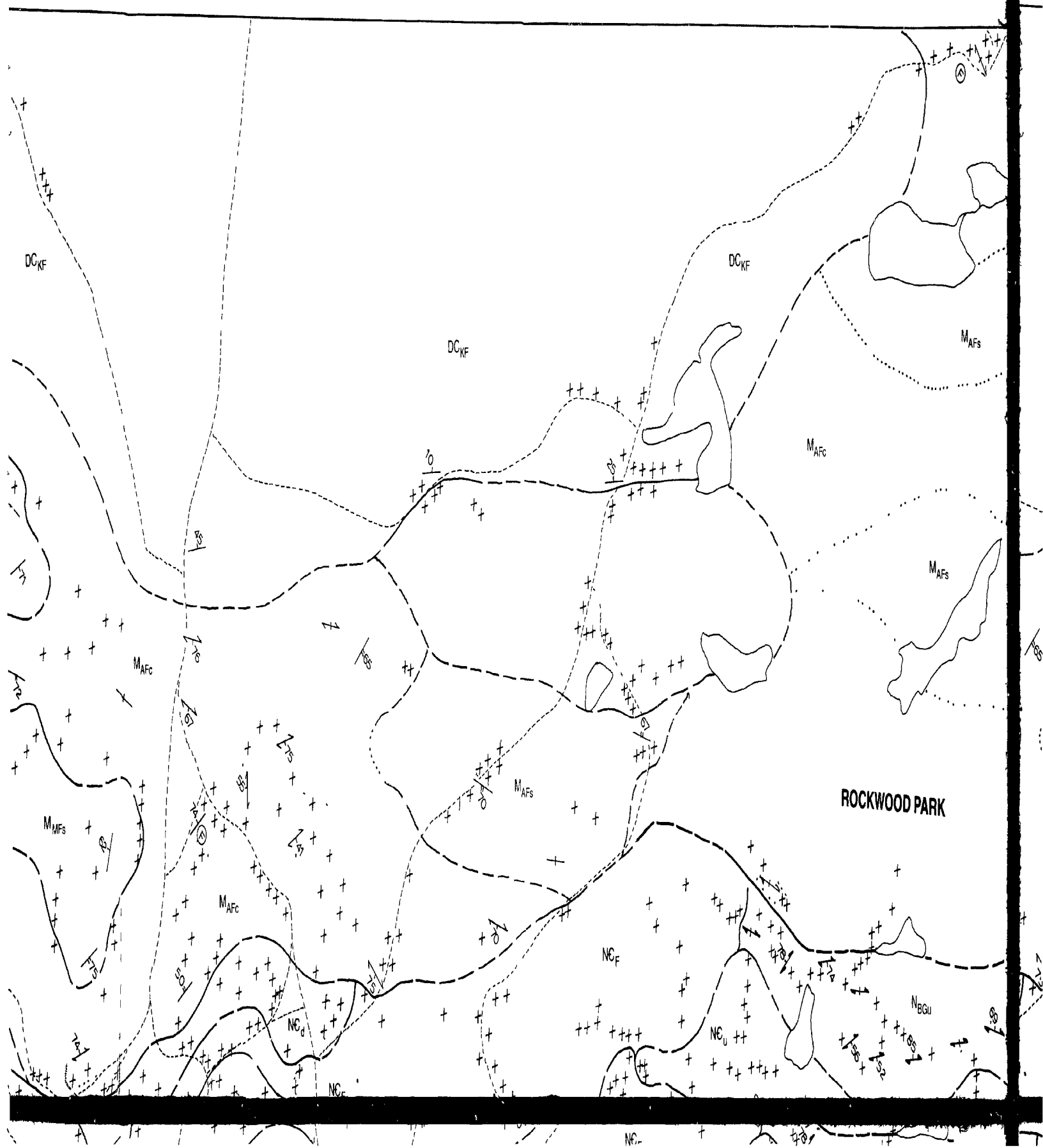


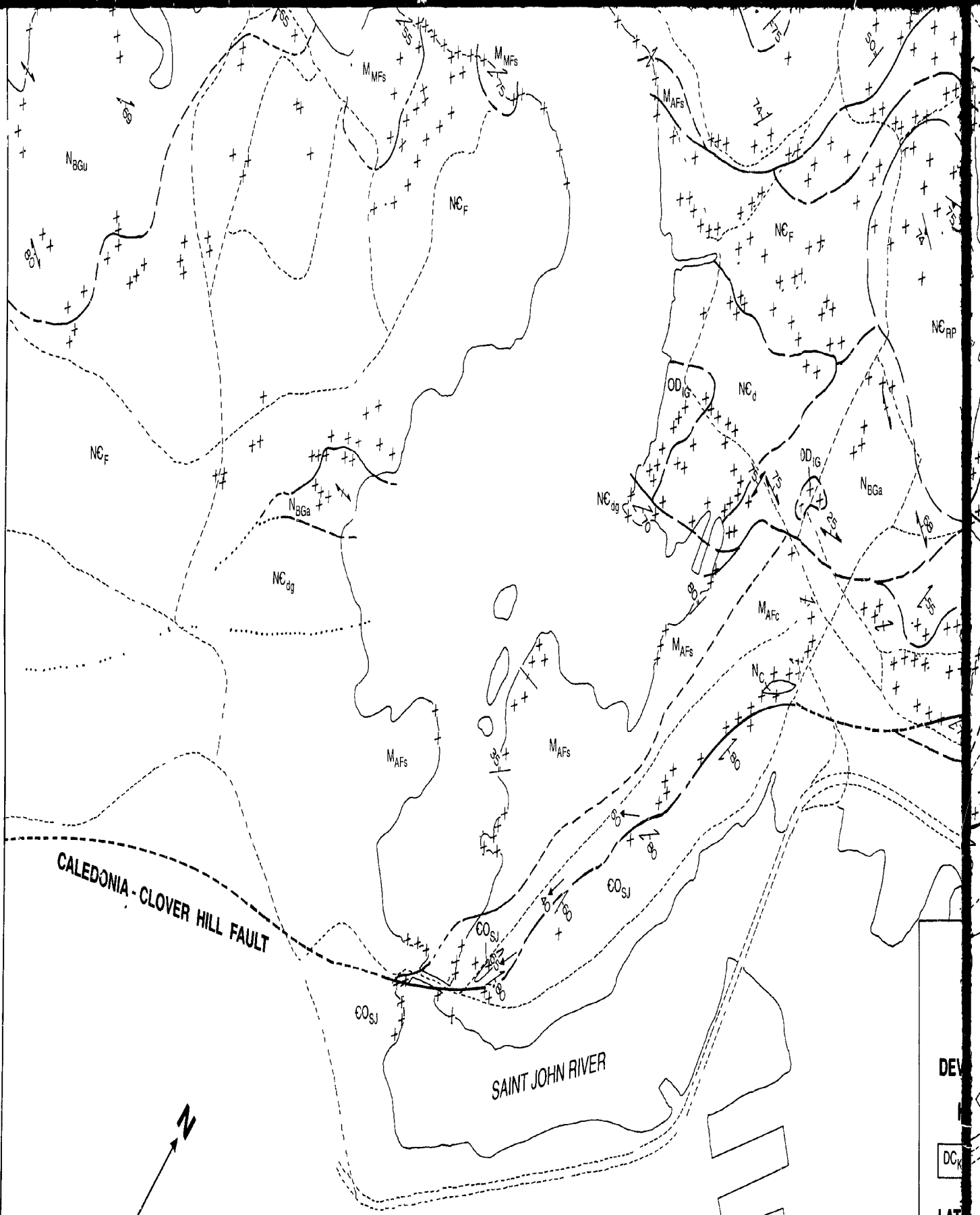
GREEN
HEAD
ISLAND

SAINT JOHN RIVER

The Narrows







CALEDONIA-CLOVER HILL FAULT

SAINT JOHN RIVER

0 0.5 1.0

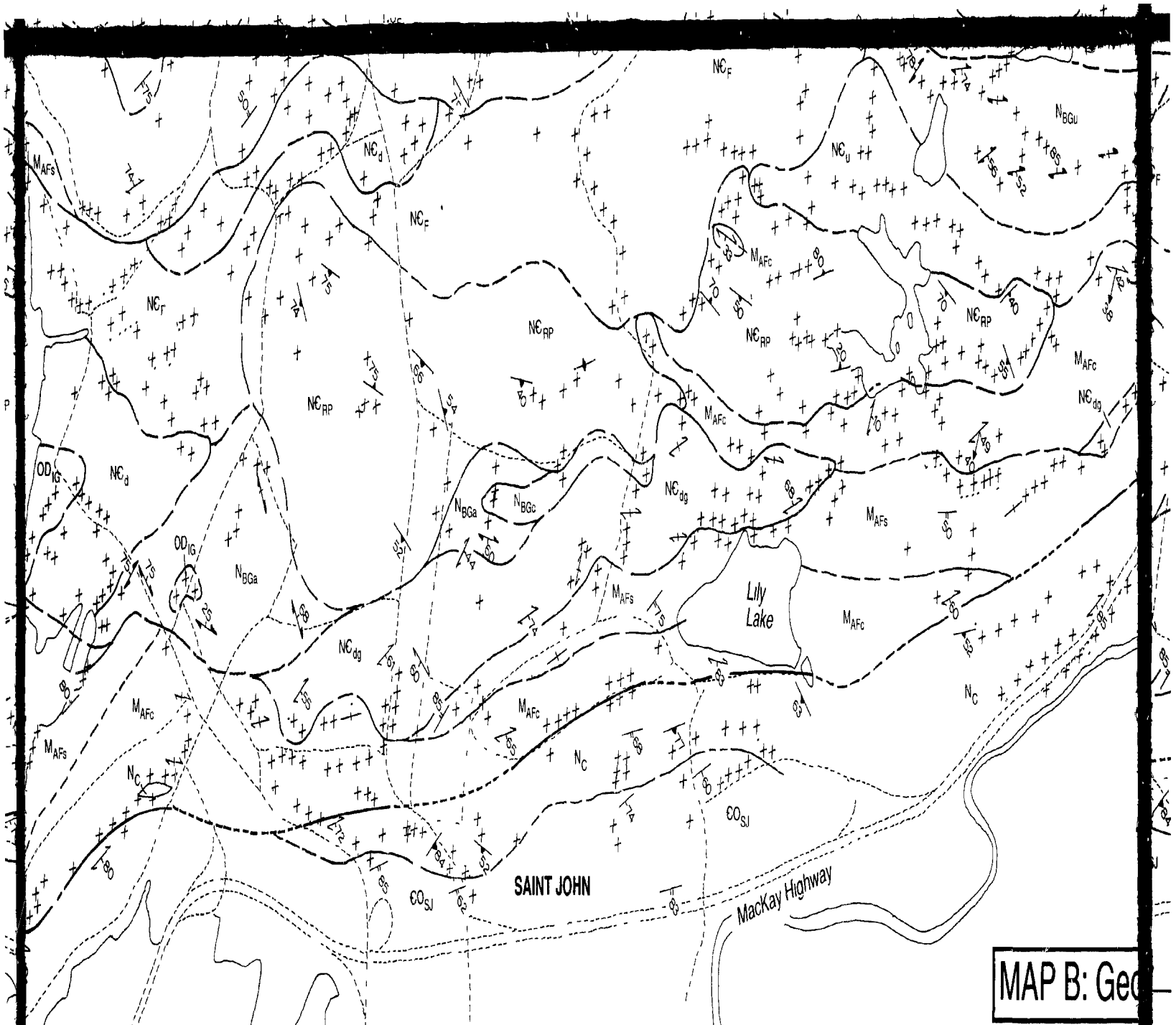


SYMBOLS

X X Outcrop, area of outcrop

 Flow foliation or volcanic layering

DEV
DC
LAT
B
N_{BG}



MAP B: Geo

BROOKVILLE TERRANE LEGEND

STRATIFIED UNITS

PLUTONIC UNITS

DEVONIAN TO CARBONIFEROUS

MESOPROTEROZOIC

ORDOVICIAN TO DEVONIAN (?)

Kennebecasis Formation

Green Head Group

OD_{IG} Indiantown Gabbro

DC_{KF} conglomerate, sandstone, siltstone; minor limestone

Asburn Formation

LATE NEOPROTEROZOIC TO CAMBRIAN

LATE NEOPROTEROZOIC

MA_{FC} mainly carbonate rocks: calcite and dolomite marble

NC_{dg} deformed granitoid rocks

Brookville Gneiss

MA_{FS} mainly siliciclastic rocks: quartzite, meta-siltstone, and spotted hornfels

NC_{ML} Mayflower Lake Tonalite

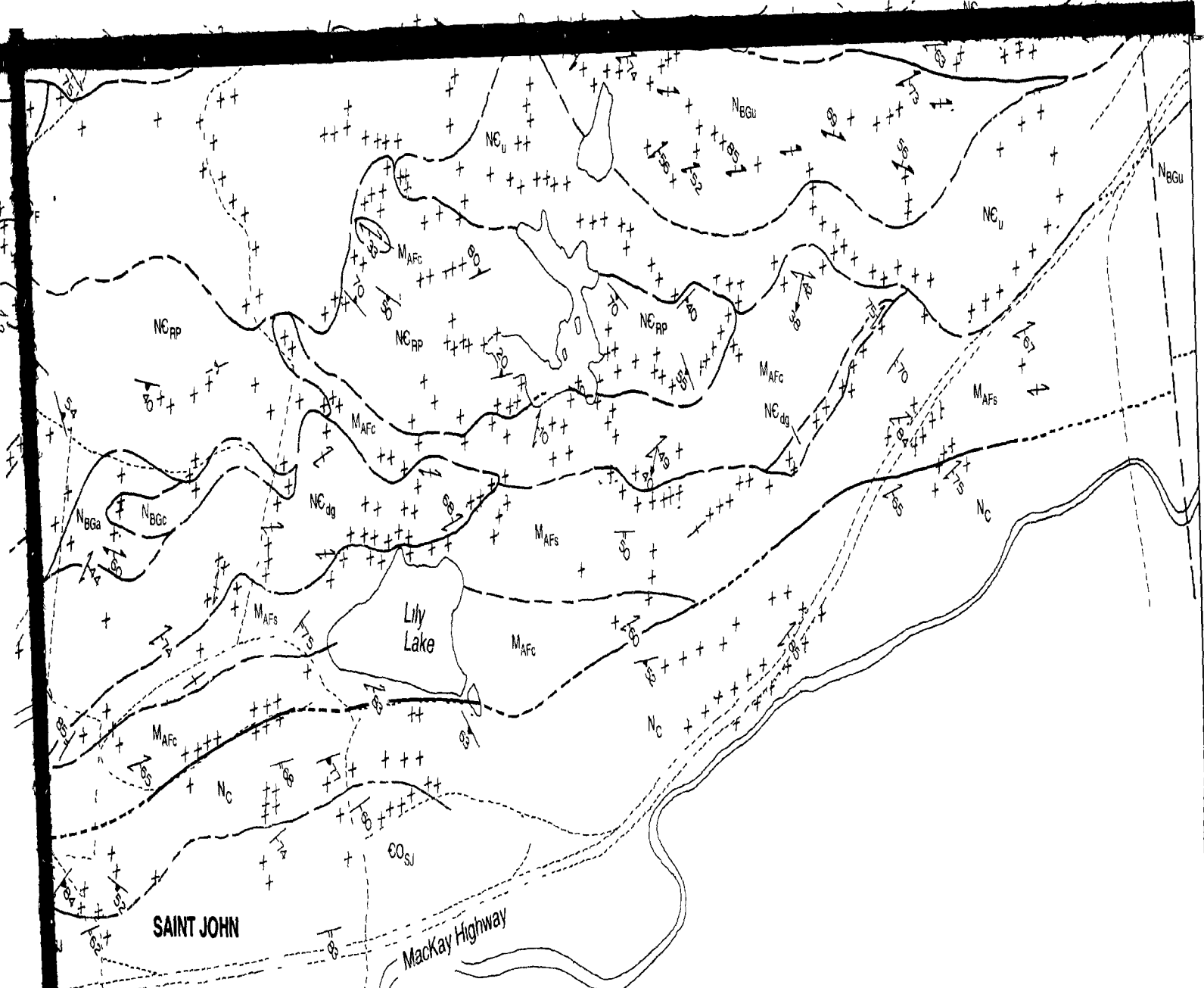
NB_{GU} undivided orthogneiss,

Martin Formation

NC_N Narrows Tonalite

BOLS

Flow foliation or volcanic layering



MAP B: Geology of the Saint John area

BROOKVILLE TERRANE LEGEND

STRATIFIED UNITS

PLUTONIC UNITS

PRECAMBRIAN

MESOPROTEROZOIC

ORDOVICIAN TO DEVONIAN (?)

Formation

Green Head Group

OD_{IG} Indiantown Gabbro

shale, sandstone, siltstone; limestone

Asburn Formation

LATE NEOPROTEROZOIC TO CAMBRIAN

NEOPROTEROZOIC

M_{AFC} mainly carbonate rocks: calcite and dolomite marble

NC_{dg} deformed granitoid rocks

NC_{ML} Mayflower Lake Tonalite

NC_N Narrows Tonalite

NC_U undivided dioritic and

CALEDONIA TERRANE LEGEND

STRATIFIED UNITS

CAMBRIAN TO ORDOVICIAN

Saint John Group

CO_{SJ} shale, siltstone, sandstone, minor limestone

LATE NEOPROTEROZOIC

Coldbrook Group

NC dacitic flows, tuffs, and minor chert and ash

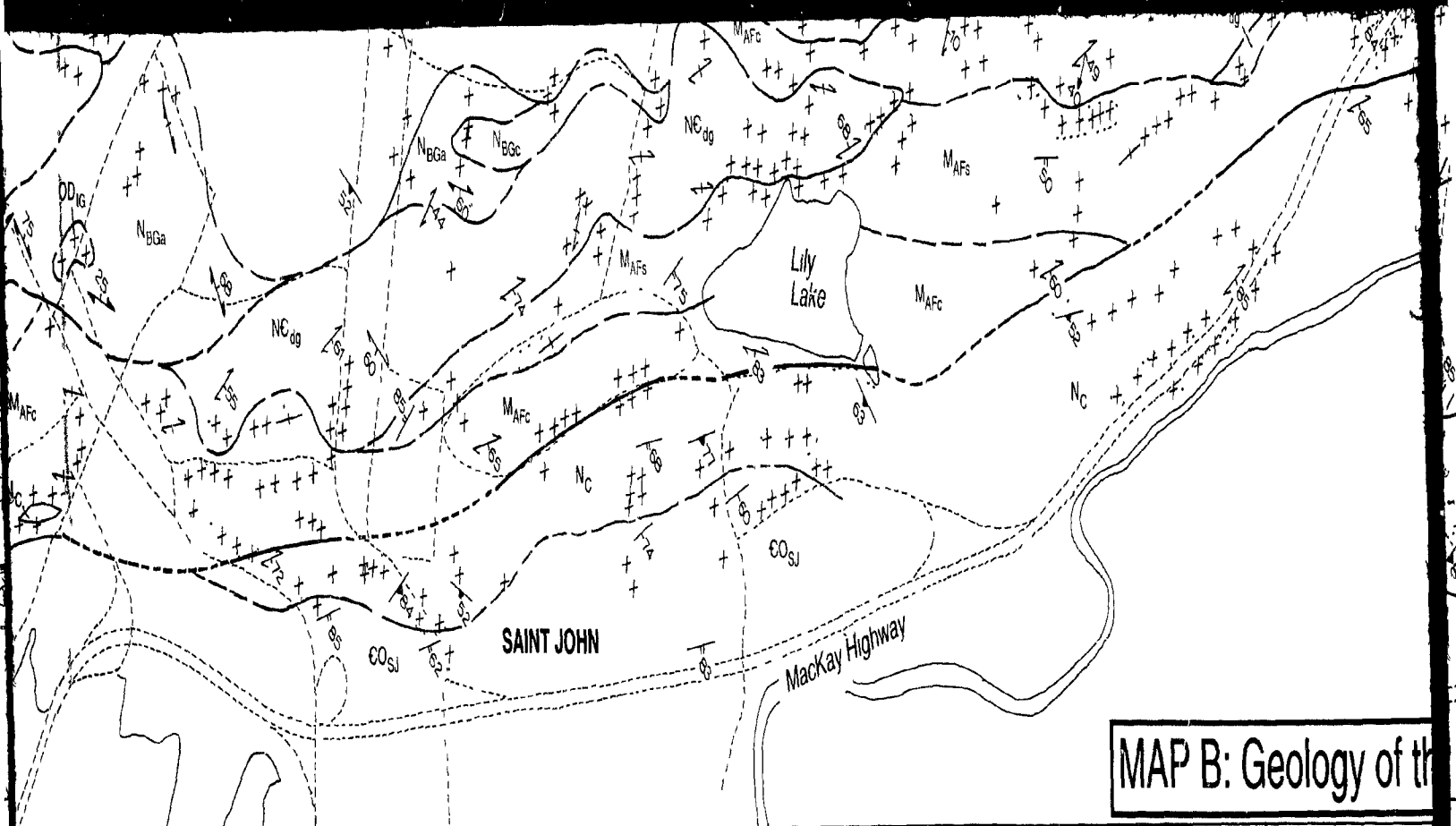
gneiss, and marble

Flow foliation or volcanic layering

N_{BGu}

undivided orthogneiss, paragneiss, and marble

Martin Formation



MAP B: Geology of the

BROOKVILLE TERRANE LEGEND

STRATIFIED UNITS

DEVONIAN TO CARBONIFEROUS

Kennebecasis Formation

DC_{KF} conglomerate, sandstone, siltstone; minor limestone

LATE NEOPROTEROZOIC

Brookville Gneiss

N_{BGu} undivided orthogneiss, paragneiss, and marble

N_{BGa} amphibolite

N_{BGc} carbonate rocks

MESOPROTEROZOIC

Green Head Group

Asburn Formation

M_{AFc} mainly carbonate rocks: calcite and dolomite marble

M_{AFs} mainly siliciclastic rocks: quartzite, meta-siltstone, and spotted hornfels

Martin Formation

M_{MFG} mainly siliciclastic rocks: quartzite, meta-siltstone, and spotted hornfels

M_{MFC} mainly carbonate rocks: calcite and dolomite marble

PLUTONIC UNITS

ORDOVICIAN TO DEVONIAN (?)

OD_{IG} Indiantown Gabbro

LATE NEOPROTEROZOIC TO CAMBRIAN

NC_{dg} deformed granitoid rocks

NC_{ML} Mayflower Lake Tonalite

NC_N Narrows Tonalite

NC_U undivided dioritic and granitic rocks

NC_d dioritic rocks (equivalent to the French Village Quartz Diorite)

NC_{RP} Rockwood Park Granodiorite

NC_F Fairville Granite

CALEDONIA

STRAT

CAMBRIAN

Saint John

CO_{SJ} shale, minor

LATE NEOPROTEROZOIC

Coldbrook

NC dacitic chert

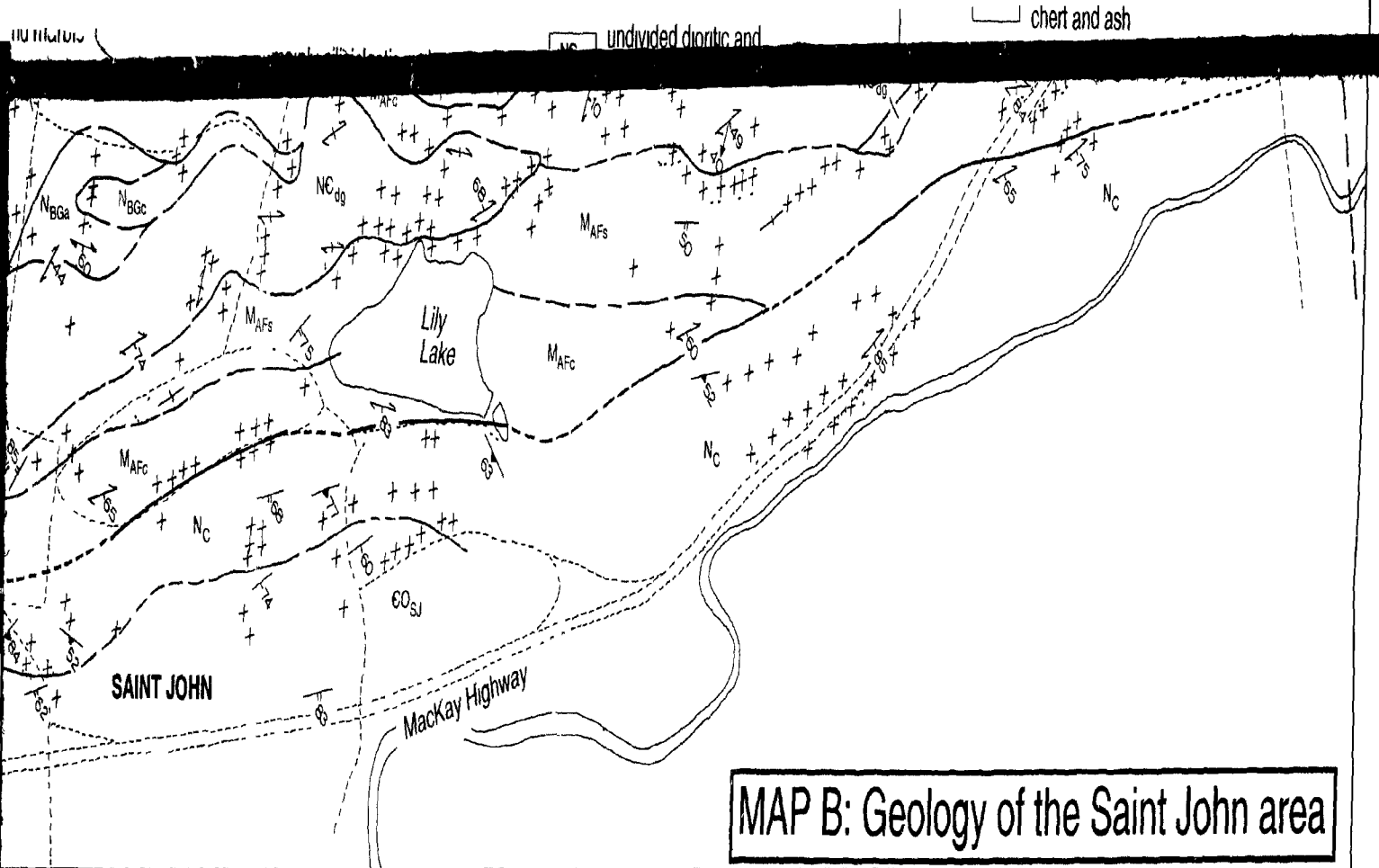
Flow foliation or volcanic layering

Positivity

Stretching lineation

Stromatolite

Lead



MAP B: Geology of the Saint John area

BROOKVILLE TERRANE LEGEND

STRATIFIED UNITS

BONIFEROUS

Formation
sandstone, siltstone;
shale

PROTEROZOIC

gneiss,
marble

MESOPROTEROZOIC

Green Head Group

Asburn Formation

MAFc mainly carbonate rocks: calcite and dolomite marble

MAFs mainly siliciclastic rocks: quartzite, meta-siltstone, and spotted hornfels

Martinon Formation

M_{MFS} mainly siliciclastic rocks: quartzite, meta-siltstone, and spotted hornfels

M_{MFC} mainly carbonate rocks: calcite and dolomite marble

PLUTONIC UNITS

ORDOVICIAN TO DEVONIAN (?)

OD_{IG} Indiantown Gabbro

LATE NEOPROTEROZOIC TO CAMBRIAN

NC_{dg} deformed granitoid rocks

NC_{ML} Mayflower Lake Tonalite

NC_N Narrows Tonalite

NC_U undivided dioritic and granitic rocks

NC_d dioritic rocks (equivalent to the French Village Quartz Diorite)

NC_{RP} Rockwood Park Granodiorite

NC_F Fairville Granite

CALEDONIA TERRANE LEGEND

STRATIFIED UNITS

CAMBRIAN TO ORDOVICIAN

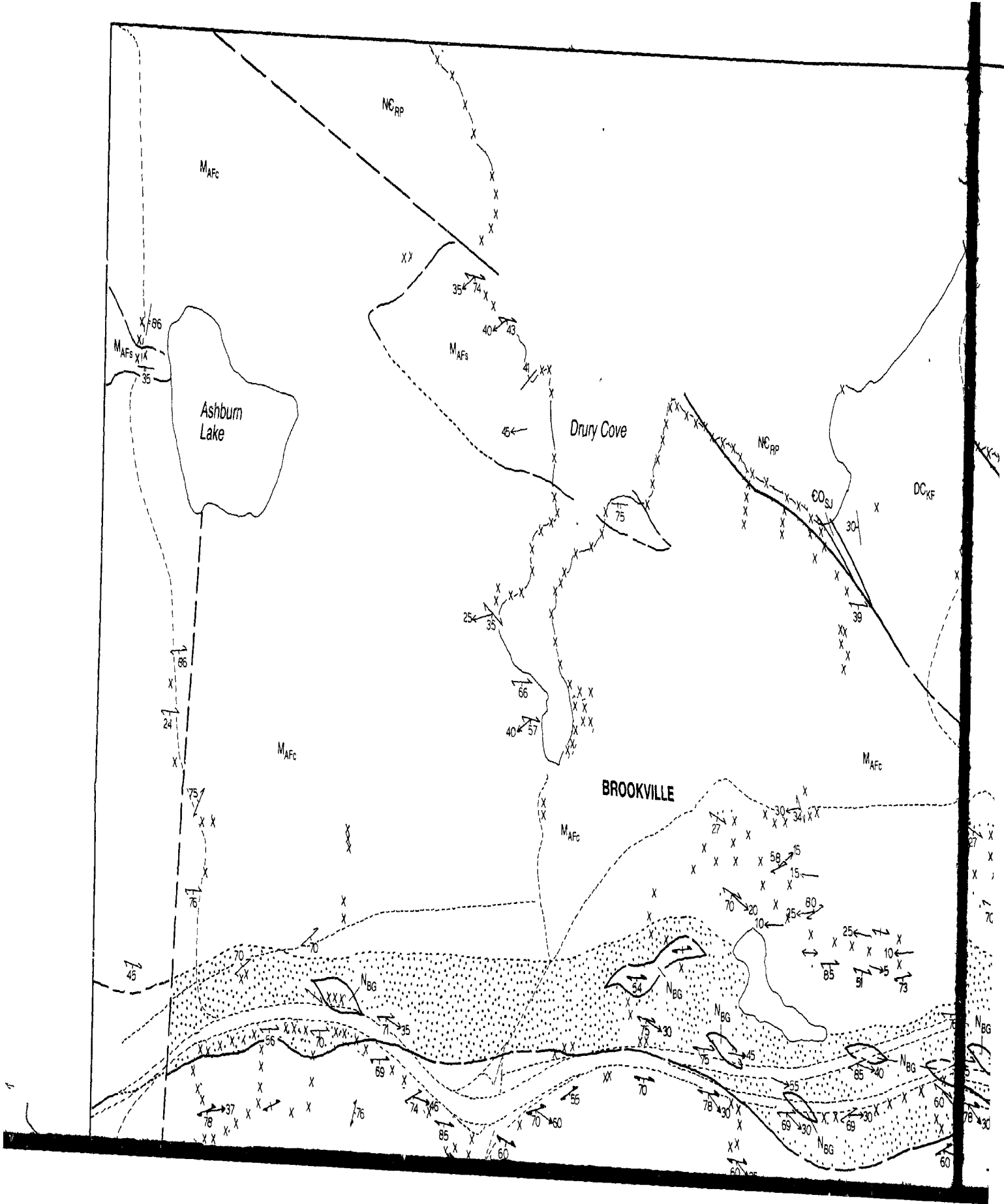
Saint John Group

CO_{SJ} shale, siltstone, sandstone; minor limestone

LATE NEOPROTEROZOIC

Coldbrook Group

N_C dacitic flows, tuffs, and minor chert and ash



KENNEBECASIS BAY

NC_{RP}

X
X
X

XX

X

X

X
X
X
X
X
X
68

NC_{RP}

DC_{KF}

TORRYBURN

NC_{RP}

XX

#

85

N_{BG}



80

50

N_{BG}

20

N_{BG}

Mackay Highway

76

66

61

60

45

84

82

54

40

56

40

70

58

75

75

72

82

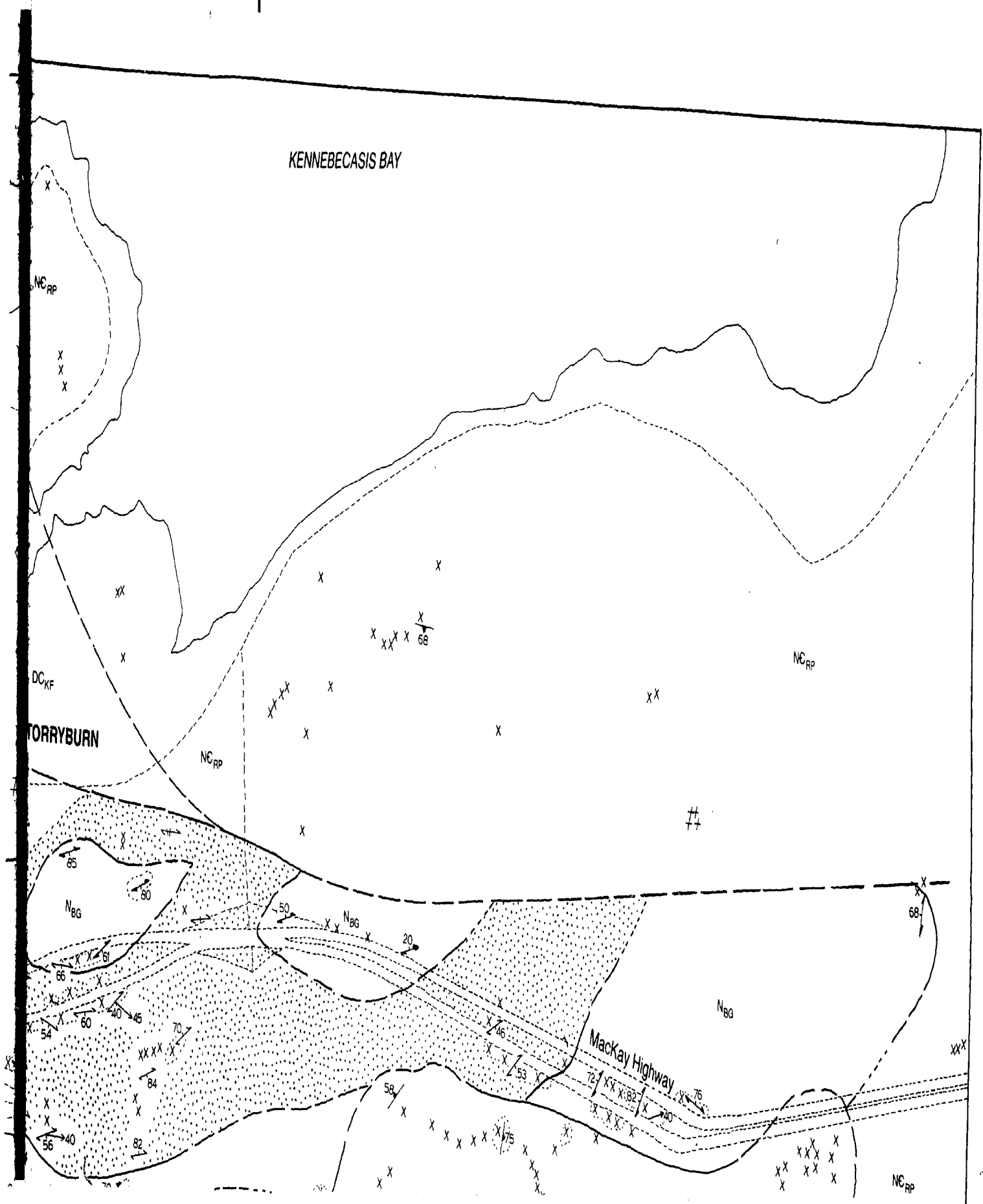
70

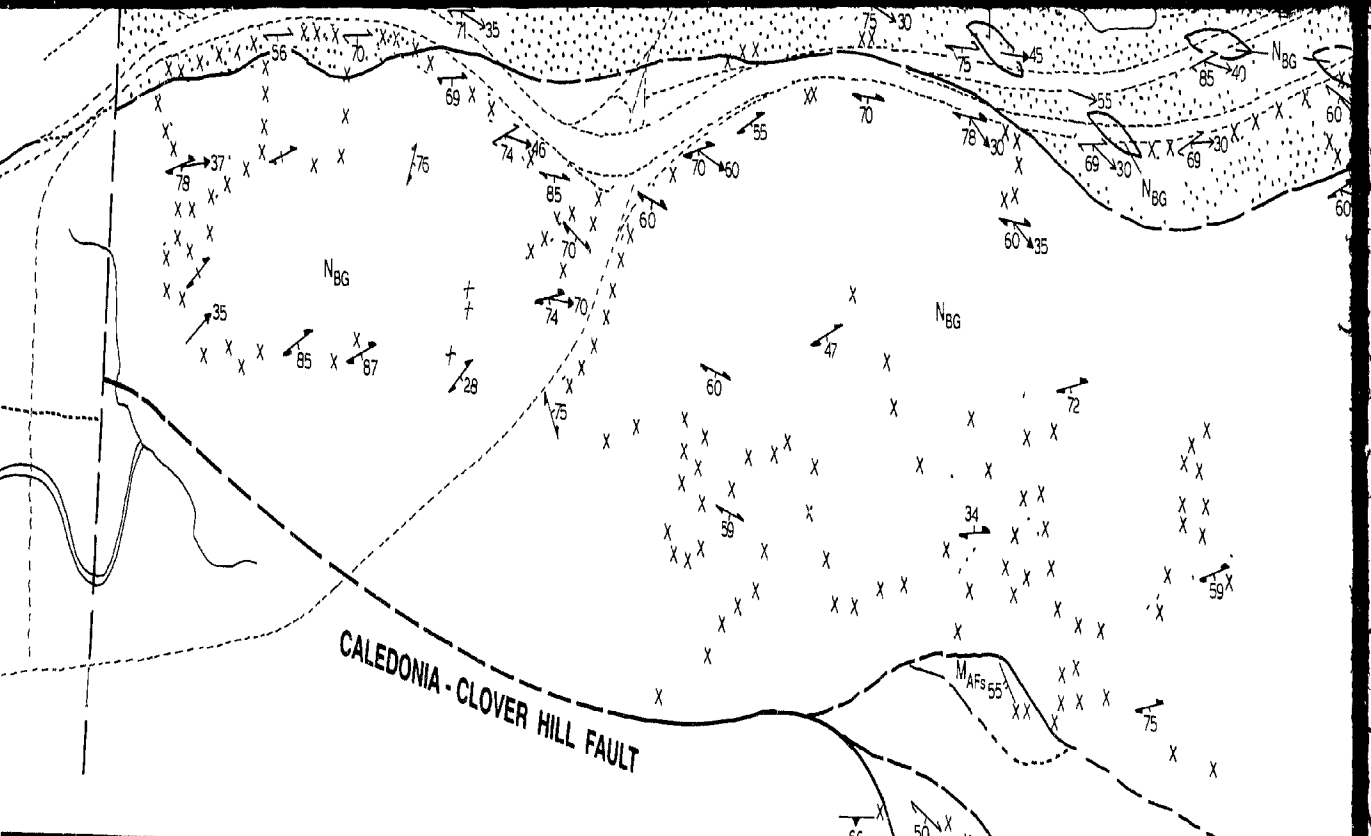
70

NC_{RP}

XX

68





MAP C: Mackay Highway shear zone

LEGEND

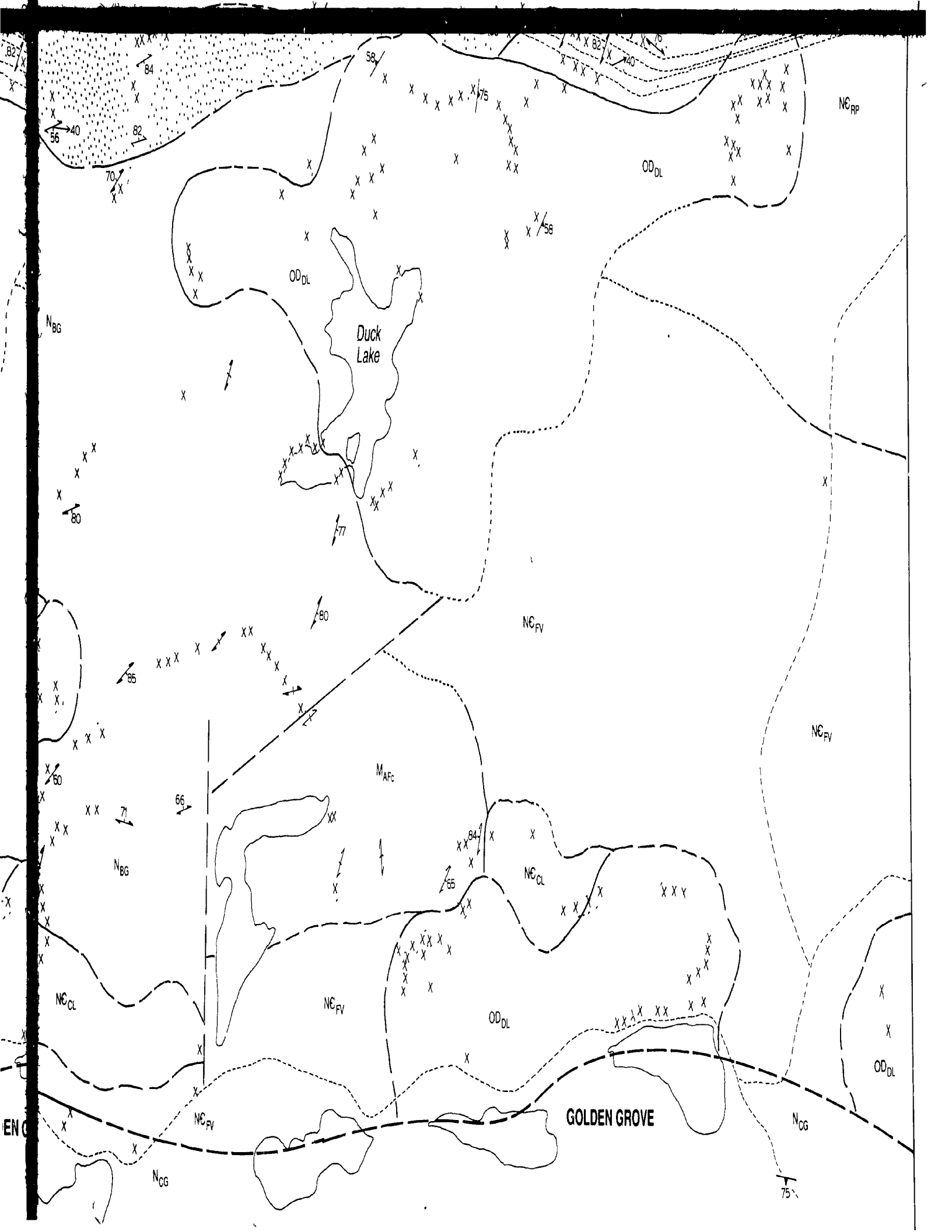
DEVONIAN TO CARBONIFEROUS	
DC _{KF}	Kennebecasis Formation
ORDOVICIAN TO DEVONIAN (?)	
OD _{DL}	Duck Lake Pluton
CAMBRIAN TO ORDOVICIAN	
CO _{SJ}	Saint John Group
LATE NEOPROTEROZOIC TO CAMBRIAN	
NC _{dg}	deformed granitoid rocks
NC _{PP}	Renforth Pluton
NC _{FV}	French Village Quartz Diorite
NC _{CL}	Chalet Lake Granite
[Dotted Pattern]	Mackay Highway shear zone
LATE NEOPROTEROZOIC	
N _{BG}	Brookville Gneiss
N _{CG}	Coldbrook Group

SYMBOLS

X : X	Outcrop, area of outcrop
---	Geological contact (defined, approximate, assumed)
- - -	Fault (defined, approximate)
/ ₂₃ / ₃₄	Bedding (tops known, unknown)
/ ₄₅	Foliation
/ ₆₇	Flow foliation or volcanic layering







MAP C: MacKay Highway shear zone

LEGEND

DEVONIAN TO CARBONIFEROUS

DC_{KF} Kennebecasis Formation

ORDOVICIAN TO DEVONIAN (?)

OD_{DL} Duck Lake Pluton

CAMBRIAN TO ORDOVICIAN

CO_S Saint John Group


LATE NEOPROTEROZOIC TO CAMBRIAN

NC_{dg} deformed granitoid rocks

NC_{RP} Renforth Pluton

NC_{FV} French Village Quartz Diorite

NC_{CL} Chalet Lake Granite

 MacKay Highway shear zone

LATE NEOPROTEROZOIC

N_{BG} Brookville Gneiss

N_{CG} Coldbrook Group

MESOPROTEROZOIC


Asburn Formation


MA_{FC} mainly carbonate rocks: calcite, marble and dolomite

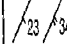
MA_{FS} mainly siliciclastic rocks: quartzite, siltstone, and schist


SYMBOLS


X . X Outcrop, area of outcrop


 Geological contact (defined, approximate, assumed)


 Fault (defined, approximate)


 Bedding (tops known, unknown)

 Foliation

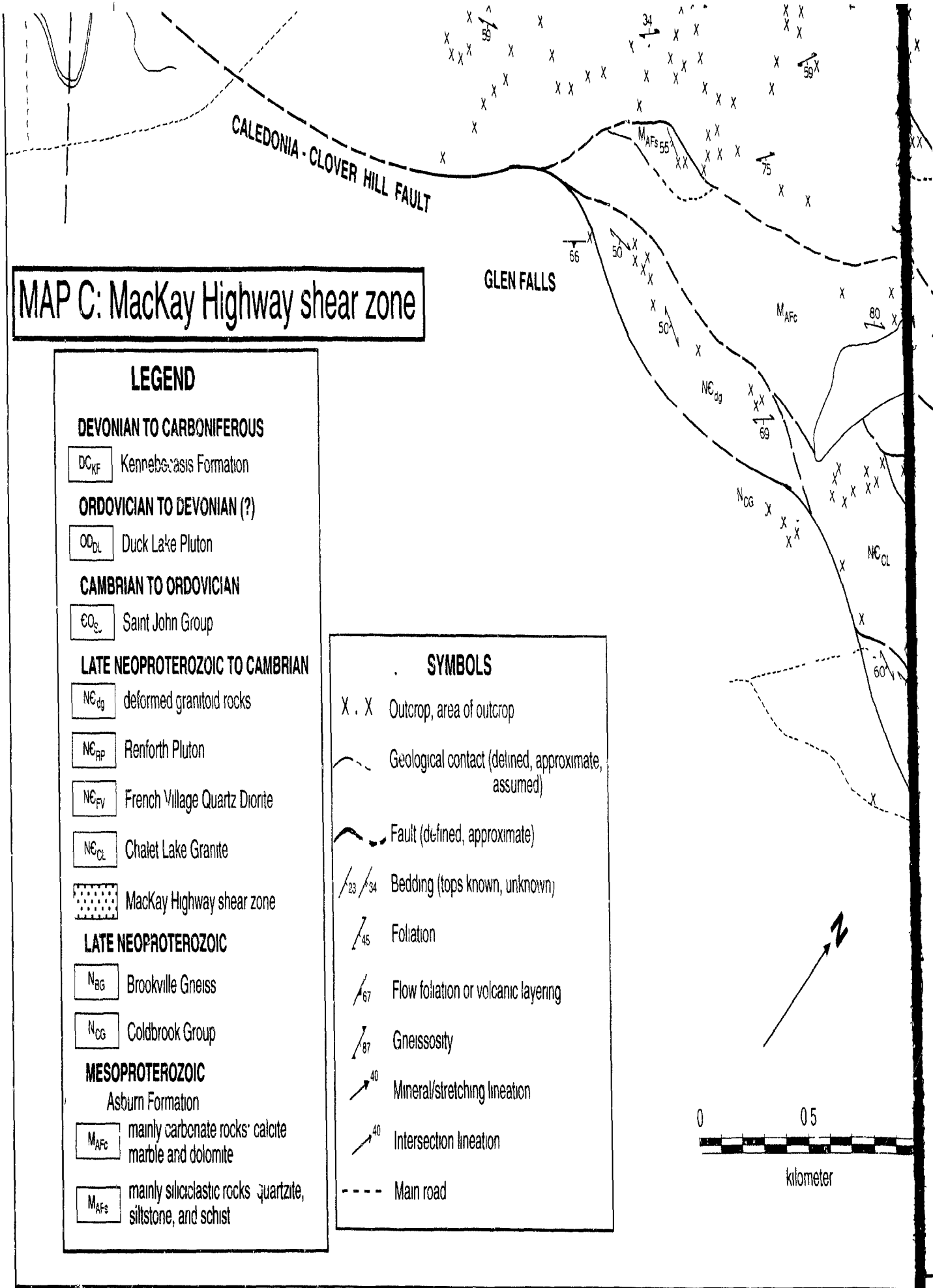
 Flow foliation or volcanic layering

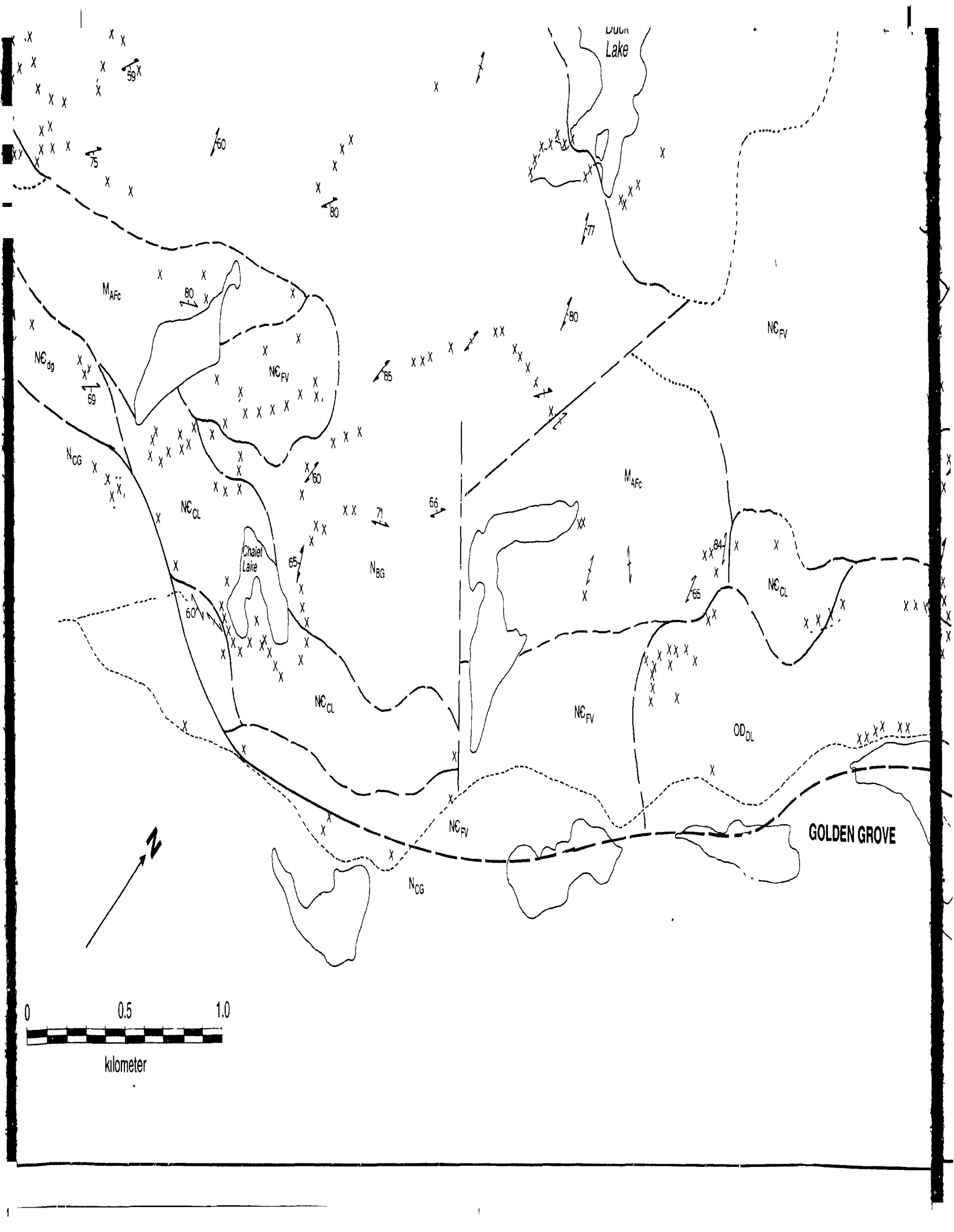
 Gneissosity

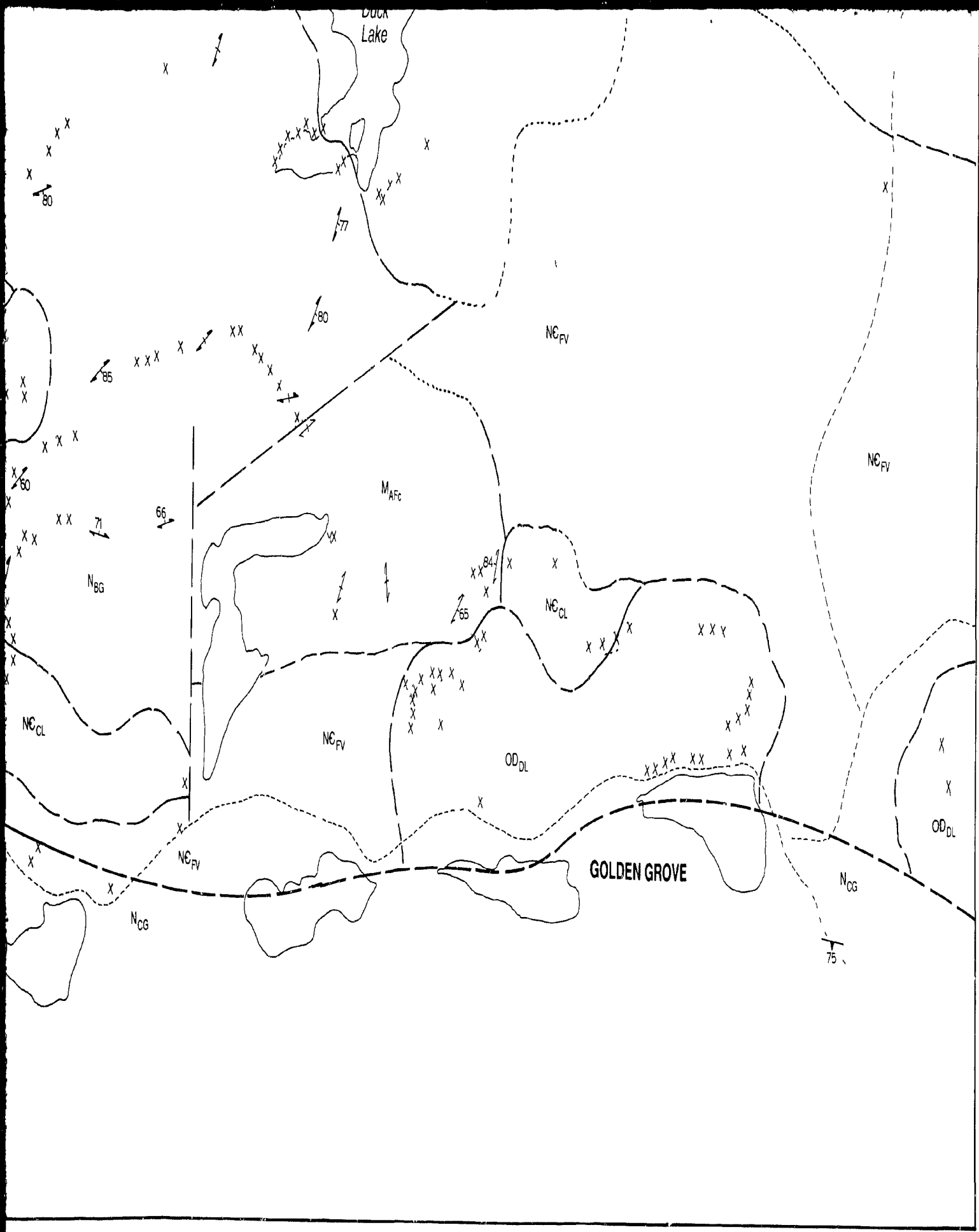
 Mineral/stretching lineation

 Intersection lineation

--- Main road







LEGEND

STRATIFIED UNITS

PLUTONIC UNITS

TRIASSIC

T_{LF} Lepreau Formation

CARBONIFEROUS

C_{LF} Lancaster Formation

C_{BLF} Balls Lake Formation

C_{PF} Parleeville Formation

DEVONIAN TO CARBONIFEROUS

DC_{MF} Memramcook Formation

DC_{KF} Kennebecasis Formation

CAMBRIAN TO ORDOVICIAN

Saint John Group

EO_{KSF} King Square Formation

EO_{FHF} Forest Hills Formation

LATE PROTEROZOIC

Dipper Harbour volcanic unit

P_{DHr} rhyolitic rocks

P_{DHnd} andesitic to dacitic rocks

P_{DHsr} andesitic to rhyolitic rocks with minor sedimentary rocks

Brookville Gneiss

P_{BCpo} paragneiss and orthogneiss

P_{BGa} amphibolite

PROTEROZOIC

Green Head Group

P_{AF} Ashburn Formation

P_{MF} Martinon Formation

CT CALEDONIA TERRANE

KC KINGSTON COMPLEX

ORDOVICIAN TO SILURIAN (?)

Gabbro and Ultramafic rocks

OS_{DL} Duck Lake Pluton

OS_I Indiantown Pluton

LATE PROTEROZOIC TO CAMBRIAN

PE_{dg} Deformed granitoid rocks

Syenogranite to Monzogranite

PE_{HH} Harvey Hill Syenogranite

PE_{PW} Prince of Wales Granite

PE_{CH} Cranberry Head Syenogranite

PE_{JL} Jarvies Lake Syenogranite

PE_{MH} Musquash Harbour Granite (d = diorite)

PE_{HB} Henderson Brook Granite

Monzogranite to Granodiorite

PE_{LH} Lepreau Harbour Granodiorite

PE_L Lepreau Pluton

PE_{HS} Hanson Stream Granodiorite

PE_{MHP} Milkish Head Pluton

PE_{HR} Hammond River Granite

PE_{CL} Chalet Lake Granite

PE_F Fairville Granite

Diorite to Granodiorite

PE_A Acamac Tonalite

PE_N Narrows Tonalite

PE_{ML} Mayflower Lake Tonalite

PE_R Renforth Pluton

PE_{TR} Talbot Road Granodiorite

PE_{SL} Shadow Lake Granodiorite (e = enclave)

PE_{PL} Perch Lake Granodiorite (e = enclave)

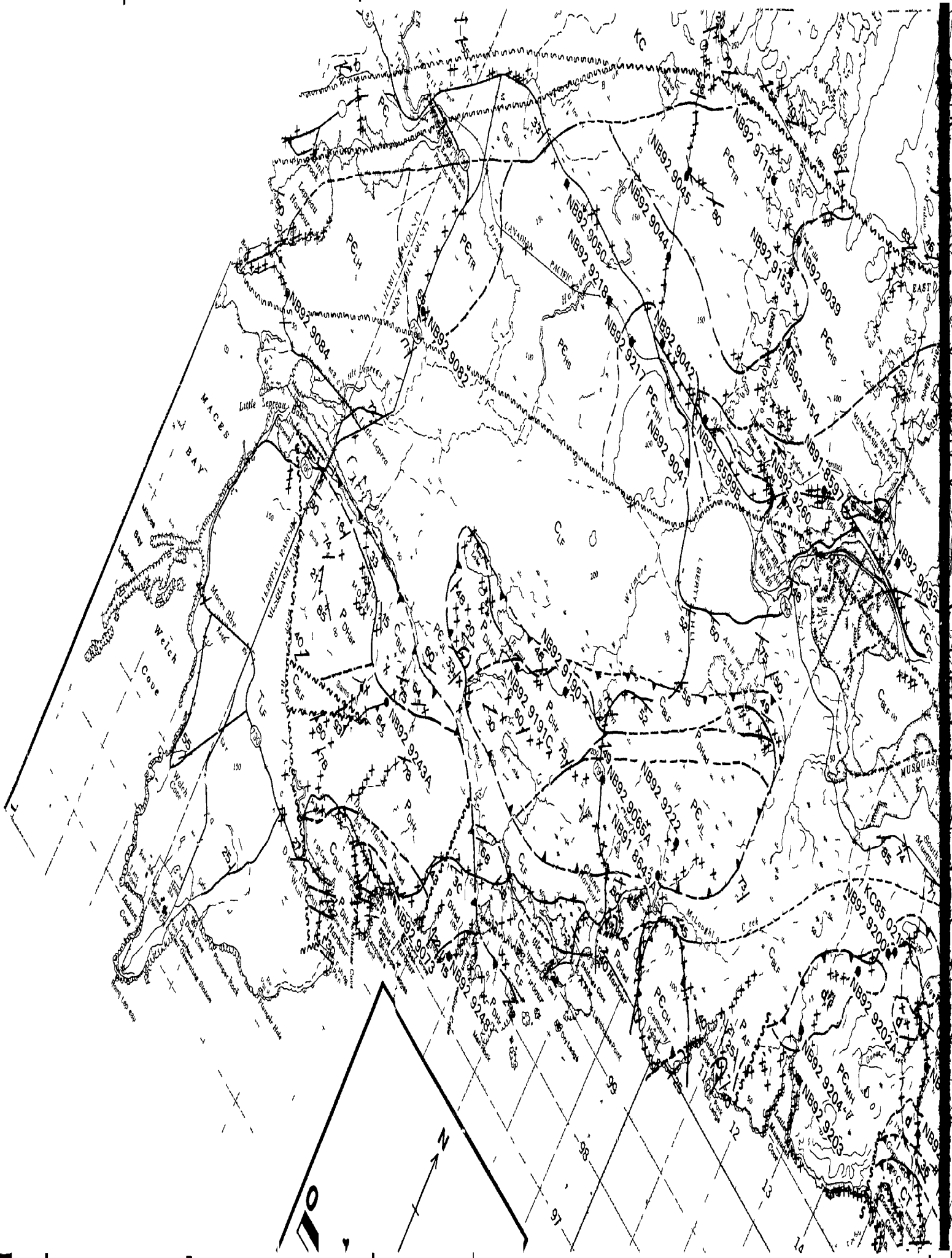
PE_B Belmont Tonalite

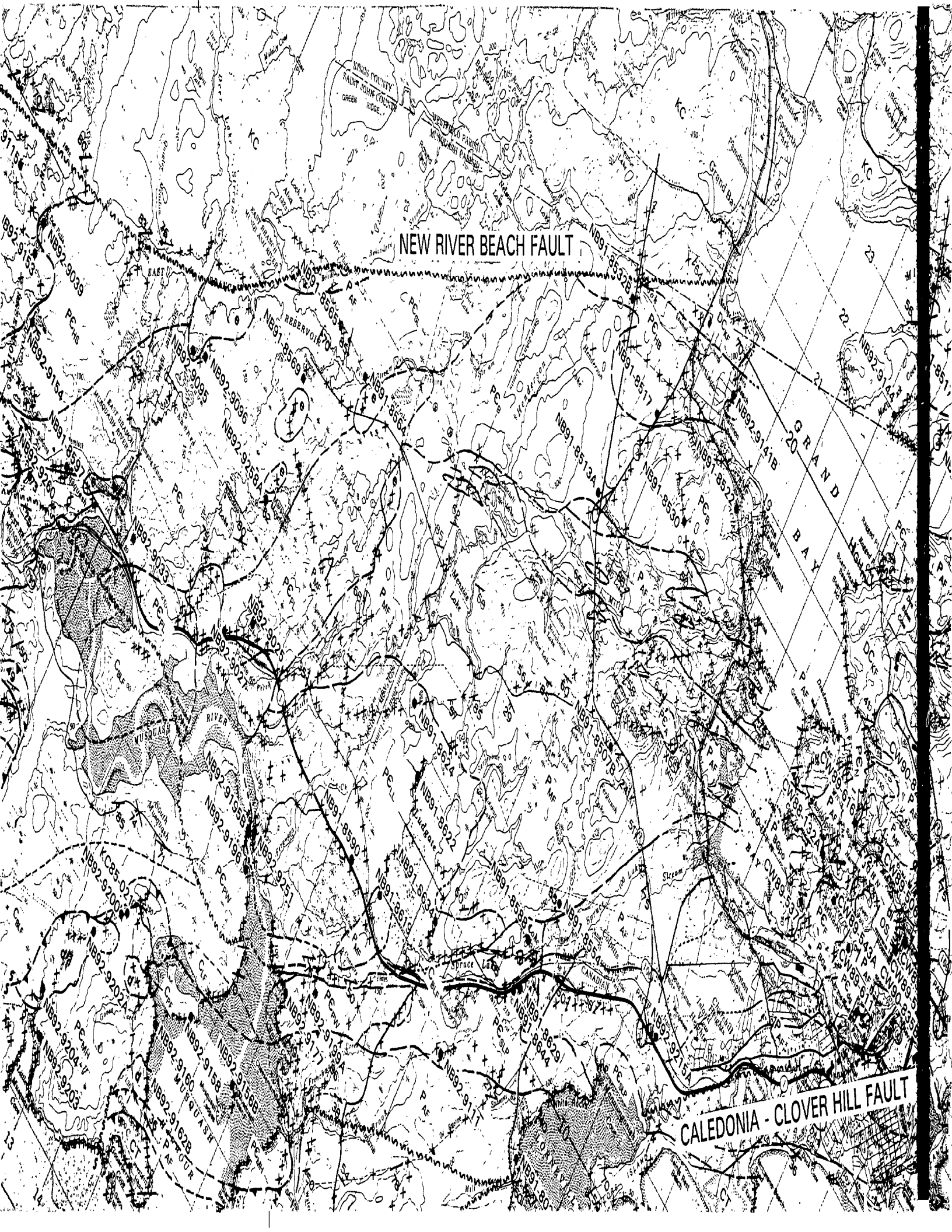
PE_{FV} French Village Quartz Diorite and equivalent units (di)

PE_{RP} Rockwood Park Granodiorite

PE_{SLP} Spruce Lake Pluton

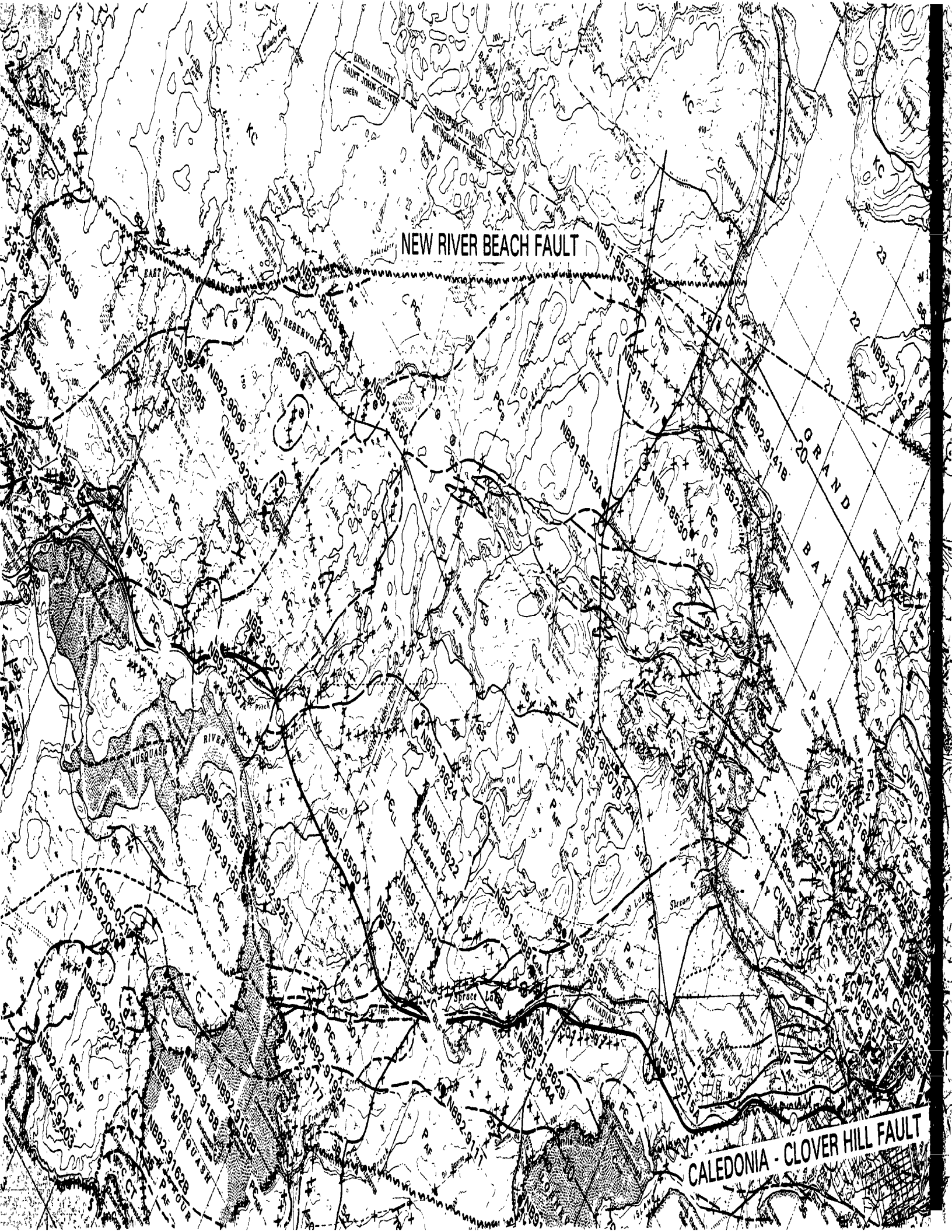
PE_{LI} Ludgate Lake Granodiorite





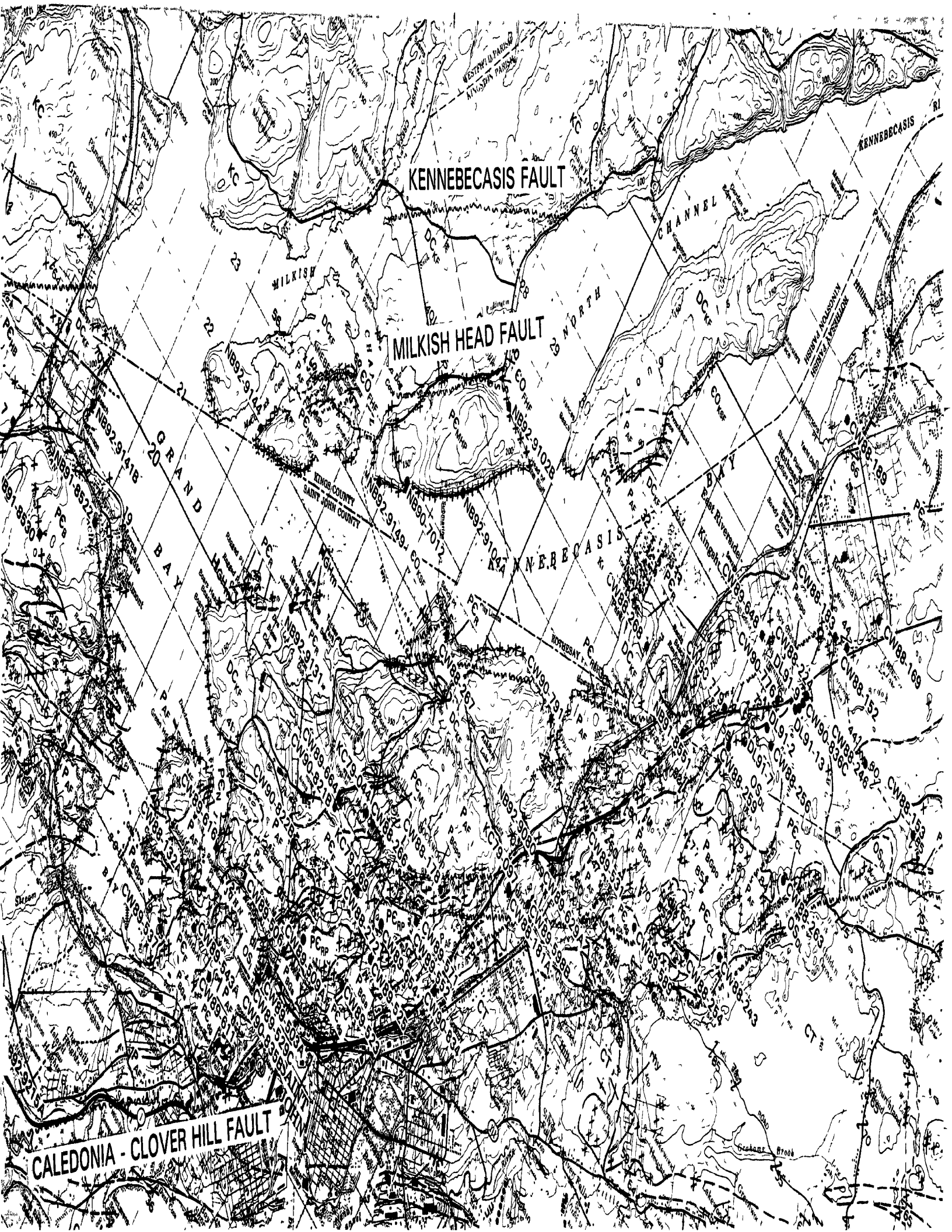
NEW RIVER BEACH FAULT

CALEDONIA - CLOVER HILL FAULT



NEW RIVER BEACH FAULT

CALEDONIA - CLOVER HILL FAULT



KENNEBECASIS FAULT

MILKISH HEAD FAULT

CALEDONIA - CLOVER HILL FAULT

GRAND BAY

KENNEBECASIS

KENNEBECASIS

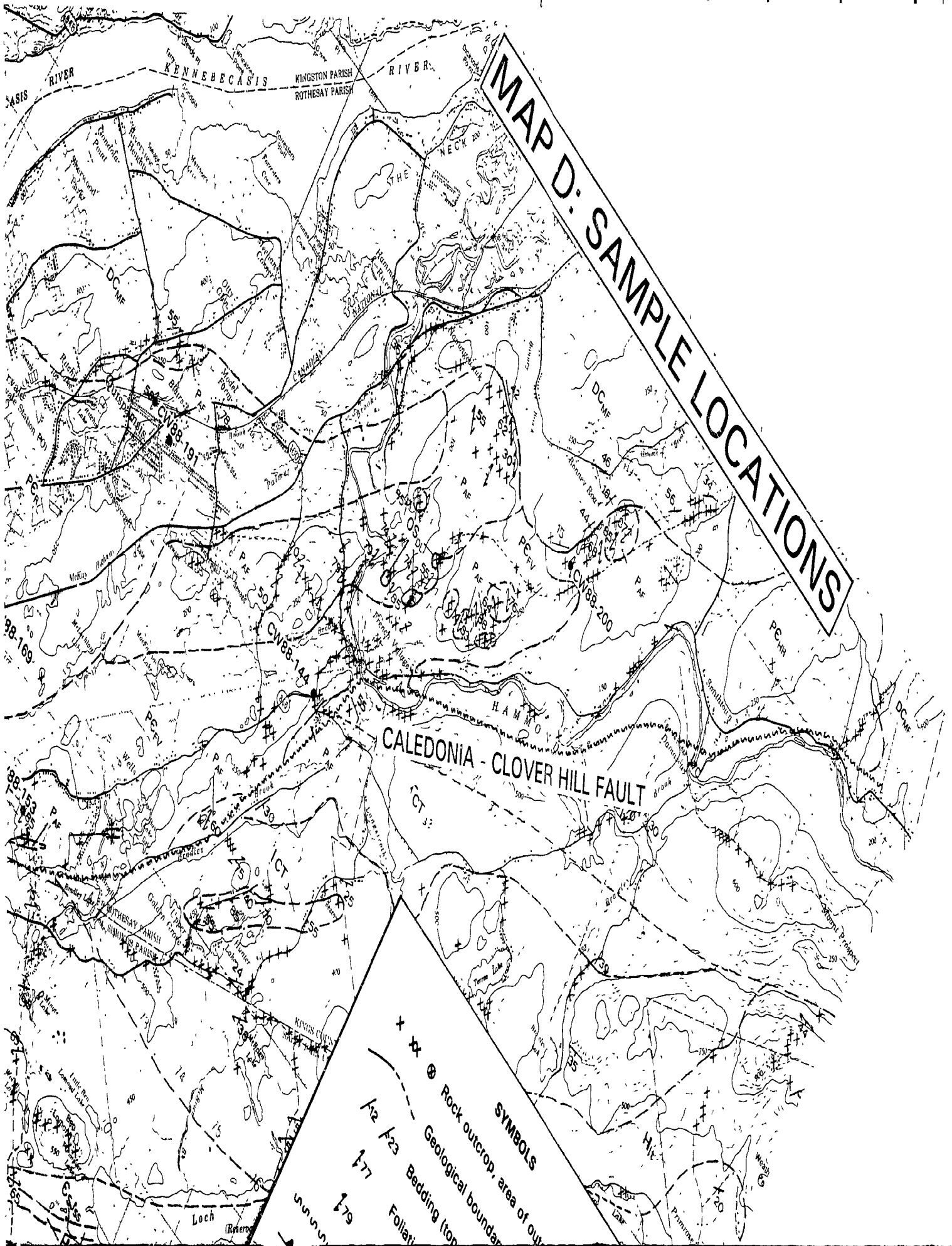
MILKISH

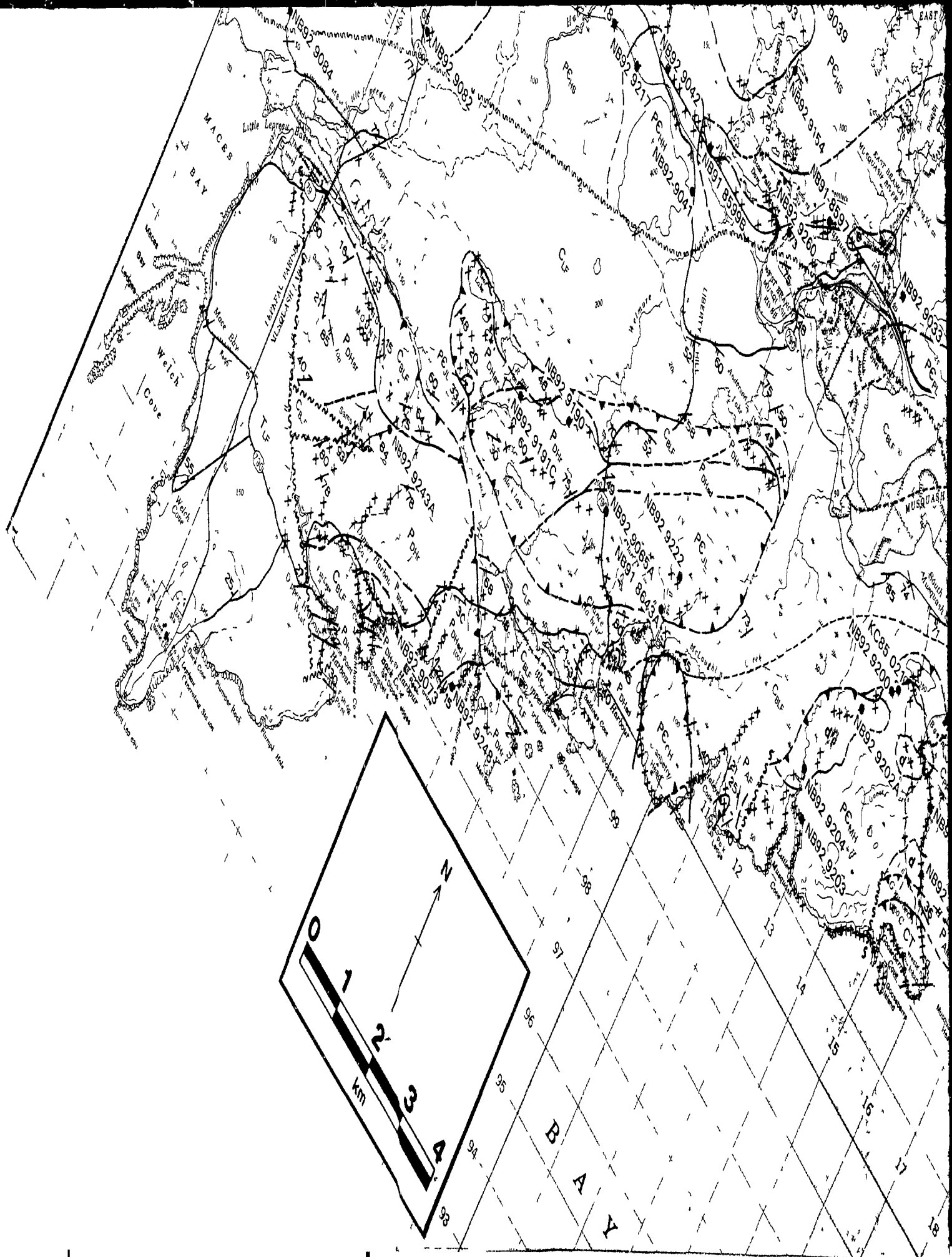
NORTH

RINGS COUNTY
SAINT JOHN COUNTY

Stoughton Brook

MAP D: SAMPLE LOCATIONS







MILKISH HEAD FAULT

GRAND BAY

NERECASIS

CALEDONIA - CLOVER HILL FAULT

SAINT JOHN HARBOUR

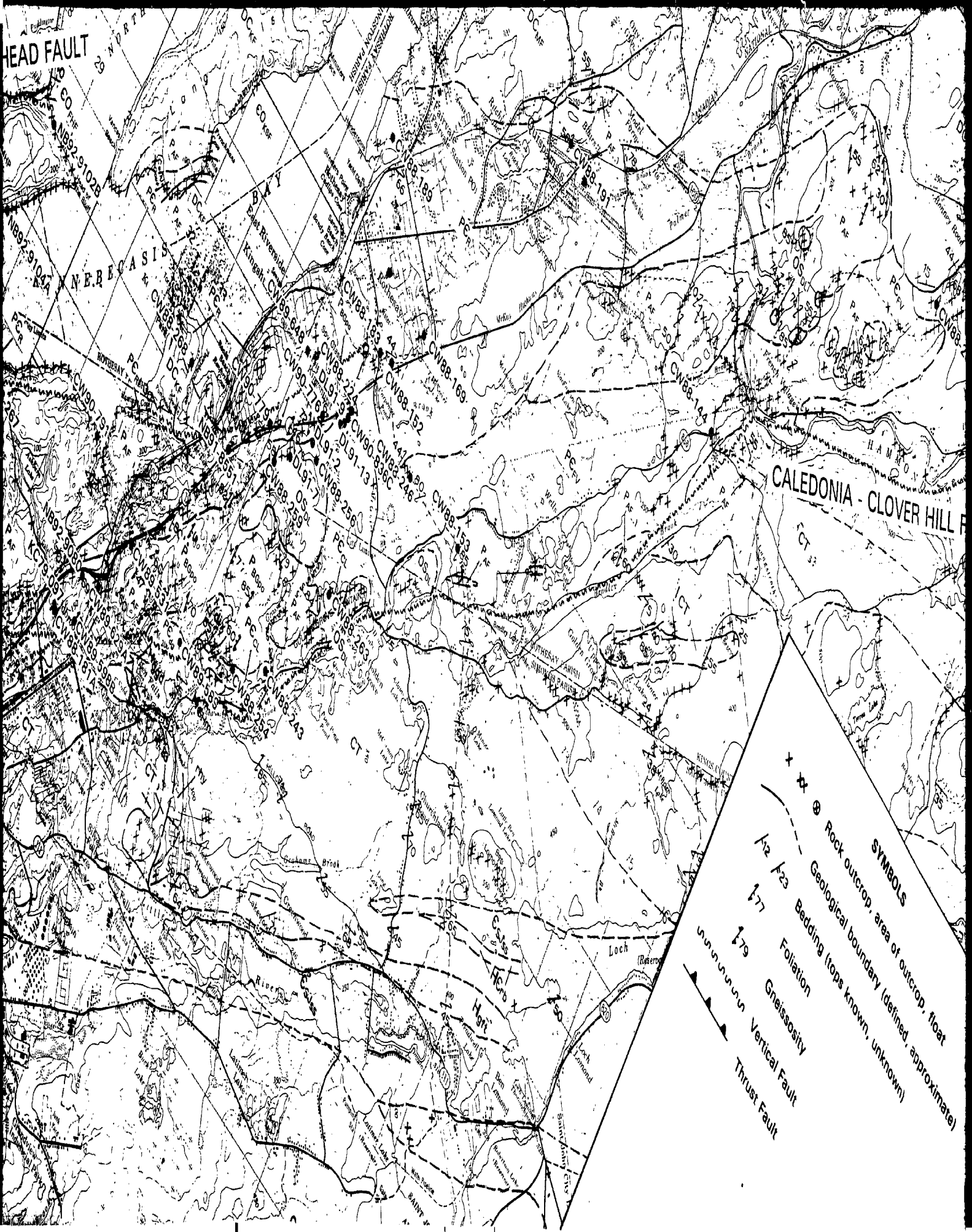
HEAD FAULT

NEBECA S I S

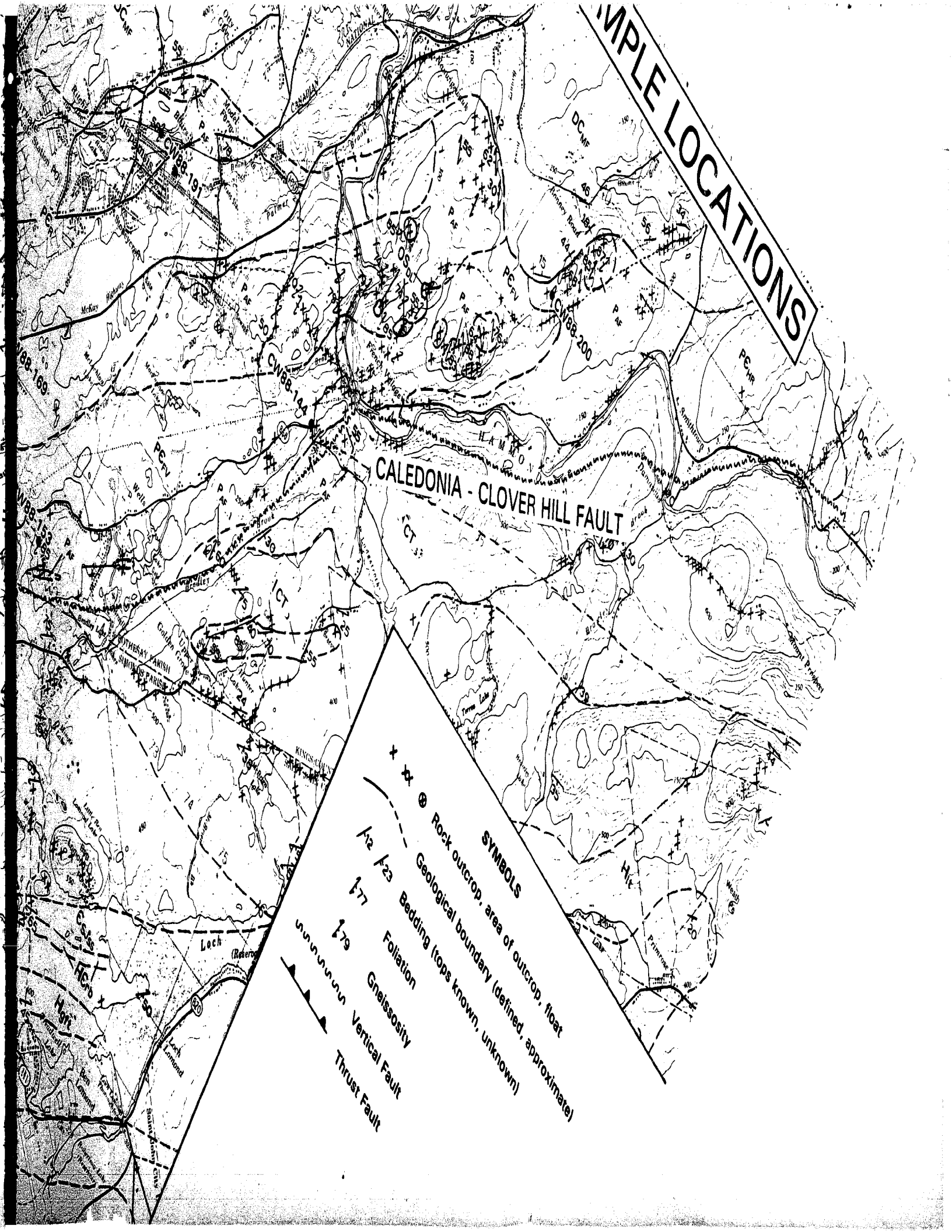
CALEDONIA - CLOVER HILL F

SYMBOLS

- x ⊗ Rock outcrop, area of outcrop, float
- - - Geological boundary (defined, approximate)
- 1/2 1/2 Bedding (tops known, unknown)
- 1/7 Foliation
- 1/9 Gneissosity
- Vertical Fault
- Thrust Fault



WATER SAMPLE LOCATIONS

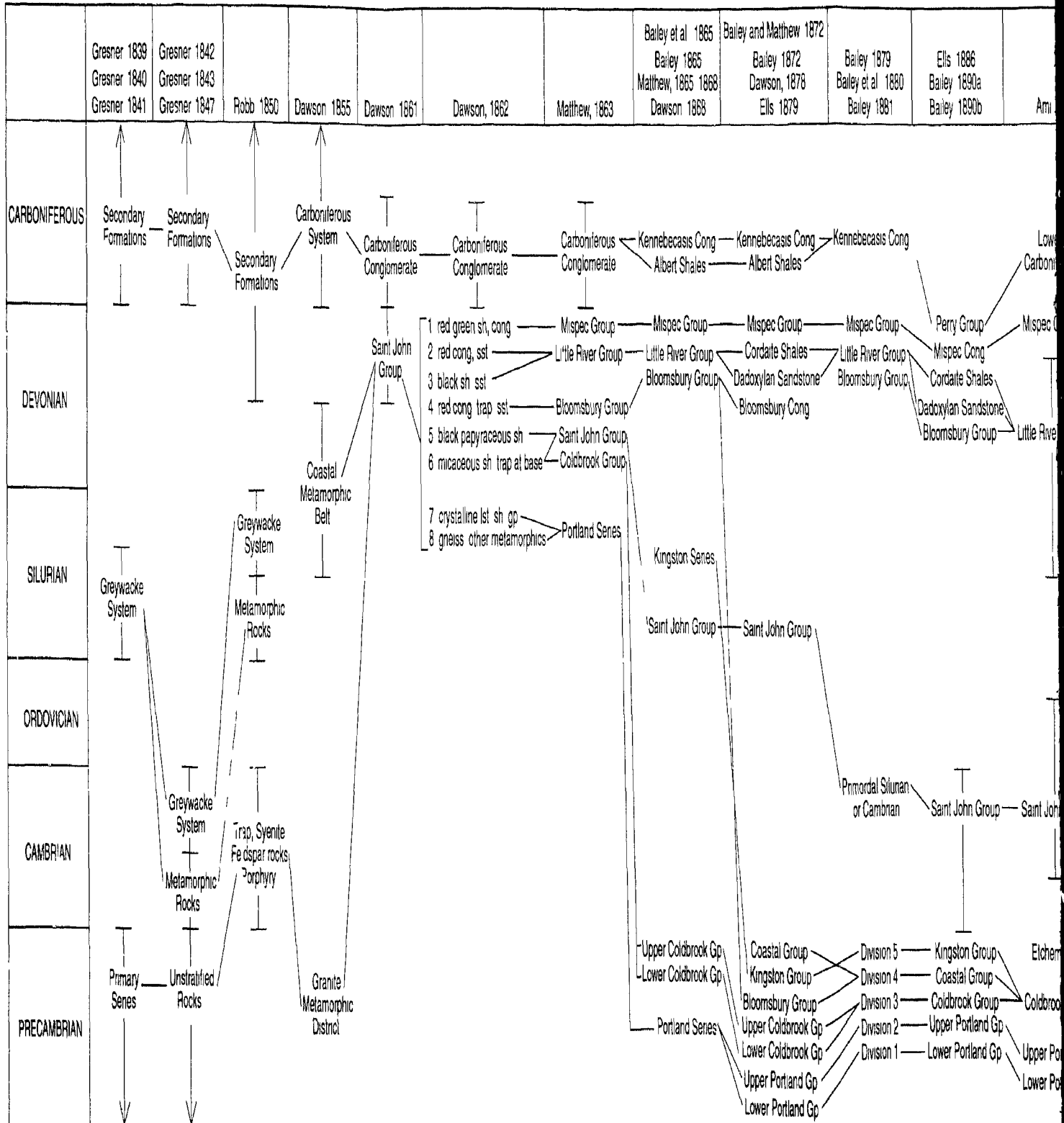


CALEDONIA - CLOVER HILL FAULT

SYMBOLS

- x x o Rock outcrop, area of outcrop, float
- - - Geological boundary (defined, approximate)
- 1/2 1/2 Bedding (tops known, unknown)
- 1/7 Foliation
- 1/9 Gneissosity
- Vertical Fault
- Thrust Fault

Table A1 1 Summary chart for stratigraphic correlation and history of interpretation for southern New Brunswick



Bailey et al., 1865 Bailey, 1865 Matthew, 1865, 1868 Dawson, 1868	Bailey and Matthew, 1872 Bailey, 1872 Dawson, 1878 Ells 1879	Bailey 1879 Bailey et al., 1880 Bailey 1881	Ells 1886 Bailey 1890a Bailey 1890b	Ami 1900	Ells 1906 Ells 1907 Ells 1908	Matthew 1908a Matthew 1908b	Hayes 1914	Bailey and Matthew 1919 Matthew 1921	Hayes and Howell 1937	Alcock 1938 Alcock, 1948 Smith, 1966
--	---	---	---	----------	-------------------------------------	--------------------------------	------------	---	-----------------------	--

